

**DIFFUSION STUDY ON MEASURING AND MITIGATING THE
INTERACTIONS BETWEEN NEODYMIUM AND STEEL
CLADDING MATERIALS**

A Thesis

by

GRANT WILSON HELMREICH

Submitted to the Office of Graduate and Professional Studies of
Texas A&M University
in partial fulfillment of the requirements for the degree of

DOCTOR OF PHILOSOPHY

Chair of Committee,	Sean M. McDeavitt
Committee Members,	Lin Shao
	Xinghang Zhang
	Delia Perez-Nunez
Head of Department,	Ibrahim Karaman

May 2014

Major Subject: Materials Science

Copyright 2014 Grant Wilson Helmreich

ABSTRACT

One of the challenges facing the development of ultra-high burnup fast reactors, such as the Travelling Wave Reactor, is Fuel-Cladding Chemical Interactions (FCCI) between lanthanide fission products and steel cladding materials. At higher burnup, the fission product inventory increases dramatically, which in turn increases the chemical activity of each element and exacerbates the challenges associated with FCCI. This interaction forms a brittle intermetallic within the cladding which may limit fuel performance and durability. To better understand the mechanisms of lanthanide interactions with various steel alloys and the methods by which those interactions may be prevented, diffusion couples composed of neodymium, various steel alloys, and various refractory metal diffusion barriers were annealed for 17.5 to 56 days at temperatures from 550°C to 700°C and analyzed. In total, 204 diffusion couples including 476 interfaces were annealed and analyzed, approximately half of which successfully bonded. Elemental profiles acquired by Electron Probe MicroAnalysis (EPMA) were used to characterize the four intermetallic diffusion zones formed between steel alloys and neodymium, including the effects of alloying elements on growth rates. In addition, diffusion coefficients for potential diffusion barrier materials, which ranged from $3\text{E-}20$ m²/s to $6\text{E-}19$ m²/sec, were determined to ascertain their effectiveness in preventing lanthanide/steel interaction. Of the liner materials tested, tungsten, molybdenum, and zirconium interacted the least with neodymium. Simulations of the thermal and neutronic effects of these liner materials on reactor performance were also performed to provide a more complete perspective on their implementation. These simulations demonstrated that minimization of deleterious

effects from the addition of a liner depends primarily on minimizing liner thickness, not the material used.

DEDICATION

This thesis is dedicated to Carissa, whose unfailing support and patience made finishing this monumental task possible, and whose insightful assistance was, as always, invaluable.

ACKNOWLEDGEMENTS

- Funding for this project was provided by TerraPower LLC., based in Bellevue, WA, USA to support work on the Traveling Wave Reactor (TWR).
- Preliminary sample preparation and heat treatment were performed at Intellectual Ventures Laboratory by Rob Corbin and Jeff Dallas.
- Sample analysis was performed at Texas A&M University using equipment from the Department of Geology and Geophysics.
- Expert advice regarding EPMA methods was provided by Dr. Ray Guillemette from the Texas A&M University Department of Geology and Geophysics.

NOMENCLATURE

FCCI – Fuel Cladding Chemical Interactions

EPMA – Electron Probe Micro Analysis

WDS – Wavelength Dispersive Spectroscopy

EDS – Electron Dispersive Spectroscopy

BSE – Back Scatter Electron

SFR – Sodium Fast Reactor

TWR – Traveling Wave Reactor

TABLE OF CONTENTS

	Page
ABSTRACT	ii
DEDICATION	iv
ACKNOWLEDGEMENTS.....	v
NOMENCLATURE	vi
TABLE OF CONTENTS	vii
LIST OF FIGURES.....	xvi
LIST OF TABLES.....	xxii
1 INTRODUCTION	1
2 BACKGROUND.....	4
2.1 High-Burnup Sodium Fast Reactors.....	4
2.1.1 Potential Design Benefits	5
2.1.2 Potential Design Challenges.....	5
2.1.3 Traveling Wave Reactor	7
2.2 Previous SFR FCCI Data.....	9
2.2.1 Lanthanide Penetration into Cladding	10
2.2.2 Intermetallic Formation.....	12
2.2.3 Fuel Performance Implications	12
2.3 Diffusion Barrier Liner Experience with Nuclear Fuel.....	16
2.4 Existing Diffusion Couple Data	18
2.4.1 Steel/Lanthanide Diffusion.....	19
2.4.2 Diffusion Barrier Liner Diffusion	22
2.5 Computation of Diffusion Parameters	26
2.5.1 Simple Fick’s Law Diffusion.....	27
2.5.2 Line Compound Diffusion.....	28
3 EXPERIMENTAL METHODS.....	31
3.1 Fabrication of Diffusion Couples	31
3.2 Heat Treatment of Diffusion Couples	35
3.3 Electron Microscopy of Diffusion Couples.....	38
3.4 Analysis of Electron Microscopy Data	41

	Page
3.4.1	Average Zone Width Measurement..... 41
3.4.2	WDS False-Positive Correction 42
3.4.3	Determination of Fick's Law Diffusion Coefficients..... 43
3.4.4	Attempted Analysis of Broken Diffusion Interfaces..... 47
3.4.5	Determination of Line Compound Diffusion Coefficients 48
3.5	Combination of Calculated Diffusion Coefficients 48
3.5.1	Averaging Multiple Diffusion Coefficients..... 48
3.5.2	Propagation of Error for Arrhenius Equation..... 50
4	RESULTS52
4.1	Neodymium/Steel Diffusion..... 54
4.1.1	Neodymium Diffusion with HT-9..... 55
4.1.2	Neodymium Diffusion with G.91 63
4.1.3	Neodymium Diffusion with SS-316 70
4.1.4	Neodymium Diffusion with Iron..... 76
4.2	Neodymium/Liner Diffusion..... 77
4.2.1	Neodymium Diffusion with Vanadium 77
4.2.2	Neodymium Diffusion with Zirconium 83
4.2.3	Neodymium Diffusion with Titanium..... 88
4.2.4	Neodymium Diffusion with Molybdenum..... 93
4.2.5	Neodymium Diffusion with Tungsten 98
4.2.6	Neodymium Diffusion with Tantalum..... 103
4.3	Steel/Liner Diffusion 108
4.3.1	Steel Diffusion with Vanadium..... 109
4.3.2	Steel Diffusion with Zirconium 112
4.3.3	Steel Diffusion with Titanium 116
4.3.4	Steel Diffusion with Molybdenum 120
4.3.5	Steel Diffusion with Tungsten..... 121
4.3.6	Steel Diffusion with Tantalum 124
4.4	Liner/Liner Diffusion 126
4.4.1	Vanadium Diffusion with Zirconium 126
4.4.2	Vanadium Diffusion with Titanium..... 129
4.4.3	Vanadium Diffusion with Molybdenum..... 131
4.4.4	Vanadium Diffusion with Tungsten 131
4.4.5	Vanadium Diffusion with Tantalum..... 134
5	DISCUSSION135
5.1	Nd/Steel Intermetallic Phases..... 139

	Page
5.1.1 Nd ₂ (Fe+Cr) ₁₇ Phase.....	140
5.1.2 NdFe ₂ Phase	151
5.1.3 Nd ₅ Fe ₁₇ Phase.....	153
5.1.4 Nd ₃ Ni Phase.....	155
5.1.5 Extent of Interaction for SS-316 vs. HT-9/G.91	158
5.2 Liner Diffusion with Neodymium.....	159
5.3 Liner Diffusion with Steel	160
5.4 Comparative Reactor Impact of Liners Tested	161
5.4.1 Required Thicknesses	161
5.4.2 Neutronic Impact	163
5.4.3 Heat Transfer Impact.....	167
6 CONCLUSIONS.....	169
REFERENCES.....	172
APPENDIX A: DIFFUSION CALCULATION MACROS.....	180
A.1 Macro for Boltzmann-Matano Diffusion Coefficient Calculation.....	180
A.2 Macro for Diffusion Coefficient Calculation on Split Interface	192
A.3 Macro for Combination of Diffusion Coefficients and Calculation of Q	196
APPENDIX B: SUMMARY OF HT-9 INTERFACES.....	201
B.1 HT-9/Nd After 17.5 Days at 550°C.....	201
B.2 HT-9/V/Nd After 17.5 Days at 550°C.....	204
B.3 HT-9/Zr/V/Nd After 17.5 Days at 550°C	205
B.4 HT-9/Zr/Nd After 17.5 Days at 550°C	205
B.5 HT-9/Ti/V/Nd After 17.5 Days at 550°C.....	205
B.6 HT-9/Ti/Nd After 17.5 Days at 550°C.....	205
B.7 HT-9/Ta/V/Nd After 17.5 Days at 550°C	206
B.8 HT-9/Ta/Nd After 17.5 Days at 550°C	207
B.9 HT-9/Mo/V/Nd After 17.5 Days at 550°C	207
B.10 HT-9/Mo/Nd After 17.5 Days at 550°C.....	208
B.11 HT-9/W/V/Nd After 17.5 Days at 550°C	210
B.12 HT-9/W/Nd After 17.5 Days at 550°C.....	210
B.13 HT-9/Nd After 28 Days at 550°C.....	211
B.14 HT-9/V/Nd After 28 Days at 550°C.....	214
B.15 HT-9/Zr/V/Nd After 28 Days at 550°C	215
B.16 HT-9/Zr/Nd After 28 Days at 550°C	215
B.17 HT-9/Ti/V/Nd After 28 Days at 550°C.....	216

	Page
B.18 HT-9/Ti/Nd After 28 Days at 550°C	216
B.19 HT-9/Ta/V/Nd After 28 Days at 550°C	217
B.20 HT-9/Ta/Nd After 28 Days at 550°C	217
B.21 HT-9/Mo/V/Nd After 28 Days at 550°C	218
B.22 HT-9/Mo/Nd After 28 Days at 550°C.....	218
B.23 HT-9/W/V/Nd After 28 Days at 550°C	219
B.24 HT-9/W/Nd After 28 Days at 550°C.....	219
B.25 HT-9/Nd After 56 Days at 550°C.....	220
B.26 HT-9/V/Nd After 56 Days at 550°C.....	225
B.27 HT-9/Zr/V/Nd After 56 Days at 550°C	226
B.28 HT-9/Zr/Nd After 56 Days at 550°C	226
B.29 HT-9/Ti/V/Nd After 56 Days at 550°C.....	227
B.30 HT-9/Ti/Nd After 56 Days at 550°C.....	229
B.31 HT-9/Ta/V/Nd After 56 Days at 550°C.....	230
B.32 HT-9/Ta/Nd After 56 Days at 550°C	230
B.33 HT-9/Mo/V/Nd After 56 Days at 550°C	231
B.34 HT-9/Mo/Nd After 56 Days at 550°C.....	231
B.35 HT-9/W/V/Nd After 56 Days at 550°C	232
B.36 HT-9/W/Nd After 56 Days at 550°C.....	233
B.37 HT-9/Nd After 28 Days at 625°C.....	234
B.38 HT-9/V/Nd After 28 Days at 625°C.....	237
B.39 HT-9/Zr/V/Nd After 28 Days at 625°C	237
B.40 HT-9/Zr/Nd After 28 Days at 625°C	237
B.41 HT-9/Ti/V/Nd After 28 Days at 625°C.....	238
B.42 HT-9/Ti/Nd After 28 Days at 625°C.....	238
B.43 HT-9/Ta/V/Nd After 28 Days at 625°C.....	238
B.44 HT-9/Ta/Nd After 28 Days at 625°C	239
B.45 HT-9/Mo/V/Nd After 28 Days at 625°C	240
B.46 HT-9/Mo/Nd After 28 Days at 625°C.....	240
B.47 HT-9/W/V/Nd After 28 Days at 625°C	241
B.48 HT-9/W/Nd After 28 Days at 625°C.....	242
B.49 HT-9/Nd After 28 Days at 700°C.....	243
B.50 HT-9/V/Nd After 28 Days at 700°C.....	250
B.51 HT-9/Zr/V/Nd After 28 Days at 700°C	251
B.52 HT-9/Zr/Nd After 28 Days at 700°C	251
B.53 HT-9/Ti/V/Nd After 28 Days at 700°C.....	253
B.54 HT-9/Ti/Nd After 28 Days at 700°C.....	253
B.55 HT-9/Ta/V/Nd After 28 Days at 700°C.....	254

	Page
B.56 HT-9/Ta/Nd After 28 Days at 700°C	254
B.57 HT-9/Mo/V/Nd After 28 Days at 700°C	255
B.58 HT-9/Mo/Nd After 28 Days at 700°C.....	255
B.59 HT-9/W/V/Nd After 28 Days at 700°C	256
B.60 HT-9/W/Nd After 28 Days at 700°C.....	256
APPENDIX C: SUMMARY OF G.91 INTERFACES	258
C.1 G.91/Nd After 28 Days at 550°C	258
C.2 G.91/V/Nd After 28 Days at 550°C.....	262
C.3 G.91/Zr/V/Nd After 28 Days at 550°C	262
C.4 G.91/Zr/Nd After 28 Days at 550°C	263
C.5 G.91/Ti/V/Nd After 28 Days at 550°C.....	264
C.6 G.91/Ti/Nd After 28 Days at 550°C	264
C.7 G.91/Ta/V/Nd After 28 Days at 550°C	265
C.8 G.91/Ta/Nd After 28 Days at 550°C	266
C.9 G.91/Mo/V/Nd After 28 Days at 550°C.....	267
C.10 G.91/Mo/Nd After 28 Days at 550°C.....	268
C.11 G.91/W/V/Nd After 28 Days at 550°C.....	269
C.12 G.91/W/Nd After 28 Days at 550°C.....	269
C.13 G.91/Nd After 56 Days at 550°C.....	269
C.14 G.91/V/Nd After 56 Days at 550°C.....	273
C.15 G.91/Zr/v/Nd After 56 Days at 550°C.....	273
C.16 G.91/Zr/Nd After 56 Days at 550°C	274
C.17 G.91/Ti/V/Nd After 56 Days at 550°C.....	274
C.18 G.91/Ti/Nd After 56 Days at 550°C.....	274
C.19 G.91/Ta/V/Nd After 56 Days at 550°C	275
C.20 G.91/Ta/Nd After 56 Days at 550°C	276
C.21 G.91/Mo/V/Nd After 56 Days at 550°C.....	277
C.22 G.91/Mo/Nd After 56 Days at 550°C.....	277
C.23 G.91/W/V/Nd After 56 Days at 550°C.....	278
C.24 G.91/W/Nd After 56 Days at 550°C.....	278
C.25 G.91/Nd After 28 Days at 625°C	279
C.26 G.91/V/Nd After 28 Days at 625°C.....	282
C.27 G.91/Zr/V/Nd After 28 Days at 625°C	282
C.28 G.91/Zr/Nd After 28 Days at 625°C	283
C.29 G.91/Ti/V/Nd After 28 Days at 625°C.....	283
C.30 G.91/Ti/Nd After 28 Days at 625°C	284
C.31 G.91/Ta/V/Nd After 28 Days at 625°C	285

	Page
C.32 G.91/Ta/Nd After 28 Days at 625°C	285
C.33 G.91/Mo/V/Nd After 28 Days at 625°C.....	285
C.34 G.91/Mo/Nd After 28 Days at 625°C.....	286
C.35 G.91/W/V/Nd After 28 Days at 625°C.....	287
C.36 G.91/W/Nd After 28 Days at 625°C.....	288
C.37 G.91/Nd After 28 Days at 700°C.....	288
C.38 G.91/V/Nd After 28 Days at 700°C.....	290
C.39 G.91/Zr/V/Nd After 28 Days at 700°C	292
C.40 G.91/Zr/Nd After 28 Days at 700°C	293
C.41 G.91/Ti/V/Nd After 28 Days at 700°C.....	293
C.42 G.91/Ti/Nd After 28 Days at 700°C.....	294
C.43 G.91/Ta/V/Nd After 28 Days at 700°C	295
C.44 G.91/Ta/Nd After 28 Days at 700°C	295
C.45 G.91/Mo/V/Nd After 28 Days at 700°C.....	296
C.46 G.91/Mo/Nd After 28 Days at 700°C.....	297
C.47 G.91/W/V/Nd After 28 Days at 700°C.....	298
C.48 G.91/W/Nd After 28 Days at 700°C.....	298
APPENDIX D: SUMMARY OF SS-316 INTERFACES.....	300
D.1 SS-316/Nd After 28 Days at 550°C.....	300
D.2 SS-316/V/Nd After 28 Days at 550°C	304
D.3 SS-316/Zr/V/Nd After 28 Days at 550°C.....	304
D.4 SS-316/Zr/Nd After 28 Days at 550°C.....	304
D.5 SS-316/Ti/V/Nd After 28 Days at 550°C	305
D.6 SS-316/Ti/Nd After 28 Days at 550°C.....	307
D.7 SS-316/Ta/V/Nd After 28 Days at 550°C.....	307
D.8 SS-316/Ta/Nd After 28 Days at 550°C.....	308
D.9 SS-316/Mo/V/Nd After 28 Days at 550°C.....	308
D.10 SS-316/Mo/Nd After 28 Days at 550°C	309
D.11 SS-316/W/V/Nd After 28 Days at 550°C	310
D.12 SS-316/W/Nd After 28 Days at 550°C	310
D.13 SS-316/Nd After 56 Days at 550°C.....	311
D.14 SS-316/V/Nd After 56 Days at 550°C	316
D.15 SS-316/Zr/V/Nd After 56 Days at 550°C.....	316
D.16 SS-316/Zr/Nd After 56 Days at 550°C.....	317
D.17 SS-316/Ti/V/Nd After 56 Days at 550°C	318
D.18 SS-316/Ti/Nd After 56 Days at 550°C.....	318
D.19 SS-316/Ta/V/Nd After 56 Days at 550°C.....	319

	Page
D.20 SS-316/Ta/Nd After 56 Days at 550°C.....	319
D.21 SS-316/Mo/V/Nd After 56 Days at 550°C.....	319
D.22 SS-316/Mo/Nd After 56 Days at 550°C.....	320
D.23 SS-316/W/V/Nd After 56 Days at 550°C.....	321
D.24 SS-316/W/Nd After 56 Days at 550°C.....	322
D.25 SS-316/Nd After 28 Days at 625°C.....	322
D.26 SS-316/V/Nd After 28 Days at 625°C.....	326
D.27 SS-316/Zr/V/Nd After 28 Days at 625°C.....	327
D.28 SS-316/Zr/Nd After 28 Days at 625°C.....	327
D.29 SS-316/Ti/V/Nd After 28 Days at 625°C.....	328
D.30 SS-316/Ti/Nd After 28 Days at 625°C.....	329
D.31 SS-316/Ta/V/Nd After 28 Days at 625°C.....	330
D.32 SS-316/Ta/Nd After 28 Days at 625°C.....	330
D.33 SS-316/Mo/V/Nd After 28 Days at 625°C.....	330
D.34 SS-316/Mo/Nd After 28 Days at 625°C.....	331
D.35 SS-316/W/V/Nd After 28 Days at 625°C.....	331
D.36 SS-316/W/Nd After 28 Days at 625°C.....	331
D.37 SS-316/Nd After 28 Days at 700°C.....	332
D.38 SS-316/V/Nd After 28 Days at 700°C.....	335
D.39 SS-316/Zr/V/Nd After 28 Days at 700°C.....	336
D.40 SS-316/Zr/Nd After 28 Days at 700°C.....	337
D.41 SS-316/Ti/V/Nd After 28 Days at 700°C.....	338
D.42 SS-316/Ti/Nd After 28 Days at 700°C.....	339
D.43 SS-316/Ta/V/Nd After 28 Days at 700°C.....	341
D.44 SS-316/Ta/Nd After 28 Days at 700°C.....	342
D.45 SS-316/Mo/V/Nd After 28 Days at 700°C.....	342
D.46 SS-316/Mo/Nd After 28 Days at 700°C.....	343
D.47 SS-316/W/V/Nd After 28 Days at 700°C.....	343
D.48 SS-316/W/Nd After 28 Days at 700°C.....	343
APPENDIX E: SUMMARY OF IRON INTERFACES.....	344
E.1 Fe/Nd After 28 Days at 550°C.....	344
E.2 Fe/V/Nd After 28 Days at 550°C.....	344
E.3 Fe/Zr/V/Nd After 28 Days at 550°C.....	344
E.4 Fe/Zr/Nd After 28 Days at 550°C.....	345
E.5 Fe/Ti/V/Nd After 28 Days at 550°C.....	346
E.6 Fe/Ti/Nd After 28 Days at 550°C.....	347
E.7 Fe/Ta/V/Nd After 28 Days at 550°C.....	348

	Page
E.8 Fe/Ta/Nd After 28 Days at 550°C	348
E.9 Fe/Mo/V/Nd After 28 Days at 550°C	348
E.10 Fe/Mo/Nd After 28 Days at 550°C.....	348
E.11 Fe/W/V/Nd After 28 Days at 550°C	349
E.12 Fe/W/Nd After 28 Days at 550°C.....	350
E.13 Fe/Nd After 56 Days at 550°C.....	351
E.14 Fe/V/Nd After 56 Days at 550°C.....	351
E.15 Fe/Zr/V/Nd After 56 Days at 550°C	352
E.16 Fe/Zr/Nd After 56 Days at 550°C	353
E.17 Fe/Ti/V/Nd After 56 Days at 550°C.....	353
E.18 Fe/Ti/Nd After 56 Days at 550°C.....	354
E.19 Fe/Ta/V/Nd After 56 Days at 550°C.....	355
E.20 Fe/Ta/Nd After 56 Days at 550°C	355
E.21 Fe/Mo/V/Nd After 56 Days at 550°C	355
E.22 Fe/Mo/Nd After 56 Days at 550°C.....	356
E.23 Fe/W/V/Nd After 56 Days at 550°C	356
E.24 Fe/W/Nd After 56 Days at 550°C.....	356
E.25 Fe/Nd After 28 Days at 625°C.....	357
E.26 Fe/V/Nd After 28 Days at 625°C.....	357
E.27 Fe/Zr/V/Nd After 28 Days at 625°C	358
E.28 Fe/Zr/Nd After 28 Days at 625°C	360
E.29 Fe/Ti/V/Nd After 28 Days at 625°C.....	361
E.30 Fe/Ti/Nd After 28 Days at 625°C.....	361
E.31 Fe/Ta/V/Nd After 28 Days at 625°C.....	362
E.32 Fe/Ta/Nd After 28 Days at 625°C	362
E.33 Fe/Mo/V/Nd After 28 Days at 625°C	362
E.34 Fe/Mo/Nd After 28 Days at 625°C.....	362
E.35 Fe/W/V/Nd After 28 Days at 625°C	363
E.36 Fe/W/Nd After 28 Days at 625°C.....	364
E.37 Fe/Nd After 28 Days at 700°C.....	365
E.38 Fe/V/Nd After 28 Days at 700°C.....	365
E.39 Fe/Zr/V/Nd After 28 Days at 700°C	365
E.40 Fe/Zr/Nd After 28 Days at 700°C	366
E.41 Fe/Ti/V/Nd After 28 Days at 700°C.....	366
E.42 Fe/Ti/Nd After 28 Days at 700°C.....	367
E.43 Fe/Ta/V/Nd After 28 Days at 700°C.....	367
E.44 Fe/Ta/Nd After 28 Days at 700°C	367
E.45 Fe/Mo/V/Nd After 28 Days at 700°C	367

	Page
E.46 Fe/Mo/Nd After 28 Days at 700°C.....	367
E.47 Fe/W/V/Nd After 28 Days at 700°C	368
E.48 Fe/W/Nd After 28 Days at 700°C.....	368

LIST OF FIGURES

	Page
Figure 2-1. Cutaway diagram of conceptual TWR design [12].	8
Figure 2-2. Top-down view of assemblies in hypothetical TWR core [12].	9
Figure 2-3. Fuel-cladding interface showing lanthanide buildup and cladding penetration [20].	10
Figure 2-4. EPMA of fuel/cladding interface from EBR-II [46].	11
Figure 2-5. Impact tested cladding specimen showing increased hardness in intermetallic zone [20].	13
Figure 2-6. Cracking in fuel cladding due to intermetallic formation and decarburization [48].	14
Figure 2-7. Iron-neodymium phase diagram [50].	15
Figure 2-8. Iron-cerium phase diagram [49].	16
Figure 2-9. Transverse section of fuel with partially intact zirconium sheath from casting [51].	18
Figure 2-10. Neodymium/iron elemental profile after 9 hours at 780°C [56].	20
Figure 2-11. Neodymium/iron elemental profile after 25 hours at 680°C [56].	20
Figure 2-12. Neodymium/steel interface after 6 hours at 700°C [59].	22
Figure 2-13. Zirconium interaction with U-10Zr after 25 hours at 800°C [53].	23
Figure 2-14. Niobium interaction with U-10Zr after 25 hours at 800°C [53].	24
Figure 2-15. Titanium interaction with U-10Zr and HT-9 after 25 hours at 800°C [53].	24
Figure 2-16. Molybdenum interaction with U-10Zr after 25 hours at 800°C [53].	25
Figure 2-17. Tantalum interaction with U-10Zr after 25 hours at 800°C [53].	25
Figure 2-18. Vanadium interaction with HT-9 after 25 hours at 800°C [53].	26
Figure 2-19. Chromium with U-10Zr and HT-9 after 25 hours at 800°C [53].	26
Figure 2-20. Superposition of infinite planar sources to form concentration curve [63].	27

	Page
Figure 2-21. Series of two line compounds (β, γ) between two terminal solutions (α, δ) [64].	29
Figure 2-22. Example profile for application of Equation 2-2.	30
Figure 3-1. Schematic of assembled diffusion couple stack.	33
Figure 3-2. Schematic of loaded diffusion couple jig.	33
Figure 3-3. Assembled diffusion couple stack in jig.	34
Figure 3-4. Diffusion couples loaded into kiln prior to heat treatment.	36
Figure 3-5. Diffusion couple sectioning using diamond saw.	39
Figure 3-6. Example of false-positive chromium signal in vanadium.	43
Figure 3-7. Nd/V diffusion interface with adjusted composition for error analysis.	45
Figure 3-8. Nd/V diffusion interface with adjusted position for error analysis.	46
Figure 4-1. HT-9/Nd interface after 17.5 days at 550°C.	56
Figure 4-2. Composition of major elements for Nd/HT-9 after 17.5 days at 550°C.	57
Figure 4-3. HT-9/Nd interface after 28 days at 550°C.	58
Figure 4-4. Composition of major elements for Nd/HT-9 after 28 days at 550°C.	58
Figure 4-5. HT-9/Nd interface after 56 days at 550°C.	59
Figure 4-6. Composition of major elements for Nd/HT-9 after 56 days at 550°C.	60
Figure 4-7. Broken HT-9/Nd interface after 28 days at 625°C.	61
Figure 4-8. Broken HT-9/Nd interface after 28 days at 700°C.	62
Figure 4-9. G.91/Nd diffusion interface after 28 days at 550°C.	64
Figure 4-10. Composition of major elements for Nd/G.91 after 28 days at 550°C.	64
Figure 4-11. G.91/Nd interface after 56 days at 550°C.	66
Figure 4-12. Composition of major elements for Nd/G.91 after 56 days at 550°C.	66
Figure 4-13. G.91/Nd interface after 28 days at 625°C.	67
Figure 4-14. Composition of major elements for Nd/G.91 after 28 days at 625°C.	68

	Page
Figure 4-15. Broken G.91/Nd interface after 28 days at 700°C.	69
Figure 4-16. SS-316/Nd interface after 28 days at 550°C.....	71
Figure 4-17. Composition of major elements for SS-316/Nd interface after 28 days at 550°C.....	72
Figure 4-18. SS-316/Nd interface after 56 days at 550°C.....	73
Figure 4-19. SS-316/Nd interface after 28 days at 625°C.....	74
Figure 4-20. SS-316/Nd interface after 28 days at 700°C.....	75
Figure 4-21. Remaining iron disk following exposure to Nd for 28 days at 550°C.	77
Figure 4-22. Model vs. WDS data for V/Nd interface after 28 days at 550°C.....	78
Figure 4-23. Model vs. WDS data for V/Nd interface after 56 days at 550°C.....	79
Figure 4-24. Model vs. WDS data for V/Nd interface after 28 days at 625°C.....	80
Figure 4-25. Model vs. WDS data for V/Nd interface after 28 days at 700°C.....	81
Figure 4-26. BSE image of V/Nd interface following 28 days at 550°C.	83
Figure 4-27. Model vs. WDS data for Zr/Nd interface after 28 days at 550°C.	84
Figure 4-28. Model vs. WDS data for Zr/Nd interface after 56 days at 550°C.	84
Figure 4-29. Model vs. WDS data for Zr/Nd interface after 28 days at 625°C.	85
Figure 4-30. Model vs. WDS data for Zr/Nd interface after 28 days at 700°C.	86
Figure 4-31. BSE image of Zr/Nd interface following 28 days at 625°C.....	87
Figure 4-32. Model vs. WDS data for Ti/Nd interface after 28 days at 550°C.	88
Figure 4-33. Model vs. WDS data for Ti/Nd interface after 56 days at 550°C.	89
Figure 4-34. Model vs. WDS data for Ti/Nd interface after 28 days at 625°C.	90
Figure 4-35. Model vs. WDS data for Ti/Nd interface after 28 days at 700°C.	91
Figure 4-36. BSE image of Ti/Nd interface following 56 days at 550°C.	92
Figure 4-37. Model vs. WDS data for Mo/Nd interface after 28 days at 550°C.....	93
Figure 4-38. Model vs. WDS data for Mo/Nd interface after 56 days at 550°C.....	94

Figure 4-39. Model vs. WDS data for Mo/Nd interface after 28 days at 625°C.....	95
Figure 4-40. Model vs. WDS data for Mo/Nd interface after 28 days at 700°C.....	96
Figure 4-41. BSE image of Mo/Nd interface following 28 days at 700°C.....	97
Figure 4-42. Model vs. WDS data for W/Nd interface after 28 days at 550°C.....	98
Figure 4-43. Model vs. WDS data for W/Nd interface after 56 days at 550°C.....	99
Figure 4-44. Model vs. WDS data for W/Nd interface after 28 days at 625°C.....	100
Figure 4-45. Model vs. WDS data for W/Nd interface after 28 days at 700°C.....	101
Figure 4-46. BSE image of W/Nd interface following 56 days at 550°C.....	102
Figure 4-47. Model vs. WDS data for Ta/Nd interface after 17.5 days at 550°C.	103
Figure 4-48. Model vs. WDS data for Ta/Nd interface after 28 days at 550°C.	104
Figure 4-49. Model vs. WDS data for Ta/Nd interface after 28 days at 625°C.	105
Figure 4-50. Model vs. WDS data for Ta/Nd interface after 28 days at 700°C.	106
Figure 4-51. BSE image of Ta/Nd interface following 28 days at 550°C.	108
Figure 4-52. Model vs. WDS data for V/HT-9 interface after 56 days at 550°C.	109
Figure 4-53. Model vs. WDS data for V/SS-316 interface after 28 days at 625°C.....	110
Figure 4-54. Model vs. WDS data for V/HT-9 interface after 28 days at 700°C.	111
Figure 4-55. Model vs. WDS data for V/G.91 interface after 28 days at 700°C.	111
Figure 4-56. Model vs. WDS data for Zr/SS-316 interface after 56 days at 550°C.....	113
Figure 4-57. Model vs. WDS data for Zr/Fe interface after 56 days at 550°C.....	113
Figure 4-58. Model vs. WDS data for Zr/Fe interface after 28 days at 625°C.....	114
Figure 4-59. Model vs. WDS data for Zr/SS-316 interface after 28 days at 700°C.....	115
Figure 4-60. Model vs. WDS data for Ti/HT-9 interface after 56 days at 550°C.....	117
Figure 4-61. Model vs. WDS data for Ti/G.91 interface after 28 days at 550°C.....	117
Figure 4-62. Model vs. WDS data for Ti/SS-316 interface after 28 days at 550°C.	118
Figure 4-63. Model vs. WDS data for Ti/Fe interface after 28 days at 550°C.....	118
Figure 4-64. Model vs. WDS data for Ti/G.91 interface after 28 days at 625°C.....	119

	Page
Figure 4-65. Model vs. WDS data for Mo/SS-316 interface after 28 days at 625°C.	121
Figure 4-66. Model vs. WDS data for W/SS-316 interface after 56 days at 550°C.	122
Figure 4-67. Model vs. WDS data for W/SS-316 interface after 28 days at 625°C.	123
Figure 4-68. Model vs. WDS data for Ta/G.91 interface after 56 days at 550°C.	124
Figure 4-69. Model vs. WDS data for Ta/SS-316 interface after 28 days at 625°C. ...	125
Figure 4-70. Model vs. WDS data for V/Zr interface after 56 days at 550°C.	127
Figure 4-71. Model vs. WDS data for V/Zr interface after 28 days at 625°C.	127
Figure 4-72. Model vs. WDS data for V/Zr interface after 28 days at 625°C.	128
Figure 4-73. Model vs. WDS data for V/Ti interface after 56 days at 550°C.	129
Figure 4-74. Model vs. WDS data for V/Ti interface after 28 days at 625°C.	130
Figure 4-75. Model vs. WDS data for V/Mo interface after 56 days at 550°C.	131
Figure 4-76. Model vs. WDS data for V/W interface after 56 days at 550°C.	132
Figure 4-77. Model vs. WDS data for V/W interface after 28 days at 625°C.	133
Figure 5-1. Nd concentration across Nd ₂ (Fe+Cr) ₁₇ phase after 17.5 days at 550°C with HT-9.	142
Figure 5-2. Nd concentration across Nd ₂ (Fe+Cr) ₁₇ phase after 28 days at 550°C with HT-9.	143
Figure 5-3. Nd concentration across Nd ₂ (Fe+Cr) ₁₇ phase after 56 days at 550°C with HT-9.	143
Figure 5-4. Nd concentration across Nd ₂ (Fe+Cr) ₁₇ phase after 28 days at 625°C with HT-9.	145
Figure 5-5. Nd concentration across Nd ₂ (Fe+Cr) ₁₇ phase after 28 days at 700°C with HT-9.	145
Figure 5-6. Nd concentration across Nd ₂ (Fe+Cr) ₁₇ phase after 28 days at 550°C with SS-316.	146
Figure 5-7. Nd concentration across Nd ₂ (Fe+Cr) ₁₇ phase after 56 days at 550°C with SS-316.	147

	Page
Figure 5-8. Nd concentration across $\text{Nd}_2(\text{Fe}+\text{Cr})_{17}$ phase after 28 days at 625°C with SS-316.....	148
Figure 5-9. Nd concentration across $\text{Nd}_2(\text{Fe}+\text{Cr})_{17}$ phase after 28 days at 700°C with SS-316.....	149
Figure 5-10. SS-316/Nd interface after 28 days at 700°C.....	150
Figure 5-11. CeGa_2Al_2 type crystal structure where $\text{R}=\text{Nd}$; $\text{T}=\text{Fe}$, Mn , or Cr ; and $\text{X}=\text{Si}$ [73].	152
Figure 5-12. Cubic Laves structure of NdFe_2 , where Nd is gray and Fe is red [74].	152
Figure 5-13. Calculated Ni-Nd intermetallic Gibbs energies at 800°C [79].....	156
Figure 5-14. TII type crystal structure of NdNi [81].	157
Figure 5-15. Fe_3C type crystal structure of Nd_3Ni [82].	158
Figure 5-16. Liner/Nd diffusion coefficients vs. liner melting point.	160
Figure 5-17. Required liner thicknesses for various fuel lifetimes.....	163
Figure 5-18. Top-down schematic of MCNP simulated core with fuel pins (blue) and coolant (orange).....	164
Figure 5-19. Neutronic impact of various liners.....	166
Figure 5-20. Thermal effects of various liners at fuel-cladding interface.	168

LIST OF TABLES

	Page
Table 2-1. Relative fission yields of the lanthanide series [47].	12
Table 3-1. Composition of alloying components in each steel alloy (at%).	32
Table 3-2. Thermal expansion calculation for HT-9 diffusion couple stack.	35
Table 3-3. Summary of all diffusion couples with corresponding appendices.	37
Table 3-4. Polishing steps used in sample preparation.	39
Table 3-5. WDS parameters used for quantitative analysis.	40
Table 4-1. Summary of all diffusion assemblies with corresponding appendices.	53
Table 4-2. Integrated diffusion coefficients for HT-9/Nd.	63
Table 4-3. Integrated diffusion coefficients for G.91/Nd.	70
Table 4-4. Integrated diffusion coefficients for SS-316/Nd.	76
Table 4-5. Average diffusion coefficients for the V/Nd system.	82
Table 4-6. Average diffusion coefficients for the Zr/Nd system.	87
Table 4-7. Average diffusion coefficients for the Ti/Nd system.	92
Table 4-8. Average diffusion coefficients for the Mo/Nd system.	97
Table 4-9. Average diffusion coefficients for the W/Nd system.	102
Table 4-10. Average diffusion coefficients for the Ta/Nd system.	107
Table 4-11. Average diffusion coefficients for V with steel alloys and Fe.	112
Table 4-12. Average diffusion coefficients for Zr with steel alloys and Fe.	116
Table 4-13. Average diffusion coefficients for Ti with steel alloys and Fe.	120
Table 4-14. Average diffusion coefficients for W with steel alloys and Fe.	124
Table 4-15. Average diffusion coefficients for Ta with steel alloys and Fe.	126
Table 4-16. Average diffusion coefficients for V with Zr.	129
Table 4-17. Average diffusion coefficients for V with Ti.	130
Table 4-18. Average diffusion coefficients for V with W.	133
Table 5-1. Summary of diffusion data for steel with neodymium.	136

	Page
Table 5-2. Summary of diffusion data for liners with neodymium.	137
Table 5-3. Summary of diffusion data for liners with steel alloys and iron.	138
Table 5-4. Summary of diffusion data for dual-layer liners.....	139
Table 5-5. Neutronic impact of various liners.....	165
Table 5-6. Thermal effects of various liners at fuel-cladding interface.	167

1 INTRODUCTION

One of the prominent nuclear energy systems under investigation for future applications is the Sodium-cooled Fast Reactor (SFR) [1, 2, 3, 4, 5, 6, 7]. There are promising design features which may be achievable using SFR's, including increased utilization of fissionable fuel content, breeding of further fissile fuel content, high neutronic efficiency, more efficient burning of undesirable radioactive waste in-reactor, and the elimination of water-cladding interactions which may pose safety concerns for water-cooled reactor designs [5, 8, 9, 10]. Some of these benefits, most notably the conversion of fertile isotopes to fissile isotopes and the reduction in overall radioactive waste, are most realized at extended fuel lifetimes when fertile to fissile breeding processes will eventually dominate reactor performance and the inventories of many radioactive fission products in the fuel will have effectively plateaued [11, 12]. Thus, the extension of fuel lifetimes for SFR designs to periods on the order of ten to forty years will have a strong impact on the sustainability and efficiency of the designs [11]. However, the current experience on which future SFR designs are based is primarily limited to significantly shorter fuel lifetimes, on the order of one to two years with up to 20% burnup [13]. Thus, one of the great challenges in designing advanced SFR's lies in addressing how fuel performance and integrity can be assured over fuel lifetimes much longer than those previously used [10].

Addressing this challenge requires substantial work on several related technical challenges including:

- Fuel and cladding durability following exposure to exceptionally high radiation fluence [10].

- Accommodation of fission product swelling at very high burnups without inducing undue mechanical strain in the cladding [14].
- Maintaining sufficient thermal conductivity within the fuel following long-term thermal and radiation driven restructuring and the introduction of significant quantities of solid and gaseous fission products [14].
- Prevention of chemical interactions between fuel and cladding which may lead to reduced fuel melting temperatures or reduction in cladding integrity [14].

Fuel-Cladding Chemical Interactions (FCCI) may be generalized into two broad categories. First, eutectic interactions between the steel cladding materials commonly used in SFR's and metallic uranium fuel may result in significantly lowered fuel melting temperatures [15]. There are two iron-uranium eutectics, one of which at 67 at% U melts at 725°C [16], which is above the nominal fuel-cladding interface temperature for most SFR designs of 400 to 550°C [11]; however, the nominal fuel-cladding interface temperature may be exceeded in transient accident scenarios, which makes the prevention of eutectic interactions necessary to ensure reactor safety [17]. This issue is generally addressed by the addition of zirconium to the uranium fuel, which effectively increased the eutectic melting temperature as well as reducing anisotropic fuel swelling [18].

The second general form of FCCI is diffusive interactions between cladding and fission products present in the fuel. There is a broad bimodal distribution (by mass number) of fission products which is similar for all types of nuclear reactor systems, but the fission product yields do vary slightly dependent upon the neutron spectrum and the isotopic composition of the fuel [19]. The fission products which are primarily responsible for FCCI may be generalized into several categories. Based on previous reactor experience, the category of fission products most responsible for weakening of cladding are the rare earth isotopes, or lanthanides [20,

14, 17]. They are elements from lanthanum to ytterbium (atomic numbers 57 to 70) that are chemically reactive and, in many cases, strong neutron absorbers. Post-Irradiation Examination (PIE) of used SFR fuel has shown that lanthanides diffuse to the fuel-cladding interface to form iron-lanthanide intermetallics within the cladding [14, 20]. Diffusion of lanthanides out of the uranium alloy fuel to the fuel-cladding interface is driven by thermodynamic instability of lanthanides in the uranium alloy fuel and accelerated by radiation-enhanced diffusion [20]. This intermetallic is hard and brittle compared to the original steel cladding, and in some fuel pins exposed to increased temperatures, this interaction resulted in rupture of the cladding tube under excessive hoop stress due to fuel swelling [17, 21, 20, 22].

The central focus of the work reported in this document is the study of the rate of intermetallic formation between a lanthanide and several representative cladding steels. Neodymium is used as the primary lanthanide for this study to simplify the test matrix based on its observed behavior relative to the other lanthanides in past FCCI studies on used fuel [20, 17]. In addition, the interaction of lanthanides (i.e., Nd) with vanadium, titanium, zirconium, molybdenum, tantalum, and tungsten is characterized to enable their consideration as liners for the prevention of intermetallic formation. Diffusion couples of these materials were heat treated for 17.5 to 56 days at temperatures of 550 to 700°C. The resulting diffusion interfaces which formed were then sectioned and analyzed using Electron Probe Microanalysis (EPMA). Wavelength Dispersive Spectroscopy (WDS) line scan analyses were completed across the interfaces to provide elemental concentration profiles for the diffusing elements. These concentration profiles were analyzed to determine the governing diffusion coefficients and activation energies in each system. These results may be used to better model and understand the formation of lanthanide intermetallics in SFR cladding, and to design diffusion barrier liners for prevention of intermetallic formation.

2 BACKGROUND

2.1 High-Burnup Sodium Fast Reactors

Sodium Fast Reactors (SFRs) are a prominent area of research and development for the next generation of nuclear reactors. There are many variations in SFR designs, but there are several defining commonalities between them. All SFR designs use sodium coolant, with typical operating temperatures around 400 to 550°C [11]. The fuel for SFR designs is typically either a metallic alloy consisting of uranium, plutonium, zirconium, and/or molybdenum, or a mixture of uranium and plutonium oxides [23, 24]. In either case, the fuel is typically sealed within tubes of steel cladding, which provides very low interaction with the sodium coolant and low irradiation swelling [14, 23, 24]. At beginning of life, power production in SFRs is typically dominated by the fissioning of initially loaded fissile material, such as U-235, with some contribution from the fissioning of initially loaded fissionable material, such as U-238. However, as fuel is irradiated, U-238 atoms absorb neutrons and undergo successive beta decays to breed isotopes of plutonium [12, 2]. As the initially loaded fissile material is fissioned, the growing inventory of bred plutonium becomes the predominant source of power within the reactor [12, 2]. This bred fuel may be kept in-reactor to continue providing power, or removed for reprocessing to form new fuel elements. To provide the maximum efficiency for this breeding and burning of fuel, SFRs are designed to have a fast neutron spectrum, which is reflected in the selection of low moderating coolant and fuels [14, 7, 5].

Experimental SFR's were built by several countries around the world, including the United States [25, 26, 27], Russia [3], China [28], the United Kingdom [29], India [4], Japan [30, 31], Germany [32], and France [33, 34]. The overall goal for most of these reactors has been to develop the technology necessary for

implementation of SFR's for electrical power generation with the capacity to close the fuel cycle by recycling minor actinides [35].

2.1.1 Potential Design Benefits

One of the primary benefits achieved with an SFR over current thermal (non-fast) reactor designs is the breeding and burning of fissile isotopes, as it potentially allows greatly increased fuel efficiency [36, 12]. This process increases the utilization of energy present within natural uranium by consuming a far greater fraction of U-238 than is typically consumed by conventional reactors [7, 12]. If carefully managed, fast reactor fuel has the potential to create more fissile material through the transmutation of U-238 to Pu-239 than is initially loaded into the reactor [12]. If the bred-in fissile material can then be burned, either through shuffling of fuel pins or reprocessing into new fuel, SFR's have the potential to drive a self-sustaining fuel cycle, requiring only the addition of further natural or depleted uranium [12, 2, 37]. This fuel cycle would possess a significant benefit over the conventional nuclear fuel cycle, as its requirements for uranium enrichment, which poses both economic and nuclear proliferation concerns, would be significantly reduced [5].

In addition to increasing fuel usage efficiency, SFR's have the potential to produce a reduced quantity of nuclear waste compared to conventional reactors [38, 8]. In SFRs, actinides and other radioactive elements produced in nuclear fuels are destroyed, either by transmutation or by fissioning, reducing the quantity of radioactive waste produced by the fuel cycle. This feature would in theory also allow SFRs to consume some fraction of the radioactive waste produced by conventional reactors [38].

2.1.2 Potential Design Challenges

There are several key design challenges which must be overcome for the successful implementation of SFRs to generate power. One of the primary

challenges encountered by early SFR developers was maintaining metal fuel stability and mitigating the deleterious effects of fuel swelling under irradiation [14, 39]. These issues were overcome, in part, by alloying uranium with zirconium or molybdenum to reduce anisotropic α -phase uranium swelling and to anneal out any initial metallographic texture within the fuel caused by fabrication [14, 39]. In addition, the fuel smear density was reduced and a large sodium-filled gap was created between the fuel and cladding to accommodate isotropic swelling due to solid and gaseous fission product accumulation [14]. While this approach has been successful, these steps have the negative effect of reducing the density of fissile and fissionable materials, reducing the effectiveness of breeding and burning fissile material.

Another challenge arises due to the well-known reactive nature of the sodium coolant [40]. Preventing contact between the liquid sodium and air or water is a significant design requirement. Some past SFRs, such as the Monju reactor in Japan, have experienced major fires due to sodium leaks [41]. On the other hand, the Experimental Breeder Reactor II (EBR-II) at Argonne National Laboratory – West operated sodium-water heat exchangers for decades without incident. Safe implementation of SFRs requires careful design to both prevent the occurrence of sodium leaks and minimize the adverse effects of any leaks which do occur.

One of the greatest challenges under consideration for SFRs is the extension of fuel lifetime and burnup significantly past what has previously been achieved [42, 12]. Past reactor experience has shown that burnups of up to 20%, equivalent to roughly ~200 GWd per metric ton of heavy metal fuel, can be reliably achieved [13, 43]. Due to the breeding of plutonium within the fuel, SFR fuel pins have the theoretical ability to remain active within the reactor for much longer than conventional fuel pins, potentially reaching 40% burnup [12]. However, reaching this level of burnup will necessitate overcoming significant challenges. First,

extending fuel lifetimes will significantly increase the radiation fluence to which fuel and cladding are exposed, taking them beyond currently established databases for radiation damage in materials (from ~200 displacements per atom to over 400) [10, 12]. Second, fuel stability and performance in the presence of significant quantities of fission products must be assured so that fuel remains contained within its cladding and heat is efficiently conducted into the coolant [44]. Finally, chemical interactions between fuel and cladding must be mitigated to prevent potential rupture of cladding before the end of extended fuel lifetimes due to fuel swelling and the degradation of cladding strength from irradiation and chemical attack [14, 45].

2.1.3 Traveling Wave Reactor

The Traveling Wave Reactor (TWR) under development by Terrapower, LLC. is an SFR design which seeks to improve on existing SFR technology in a manner which allows for sustainable energy production by greatly increasing fuel lifetime beyond previous SFR's [12, 2]. The conceptual design would operate by maintaining a perpetual wave of reactivity within the fuel by continually breeding fissile material by fissioning previously created fissile material. In this manner, a relatively small amount of initially enriched material could be used to extract energy from a large amount of fertile material [2, 12, 37].

A cutaway diagram of a simple model of the potential TWR design is given in Figure 2-1. The core, which is the red zone near the bottom of the image, is to be submerged in a pool of liquid sodium circulated by the primary pumps to remove heat from the core for energy generation [12]. A top-down diagram of the assemblies within the core is given in Figure 2-2. In this diagram, the inner circle would initially consist primarily of fuel assemblies 20% enriched in U-235, while the outer circle would consist of assemblies with depleted uranium fuel [12]. As

plutonium is bred into the outer assemblies, they would be shuffled into the center of the core to provide further power and maintain a relatively constant power profile over the core lifetime. By careful fuel management, simulations have shown that such a core could maintain power for up to forty years without the addition of further fuel [2, 12].

While this is achievable in computer-based nuclear reactor simulations, it will push the limits of prior experience for structural materials and fuel performance. While prior fast reactors have achieved 20% burnup and up to 200 dpa for structural materials, the TWR will require *at least* 28% burnup and over 400 dpa [12]. The need to understand and mitigate FCCI mechanisms for such long-lived fuel was the primary motivation behind this work.



Figure 2-1. Cutaway diagram of conceptual TWR design [12].

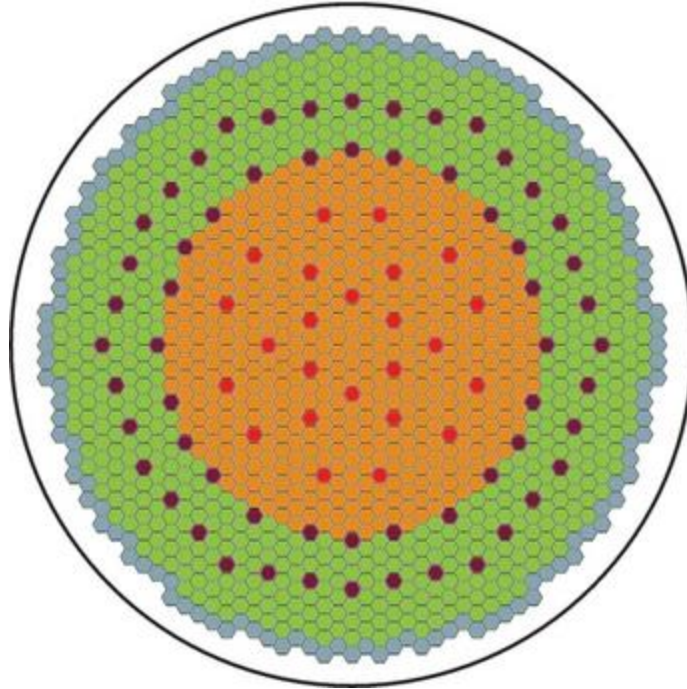


Figure 2-2. Top-down view of assemblies in hypothetical TWR core [12].

2.2 Previous SFR FCCI Data

Post-irradiation examination studies of fuel pins from prototype SFR's has provided data regarding the fuel-cladding chemical reactions which occur in steel-clad metal fuels. Unfortunately, due to the nature of reactor operations and the difficulties which necessarily accompany the examination of highly radioactive fuel, the limited quantity of data falls short of providing a comprehensive understanding of the mechanisms and behavior of FCCI needed for extension to future systems with varying operating temperatures, burnup, and cladding materials. However, due to the complex interplay of numerous environmental factors in reactor cores that are challenging to reproduce in laboratory settings, this data remains critical to understanding FCCI in SFR systems.

2.2.1 Lanthanide Penetration into Cladding

One of the primary sources of FCCI data for uranium alloy/steel interfaces in an SFR is post-irradiation examination performed on fuel pins from EBR-II [20, 17, 14]. Analysis of cross-sections of these fuel pins using EPMA found that lanthanide fission products tend to build up at the fuel-cladding interface, due to their limited solubility within the uranium alloy fuel, and then diffuse into the cladding to form intermetallics with iron [20, 46]. These effects are demonstrated in the optical microscopy image from a fuel pin cross-section shown in Figure 2-3, in which the lanthanide rich regions adjacent to the cladding are dark gray, and the diffusion zone into the cladding is next to the arrows.

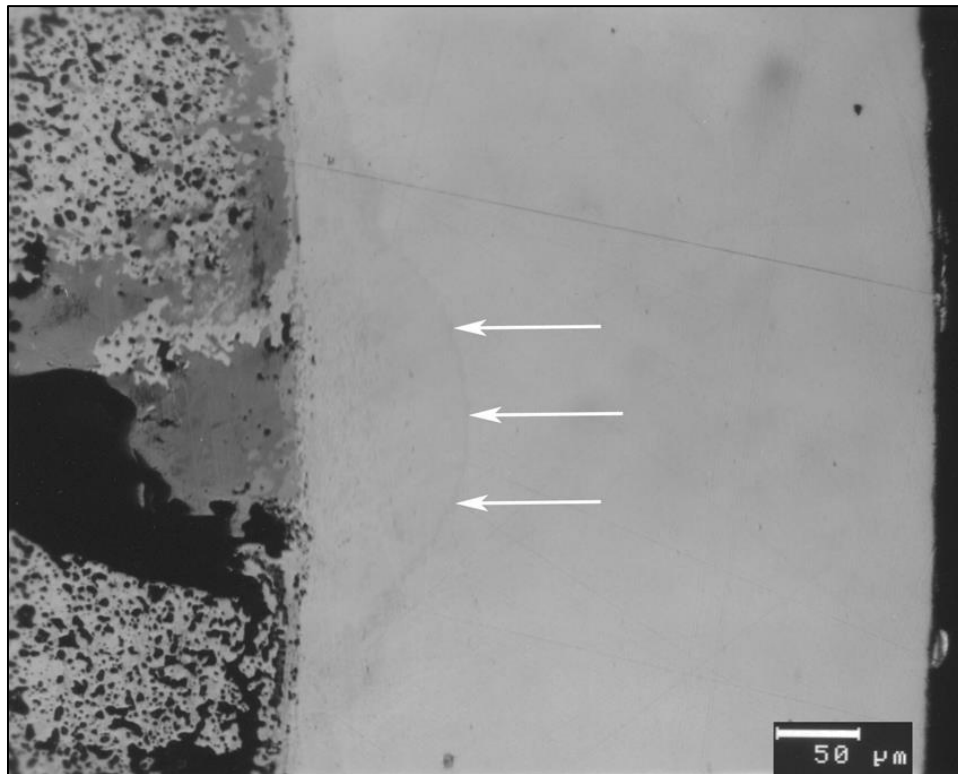


Figure 2-3. Fuel-cladding interface showing lanthanide buildup and cladding penetration [20].

Elemental profiles across the fuel-cladding interface in areas with FCCI showed that of all the elements within the fuel, lanthanides were the furthest penetrating and the greatest fraction within the cladding. Cerium and neodymium were the most prevalent lanthanides in the cladding, due in part to their higher fission yields which are given in Table 2-1 [20, 47]. However, most of the lanthanides appear to have diffused uniformly as a group into the characterized cladding sections [20]. Some counter-diffusion of steel elements into the fuel was also observed, primarily iron and nickel [20, 46]. An example of the elemental profiles found between at the fuel-cladding interface is given in Figure 2-4.

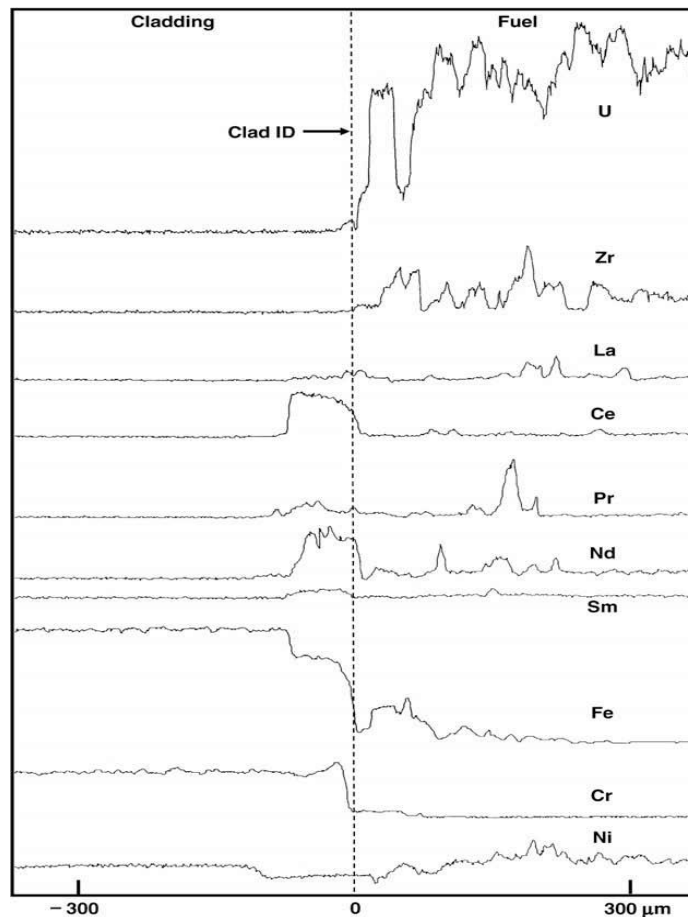


Figure 2-4. EPMA of fuel/cladding interface from EBR-II [46].

Table 2-1. Relative fission yields of the lanthanide series [47].

	Y	La	Ce	Pr	Nd	Pm	Sm	Eu	Gd
Relative Yield	4.0%	12.5%	22.3%	11.4%	35.9%	1.2%	10.4%	1.2%	1.1%

2.2.2 Intermetallic Formation

Analysis of various EBR-II fuel pins found that FCCI regions were typically 20 to 100 μm thick, with greater thicknesses found in areas exposed to higher temperatures [20]. This effect was attributed to more rapid diffusion of the lanthanides through the fuel to the fuel-cladding interface at higher temperatures [48]. Within the FCCI interdiffusion region, several distinct zones were found. The largest zone was found to form within the cladding, with a composition close to $Ln_2(Fe+Cr)_{17}$, corresponding to the Ce_2Fe_{17} or Nd_2Fe_{17} intermetallics [20, 49, 50]. Within this intermetallic phase, there were often lanthanide-rich precipitates and an increase in chromium concentration relative to the bulk steel.

2.2.3 Fuel Performance Implications

Three primary effects on fuel performance were observed in areas with significant lanthanide-based FCCI [14, 48]. First, the intermetallic phases created by lanthanide penetration into the steel were found to be significantly harder than the original steel, as shown by the impact hardness tests performed on cladding with intermetallic penetration in Figure 2-5. This increase in hardness made the cladding in areas affected by FCCI much more susceptible to cracking under stress [20, 48].

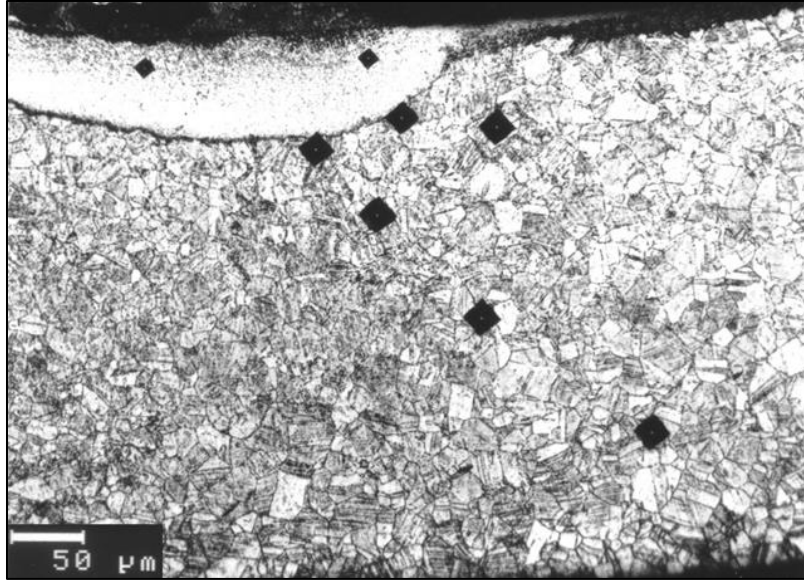


Figure 2-5. Impact tested cladding specimen showing increased hardness in intermetallic zone [20].

The second fuel performance issue generated by FCCI was decarburization which was observed in cladding near FCCI regions [48]. Post-irradiation examination of EBR-II fuel elements found decarburized zones with a large, soft grain structure in steel up to 60 μm past the reaction front of the lanthanide penetration. When coupled with the brittle intermetallics formed within the cladding, this decarburization further reduced the integrity of the cladding [48]. An optical microscopy image of fuel cladding that nearly ruptured due to these effects is shown in Figure 2-6. In this image, the fuel was originally on the bottom side of the cladding shown. The intermetallic region is visible in the bottom section of the cladding as a lighter region in the upper image and a darker region in the etched lower image. The decarburized zone, characterized by larger grains, is visible above the intermetallic region in the etched lower image. The scale bar in the image is approximate, and was added to provide a general idea of the depth of intermetallic formation and decarburization.

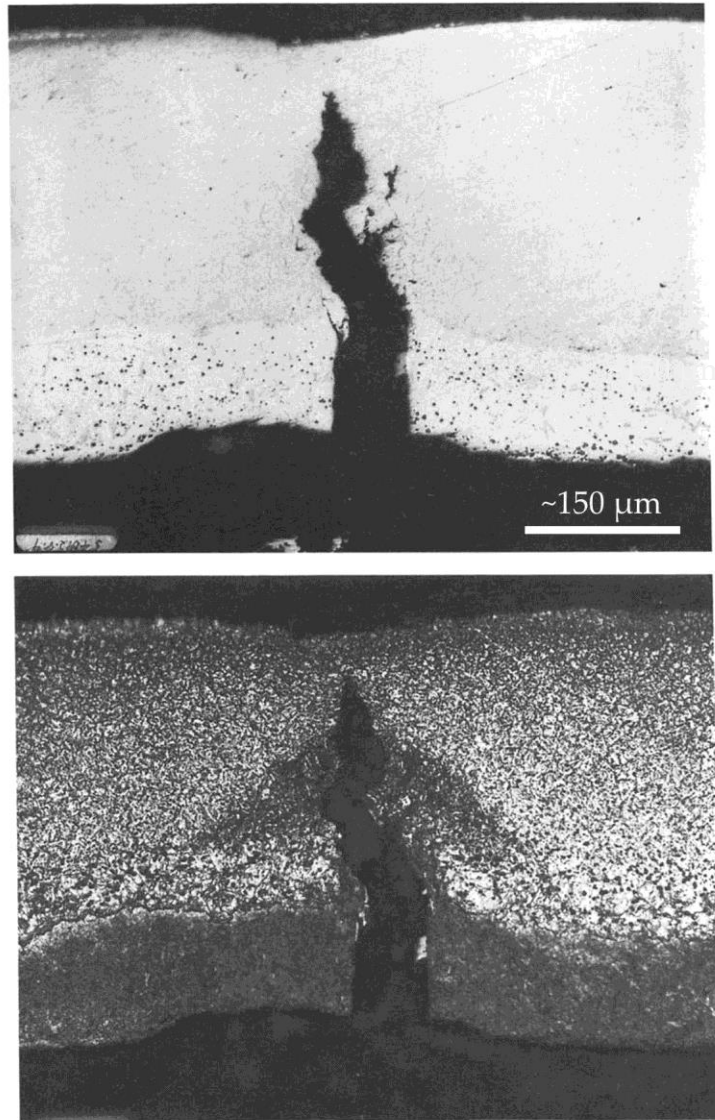


Figure 2-6. Cracking in fuel cladding due to intermetallic formation and decarburization [48].

The final (for this review) performance issue generated by lanthanide intermetallic formation within cladding is the possibility of eutectic melting at the fuel-cladding interface at lower than normal temperatures [46, 9, 24, 38, 17, 51, 14]. Intermetallics between iron and lanthanide elements undergo eutectic melting between 600 to 700°C, as shown for neodymium and cerium in Figure 2-7 and Figure

2-8, respectively. Given a nominal fuel-cladding interface temperature of 400 to 550°C for SFR's, this poses a greatly increased risk of eutectic melting at the fuel-cladding interface during reactor transients in which temperatures increase [17].

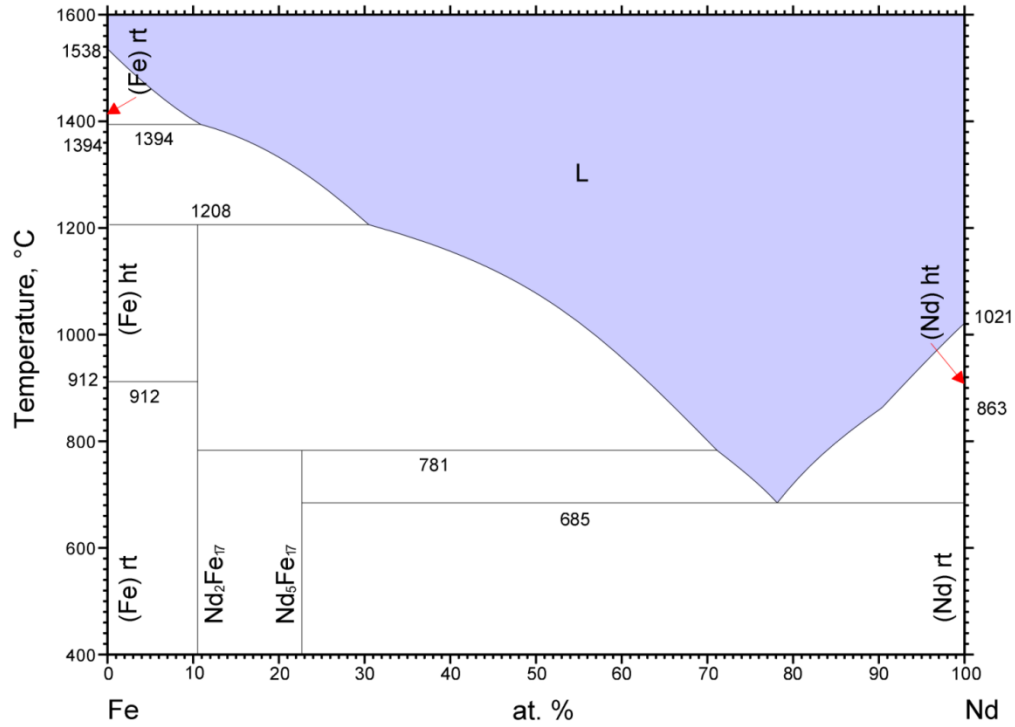


Figure 2-7. Iron-neodymium phase diagram [50].

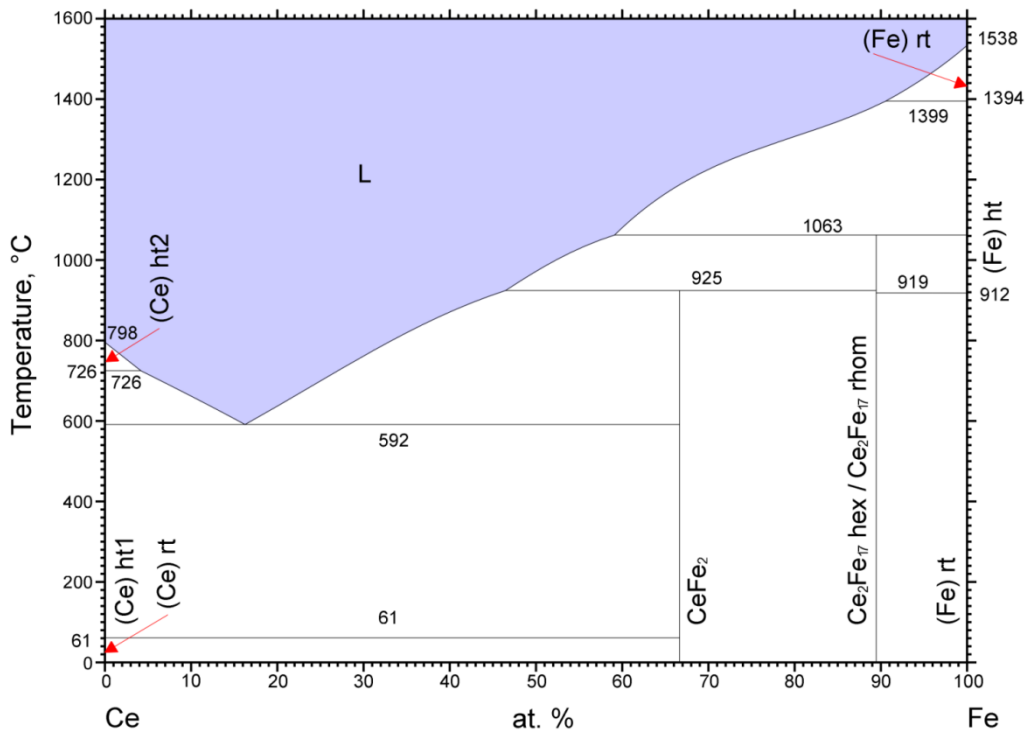


Figure 2-8. Iron-cerium phase diagram [49].

2.3 Diffusion Barrier Liner Experience with Nuclear Fuel

The concept of using refractory metals as diffusion barrier liners between fuel and cladding for fast reactor designs has a long history [24, 21, 15, 22, 18, 52]. During development for EBR-II, prototype fuel elements were fabricated using tungsten and vanadium as liner materials. Fuel cladding was fabricated with a ~40 μm layer of vapor-deposited tungsten or with a ~13 μm foil layer of vanadium. In reactor tests of twenty-one of these prototype fuel elements containing uranium, plutonium, and a mixture of fission products for burnups of 400 to 2600 MWd met with mixed results [52]. FCCI was prevented in most cases by the vanadium foils; however, pinhole defects within the vapor-deposited tungsten layer resulted in unreliable behavior for those fuel elements [52]. In the tungsten-coating fuel

elements, FCCI through pinhole defects resulted in extensive eutectic formation, the formation of small holes within the cladding, or in some cases longitudinal splits in the cladding through which fuel could protrude [52].

The idea of using refractory metal diffusion barrier liners was revived near the end of EBR-II operation based on experience with fuel pins cast into zirconium molds [51]. Although the initial goal of the project was to minimize waste associated with quartz molds during injection casting of fuel pins, it was found that the process resulted in a sheath of zirconium surrounding the cast fuel which was quasi-effective in reducing FCCI. Wherever the zirconium sheath remained intact, FCCI was prevented; however, the sheath was often broken in several radial locations around the fuel pin, resulting in wedge-shaped cracks through which FCCI occurred. A transverse section of an irradiated fuel pin with a zirconium sheath is given in Figure 2-9, in which the outer white ring is the steel cladding and the inner ring is the mostly intact zirconium sheath. This breakage was likely due to plastic deformation of the zirconium sheath during swelling of the fuel pins [51, 17].

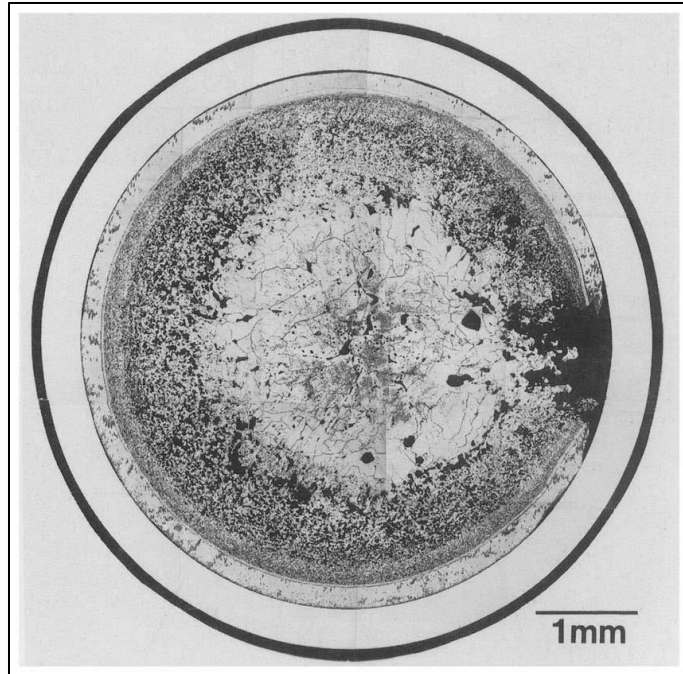


Figure 2-9. Transverse section of fuel with partially intact zirconium sheath from casting [51].

Based on this experience, the concept of refractory metal diffusion liners was again investigated at EBR-II the following year [21]. A set of experimental fuel elements featuring a vanadium liner to prevent FCCI were fabricated for testing in the reactor. Unfortunately, the data from these tests, if they were completed, has not been published [21].

2.4 Existing Diffusion Couple Data

Several prior studies have been completed using diffusion systems relevant to FCCI, including both diffusion between steel alloys and various lanthanides as well as the diffusive behavior of potential diffusion barrier liner materials [15, 47, 22, 18, 53, 54]. In general, these studies have been conducted at or above typical reactor operating temperatures, either to increase the degree of diffusion observed or to simulate reactor transient temperature increases. Studies which have performed

long-term diffusion anneals of greater than a few days at reactor operating temperatures are relatively rare.

2.4.1 Steel/Lanthanide Diffusion

Diffusion couple studies performed using pure iron with various lanthanides, including cerium and neodymium confirmed the existence of several intermetallic phases which form depending on the lanthanide present. While cerium and neodymium, represented as 'Ln', both form $\text{Ln}_2\text{Fe}_{17}$ and LnFe_2 intermetallics with iron, neodymium has also been observed to form $\text{Nd}_5\text{Fe}_{17}$ [55]. In some studies, the $\text{Nd}_5\text{Fe}_{17}$ was only observed to form when annealed at temperatures below 700°C [56]. When a mixture of lanthanides, rather than single elements, was used in diffusion couples with iron the $\text{Ln}_2\text{Fe}_{17}$ and LnFe_2 intermetallics were both observed to form. The lack of an $\text{Nd}_5\text{Fe}_{17}$ intermetallic in these experiments is not surprising, given that neodymium is the only lanthanide to form that type of intermetallic with iron and it accounted for less than a quarter of the lanthanide mixture [57]. Examples of elemental profiles generated by diffusion between neodymium and iron demonstrating the formation of the $\text{Nd}_2\text{Fe}_{17}$ phase alone at high temperatures (780°C) and the formation of both the $\text{Nd}_5\text{Fe}_{17}$ and $\text{Nd}_2\text{Fe}_{17}$ phases at low temperatures (680°C) are given in Figure 2-10 and Figure 2-11 respectively. These elemental profiles also demonstrate the typical behavior seen for all lanthanide-iron diffusion couples, regardless of temperatures, of a series of intermetallic zones with narrow composition bands.

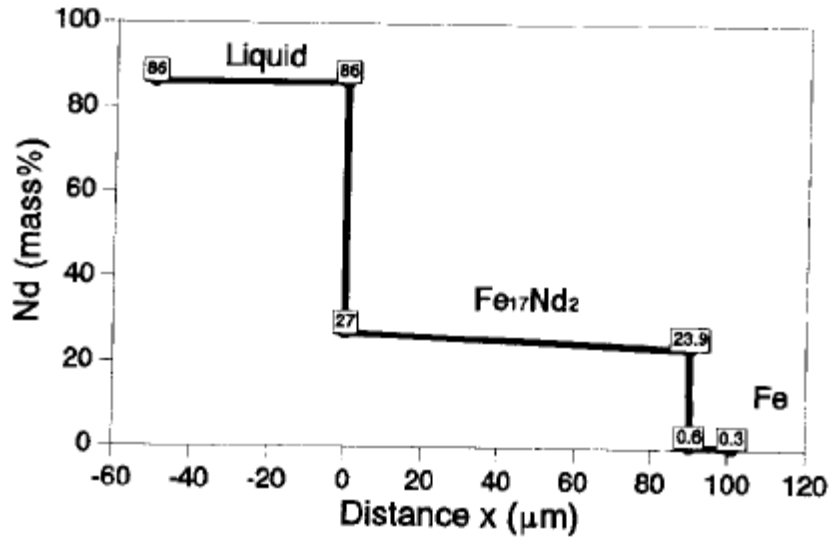


Figure 2-10. Neodymium/iron elemental profile after 9 hours at 780°C [56].

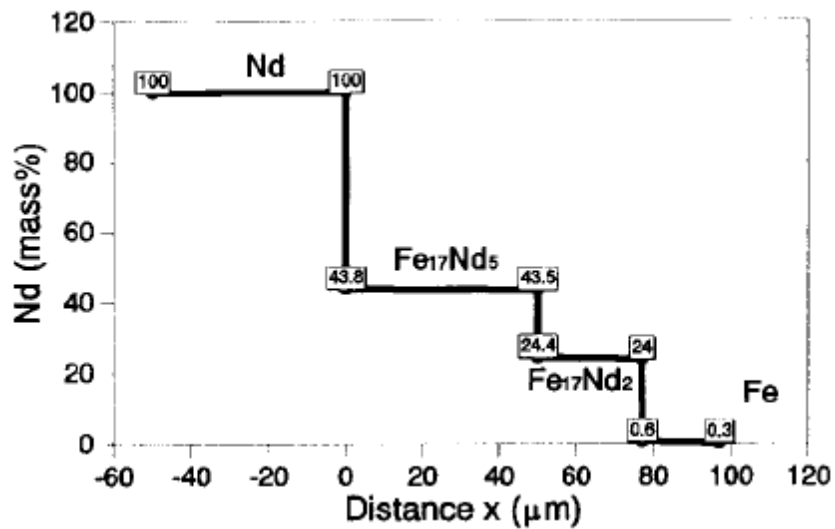


Figure 2-11. Neodymium/iron elemental profile after 25 hours at 680°C [56].

The diffusion of dilute amounts of iron and other elements from the first transition row in lanthanides has also been studied using radioactive tracers to compare the vacancy and interstitial diffusion mechanisms [58]. In these tests, elements from the first transition metal series (scandium through copper) were

found to diffuse significantly faster through lanthanides than the self-diffusion rates of the lanthanides themselves. This accelerated diffusion was ascribed to interstitial diffusion mechanisms for the smaller atoms moving through the lanthanide crystal structure [58]. Additional diffusion couples between cerium and various binary alloys of iron, nickel and chromium found that nickel diffuses significantly faster with cerium than either iron or chromium. The intermetallic phases formed by these diffusion couples did not generally match with the expected phases from the cerium-iron phase diagram; however, the CeFe_2 phase did consistently form [54]. These results indicate that rapid diffusion should be expected for elements from the first transition row, and nickel in particular, with lanthanides due to rapid interstitial diffusion mechanisms.

Diffusion couples between a ferritic-martensitic steel alloy (G.92) and lanthanides found that, as with diffusion between pure iron and lanthanide mixtures, the $\text{Ln}_2\text{Fe}_{17}$ and LnFe_2 intermetallic phases were formed [59, 60]. In these diffusion couples, increases in chromium concentration in the $\text{Ln}_2\text{Fe}_{17}$ phase due to low chromium content in the LnFe_2 phase resulted in a cubic rate law for phase growth, rather than the parabolic rate law predicted for diffusion controlled systems [60]. Further diffusion couples using G.92 and neodymium found the $\text{Nd}_2\text{Fe}_{17}$ and $\text{Nd}_5\text{Fe}_{17}$ phases to form, but not the NdFe_2 phase, which would be expected [59]. In both of these studies, deviations in the form of cubic rather than parabolic rate laws and expected phases not forming may have been the result of using relatively short annealing times (typically less than one day, and at most five days) at elevated temperatures (660-800°C). A BSE image of the interaction zone observed between steel and neodymium after six hours at 700°C is given in Figure 2-12, along with the corresponding elemental profile.

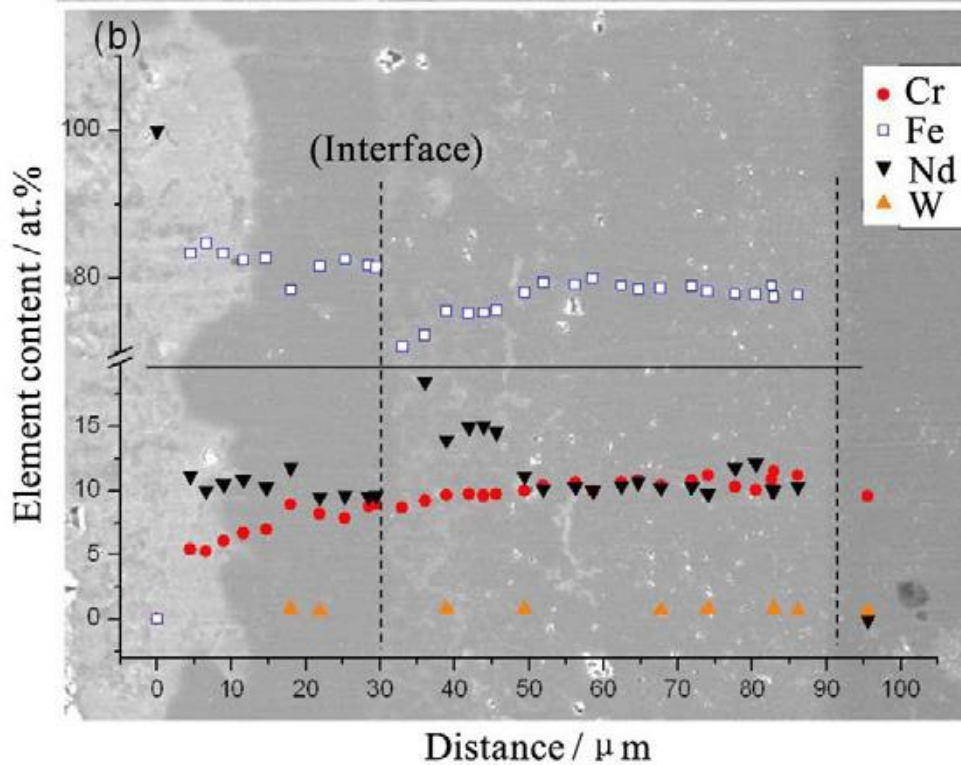


Figure 2-12. Neodymium/steel interface after 6 hours at 700°C [59].

2.4.2 Diffusion Barrier Liner Diffusion

Several diffusion couple studies involving the performance of refractory metals, including zirconium, vanadium, niobium, titanium, molybdenum, tantalum, and chromium, as liners have been conducted [53, 61, 62, 22]. These studies have typically used uranium-zirconium alloys and steel cladding materials to test the compatibility of the liner materials with both fuel and cladding. Some attempts have been made to use fuel alloys with some fraction of dissolved lanthanides to simulate high-burnup fuel. However, the tendency of the lanthanides to form into isolated particles within the fuel alloy prevented any interactions from occurring between the lanthanides and the liners [53]. Thus, diffusion data for liner materials

has been generated primarily for diffusion with uranium-zirconium alloys and steel cladding materials.

Overall, these diffusion studies have found vanadium and chromium to be the best candidates, based primarily on their extent of interaction with uranium alloys [53]. Zirconium, niobium, titanium, molybdenum, and tantalum barriers placed between U-10Zr and HT-9 for 25 hours at 800°C were found to form significant diffusive interaction zones with U-10Zr, as shown in Figure 2-13, Figure 2-14, Figure 2-15, Figure 2-16, and Figure 2-17. On the other hand, vanadium and chromium under the same conditions were found to react in a very limited manner with either the U-10Zr or the HT-9, as shown in Figure 2-18 and Figure 2-19.

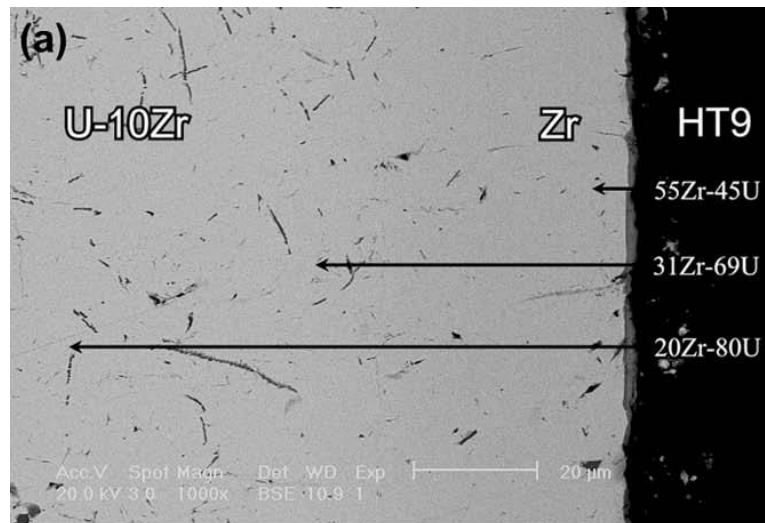


Figure 2-13. Zirconium interaction with U-10Zr after 25 hours at 800°C [53].

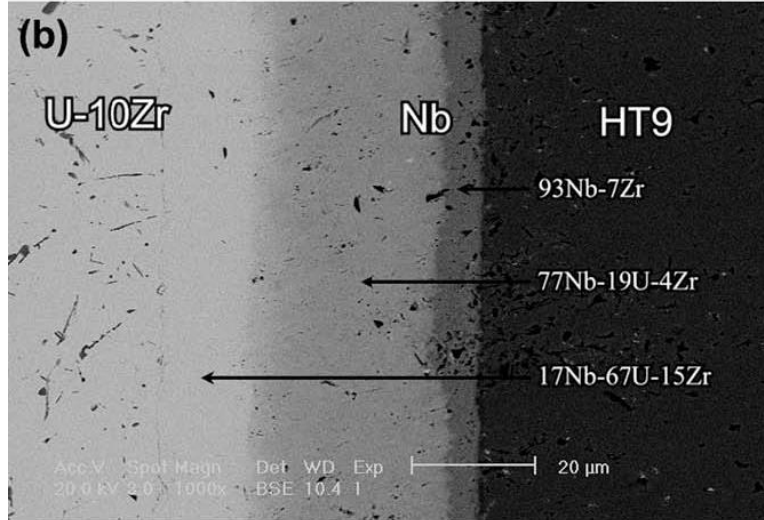


Figure 2-14. Niobium interaction with U-10Zr after 25 hours at 800°C [53].

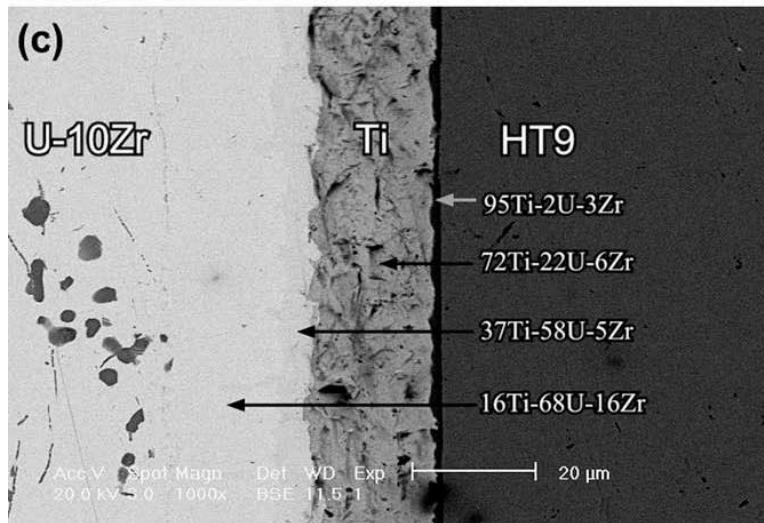


Figure 2-15. Titanium interaction with U-10Zr and HT-9 after 25 hours at 800°C [53].

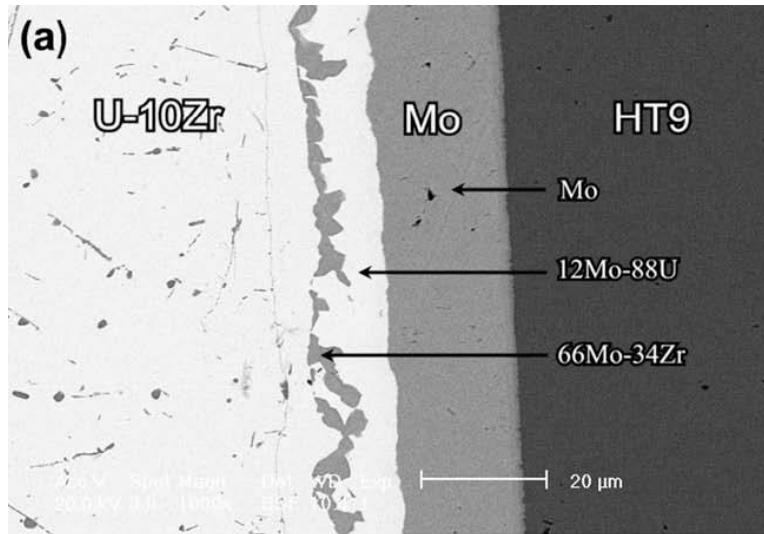


Figure 2-16. Molybdenum interaction with U-10Zr after 25 hours at 800°C [53].

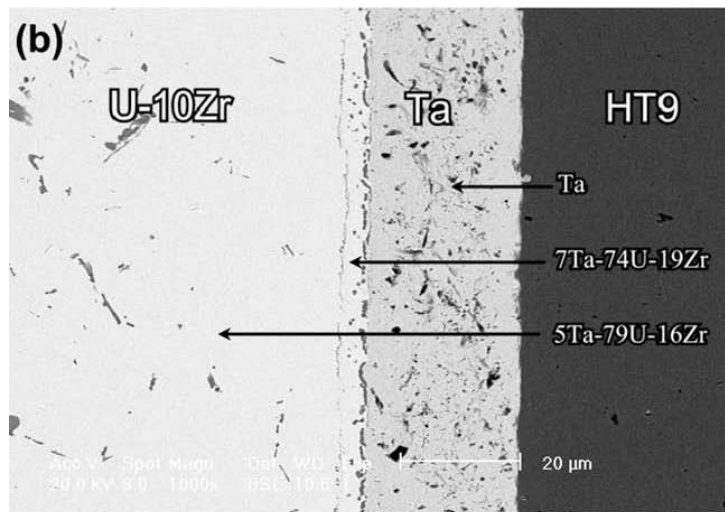


Figure 2-17. Tantalum interaction with U-10Zr after 25 hours at 800°C [53].

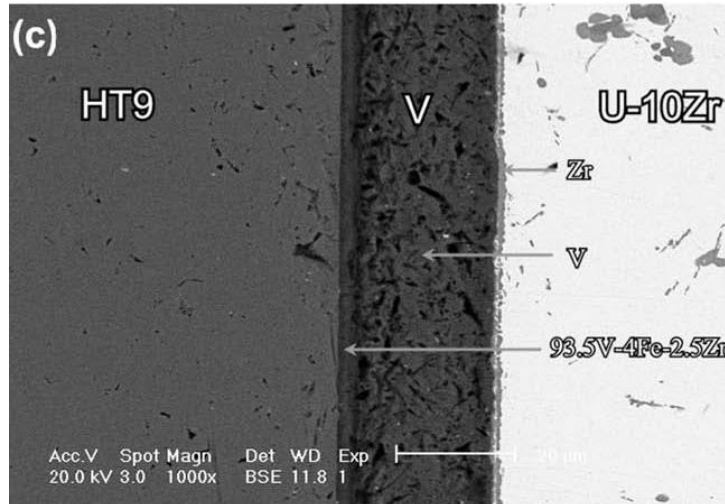


Figure 2-18. Vanadium interaction with HT-9 after 25 hours at 800°C [53].

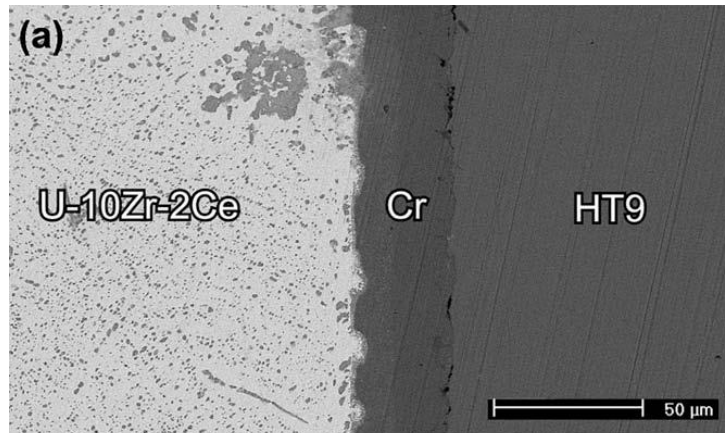


Figure 2-19. Chromium with U-10Zr and HT-9 after 25 hours at 800°C [53].

2.5 Computation of Diffusion Parameters

Two discrete methods were used in this work for analyzing the diffusion results and determining diffusion coefficients. In most of the diffusion interfaces in this work, no intermetallic phases were formed, and elemental profiles followed smooth curves which were easily represented using the simple diffusion methods

described in Section 2.5.1. For the remaining diffusion interfaces, a series of line compound intermetallic phases formed and an alternate method based on phase widths and elemental concentrations in each intermetallic was used, as described in Section 2.5.2.

2.5.1 Simple Fick's Law Diffusion

Diffusion between two planar semi-infinite sources may be modelled in a straightforward manner by assuming that the governing interdiffusion coefficients are independent of concentration [63]. This assumption is accurate either for diffusion between systems with only minor initial differences in concentration, or for systems in which ideal randomized mixing between materials occurs. In this case, each of the semi-infinite sources may be considered as a series of infinitely thin planar sources, each of which contributes to the final concentration curve an individual Gaussian curve centered on itself, as shown in Figure 2-20. As shown in this figure, as diffusion progresses with time, new planar sources are generated along the advancing diffusional interaction front.

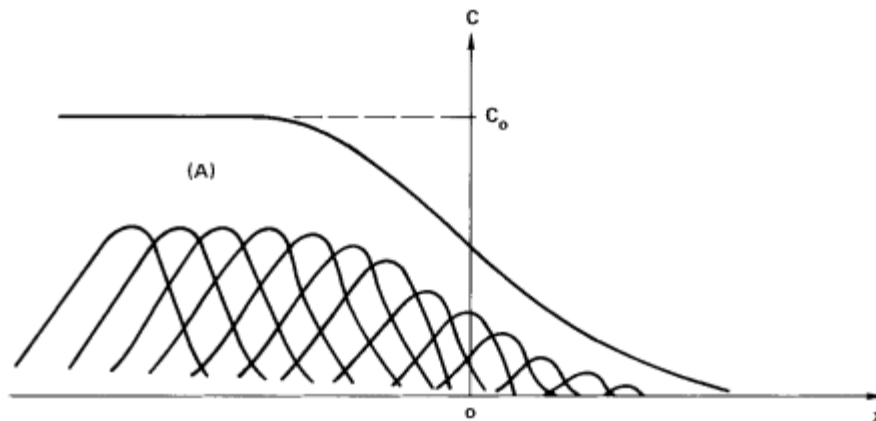


Figure 2-20. Superposition of infinite planar sources to form concentration curve [63].

The integration of all the Gaussians into a composite composition curve results in the single expression for elemental concentration as a function of time and position given in Equation 2-1, in which $C(x,t)$ is the concentration at a given position x and time t , C_0 is the concentration in the bulk material, and D is the interdiffusion coefficient [63]. In this solution, the position, x , is set to zero at the original diffusion interface in the center of the diffusion couple.

Equation 2-1

$$C(x, t) = \frac{C_0}{2} \operatorname{erfc} \frac{x}{2\sqrt{Dt}}$$

2.5.2 Line Compound Diffusion

Diffusion interfaces which form into a series of line compounds, such as intermetallic systems, require special analysis methods [64, 65, 66, 67, 68]. While general diffusion solutions are based on randomized mixing of originally separate materials due to concentration gradients, the driving force for intermetallic diffusion is the chemical energy of formation accompanying the creation of the new phase [63]. As such, diffusion in intermetallic systems generally produces a series of phases with relatively constant elemental concentrations near the stoichiometric balance, as shown in Figure 2-21.

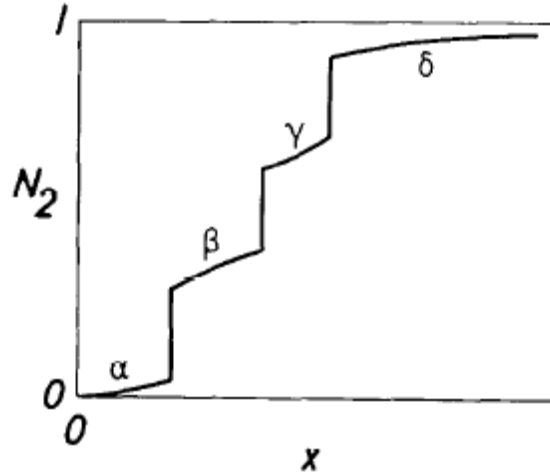


Figure 2-21. Series of two line compounds (β, γ) between two terminal solutions (α, δ) [64].

One of the foundational analysis methods for line compound diffusion developed by C. Wagner allows for the calculation of integrated diffusion coefficients for serial interdiffusion phases, such as are formed by intermetallics, so long as local equilibrium exists at each of the interphases between phases [64]. Based on this approach, the integrated diffusion coefficient for a given phase i is given by Equation 2-2, where D_i is the integrated diffusion coefficient for phase i , N^i is the concentration in phase i , $N^{(i-1)'}$ is the concentration in the preceding phase $i-1$ immediately adjacent to phase i , $N^{(i+1)'}$ is the concentration in the following phase $i+1$ immediately adjacent to phase i , Δx^i is the width of phase i , and t is the annealing time. An example elemental profile with the appropriate variables for Equation 2-2 labeled is given in Figure 2-22.

Equation 2-2

$$D_i = \frac{(N^{(i)} - N^{(i-1)'}) (N^{(i+1)' } - N^{(i)}) (\Delta x^i)^2}{(N^{(i+1)' } - N^{(i-1)'}) 2t}$$

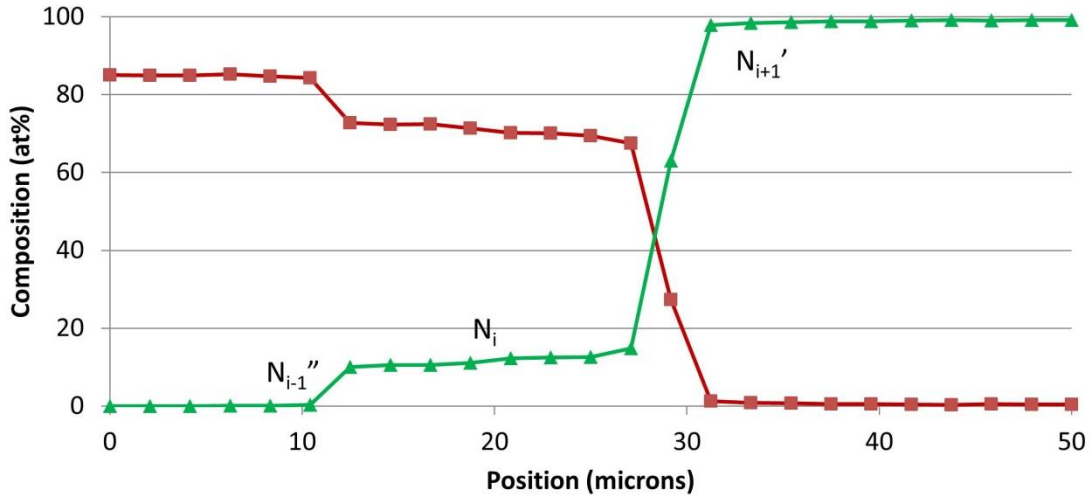


Figure 2-22. Example profile for application of Equation 2-2.

Although Wagner's method was initially developed assuming narrow concentration bands for each interdiffusion zone, later work expanded upon this and demonstrated that the resulting equations could be applied without error to diffusion systems in which deviations from ideal behavior were observed [68, 69].

3 EXPERIMENTAL METHODS

3.1 Fabrication of Diffusion Couples

The diffusion couples prepared for this project were assembled at Intellectual Ventures Laboratory by Jeff Dallas using disks of steel, iron, and neodymium along with foils of vanadium, zirconium, titanium, molybdenum, tantalum, and titanium. Bulk plates of HT-9 and G.91 were obtained from Oak Ridge National Laboratory and cut into 3.2 mm (0.125 inch) thick, 12.7 mm (0.5 inch) square disks by Electrical Discharge Machining (EDM). A 12.7 mm (0.5 inch) diameter rod of SS-316 and a 0.625 inch diameter rod of pure iron obtained from McMaster-Carr were cut into 3.2 mm (0.125 inch) thick disks using EDM. Nominal composition ranges for alloying components in each of the three steels used are given in Table 3-1. Finally, a rod of neodymium (99.5%) obtained from Alfa-Aesar was cut into 3.2 mm (0.125 inch) thick disks using EDM. As this cutting process produces extremely smooth surfaces, comparable to a 10 μm polish, no polishing of the disk faces was performed. Following cutting, all materials were immediately stored in an inert-atmosphere glovebox to prevent surface oxidation. Foils approximately 100 μm thick of vanadium (99.8%), zirconium (99.5%), titanium (99%), molybdenum (99.95%), tantalum (99.95%), and tungsten (99.95%) were obtained from Alfa-Aesar. These foils were cut into 15.9 mm (0.625 inch) diameter disks using a shim punch. No polishing was performed on the foils, and all foils were stored in an inert-atmosphere glovebox to prevent oxidation. Based on the analyzed diffusion interfaces, no significant surface oxidation was apparent.

Table 3-1. Composition of alloying components in each steel alloy (at%).

	Cr	Ni	C	Mn	Cu	Mo	Si	S	P	N	V	W
HT-9	11- 12	0.5- 0.6	0.18- 0.22	0.45- 0.85	0- 0.02	0.85- 0.95	0.1- 0.3	0- 0.003	0- 0.01	0.01- 0.03	0.25- 0.55	0.45- 0.55
G.91	8- 9.5	0- 0.4	0.08- 0.12	0.3- 0.6	0- 0.02	0.85- 1.05	0.2- 0.5	0-0.1	0- 0.01	0.03- 0.07	0.18- 0.25	0-0.1
SS-316	16- 18	10- 14	0- 0.08	0-2	0- 0.75	0-3	0-1	0.03	0- 0.045	0-0.1	N/A	N/A

Once the requisite materials were prepared, diffusion couples were assembled into stacks, as shown in Figure 3-1, using disks of a single steel alloy or iron, as well as neodymium disks and an assortment of foil disks. Each stack included six neodymium disks, sandwiched on either side by foils and steel disks. One steel/neodymium interface on each stack was left without a foil barrier to provide a base-case for the interaction between steel and neodymium without a liner. Six steel/neodymium interfaces in each stack included a single foil barrier, matching the six liner materials tested, while five steel/neodymium interfaces in each stack included a dual-foil barrier. These dual barriers each consisted of a vanadium foil disk paired with one of the other six liner materials. In each case, the vanadium foil was placed facing the neodymium disk while the other foil was placed facing the steel disk.

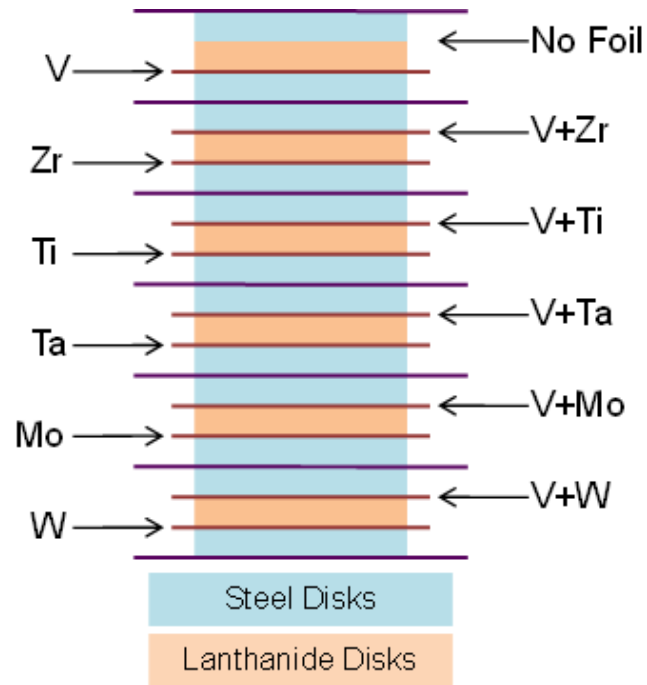


Figure 3-1. Schematic of assembled diffusion couple stack.

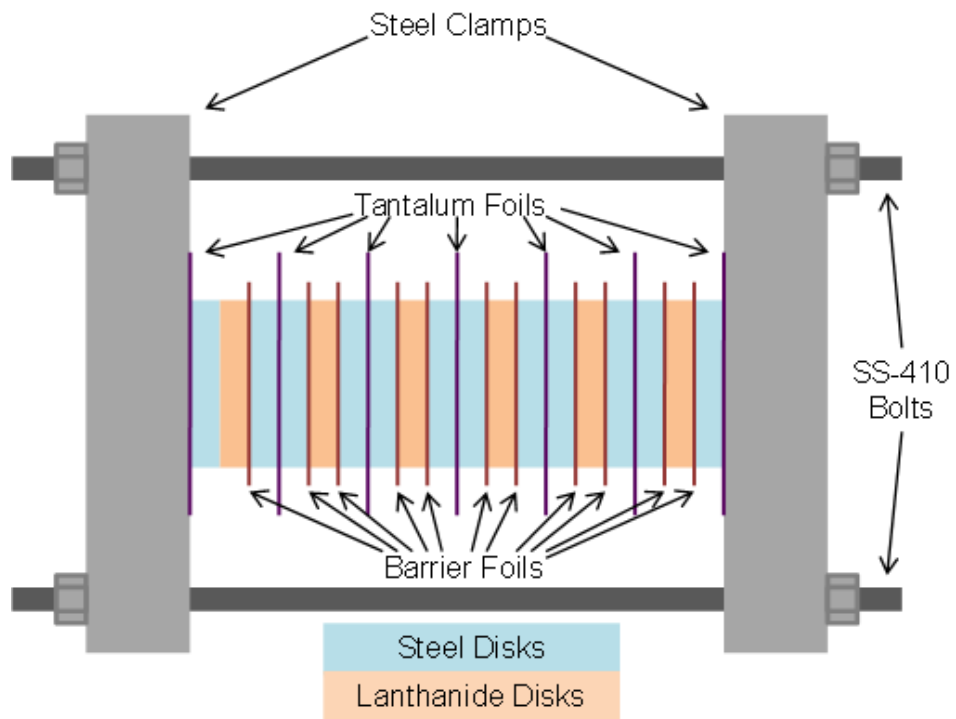


Figure 3-2. Schematic of loaded diffusion couple jig.

The assembled diffusion couple stacks were placed into jigs, as shown in Figure 3-2 and Figure 3-3. The end-plates of the jigs were disks of SS-316, while the rods and nuts were SS-410. These materials were selected to closely match the thermal expansion of the diffusion couple stack, providing a slight compressive force during diffusion annealing, example calculations for which are given in Table 3-2. Boron nitride lubricant was applied to the ends of each rod, and the nuts on each jig were tightened to a torque of 0.23 kg*m (20 in-lbs), providing an initial compressive force of 94 MPa.



Figure 3-3. Assembled diffusion couple stack in jig.

Table 3-2. Thermal expansion calculation for HT-9 diffusion couple stack.

	α_L ($\mu\text{m}/\text{m}\cdot\text{K}$)	Thickness (mm)	ΔT ($^{\circ}\text{C}$)	Thermal Expansion (μm)
Nd disks	9.6	19.05	675	123.4
HT-9 disks	9.9	38.1	675	254.6
Foils	6.4	2.3	675	9.9
SS-316 end-plates	16	12.7	675	137.2
SS-410 Rods	9.9	72.15	675	482.1
Total Compression (μm)				43.0
Compressive Force (MPa)				119.2

3.2 Heat Treatment of Diffusion Couples

Assembled diffusion couple stacks in jigs were placed into flanged steel chambers while still inside an inert atmosphere glovebox. A total of four flanged chambers were used for each heat treatment, each of which held a diffusion couple stack with one of the three steel alloys or iron. Once sealed, the loaded chambers were removed from the inert atmosphere glovebox and loaded into a kiln for heat treatment. Fittings on each flange were used to connect the four nipples together in series with steel tubing. One end of the series was then connected to an argon supply line, while the other end was connected to a crimped tube designed to allow low but steady flow of gas through the system. A picture of the loaded kiln before heat treatment is shown in Figure 3-4.

The argon supply line for the system included two tanks of argon gas configured such that each could be isolated from the system for replacement and purging of the lines. The argon from these tanks was purified through moisture and oxygen traps (Alltech model numbers AT8128 and AT7215) in series before entering the diffusion couple system to minimize the presence of any reactive gases. During

heat treatments, the system was pressurized to 103 kPa (15 psig) with a steady slow flow of gas through the system.



Figure 3-4. Diffusion couples loaded into kiln prior to heat treatment.

Heat treatments were performed for (1) 17.5 days at 550°C, (2) 28 days at 550°C, (3) 56 days at 550°C, (4) 28 days at 625°C, and (5) 28 days at 700°C. For each of these heat treatments, diffusion couple stacks containing each of the three steel alloys and iron were included, with the exception of the 17.5 day heat treatment at 550°C for which there was only enough material to include the HT-9 diffusion couple stack. Heat treatments were brought to temperature using a ramp rate of 10°C/min and allowed to cool naturally when completed. During heat treatment, temperature was monitored continuously with two thermocouples. A summary of

all of the diffusion couples and heat treatments is provided in Table 3-3, along with the corresponding appendix section for each in which further data may be found.

Table 3-3. Summary of all diffusion couples with corresponding appendices.

	17.5 Days @ 550°C	28 Days @ 550°C	56 Days @ 550°C	28 Days @ 625°C	28 Days @ 700°C
HT-9/Nd	B.1	B.13	B.25	B.37	B.49
HT-9/V/Nd	B.2	B.14	B.26	B.38	B.50
HT-9/Zr/V/Nd	B.3	B.15	B.27	B.39	B.51
HT-9/Zr/Nd	B.4	B.16	B.28	B.40	B.52
HT-9/Ti/V/Nd	B.5	B.17	B.29	B.41	B.53
HT-9/Ti/Nd	B.6	B.18	B.30	B.42	B.54
HT-9/Ta/V/Nd	B.7	B.19	B.31	B.43	B.55
HT-9/Ta/Nd	B.8	B.20	B.32	B.44	B.56
HT-9/Mo/V/Nd	B.9	B.21	B.33	B.45	B.57
HT-9/Mo/Nd	B.10	B.22	B.34	B.46	B.58
HT-9/W/V/Nd	B.11	B.23	B.35	B.47	B.59
HT-9/W/Nd	B.12	B.24	B.36	B.48	B.60
	17.5 Days @ 550°C	28 Days @ 550°C	56 Days @ 550°C	28 Days @ 625°C	28 Days @ 700°C
G.91/Nd	N/A	C.1	C.13	C.25	C.37
G.91/V/Nd	N/A	C.2	C.14	C.26	C.38
G.91/Zr/V/Nd	N/A	C.3	C.15	C.27	C.39
G.91/Zr/Nd	N/A	C.4	C.16	C.28	C.40
G.91/Ti/V/Nd	N/A	C.5	C.17	C.29	C.41
G.91/Ti/Nd	N/A	C.6	C.18	C.30	C.42
G.91/Ta/V/Nd	N/A	C.7	C.19	C.31	C.43
G.91/Ta/Nd	N/A	C.8	C.20	C.32	C.44
G.91/Mo/V/Nd	N/A	C.9	C.21	C.33	C.45
G.91/Mo/Nd	N/A	C.10	C.22	C.34	C.46
G.91/W/V/Nd	N/A	C.11	C.23	C.35	C.47
G.91/W/Nd	N/A	C.12	C.24	C.36	C.48
	17.5 Days @ 550°C	28 Days @ 550°C	56 Days @ 550°C	28 Days @ 625°C	28 Days @ 700°C
SS-316/Nd	N/A	D.1	D.13	D.25	D.37
SS-316/V/Nd	N/A	D.2	D.14	D.26	D.38
SS-316/Zr/V/Nd	N/A	D.3	D.15	D.27	D.39

Table 3-3 Continued

	17.5 Days @ 550°C	28 Days @ 550°C	56 Days @ 550°C	28 Days @ 625°C	28 Days @ 700°C
SS-316/Zr/Nd	N/A	D.4	D.16	D.28	D.40
SS-316/Ti/V/Nd	N/A	D.5	D.17	D.29	D.41
SS-316/Ti/Nd	N/A	D.6	D.18	D.30	D.42
SS-316/Ta/V/Nd	N/A	D.7	D.19	D.31	D.43
SS-316/Ta/Nd	N/A	D.8	D.20	D.32	D.44
SS-316/Mo/V/Nd	N/A	D.9	D.21	D.33	D.45
SS-316/Mo/Nd	N/A	D.10	D.22	D.34	D.46
SS-316/W/V/Nd	N/A	D.11	D.23	D.35	D.47
SS-316/W/Nd	N/A	D.12	D.24	D.36	D.48
	17.5 Days @ 550°C	28 Days @ 550°C	56 Days @ 550°C	28 Days @ 625°C	28 Days @ 700°C
Fe/Nd	N/A	E.1	E.13	E.25	E.37
Fe/V/Nd	N/A	E.2	E.14	E.26	E.38
Fe/Zr/V/Nd	N/A	E.3	E.15	E.27	E.39
Fe/Zr/Nd	N/A	E.4	E.16	E.28	E.40
Fe/Ti/V/Nd	N/A	E.5	E.17	E.29	E.41
Fe/Ti/Nd	N/A	E.6	E.18	E.30	E.42
Fe/Ta/V/Nd	N/A	E.7	E.19	E.31	E.43
Fe/Ta/Nd	N/A	E.8	E.20	E.32	E.44
Fe/Mo/V/Nd	N/A	E.9	E.21	E.33	E.45
Fe/Mo/Nd	N/A	E.10	E.22	E.34	E.46
Fe/W/V/Nd	N/A	E.11	E.23	E.35	E.47
Fe/W/Nd	N/A	E.12	E.24	E.36	E.48

3.3 Electron Microscopy of Diffusion Couples

Following heat treatment, diffusion couples were removed from their jigs and prepared for electron microscopy. Each stack of diffusion couples was divided into six sections, each of which featured a neodymium disk sandwiched between two steel disks and some foils. If possible these sandwiches were kept intact; however, in some cases they broke apart upon removal from the jig. The components of these broken diffusion couples were maintained and mounted together with their original

order and facing. Each diffusion couple was sectioned across its midsection, as shown in Figure 3-5, then mounted in epoxy. The mounted samples were polished up to a 1 μm diamond grit suspension following the steps outlined in Table 3-4. Polishing was performed by hand using a rotary grinder/polisher. Minimal force was used on the samples, especially during the initial grinding step, to minimize damage to brittle interdiffusion phases.



Figure 3-5. Diffusion couple sectioning using diamond saw.

Table 3-4. Polishing steps used in sample preparation.

Polishing Medium	Lubricant	Speed	Duration
180 grit SiC paper	200 proof ethanol	100 rpm	5-10 minutes
240 grit SiC paper	200 proof ethanol	100 rpm	2-3 minutes
320 grit SiC paper	200 proof ethanol	100 rpm	2-3 minutes
400 grit SiC paper	200 proof ethanol	100 rpm	2-3 minutes
600 grit SiC paper	200 proof ethanol	150 rpm	3-5 minutes
800 grit SiC paper	200 proof ethanol	150 rpm	3-5 minutes
1200 grit SiC paper	200 proof ethanol	150 rpm	3-5 minutes
3 μm diamond suspension	None	200 rpm	5-10 minutes
1 μm diamond suspension	None	200 rpm	5-10 minutes

Polished samples were carbon-coated to prevent surface charging, then imaged and analyzed using a Cameca SX-50 Electron Microprobe. BSE images and X-ray maps were acquired to qualitatively evaluate each diffusion interface. Quantitative composition analysis of diffusion interfaces was acquired by taking series of WDS measurements at points across the diffusion interfaces. These WDS linescans were performed using a 1 μm diameter electron beam at 15 keV with a beam current of either 20 or 40 nA, depending on the sample and a step size between points of 1 μm or more. The WDS parameters used for quantitative analysis of each element are given in Table 3-5.

Table 3-5. WDS parameters used for quantitative analysis.

Element	X-ray	Diffracting Crystal	Background Position	Mode	Differential Window
Si	K α	PET	+800/-800	Differential	1500
Ti	K α	PET	+500/-500	Integral	N/A
V	K α	LiF	+900/-900	Differential	1500
Cr	K α	LiF	+800/-800	Differential	1500
Mn	K α	LiF	+1000/-1000	Differential	1500
Fe	K α	LiF	+500/-500	Integral	N/A
Ni	K α	LiF	+1000/-1000	Integral	N/A
Zr	L α	PET	+1100/-1100	Differential	1500
Mo	L α	PET	+900/-900	Differential	1500
Nd	L α	LiF	+600/-600	Integral	N/A
Ta	M α	TAP	+500/-500	Differential	2500
W	M α	PET	+800/-800	Differential	1500

The diffracting crystals used were PET (pentaerythriol), LiF (Lithium Fluoride), and TAP (Thallium Acid Phthalate). The background position for each element defined the points at which background counts for the diffracting crystal

were taken in terms of the sine of the diffracting angle. The background points on either side were averaged for each element and subtracted from the counts on-peak at each WDS measurement point. Differential and Integral mode determined the operation of the pulse height analysis for each element. In Differential mode, X-rays with wavelengths which are near to a multiple of the wavelength of the X-ray being measured are filtered out, while in Integral mode they are not. When Differential mode is active, the Differential Window determines the range of angles (in terms of the sine of the angle) over which X-rays are discriminated against.

3.4 Analysis of Electron Microscopy Data

Conversion of electron microscopy data gathered for diffusion interfaces into measured diffusion coefficients required a specific series of analytical steps depending on the type of interface.

3.4.1 Average Zone Width Measurement

For diffusion interfaces consisting of a series of line compound zones, analysis required an accurate measurement of the thickness of each diffusion zone. This measurement was performed using two methods, the results of which were then compared for agreement. First, the width of each zone was estimated based on the WDS line scans taken across the zone. Each zone was identified within WDS line scans based on composition, and the average width over all line scans of that interface was taken as the width of a given zone. Second, zone widths were estimated based on the BSE images taken of each diffusion interface. This method required different interaction zones to possess a large enough difference in composition to be visually distinguishable from each other in a BSE image. The benefit of this method is that instead of using the scale bar to determine zone width at a single point across an interface, the area of an entire zone in a BSE image was measured by counting the number of pixels it contains. This area was then

converted into an average zone width across the full BSE image then converted from pixels back into micrometers based on the scale bar.

3.4.2 WDS False-Positive Correction

While WDS generally provides highly accurate compositional data, there are some cases in which systematic errors occur due to the energies of characteristic X-rays for the elements being analyzed. When secondary X-rays for one element are close in energy to the primary X-rays for another element, a false-positive reading for the second element may be generated by the presence of the first. To correct for this effect, WDS measurements were taken deep in the bulk region of the interfering element where the expected concentration of the false-positive element is known. The apparent concentration of the false-positive element was then compared to the measured concentration of the interfering element to determine the magnitude of the false-positive signal in wt% per wt% of the interfering element. This measured false-positive ratio was then used to correct WDS data wherever the interfering element was present. A total of three pairs of interfering and false-positive elements were identified: 0.201 wt% Cr per wt% V, 0.002 wt% Mn per wt% Nd, and 0.226 wt% W per wt% Ta. An example of this false positive reading is given in Figure 3-6, in which the false-positive chromium signal is consistently ~2% of the actual vanadium signal. In this case, the chromium concentration at each point was corrected based on the measured false-positive ratio and the concentration of vanadium. The concentrations for each of the element were then rescaled to make the total concentration at each point 100%.

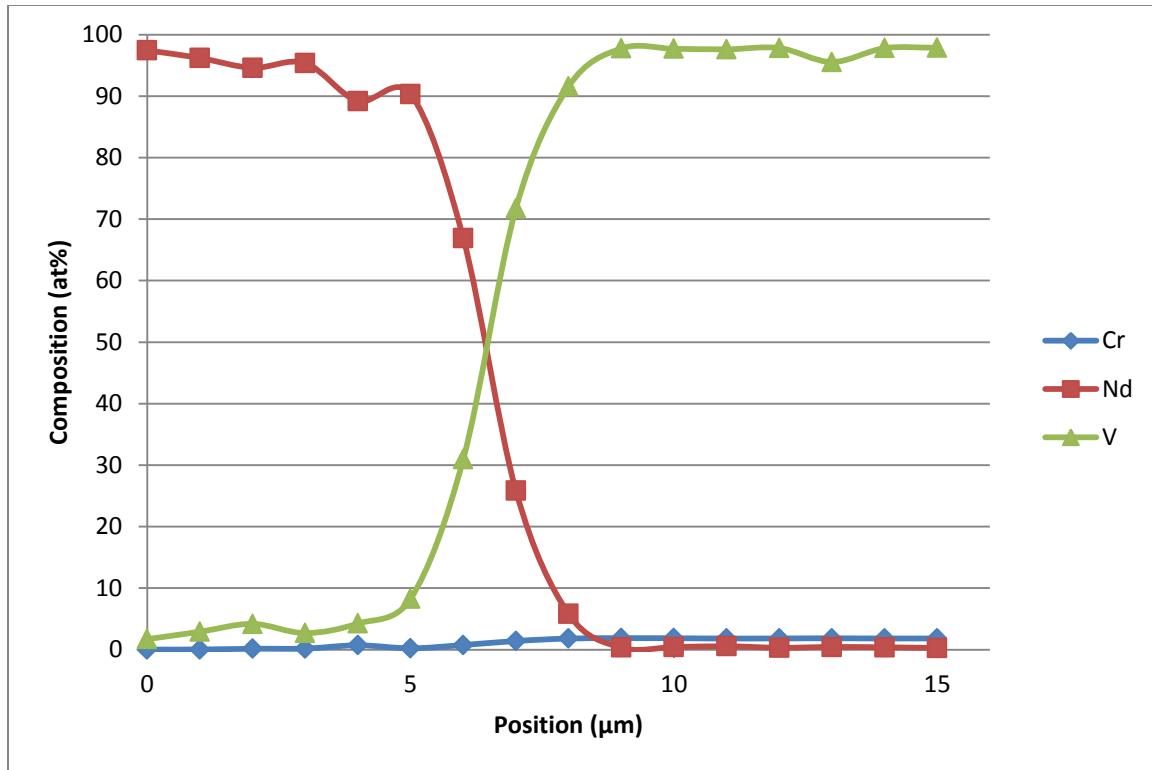


Figure 3-6. Example of false-positive chromium signal in vanadium.

3.4.3 Determination of Fick's Law Diffusion Coefficients

The theoretical equations used for calculating Fick's Law diffusion coefficients are given in Section 2.5.1. The traditional method for applying these equations to data is to evaluate the Boltzmann-Matano equation continuously at each point along the diffusion curve using the Matano plane as a reference point. However, this approach becomes impractical for use when applied to the extremely narrow diffusion zones observed in this work due to the relatively low diffusion coefficients involved and the minimum spacing between WDS analysis points of 1 μm.

To overcome this issue, a new method was approached based on fitting the equations given in Section 2.5.1 to each diffusion curve. Elements along WDS line

scans were summed into two groups to produce a pair of diffusion curves across the interface. These curves were then fit to high order polynomials that could be integrated to determine the exact point of mass-balance along each curve, which corresponded to the Matano interface. Using the interface position for each curve as a reference point, Equation 2-1 was then fit to each of the diffusion curves by varying their diffusion coefficients until the best fit was obtained. This method produced one calculated diffusion coefficient for each of the two diffusion curves at each interface.

Estimation of the associated error for each calculated diffusion coefficient was carried out by considering the systematic errors in position and composition inherent in the microprobe analysis for each curve separately then combining the estimated errors. Error in the diffusion coefficient due to position errors was estimated by refitting Equation 2-1 to the data for each curve after shifting the position values for each point either toward or away from the Matano plane by the maximum estimated error in position of 0.05 μm . An upper limit on the diffusion coefficient was determined by shifting points away from the Matano plane, while a lower limit was determined by shifting points toward the Matano plane. Error in the diffusion coefficient due to concentration errors was estimated by refitting Equation 2-1 to the data for each curve after shifting concentration values for each point either up or down by the estimated error associated with each element. An upper limit on the diffusion coefficient was determined by increasing concentrations below 50at% by the estimated error and decreasing concentrations above 50at% by the estimated error, while a lower limit was determined by performing the inverse.

This process is shown graphically for a vanadium/neodymium diffusion interface in Figure 3-7 and Figure 3-8. In Figure 3-7, the composition of vanadium and neodymium have been adjusted on either side of the diffusion interface either inwards (toward 50%) or outwards (away from 50%). This results in two additional

diffusion curves for both vanadium and neodymium, one pair of which has a diffusion coefficient larger than the original data (adjusted out) and one pair of which has a diffusion coefficient smaller than the original data (adjusted in). Likewise, in Figure 3-8, the position of each point has been adjusted either outwards (away from the diffusion interface) or inwards (toward the diffusion interface). Again, this produces two additional diffusion curves for both vanadium and neodymium, one pair of which has a diffusion coefficient larger than the original data (adjusted out) and one pair of which has a diffusion coefficient smaller than the original data (adjusted in). Note that in Figure 3-8 the adjustments to position have been exaggerated by a factor of four to make the difference more easily visible.

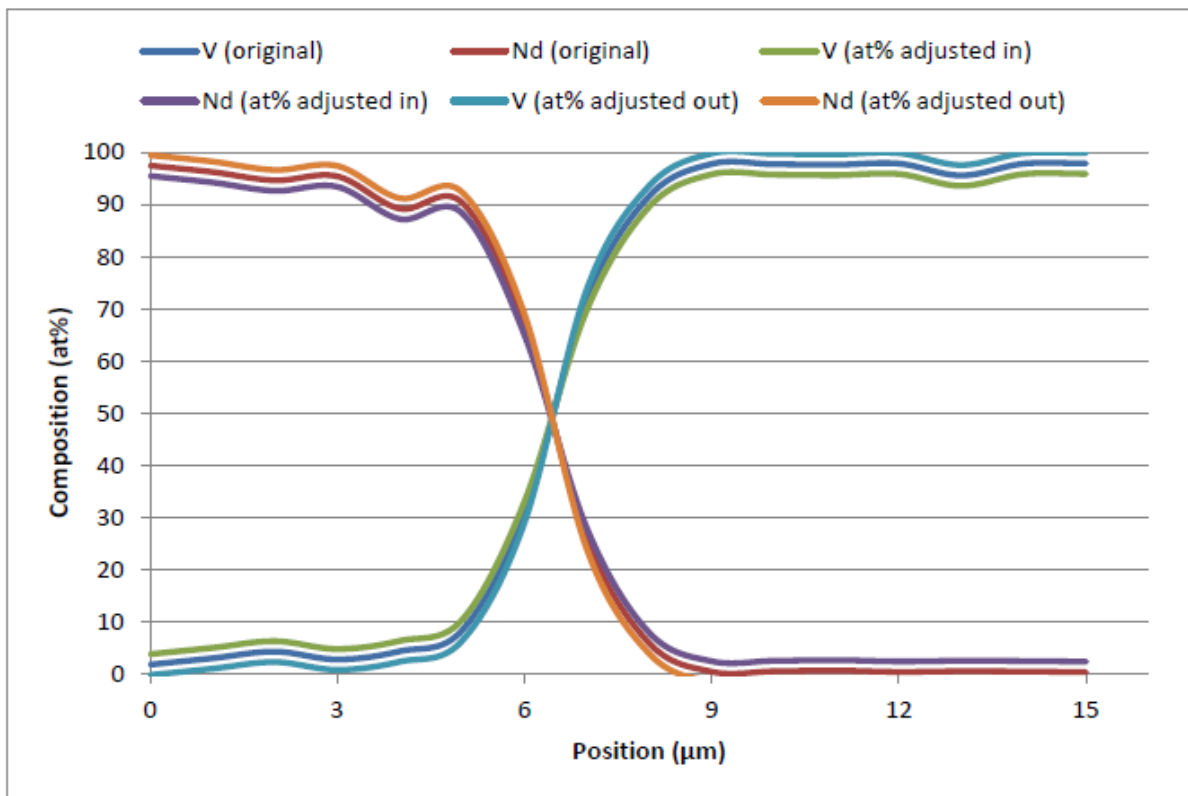


Figure 3-7. Nd/V diffusion interface with adjusted composition for error analysis.

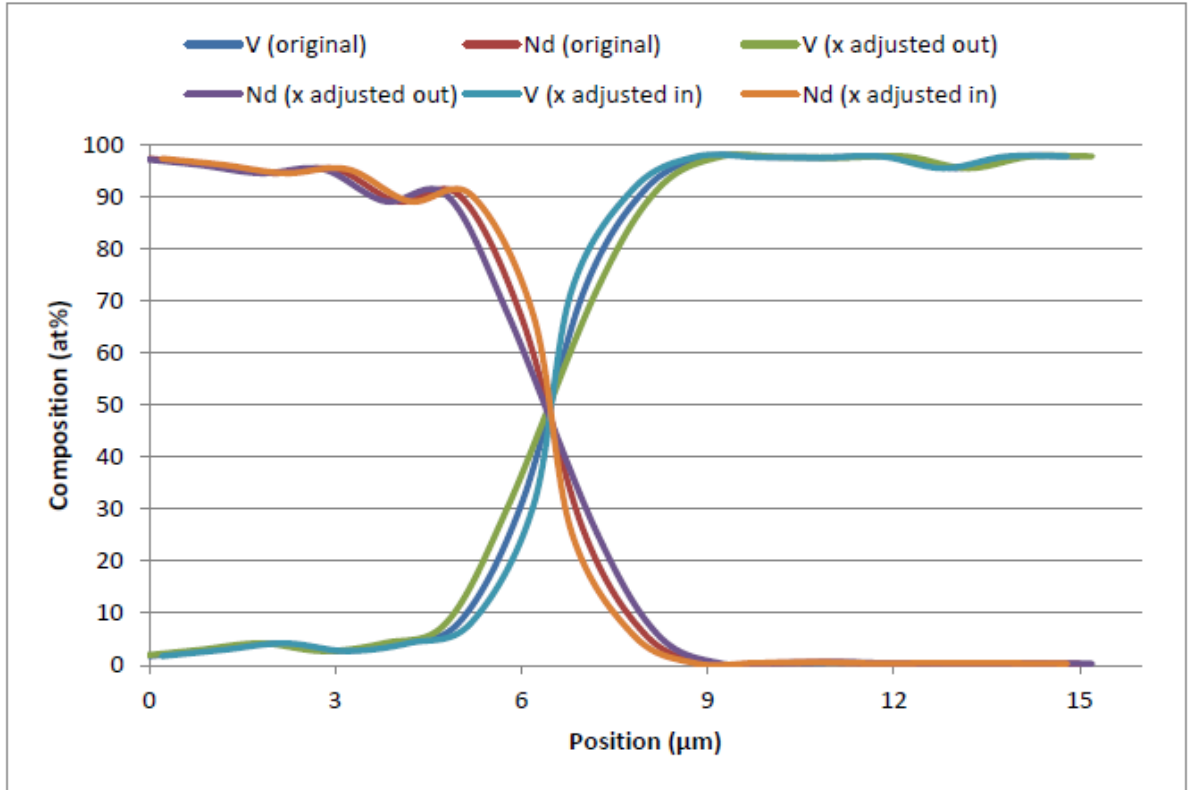


Figure 3-8. Nd/V diffusion interface with adjusted position for error analysis.

As a result of these steps, a total of four revised diffusion coefficients were calculated for each diffusion curve. The upper and lower bound coefficients for both position and concentration errors were each compared to the original calculated diffusion coefficient, and the root mean square of the difference from the original coefficient for the upper and lower bounds of each source of error was calculated. These root mean square values for error due to position and error were then combined by taking the square root of the sum of their squares to provide a final estimated error for the calculated diffusion coefficient for each curve.

3.4.4 Attempted Analysis of Broken Diffusion Interfaces

In some cases, diffusion couples failed to bond together or broke apart during removal from the furnace. Due to the relatively large number of cases (~50% of all diffusion interfaces) in which this happened and the impracticality of repeating heat treatments for failed diffusion couples, an attempt was made to glean enough information from the split interfaces to determine possibly-meaningful diffusion data.

For split interfaces, WDS line scans were performed from the edges of the broken interfaces to a depth of several μm into the materials. These scans typically revealed trace amounts of the diffusing material from the opposing side of the interface, in some cases up to ~3 at%. As these traces represented the tail ends of diffusion curves an attempt was made to analyze them in a manner similar to that covered in Section 3.5.3.

First, the available data from one interface was mirrored to produce the opposing tail end of the diffusion curves with inverted compositions. The spacing between the available data and its mirrored copy was then set to be variable, thus providing the two extreme portions of the diffusion curve while leaving a central portion of indeterminate width blank. The fitting method described in Section 3.5.3 was then applied, with the added caveat that the width of the unknown central portion was an additional variable in the fitting of Equation 2-1.

Although this approach was capable of determining approximate diffusion coefficients given limited data, it was not generally applied for two reasons. First, it was found to lack accuracy when tested on unbroken diffusion curves with the central portion of data artificially removed. The split-interface results were consistently within an order of magnitude of the full curve results; however, no method could be determined to ensure better accuracy. Second, the method was found to be susceptible to very slight changes in concentration at one or two points.

This was due to the fact that the calculation was highly dependent on the points closest to the broken interface. Changes of only 0.5 at% at those points could result in order of magnitude changes in the calculated diffusion coefficients.

3.4.5 Determination of Line Compound Diffusion Coefficients

As outlined in Section 2.5.2, a special approach is required for the calculation of diffusion coefficients governing the growth of line compound interaction zones. This method requires knowledge of elemental concentrations of diffusing elements at a few points in each of the interaction zones, as well as the average width of each zone. Zone widths for each interaction zone were determined as described in Section 3.5.1. The required elemental concentration values for each zone were determined by averaging across all line scans taken. Compositions on the edges of zones were determined by taking the two WDS analysis points nearest the edge of that zone, while zone-wide average compositions were found by averaging all WDS analysis points within the given zone.

3.5 Combination of Calculated Diffusion Coefficients

Given the large number of diffusion couples included within this research, the combination and propagation of error for multiple diffusion coefficients found for each given system was highly important.

3.5.1 Averaging Multiple Diffusion Coefficients

Rather than taking the simple arithmetical mean of multiple diffusion coefficients measured for a given system at a given temperature, the Maximum Likelihood Method (MLM) [70] was applied to provide an estimate of the true mean value with the minimum possible error. For this method, it is necessary to assume a statistical distribution for the variation in the data points considered. Given the

typical behavior of statistical variance in experimental data, it was assumed that a normal or Gaussian distribution would be a reasonable match.

To estimate the true mean of a set of data, the MLM applies the assumed statistical distribution for variation to the data set to determine the likelihood of each data point being measured for apparent values of the true mean. The cumulative likelihood for all data points is then maximized by varying the value of the apparent true mean. The estimate of the true mean which provides the highest cumulative likelihood for the data set is taken as the estimated true mean as provided by the MLM. For a Gaussian distribution, this value will be given by Equation 3-1, where α is the estimated true mean, x_i are the data points measured, and σ_i are the standard deviations of each data point. This is simply the inverse variance weighted average of the data, and simplifies to the unweighted average in the case where the variance for each data point is identical. Propagation of errors for the weighted average leads to Equation 3-2, which defines the variance of the estimated true mean σ_α in terms of the variance for each data point in the set.

Equation 3-1

$$\alpha = \frac{\sum_{i=1}^n x_i / \sigma_i^2}{\sum_{i=1}^n 1 / \sigma_i^2}$$

Equation 3-2

$$\sigma_\alpha = \frac{1}{\sum_{i=1}^n 1 / \sigma_i^2}$$

In applying this method to diffusion coefficients, the estimated error for each diffusion coefficient determined as described in Section 3.5.3 was taken as the standard deviation for each diffusion coefficient.

3.5.2 Propagation of Error for Arrhenius Equation

Combination of mean diffusion coefficients determined at various temperatures for each diffusive system was performed using a least-squares fit of a linearized version of the Arrhenius equation. The Arrhenius equation was linearized by taking the natural logarithm of both sides of the equation, producing Equation 3-3, where $D(T)$ is the diffusion coefficient at temperature T , D_0 is a constant, R is the gas constant, and Q is the activation energy.

Equation 3-3

$$\ln(D(T)) = \ln(D_0) - \frac{Q}{R}T$$

In this form, the least squares fit for D_0 and Q can be found from the measured diffusion coefficients D_i and their associated temperatures T_i from Equation 3-4 and Equation 3-5, respectively, where n represents the number of data points being fit.

Equation 3-4

$$\ln(D_0) = \frac{\sum_{i=1}^n \ln(D_i) \sum_{i=1}^n T_i^2 - \sum_{i=1}^n \ln(D_i) T_i \sum_{i=1}^n T_i}{n \sum_{i=1}^n T_i^2 - (\sum_{i=1}^n T_i)^2}$$

Equation 3-5

$$-\frac{Q}{R} = \frac{n \sum_{i=1}^n \ln(D_i) T_i - \sum_{i=1}^n \ln(D_i) \sum_{i=1}^n T_i}{n \sum_{i=1}^n T_i^2 - (\sum_{i=1}^n T_i)^2}$$

Propagation of errors for Equation 3-4 and Equation 3-5 then leads to Equation 3-6 and Equation 3-7, which determine the error in D_0 , given by σ_{D_0} , and the error in Q , given by σ_Q , respectively based on the error in each diffusion coefficient σ_i .

Equation 3-6

$$\ln(\sigma_{D_0})^2 = \frac{\sum_{i=1}^n \frac{T_i^2}{\ln(\sigma_i)^2}}{\sum_{i=1}^n \frac{1}{\ln(\sigma_i)^2} \sum_{i=1}^n \frac{T_i^2}{\ln(\sigma_i)^2} - \left(\sum_{i=1}^n \frac{T_i}{\ln(\sigma_i)^2} \right)^2}$$

Equation 3-7

$$\sigma_Q^2 = R^2 \frac{\sum_{i=1}^n \frac{1}{\ln(\sigma_i)^2}}{\sum_{i=1}^n \frac{1}{\ln(\sigma_i)^2} \sum_{i=1}^n \frac{T_i^2}{\ln(\sigma_i)^2} - \left(\sum_{i=1}^n \frac{T_i}{\ln(\sigma_i)^2} \right)^2}$$

Based on these results, the coefficients of the Arrhenius equation and their associated errors were determined for each diffusion system using the diffusion coefficients and associated errors determined by combining data from multiple WDS line scans of each system for each temperature studied.

4 RESULTS

In total, 204 diffusion assemblies featuring 476 diffusion interfaces were annealed in this study. Of the 476 attempted interfaces, ~50% did not successfully bond, potentially due to several factors including the unconventionally long diffusion couple stacks, excess force applied upon removal from the diffusion jigs, and the low diffusivities of many of the materials involved. All diffusion couples, both bonded and broken, have been analyzed using an electron microprobe, and the resulting data is compiled in the appendices as given in in Table 4-1.

In the following sections, a detailed review of the data gathered has been collated into technical categories and is presented in the next subsections as follows:

- 4.1 Interactions between neodymium and steel alloys simulating FCCI
- 4.2 Interactions between neodymium and candidate liner materials (i.e. V, Zr, Ti, Mo, Ta, and W)
- 4.3 Interactions between steel alloys and candidate liner materials (i.e. V, Zr, Ti, Mo, Ta, and W)
- 4.4 Diffusion between candidate liner materials in dual-liner couples

Table 4-1. Summary of all diffusion assemblies with corresponding appendices.

	17.5 Days @ 550°C	28 Days @ 550°C	56 Days @ 550°C	28 Days @ 625°C	28 Days @ 700°C
HT-9/Nd	B.1	B.13	B.25	B.37	B.49
HT-9/V/Nd	B.2	B.14	B.26	B.38	B.50
HT-9/Zr/V/Nd	B.3	B.15	B.27	B.39	B.51
HT-9/Zr/Nd	B.4	B.16	B.28	B.40	B.52
HT-9/Ti/V/Nd	B.5	B.17	B.29	B.41	B.53
HT-9/Ti/Nd	B.6	B.18	B.30	B.42	B.54
HT-9/Ta/V/Nd	B.7	B.19	B.31	B.43	B.55
HT-9/Ta/Nd	B.8	B.20	B.32	B.44	B.56
HT-9/Mo/V/Nd	B.9	B.21	B.33	B.45	B.57
HT-9/Mo/Nd	B.10	B.22	B.34	B.46	B.58
HT-9/W/V/Nd	B.11	B.23	B.35	B.47	B.59
HT-9/W/Nd	B.12	B.24	B.36	B.48	B.60
	17.5 Days @ 550°C	28 Days @ 550°C	56 Days @ 550°C	28 Days @ 625°C	28 Days @ 700°C
G.91/Nd	N/A	C.1	C.13	C.25	C.37
G.91/V/Nd	N/A	C.2	C.14	C.26	C.38
G.91/Zr/V/Nd	N/A	C.3	C.15	C.27	C.39
G.91/Zr/Nd	N/A	C.4	C.16	C.28	C.40
G.91/Ti/V/Nd	N/A	C.5	C.17	C.29	C.41
G.91/Ti/Nd	N/A	C.6	C.18	C.30	C.42
G.91/Ta/V/Nd	N/A	C.7	C.19	C.31	C.43
G.91/Ta/Nd	N/A	C.8	C.20	C.32	C.44
G.91/Mo/V/Nd	N/A	C.9	C.21	C.33	C.45
G.91/Mo/Nd	N/A	C.10	C.22	C.34	C.46
G.91/W/V/Nd	N/A	C.11	C.23	C.35	C.47
G.91/W/Nd	N/A	C.12	C.24	C.36	C.48
	17.5 Days @ 550°C	28 Days @ 550°C	56 Days @ 550°C	28 Days @ 625°C	28 Days @ 700°C
SS-316/Nd	N/A	D.1	D.13	D.25	D.37
SS-316/V/Nd	N/A	D.2	D.14	D.26	D.38
SS-316/Zr/V/Nd	N/A	D.3	D.15	D.27	D.39
SS-316/Zr/Nd	N/A	D.4	D.16	D.28	D.40
SS-316/Ti/V/Nd	N/A	D.5	D.17	D.29	D.41
SS-316/Ti/Nd	N/A	D.6	D.18	D.30	D.42
SS-316/Ta/V/Nd	N/A	D.7	D.19	D.31	D.43
SS-316/Ta/Nd	N/A	D.8	D.20	D.32	D.44
SS-316/Mo/V/Nd	N/A	D.9	D.21	D.33	D.45

Table 4-1 Continued

	17.5 Days @ 550°C	28 Days @ 550°C	56 Days @ 550°C	28 Days @ 625°C	28 Days @ 700°C
SS-316/Mo/Nd	N/A	D.10	D.22	D.34	D.46
SS-316/W/V/Nd	N/A	D.11	D.23	D.35	D.47
SS-316/W/Nd	N/A	D.12	D.24	D.36	D.48
	17.5 Days @ 550°C	28 Days @ 550°C	56 Days @ 550°C	28 Days @ 625°C	28 Days @ 700°C
Fe/Nd	N/A	E.1	E.13	E.25	E.37
Fe/V/Nd	N/A	E.2	E.14	E.26	E.38
Fe/Zr/V/Nd	N/A	E.3	E.15	E.27	E.39
Fe/Zr/Nd	N/A	E.4	E.16	E.28	E.40
Fe/Ti/V/Nd	N/A	E.5	E.17	E.29	E.41
Fe/Ti/Nd	N/A	E.6	E.18	E.30	E.42
Fe/Ta/V/Nd	N/A	E.7	E.19	E.31	E.43
Fe/Ta/Nd	N/A	E.8	E.20	E.32	E.44
Fe/Mo/V/Nd	N/A	E.9	E.21	E.33	E.45
Fe/Mo/Nd	N/A	E.10	E.22	E.34	E.46
Fe/W/V/Nd	N/A	E.11	E.23	E.35	E.47
Fe/W/Nd	N/A	E.12	E.24	E.36	E.48

4.1 Neodymium/Steel Diffusion

The phase morphologies observed between pure neodymium metal and HT-9, G.91, and SS-316 regularly contained a sequence of intermetallic diffusion zones. Each of these interaction zones were characterized by nearly constant composition profiles indicating the presence of intermetallic line compounds from the associated phase diagrams. The widest interaction zone observed in all Nd-Steel diffusion couples corresponds to the $\text{Nd}_2\text{Fe}_{17}$ ("2-17") intermetallic. The second interaction zone observed in all unbroken diffusion couples corresponded to the NdFe_2 ("1-2") intermetallic with ~4% Si, ~3% Cr, and ~0.5% Mn, which may have been $\text{Cr}_2\text{Si}_2\text{Nd}$ and $\text{Mn}_2\text{Si}_2\text{Nd}$ by composition. In addition to these two common phases, additional interaction phases were observed in some couples that correspond to $\text{Nd}_5\text{Fe}_{17}$ ("5-17") and Ni_3Nd ("3-1") intermetallics.

The elemental compositions given in the following sections for each observed interaction zone are each based on the average of several WDS linescans across the interfaces. The systematic error in each of the individual measurements is quite low (<0.1 at%) due to the inherent accuracy and precision of WDS; however, there was typically minor variance (~1 at%) between different WDS linescans of the same interface. Similarly, the widths of the interaction zones varied somewhat (by up to 10% of the zone width) depending on position due to the boundaries between zones not being perfectly straight.

In referring to the series of intermetallic zones observed in diffusion couples in the following sections, they are considered starting with the zone nearest to the bulk steel, then progressing toward the bulk neodymium. For example, if the diffusion couple included bulk steel, $\text{Nd}_2\text{Fe}_{17}$, $\text{Nd}_5\text{Fe}_{17}$, NdFe_2 , and bulk neodymium in that order, $\text{Nd}_2\text{Fe}_{17}$ would be referred to as the first interaction zone, $\text{Nd}_5\text{Fe}_{17}$ would be referred to as the second interaction zone, and NdFe_2 would be referred to as the third interaction zone.

4.1.1 Neodymium Diffusion with HT-9

After annealing for 17.5 days at 550°C, the interface between HT-9 and Nd included two interaction zones, as shown in Figure 4-1 and Figure 4-2. The first interaction zone was ~10 μm wide (based on 4 WDS linescans and image analysis), and had a composition of $\text{Nd}_2(\text{Fe}+\text{Cr})_{17}$. Relative to the bulk HT-9, this zone was slightly enriched in Mo, W, Cr, and V and strongly depleted in Ni. While the steel-end of this interaction zone matched the expected composition of 10.5 at% Nd, the remainder of the zone was super-stoichiometric in Nd, reaching up to ~16 at%. As the Nd concentration increased, $\text{Nd}_5(\text{Fe}+\text{Cr})_{17}$ precipitates were observed within the zone, culminating in nearly complete $\text{Nd}_5(\text{Fe}+\text{Cr})_{17}$ over the last micron. The second interaction zone was ~3 μm wide (based on 4 WDS linescans and image analysis),

and had a composition of NdFe_2 . Relative to the bulk HT-9, this zone was strongly depleted in all alloying elements except Mn.

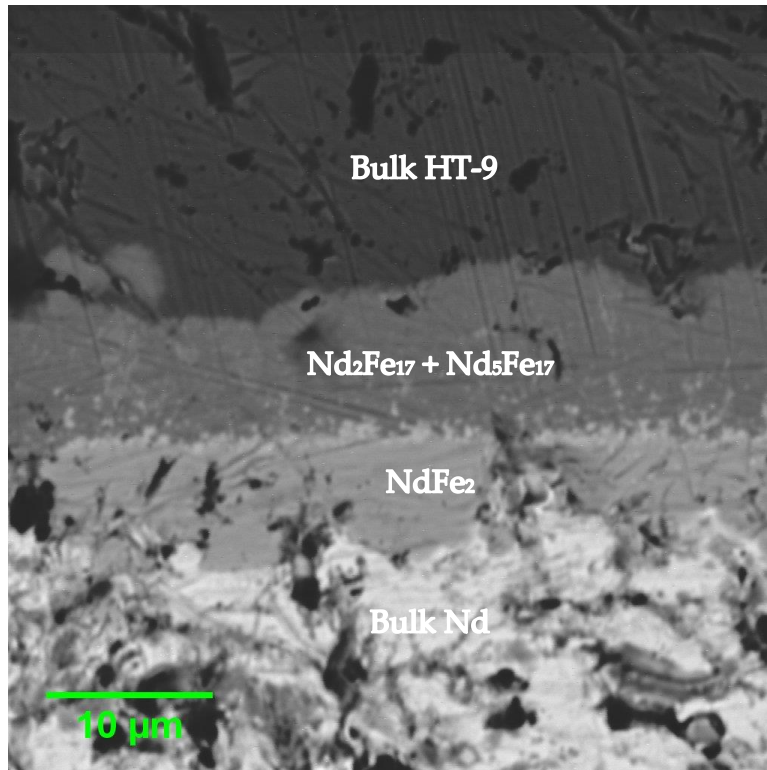


Figure 4-1. HT-9/Nd interface after 17.5 days at 550°C.

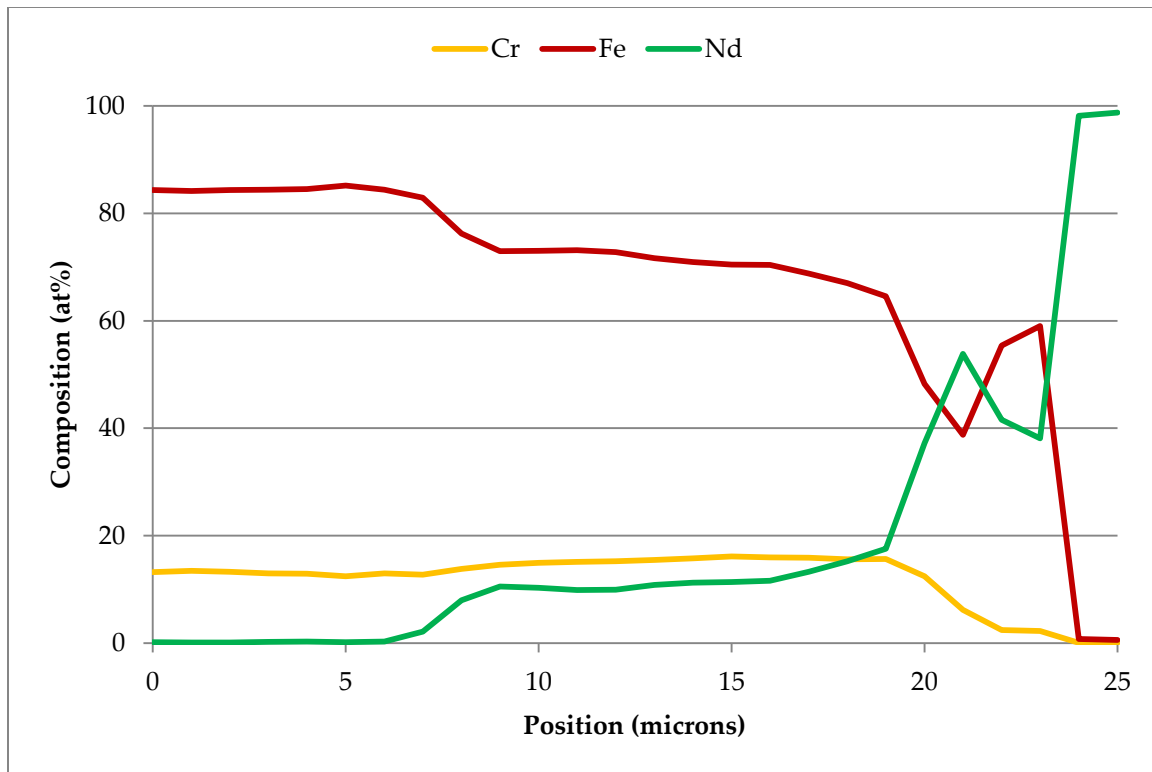


Figure 4-2. Composition of major elements for Nd/HT-9 after 17.5 days at 550°C.

After annealing for 28 days at 550°C, the interface between HT-9 and Nd once again included two interaction zones, as shown in Figure 4-3 and Figure 4-4. The first interaction zone, $\text{Nd}_2(\text{Fe}+\text{Cr})_{17}$ was ~12 μm wide (based on 5 WDS linescans and image analysis), and was once again slightly enriched in Mo, W, Cr, and V and strongly depleted in Ni. Again, the steel-end matched the expected composition of 10.5at% Nd, while the remainder of the zone was super-stoichiometric in Nd with $\text{Nd}_5(\text{Fe}+\text{Cr})_{17}$ precipitates. In some areas, the $\text{Nd}_5(\text{Fe}+\text{Cr})_{17}$ precipitates formed a separate zone up to 2 μm wide. The third zone, Fe_2Nd was ~4 μm wide (based on 5 WDS linescans and image analysis) and once again was strongly depleted in all alloying elements except Mn relative to bulk HT-9.

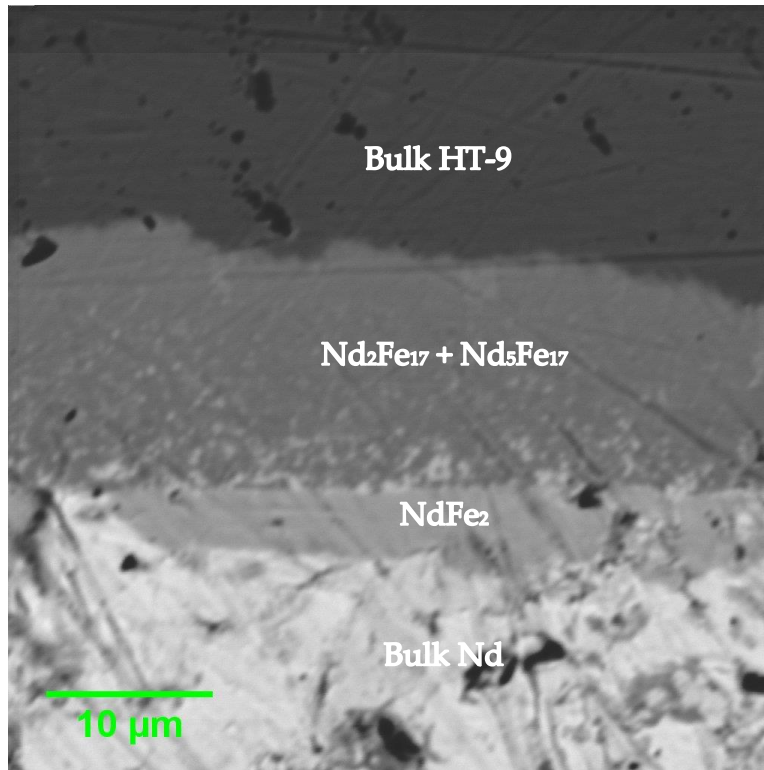


Figure 4-3. HT-9/Nd interface after 28 days at 550°C.

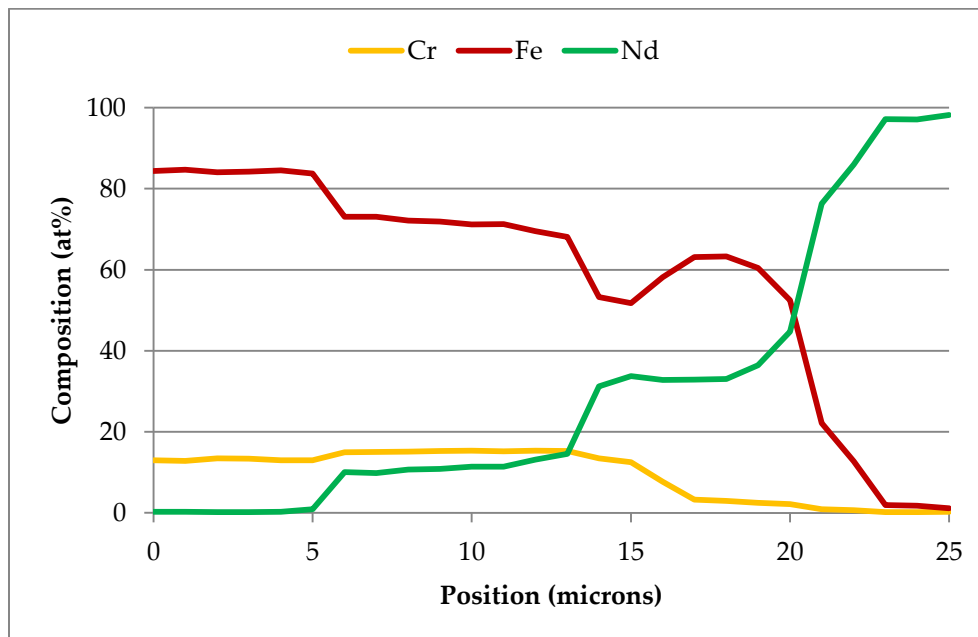


Figure 4-4. Composition of major elements for Nd/HT-9 after 28 days at 550°C.

After annealing for 56 days at 550°C, the same interaction zones were observed with similar compositions, as shown in Figure 4-5 and Figure 4-6. The $\text{Nd}_2(\text{Fe}+\text{Cr})_{17}$ zone was $\sim 18 \mu\text{m}$ wide, the $\text{Nd}_5(\text{Fe}+\text{Cr})_{17}$ zone was $\sim 8 \mu\text{m}$ wide, and the Fe_2Nd zone was $\sim 5 \mu\text{m}$ wide (each based on 6 WDS linescans and image analysis). While the $\text{Nd}_2(\text{Fe}+\text{Cr})_{17}$ phase still contained $\text{Nd}_5(\text{Fe}+\text{Cr})_{17}$ precipitates, unlike the shorter anneals at 550°C, the intermediate $\text{Nd}_5(\text{Fe}+\text{Cr})_{17}$ phase developed consistently across the full interface, and to a much greater thickness, as shown in Figure 4-5.

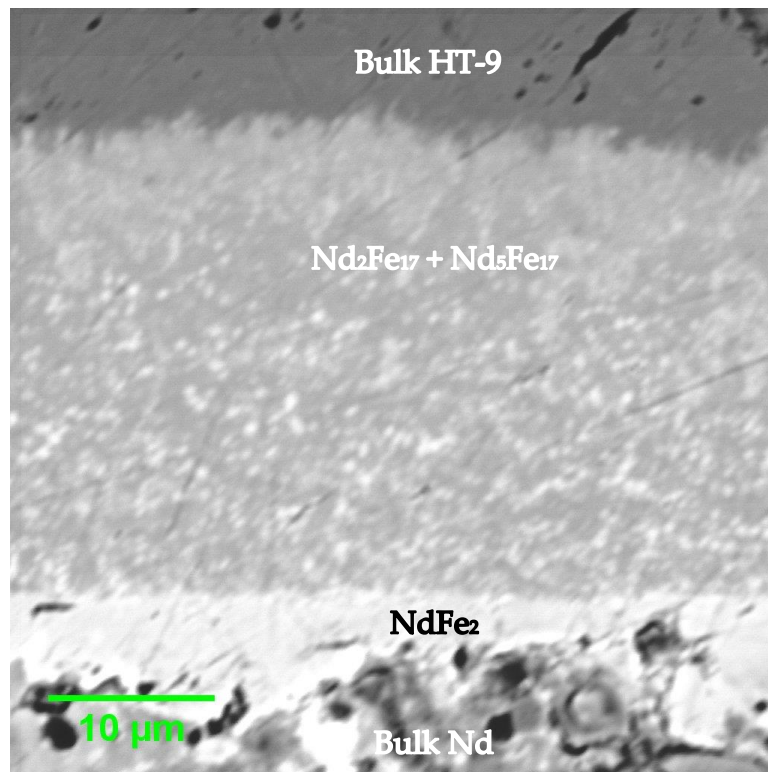


Figure 4-5. HT-9/Nd interface after 56 days at 550°C.

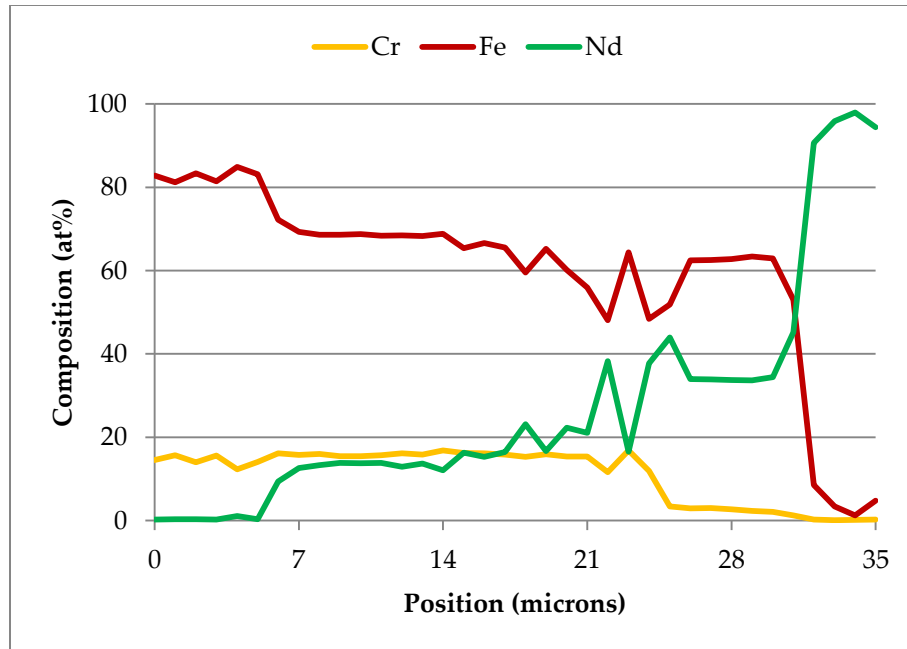


Figure 4-6. Composition of major elements for Nd/HT-9 after 56 days at 550°C.

After annealing for 28 days at 625°C a significant interaction zone developed between the HT-9 and Nd, as shown in Figure 4-7; however, due to the brittle nature of the interaction zones the diffusion couple broke apart upon removal from the furnace. The first $\text{Nd}_2(\text{Fe}+\text{Cr})_{17}$ phase remained mostly intact, with a zone width of ~40 μm (based on two WDS linescans and image analysis). In contrast to the lower temperature couples, the Nd content in this phase remained fairly close to the expected stoichiometric ratio, increasing to super-stoichiometric amounts only over the last few micrometers of the phase. Small portions of additional $\text{Nd}_5(\text{Fe}+\text{Cr})_{17}$ and Fe_2Nd phases were found past the $\text{Nd}_2(\text{Fe}+\text{Cr})_{17}$ phase on the broken edge of the interface.

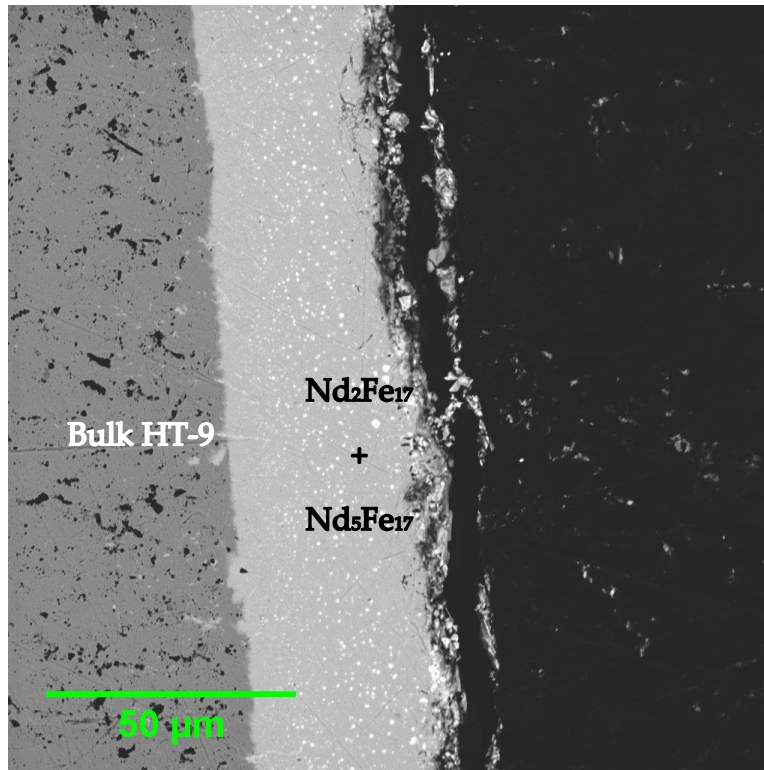


Figure 4-7. Broken HT-9/Nd interface after 28 days at 625°C.

After annealing for 28 days at 700°C there was once again a significant interaction zone which broke upon removal from the furnace, as shown in Figure 4-8. Only the $\text{Nd}_2(\text{Fe}+\text{Cr})_{17}$ phase remained intact, with a zone width of $\sim 530 \mu\text{m}$ (based on two WDS linescans and image analysis). Similar to the diffusion couple annealed at 625°C, the Nd content across the interaction zone remained consistently near to the stoichiometric value of 10.5 at%.

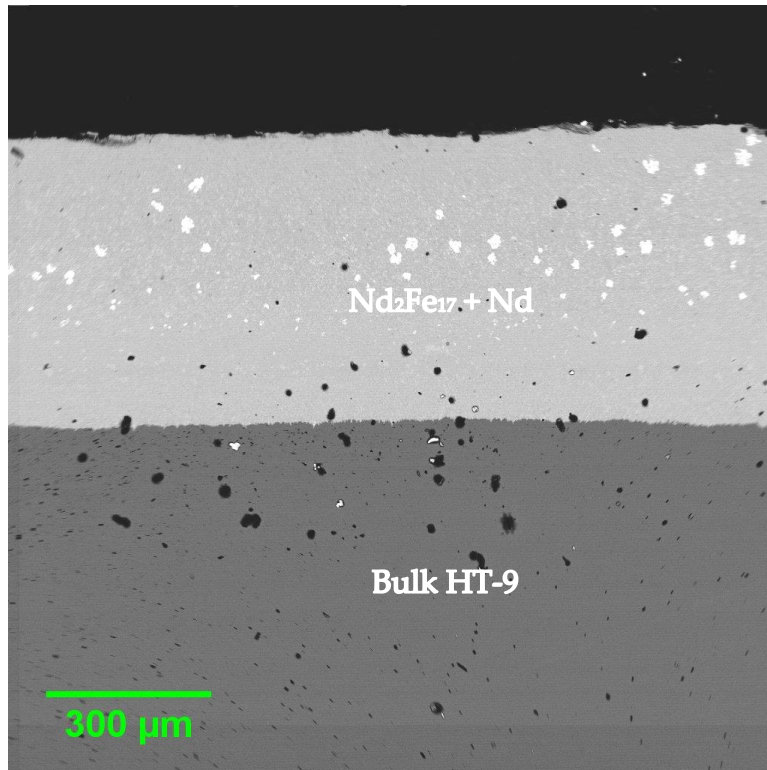


Figure 4-8. Broken HT-9/Nd interface after 28 days at 700°C.

The methods described in Section 2.5.2 were applied to the HT-9/Nd diffusion data to determine integrated diffusion coefficients for each interdiffusion zone which remained intact. The resulting integrated diffusion coefficients are given in Table 4-2.

Table 4-2. Integrated diffusion coefficients for HT-9/Nd.

	Nd ₂ (Fe+Cr) ₁₇		Nd ₅ (Fe+Cr) ₁₇		NdFe ₂	
	D (m ² /s)	±	D (m ² /s)	±	D (m ² /s)	±
17.5 days at 550°C	2.22E-16	4.6E-17	4.04E-18	1.33E-18	2.97E-17	2.38E-17
28 days at 550°C	2.23E-16	5.1E-17	4.71E-18	1.33E-18	3.30E-17	1.57E-17
56 days at 550°C	1.80E-16	4.2E-17	4.74E-17	1.14E-17	2.58E-17	1.15E-17
28 days at 625°C	1.84E-15	4.2E-16	N/A	N/A	N/A	N/A
28 days at 700°C	3.21E-13	4.1E-14	N/A	N/A	N/A	N/A

4.1.2 Neodymium Diffusion with G.91

The diffusive behavior of G.91 with Nd was very similar to that of HT-9. After annealing for 28 days at 550°C, the first interaction zone was ~13 μm wide (based on four WDS linescans and image analysis) with a composition matching Nd₂(Fe+Cr)₁₇, as shown in Figure 4-9 and Figure 4-10. Relative to the bulk G.91, this zone was slightly enriched in Cr and Mo. This zone was slightly superstoichiometric in Nd with an average concentration of 14.0 at%, and in some areas included Nd₅(Fe+Cr)₁₇ precipitates. In the last few microns of the zone, these precipitates were dense enough in some areas to effectively form a second Nd₅(Fe+Cr)₁₇ zone, up to ~2 μm wide. The third and final interaction zone was ~2 μm wide (based on four WDS linescans and image analysis) with a composition matching Fe₂Nd. This zone was depleted in most alloying elements from the G.91, with the exception of Mn, which had a concentration roughly equal to the bulk G.91, and Si, which was present at a concentration several times higher than the bulk G.91.

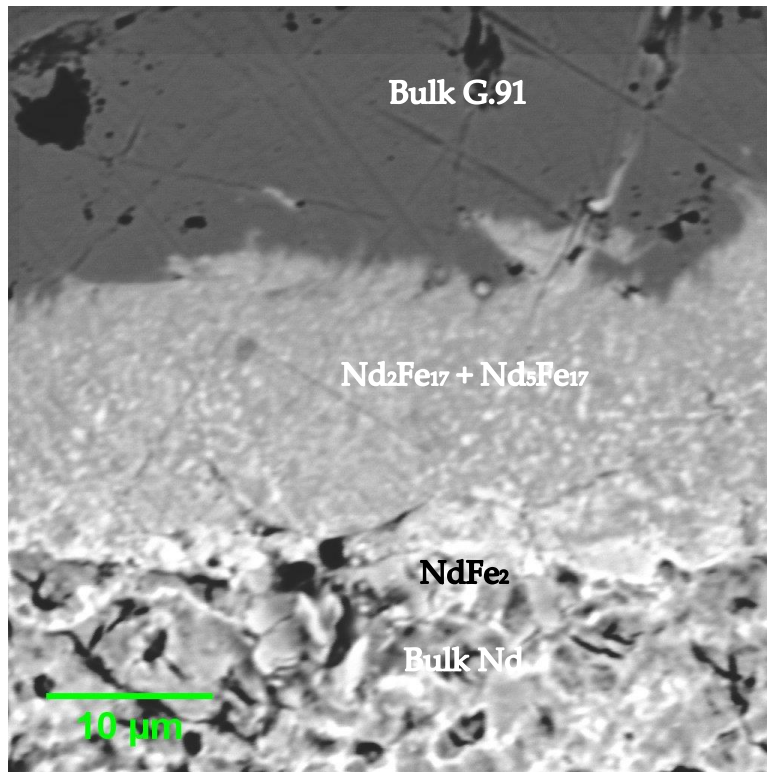


Figure 4-9. G.91/Nd diffusion interface after 28 days at 550°C.

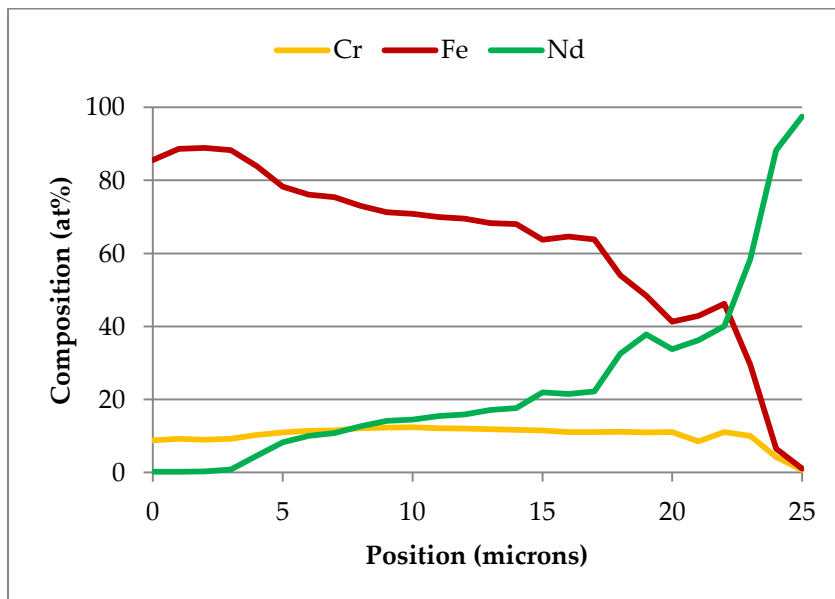


Figure 4-10. Composition of major elements for Nd/G.91 after 28 days at 550°C.

After annealing for 56 days at 550°C a similar set of interaction zones were observed, as shown in Figure 4-11 and Figure 4-12. The first zone was ~16 μm wide (based on five WDS linescans and image analysis) and had a composition matching $\text{Nd}_2(\text{Fe}+\text{Cr})_{17}$ with $\text{Nd}_5(\text{Fe}+\text{Cr})_{17}$ precipitates. As in the 28 day test at 550°C, this zone was enriched in Cr, and Mo relative to the bulk G.91 and was super-stoichiometric in Nd with an average concentration of 13.52at%. The second zone was ~3 μm wide (based on five WDS linescans and image analysis), and had a composition matching $\text{Nd}_5(\text{Fe}+\text{Cr})_{17}$. As in the 28 day test at 550°C, the second interaction zone was slightly enriched in Cr and Mo. The third interaction zone was ~ 3 μm wide (based on five WDS linescans and image analysis) with a composition matching Fe_2Nd . Once again, this zone was depleted in all alloying elements relative to bulk G.91, with only the exceptions of Mn, which had a concentration very close to the bulk G.91, and Si, which had a concentration that was several times higher than in the bulk G.91.

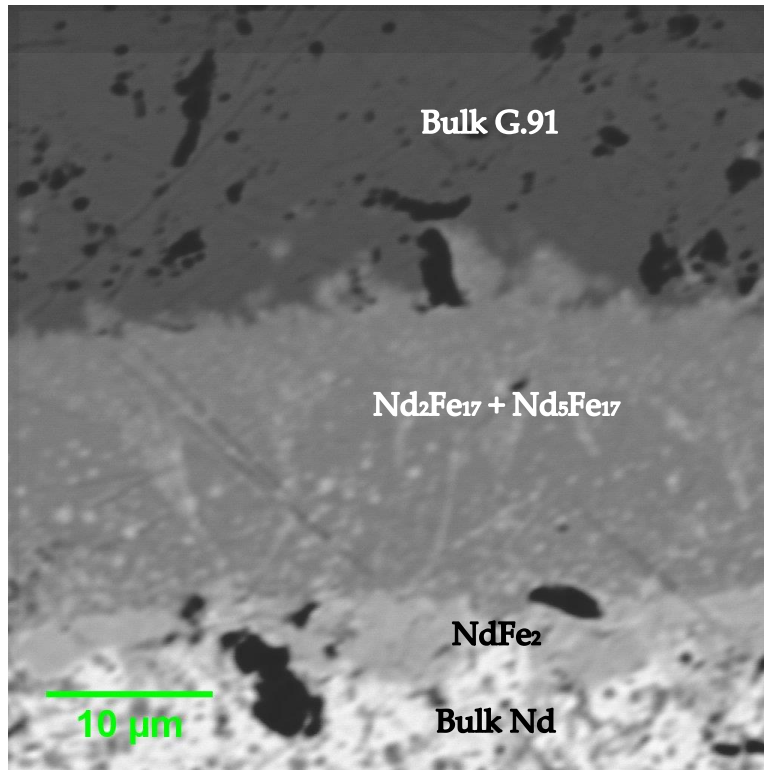


Figure 4-11. G.91/Nd interface after 56 days at 550°C.

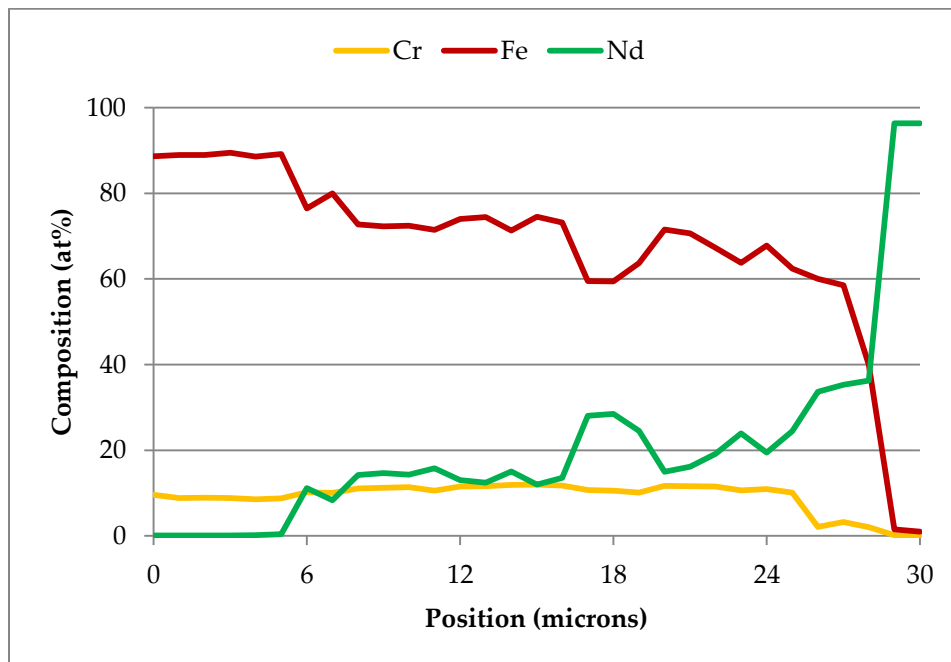


Figure 4-12. Composition of major elements for Nd/G.91 after 56 days at 550°C.

Unlike the HT-9/Nd diffusion couple annealed for 28 days at 625°C, the G.91/Nd diffusion couple annealed for 28 days at 625°C remained intact across the full diffusion interface, as shown in Figure 4-13 and Figure 4-14. The first interaction zone observed was ~38 μm wide (based on four WDS linescans and image analysis), with a composition matching $\text{Nd}_2(\text{Fe}+\text{Cr})_{17}$. Relative to the bulk G.91, this zone was slightly enriched in Cr and Mo, and slightly depleted in Si. The interaction zone was only slightly super-stoichiometric in Nd, with an average concentration of 11.9 at%. In contrast to the lower temperature diffusion couples no $\text{Nd}_5(\text{Fe}+\text{Cr})_{17}$ phase was observed. The second interaction zone had a composition matching Fe_2Nd , with a zone width of ~4 μm (based on four WDS linescans and image analysis). This zone was strongly depleted in alloying elements, with the exception of Mn, which had a concentration similar to the bulk G.91, and Si, which had a concentration several times higher than in the bulk G.91.

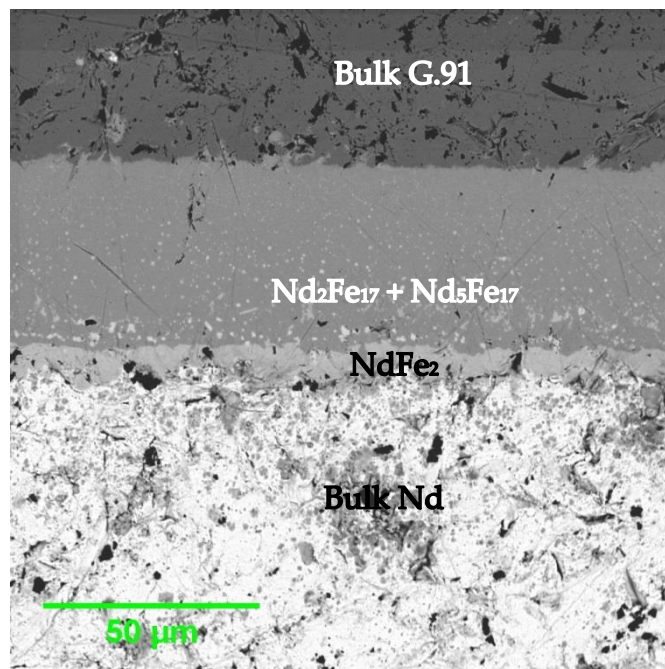


Figure 4-13. G.91/Nd interface after 28 days at 625°C.

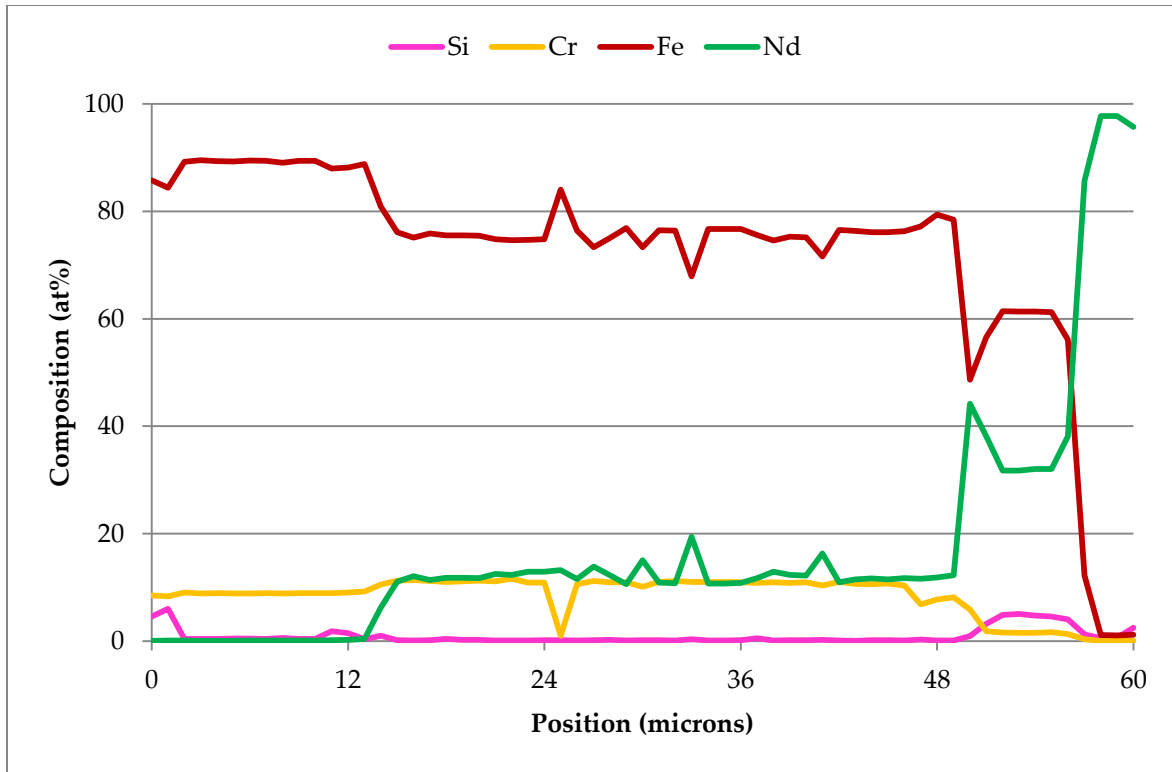


Figure 4-14. Composition of major elements for Nd/G.91 after 28 days at 625°C.

The G.91/Nd diffusion couple annealed for 28 days at 700°C broke upon removal from the furnace, leaving only the first interaction zone intact, as shown in Figure 4-15. The remaining portion of this zone was ~640 μm wide (based on two WDS linescans and image analysis), with a composition matching $\text{Nd}_2(\text{Fe}+\text{Cr})_{17}$. This zone was slightly enriched in Mo and Cr relative to the bulk G.91, and possessed an almost perfectly stoichiometric Nd content, with an average concentration of 10.7 at%.

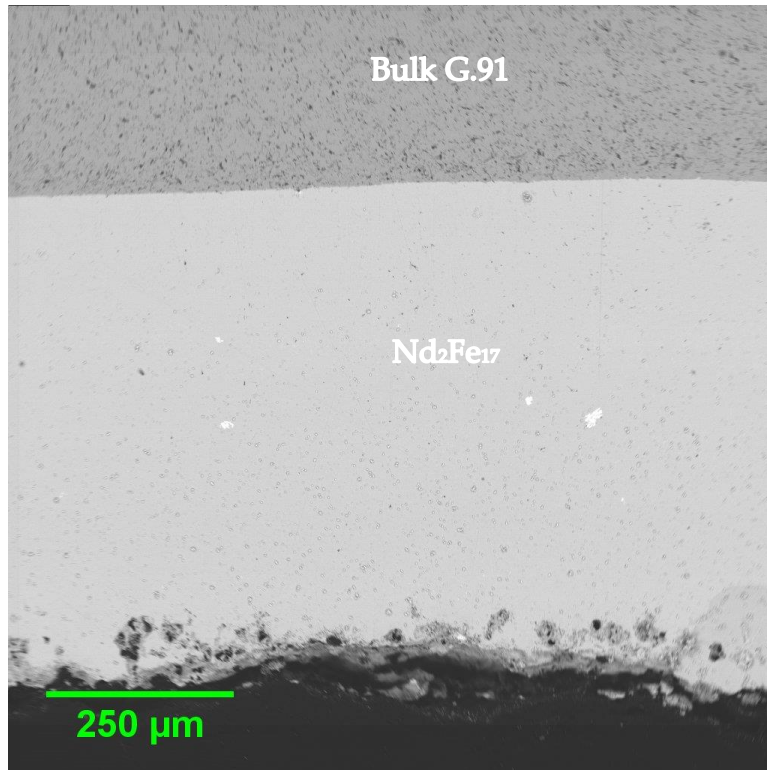


Figure 4-15. Broken G.91/Nd interface after 28 days at 700°C.

The methods described in Section 2.5.2 were applied to the G.91/Nd diffusion data to determine integrated diffusion coefficients for each interdiffusion zone which remained intact. The resulting integrated diffusion coefficients are given in Table 4-3.

Table 4-3. Integrated diffusion coefficients for G.91/Nd.

	Nd ₂ (Fe+Cr) ₁₇		Nd ₅ (Fe+Cr) ₁₇		NdFe ₂	
	D (m ² /s)	±	D (m ² /s)	±	D (m ² /s)	±
28 days at 550°C	1.09E-16	2.6E-17	1.06E-17	2.5E-18	8.25E-18	4.04E-18
56 days at 550°C	1.09E-16	2.1E-17	1.43E-17	4.0E-18	9.28E-18	4.33E-18
28 days at 625°C	2.02E-15	4.4E-16	N/A	N/A	3.30E-17	1.51E-17
28 days at 700°C	4.67E-13	7.5E-14	N/A	N/A	N/A	N/A

4.1.3 Neodymium Diffusion with SS-316

While the two ferritic-martensitic alloys formed a similar series of diffusion interaction zones with Nd, SS-316 performed very differently. When annealed for 28 days at 550°C, the SS-316/Nd diffusion couple formed into three diffusion interaction zones, as shown in Figure 4-16 and Figure 4-17. The first zone was ~52 μm wide (based on two WDS linescans and image analysis), with a composition matching Nd₂(Fe+Cr)₁₇. Unlike the ferritic-martensitic alloy diffusion couples for which this zone was typically super-stoichiometric in Nd with Nd₅(Fe+Cr)₁₇ precipitates, in the SS-316/Nd diffusion couple this zone was almost exactly stoichiometrically balanced, with an average Nd concentration of 10.7at%. Relative to the bulk SS-316, this zone was slightly enriched in Cr and strongly depleted in Ni. The second interaction zone was ~21 μm wide (based on two WDS linescans and image analysis), with a composition matching Fe₂Nd. Relative to the bulk SS-316, this zone was enriched in Si and strongly depleted in Cr, Mo, Ni, and V. Finally, the third interaction zone observed was ~15 μm wide (based on two WDS linescans and image analysis), with a composition matching Nd₃(Ni+Fe). This phase was not

observed in any of the ferritic-martensitic alloy diffusion couples, which is unsurprising given the very low Ni concentration in those alloys.

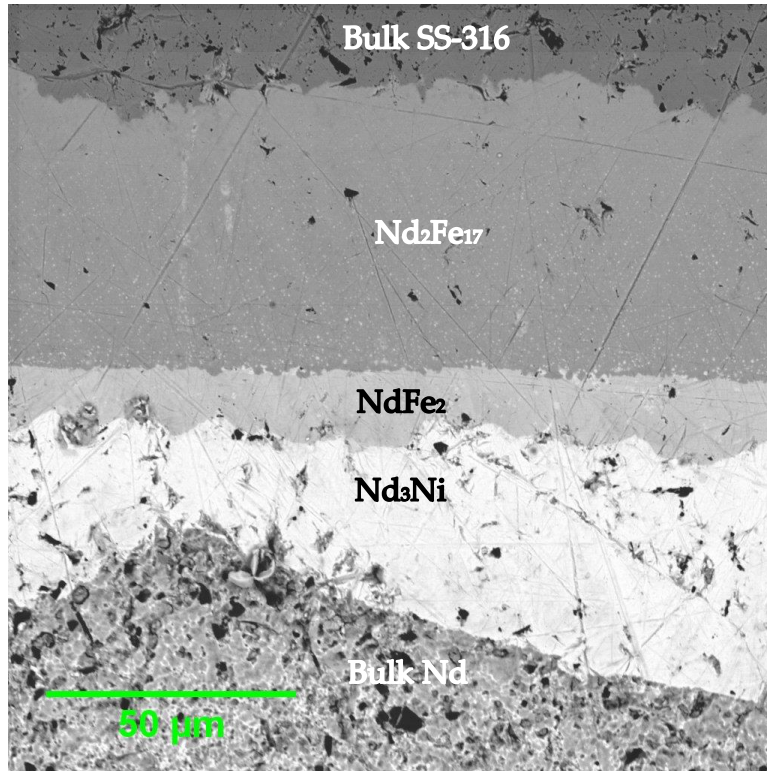


Figure 4-16. SS-316/Nd interface after 28 days at 550°C.

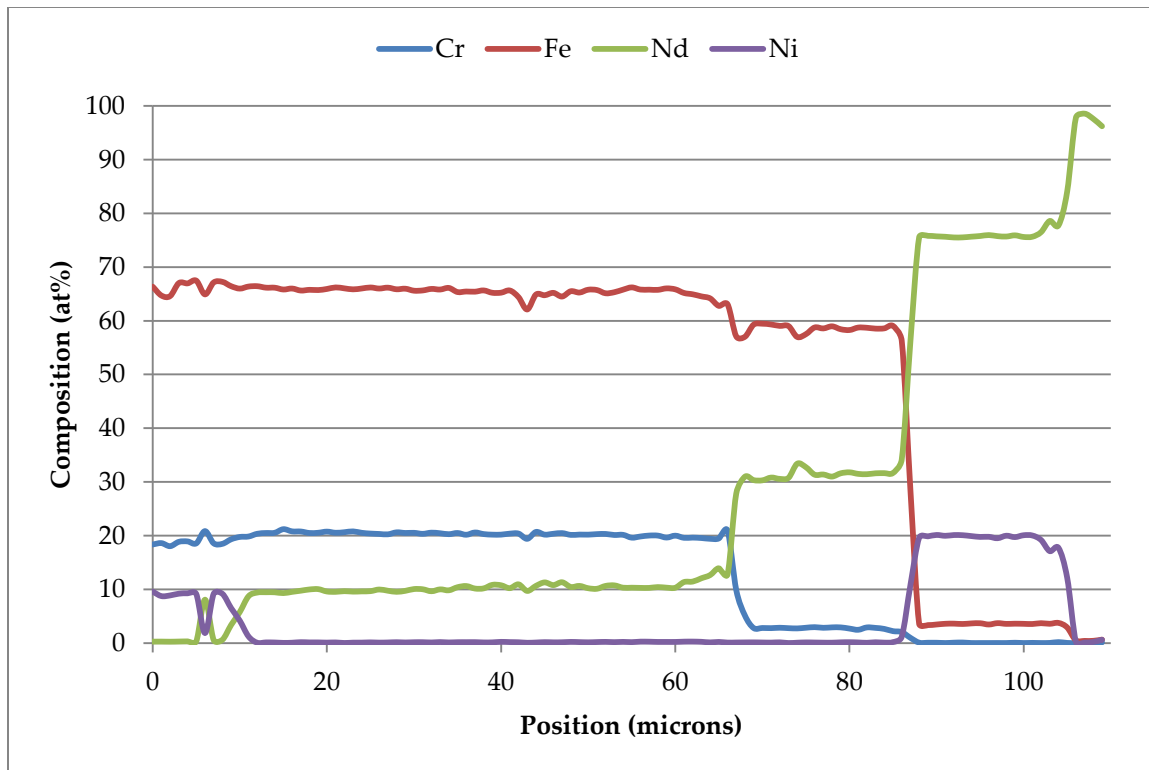


Figure 4-17. Composition of major elements for SS-316/Nd interface after 28 days at 550°C.

When annealed for 56 days at 550°C, three interaction zones were once again observed for the SS-316/Nd diffusion couple, as shown in Figure 4-18. The first interaction zone, which had a composition matching $\text{Nd}_2(\text{Fe}+\text{Cr})_{17}$, was $\sim 87 \mu\text{m}$ wide (based on two WDS linescans and image analysis) and was nearly stoichiometrically balanced with an average Nd concentration of 10.8at%. Once again, this zone was slightly enriched in Cr and strongly depleted in Ni relative to the bulk SS-316. The second interaction zone, which had a composition matching Fe_2Nd , was $\sim 21 \mu\text{m}$ wide (based on two WDS linescans and image analysis). Relative to the bulk SS-316, this zone was enriched in Si and strongly depleted in Mo, Cr, V and Ni. The third interaction zone observed had a composition matching $\text{Nd}_3(\text{Ni}+\text{Fe})$ and was $\sim 22 \mu\text{m}$ wide (based on two WDS linescans and image analysis).

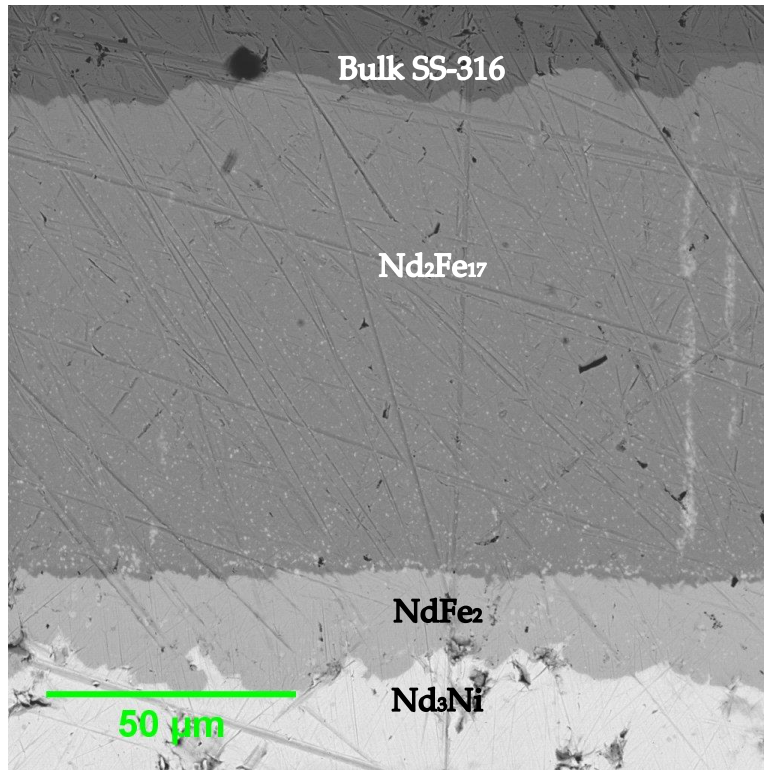


Figure 4-18. SS-316/Nd interface after 56 days at 550°C.

The diffusion interface of the SS-316/Nd diffusion couple annealed for 28 days at 625°C broke apart upon removal from the furnace, rendering full analysis of the developed phases impossible. The remainder of the interface included two interaction zones, as shown in Figure 4-19. First, a zone matching $\text{Nd}_2(\text{Fe}+\text{Cr})_{17}$ by composition extended for $\sim 500 \mu\text{m}$ (based on one WDS linescan and image analysis). As in the lower temperature diffusion couples, this zone was slightly enriched in Cr and strongly depleted in Ni relative to the bulk SS-316. The stoichiometry of this zone was, however, different than that observed at lower temperatures. On average, the Nd concentration in the zone was 10.85 at%, which is very close to stoichiometric; however, there was significant variation across the zone, ranging between ~ 8 at% Nd near the SS-316 interface up to ~ 13 at% at the other end. The

second interaction zone matched $\text{Nd}_5(\text{Fe}+\text{Cr}+\text{Ni})_{17}$ by composition, but was only partially intact so its width was unmeasurable. No similar phase was observed in SS-316/Nd diffusion couples annealed at 550°C; however, this phase was similar to the $\text{Nd}_5(\text{Fe}+\text{Cr})_{17}$ phase observed in ferritic-martensitic alloy diffusion couples, with the exception of the ~10.6at% of Ni which was present in the zone.

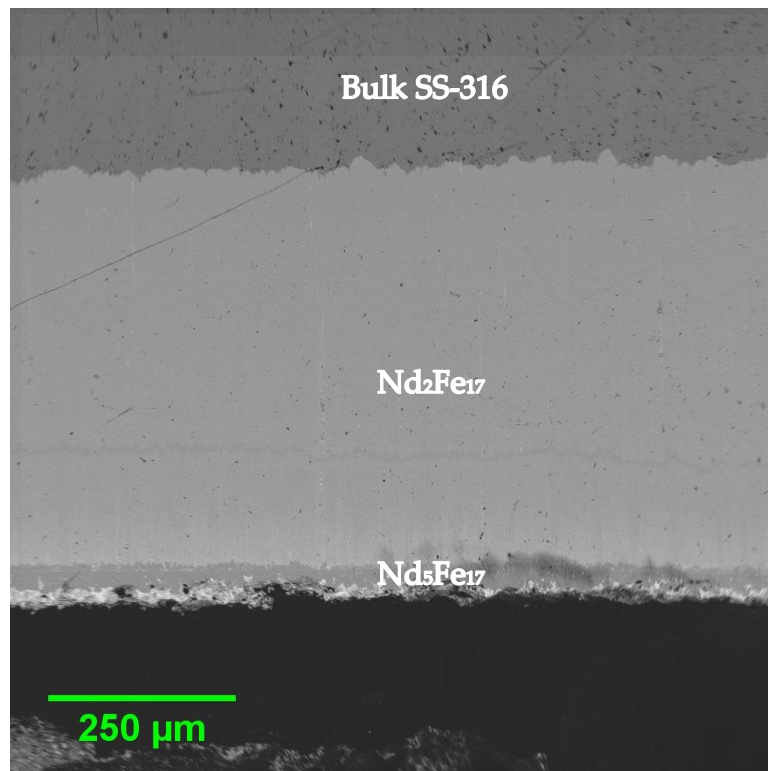


Figure 4-19. SS-316/Nd interface after 28 days at 625°C.

The diffusion interface of the SS-316/Nd diffusion couple annealed for 28 days at 700°C also broke apart upon removal from the furnace. The remaining interface contained a region that was approximately ~780 μm in width (based on WDS linescan and image analysis) and was predominantly $\text{Nd}_2(\text{Fe}+\text{Cr})_{17}$ by

composition with some precipitates of $\text{Nd}_5(\text{Fe}+\text{Cr}+\text{Ni})_{17}$, as shown in Figure 4-20. The $\text{Nd}_2(\text{Fe}+\text{Cr})_{17}$ was once again slightly enriched in Cr and strongly depleted in Ni. Uniquely, this phase was divided into two regions with widely varying characteristics. In the $\sim 300\ \mu\text{m}$ closest to the SS-316, the concentration of Nd followed a gradient from $\sim 8\ \text{at}\%$ closest to the SS-316 up to $\sim 16\ \text{at}\%$. After this first region, the remainder of the $\text{Nd}_2(\text{Fe}+\text{Cr})_{17}$ phase was very substoichiometric in Nd, at $\sim 8\ \text{at}\%$, with scattered $\text{Nd}_5(\text{Fe}+\text{Cr}+\text{Ni})_{17}$ precipitates.

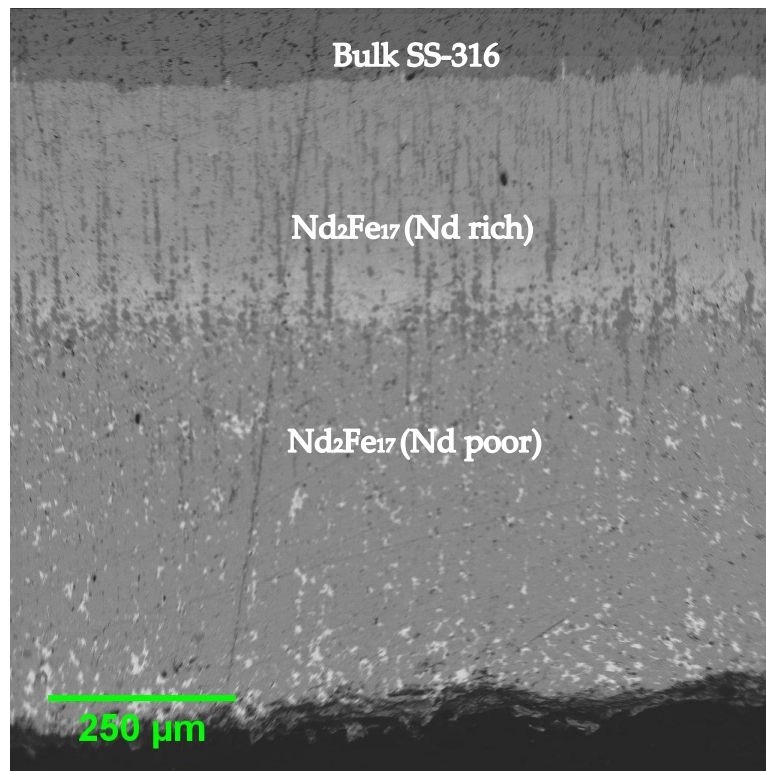


Figure 4-20. SS-316/Nd interface after 28 days at 700°C.

The methods described in Section 2.5.2 were applied to the G.91/Nd diffusion data to determine integrated diffusion coefficients for each interdiffusion zone

which remained intact. The resulting integrated diffusion coefficients are given in Table 4-4.

Table 4-4. Integrated diffusion coefficients for SS-316/Nd.

	Nd ₂ (Fe+Cr) ₁₇		NdFe ₂	
	D (m ² /s)	±	D (m ² /s)	±
28 days at 550°C	3.08E-15	3.9E-16	9.09E-16	4.4E-16
56 days at 550°C	4.32E-15	5.2E-16	4.55E-16	2.2E-16
28 days at 625°C	2.85E-13	3.7E-14	N/A	N/A
28 days at 700°C	6.91E-13	6.5E-14	N/A	N/A

4.1.4 Neodymium Diffusion with Iron

All of the Nd/Fe diffusion couples crumbled upon removal from the furnace, rendering analysis impossible. This was likely due to a combination of a more rapid interaction with Nd in the absence of alloying elements present in steel as well as the brittle nature of the Fe-Nd intermetallic. The optical microscopy image showing the area of the original Fe disk consumed by interaction with Nd following 28 days at 550°C given in Figure 4-21 demonstrates the extent of the interaction and is representative for all Nd-Fe samples.



Figure 4-21. Remaining iron disk following exposure to Nd for 28 days at 550°C.

4.2 Neodymium/Liner Diffusion

Diffusion between Nd and the six liner materials tested (V, Zr, Ti, Mo, Ta, and W) occurred in a regular manner consistent with binary diffusion theory (Fick's Law) and the standard Matano analysis method (Section 2.5.1) was possible. Although the liner metals and Nd did not remain intact for every sample upon removal from the furnace, the multiple tests for each combination of liner and Nd at each temperature and time due to the four different steel alloys tested produced analyzable diffusion data for most cases.

4.2.1 Neodymium Diffusion with Vanadium

Vanadium diffused consistently with Nd and was the second-most diffusive of the liner materials tested with Nd. Diffusion between V and Nd at 550°C was measured for both 28 and 56 days. Representative graphs showing WDS line scan data and associated models for V and Nd following 28 and 56 day anneals at 550°C

are given in Figure 4-22 and Figure 4-23, respectively. As expected, doubling the duration of the diffusion anneal resulted in an approximate increase in diffusion by a factor of the square-root of 2.

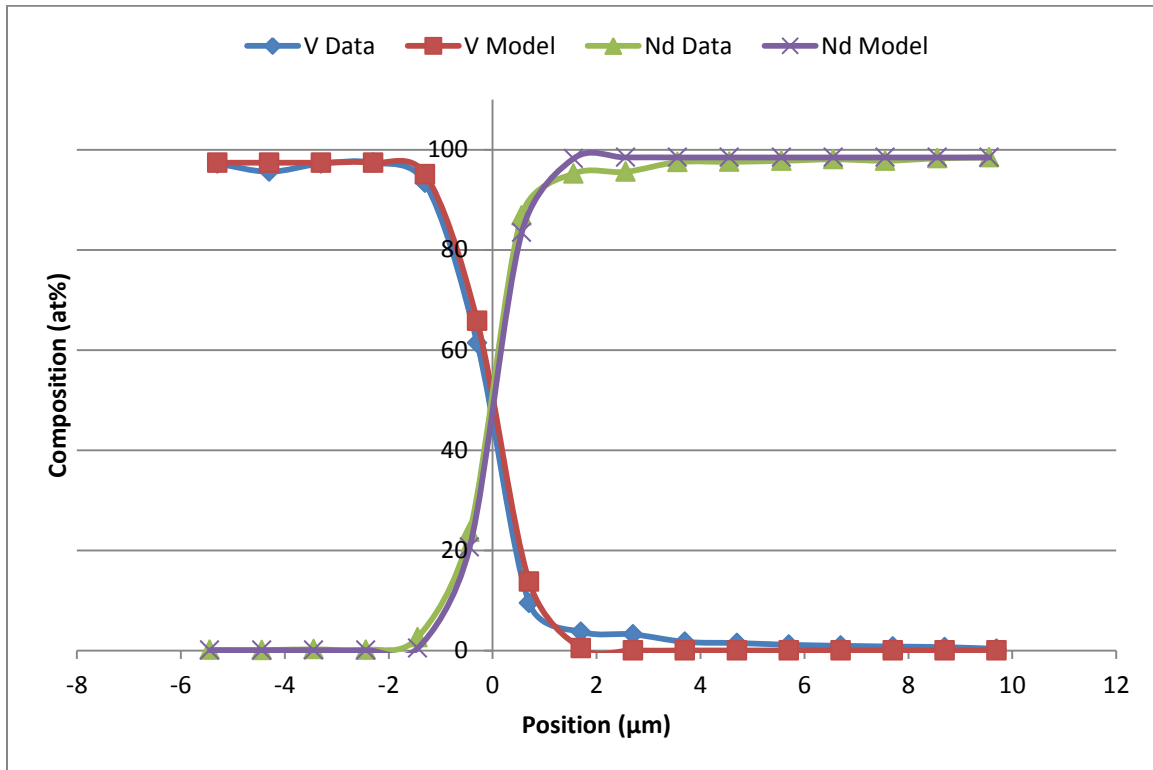


Figure 4-22. Model vs. WDS data for V/Nd interface after 28 days at 550°C.

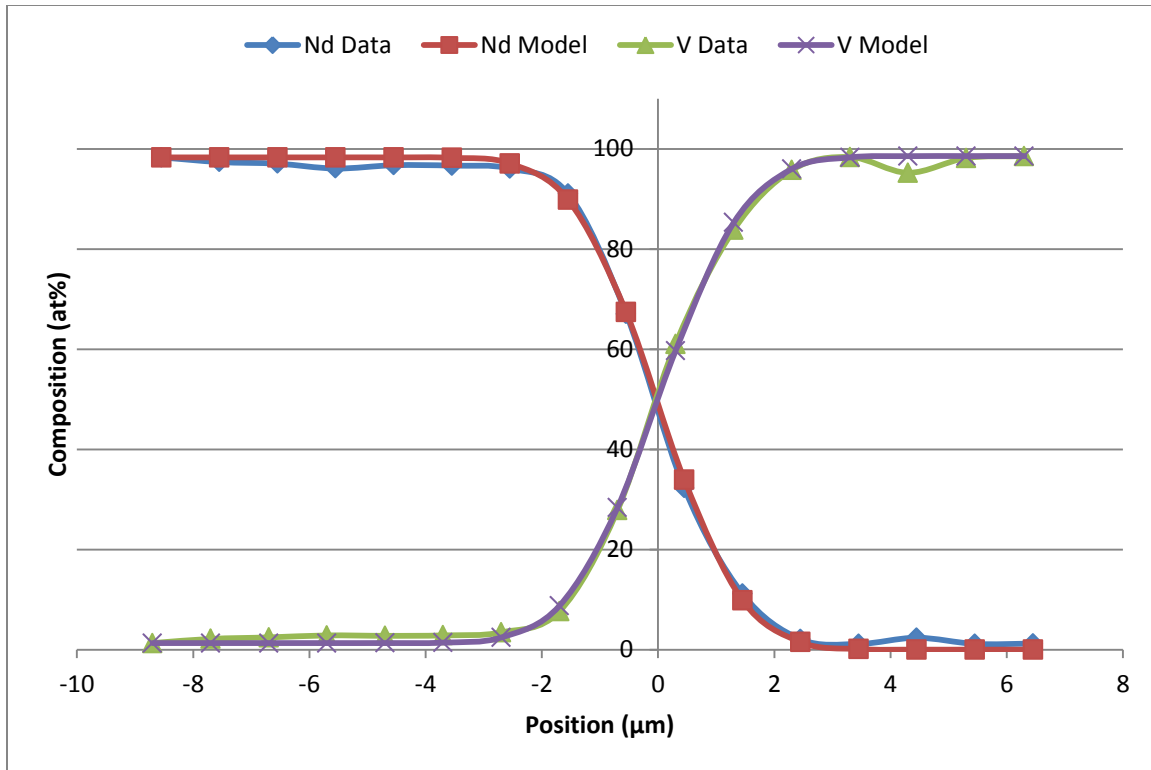


Figure 4-23. Model vs. WDS data for V/Nd interface after 56 days at 550°C.

After 28 days at 625°C, the diffusion between V and Nd progressed further than after 28 days at 550°C, as would be expected. A representative graph showing the WDS data and associated models for the V/Nd interface after 28 days at 625°C is given in Figure 4-24.

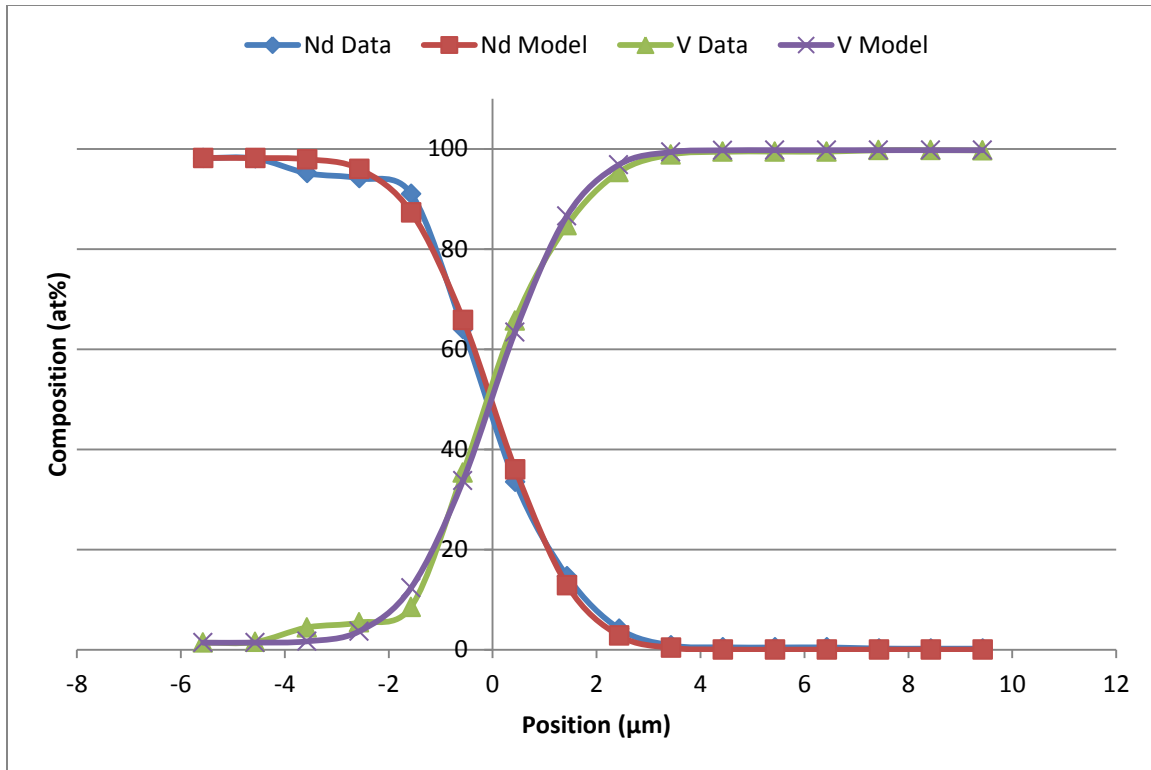


Figure 4-24. Model vs. WDS data for V/Nd interface after 28 days at 625°C.

Once again following the expected diffusive behavior with increasing temperature, the V/Nd interface annealed for 28 days at 700°C showed more interaction than either of the lower temperature cases. A representative graph showing the WDS data and associated models for the V/Nd interface after 28 days at 625°C is given in Figure 4-25.

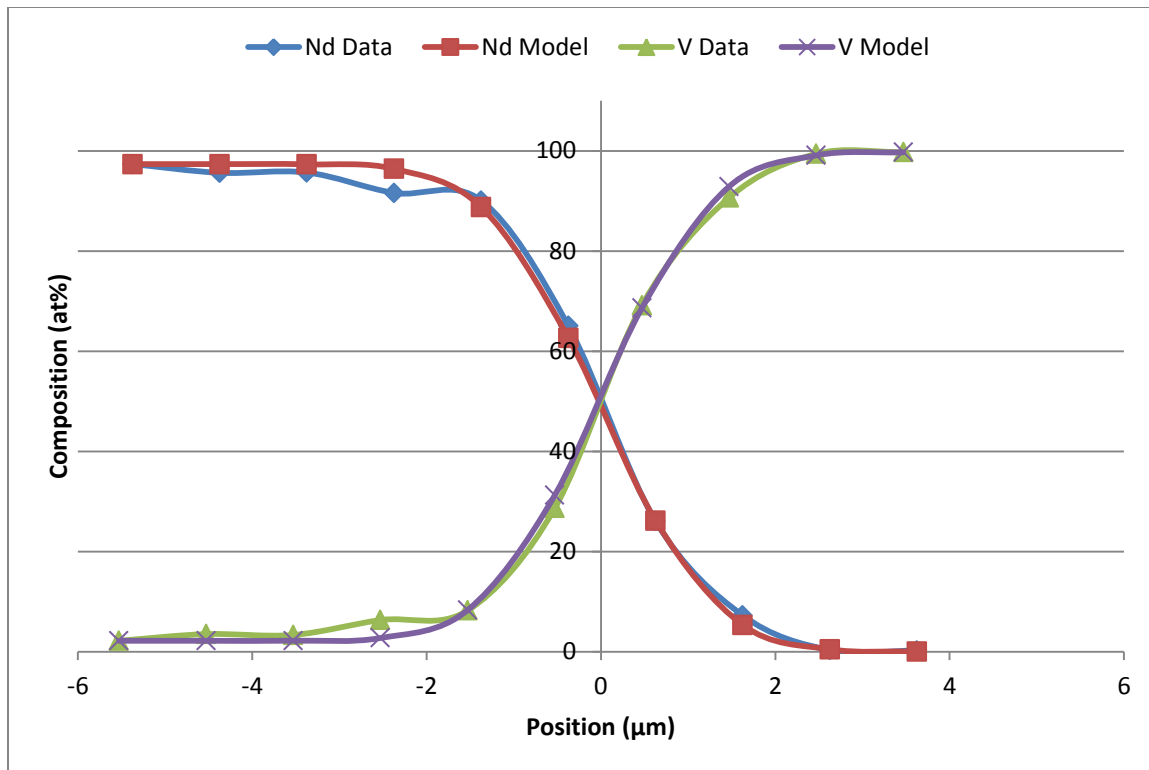


Figure 4-25. Model vs. WDS data for V/Nd interface after 28 days at 700°C.

The average measured diffusion coefficients for each temperature for the V/Nd system (averaged using the Maximum Likelihood Method described in Section 3.5), along with their calculated errors, are given in Table 4-5. Diffusion coefficients were averaged from six WDS linescans at 550°C, four WDS linescans at 625°C, and two WDS linescans at 700°C. Based on these results, the activation energy governing the diffusion of the V/Nd system was calculated to be 68.4 ± 5.3 kJ/mol, with a pre-exponential factor of $2.5E-15 \pm 1.8E-15$ m²/s.

Table 4-5. Average diffusion coefficients for the V/Nd system.

T (°C)	D (m ² /s)	±
550	9.95E-20	7.0E-21
625	3.38E-19	2.0E-20
700	4.54E-19	4.9E-20

Although the diffusion between V and Nd was not directly visible (i.e. no region of intermediate shading was visible between the two materials) , a representative BSE image of the V/Nd interface after 28 days at 550°C is given in Figure 4-26. The very dark spots in the V and Nd in the image are pores created during the sample preparation process. The additional color variation within the Nd in the image is due to localized oxidation of the surface following polishing. This localized oxidation was not observed in the several microns nearest the V/Nd interface, indicating that a small amount of dissolved V may have been responsible for hindering oxidation.

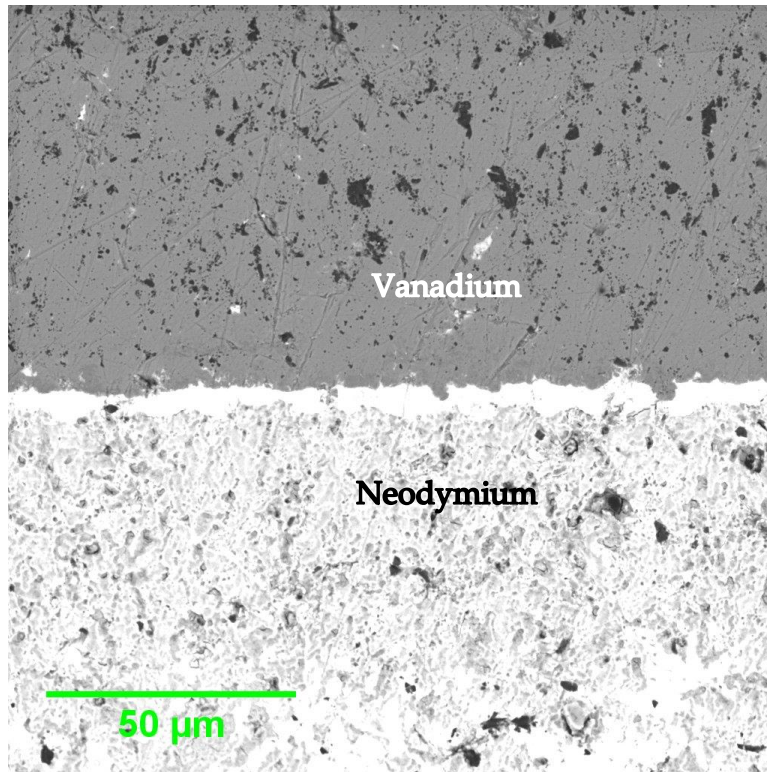


Figure 4-26. BSE image of V/Nd interface following 28 days at 550°C.

4.2.2 Neodymium Diffusion with Zirconium

Relative to the other liner materials tested, Zr diffused a moderate amount with Nd. Diffusion between Zr and Nd at 550°C was measured for periods of both 28 and 56 days, over which it followed the expected dependence of diffusion on the square root of time. Representative WDS data and associated models for Zr/Nd diffusion at 550°C for 28 and 56 days are given in Figure 4-27 and Figure 4-28, respectively.

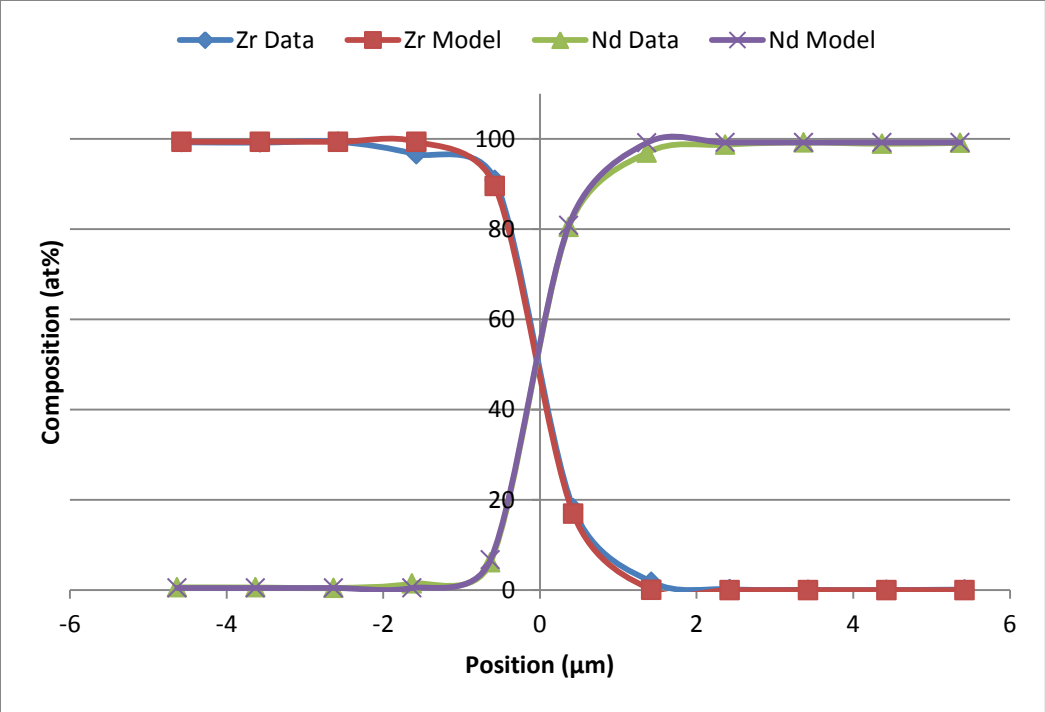


Figure 4-27. Model vs. WDS data for Zr/Nd interface after 28 days at 550°C.

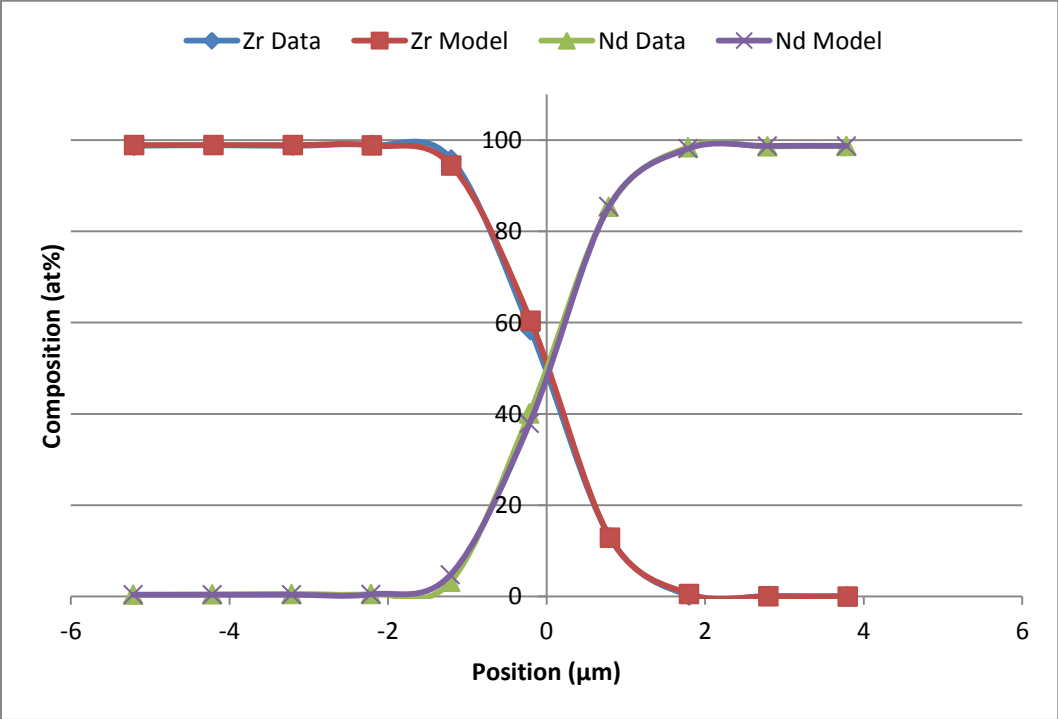


Figure 4-28. Model vs. WDS data for Zr/Nd interface after 56 days at 550°C.

After 28 days at 625°C, the diffusion between Zr and Nd progressed further than after the same period at 550°C, as would be expected. Representative WDS data and the associated models for Zr/Nd diffusion after 28 days at 625°C are given in Figure 4-29.

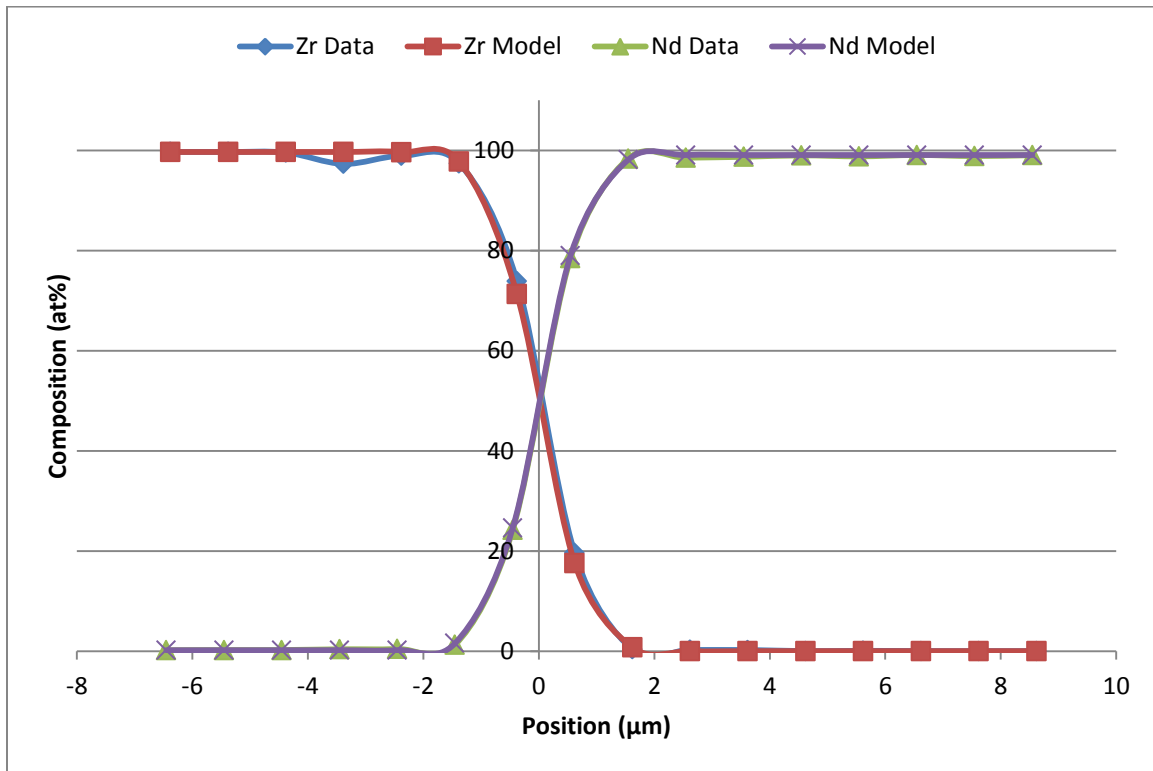


Figure 4-29. Model vs. WDS data for Zr/Nd interface after 28 days at 625°C.

After 28 days at 700°C, the diffusive interaction between Zr and Nd was greater than at either of the lower temperatures tested for that duration. Representative WDS data and the associated models for Zr/Nd diffusion for 28 days at 700°C are given in Figure 4-30.

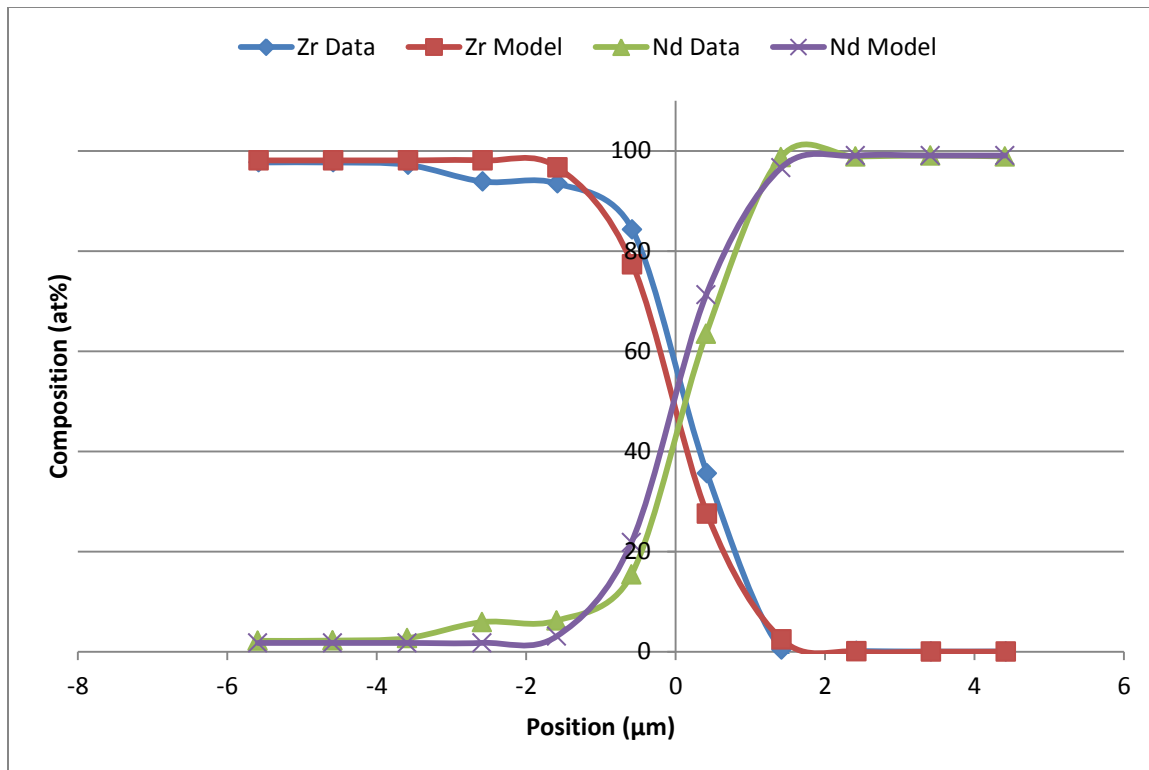


Figure 4-30. Model vs. WDS data for Zr/Nd interface after 28 days at 700°C.

The average measured diffusion coefficients for each temperature for the Zr/Nd system (averaged using the Maximum Likelihood Method described in Section 3.5), along with their calculated errors, are given in Table 4-6. Diffusion coefficients were averaged from fourteen WDS linescans at 550°C, four WDS linescans at 625°C, and six WDS linescans at 700°C. Based on these results, the activation energy governing the diffusion of the Zr/Nd system was calculated to be 37.1 ± 3.6 kJ/mol, with a pre-exponential factor of $1.16E-17 \pm 5.6E-18$ m²/s.

Table 4-6. Average diffusion coefficients for the Zr/Nd system.

T (°C)	D (m ² /s)	±
550	5.61E-20	3.2E-21
625	6.61E-20	7.6E-21
700	1.32E-19	8E-21

A representative BSE image of the Zr/Nd diffusion interface after 28 days at 625°C is given in Figure 4-31. In this image, the plane of interaction between the two elements is just visible between the two halves of the diffusion couple. As before, the very dark spots in the Nd and Zr are pores generated during sample preparation, while the other color variation within the Nd is a result of heterogeneous surface oxidation following polishing.

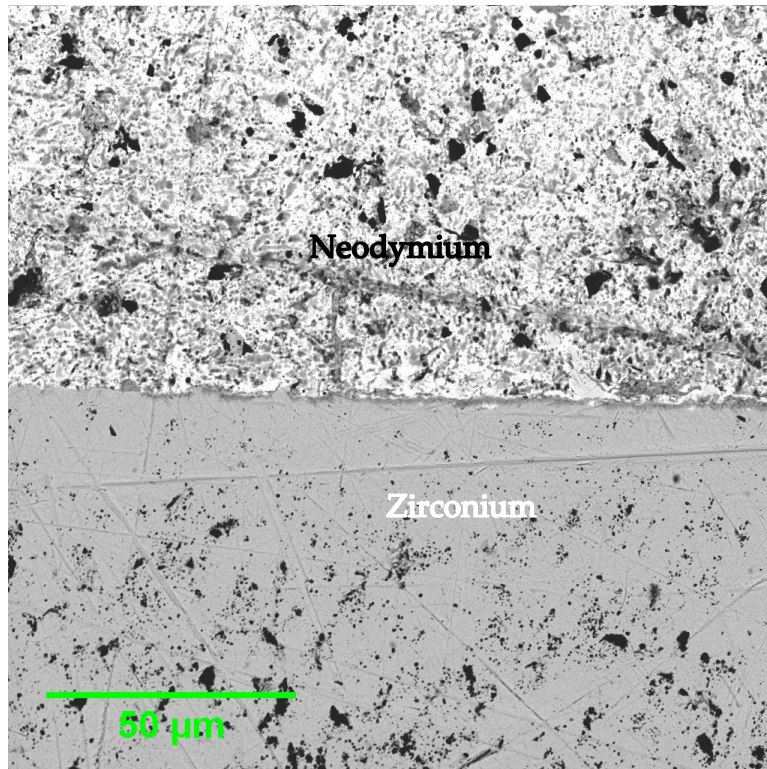


Figure 4-31. BSE image of Zr/Nd interface following 28 days at 625°C.

4.2.3 Neodymium Diffusion with Titanium

Titanium was the most diffusive of all the liners tested with Nd and was observed to bond consistently with the Nd in most diffusion couples. Diffusion between Ti and Nd at 550°C was measured for periods of both 28 and 56 days, over which it followed the expected dependence of diffusion on the square root of time. Representative WDS data and associated models for Ti/Nd diffusion at 550°C for 28 and 56 days are given in Figure 4-32 and Figure 4-33, respectively.

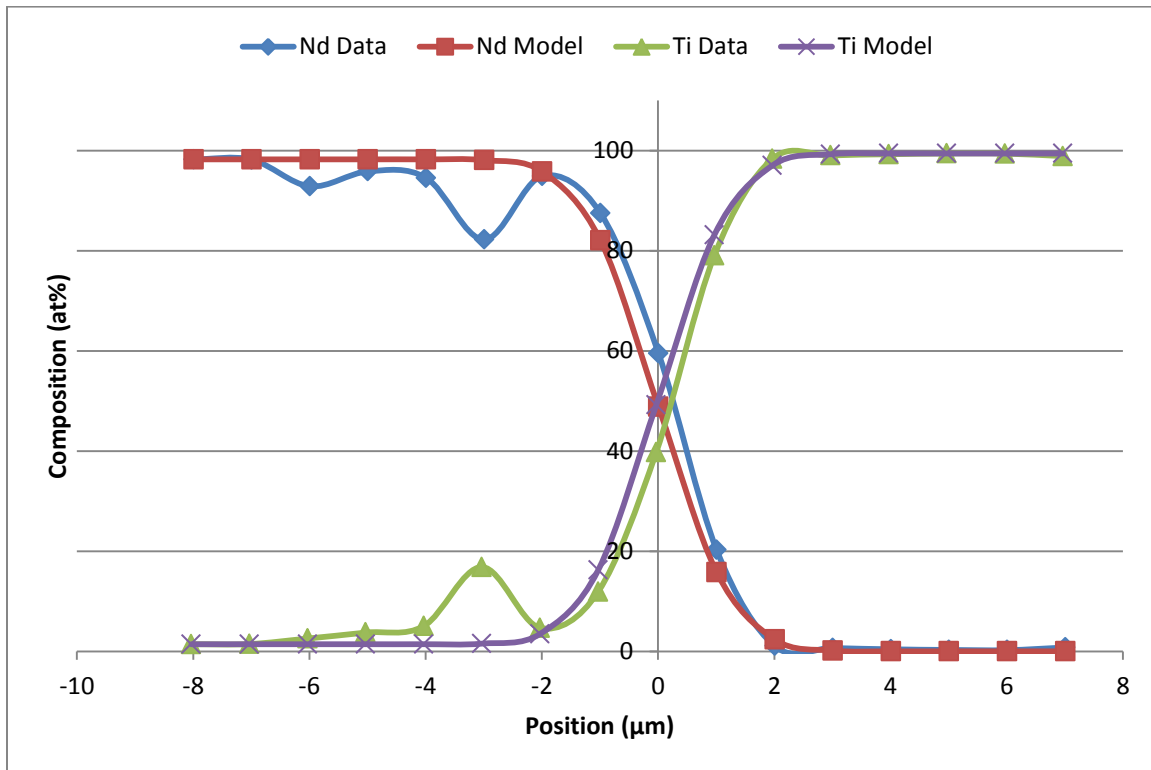


Figure 4-32. Model vs. WDS data for Ti/Nd interface after 28 days at 550°C.

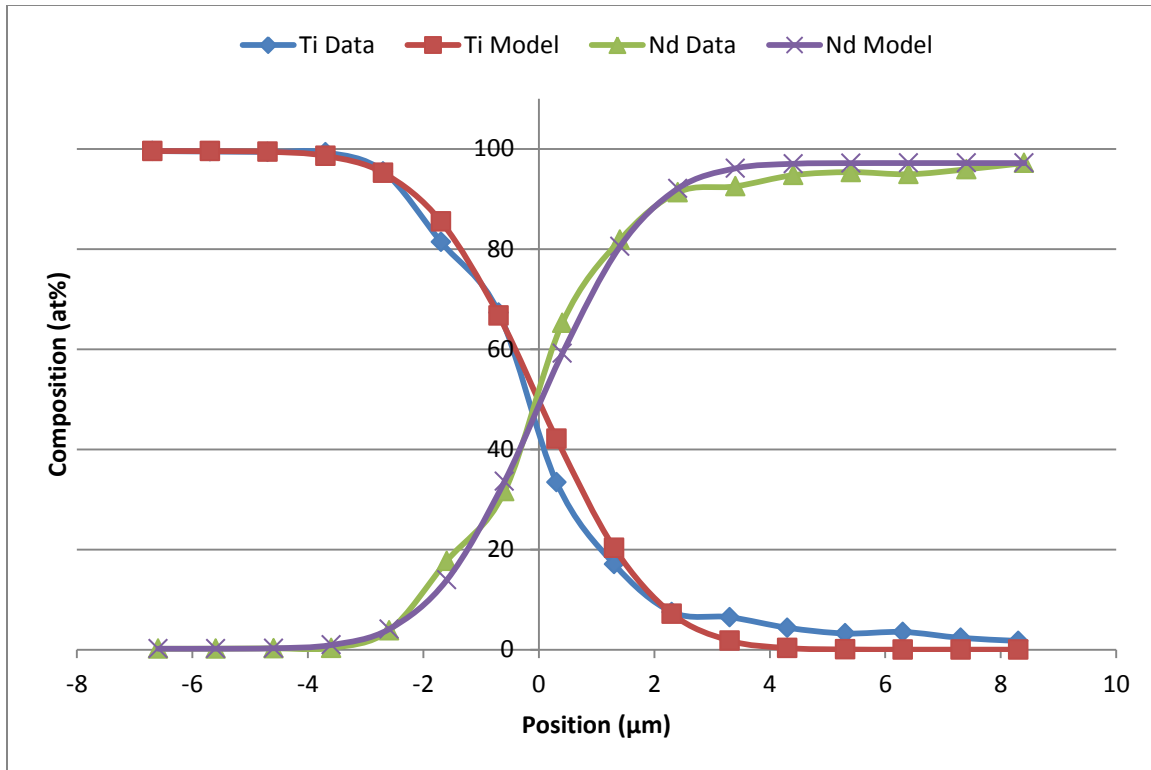


Figure 4-33. Model vs. WDS data for Ti/Nd interface after 56 days at 550°C.

After 28 days at 625°C, the diffusion between Ti and Nd progressed further than after the same period at 550°C, as would be expected. Representative WDS data and the associated models for Ti/Nd diffusion after 28 days at 625°C are given in Figure 4-34.

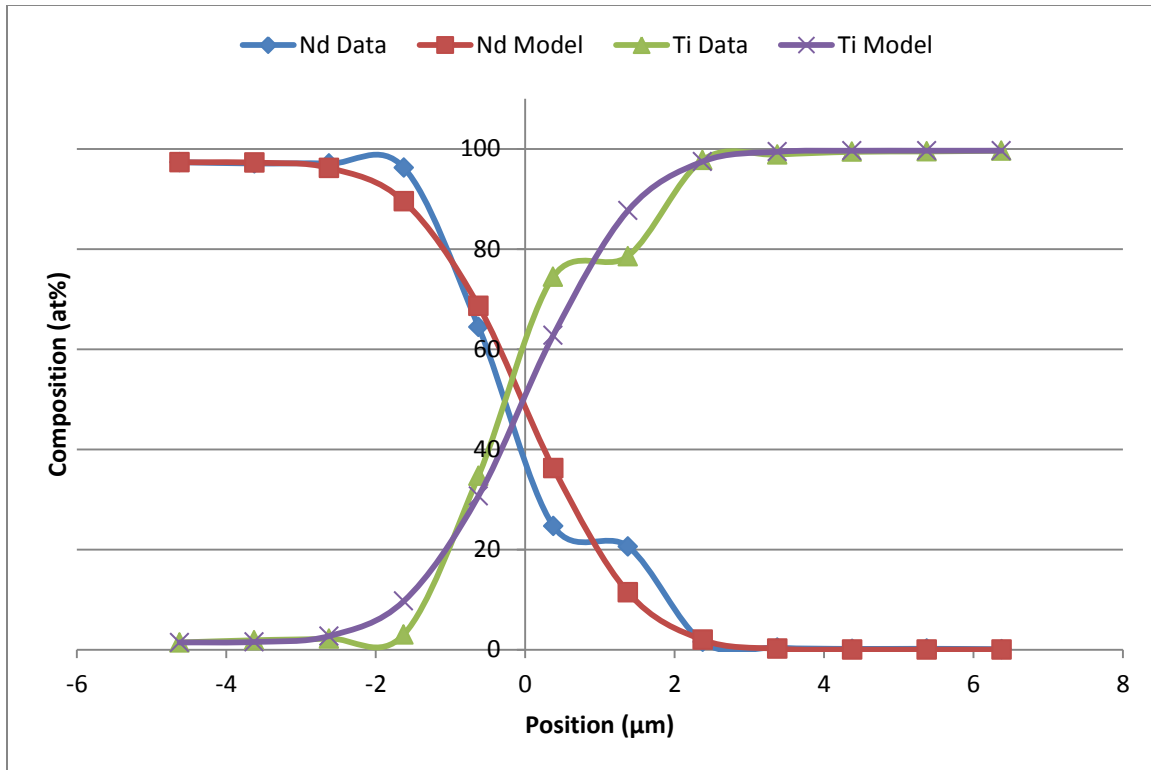


Figure 4-34. Model vs. WDS data for Ti/Nd interface after 28 days at 625°C.

After 28 days at 700°C, the diffusive interaction between Ti and Nd was greater than at either of the lower temperatures tested for that duration. Representative WDS data and the associated models for Ti/Nd diffusion for 28 days at 700°C are given in Figure 4-35.

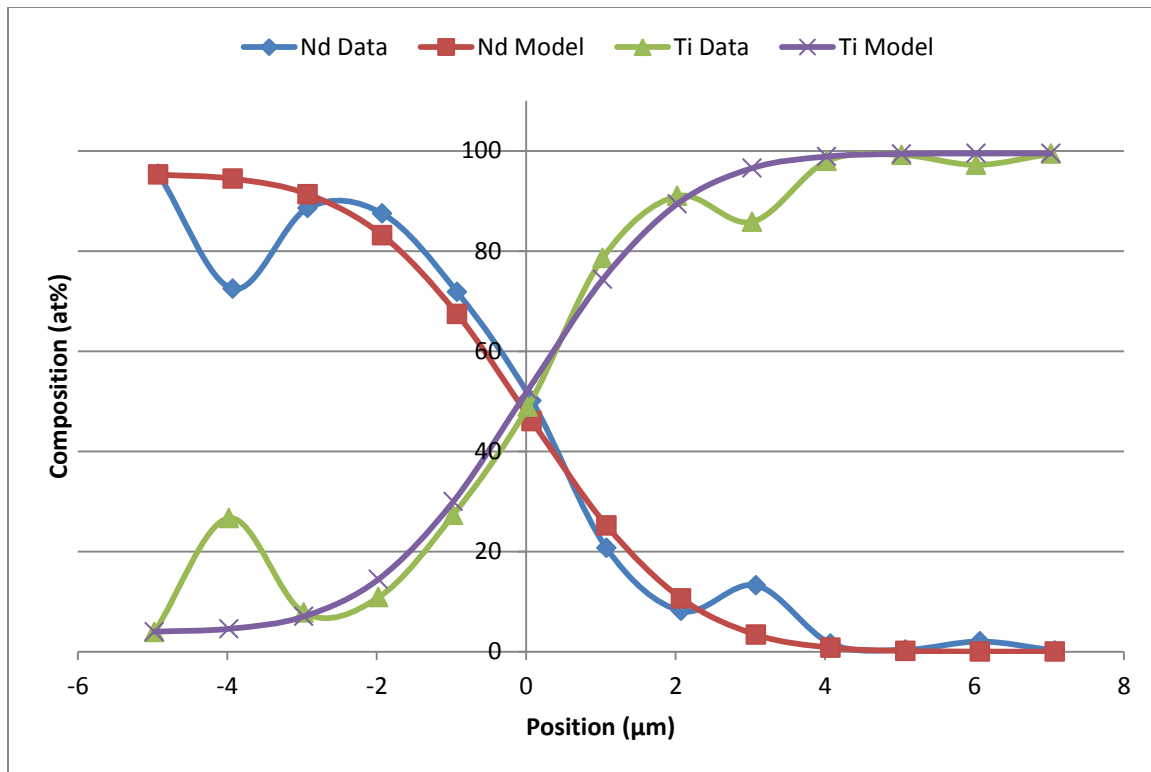


Figure 4-35. Model vs. WDS data for Ti/Nd interface after 28 days at 700°C.

The average calculated diffusion coefficients for each temperature for the Ti/Nd system (averaged using the Maximum Likelihood Method described in Section 3.5), along with their calculated errors, are given in Table 4-7. Diffusion coefficients were averaged from six WDS linescans at 550°C, four WDS linescans at 625°C, and two WDS linescans at 700°C. Based on these results, the activation energy governing the diffusion of the Ti/Nd system was calculated to be 37.7 ± 4.5 kJ/mol, with a pre-exponential factor of $5.4E-17 \pm 3.4E-17$ m²/s.

Table 4-7. Average diffusion coefficients for the Ti/Nd system.

T (°C)	D (m ² /s)	±
550	2.38E-19	1.1E-20
625	2.82E-19	1.9E-20
700	5.65E-19	6.0E-20

A representative BSE image of the Ti/Nd diffusion interface after 56 days at 550°C is given in Figure 4-36. As before, the very dark spots in the Nd and Ti are pores generated during sample preparation, while the other color variation within the Nd is a result of heterogeneous surface oxidation following polishing.

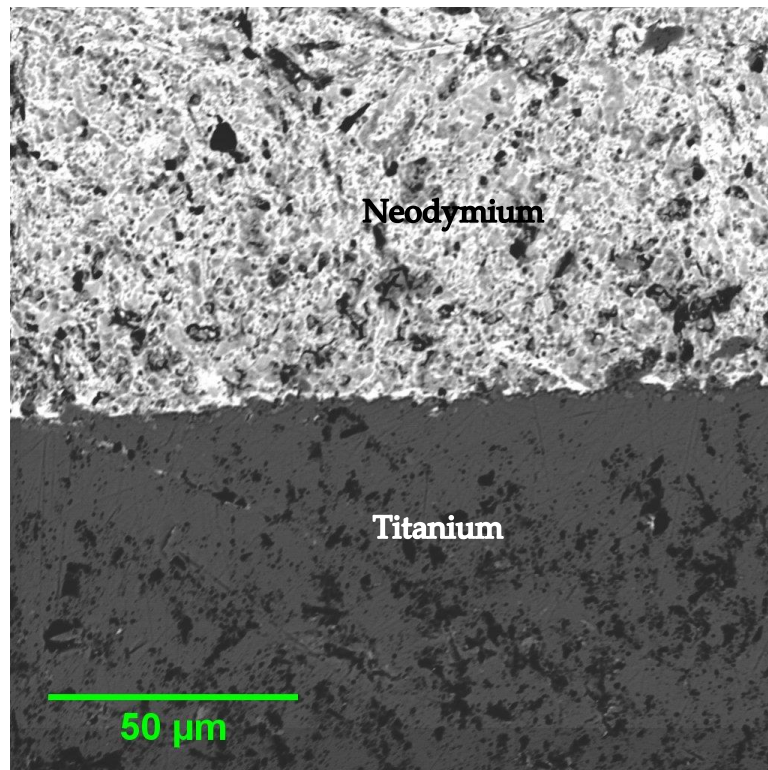


Figure 4-36. BSE image of Ti/Nd interface following 56 days at 550°C.

4.2.4 Neodymium Diffusion with Molybdenum

Relative to the other liner materials tested, Mo-Nd interdiffusion proceeded at a moderate rate. Diffusion between Mo and Nd at 550°C was measured for periods of both 28 and 56 days, over which it followed the expected dependence of diffusion on the square root of time. Representative WDS data and associated models for Mo/Nd diffusion at 550°C for 28 and 56 days are given in Figure 4-37 and Figure 4-38, respectively.

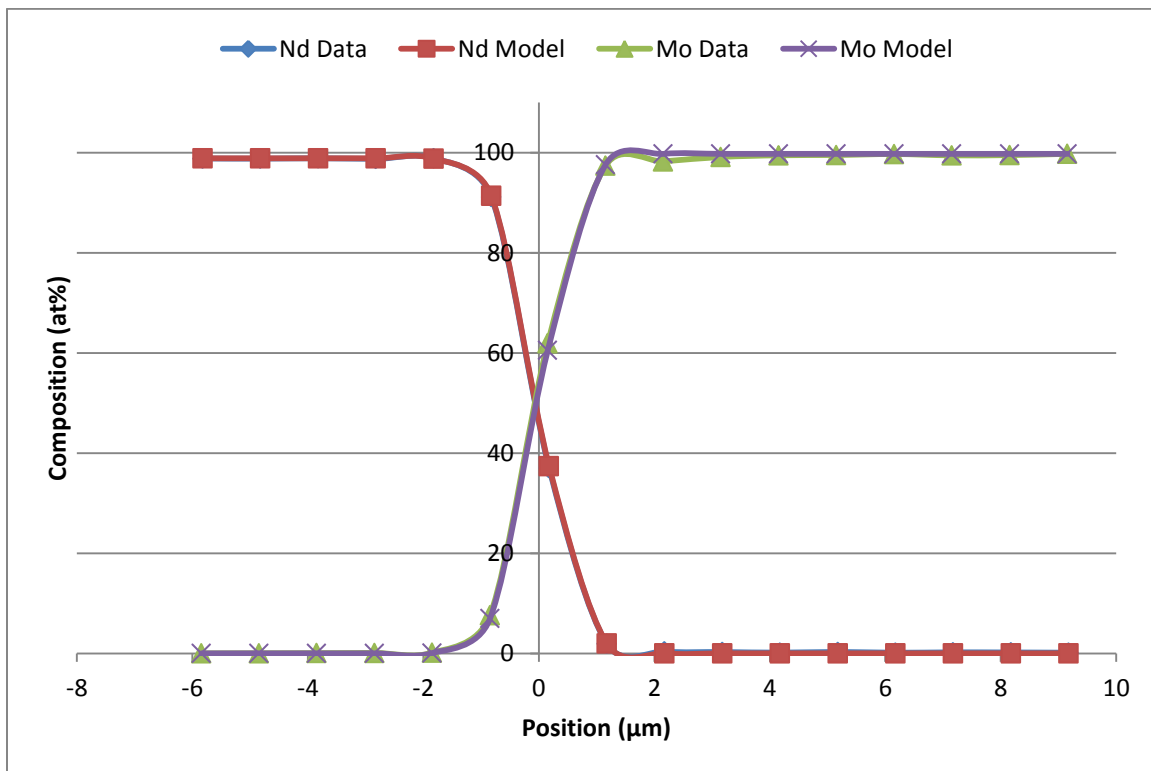


Figure 4-37. Model vs. WDS data for Mo/Nd interface after 28 days at 550°C.

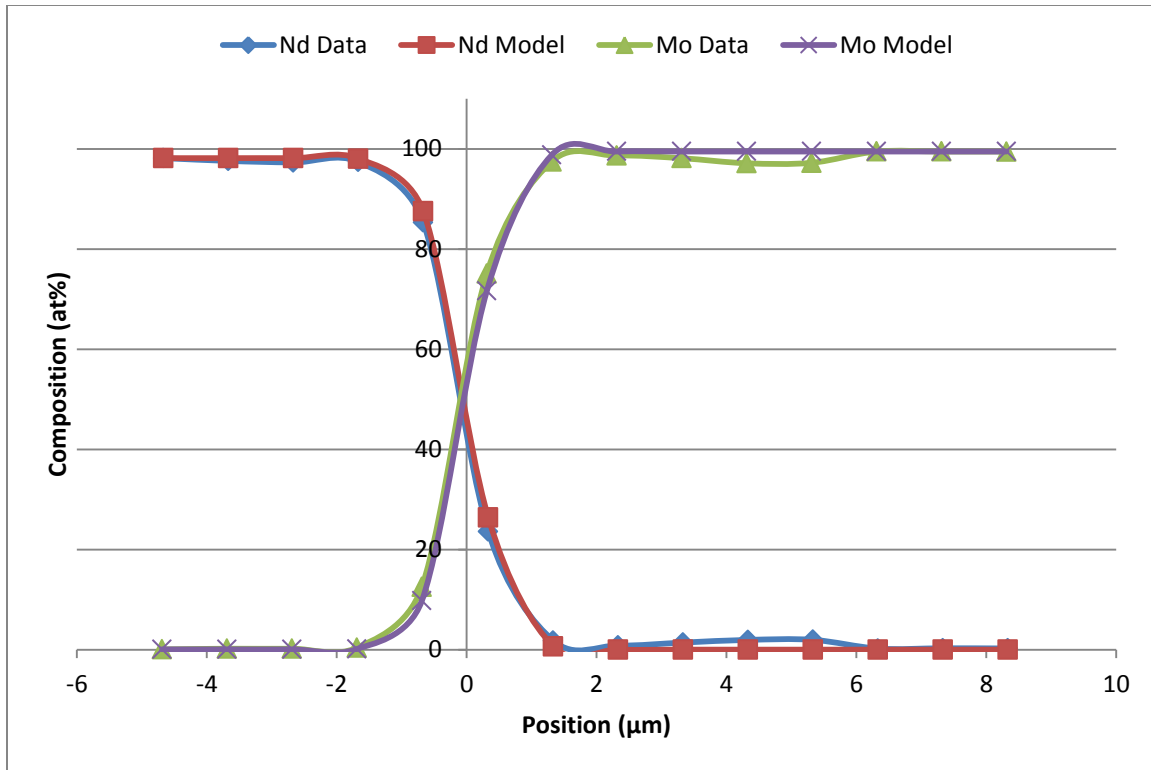


Figure 4-38. Model vs. WDS data for Mo/Nd interface after 56 days at 550°C.

After 28 days at 625°C, the diffusion between Mo and Nd progressed further than after the same period at 550°C, as would be expected. Representative WDS data and the associated models for Mo/Nd diffusion after 28 days at 625°C are given in Figure 4-39.

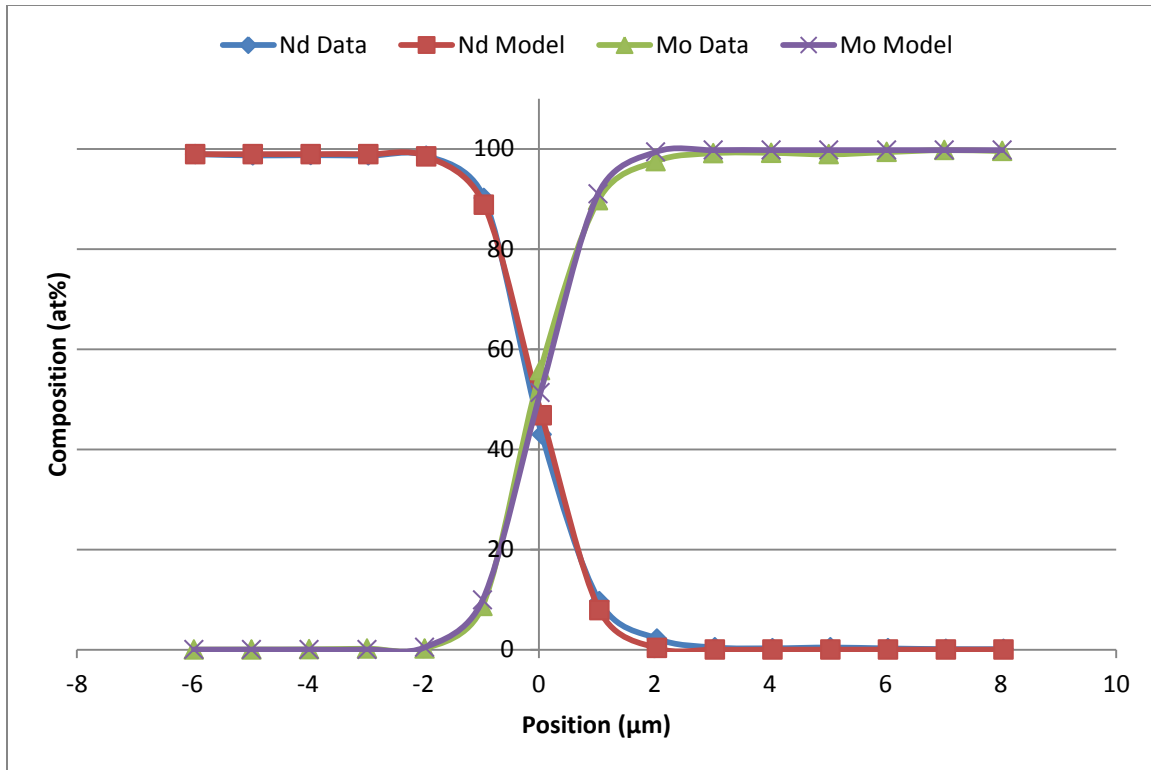


Figure 4-39. Model vs. WDS data for Mo/Nd interface after 28 days at 625°C.

After 28 days at 700°C, the diffusive interaction between Mo and Nd was greater than at either of the lower temperatures tested for that duration. Representative WDS data and the associated models for Mo/Nd diffusion for 28 days at 700°C are given in Figure 4-40.

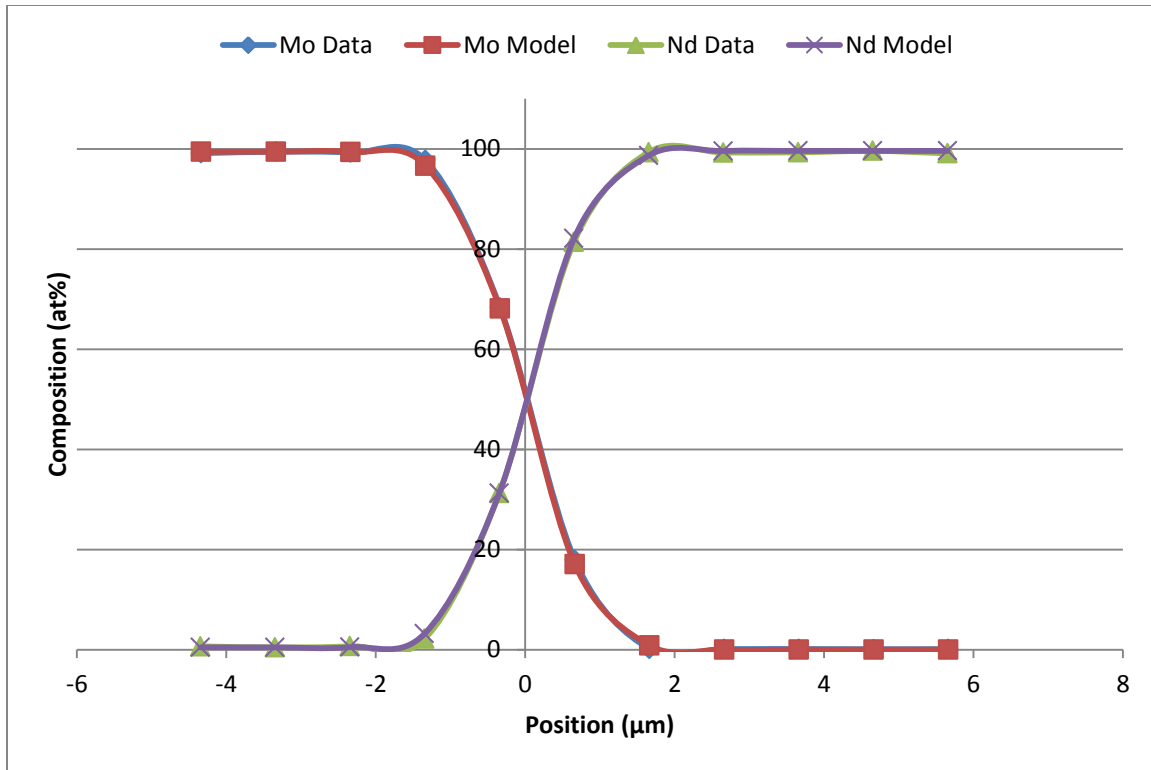


Figure 4-40. Model vs. WDS data for Mo/Nd interface after 28 days at 700°C.

The average measured diffusion coefficients for each temperature for the Mo/Nd system (averaged using the Maximum Likelihood Method described in Section 3.5), along with their calculated errors, are given in Table 4-8. Diffusion coefficients were averaged from twelve WDS linescans at 550°C, ten WDS linescans at 625°C, and four WDS linescans at 700°C. Based on these results, the activation energy governing the diffusion of the Mo/Nd system was calculated to be 41.0 ± 3.5 kJ/mol, with a pre-exponential factor of $1.85E-17 \pm 9.0E-18$ m²/s.

Table 4-8. Average diffusion coefficients for the Mo/Nd system.

T (°C)	D (m ² /s)	±
550	4.13E-20	1.6E-21
625	9.98E-20	4.9E-21
700	1.02E-19	8E-21

A representative BSE image of the Mo/Nd diffusion interface after 28 days at 700°C is given in Figure 4-41. As before, the very dark spots in the Nd and Mo are pores generated during sample preparation, while the other color variation within the Nd is a result of heterogeneous surface oxidation following polishing.

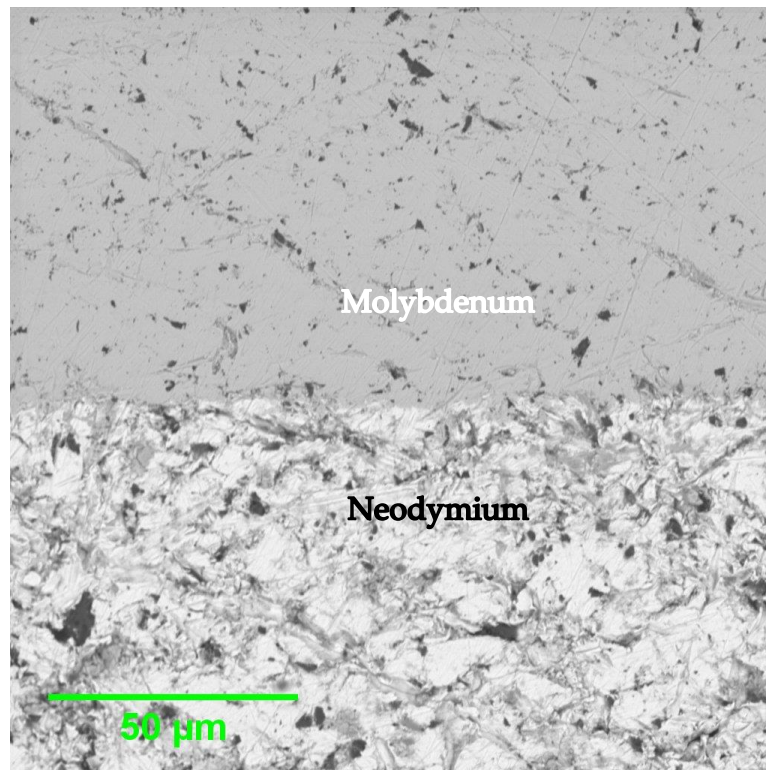


Figure 4-41. BSE image of Mo/Nd interface following 28 days at 700°C.

4.2.5 Neodymium Diffusion with Tungsten

Relative to the other liner materials tested, W diffused very little with Nd. Diffusion between W and Nd at 550°C was measured for periods of both 28 and 56 days, over which it followed the expected dependence of diffusion on the square root of time. Representative WDS data and associated models for W/Nd diffusion at 550°C for 28 and 56 days are given in Figure 4-42 and Figure 4-43, respectively.

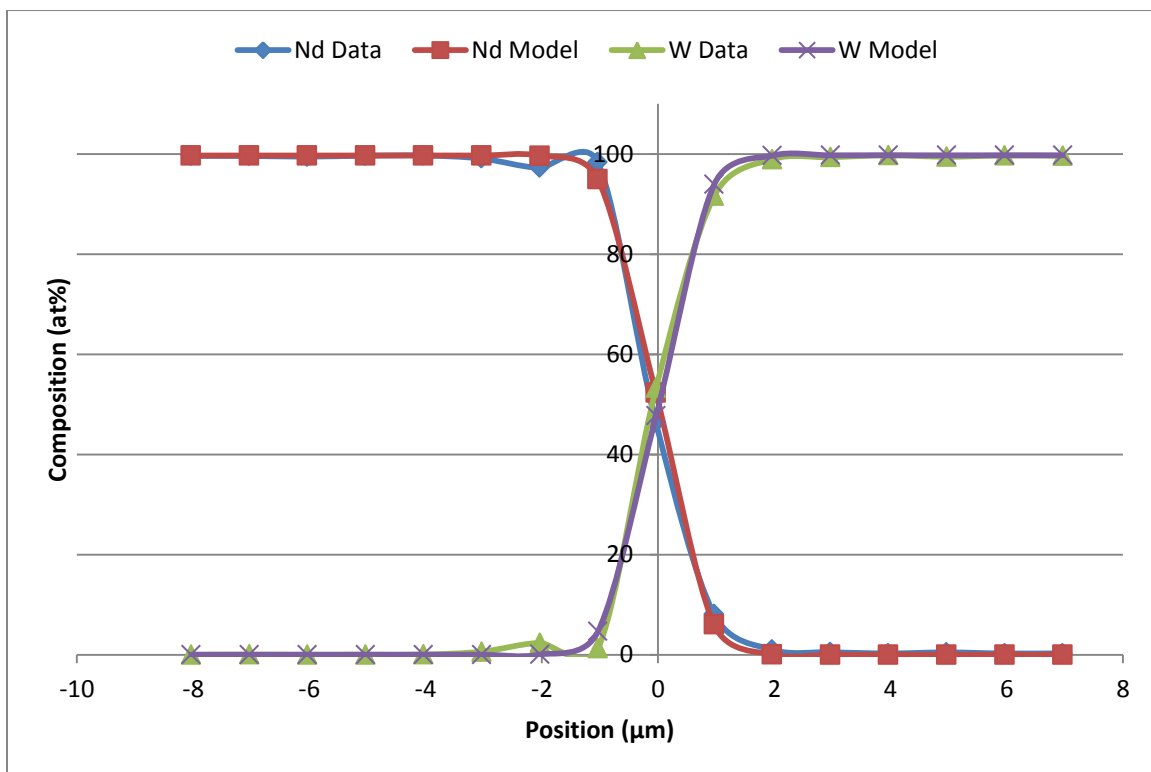


Figure 4-42. Model vs. WDS data for W/Nd interface after 28 days at 550°C.

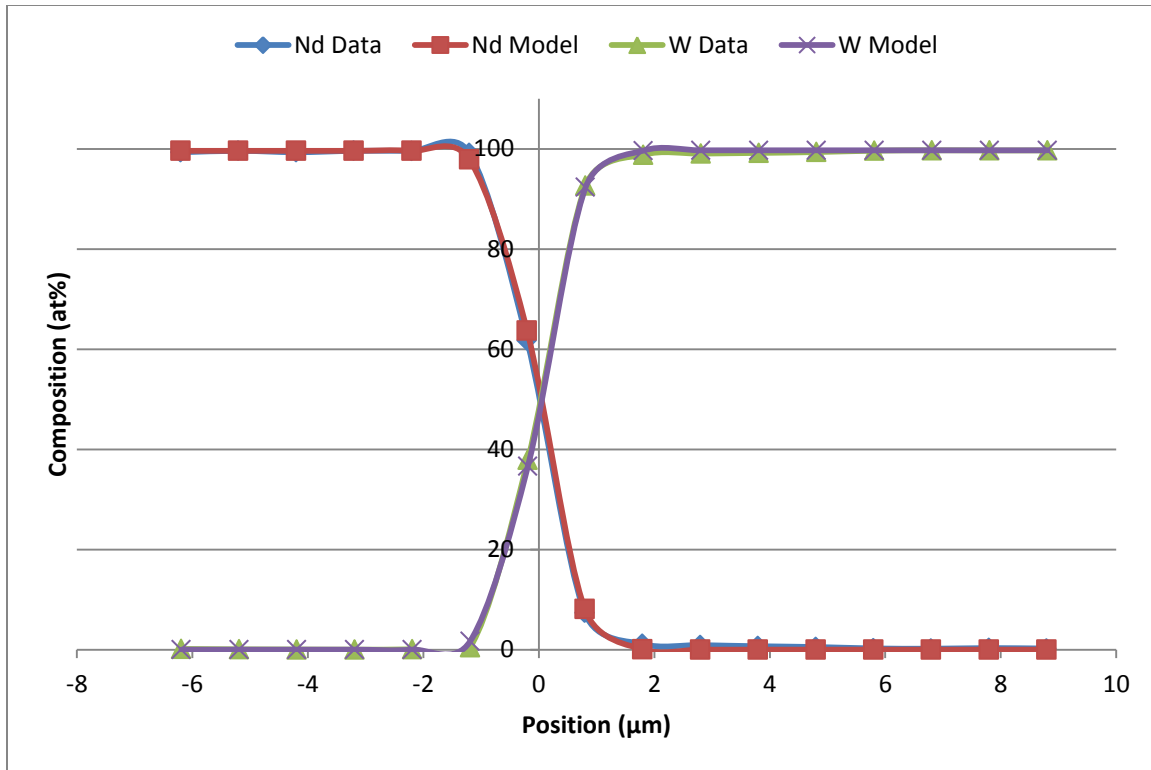


Figure 4-43. Model vs. WDS data for W/Nd interface after 56 days at 550°C.

After 28 days at 625°C, the diffusion between W and Nd progressed further than after the same period at 550°C, as would be expected. Representative WDS data and the associated models for W/Nd diffusion after 28 days at 625°C are given in Figure 4-44.

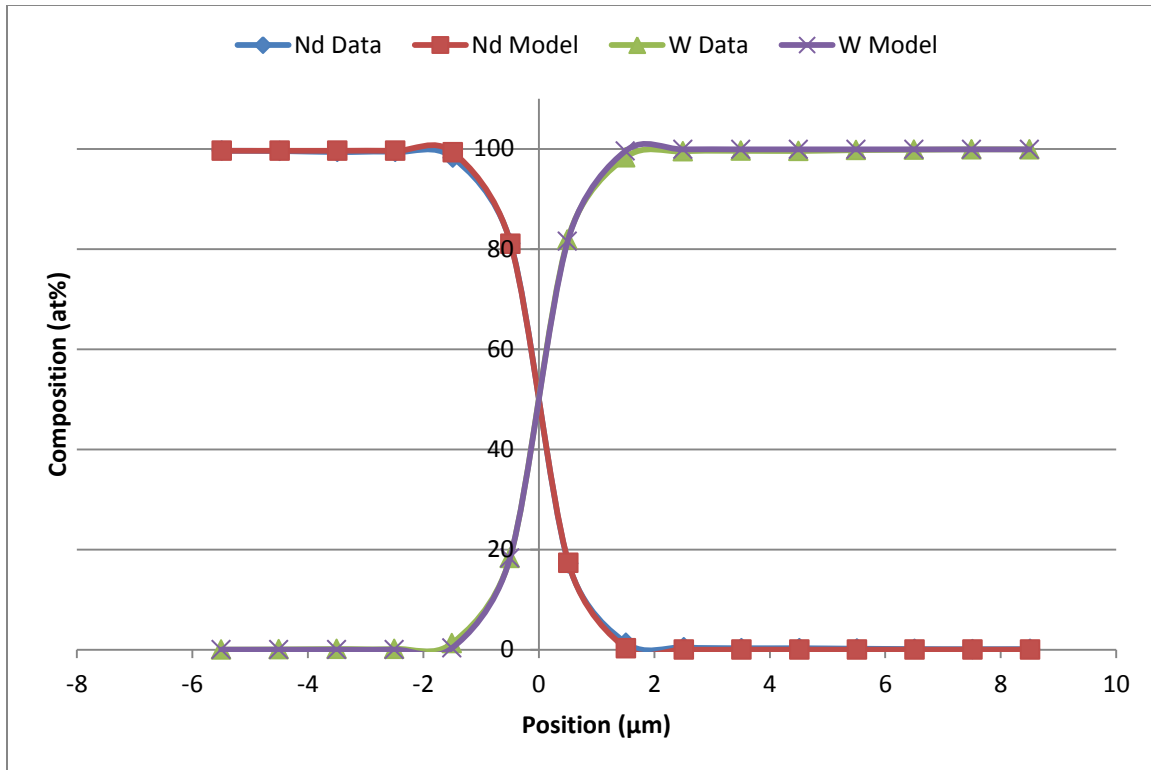


Figure 4-44. Model vs. WDS data for W/Nd interface after 28 days at 625°C.

After 28 days at 700°C, the diffusive interaction between W and Nd was greater than at either of the lower temperatures tested for that duration. Representative WDS data and the associated models for W/Nd diffusion for 28 days at 700°C are given in Figure 4-45.

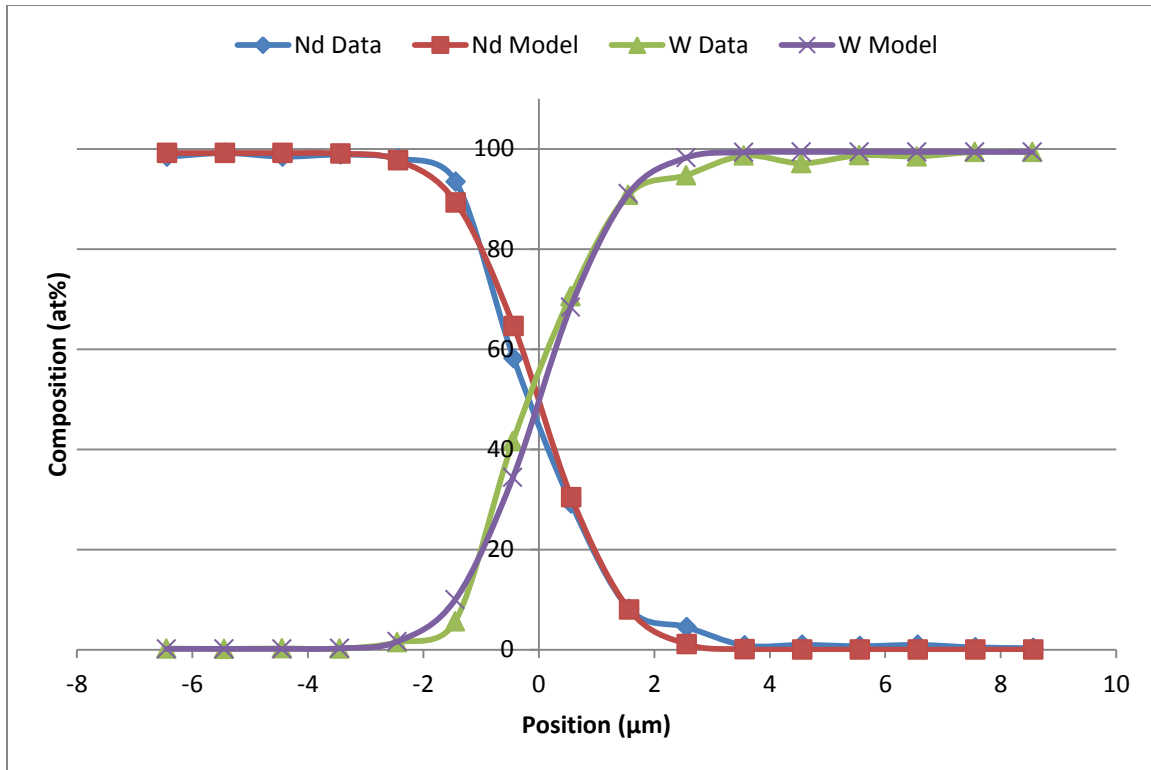


Figure 4-45. Model vs. WDS data for W/Nd interface after 28 days at 700°C.

The average measured diffusion coefficients for each temperature for the W/Nd system (averaged using the Maximum Likelihood Method described in Section 3.5), along with their calculated errors, are given in Table 4-9. Diffusion coefficients were averaged from fourteen WDS linescans at 550°C, eight WDS linescans at 625°C, and five WDS linescans at 700°C. Based on these results, the activation energy governing the diffusion of the W/Nd system was calculated to be 30.0 ± 5.0 kJ/mol, with a pre-exponential factor of $3.0E-18 \pm 2.1E-18$ m²/s.

Table 4-9. Average diffusion coefficients for the W/Nd system.

T (°C)	D (m ² /s)	±
550	3.93E-20	1.9E-21
625	4.66E-20	4.6E-21
700	7.82E-20	8.7E-21

A representative BSE image of the W/Nd diffusion interface after 56 days at 550°C is given in Figure 4-46. As before, the very dark spots in the Nd and W are pores generated during sample preparation, while the other color variation within the Nd is a result of heterogeneous surface oxidation following polishing.

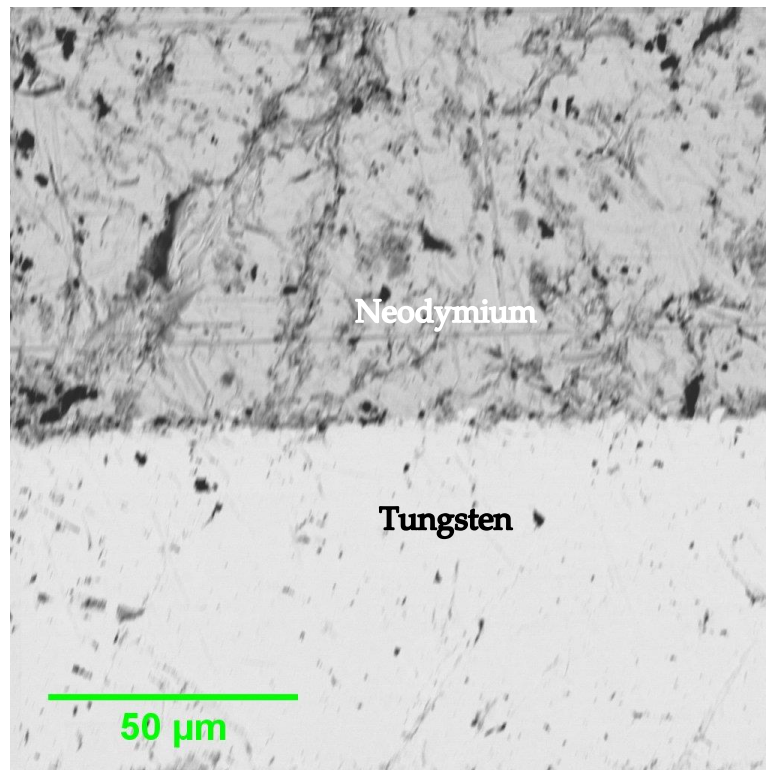


Figure 4-46. BSE image of W/Nd interface following 56 days at 550°C.

4.2.6 Neodymium Diffusion with Tantalum

Relative to the other liner materials tested, Ta diffused very little with Nd. Diffusion between Ta and Nd at 550°C was measured for periods of both 17.5 and 28 days, over which it followed the expected dependence of diffusion on the square root of time. Representative WDS data and associated models for Ta/Nd diffusion at 550°C for 17.5 and 28 days are given in Figure 4-47 and Figure 4-48, respectively.

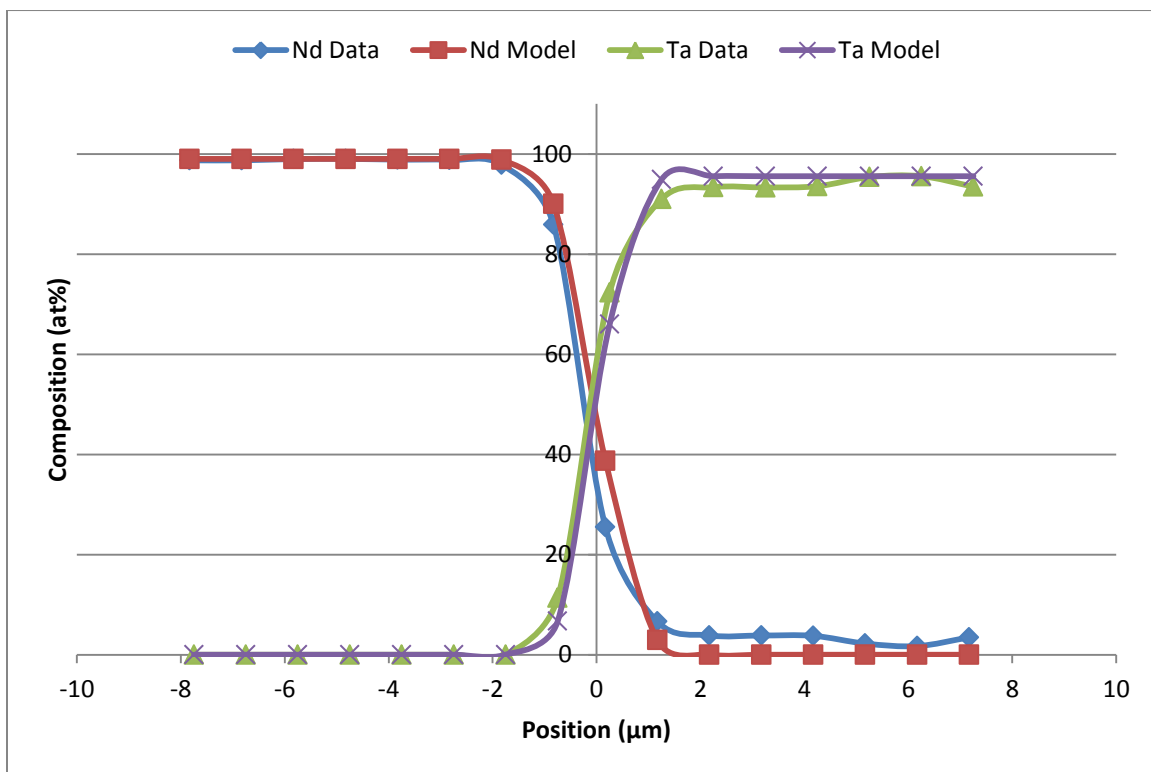


Figure 4-47. Model vs. WDS data for Ta/Nd interface after 17.5 days at 550°C.

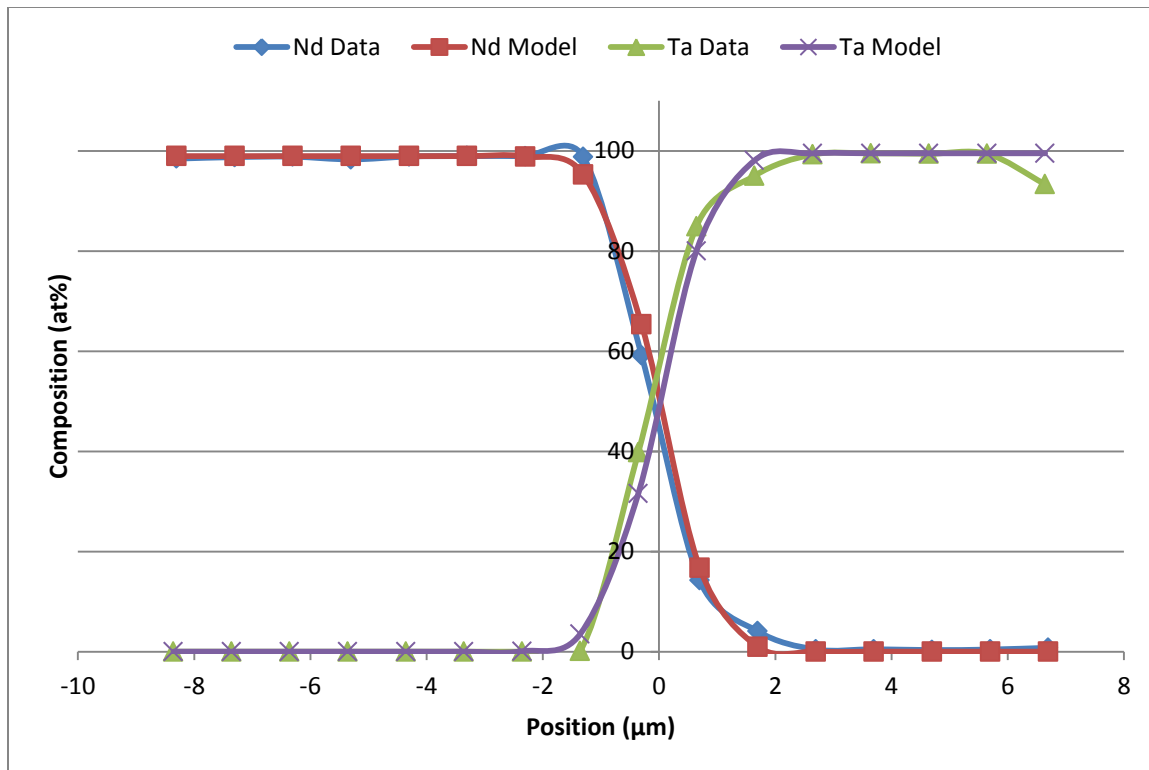


Figure 4-48. Model vs. WDS data for Ta/Nd interface after 28 days at 550°C.

After 28 days at 625°C, the diffusion between Ta and Nd progressed slightly less than after the same period at 550°C, contrary to the expected behavior. Representative WDS data and the associated models for Ta/Nd diffusion after 28 days at 625°C are given in Figure 4-49.

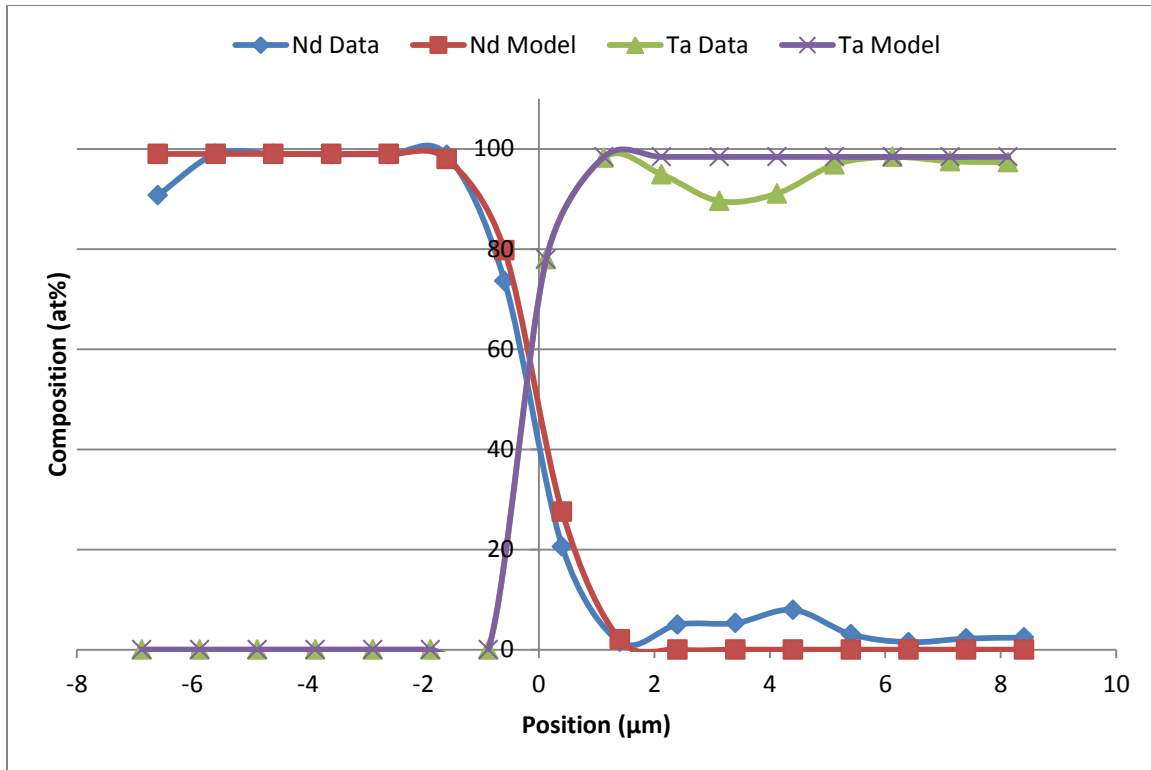


Figure 4-49. Model vs. WDS data for Ta/Nd interface after 28 days at 625°C.

After 28 days at 700°C, the diffusive interaction between Ta and Nd was less than at either of the lower temperatures tested for that duration, contrary to the expected behavior. Representative WDS data and the associated models for Ta/Nd diffusion for 28 days at 700°C are given in Figure 4-50.

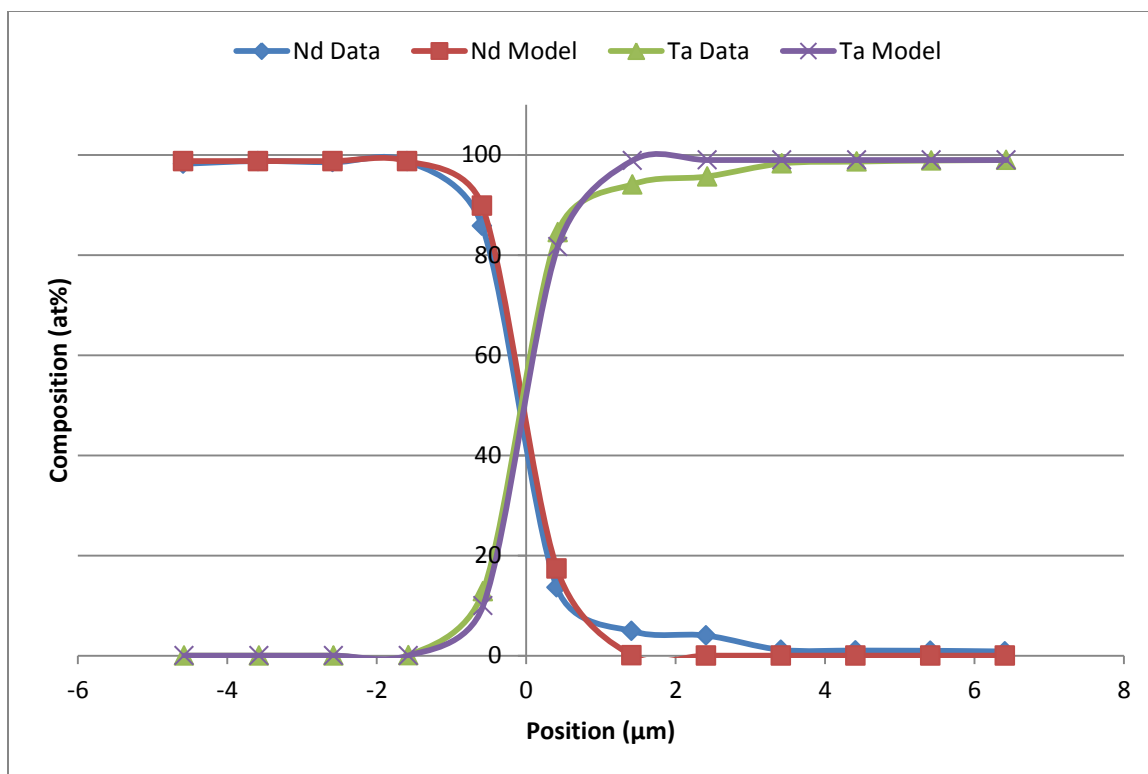


Figure 4-50. Model vs. WDS data for Ta/Nd interface after 28 days at 700°C.

The average measured diffusion coefficients for each temperature for the Ta/Nd system (averaged using the Maximum Likelihood Method described in Section 3.5), along with their calculated errors, are given in Table 4-10. Diffusion coefficients were averaged from four WDS linescans at 550°C, one WDS linescans at 625°C, and six WDS linescans at 700°C. Based on these results, the apparent activation energy governing the diffusion of the Ta/Nd system was found to be -45.0 ± 6.7 kJ/mol, with a pre-exponential factor of $1.8E-22 \pm 1.6E-22$ m²/s. The apparent negative activation energy was a result of the reduced rate of diffusion observed with increasing temperature between Ta and Nd. This result is highly unusual for diffusion couples; however, the measured coefficients at 550°C and 700°C were based on multiple measurements in good agreement across several different

diffusion couples (the data at 625°C is less conclusive). As explained in Section 5.2, this behavior may have resulted from residual vacancies in the tantalum foil from manufacturing annealing out at elevated temperatures.

Table 4-10. Average diffusion coefficients for the Ta/Nd system.

T (°C)	D (m ² /s)	±
550	1.09E-19	1.3E-20
625	9.81E-20	8.51E-20
700	3.85E-20	3.7E-21

A representative BSE image of the Ta/Nd diffusion interface after 28 days at 550°C is given in Figure 4-51. As before, the very dark spots in the Nd and Ta are pores generated during sample preparation, while the other color variation within the Nd is a result of heterogeneous surface oxidation following polishing.

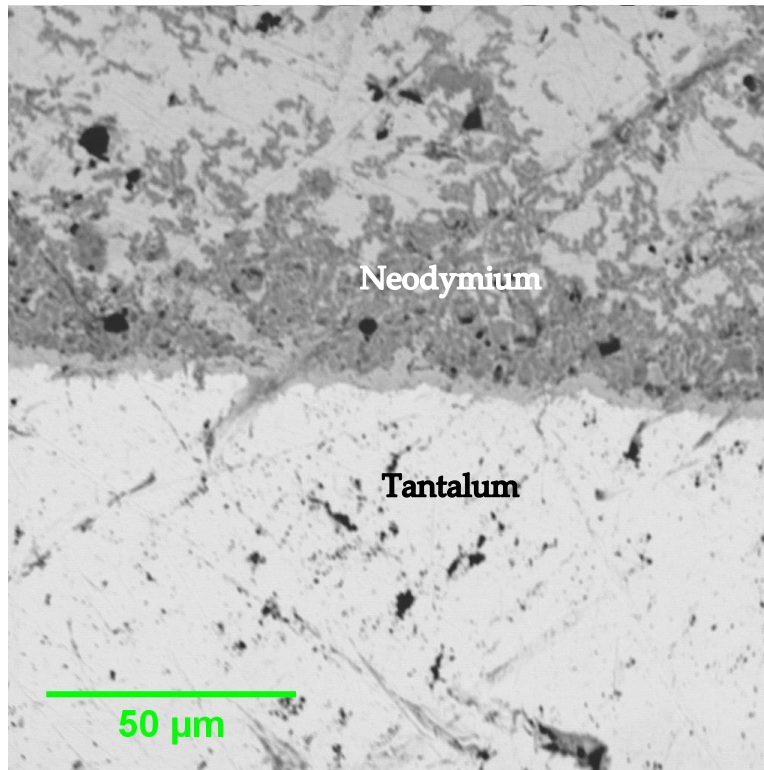


Figure 4-51. BSE image of Ta/Nd interface following 28 days at 550°C.

4.3 Steel/Liner Diffusion

Data for diffusion between the six liner materials and the three steel alloys and iron was less complete than data for diffusion between the liner materials and neodymium. This was in part due to a higher fraction of liner materials successfully diffusion bonding to neodymium than to steel, and in part due to the fact that for each time and temperature there were multiple tests of each liner with neodymium but only one or two tests of each liner with each steel alloy. Since the diffusion behavior of each steel alloy will be slightly different, diffusion data is presented for each steel alloy individually.

4.3.1 Steel Diffusion with Vanadium

For the nine V/Steel diffusion couples annealed at 550°C, diffusion data for V was only successfully acquired with HT-9. Representative WDS data and the associated models for V/HT-9 diffusion after 56 days at 550°C are given in Figure 4-52.

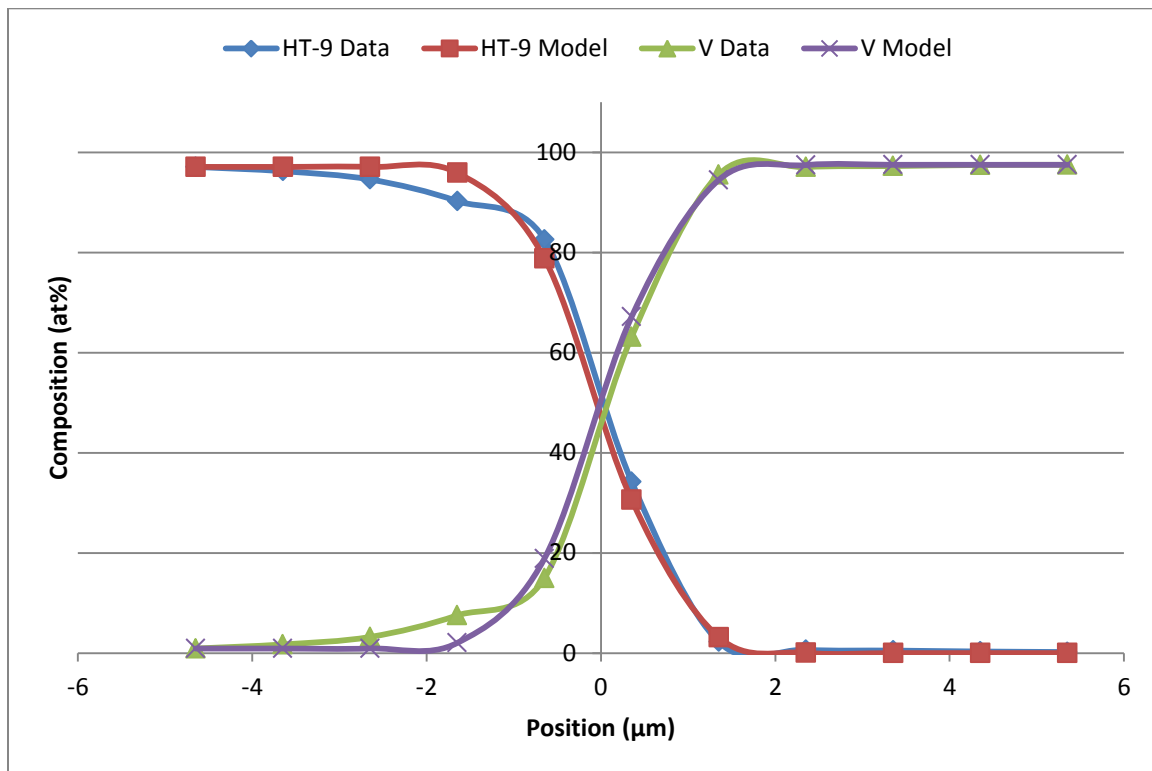


Figure 4-52. Model vs. WDS data for V/HT-9 interface after 56 days at 550°C.

For the four V/Steel diffusion couples annealed at 625°C, diffusion data was only successfully acquired with SS-316. Representative WDS data and the associated models for V/SS-316 diffusion after 28 days at 625°C are given in Figure 4-53.

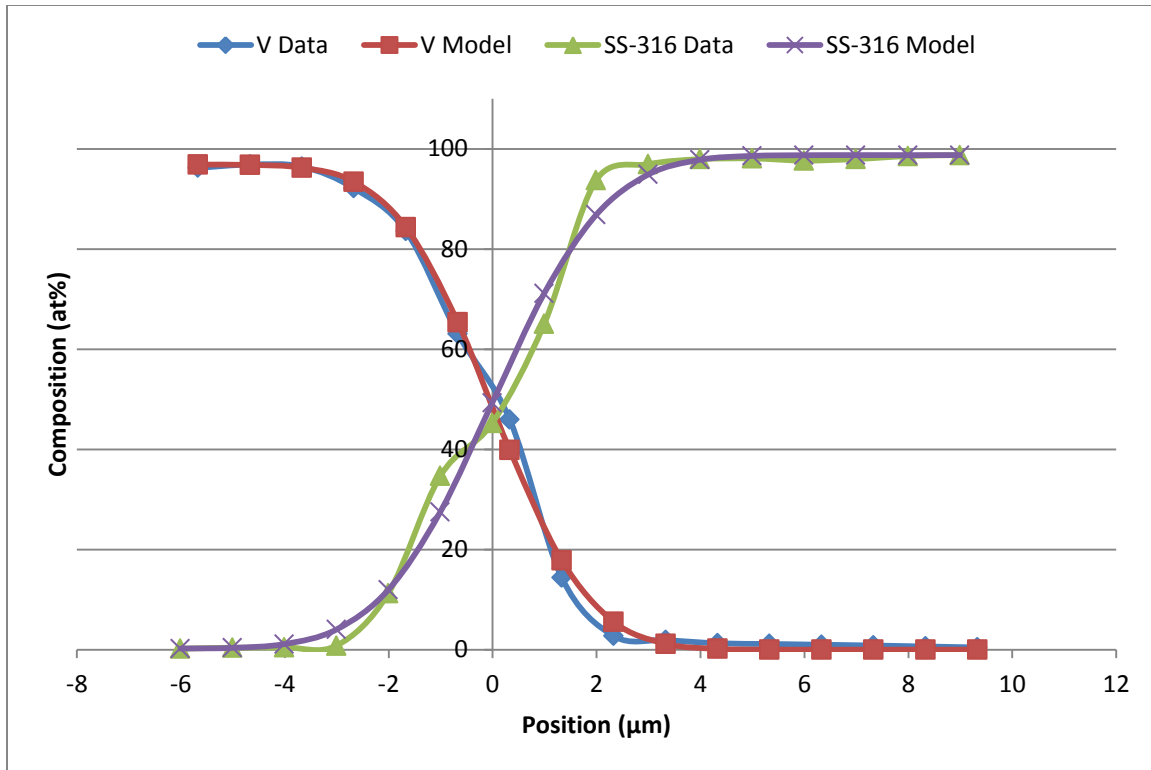


Figure 4-53. Model vs. WDS data for V/SS-316 interface after 28 days at 625°C.

For the four V/Steel diffusion couples annealed at 700°C, diffusion data for V was successfully acquired with HT-9 and G.91. Representative WDS data and the associated models for V/HT-9 and V/G.91 diffusion after 28 days at 700°C are given in Figure 4-54 and Figure 4-55 respectively.

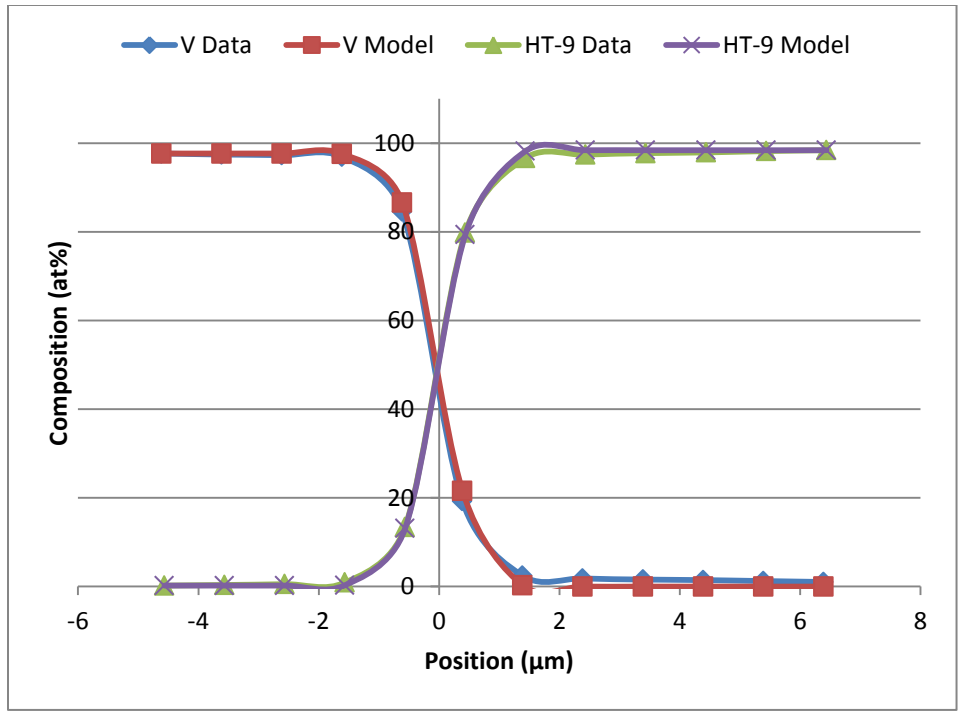


Figure 4-54. Model vs. WDS data for V/HT-9 interface after 28 days at 700°C.

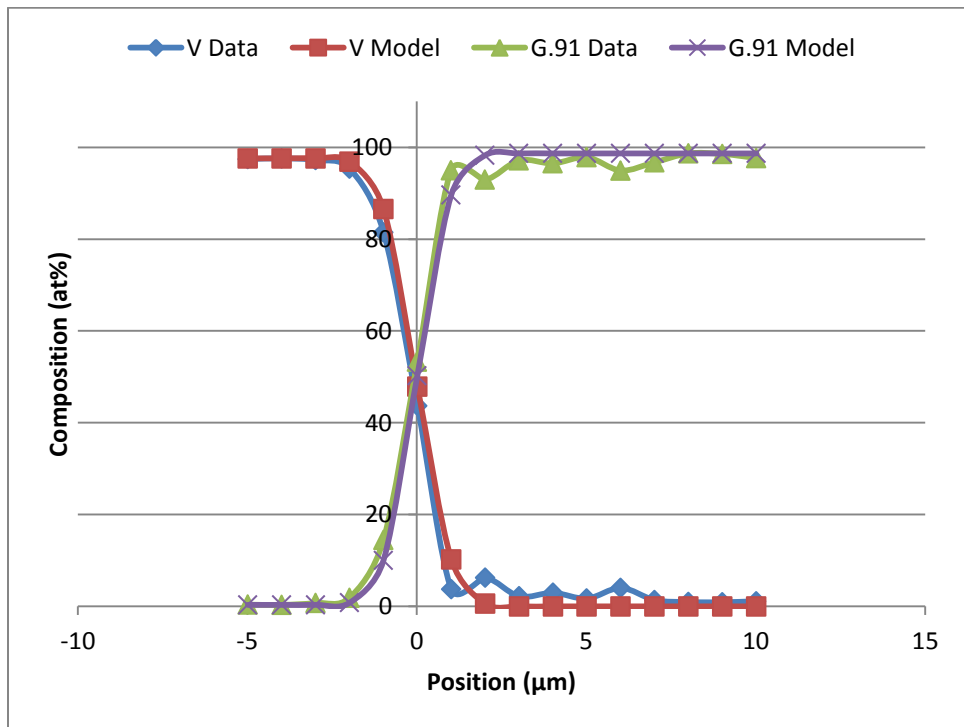


Figure 4-55. Model vs. WDS data for V/G.91 interface after 28 days at 700°C.

The average diffusion coefficients for V/HT-9, V/G.91, V/SS-316, and V/Fe (averaged using the Maximum Likelihood Method described in Section 3.5) for all available temperatures are given in Table 4-11. Since data for multiple temperatures was only available for V/HT-9, it was the only system for which an activation energy could be calculated. Based on the measured diffusion coefficients, V/HT-9 diffusion had an activation energy of 30.8 ± 8.2 kJ/mol with a pre-exponential factor of $2.2E-18 \pm 2.6E-18$ m²/s.

Table 4-11. Average diffusion coefficients for V with steel alloys and Fe.

T (°C)	V/HT-9		V/G.91		V/SS-316		V/Fe	
	D (m ² /s)	±	D (m ² /s)	±	D (m ² /s)	±	D (m ² /s)	±
550	2.44E-20	2.1E-21	N/A	N/A	N/A	N/A	N/A	N/A
625	N/A	N/A	N/A	N/A	5.22E-19	3.3E-20	N/A	N/A
700	4.90E-20	8.0E-21	5.48E-20	4.7E-21	N/A	N/A	N/A	N/A

4.3.2 Steel Diffusion with Zirconium

For the eighteen Zr/Steel diffusion couples run at 550°C, diffusion data for Zr was only successfully acquired with SS-316 and Fe. Representative WDS data and the associated models for Zr/SS-316 and Zr/Fe diffusion after 56 days at 550°C are given in Figure 4-56 and Figure 4-57, respectively.

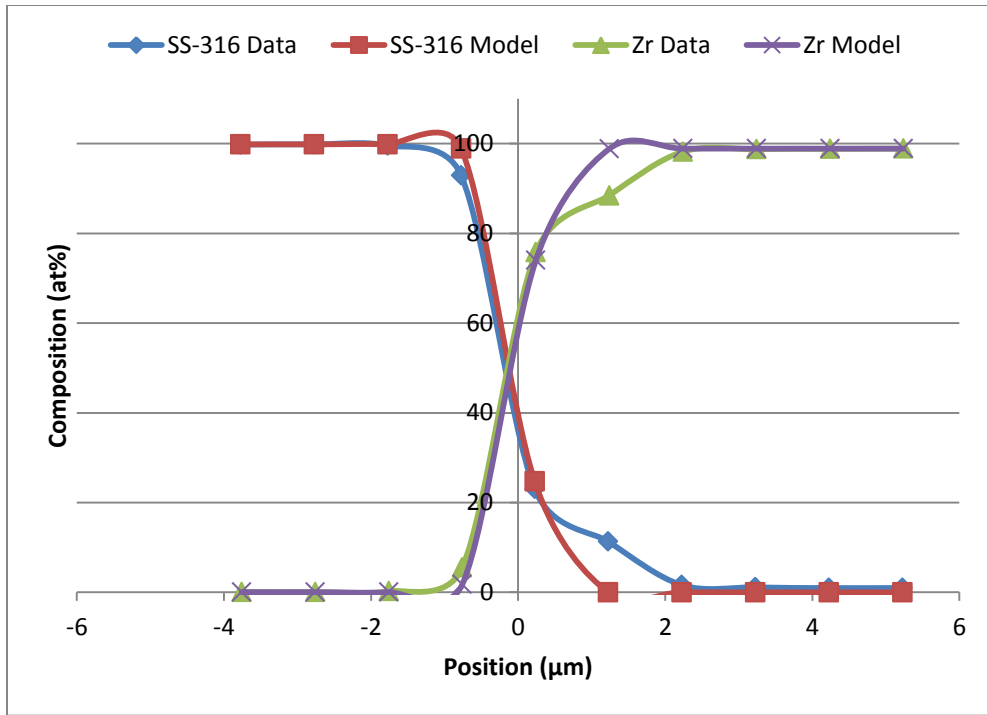


Figure 4-56. Model vs. WDS data for Zr/SS-316 interface after 56 days at 550°C.

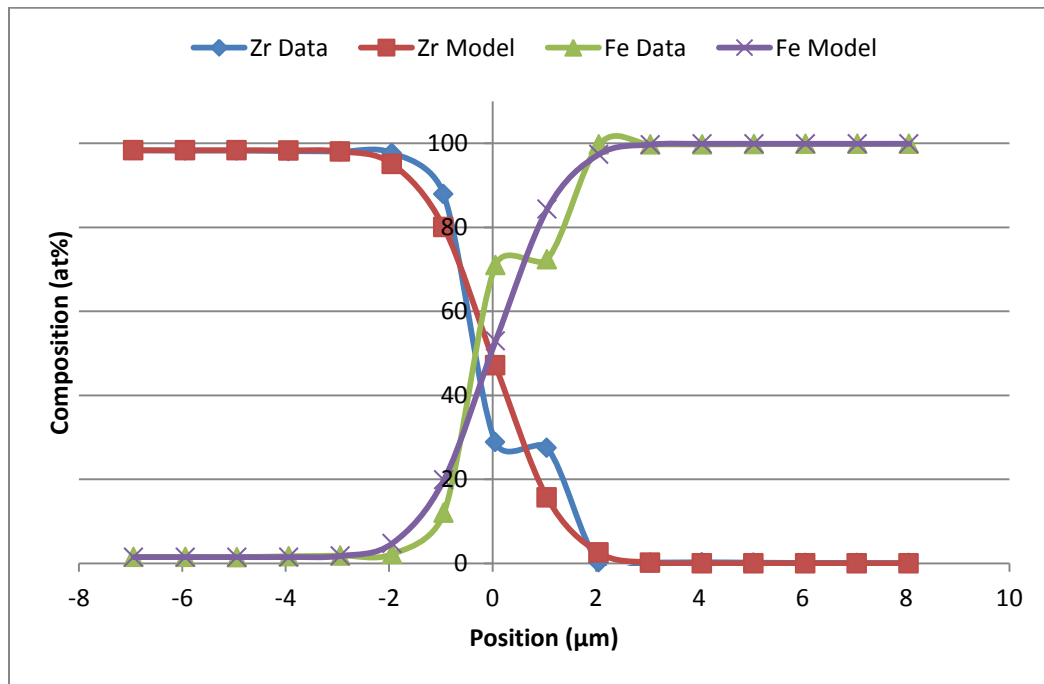


Figure 4-57. Model vs. WDS data for Zr/Fe interface after 56 days at 550°C.

For the eight Zr/Steel diffusion couples run at 625°C, diffusion data for Zr was only successfully acquired with Fe. Representative WDS data and the associated models for Zr/Fe diffusion after 28 days at 625°C are given in Figure 4-58.

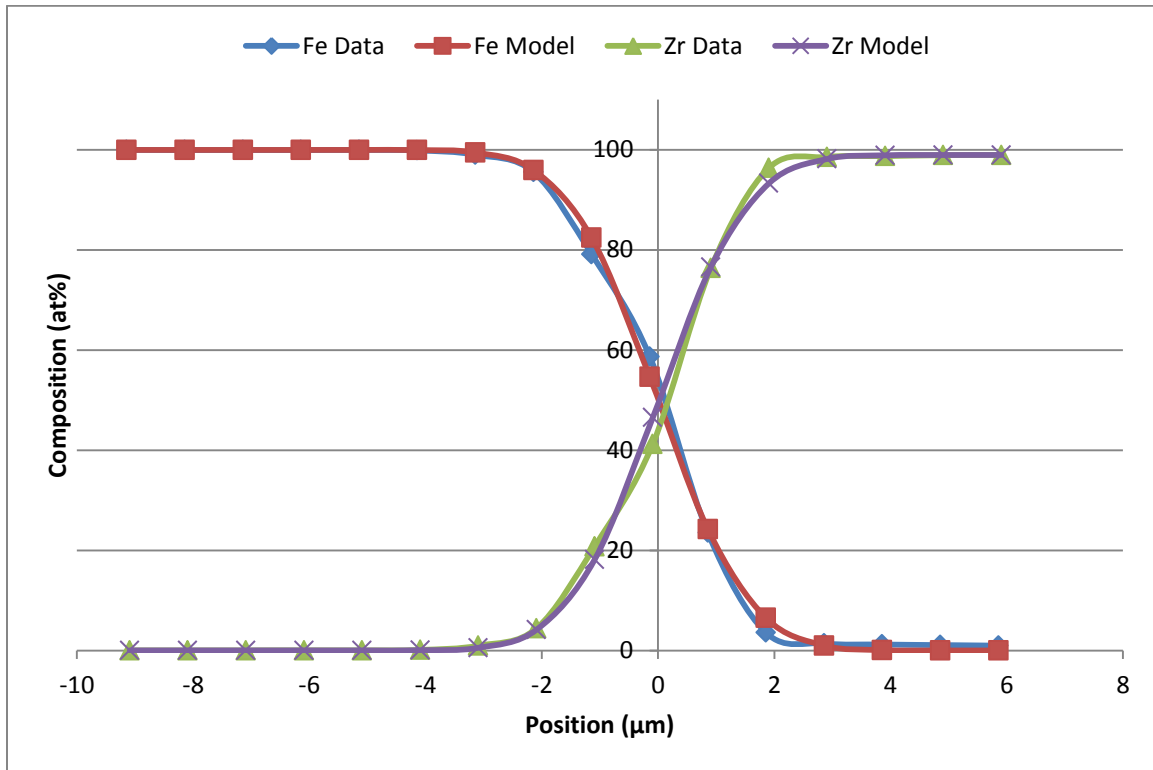


Figure 4-58. Model vs. WDS data for Zr/Fe interface after 28 days at 625°C.

For the eight Zr/Steel diffusion couples run at 700°C, diffusion data for Zr was only successfully acquired with SS-316. Representative WDS data and the associated models for Zr/SS-316 diffusion after 28 days at 700°C are given in Figure 4-59.

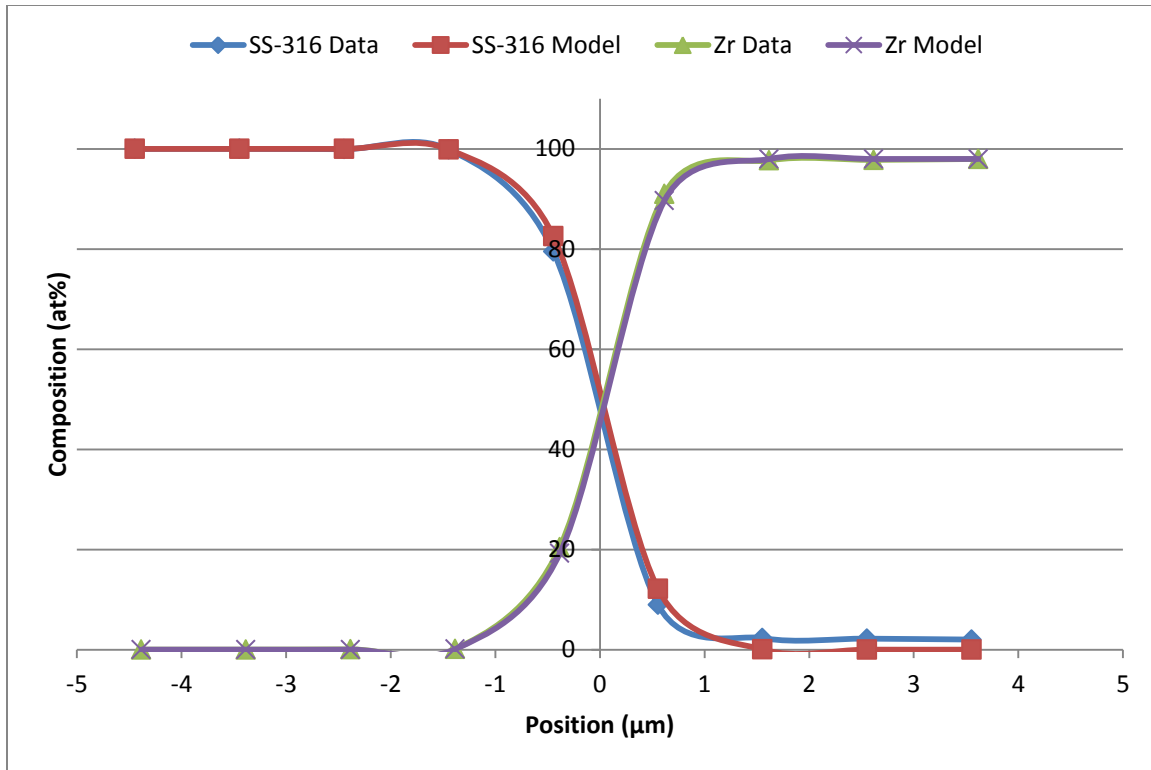


Figure 4-59. Model vs. WDS data for Zr/SS-316 interface after 28 days at 700°C.

The average diffusion coefficients for Zr/HT-9, Zr/G.91, Zr/SS-316 (averaged using the Maximum Likelihood Method described in Section 3.5), and Zr/Fe for all available temperatures are given in Table 4-12. Since data for multiple temperatures was only available for Zr/SS-316 and Zr/Fe they were the only systems for which activation energies could be calculated. Based on the measured diffusion coefficients, Zr/SS-316 diffusion had an activation energy of 55.3 ± 19.8 kJ/mol with a pre-exponential factor of $4.09E-17 \pm 1.0E-16$ m²/s, while Zr/Fe diffusion had an activation energy of 78.9 ± 5.5 kJ/mol with a pre-exponential factor of $1.12E-14 \pm 8.6E-15$ m²/s.

Table 4-12. Average diffusion coefficients for Zr with steel alloys and Fe.

T (°C)	Zr/HT-9		Zr/G.91		Zr/SS-316		Zr/Fe	
	D (m ² /s)	±	D (m ² /s)	±	D (m ² /s)	±	D (m ² /s)	±
550	N/A	N/A	N/A	N/A	1.45E-20	5.8E-21	1.11E-19	5E-21
625	N/A	N/A	N/A	N/A	N/A	N/A	2.90E-19	1.4E-20
700	N/A	N/A	N/A	N/A	4.37E-20	6.8E-21	N/A	N/A

4.3.3 Steel Diffusion with Titanium

For the eighteen Ti/Steel diffusion couples run at 550°C, diffusion data for Ti was successfully acquired in diffusion couples with HT-9, G.91, SS-316, and Fe. Representative WDS data and the associated models for Ti/HT-9, Ti/G.91, Ti/SS-316, and Ti/Fe diffusion after 28 or 56 days at 550°C are given in Figure 4-60, Figure 4-61, Figure 4-62, and Figure 4-63, respectively.

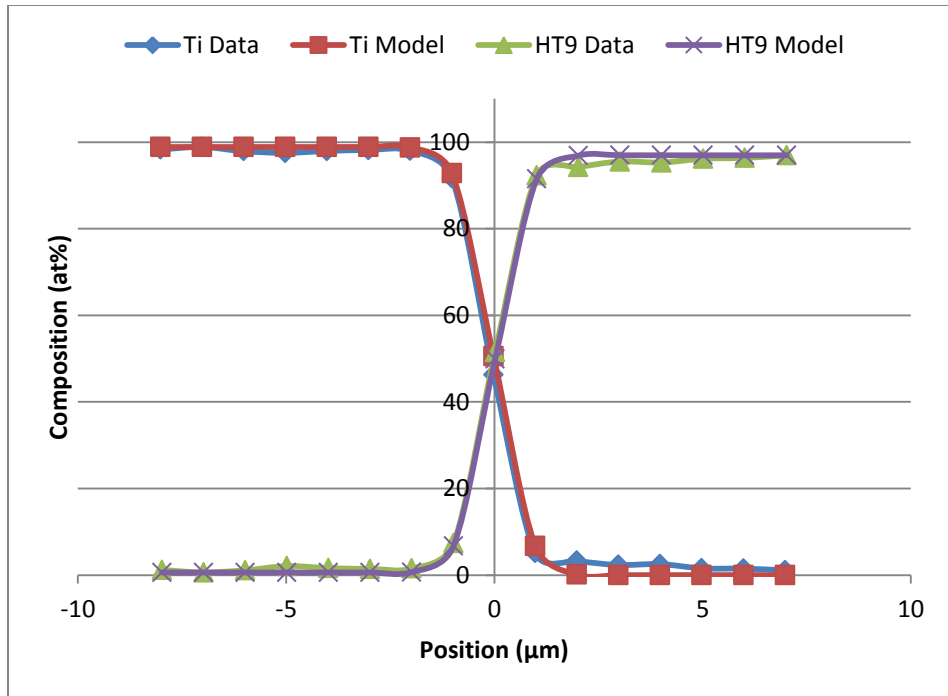


Figure 4-60. Model vs. WDS data for Ti/HT-9 interface after 56 days at 550°C.

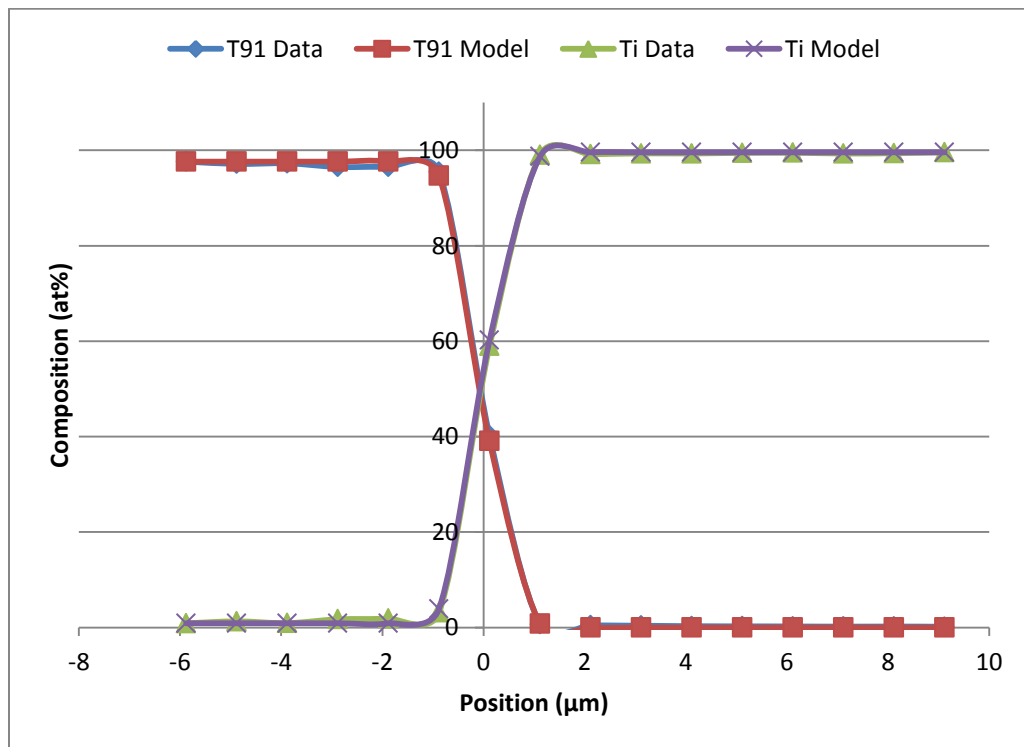


Figure 4-61. Model vs. WDS data for Ti/G.91 interface after 28 days at 550°C.

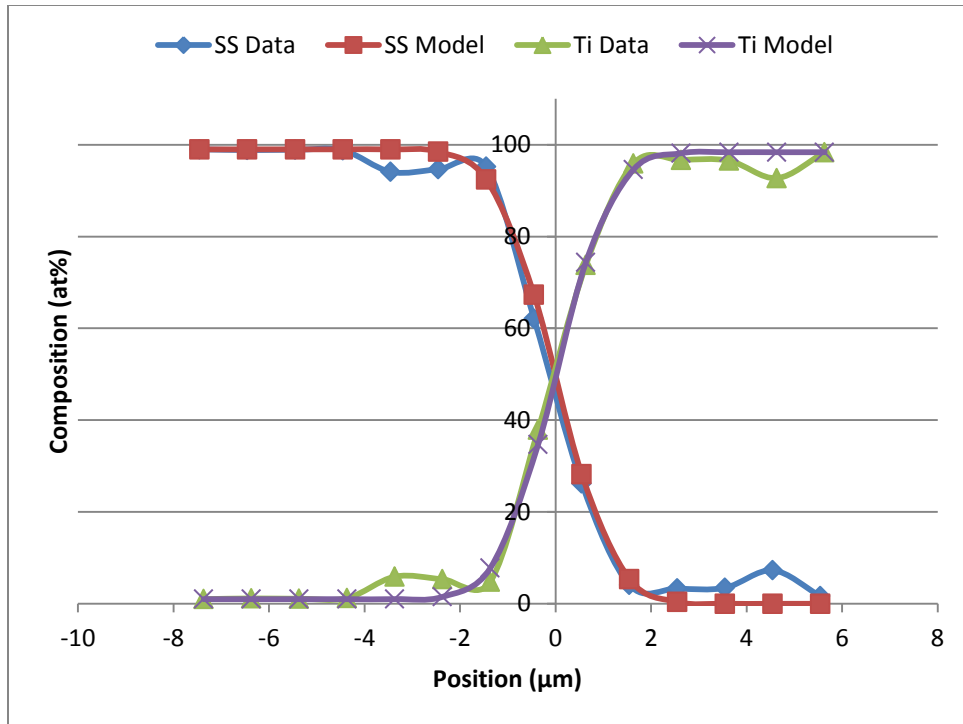


Figure 4-62. Model vs. WDS data for Ti/SS-316 interface after 28 days at 550°C.

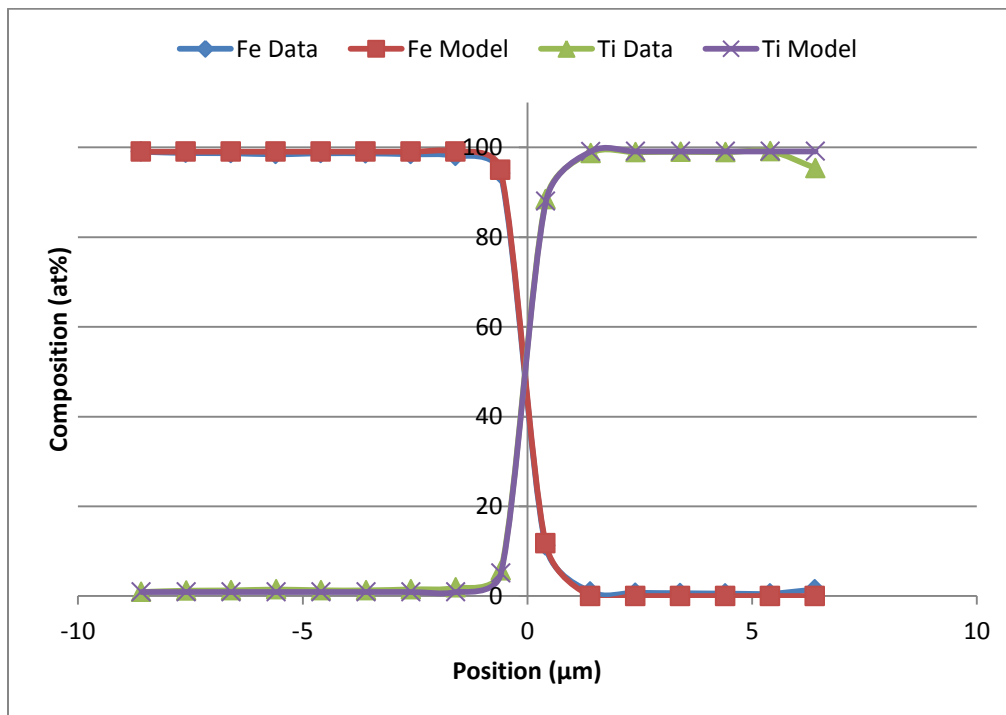


Figure 4-63. Model vs. WDS data for Ti/Fe interface after 28 days at 550°C.

For the eight Ti/Steel diffusion couples run at 625°C, diffusion data for Ti was only successfully acquired with G.91. Representative WDS data and the associated models for Ti/G.91 diffusion after 28 days at 625°C is given in Figure 4-64.

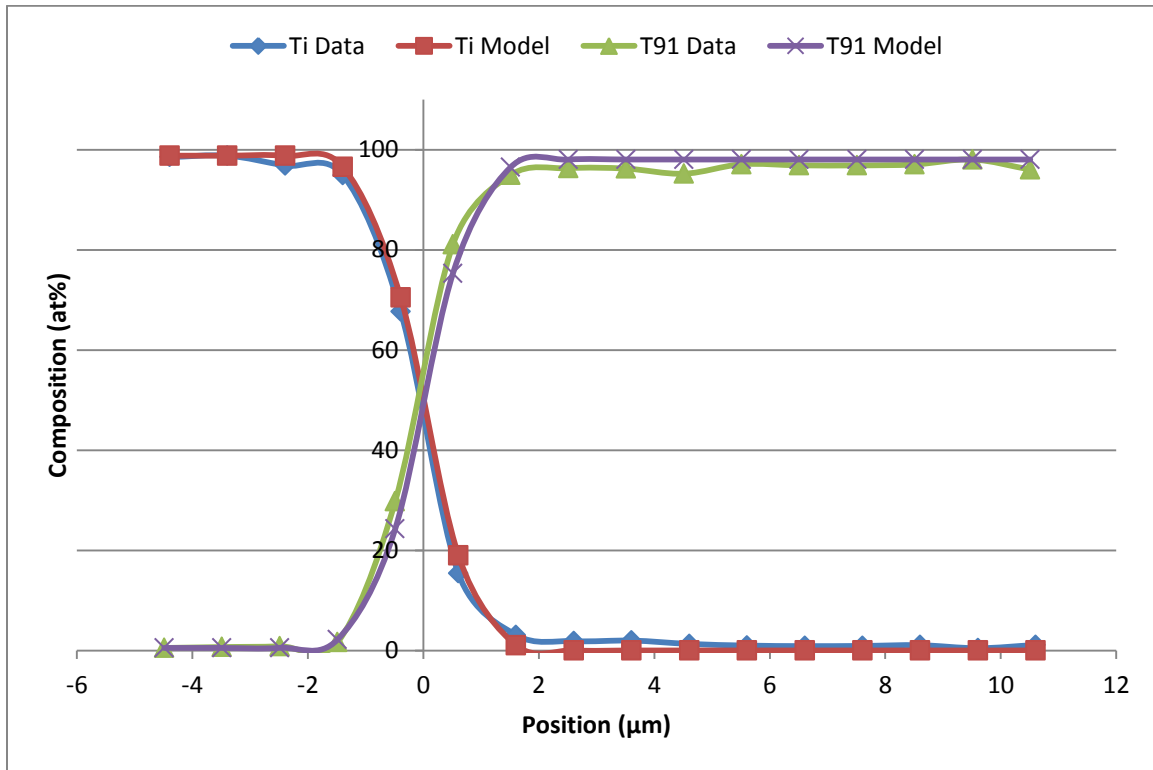


Figure 4-64. Model vs. WDS data for Ti/G.91 interface after 28 days at 625°C.

For the eight Ti/Steel diffusion couples run at 700°C, diffusion data for Ti was not successfully acquired for any of the steel alloys tested or iron.

The average diffusion coefficients for Ti/HT-9, Ti/G.91, Ti/SS-316, and Ti/Fe (averaged using the Maximum Likelihood Method described in Section 3.5) for all available temperatures are given in Table 4-13. Since data for multiple temperatures was only available for Ti/G.91, it was the only system for which an activation energy

could be calculated. Based on the measured diffusion coefficients, Ti/G.91 diffusion had an activation energy of 20 ± 27 kJ/mol with a pre-exponential factor of $8.5E-19 \pm 3.19E-18$ m²/s.

Table 4-13. Average diffusion coefficients for Ti with steel alloys and Fe.

T (°C)	Ti/HT-9		Ti/G.91		Ti/SS-316		Ti/Fe	
	D (m ² /s)	±	D (m ² /s)	±	D (m ² /s)	±	D (m ² /s)	±
550	3.22E-20	1.8E-21	4.56E-20	1.32E-20	1.76E-19	1.5E-20	1.42E-20	2.0E-21
625	N/A	N/A	5.83E-20	1.14E-20	N/A	N/A	N/A	N/A
700	N/A	N/A	N/A	N/A	N/A	N/A	N/A	N/A

4.3.4 Steel Diffusion with Molybdenum

Out of the eighteen Mo/Steel diffusion couples run at 550C, eight Mo/Steel diffusion couples run at 625C, and nine Mo/Steel diffusion couples run at 700C, diffusion data for Mo was only successfully acquired in diffusion couples with SS-316 at 625°C. No data was successfully acquired for other steel alloys or Fe, nor for other temperatures. Representative WDS data and the associated models for Mo/SS-316 diffusion after 28 days at 625°C are given in Figure 4-65. The averaged diffusion coefficients for Mo/SS-316 at 625°C was $2.80E-19 \pm 2.4E-20$ m²/s. Since data for multiple temperatures was not found, no activation energy could be calculated.

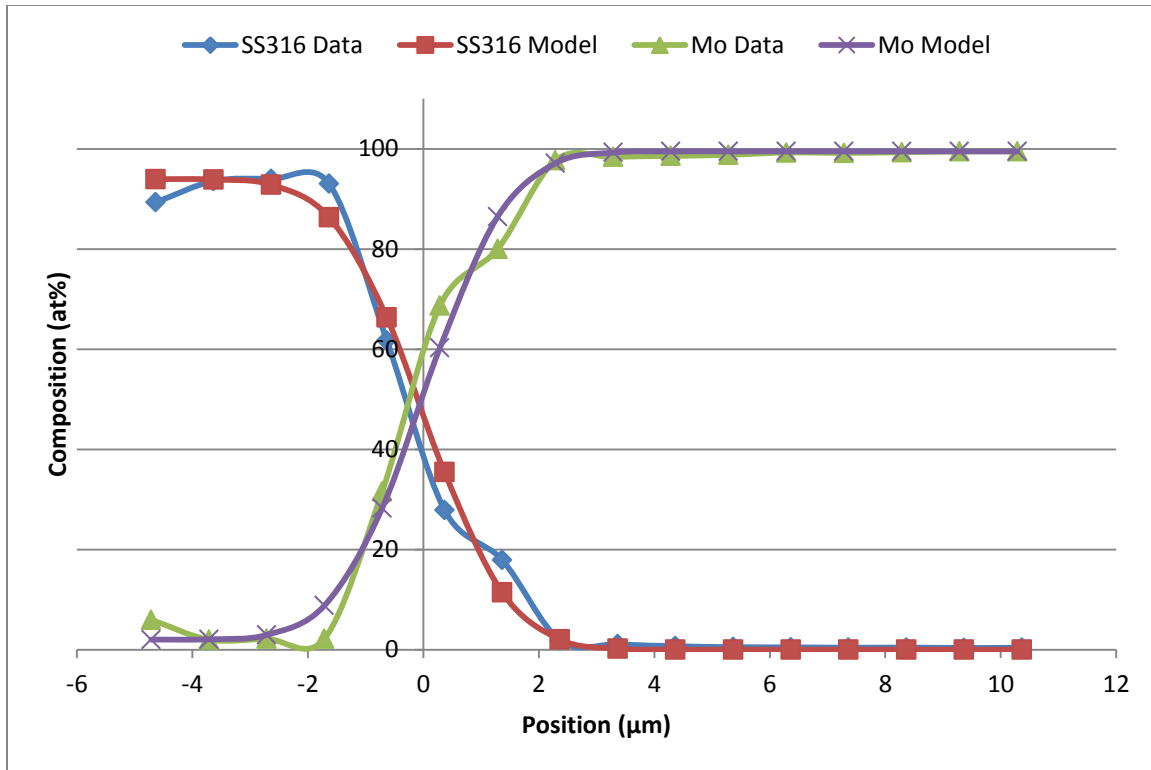


Figure 4-65. Model vs. WDS data for Mo/SS-316 interface after 28 days at 625°C.

4.3.5 Steel Diffusion with Tungsten

For the eighteen W/Steel diffusion couples run at 550°C, diffusion data for W was only successfully acquired with SS-316. Representative WDS data and the associated models for W/SS-316 diffusion after 56 days at 550°C is given in Figure 4-66.

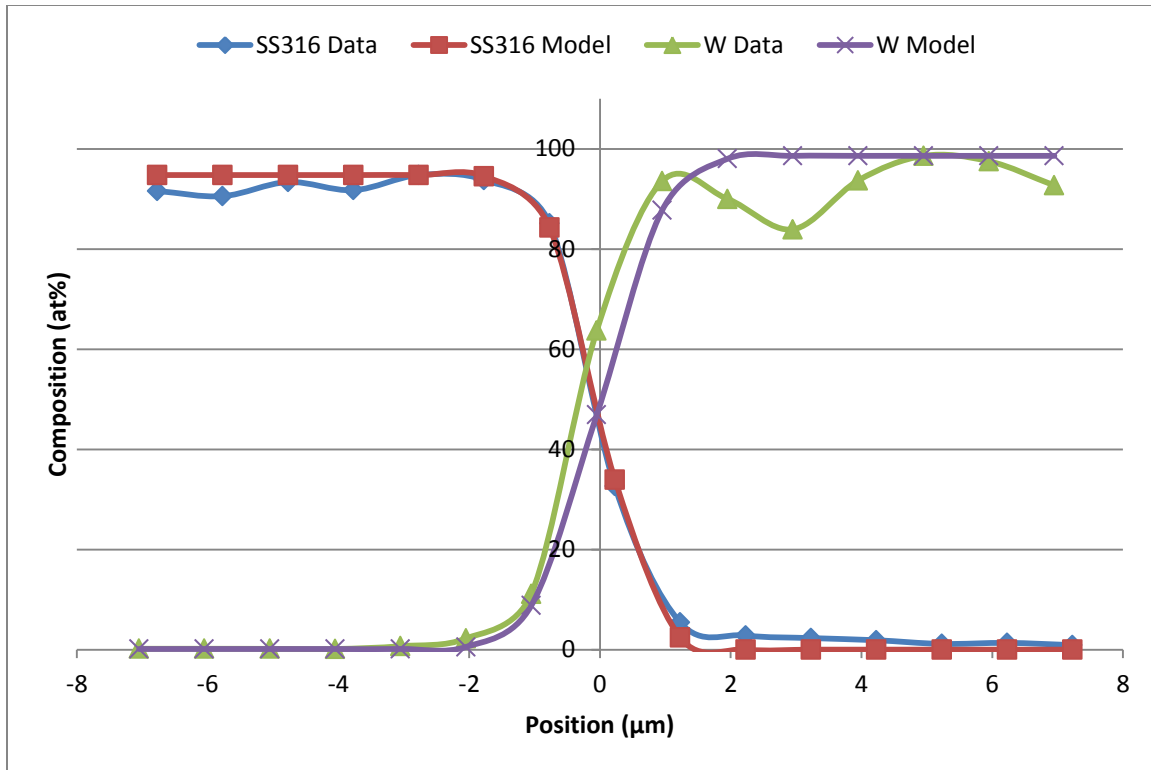


Figure 4-66. Model vs. WDS data for W/SS-316 interface after 56 days at 550°C.

For the eight W/Steel diffusion couples run at 625°C, diffusion data for W was only successfully acquired with SS-316. Representative WDS data and the associated models for W/SS-316 diffusion after 28 days at 625°C is given in Figure 4-67.

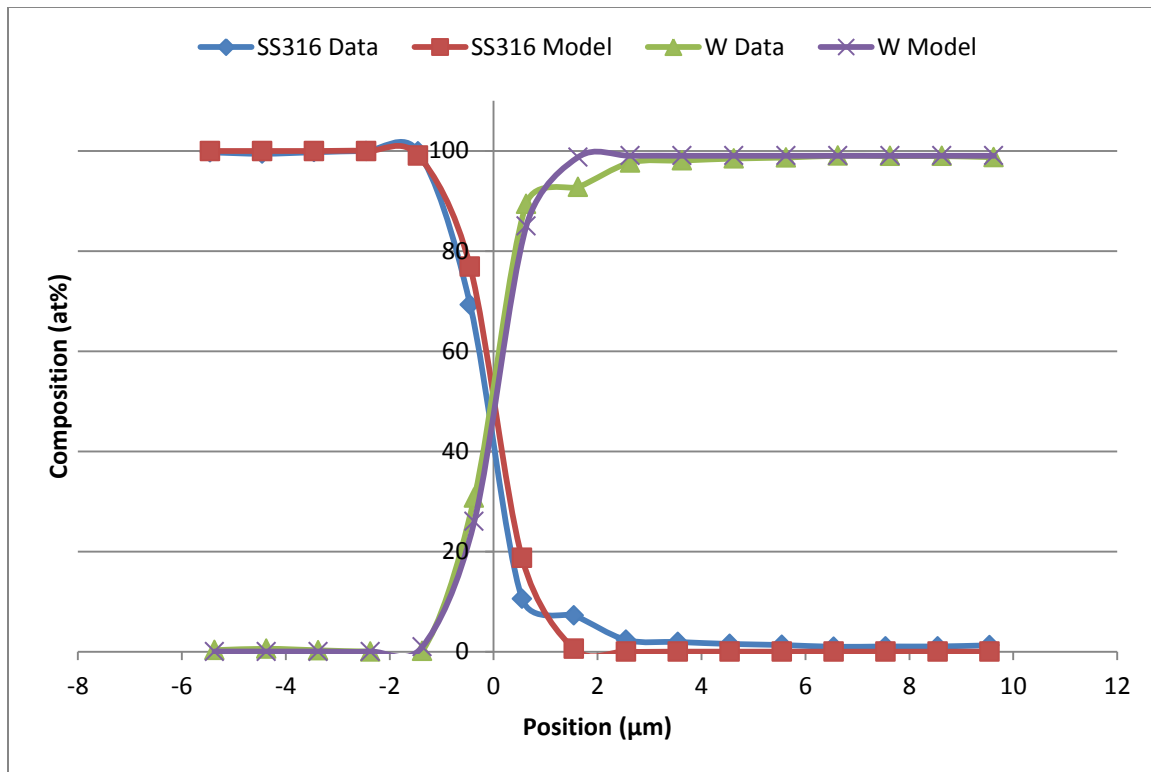


Figure 4-67. Model vs. WDS data for W/SS-316 interface after 28 days at 625°C.

For the eight W/Steel diffusion couples run at 700°C, diffusion data for W was not successfully acquired for any of the steel alloys tested or iron. The average diffusion coefficients for W/HT-9, W/G.91, W/SS-316, and W/Fe (averaged using the Maximum Likelihood Method described in Section 3.5) for all available temperatures are given in Table 4-14. Since data for multiple temperatures was only available for W/SS-316, it was the only system for which an activation energy could be calculated. Based on the measured diffusion coefficients, W/SS-316 diffusion had an activation energy of 20 ± 22 kJ/mol with a pre-exponential factor of $1.1E-18 \pm 3.5E-18$ m²/s.

Table 4-14. Average diffusion coefficients for W with steel alloys and Fe.

T (°C)	W/HT-9		W/G.91		W/SS-316		W/Fe	
	D (m ² /s)	±	D (m ² /s)	±	D (m ² /s)	±	D (m ² /s)	±
550	N/A	N/A	N/A	N/A	5.79E-20	1.27E-20	N/A	N/A
625	N/A	N/A	N/A	N/A	7.42E-20	1.21E-20	N/A	N/A
700	N/A	N/A	N/A	N/A	N/A	N/A	N/A	N/A

4.3.6 Steel Diffusion with Tantalum

For the eighteen Ta/Steel diffusion couples run at 550°C, diffusion data for Ta was only successfully acquired with G.91. Representative WDS data and the associated models for Ta/G.91 diffusion after 56 days at 550°C is given in Figure 4-68.

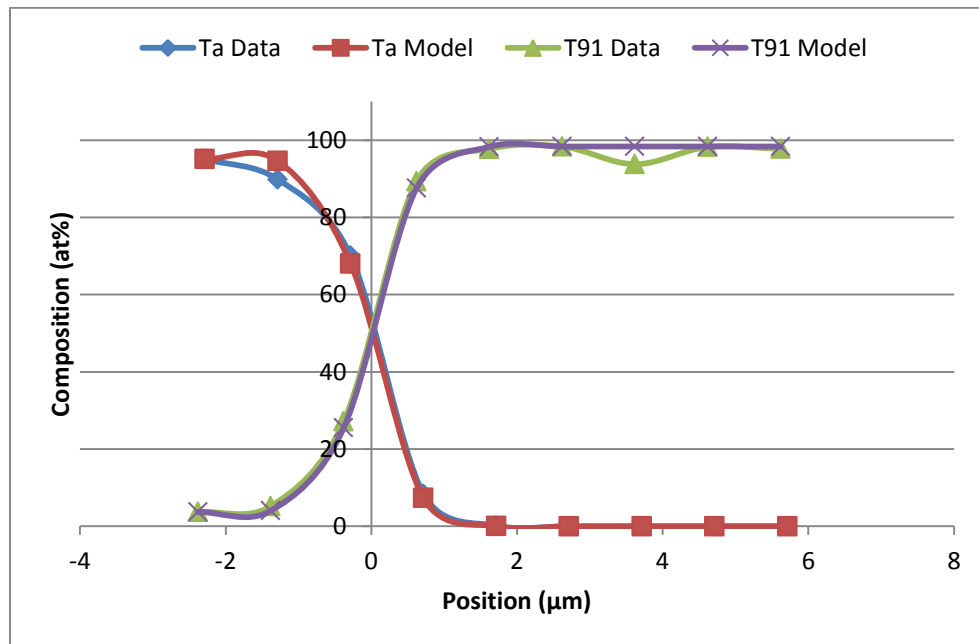


Figure 4-68. Model vs. WDS data for Ta/G.91 interface after 56 days at 550°C.

For the eight Ta/Steel diffusion couples run at 625°C, diffusion data for Ta was only successfully acquired with SS-316. Representative WDS data and the associated models for Ta/SS-316 diffusion after 28 days at 625°C is given in Figure 4-69.

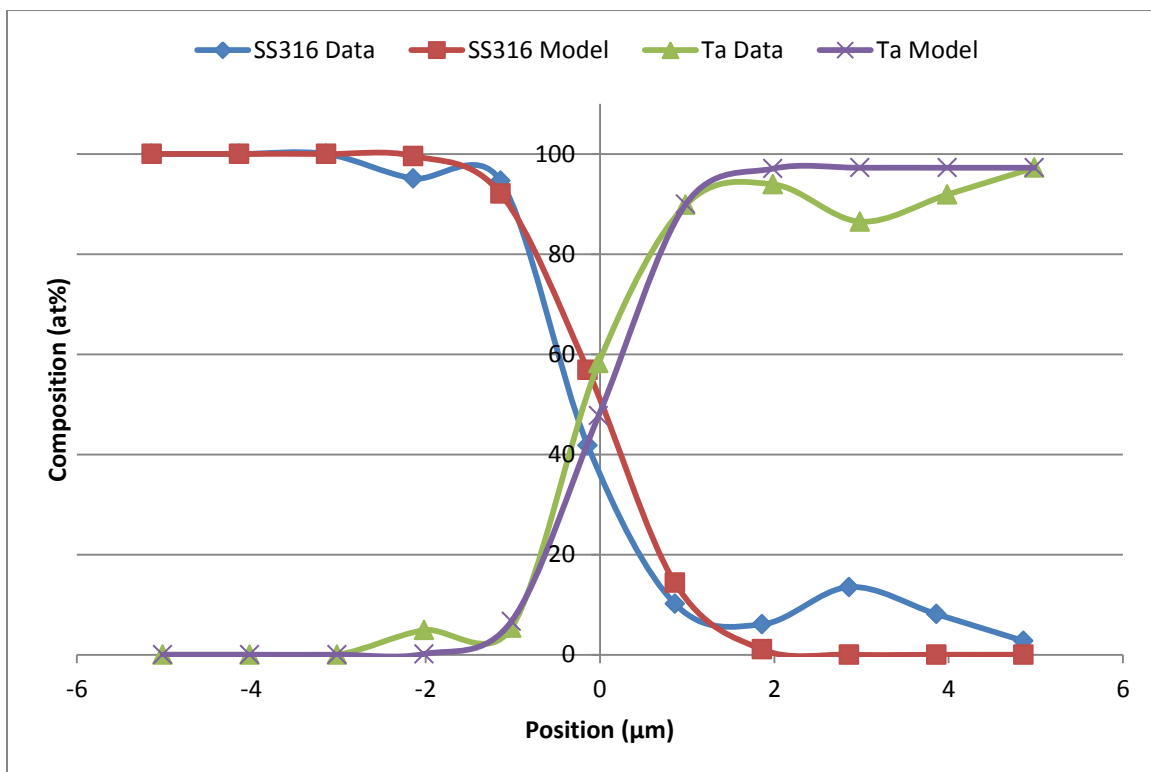


Figure 4-69. Model vs. WDS data for Ta/SS-316 interface after 28 days at 625°C.

For the eight Ta/Steel diffusion couples run at 700°C, diffusion data for Ta was not successfully acquired for any of the steel alloys tested or iron. The average diffusion coefficients for Ta/HT-9, Ta/G.91, Ta/SS-316, and Ta/Fe (averaged using the

Maximum Likelihood Method described in Section 3.5) for all available temperatures are given in Table 4-15. Since data for multiple temperatures was not found for any steel alloy, activation energies could not be calculated.

Table 4-15. Average diffusion coefficients for Ta with steel alloys and Fe.

T (°C)	Ta/HT-9		Ta/G.91		Ta/SS-316		Ta/Fe	
	D (m ² /s)	±	D (m ² /s)	±	D (m ² /s)	±	D (m ² /s)	±
550	N/A	N/A	2.78E-20	4.0E-21	N/A	N/A	N/A	N/A
625	N/A	N/A	N/A	N/A	1.54E-19	1.2E-20	N/A	N/A
700	N/A	N/A	N/A	N/A	N/A	N/A	N/A	N/A

4.4. Liner/Liner Diffusion

Diffusion between vanadium and other liner materials was characterized by typical interdiffusion curves. In some cases, the two liners failed to bond or broke apart upon removal from the furnace; however, since each combination was repeated four times for each time and temperature combination, diffusion data was acquired for most cases.

4.4.1 Vanadium Diffusion with Zirconium

Diffusion curves between V and Zr were successfully acquired for each temperature studied. Representative WDS data along with the associated models for V/Zr diffusion aft 56 days at 550°C and 28 days at 625°C and 700°C are given in Figure 4-70, Figure 4-71, and Figure 4-72, respectively.

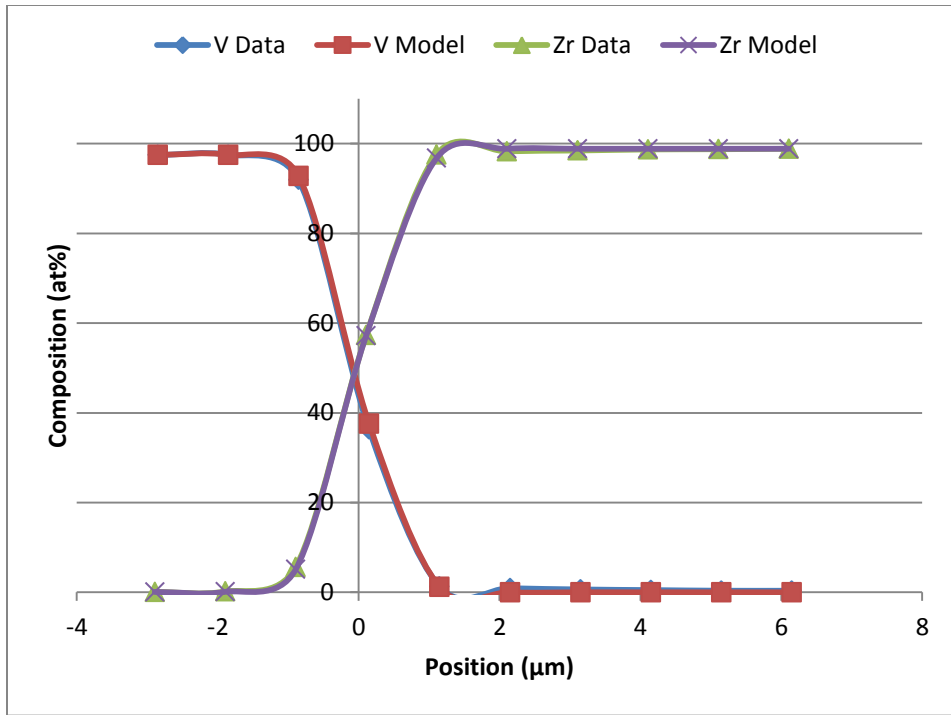


Figure 4-70. Model vs. WDS data for V/Zr interface after 56 days at 550°C.

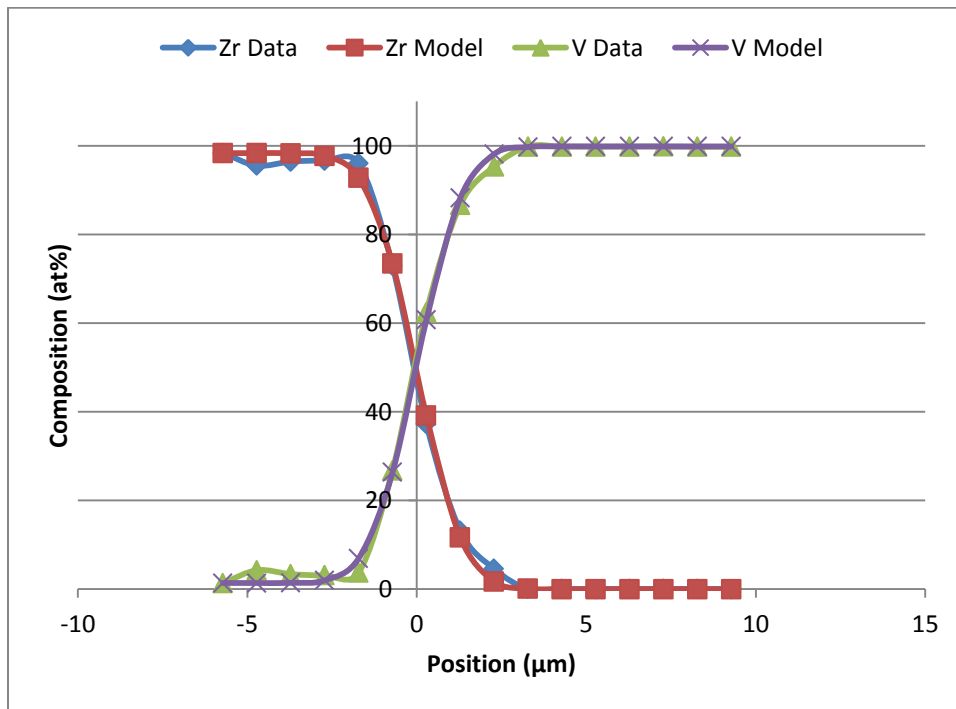


Figure 4-71. Model vs. WDS data for V/Zr interface after 28 days at 625°C.

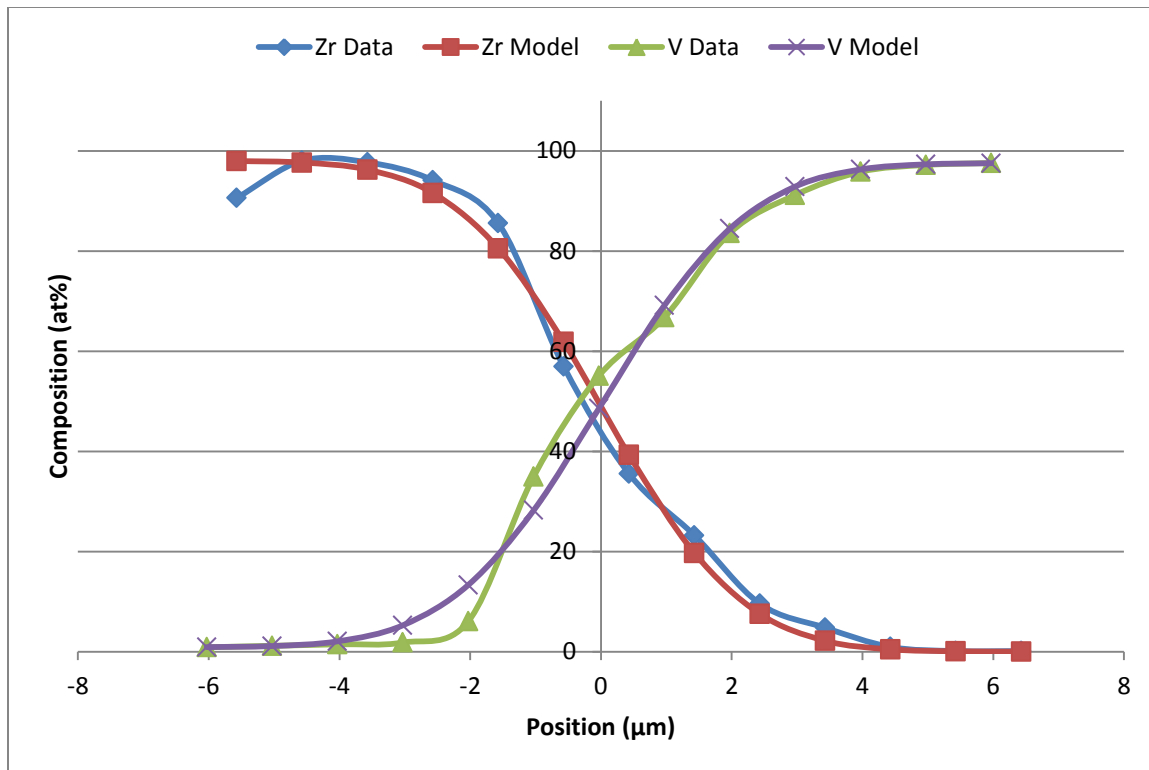


Figure 4-72. Model vs. WDS data for V/Zr interface after 28 days at 625°C.

Average values for V/Zr diffusion (averaged using the Maximum Likelihood Method described in Section 3.5) at each temperature are given in Table 4-16. Based on these measured diffusion coefficients, the activation energy for V/Zr diffusion was calculated to be 136.3 ± 6.3 kJ/mol with a pre-exponential factor of $1.6E-11 \pm 1.4E-11$ m²/s.

Table 4-16. Average diffusion coefficients for V with Zr.

T (°C)	D (m ² /s)	±
550	3.12E-20	3.8E-21
625	2.60E-19	1.2E-20
700	6.55E-19	5.4E-20

4.4.2 Vanadium Diffusion with Titanium

Diffusion curves between V and Ti were successfully acquired for 550°C and 625°C, but not 700°C. Representative WDS data along with the associated models for V/Ti diffusion after 56 days at 550°C and 28 days at 625°C are given in Figure 4-73 and Figure 4-74, respectively.

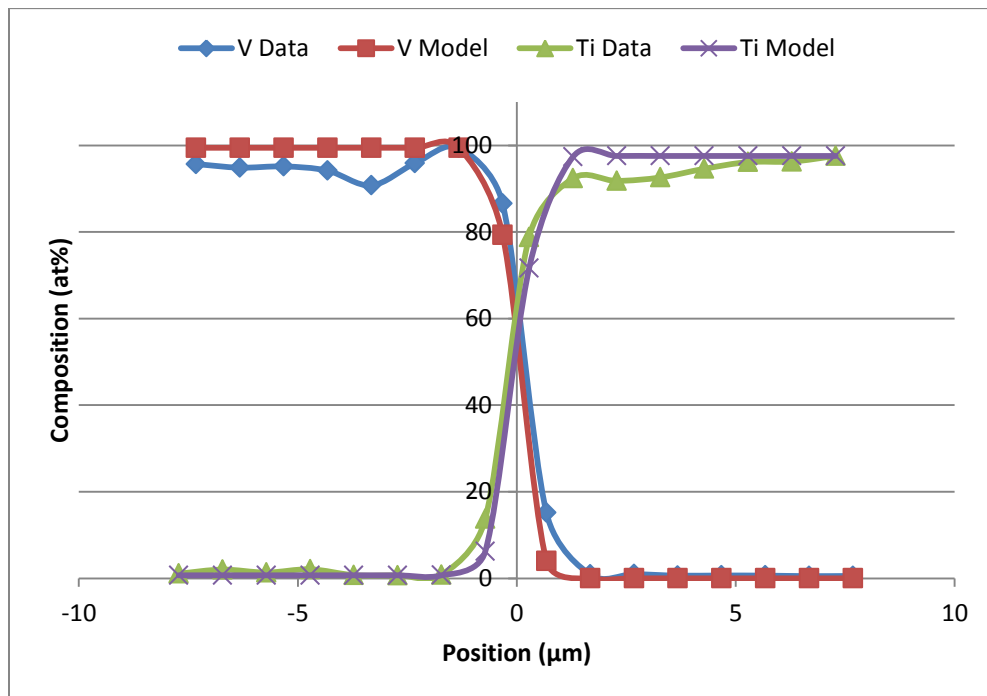


Figure 4-73. Model vs. WDS data for V/Ti interface after 56 days at 550°C.

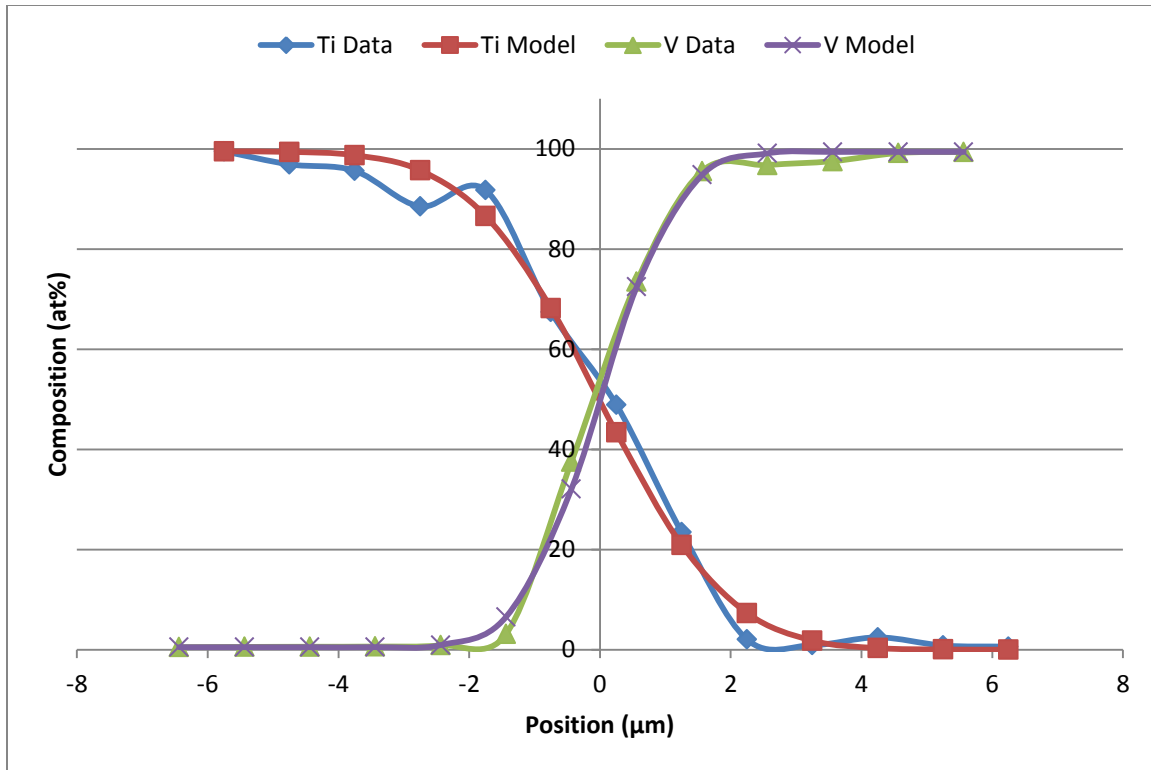


Figure 4-74. Model vs. WDS data for V/Ti interface after 28 days at 625°C.

Average values for V/Ti diffusion (averaged using the Maximum Likelihood Method described in Section 3.5) at each temperature are given in Table 4-17. Based on these measured diffusion coefficients, the activation energy for V/Ti diffusion was calculated to be 96.9 ± 19.0 kJ/mol with a pre-exponential factor of $3.6\text{E-}14 \pm 9.26\text{E-}13$ m²/s.

Table 4-17. Average diffusion coefficients for V with Ti.

T (°C)	D (m ² /s)	±
550	2.54E-20	5.1E-21
625	8.28E-20	9.4E-21
700	N/A	N/A

4.4.3 Vanadium Diffusion with Molybdenum

Diffusion curves between V and Mo were successfully acquired only at 550°C. Representative WDS data along with the associated models for V/Mo diffusion after 17.5 days at 550°C are given in Figure 4-75. The averaged diffusion coefficient for V/Mo at 550°C was $2.01\text{E-}19 \pm 2.7\text{E-}20$ m²/s. Since data was available for only one temperature, no activation energy could be calculated.

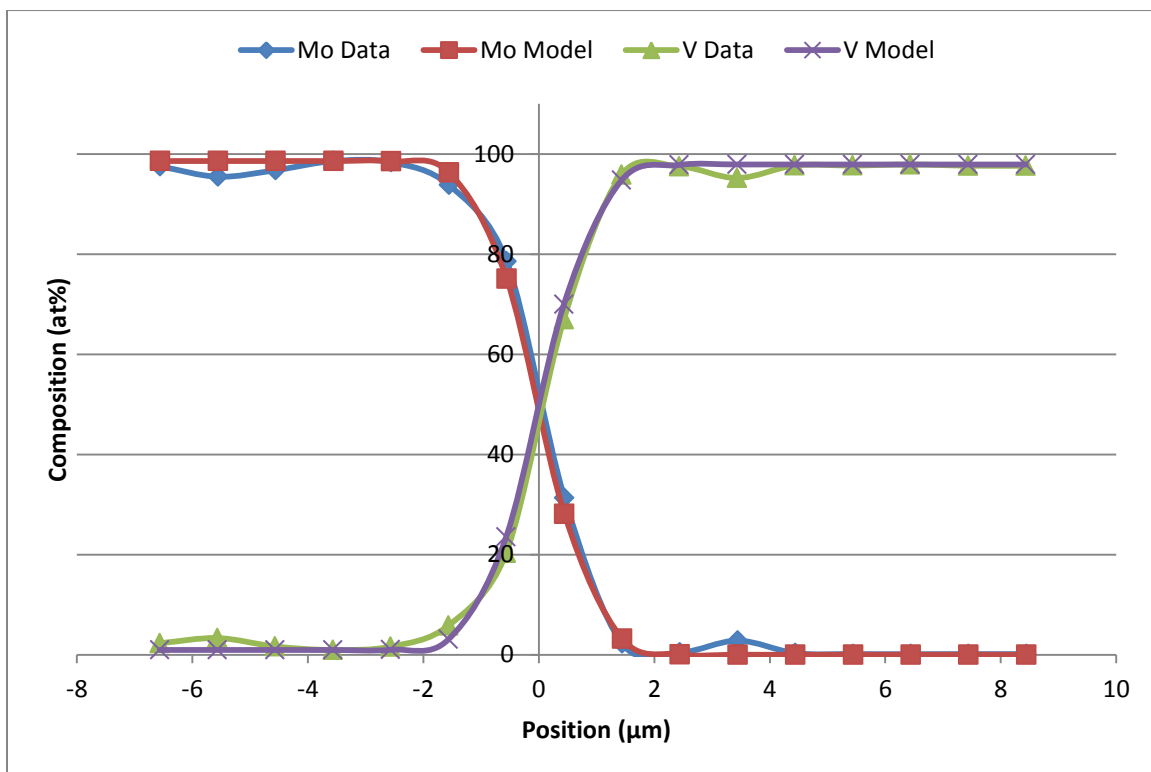


Figure 4-75. Model vs. WDS data for V/Mo interface after 56 days at 550°C.

4.4.4 Vanadium Diffusion with Tungsten

Diffusion curves between V and W were successfully acquired for 550°C and 625°C, but not 700°C. Representative WDS data along with the associated models

for V/W diffusion after 56 days at 550°C and 28 days at 625°C are given in Figure 4-76 and Figure 4-77, respectively.

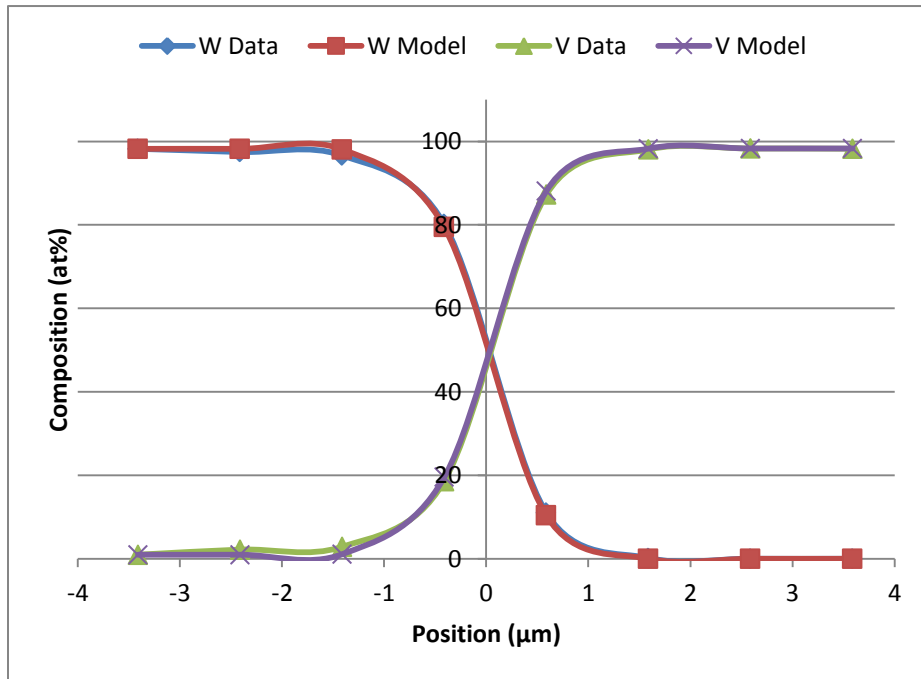


Figure 4-76. Model vs. WDS data for V/W interface after 56 days at 550°C.

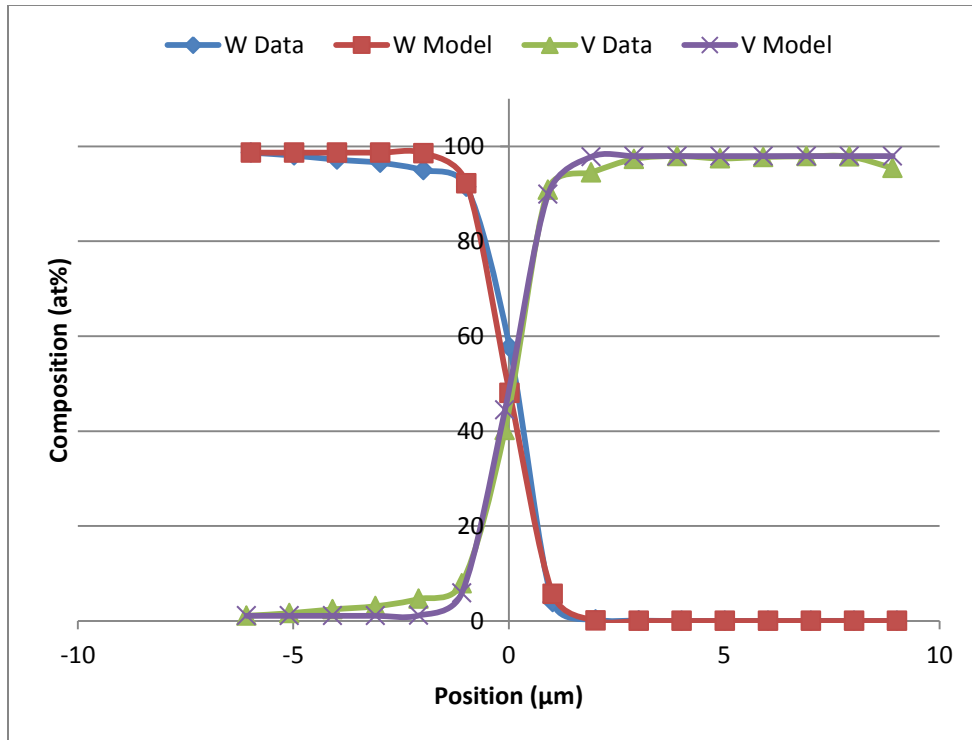


Figure 4-77. Model vs. WDS data for V/W interface after 28 days at 625°C.

Average values for V/W diffusion (averaged using the Maximum Likelihood Method described in Section 3.5) at each temperature are given in Table 4-18. Based on these measured diffusion coefficients, the activation energy for V/W diffusion was calculated to be 117.0 ± 14.9 kJ/mol with a pre-exponential factor of $6.1E-11 \pm 1.25E-12$ m²/s.

Table 4-18. Average diffusion coefficients for V with W.

T (°C)	D (m ² /s)	±
550	2.28E-20	3.5E-21
625	9.52E-20	9.2E-21
700	N/A	N/A

4.4.5 Vanadium Diffusion with Tantalum

Vanadium did not successfully bond with tantalum in any of the seventeen V/Ta diffusion couples tested. Thus, no data on V/Ta diffusion was collected.

5 DISCUSSION

The extensive set of diffusion interfaces analyzed above has revealed new diffusion parameters for the systems of interest. Table 5-1, Table 5-2, Table 5-3, and Table 5-4 summarize all of the calculated diffusion coefficients and the activation energies and pre-exponential values that were reported separately throughout Section 4. These values provide new information that is valuable for the prediction of FCCI performance in advanced metallic fuel systems. In addition to the creation of this new engineering information, several observations will be discussed below that reveal new and deeper understanding of the diffusion behavior recorded in Section 4. Section 5.1 discusses the impact of the Nd-steel intermetallic formations, including the observation of the $\text{Nd}_5\text{Fe}_{17}$ phase not commonly observed in prior FCCI diffusion studies and the Nd_3Ni phase which has never previously been observed in FCCI diffusion studies. Sections 5.2 and 5.3 examine the comparative diffusive behavior of the liner materials studied with neodymium and steel, respectively. Finally, Section 5.4 provides a brief set of simple comparative studies as a companion to the diffusion data that summarize additional impacts from liner thickness and material on nuclear reactivity and thermal energy transport.

Table 5-1. Summary of diffusion data for steel with neodymium.

		Nd ₂ (Fe+Cr) ₁₇		Nd ₅ (Fe+Cr) ₁₇		NdFe ₂	
		D (m ² /s)	±	D (m ² /s)	±	D (m ² /s)	±
HT-9/Nd	17.5 days at 550°C	2.22E-16	4.60E-17	4.04E-18	1.33E-18	2.97E-17	2.38E-17
	28 days at 550°C	2.23E-16	5.10E-17	4.71E-18	1.33E-18	3.30E-17	1.57E-17
	56 days at 550°C	1.80E-16	4.20E-17	4.74E-17	1.14E-17	2.58E-17	1.15E-17
	28 days at 625°C	1.84E-15	4.20E-16	N/A	N/A	N/A	N/A
	28 days at 700°C	3.21E-13	4.10E-14	N/A	N/A	N/A	N/A
		Nd ₂ (Fe+Cr) ₁₇		Nd ₅ (Fe+Cr) ₁₇		NdFe ₂	
		D (m ² /s)	±	D (m ² /s)	±	D (m ² /s)	±
G.91/Nd	28 days at 550°C	1.09E-16	2.60E-17	1.06E-17	2.50E-18	8.25E-18	4.04E-18
	56 days at 550°C	1.09E-16	2.10E-17	1.43E-17	4.00E-18	9.28E-18	4.33E-18
	28 days at 625°C	2.02E-15	4.40E-16	N/A	N/A	3.30E-17	1.51E-17
	28 days at 700°C	4.67E-13	7.50E-14	N/A	N/A	N/A	N/A
		Nd ₂ (Fe+Cr) ₁₇		Nd ₅ (Fe+Cr) ₁₇		NdFe ₂	
		D (m ² /s)	±	D (m ² /s)	±	D (m ² /s)	±
SS-316/Nd	28 days at 550°C	3.08E-15	3.90E-16	N/A	N/A	9.09E-16	4.40E-16
	56 days at 550°C	4.32E-15	5.20E-16	N/A	N/A	4.55E-16	2.20E-16
	28 days at 625°C	2.85E-13	3.70E-14	N/A	N/A	N/A	N/A
	28 days at 700°C	6.91E-13	6.50E-14	N/A	N/A	N/A	N/A

Table 5-2. Summary of diffusion data for liners with neodymium.

	V/Nd		Zr/Nd		Ti/Nd	
T (°C)	D (m ² /s)	±	D (m ² /s)	±	D (m ² /s)	±
550	9.95E-20	7.0E-21	5.61E-20	3.2E-21	2.38E-19	1.1E-20
625	3.38E-19	2.0E-20	6.61E-20	7.6E-21	2.82E-19	1.9E-20
700	4.54E-19	4.9E-20	1.32E-19	8E-21	5.65E-19	6.0E-20
	Q (kJ/mol)	±	Q (kJ/mol)	±	Q (kJ/mol)	±
	68.4	5.3	37.1	3.6	37.7	4.5
	D ₀ (m ² /s)	±	D ₀ (m ² /s)	±	D ₀ (m ² /s)	±
	2.5E-15	1.8E-15	1.16E-17	5.6E-18	5.4E-17	3.4E-17
	Mo/Nd		W/Nd		Ta/Nd	
T (°C)	D (m ² /s)	±	D (m ² /s)	±	D (m ² /s)	±
550	4.13E-20	1.6E-21	3.93E-20	1.9E-21	1.09E-19	1.3E-20
625	9.98E-20	4.9E-21	4.66E-20	4.6E-21	9.81E-20	8.51E-20
700	1.02E-19	8E-21	7.82E-20	8.7E-21	3.85E-20	3.7E-21
	Q (kJ/mol)	±	Q (kJ/mol)	±	Q (kJ/mol)	±
	41.0	3.5	30.0	5.0	-45.0	6.7
	D ₀ (m ² /s)	±	D ₀ (m ² /s)	±	D ₀ (m ² /s)	±
	1.85E-17	9.0E-18	3.0E-18	2.1E-18	1.8E-22	1.6E-22

Table 5-3. Summary of diffusion data for liners with steel alloys and iron.

T (°C)	V/HT-9		V/G.91		V/SS-316		V/Fe	
	D (m ² /s)	±	D (m ² /s)	±	D (m ² /s)	±	D (m ² /s)	±
550	2.44E-20	2.1E-21	N/A	N/A	N/A	N/A	N/A	N/A
625	N/A	N/A	N/A	N/A	5.22E-19	3.3E-20	N/A	N/A
700	4.90E-20	8.0E-21	5.48E-20	4.7E-21	N/A	N/A	N/A	N/A
T (°C)	Zr/HT-9		Zr/G.91		Zr/SS-316		Zr/Fe	
	D (m ² /s)	±	D (m ² /s)	±	D (m ² /s)	±	D (m ² /s)	±
550	N/A	N/A	N/A	N/A	1.45E-20	5.8E-21	1.11E-19	5E-21
625	N/A	N/A	N/A	N/A	N/A	N/A	2.90E-19	1.4E-20
700	N/A	N/A	N/A	N/A	4.37E-20	6.8E-21	N/A	N/A
T (°C)	Ti/HT-9		Ti/G.91		Ti/SS-316		Ti/Fe	
	D (m ² /s)	±	D (m ² /s)	±	D (m ² /s)	±	D (m ² /s)	±
550	3.22E-20	1.8E-21	4.56E-20	1.32E-20	1.76E-19	1.5E-20	1.42E-20	2.0E-21
625	N/A	N/A	5.83E-20	1.14E-20	N/A	N/A	N/A	N/A
700	N/A	N/A	N/A	N/A	N/A	N/A	N/A	N/A
T (°C)	Mo/HT-9		Mo/G.91		Mo/SS-316		Mo/Fe	
	D (m ² /s)	±	D (m ² /s)	±	D (m ² /s)	±	D (m ² /s)	±
550	N/A	N/A	N/A	N/A	N/A	N/A	N/A	N/A
625	N/A	N/A	N/A	N/A	2.80E-19	2.4E-20	N/A	N/A
700	N/A	N/A	N/A	N/A	N/A	N/A	N/A	N/A
T (°C)	W/HT-9		W/G.91		W/SS-316		W/Fe	
	D (m ² /s)	±	D (m ² /s)	±	D (m ² /s)	±	D (m ² /s)	±
550	N/A	N/A	N/A	N/A	5.79E-20	1.27E-20	N/A	N/A
625	N/A	N/A	N/A	N/A	7.42E-20	1.21E-20	N/A	N/A
700	N/A	N/A	N/A	N/A	N/A	N/A	N/A	N/A
T (°C)	Ta/HT-9		Ta/G.91		Ta/SS-316		Ta/Fe	
	D (m ² /s)	±	D (m ² /s)	±	D (m ² /s)	±	D (m ² /s)	±
550	N/A	N/A	2.78E-20	4.0E-21	N/A	N/A	N/A	N/A
625	N/A	N/A	N/A	N/A	1.54E-19	1.2E-20	N/A	N/A
700	N/A	N/A	N/A	N/A	N/A	N/A	N/A	N/A

Table 5-4. Summary of diffusion data for dual-layer liners.

	V/Zr		V/Ti		V/Mo	
T (°C)	D (m ² /s)	±	D (m ² /s)	±	D (m ² /s)	±
550	3.12E-20	3.8E-21	2.54E-20	5.10E-21	2.01E-19	2.7E-20
625	2.60E-19	1.2E-20	8.28E-20	9.40E-21	N/A	N/A
700	6.55E-19	5.4E-20	N/A	N/A	N/A	N/A
	Q (kJ/mol)	±	Q (kJ/mol)	±	Q (kJ/mol)	±
	136.3	6.3	96.9	19.0	N/A	N/A
	D ₀ (m ² /s)	±	D ₀ (m ² /s)	±	D ₀ (m ² /s)	±
	1.6E-11	1.4E-11	3.60E-14	9.26E-13	N/A	N/A
	V/W		V/Ta			
T (°C)	D (m ² /s)	±	D (m ² /s)	±		
550	2.28E-20	3.50E-21	N/A	N/A		
625	9.52E-20	9.20E-21	N/A	N/A		
700	N/A	N/A	N/A	N/A		
	Q (kJ/mol)	±	Q (kJ/mol)	±		
	117.0	14.9	N/A	N/A		
	D ₀ (m ² /s)	±	D ₀ (m ² /s)	±		
	6.10E-11	1.25E-12	N/A	N/A		

5.1 Nd/Steel Intermetallic Phases

One of the significant results revealed by the diffusion data described in Section 4 (beyond the comprehensive engineering parameters summarized in Table 5-1, Table 5-2, Table 5-3, and Table 5-4) is the improved understanding of the intermetallic phases that form between Nd and steel. First, the inclusion of multiple steel alloys (i.e., HT-9, G.91, and SS-316) illuminated of the impact of various alloying elements on the formation of intermetallic diffusion phases. Second, couples annealed at multiple temperatures allowed for the determination of governing activation energies as well as the dependence of intermetallic zone composition on temperature; this is especially important when considering fuel

performance predictions at long operation times or at very high burnup levels. The inclusion of a range of diffusion annealing times, especially times significantly longer than those in previously published research [60, 59], allowed for the elucidation of the development with time of multiple intermetallic phases as well as the identification of intermetallic phases not previously observed. The following sections elaborate on each of these points.

5.1.1 $\text{Nd}_2(\text{Fe}+\text{Cr})_{17}$ Phase

The $\text{Nd}_2(\text{Fe}+\text{Cr})_{17}$ was the broadest of the observed intermetallic diffusion phases to form, as well as being the analogue to the phase most commonly observed in FCCI in actual reactors [20]. Therefore, this particular “2-17” intermetallic phase and the factors controlling its development are the most critical when considering lanthanide/cladding interactions in reactors. The thermodynamic driving force for the diffusive interaction between steel and neodymium to form the 2-17 phase is the Gibbs Free Energy of formation for the $\text{Nd}_2\text{Fe}_{17}$ intermetallic. In some cases, the 2-17 phase was in apparent thermodynamic equilibrium with fine 5-17 precipitants dispersed within the diffusion zone, as shown in Figure 4-5. This occurred in some cases at low temperatures (e.g. HT-9/Nd at 550°C, Figure 4-5), but not in others (e.g. SS-316/Nd at 550°C, Figure 4-18), and in some cases at high temperatures (e.g. SS-316/Nd at 700°C Figure 4-20), but not in others (e.g. HT-9/Nd at 700°C, Figure 4-8). This varied behavior indicates that the determining factor for the precipitation of the 5-17 phase within the 2-17 phase is not a change in thermodynamics with temperature, but rather is a product of the kinetics of the diffusion reaction and the resulting higher local elemental compositions in each zone.

The rate-limiting factor controlling the growth of the $\text{Nd}_2(\text{Fe}+\text{Cr})_{17}$ phase is the diffusion of Nd through the phase. This becomes clear when examining the observable behavior of the $\text{Nd}_2(\text{Fe}+\text{Cr})_{17}$ phase in the three Nd/HT-9 couples

performed at 550°C. As shown in Figure 5-1, in the shortest diffusion anneal of 17.5 days at 550°C, the Nd concentration at the HT-9 edge of the $\text{Nd}_2(\text{Fe}+\text{Cr})_{17}$ phase was consistent with the theoretical 10.5 atom %Nd expected for the phase. However, across the width of the 2-17 phase, the Nd concentration gradually increased until it reaches ~15at% immediately adjacent to the $\text{Nd}_5(\text{Fe}+\text{Cr})_{17}$ phase. The excess Nd in the $\text{Nd}_2(\text{Fe}+\text{Cr})_{17}$ phase indicates that the diffusion of Nd into the 2-17 phase from bulk Nd is not rate-limiting. Additionally, the stoichiometric balance at the $\text{Nd}_2(\text{Fe}+\text{Cr})_{17}$ /HT-9 interface indicates that interaction of the bulk HT-9 with Nd at the leading edge of the diffusion zone (as evidenced by the 2-17 phase formation) is not the rate-limiting step. Thus, the rate-limiting step in the growth of the $\text{Nd}_2(\text{Fe}+\text{Cr})_{17}$ phase appears to be the diffusion of Nd through the phase to combine with HT-9 components to advance the leading edge of the reaction zone.

While in some areas Nd above the expected 10.5 at% for the 2-17 phase appears to have been incorporated into the phase, based on the BSE images of the interfaces there were also contained fine precipitates of the 5-17 phase in some areas. These precipitates were typically too small to be analyzed by WDS, but their contribution to the smear compositions over the 1 μm beam diameter effectively increased the Nd concentration measured in the 2-17 phase.

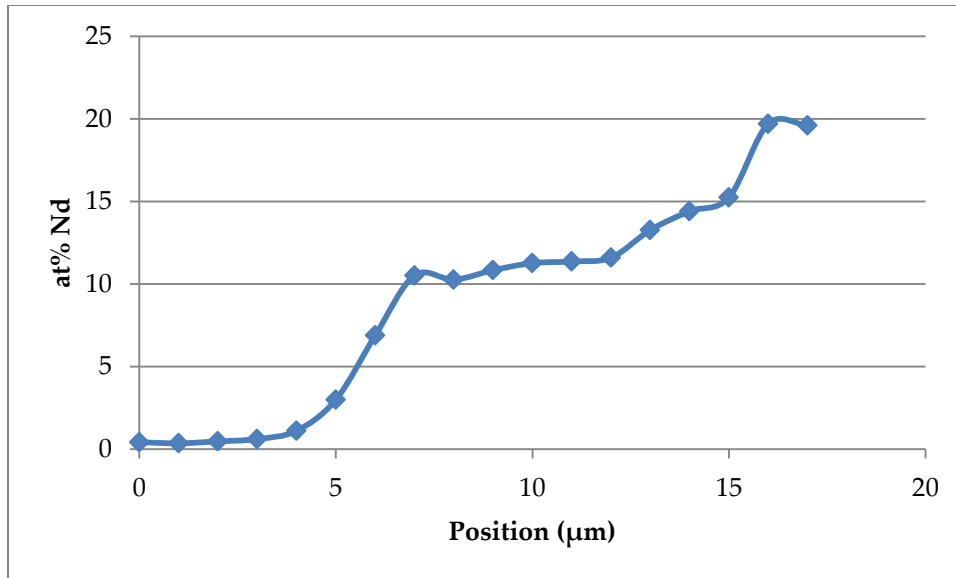


Figure 5-1. Nd concentration across $\text{Nd}_2(\text{Fe}+\text{Cr})_{17}$ phase after 17.5 days at 550°C with HT-9.

For the cases where the diffusion anneal at 550°C was increased to 28 and 56 days, the trend observed after 17.5 days continued and became even more pronounced, as shown in Figure 5-2 and Figure 5-3. In both cases, the $\text{Nd}_2(\text{Fe}+\text{Cr})_{17}$ grew with time and the Nd concentration adjacent to the HT-9 was precisely 10.5 at% Nd (stoichiometric $\text{Nd}_2(\text{Fe}+\text{Cr})_{17}$). However, the internal Nd concentration in the 2-17 phase increased across the width of the phase indicating that as the $\text{Nd}_2(\text{Fe}+\text{Cr})_{17}$ phase grows adjacent to HT-9 at 550°C, Nd diffusion across the phase remains the rate-limiting factor. Unsurprisingly, given their similar compositions, nearly identical results were seen with G.91/Nd diffusion couples annealed for 28 and 58 days at 550°C.

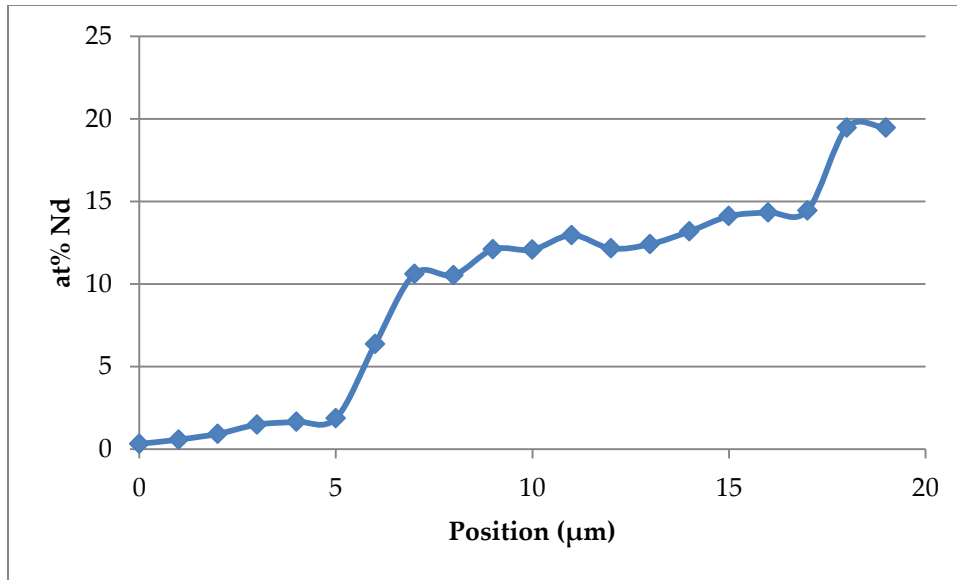


Figure 5-2. Nd concentration across $Nd_2(Fe+Cr)_{17}$ phase after 28 days at 550°C with HT-9.

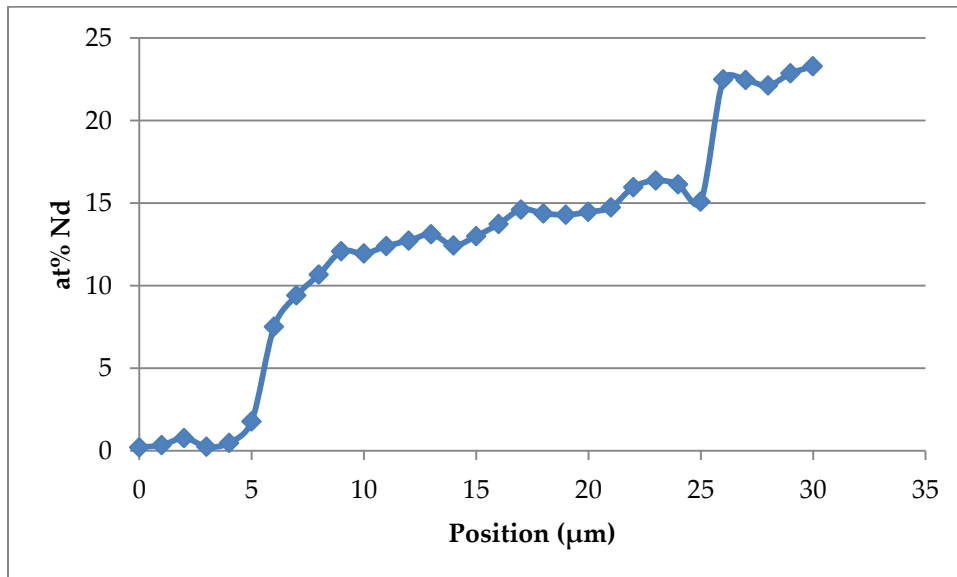


Figure 5-3. Nd concentration across $Nd_2(Fe+Cr)_{17}$ phase after 56 days at 550°C with HT-9.

The observed composition of the nominal $Nd_2(Fe+Cr)_{17}$ phase across the width of the phase field changed considerably at higher annealing temperatures for

HT-9/Nd and G.91/Nd diffusion couples. The concentration of Nd in the $\text{Nd}_2(\text{Fe}+\text{Cr})_{17}$ phase of the HT-9/Nd diffusion couple annealed for 28 days at 625°C is shown in Figure 5-4. As in the HT-9/Nd diffusion couples annealed at 550°C, the Nd concentration in the $\text{Nd}_2(\text{Fe}+\text{Cr})_{17}$ phase at the HT-9 interface was stoichiometrically correct. However, unlike the lower temperature diffusion couples, the Nd concentration across the span of the $\text{Nd}_2(\text{Fe}+\text{Cr})_{17}$ phase was also approximately stoichiometric with some minor variations. When the annealing temperature for the HT-9/Nd diffusion couple was 700°C for 28 days, this trend toward the stoichiometric Nd concentration across the $\text{Nd}_2(\text{Fe}+\text{Cr})_{17}$ phase continued, as shown in Figure 5-5. Once again, the G.91/Nd diffusion couples at these temperatures displayed behavior similar to the HT-9/Nd diffusion couples, remaining approximately stoichiometrically balanced across the $\text{Nd}_2(\text{Fe}+\text{Cr})_{17}$ phase, as shown by the data in Appendix C.

This notable difference in the Nd content across the $\text{Nd}_2(\text{Fe}+\text{Cr})_{17}$ phase bands in the HT-9/Nd and G.91/Nd diffusion couples at 550°C compared to 625°C and 700°C indicates a change in the rate-limiting diffusion step above 550°C. While at the lower temperatures growth of the $\text{Nd}_2(\text{Fe}+\text{Cr})_{17}$ phase was limited by the diffusion of Nd across the phase, as evidenced by the Nd composition gradient, as temperature increased the diffusion of Nd accelerated to the point that it remained stoichiometrically balanced across the full phase. This remained true even when the $\text{Nd}_2(\text{Fe}+\text{Cr})_{17}$ phase grew to widths an order of magnitude greater than those observed at lower temperatures.

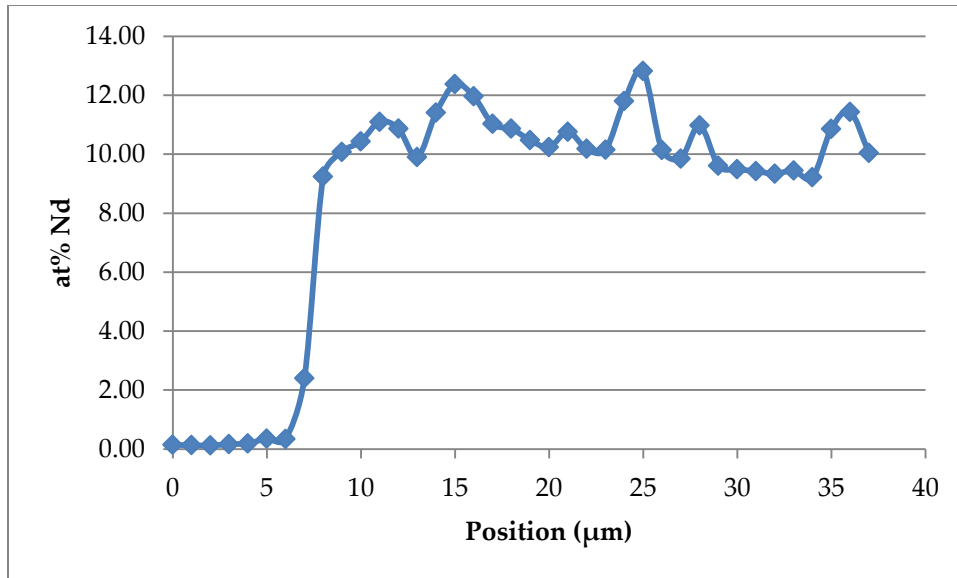


Figure 5-4. Nd concentration across $\text{Nd}_2(\text{Fe}+\text{Cr})_{17}$ phase after 28 days at 625°C with HT-9.

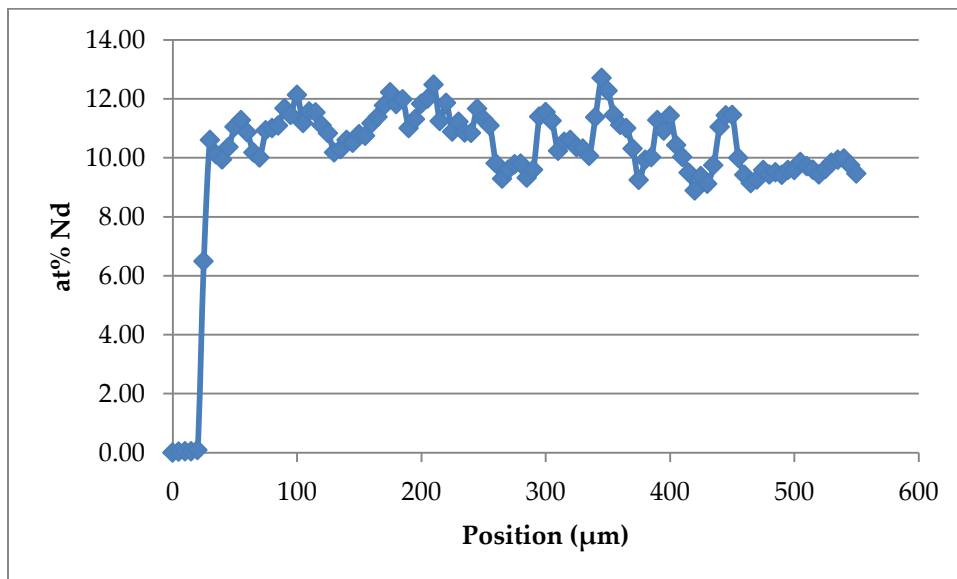


Figure 5-5. Nd concentration across $\text{Nd}_2(\text{Fe}+\text{Cr})_{17}$ phase after 28 days at 700°C with HT-9.

While the $\text{Nd}_2(\text{Fe}+\text{Cr})_{17}$ phase in HT-9/Nd and G.91/Nd diffusion couples performed similarly, the observed phase composition and growth were very

different in SS-316/Nd diffusion couples. When annealed for 28 days and 56 days at 550°C, the $\text{Nd}_2(\text{Fe}+\text{Cr})_{17}$ phase in SS-316/Nd diffusion couples remained stoichiometrically balanced with minor variations in Nd concentration around 10.5 at%, as shown in Figure 5-6 and Figure 5-7. This indicates that unlike HT-9/Nd and G.91/Nd diffusion couples annealed at 550°C, Nd diffusion across the $\text{Nd}_2(\text{Fe}+\text{Cr})_{17}$ phase was not rate-limiting for SS-316/Nd at 550°C. This was likely due to the effects of Ni present in the SS-316, as described in Section 5.1.5

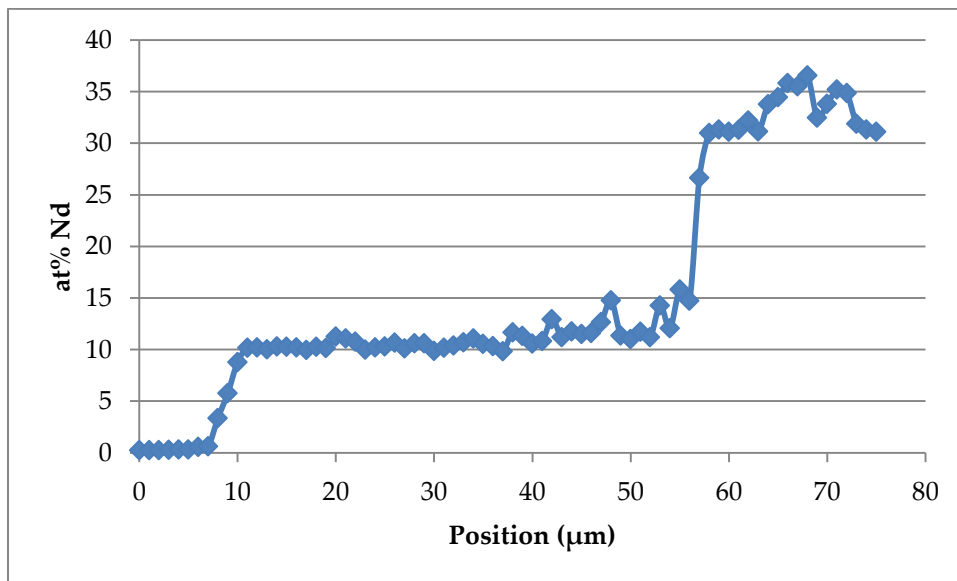


Figure 5-6. Nd concentration across $\text{Nd}_2(\text{Fe}+\text{Cr})_{17}$ phase after 28 days at 550°C with SS-316.

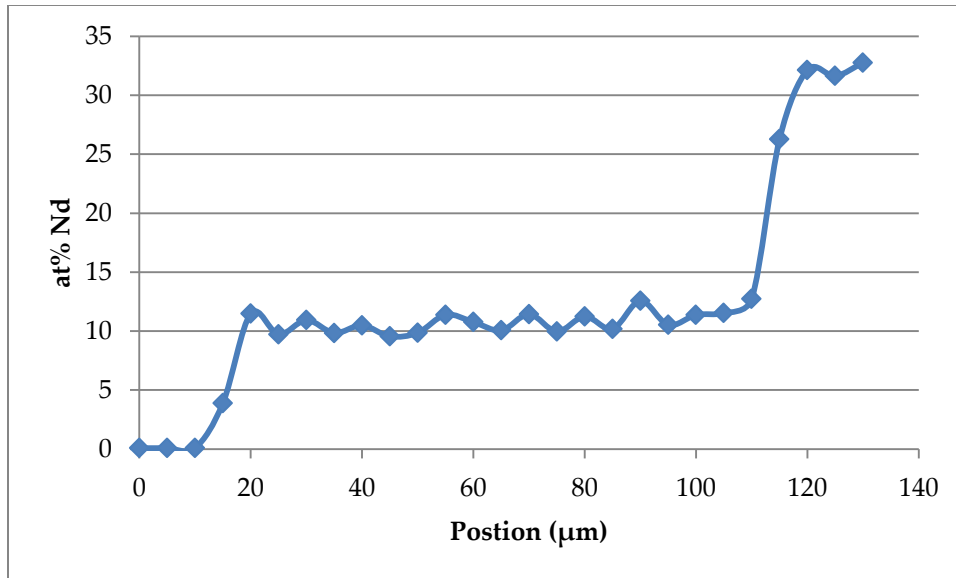


Figure 5-7. Nd concentration across $\text{Nd}_2(\text{Fe}+\text{Cr})_{17}$ phase after 56 days at 550°C with SS-316.

After 28 days at 625°C, the $\text{Nd}_2(\text{Fe}+\text{Cr})_{17}$ phase of the SS-316/Nd diffusion couple at the SS-316 interface was substoichiometric in Nd, approximately stoichiometric across the central portion of the phase, and superstoichiometric at the interface with the next phase, $\text{Nd}_5(\text{Fe}+\text{Cr})_{17}$. The deviations from stoichiometry at either end of the $\text{Nd}_2(\text{Fe}+\text{Cr})_{17}$ phase were a result of the broader diffusion pathway for Nd across the phase as it widened significantly beyond what was observed at lower temperatures.

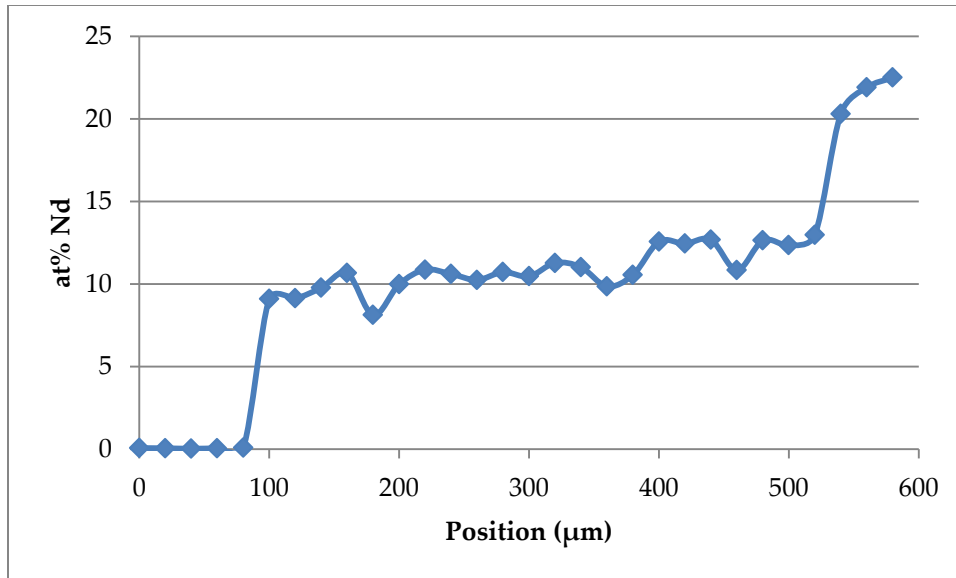


Figure 5-8. Nd concentration across $\text{Nd}_2(\text{Fe}+\text{Cr})_{17}$ phase after 28 days at 625°C with SS-316.

The $\text{Nd}_2(\text{Fe}+\text{Cr})_{17}$ phase in the SS-316/Nd diffusion couple annealed for 28 days at 700°C displayed unique behavior, as shown in Figure 5-9. As for the SS-316/Nd diffusion couple annealed for 28 days at 625°C, the portion of the $\text{Nd}_2(\text{Fe}+\text{Cr})_{17}$ phase nearest to the SS-316 was substoichiometric in Nd; however, over the next 300 μm, the Nd concentration steadily rose until it reached ~16 at%. Over the remaining 500 μm of the $\text{Nd}_2(\text{Fe}+\text{Cr})_{17}$ phase, the Nd concentration was in general substoichiometric with periodic spikes to ~20 at%. Each of these spikes corresponded with both an increase in Ni concentration and a decrease in Cr concentration, as did the increasing Nd concentration over the 300 μm closest to the SS-316. The composition at these points corresponded to $\text{Nd}_5(\text{Fe}+\text{Cr}+\text{Ni})_{17}$, rather than $\text{Nd}_2(\text{Fe}+\text{Cr})_{17}$. This compositional pattern indicates that although the solubility for Ni in $\text{Nd}_2(\text{Fe}+\text{Cr})_{17}$ is very low, Ni is highly soluble in $\text{Nd}_5(\text{Fe}+\text{Cr})_{17}$, averaging ~12.5 at% in the observed $\text{Nd}_5(\text{Fe}+\text{Cr}+\text{Ni})_{17}$ regions. In addition, the solubility of Cr

in $\text{Nd}_5(\text{Fe}+\text{Cr}+\text{Ni})_{17}$ regions was limited, averaging only ~11.5 at% relative to an average concentration in $\text{Nd}_2(\text{Fe}+\text{Cr})_{17}$ of ~20.7 at%.

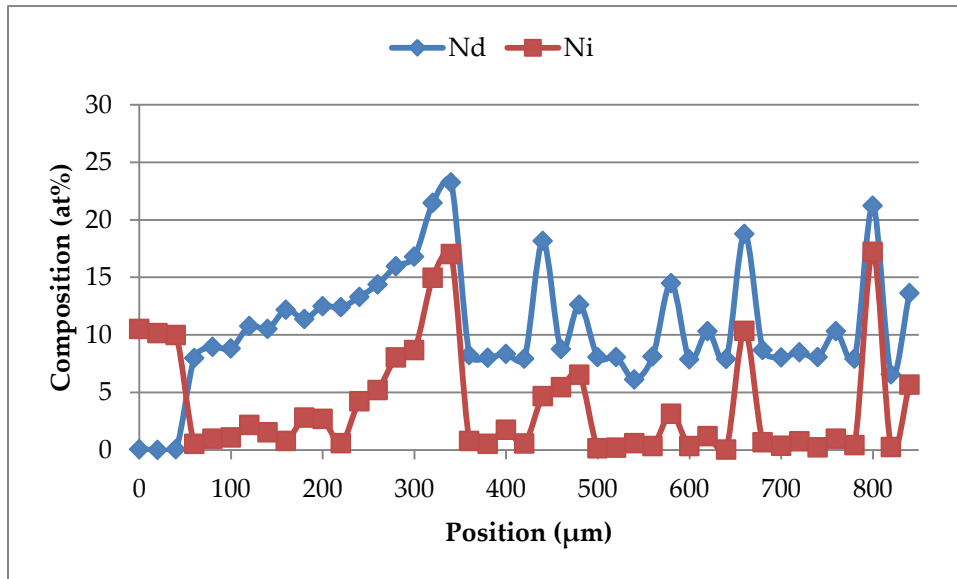


Figure 5-9. Nd concentration across $\text{Nd}_2(\text{Fe}+\text{Cr})_{17}$ phase after 28 days at 700°C with SS-316.

The BSE image of the $\text{Nd}_2(\text{Fe}+\text{Cr})_{17}$ phase, given in Figure 5-10, shows the bulk SS-316 on top, then the first 300 μm of $\text{Nd}_2(\text{Fe}+\text{Cr})_{17}$ with gradually increasing Nd concentration, then the remaining 500 μm of $\text{Nd}_2(\text{Fe}+\text{Cr})_{17}$ with bright $\text{Nd}_5(\text{Fe}+\text{Cr})_{17}$ precipitates. Within the first 300 μm, there are a series of lines running across the region which are darker than the surrounding $\text{Nd}_2(\text{Fe}+\text{Cr})_{17}$. WDS analysis of these dark regions showed they were on average 53 at% Fe and 38 at% Cr, with the remainder being Mo, Nd, Ni, and Mn.

These dark zones indicate that Ni in the SS-316 is apparently being removed from the bulk steel to form $\text{Nd}_5(\text{Fe}+\text{Cr}+\text{Ni})_{17}$, leaving behind the dark Fe+Cr regions. The fact that these dark lines are present only in the high-Nd region of the

$\text{Nd}_2(\text{Fe}+\text{Cr})_{17}$ phase indicates that a relatively high concentration of Nd is required for the formation of $\text{Nd}_5(\text{Fe}+\text{Cr}+\text{Ni})_{17}$.

Discerning the microstructural evolution of these two multi-phase zones in $\text{Nd}_2(\text{Fe}+\text{Cr})_{17}$ phase at 700°C would require conducting further diffusion couples at this temperature with shorter annealing times. However, based on the data available it is postulated that an $\text{Nd}_2(\text{Fe}+\text{Cr})_{17}$ phase similar to that observed in other diffusion couples develops first until the Nd concentration within the phase reaches a super-stoichiometric level high enough to induce the formation of $\text{Nd}_5(\text{Fe}+\text{Cr}+\text{Ni})_{17}$. Then, Ni diffusing from the steel into the $\text{Nd}_2(\text{Fe}+\text{Cr})_{17}$ phase may interact to form $\text{Nd}_5(\text{Fe}+\text{Cr}+\text{Ni})_{17}$ precipitates, producing the second portion of the $\text{Nd}_2(\text{Fe}+\text{Cr})_{17}$ phase. Over time, this second region of the $\text{Nd}_2(\text{Fe}+\text{Cr})_{17}$ phase may consume the initial region in a reaction front moving toward the bulk SS-316.

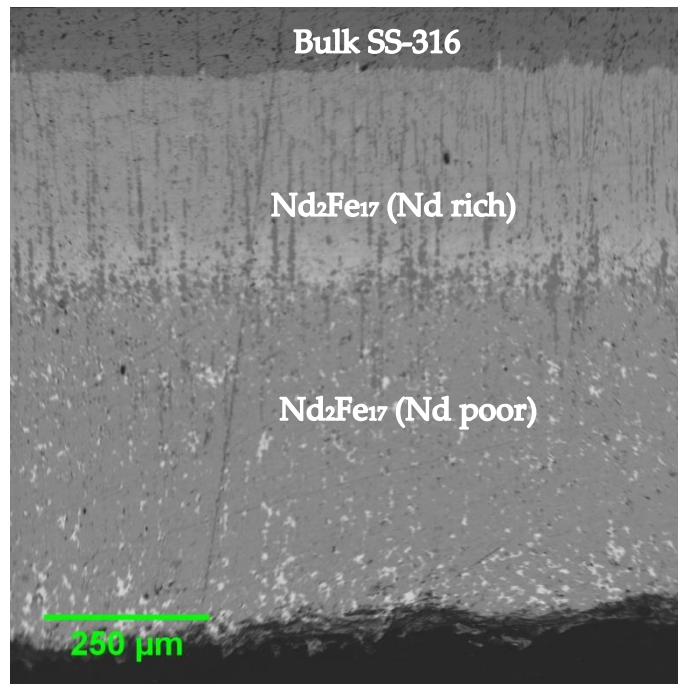


Figure 5-10. SS-316/Nd interface after 28 days at 700°C .

5.1.2 NdFe₂ Phase

The NdFe₂ phase was observed adjacent to the Nd face in all steel/Nd diffusion couples that did not break apart; it is likely that this phase did form in the broken diffusion interfaces as well. Unlike the Nd₂(Fe+Cr)₁₇ phase in which the concentrations of alloying elements, excepting Ni, remained very similar to the bulk steel, the concentration of alloying elements in the NdFe₂ phase was radically different than the bulk steel. The amount of Mo (0.02%), Cr (~2.5%), V (0.01%), W (0.03%), and Ni (0.2%) were significantly reduced, while the amount of Mn (1.4%) was roughly constant and the amount of Si (~5%) was increased.

Based on the elements present within the phase and the ternary phase systems [71, 72], the observed intermetallics may include NdFe₂Si₂, NdMn₂Si₂, and NdCr₂Si₂ as well as the parent phase of NdFe₂. The presence of Mn may be explained based on its tendency to form ternary intermetallics with Si and Nd, while the limited presence of Cr in the phase may be explained by the limited quantity of Si available to form NdCr₂Si₂ and limited solubility for Cr within the primary NdFe₂ intermetallic. Analysis of elemental ratios throughout the NdFe₂ phase demonstrates that the concentration of Si is consistently greater than the sum of Cr and Mn concentrations. NdFe₂Si₂, NdMn₂Si₂ and NdCr₂Si₂ all share the same crystal structure of the CeGa₂Al₂ type, shown in Figure 5-11, while NdFe₂ possesses a cubic Laves phase structure, shown in Figure 5-12.

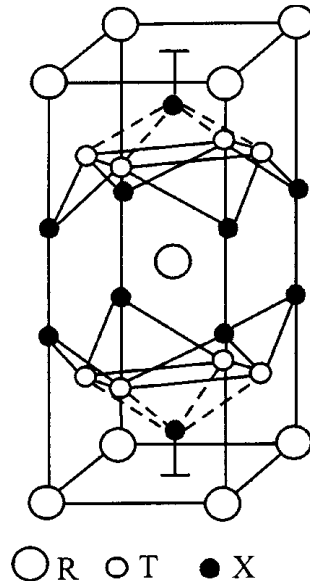


Figure 5-11. CeGa₂Al₂ type crystal structure where R=Nd; T=Fe, Mn, or Cr; and X=Si [73].

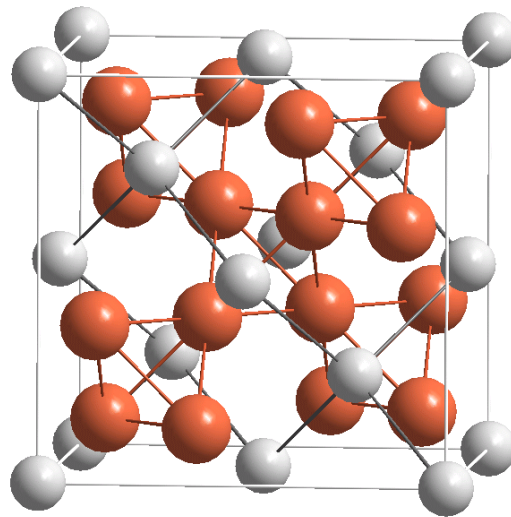


Figure 5-12. Cubic Laves structure of NdFe₂, where Nd is gray and Fe is red [74].

The limited solubility of Cr in the NdFe₂ phase due to limited Si provides an apparent cause for the slightly increased concentration of Cr relative to the bulk steel

observed in the preceding $\text{Nd}_2(\text{Fe}+\text{Cr})_{17}$ and $\text{Nd}_5(\text{Fe}+\text{Cr})_{17}$ phases. As the NdFe_2 phase formed, excess Cr would have been forced to remain behind in the $\text{Nd}_2(\text{Fe}+\text{Cr})_{17}$ and $\text{Nd}_5(\text{Fe}+\text{Cr})_{17}$ phases in which it was significantly more soluble. This increase in Cr content was observed in the $\text{Nd}_2(\text{Fe}+\text{Cr})_{17}$ and $\text{Nd}_5(\text{Fe}+\text{Cr})_{17}$ phases even in steel/Nd diffusion couples which did not remain intact and thus did not include the NdFe_2 phase. Since the NdFe_2 phase was responsible for the increase in Cr concentration in other adjacent phases, it may be concluded that the NdFe_2 phase did consistently form in all steel/Nd diffusion couples.

The limitation of Cr content in the NdFe_2 phase imposed by the available Si suggests that a reduction of the Si present in the steel alloy may have a minor effect in slowing intermetallic phase formation between steel and neodymium. Reduced accommodation of Cr in the NdFe_2 phase due to reduced availability of Si would naturally increase the degree of Cr accumulation in the preceding $\text{Nd}_2(\text{Fe}+\text{Cr})_{17}$, potentially slowing the expansion of that phase.

5.1.3 $\text{Nd}_5\text{Fe}_{17}$ Phase

The $\text{Nd}_5(\text{Fe}+\text{Cr})_{17}$ phase was only observed in a subset of diffusion systems, and it was not fully developed across the full diffusion interface after shorter annealing durations. Thus, it is not surprising that most previous steel/Nd diffusion studies have not observed this phase. The existence of the $\text{Nd}_5\text{Fe}_{17}$ phase has, however, been confirmed in several publications from thermochemical studies [75, 76], as well as some diffusion studies [77]. Additional studies have shown that $\text{Nd}_5\text{Fe}_{17}$ may be modified substitutionally by the addition of Cr, Ti, and Mn, as well as other elements [78]. Based on the steel alloying elements which successfully incorporated into the $\text{Nd}_5(\text{Fe}+\text{Cr})_{17}$ phase in diffusion couples, it appears that Mo (0.8%) , W (0.2%), and Ni (~11%) are also capable of substitutional addition to $\text{Nd}_5\text{Fe}_{17}$.

The determining factors for the formation of the $\text{Nd}_5(\text{Fe}+\text{Cr})_{17}$ phase in steel/Nd diffusion couples appears to be either a sufficient excess concentration Nd in the $\text{Nd}_2(\text{Fe}+\text{Cr})_{17}$ phase or the presence of a significant amount of Ni that is unable to be incorporated in the $\text{Nd}_2(\text{Fe}+\text{Cr})_{17}$ phase, either of which were apparently sufficient to make the 5-17 phase thermodynamically stable relative to the 2-17 phase. The requirement for excess Nd in the $\text{Nd}_2(\text{Fe}+\text{Cr})_{17}$ phase may be inferred by noting in which diffusion couples $\text{Nd}_5(\text{Fe}+\text{Cr})_{17}$ formed. In HT-9/Nd and G.91/Nd diffusion couples annealed at 550°C, the amount of excess Nd in the $\text{Nd}_2(\text{Fe}+\text{Cr})_{17}$ phase increased with increasing annealing time. Accordingly, the $\text{Nd}_5(\text{Fe}+\text{Cr})_{17}$ phase was only partially developed at shorter annealing times, in which Nd excess was limited, but formed more fully at longer annealing durations. In contrast, in HT-9/Nd and G/91/Nd diffusion couples annealed at 625°C or 700°C for which there was little to no excess Nd in the $\text{Nd}_2(\text{Fe}+\text{Cr})_{17}$ phase, only trace amounts of $\text{Nd}_5(\text{Fe}+\text{Cr})_{17}$ were found. Likewise, in SS-316/Nd diffusion couples annealed at 550°C, for which the $\text{Nd}_2(\text{Fe}+\text{Cr})_{17}$ phase was stoichiometrically balanced, no evidence of $\text{Nd}_5(\text{Fe}+\text{Cr})_{17}$ formation was found.

The only cases in which an $\text{Nd}_5\text{Fe}_{17}$ type phase was observed in the SS-316/Nd diffusion couples were those annealed at 625°C or 700°C in which some buildup of Nd in the $\text{Nd}_2(\text{Fe}+\text{Cr})_{17}$ phase was observed. However, unlike the HT-9/Nd and G.91/Nd diffusion couples the $\text{Nd}_5\text{Fe}_{17}$ phase contained significant amounts of Ni, as well as Cr, making it $\text{Nd}_5(\text{Fe}+\text{Cr}+\text{Ni})_{17}$. Interestingly, this phase appeared to remain stable even when the surrounding $\text{Nd}_2(\text{Fe}+\text{Cr})_{17}$ was depleted in Nd as evidenced by the SS-316/Nd diffusion couple annealed at 700°C. This indicates that the presence of Ni stabilizes the $\text{Nd}_5(\text{Fe}+\text{Cr}+\text{Ni})_{17}$ phase, probably due to the apparent incompatibility of Ni with $\text{Nd}_2(\text{Fe}+\text{Cr})_{17}$.

5.1.4 Nd₃Ni Phase

The Nd₃Ni phase was observed to form in both SS-316/Nd diffusion couples annealed at 550°C, and may have formed in the broken regions of the SS-316/Nd diffusion couples annealed at higher temperatures. In both cases, this phase was the formed closest to the Nd bulk. There are two reasons that the formation of this phase was surprising. First, the formation of this phase required the diffusion of a significant quantity of Ni through growing regions of intermediate phases with very low Ni solubility that eventually reached widths of more than 100 μm. Second, when a binary Nd-Ni intermetallic phase were to form, there are other intermetallics between the two which could be expected based on Gibbs Free Energies of formation.

For the diffusion of Ni from the bulk SS-316 into the Nd₃Ni phase, neither the Nd₂(Fe+Cr)₁₇ phase nor the NdFe₂ phase contained significant amounts of Ni. Thus, the diffusion of Ni was clearly driven by a chemical potential gradient, not a concentration gradient. There are two possible mechanism by which this diffusion of Ni occurred. First, Ni may have simply diffused through the intervening low concentration phases at relatively high speeds without ever reaching significant concentrations. The small amounts of Ni nearest the Nd₃Ni phase would then be incorporated into the phase, drawing further Ni through the low concentration zones. The second explanation is that localized precipitation of Nd₅(Fe+Cr+Ni)₁₇ in the Nd₂(Fe+Cr)₁₇ phase may have allowed Ni to cross. These precipitates could have progressed up the Nd concentration gradient by dissolution and resolution, driven by their increased Nd content relative to the bulk Nd₂(Fe+Cr)₁₇ from which they were formed. However, these precipitates were only observed in the SS-316/Nd diffusion couple annealed at 700°C and may not have formed at lower temperatures.

Examination of the Nd-Ni phase diagram shows that there are seven binary intermetallics which may form between the two elements, for which the Gibbs

energies of formation at 800°C have been determined [79]. These energies are plotted in Figure 5-13. Assuming that the relative ordering of these energies is unchanged at 550°C, Nd₃Ni is not the intermetallic which would be expected to form. Given that the limiting factor in Ni-Nd intermetallic formation would be the quantity of available Ni, due to the proximity of the phase to the bulk Nd, the expected intermetallic would be NdNi, as it possesses the most negative Gibbs energy of formation per mole of available Ni. Still, even the Nd₃Ni intermetallic features a significantly greater energy of formation than Nd₂Fe₁₇, which for the same temperature has an energy of formation of only ~47 kJ/mol [80].

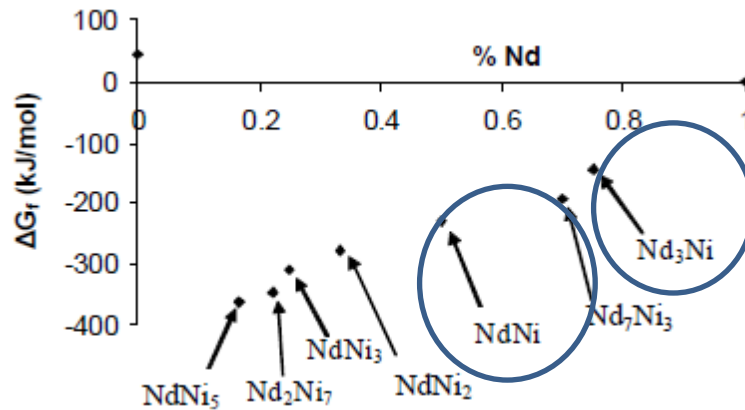


Figure 5-13. Calculated Ni-Nd intermetallic Gibbs energies at 800°C [79].

Given the energetics of the pure Nd-Ni system, it seems likely then that the factor which caused Nd₃Ni to form, rather than NdNi was the presence of additional alloying elements. As given in Appendices D.1 and D.13, the primary additional element present was Fe, which averaged 3.5 at% across the phase. Ternary phase diagrams for these three elements are not available in this composition range;

however, examination of the crystal structures of Nd_3Ni and NdNi shows that Nd_3Ni should be better able to accommodate Fe.

NdNi has the thallium iodide crystal structure, which is an orthorhombic distortion of the NaCl structure, as shown in Figure 5-14. Nd_3Ni , on the other hand, has the Fe_3C crystal structure, as shown in Figure 5-15. The relative openness of the Nd_3Ni structure as compared to the NdNi structure may be better able to accommodate the Fe present by substitution for Ni, thus compensating for its higher Gibbs energy relative to NdNi . The conclusion that Fe is substituting for Ni is supported by the fact that throughout the observed Nd_3Ni zone, the sum of Ni and Fe concentrations combined to approximately one-third the Nd concentration.

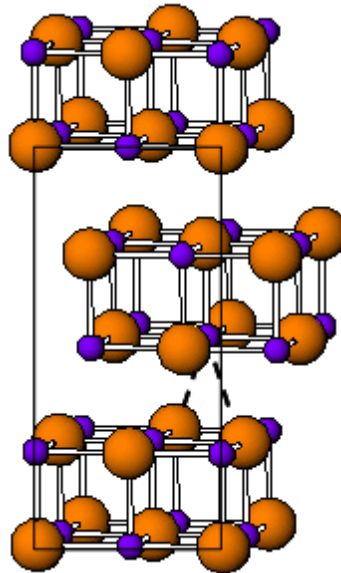


Figure 5-14. TII type crystal structure of NdNi [81].

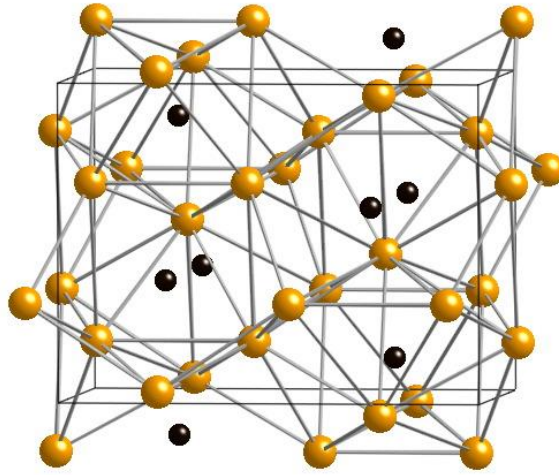


Figure 5-15. Fe₃C type crystal structure of Nd₃Ni [82].

5.1.5 Extent of Interaction for SS-316 vs. HT-9/G.91

In addition to differences in phase formation and composition, a large difference in the overall width of the interdiffusion zones was observed for SS-316/Nd diffusion couples and HT-9/Nd or G.91/Nd diffusion couples. This difference was especially pronounced in diffusion couples annealed at 550°C or 625°C, for which the SS-316/Nd interaction zones were approximately six to ten times as thick as the HT-9/Nd and G.91/Nd interaction zones. Given that the rate-limiting factor for the creation of the primary Nd₂(Fe+Cr)₁₇ phase in both the HT-9/Nd and G.91/Nd diffusion couples at lower temperatures was the diffusion of Nd across the phase, it is probable that the accelerated interaction in SS-316/Nd diffusion couples was due to the acceleration of Nd diffusion within the Nd₂(Fe+Cr)₁₇ phase.

This acceleration was likely the result of the diffusion of Ni through the Nd₂(Fe+Cr)₁₇ phase to form the Nd₃Ni phase. As Ni diffused through the

$\text{Nd}_2(\text{Fe}+\text{Cr})_{17}$ phase, driven by the chemical potential driving force to form the Nd_3Ni phase, it could accelerate the counter-diffusion of Nd in the opposite direction. This effect would have become less relevant to the interaction zone width with increasing temperature, as Nd diffusion through the $\text{Nd}_2(\text{Fe}+\text{Cr})_{17}$ phase ceased to be rate-limiting for HT-9/Nd and G.91/Nd as temperature increased.

5.2 Liner Diffusion with Neodymium

The diffusion parameters for each liner material with Nd were in general inversely correlated to the melting point of the material, as shown in Figure 5-16. This correlation is reasonable, given that melting point is closely related to bond strength, which in turn is inversely related to diffusional jump frequency. The primary deviations from this correlation were observed in Zr ($T_m=2128$ K) and Ti ($T_m=1941$ K). Diffusion between Ti and Nd was consistently higher than would be expected from the trend, while diffusion between Zr and Nd was consistently lower. Unsurprisingly for refractory metals, the diffusion rates of all the liner materials studied were very low, bordering on the minimum rates which could be measured by the techniques employed.

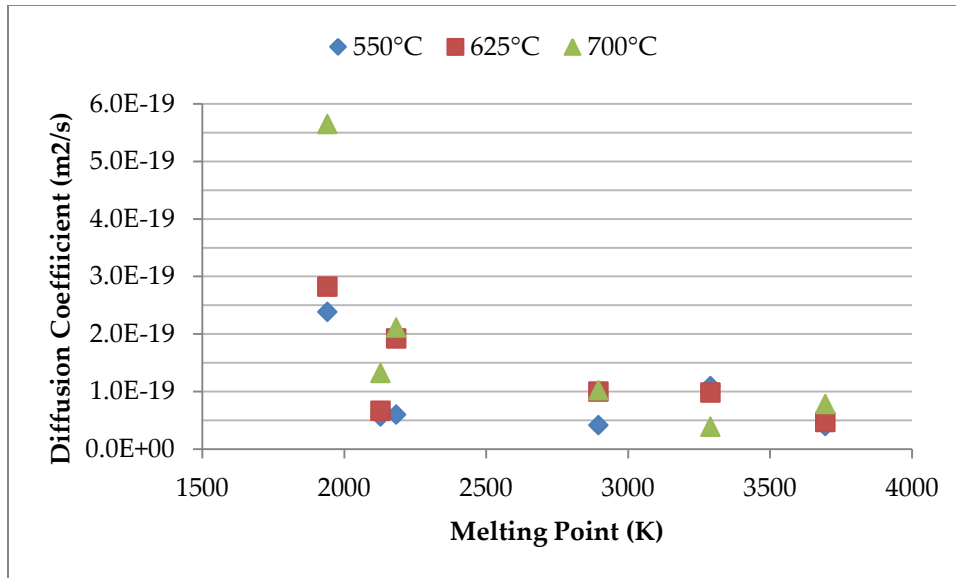


Figure 5-16. Liner/Nd diffusion coefficients vs. liner melting point.

Diffusion between each of the liners and neodymium followed the expected Arrhenius behavior with temperature, with the very unusual exception of tantalum. A slight decrease in Ta/Nd diffusion was seen from 550°C to 625°C, and a large decrease was seen from 625°C to 700°C. This odd behavior may have been the result of pre-existing microstructure, including excess vacancies, dislocations, and smaller grains, due to cold-working during manufacturing, as the tantalum foil was not annealed before use in diffusion couples. Such defects have previously been observed to increase diffusion rates at low temperatures [83]. This may explain both why Ta/Nd diffusion was faster than would be expected at lower temperatures, due to increased vacancy concentration, and why Ta/Nd diffusion rates decreased with increasing temperature, due to annihilation of excess vacancies.

5.3 Liner Diffusion with Steel

Comparative analysis of the diffusion of each liner material with the various steels tested was difficult given the limited success with which diffusion bonding

was achieved between these materials; however, some general conclusions may be drawn from the available data. First, SS-316 successfully bonded to liners with greater frequency than either of the other steel alloys tested or pure iron. In addition, for liners which successfully bonded to multiple steel alloys, diffusion coefficients with SS-316 were consistently higher than either of the other two steel alloys. Second, vanadium and titanium tended to bond to the steel alloys more regularly and with larger diffusion coefficients than the heavier elements. Finally, diffusion coefficients for each liner material were consistently higher with neodymium than with each of the steel alloys, indicating that the liner materials under consideration will tend to diffusively interact more on the fuel-side than on the cladding side.

5.4 Comparative Reactor Impact of Liners Tested

The ultimate objective for each of the liner materials tested is to provide a means of preventing FCCI due to lanthanide diffusion in SFR's. Thus, although a complete study would be necessary for implementation in a reactor, some consideration and estimation of the operational impact that will arise by implementing these liners. This section describes a set of basic simulations performed as a companion to this diffusion study to estimate the required thickness of liners required to prevent FCCI, and to simulate neutronic performance and heat transfer to coolant. These simulations were completed using a simplified reactor core model with the inclusion of different liners.

5.4.1 Required Thicknesses

An easy first parameter to consider for each liner material, which in turn controls their impacts on reactor operations, is the thickness required for each liner to prevent FCCI for a given period of reactor operation. A very simple bounding estimate of the required thicknesses may be determined based on the diffusion

coefficients calculated for each liner material by setting a maximum concentration of lanthanides allowed to reach the cladding on the opposite side. This estimate is conservative in that it considers a full layer of lanthanides to be present at the fuel-cladding interface from the start of reactor operation, reflecting the build-up of lanthanides observed at the fuel-cladding interface in fuel elements after 1 to 2 years in prior SFR's. It is also assumed that the distribution of lanthanides produced as fission products diffuse at the same rate as neodymium alone and neglects diffusion from the other side of the liner with the cladding itself. These assumptions seem reasonable, given that neodymium matches the penetration profile of the lanthanides as a whole in post-irradiation examination of fuel elements and that each liner material diffused significantly more with neodymium than with steel. The greater source of uncertainty in the estimation of required liner thicknesses based on out of reactor diffusion tests is the accelerating effect of a large radiation flux on diffusion rates. Without the means by which to estimate the magnitude of this effect, however, it must be neglected in this estimate.

Given those considerations, the estimated required thicknesses for each liner material given a maximum Nd concentration of 1at% adjacent to the cladding and a fuel-cladding interface temperature of 550°C are given for various fuel lifetimes are given in Figure 5-17.

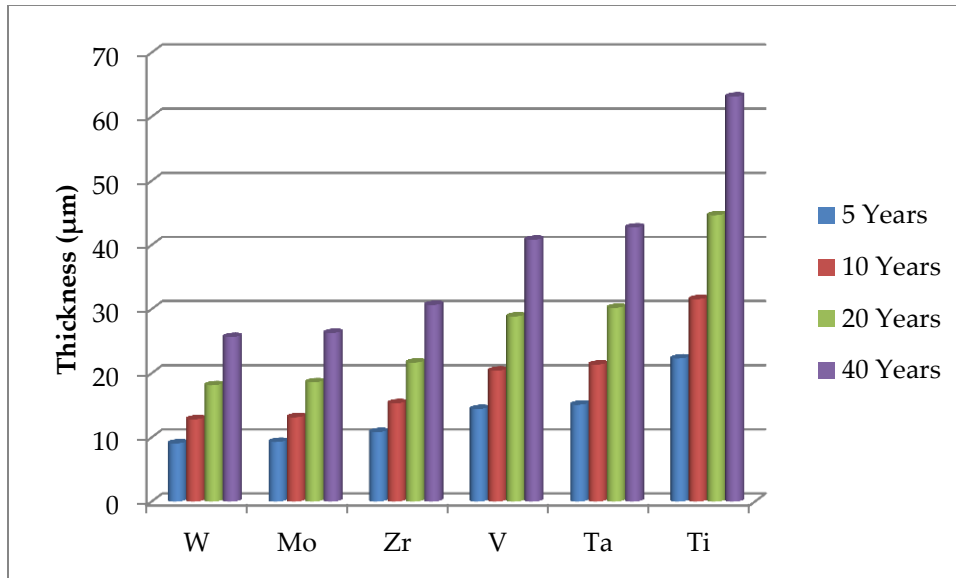


Figure 5-17. Required liner thicknesses for various fuel lifetimes.

Based on this analysis, the differences in diffusivity for each liner material with neodymium result in significant differences in the required liner thickness to prevent FCCI, especially for extended fuel lifetimes. The first-order estimates provided here do not account for the effects of radiation-enhanced diffusion, which may greatly accelerate the rate of lanthanide penetration, and thus greatly increase the required liner thickness.

5.4.2 Neutronic Impact

The impact of liners on the operational reactor physics parameters were simulated using a Monte Carlo N-Particle Version 5 (MCNP) model of one sixth of a small hypothetical core, similar to a miniature version of the Traveling Wave Reactor (TWR) core. The MCNP program is designed for simulation of radiation transport through materials based on cross sections and random number generation, and includes the ability to estimate the reactivity, or k_{eff} , of a given system [84]. Systems with a k_{eff} of 1 are referred to as 'critical', and will sustain a fission chain

reaction of constant energy. Systems with k_{eff} less than 1 are subcritical and will decrease energy production over time. Systems with k_{eff} greater than 1 are supercritical and will increase energy production over time. Reactivity increases with the amount of fissile material within the core of nuclear reactors, and decreases with the presence of neutron absorbers and leakage of neutrons.

The simulated core consisted of 15 rings of pins in a 50 cm tall hexagonal lattice with a pin pitch of 0.85 cm and liquid sodium coolant, as shown in Figure 5-18. Each pin was 0.75 cm in diameter with a 0.5 mm thick cladding and a liner of variable thickness and composition. Pins were filled with 75% U and 25% Na by volume, to simulate a sodium-bonded fuel with low smear density to allow for fission product accumulation over the fuel lifetime. The fuel was enriched to 70at% U-235.

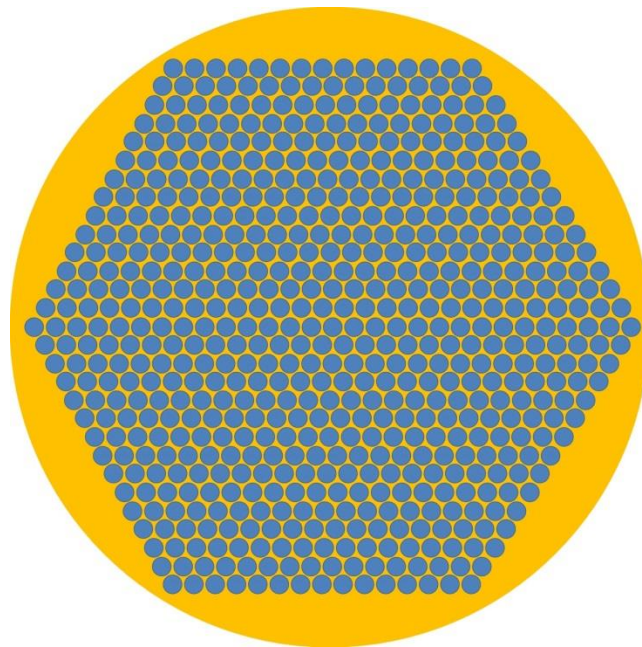


Figure 5-18. Top-down schematic of MCNP simulated core with fuel pins (blue) and coolant (orange).

The simulation process in MCNP to determine criticality is performed by simulating the interaction and travel history of a set number (cycle) of neutrons through the reactor system and tracking their progression through the core until they leak out of the core or are absorbed while tracking the number of fissions they induce. After a cycle is finished, the reactivity of the system is calculated based on the number of fissions induced and the starting position for neutrons in the next cycle is determined based on the positions of those fissions. This process is repeated until the reactivity between successive cycles is within statistical agreement. For the simulations performed in this study, 30,000 neutrons were simulated in each cycle, and a total of 100 cycles were completed for each core configuration.

Without a liner present, the simulated core was subcritical with a k_{eff} of 0.61233 ± 0.00020 . The addition of liners decreased the reactivity of the core, both by absorbing additional neutrons and by reducing the quantity of fissile material in each pin. The effects of liners of various compositions and thicknesses are given in Table 5-5 and Figure 5-19.

Table 5-5. Neutronic impact of various liners.

Liner Depth (μm)	V		Ti		Zr		Mo		W		Ta	
	Δk_{eff}	\pm	Δk_{eff}	\pm	Δk_{eff}	\pm	Δk_{eff}	\pm	Δk_{eff}	\pm	Δk_{eff}	\pm
5	-0.17%	0.03%	-0.33%	0.11%	-0.27%	0.11%	-0.22%	0.11%	-0.23%	0.03%	-0.20%	0.04%
10	-0.38%	0.03%	-0.50%	0.03%	-0.46%	0.04%	-0.41%	0.03%	-0.40%	0.03%	-0.39%	0.03%
20	-0.82%	0.04%	-1.00%	0.03%	-0.81%	0.04%	-0.79%	0.04%	-0.87%	0.03%	-0.74%	0.03%
50	-2.09%	0.03%	-2.43%	0.03%	-2.29%	0.04%	-2.05%	0.04%	-2.25%	0.03%	-1.93%	0.03%
100	-4.19%	0.03%	-4.81%	0.03%	-4.50%	0.04%	-3.98%	0.04%	-4.56%	0.03%	-3.98%	0.03%

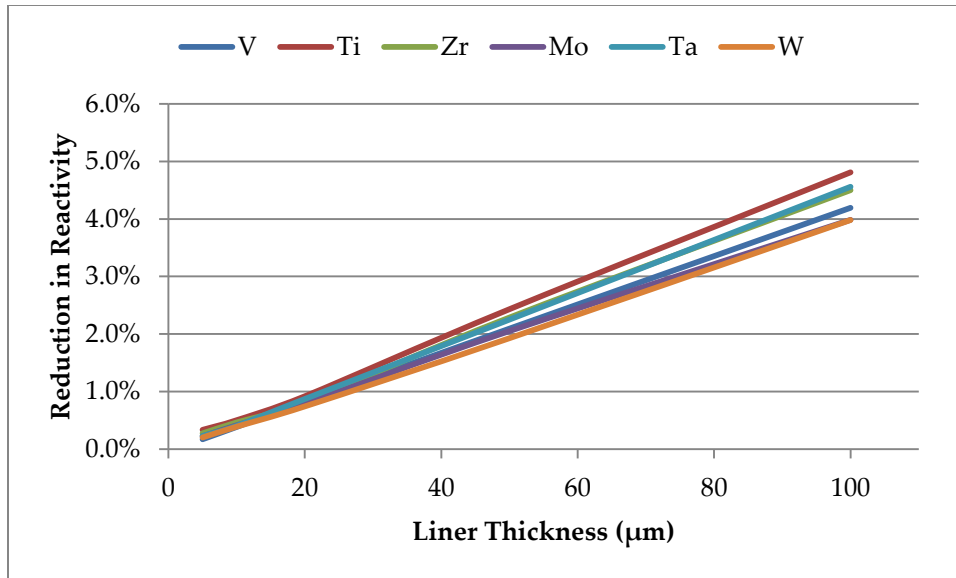


Figure 5-19. Neutronic impact of various liners

The MCNP simulations of the effects of varying liner materials and thicknesses on reactivity demonstrated that the most critical factor governing the reactivity drop due to the addition of a liner was not neutron absorption by the liner, but rather the reduction in fissile material due to a reduction in fuel pellet diameter. This factor becomes even more important as the fuel pin diameter is reduced, as fraction of fuel replaced by a liner of a given thickness will become larger.

Therefore, minimizing the negative impact of liner addition on reactivity will be achieved by selecting the liner material most resistant to diffusion, thereby minimizing the required thickness of the liner. Based on the diffusion results, this observation favors tungsten, molybdenum, or zirconium as candidates for a liner material. Further discrimination based on the MCNP simulations favors tungsten or molybdenum, as they reduced reactivity by less than zirconium for a given liner thickness.

5.4.3 Heat Transfer Impact

The impact of each liner material under consideration on the temperature at the fuel-cladding interface was estimated by calculating the temperature change for a fuel pin with an outer radius of 5 mm, 0.5 mm thick steel cladding, and a linear power of 25 kW/m. The formula for temperature change across an infinite cylinder, given in Equation 5-1, was used for these calculations.

Equation 5-1

$$\Delta T = \frac{\ln(r_o/r_i) \cdot Q}{2\pi k}$$

Based on this approach, the calculated temperature changes at the fuel-cladding interface for varying thicknesses of each liner material are given in Table 5-6 and Figure 5-20.

Table 5-6. Thermal effects of various liners at fuel-cladding interface.

Liner Depth (μm)	ΔT at Fuel-Cladding Interface ($^{\circ}\text{C}$)					
	V	Ti	Zr	Mo	W	Ta
5	0.34	0.48	0.46	0.08	0.06	0.18
10	0.68	0.95	0.92	0.15	0.12	0.36
20	1.36	1.90	1.84	0.30	0.24	0.72
50	3.37	4.72	4.57	0.75	0.60	1.80
100	6.65	9.32	9.03	1.48	1.18	3.55

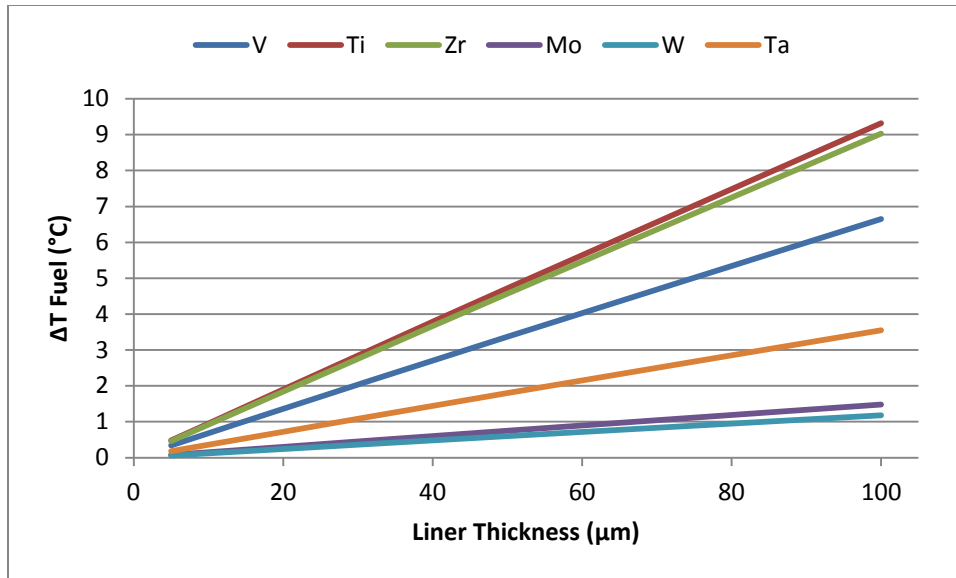


Figure 5-20. Thermal effects of various liners at fuel-cladding interface.

Due to the relatively high thermal conductivity of all the liner materials under consideration, the primary factor governing the impact of the addition of a liner on heat transfer out of fuel pins was once again the necessary thickness of the liner. However, there was more difference between the various liner materials in thermal impact than in neutronic impact. Still, the most conductive liners (with the smallest thermal impact) were also the liners with the best diffusion performance (i.e. tungsten and molybdenum). Based on this, the liners with the least negative impact on heat transfer out of fuel pins will be either tungsten or molybdenum, as they possessed both the lowest rates of diffusion with neodymium and the highest thermal conductivities.

6 CONCLUSIONS

In this study, the diffusion behaviors of HT-9, G.91, and SS-316 with neodymium for long durations at various temperatures were well characterized to aid in better understanding of lanthanide fission product interactions with steel cladding materials in nuclear reactors. The various intermetallic phases which formed were characterized based on elemental compositions and zone widths, and the resulting data was used to gain insight into the dynamics of diffusional phase formation in each system, as well as to determine diffusion coefficients and activation energies for each intermetallic.

The primary intermetallic observed in each of the diffusion couples was $\text{Nd}_2(\text{Fe}+\text{Cr})_{17}$. This intermetallic diffusion zone was the widest in each case, and the most interesting for modeling FCCI as it corresponds to the intermetallic observed forming in steel cladding in prior sodium fast reactors. The behavior of this zone was observed to depend on temperature at steel alloy. For the ferritic-martensitic alloys (i.e., HT-9 and G.91), diffusion of neodymium across the zone was the rate-limiting factor in zone growth at low temperatures (550°C), but not at higher temperatures (625°C and 700°C). In contrast, SS-316 diffusion couples formed a much more extensive $\text{Nd}_2(\text{Fe}+\text{Cr})_{17}$ interaction zone, particularly at 550°C. This more extensive reaction was due to the diffusion of nickel from the SS-316 to form a Nd_3Ni intermetallic, which accelerated neodymium diffusion in the reverse direction.

The second intermetallic observed was $\text{Nd}_5(\text{Fe}+\text{Cr})_{17}$; however, this intermetallic only formed in diffusion couples in which neodymium excess grew into the $\text{Nd}_2(\text{Fe}+\text{Cr})_{17}$ phase. In some cases $\text{Nd}_5(\text{Fe}+\text{Cr})_{17}$ developed as a separate phase, while in others it was mixed as precipitates within the $\text{Nd}_2(\text{Fe}+\text{Cr})_{17}$ phase. Since that the neodymium excess was observed only after long diffusion anneals at

low temperatures, this phase has only been observed in a small number of prior FCCI diffusion studies.

The third intermetallic observed was NdFe_2 , which based on composition was homogeneously mixed with the ternary intermetallics NdSi_2Fe_2 , NdSi_2Mn_2 , and NdSi_2Cr_2 . These additional intermetallics explained the limited solubility for chromium and manganese within the NdFe_2 phase based on the total amount of silicon.

The final intermetallic, which has not previously been reported in FCCI diffusion studies, was Nd_3Ni . Based on thermodynamic stabilities of neodymium/nickel intermetallics and the limiting factor being nickel, the expected intermetallic should be NdNi . The formation instead of Nd_3Ni was possibly due to the substitution of iron for nickel within the Nd_3Ni crystal structure, preventing the formation of NdNi either kinetically or thermodynamically.

In addition to steel/neodymium intermetallic characterization, the performance of six refractory metals as diffusion barriers between steel alloys and neodymium were tested, demonstrating that each of the tested liner materials was capable of preventing interaction between steel and neodymium while not reacting significantly with either. Diffusion coefficients for each liner material with steel and with neodymium were calculated. In general, diffusion between liners and neodymium was higher than diffusion between liners and steel alloys. Diffusion coefficients between liners and neodymium were found to correlate to the inverse of liner melting point, which is the expected result based on the relationship between melting point, cohesive energy, and bond strength.

Based on these diffusion results, as well as first-order simulations of the effects of liners on reactor neutronic and thermal performance, several key conclusions may be drawn for reactor design.

- Reduction of the concentration of nickel, and to a lesser extent of silicon, in steel alloys may effectively reduce the rate of interaction with lanthanides, making such alloys desirable for use as relatively FCCI-resistant cladding materials.
- Of the liner materials tested, tungsten, molybdenum, and zirconium displayed the least diffusion with neodymium, making those materials promising candidates for liners of minimum thickness.
- Neutronic and thermal simulation of the effects of liners on reactor performance indicate that the most critical factor is the thickness of the liner, not its material, making minimization of necessary liner thickness a priority.

Further work in this area ought to follow three primary leads. First, the diffusion performance of thinner liners, such as coatings of refractory metal nitrides, may provide superior diffusion performance with minimal negative reactor performance impact and should be studied. Second, the diffusion behavior of candidate liner materials should be tested against both pure fuel alloys and fuel alloys containing simulated fission products to confirm their continuing integrity when exposed to fuel. Finally, accurate estimation of required liner thicknesses to prevent FCCI will require in-reactor diffusion testing to account for the effects of radiation on diffusion rates.

REFERENCES

- [1] B. Triplett, E. Loewen and B. Dooies, "PRISM: a competitive small modular sodium-cooled reactor," *Nuclear Technology*, vol. 178, pp. 186-200, 2012.
- [2] P. Hejzlar, R. Petroski, J. Chetham, N. Touran and M. Cohen, "Terrapower, LLC traveling wave reactor development program overview," *Nuclear Engineering and Technology*, vol. 45, pp. 731-744, 2013.
- [3] Y. Bagdasarov and A. Kamaev, "Successive development phases for sodium-cooled fast reactors," *Atomic Energy*, vol. 111, pp. 389-397, 2012.
- [4] S. Chetal, P. Chellapandi and P. Puthiyavinayagam, "Current status of fast reactors and future plans in India," *Asian Nuclear Prospects 2010*, vol. 7, pp. 64-73, 2011.
- [5] M. Ichimiya, "The status of Generation IV sodium-cooled fast reactor technology development and its future project," *Energy Procedia*, vol. 7, pp. 79-87, 2011.
- [6] B. Raj, "Materials and manufacturing technologies for sodium cooled fast reactors and associated fuel cycle: innovations and maturity," *Energy Procedia*, vol. 7, pp. 186-198, 2011.
- [7] T. Abram and S. Ion, "Generation-IV nuclear power: a review of the state of the science," *Energy Policy*, vol. 36, pp. 4323-4330, 2008.
- [8] C. Walker and G. Nicolaou, "Transmutation of neptunium and americium in a fast neutron flux," *Journal of Nuclear Materials*, vol. 218, pp. 129-138, 1995.
- [9] T. Allen, J. Busby, R. Klueh, S. Maloy and M. Tolocsko, "Cladding and duct materials for advanced nuclear recycle reactors," *JOM*, vol. 60, pp. 15-23, 2008.
- [10] P. Yvon and F. Carre, "Structural materials challenges for advanced reactor systems," *Journal of Nuclear Materials*, vol. 385, pp. 217-222, 2009.
- [11] J. Jung, S. Kim, S. Shin and I. K. J. Bang, "Feasibility study of fuel cladding

- performance for application in ultra-long cycle fast reactor," *Journal of Nuclear Materials*, vol. 440, pp. 596-605, 2013.
- [12] T. Ellis, R. Petrowskil, P. Hejzlar and G. Zimmerman, "Fuelling the traveling wave reactor," *Nuclear Engineering International*, vol. 56, 2011.
- [13] R. Pahl, D. Porter, D. Crawford and L. Walters, "Irradiation behavior of metallic fast reactor fuels," *Journal of Nuclear Materials*, vol. 188, pp. 3-9, 1992.
- [14] G. Hofman, L. Walters and T. Bauer, "Metallic Fast Reactor Fuels," *Progress in Nuclear Energy*, vol. 31, pp. 83-110, 1997.
- [15] V. Firouzdor and L. S. K. Wilson, "Development of diffusion barrier coatings for mitigation of fuel-cladding chemical interactions," in *4th International Conference on Electrophoretic Deposition: Fundamentals and Applications*, 2012.
- [16] L. Chapman and C. Holcombe, "Revisions of the iron-uranium phase diagram," *Journal of Nuclear Materials*, 1984.
- [17] A. Cohen, H. Tsai and L. Neimark, "Fuel/cladding compatibility in U-19Pu-10Zr/HT9-clad fuel at elevated temperatures," *Journal of Nuclear Materials*, vol. 204, pp. 244-251, 1993.
- [18] R. Mariani, D. Porter, T. O'Holleran, S. Hayes and J. Kennedy, "Lanthanides in metallic nuclear fuels: Their behavior and methods for their control," *Journal of Nuclear Materials*, vol. 419, pp. 263-271, 2011.
- [19] R. Mayo, *Introduction to Nuclear Concepts for Engineers*, American Nuclear Society, 1998.
- [20] D. Keiser, "ANL-NT-240," Argonne National Laboratory, Technical Report, 2006.
- [21] A. Cohen, T. Wiencek and H. Tsai, "Vanadium-lined HT9 cladding tubes," Argonne National Laboratory, 1994.

- [22] D. Keiser and J. Cole, "An evaluation of potential liner materials for eliminating FCCI in irradiated metallic nuclear fuel elements," Idaho National Laboratory, 2007.
- [23] D. Crawford, D. Porter and S. Hayes, "Fuels for sodium-cooled fast reactors: US perspective," *Journal of Nuclear Materials*, vol. 371, pp. 202-231, 2007.
- [24] D. Burkes, R. Fielding, D. Porter, D. Crawford and M. Meyer, "A US perspective on fast reactor fuel fabrication technology and experience part I: metal fuels and assembly design," *Journal of Nuclear Materials*, vol. 389, pp. 458-469, 2009.
- [25] G. Tillett and A. Buhl, "Clinch River breeder reactor breeding characteristics," *Nuclear Technology*, vol. 28, pp. 92-97, 1976.
- [26] M. Steele, "Operating experience at Enrico Fermi Fast Breeder Reactor," *Reactor Technology*, vol. 14, 1971.
- [27] Y. Chang, "The Integral Fast Reactor," *Nuclear Technology*, vol. 88, pp. 129-138, 1989.
- [28] X. Mi, "Fast reactor technology R&D activities in China," *Nuclear Engineering and Technology*, vol. 39, pp. 187-192, 2007.
- [29] R. Moore, "Douerey prototype fast reactor," *Nuclear Engineering International*, vol. 16, 1971.
- [30] U. Wehmann and H. Kinjo, "Studies on plutonium burning in the prototype fast breeder reactor Monju," *Nuclear Science and Engineering*, vol. 140, pp. 205-222, 2002.
- [31] T. Aoyama, T. Sekine and S. Tabuchi, "Characterization of neutron field in the experimental fast reactor JOYO for fuel and structural material irradiation test," *Nuclear Engineering and Design*, vol. 228, pp. 21-34, 2004.
- [32] A. Brandste and E. Guthmann, "Prototype nuclear-power station SNR-300,"

Atomwirtschaft, vol. 17, 1972.

- [33] M. Tourasse, M. Boidron and B. Pasquet, "Fission product behavior in Phenix fuel-pins at high burnup," *Journal of Nuclear Materials*, vol. 188, pp. 49-57, 1992.
- [34] A. Camplani and A. Zambelli, "Advanced nuclear-power stations - Superphenix and fast-breeder reactors," *Endeavour*, vol. 10, pp. 132-138, 1986.
- [35] M. Lineberry and T. Allen, "The sodium-cooled fast reactor (SFR)," Argonne National Laboratory, 2002.
- [36] H. Sekimoto, K. Ryu and Y. Yoshimura, "CANDLE: The new burnup strategy," *Nuclear Science and Engineering*, vol. 139, pp. 306-317, 2001.
- [37] D. Hartanto and Y. Kim, "Spent fuel utilization in a compact traveling wave reactor," in *ICANSE 2011*, 2012.
- [38] W. Carmack and D. Porter, "Metallic Fuels for Advanced Reactors," *Journal of Nuclear Materials*, vol. 392, pp. 139-150, 2009.
- [39] J. Kittel, B. Frost and J. Mustelier, "History of fast-reactor fuel development," *Journal of Nuclear Materials*, vol. 204, pp. 1-13, 1993.
- [40] V. Poplavskii, Y. Bagdasarov and A. Kamaev, "Danger of burning sodium coolant," *Atomic Energy*, vol. 96, pp. 327-331, 2004.
- [41] K. Ito, A. Yamaguchi and Y. Wada, "Technical report on Monju's sodium leak incident," *Journal of the Atomic Energy Society of Japan*, vol. 39, pp. 704-732, 1997.
- [42] A. Kimura, H. Cho and N. Toda, "High burnup fuel cladding materials R&D for advanced nuclear systems - Nano-sized oxide dispersion strengthened steels," *Journal of Nuclear Science and Technology*, vol. 44, pp. 323-328, 2007.
- [43] D. Crawford, D. Porter and S. Hayes, "Fuels for sodium-cooled fast reactors: US perspective," *Journal of Nuclear Materials*, vol. 371, pp. 202-231, 2007.
- [44] K. Sawa and K. Minato, "An investigation of irradiation performance of high

- burnup HTGR fuel," *Journal of Nuclear Science and Technology*, vol. 36, pp. 781-791, 1999.
- [45] D. Porter and C. Hilton, "Extending sodium fast reactor driver fuels to higher temperatures," *Nuclear Technology*, vol. 173, pp. 218-225, 2011.
- [46] Y. Kim, G. Hofman and A. Yacout, "Migration of minor actinides and lanthanides in fast reactor metallic fuel," *Journal of Nuclear Materials*, vol. 392, pp. 164-170, 2009.
- [47] K. Ingaki and T. Ogata, "Reaction of lanthanide elements with Fe-Cr alloy," *Journal of Nuclear Materials*, vol. 441, pp. 574-578, 2013.
- [48] R. Pahl, C. Lahm and S. Hayes, "Performance of HT9 clad metallic fuel at high temperature," *Journal of Nuclear Materials*, vol. 204, pp. 141-147, 1993.
- [49] X. Su, "Thermodynamic modeling of the ternary Ce-Fe-Sb system: assessment of the Ce-Sb and Ce-Fe systems," *CALPHAD*, 2006.
- [50] H. Okamoto, "Fe-Nd (Iron-Neodymium)," *Journal of Phase Equilibria*, 1997.
- [51] D. Crawford, C. Lahm, H. Tsai and R. Pahl, "Performance of U-Pu-Zr fuel cast into zirconium molds," *Journal of Nuclear Materials*, vol. 204, pp. 157-164, 1993.
- [52] W. Beck and R. Fousek, "The irradiation behavior of high-burnup uranium-plutonium alloy prototype fuel elements," Argonne National Laboratory, 1968.
- [53] H. Ryu, B. Lee and S. Oh, "Performance of FCCI barrier foils for U-Zr-X metallic fuel," *Journal of Nuclear Materials*, vol. 392, pp. 206-212, 2009.
- [54] P. Tortorici and M. Dayananda, "Interdiffusion of cerium in Fe-base alloys with Ni or Cr," *Journal of Nuclear Materials*, vol. 204, pp. 165-172, 1993.
- [55] R. Marazza, P. Riani and G. Cacciamani, "Critical assessment of iron binary systems with light rare earths La, Ce, Pr, and Nd," *Inorganica Chimica Acta*, vol. 361, pp. 3800-3806, 2008.

- [56] D. Zhang, I. McColl and J. Wood, "Diffusion reactions in the iron-neodymium binary alloy system," *Philosophical Magazine A*, vol. 75, pp. 959-974, 1997.
- [57] M. Devi and K. Gupta, "The misch metal-iron system," *Journal of Alloys and Compounds*, vol. 189, pp. 145-149, 1992.
- [58] M. Dariel, "The solute diffusion of iron in the light rare-earth metals cerium, praeodymium, and neodymium," *Acta Metallurgica*, vol. 23, pp. 472-479, 1975.
- [59] J. Kim, B. Lee and C. Lee, "Formation of intermetallic compound at interface between rare earth elements," *Journal of the Rare Earths*, vol. 30, pp. 599-603, 2012.
- [60] J. Kim, J. Baek and B. Lee, "Reaction between a rare earth element and 9Cr-2W steel," *Metals and Materials International*, vol. 4, pp. 535-540, 2011.
- [61] J. Kim, H. Ryu and J. Baek, "Performance of a diffusion barrier under a fuel-clad chemical interaction (FCCI)," *Journal of Nuclear Materials*, vol. 394, pp. 144-150, 2009.
- [62] S. Yang, H. Ryu and J. Kim, "FCCI barrier performance of electroplated Cr for metallic fuel," *Journal of Nuclear Materials*, vol. 401, pp. 98-103, 2010.
- [63] R. Borg and G. Dienes, *An Introduction to Solid State Diffusion*, Academic Press, 1988.
- [64] C. Wagner, "The evaluation of data obtained with diffusion couples of binary single-phase and multiphase systems," *Acta Metallurgica*, vol. 17, pp. 99-107, 1969.
- [65] A. Paul, A. Kodentsov and F. van Loo, "Physico-chemical analysis of compound growth in a diffusion couple with two-phase end members," *Intermetallics*, vol. 14, pp. 1428-1432, 2006.
- [66] C. Ghosh and A. Paul, "A physico-chemical approach to binary solid-state interdiffusion," *Acta Materialia*, vol. 55, pp. 1927-1939, 2007.

- [67] G. Kidson, "Some aspects of the growth of diffusion layers in binary systems," *Journal of Nuclear Materials*, vol. 3, pp. 21-29, 1961.
- [68] G. Li and G. Powell, "Theory of reaction diffusion in binary systems," *Acta Metallurgica*, vol. 33, pp. 23-31, 1985.
- [69] S. Shatynski, J. Hirth and R. Rapp, "A theory of multiphase binary diffusion," *Acta Metallurgica*, vol. 24, pp. 1071-1078, 1976.
- [70] K. Gan, "Lecture 7: Some Advanced Topics using Propagation of Errors and Least Squares Fitting," 2004. [Online]. Available: <http://www.physics.ohio-state.edu/~gan/teaching/spring04/Chapter7.pdf>. [Accessed 2013].
- [71] Y. Prots, P. Salamakha, O. Sologub and O. Bodak, "The neodymium-(vanadium, chromium, manganese)-silicon systems," *Journal of Alloys and Compounds*, vol. 215, pp. 235-238, 1994.
- [72] P. Salamakha, J. StepenDamm and O. Bodak, "Isothermal section of the Nd-Fe-Si system at 870K," *Journal of Alloys and Compounds*, vol. 242, pp. L1-L2, 1996.
- [73] N. Kolmakova, "Strongly Correlated Systems and High Temperature Superconductivity," *Low Temperature Physics*, vol. 28, pp. 653-668, 2002.
- [74] "Laves Phases," Department of Chemistry, University of Konstanz, [Online]. Available: http://www.chemie.uni-konstanz.de/~agfel/3D_FEST/INTER/MGCU_L.HTML. [Accessed 19 1 2014].
- [75] F. Landgraf, "Solidification and solid state transformations in Fe-Nd," *Journal of the Less-Common Metals*, vol. 163, pp. 209-218, 1990.
- [76] J. Moreau, "A new phase in the Nd-Fe system," *Journal of the Less-Common Metals*, vol. 163, pp. 245-251, 1990.
- [77] G. Egeland, "Reducing fuel-cladding chemical interaction: The effect of palladium on the reactivity of neodymium on iron in diffusion couples," *Journal*

- of Nuclear Materials*, vol. 432, pp. 539-544, 2013.
- [78] R. Murakami, "Substitutional and interstitial modification of Nd₅Fe₁₇," *Journal of Alloys and Compounds*, vol. 443, pp. 1-6, 2007.
- [79] C. Nourry, "Formation of Ni-Nd alloys by Nd(III) Electrochemical Reduction in Molten Fluoride," *Journal of New Materials for Electrochemical Systems*, vol. 10, pp. 117-122, 2007.
- [80] T. Nagai, "Thermodynamic measurement of Nd-Fe system by double Knudsen cell mass spectrometry," *Thermochimica Acta*, vol. 516, pp. 8-12, 2011.
- [81] "Thallium(I) iodide," Wikipedia, 27 February 2013. [Online]. Available: [http://en.wikipedia.org/wiki/Thallium\(I\)_iodide](http://en.wikipedia.org/wiki/Thallium(I)_iodide). [Accessed 22 January 2014].
- [82] "Structure Type 055: Fe₃C (Cementite)," Cambridge University, [Online]. Available: <http://som.web.cmu.edu/structures/S055-Fe3C.html>. [Accessed 2014 January 2014].
- [83] O. Heusler, "Diffusion in metals at room-temperature," *ZEITSCHRIFT FUR METALLKUNDE*, vol. 85, no. 1, pp. 47-49, 1994.
- [84] "A General Monte Carlo N-Particle (MCNP) Transport Code," Los Alamos National Laboratory, 2010. [Online]. Available: mcnp.lanl.gov. [Accessed 2014].
- [85] T. Furukawa, S. Kato and E. Yoshida, "Compatibility of FBR materials with sodium," *Journal of Nuclear Materials*, vol. 392, pp. 249-254, 2009.
- [86] "Metallographic Etchants," Pace Technologies, [Online]. Available: <http://www.metallographic.com/Etchants/Etchants.htm>. [Accessed 2014].

APPENDIX A: DIFFUSION CALCULATION MACROS

A.1 Macro for Boltzmann-Matano Diffusion Coefficient Calculation

```
Sub Matano_Method_with_Error_Analysis()
```

```
' Matano_Method Macro
```

```
' This macro is designed to take position data (first column) and composition data  
' for two elements (second and third columns)
```

```
' and determine the location of the Matano plane. Once this plane is determined, an  
' erfc fit is made to each concentration
```

```
' curve. Based on this fit, a diffusion coefficient is calculated based on each curve. In  
' addition, error values are computed.
```

```
' Note: The assumed units for input are  $\mu\text{m}$  and seconds and the output diffusion  
' coefficients are in units of  $\text{m}^2/\text{s}$ 
```

```
' Note: This macro will not work unless the Solver add-in is installed, Solver has  
' been run at least once in the worksheet,
```

```
' and the Solver add-in is referenced in the VBA editor
```

```
' This macro was created by Grant Helmreich. Contact granthelmreich@gmail.com  
' for any comments or questions.
```

```
Dim num As Integer 'the number of data points
```

```
Dim r As Integer 'loop counter and current row number
```

```
Dim quit As Boolean 'loop exit variable
```

```
Dim ele1avg As Double 'Average of high and low concentrations of element 1
```

```
Dim ele2avg As Double 'Average of high and low concentrations of element 2
```

```
Dim ele1min As Double 'Lowest concentration of element 1
```

```
Dim ele2min As Double 'Lowest concentration of element 2
```

```
Dim ele1max As Double 'Highest concentration of element 1
```

```
Dim ele2max As Double 'Highest concentration of element 2
```

```
Dim swap As Double 'Temporary variable for swapping columns
```

```
Dim xm1 As Double 'Matano plane offset for element 1
```

```
Dim xm2 As Double 'Matano plane offset for element 2
```

```
Dim time As Double 'Duration of the diffusion heat treatment in seconds
```

```
Dim sigx As Double 'Error (in  $\mu\text{m}$ ) in position values
```

```
Dim sigc As Double 'Error (in at%) in concentration values
```

```

Dim target As String 'Target cell for solver
Dim source As String 'Source cell for solver

r = 0
num = 0
quit = False

Application.ScreenUpdating = False

r = 2
Do 'Loop to find total number of points
    If Cells(r, 1).Value = "" Then
        quit = True
    Else
        r = r + 1
    End If
Loop Until quit = True
quit = False
num = r - 2
r = 0

If Cells(2, 2).Value > Cells(2, 3).Value Then 'This block swaps the columns to
put them in the right order
    r = 2
    Cells(1, 4).Value = Cells(1, 2).Value
    Cells(1, 2).Value = Cells(1, 3).Value
    Cells(1, 3).Value = Cells(1, 4).Value
    Cells(1, 4).Value = ""

    Do
        swap = Cells(r, 2).Value
        Cells(r, 2).Value = Cells(r, 3).Value
        Cells(r, 3).Value = swap
        r = r + 1
    Loop Until r = num + 2
End If

ele1min = WorksheetFunction.Min(Range(Cells(2, 2), Cells(num + 1, 2))) 'Finds
minimum value for element 1

```


ele1max = WorksheetFunction.Max(Range(Cells(2, 2), Cells(num + 1, 2))) 'Finds maximum value for element 1

ele2max = WorksheetFunction.Min(Range(Cells(2, 3), Cells(num + 1, 3))) 'Finds minimum value for element 2

ele2max = WorksheetFunction.Max(Range(Cells(2, 3), Cells(num + 1, 3))) 'Finds maximum value for element 2

ele1avg = (ele1max - ele1min) / 2 'Find average of high and low values of element 1

ele2avg = (ele2max - ele2min) / 2 'Find average of high and low values of element 2

r = 2

Do

Cells(r, 4).Value = Cells(r - 1, 4).Value + Cells(r, 2).Value - ele1min
'Forward sum of element 1

Cells(r, 6).Value = Cells(r - 1, 6).Value + ele2max - Cells(r, 3).Value
'Reverse sum of element 2

Cells(num + 3 - r, 5).Value = Cells(num + 4 - r, 5) + ele1max - Cells(num + 3 - r, 2).Value 'Reverse sum of element 1

Cells(num + 3 - r, 7).Value = Cells(num + 4 - r, 7) + Cells(num + 3 - r, 3).Value - ele2min 'Forward sum of element 2

Cells(r, 8).Value = Cells(r, 1).Value 'This set of cells are the 1st-6th powers of the position values

Cells(r, 9).Value = (Cells(r, 1).Value) ^ 2 'they will be used to make a 6th order polynomial fit to the forward

Cells(r, 10).Value = (Cells(r, 1).Value) ^ 3 'and reverse sums for elements 1 and 2

Cells(r, 11).Value = (Cells(r, 1).Value) ^ 4

Cells(r, 12).Value = (Cells(r, 1).Value) ^ 5

Cells(r, 13).Value = (Cells(r, 1).Value) ^ 6

r = r + 1

Loop Until r = num + 2

Range(Cells(1, 14), Cells(1, 20)).FormulaArray = "=Linest(R2C4:R" & num + 1 & "C4,R2C8:R" & num + 1 & "C13,true,false)" 'Defines cells N1-S1 as coefficients for polynomial fit to forward sum of element 1

Range(Cells(2, 14), Cells(2, 20)).FormulaArray = "=Linest(R2C5:R" & num + 1 & "C5,R2C8:R" & num + 1 & "C13,true,false)" 'Defines cells N2-S2 as coefficients for polynomial fit to reverse sum of element 1

Range(Cells(3, 14), Cells(3, 20)).FormulaArray = "=Linest(R2C6:R" & num + 1 & "C6,R2C8:R" & num + 1 & "C13,true,false)" 'Defines cells N3-S3 as coefficients for polynomial fit to forward sum of element 2

Range(Cells(4, 14), Cells(4, 20)).FormulaArray = "=Linest(R2C7:R" & num + 1 & "C7,R2C8:R" & num + 1 & "C13,true,false)" 'Defines cells N4-S4 as coefficients for polynomial fit to reverse sum of element 2

Cells(6, 14).Value = (Cells(num + 1, 1).Value - Cells(2, 1).Value) / 2 'Starting guess for Matano plane for element 1

Cells(7, 14).Value = (Cells(num + 1, 1).Value - Cells(2, 1).Value) / 2 'Starting guess for Matano plane for element 2

Cells(6, 16).Value =
"=N1*N6^6+O1*N6^5+P1*N6^4+Q1*N6^3+R1*N6^2+S1*N6+T1" 'Value of fit for
element 1 forward sum at matano plane

Cells(6, 17).Value =
"=N2*N6^6+O2*N6^5+P2*N6^4+Q2*N6^3+R2*N6^2+S2*N6+T2" 'Value of fit for
element 1 reverse sum at matano plane

Cells(7, 16).Value =
"=N3*N7^6+O3*N7^5+P3*N7^4+Q3*N7^3+R3*N7^2+S3*N7+T3" 'Value of fit for
element 2 forward sum at matano plane

Cells(7, 17).Value =
"=N4*N7^6+O4*N7^5+P4*N7^4+Q4*N7^3+R4*N7^2+S4*N7+T4" 'Value of fit for
element 2 reverse sum at matano plane

Cells(6, 18).Value = "=abs(P6-Q6)*1000" 'Difference between forward and reverse sums for element 1

Cells(7, 18).Value = "=abs(P7-Q7)*1000" 'Difference between forward and reverse sums for element 2

SolverReset

solverok SetCell:="\$R\$6", MaxMinVal:=2, ValueOf:=0, ByChange:="\$N\$6",
Engine:=1, EngineDesc:="GRG Nonlinear" 'Solver to find element 1 Matano plane

SolverAdd CellRef:="\$N\$6", Relation:=3, FormulaText:=Cells(2, 1).Value

SolverAdd CellRef:="\$N\$6", Relation:=1, FormulaText:=Cells(num + 1, 1).Value

solversolve UserFinish:=True

xm1 = Cells(6, 14).Value 'Save matano plane position 1

```

SolverReset
solverok SetCell:="$R$7", MaxMinVal:=2, ValueOf:=0, ByChange:="$N$7",
Engine:=1, EngineDesc:="GRG Nonlinear" 'Solver to find element 2 Matano plane
SolverAdd CellRef:="$N$7", Relation:=3, FormulaText:=Cells(2, 1).Value
SolverAdd CellRef:="$N$7", Relation:=1, FormulaText:=Cells(num + 1, 1).Value
solversolve UserFinish:=True
xm2 = Cells(6, 14).Value 'Save matano plane position 2

r = 2
Do
    Cells(r, 22).Value = "=R" & r & "C1-R6C14" 'Position reset so that the
Matano plane for element 1 is at 0
    Cells(r, 26).Value = "=R" & r & "C1-R7C14" 'Position reset so that the
Matano plane for element 2 is at 0

    Cells(r, 23).Value = Cells(r, 2).Value 'Copied values of
concentrations for element 1
    Cells(r, 27).Value = Cells(r, 3).Value 'Copied values of
concentrations for element 2

    Cells(r, 24).Value = "=" & ele1max & "-ERFC(R" & r & "C22*R9C15/10000)*" &
ele1avg 'Erfc fit for element 1
    Cells(r, 28).Value = "=ERFC(R" & r & "C26*R10C15/10000)*" & ele2avg & "+" &
ele2min 'Erfc fit for element 2

    Cells(r, 25).Value = "=R" & r & "C24-R" & r & "C23)^2" 'Square of the
difference between Erfc fit and available data for element 1
    Cells(r, 29).Value = "=R" & r & "C28-R" & r & "C27)^2" 'Square of the
difference between Erfc fit and available data for element 2

    r = r + 1
Loop Until (r = num + 2)

Cells(9, 16).Value = "=Sum(R2C25:R" & num + 1 & "C25)" 'Sum of the squares of
the errors for element 1 Erfc fit
Cells(10, 16).Value = "=Sum(R2C29:R" & num + 1 & "C29)" 'Sum of the squares of
the errors for element 2 Erfc fit

SolverReset

```

solverok SetCell:="\$P\$9", MaxMinVal:=2, ValueOf:=0, ByChange:="\$O\$9",
Engine:=1, EngineDesc:="GRG Nonlinear" 'Solver to optimize the Erfc fit for
element 1

solversolve UserFinish:=True

SolverReset

solverok SetCell:="\$P\$10", MaxMinVal:=2, ValueOf:=0, ByChange:="\$O\$10",
Engine:=1, EngineDesc:="GRG Nonlinear" 'Solver to optimize the Erfc fit for element
1

solversolve UserFinish:=True

Cells(12, 15).Value = "Time (s):" 'Output descriptors (time must be entered
manually)

Cells(11, 17).Value = "Ele 1 (m²/s):"

Cells(12, 17).Value = "Ele 2 (m²/s):"

Cells(11, 18).Value = "=(5/(R9C15*1000))^2/R12C16" 'Calculation of D for
element 1

Cells(12, 18).Value = "=(5/(R10C15*1000))^2/R12C16" 'Calculation of D for
element 2

Cells(12, 16).Value = "=A1*24*3600" 'Set time (s) to equal Cell A1 (days)

'The remainder of this macro attempts to define the standard error in the
calculated diffusion coefficients.

Cells(num * 1 + 3, 1).Value = "D+(C)"

Cells(num * 2 + 5, 1).Value = "D-(C)"

Cells(num * 3 + 7, 1).Value = "D+(x)"

Cells(num * 4 + 9, 1).Value = "D-(x)"

sigx = 0.05

sigc = 2

r = 1

Do While r < num + 1 'This loop initializes the next four
data sets as copies of the first

Cells(num * 1 + 3 + r, 1).Value = Cells(r + 1, 1).Value

Cells(num * 2 + 5 + r, 1).Value = Cells(r + 1, 1).Value

Cells(num * 3 + 7 + r, 2).Value = Cells(r + 1, 2).Value

Cells(num * 4 + 9 + r, 2).Value = Cells(r + 1, 2).Value
 Cells(num * 3 + 7 + r, 3).Value = Cells(r + 1, 3).Value
 Cells(num * 4 + 9 + r, 3).Value = Cells(r + 1, 3).Value

If Cells(r + 1, 1).Value < (xm1 + xm2) / 2 Then 'Adjust x values in D+x
 and D-x
 Cells(num * 3 + 7 + r, 1).Value = Cells(r + 1, 1).Value - sigx
 Cells(num * 4 + 9 + r, 1).Value = Cells(r + 1, 1).Value + sigx
 End If

If Cells(r + 1, 1).Value > (xm1 + xm2) / 2 Then 'Adjust x values in D+x
 and D-x
 Cells(num * 3 + 7 + r, 1).Value = Cells(r + 1, 1).Value + sigx
 Cells(num * 4 + 9 + r, 1).Value = Cells(r + 1, 1).Value - sigx
 End If

If Cells(r + 1, 1).Value < xm1 Then 'Adjust C1 values in D+c and
 D-c
 Cells(num * 1 + 3 + r, 2).Value = Cells(r + 1, 2).Value + sigc
 Cells(num * 2 + 5 + r, 2).Value = Cells(r + 1, 2).Value - sigc
 End If

If Cells(r + 1, 1).Value > xm1 Then
 Cells(num * 1 + 3 + r, 2).Value = Cells(r + 1, 2).Value - sigc
 Cells(num * 2 + 5 + r, 2).Value = Cells(r + 1, 2).Value + sigc
 End If

If Cells(r + 1, 1).Value < xm2 Then 'Adjust C2 values in D+c and
 D-c
 Cells(num * 1 + 3 + r, 3).Value = Cells(r + 1, 3).Value - sigc
 Cells(num * 2 + 5 + r, 3).Value = Cells(r + 1, 3).Value + sigc
 End If

If Cells(r + 1, 1).Value > xm2 Then
 Cells(num * 1 + 3 + r, 3).Value = Cells(r + 1, 3).Value + sigc
 Cells(num * 2 + 5 + r, 3).Value = Cells(r + 1, 3).Value - sigc
 End If

Cells(num * 1 + 3 + r, 5).Value = Cells(num * 1 + 3 + r, 1).Value - xm1 'Setup
 matano plane adjusted x values for erfc() fits on all four data sets

Cells(num * 1 + 3 + r, 9).Value = Cells(num * 1 + 3 + r, 1).Value - xm2
 Cells(num * 2 + 5 + r, 5).Value = Cells(num * 2 + 5 + r, 1).Value - xm1
 Cells(num * 2 + 5 + r, 9).Value = Cells(num * 2 + 5 + r, 1).Value - xm2
 Cells(num * 3 + 7 + r, 5).Value = Cells(num * 3 + 7 + r, 1).Value - xm1
 Cells(num * 3 + 7 + r, 9).Value = Cells(num * 3 + 7 + r, 1).Value - xm2
 Cells(num * 4 + 9 + r, 5).Value = Cells(num * 4 + 9 + r, 1).Value - xm1
 Cells(num * 4 + 9 + r, 9).Value = Cells(num * 4 + 9 + r, 1).Value - xm2

Cells(num * 1 + 3 + r, 6).Value = "=" & ele1max - sigc & "-ERFC(R" & num * 1 + 3 + r & "C5*R" & num * 1 + 4 & "C13/10000)*" & ele1avg - sigc 'Setup erfc() calculators for all four data sets

Cells(num * 1 + 3 + r, 10).Value = "=ERFC(R" & num * 1 + 3 + r & "C9*R" & num * 1 + 4 & "C14/10000)*" & ele2avg - sigc & "+" & ele2min + sigc

Cells(num * 2 + 5 + r, 6).Value = "=" & ele1max + sigc & "-ERFC(R" & num * 2 + 5 + r & "C5*R" & num * 2 + 6 & "C13/10000)*" & ele1avg + sigc

Cells(num * 2 + 5 + r, 10).Value = "=ERFC(R" & num * 2 + 5 + r & "C9*R" & num * 2 + 6 & "C14/10000)*" & ele2avg + sigc & "+" & ele2min - sigc

Cells(num * 3 + 7 + r, 6).Value = "=" & ele1max & "-ERFC(R" & num * 3 + 7 + r & "C5*R" & num * 3 + 8 & "C13/10000)*" & ele1avg

Cells(num * 3 + 7 + r, 10).Value = "=ERFC(R" & num * 3 + 7 + r & "C9*R" & num * 3 + 8 & "C14/10000)*" & ele2avg & "+" & ele2min

Cells(num * 4 + 9 + r, 6).Value = "=" & ele1max & "-ERFC(R" & num * 4 + 9 + r & "C5*R" & num * 4 + 10 & "C13/10000)*" & ele1avg

Cells(num * 4 + 9 + r, 10).Value = "=ERFC(R" & num * 4 + 9 + r & "C9*R" & num * 4 + 10 & "C14/10000)*" & ele2avg & "+" & ele2min

Cells(num * 1 + 3 + r, 7).Value = "(R" & num * 1 + 3 + r & "C2-R" & num * 1 + 3 + r & "C6)^2" 'Setup square of the errors for each fit

Cells(num * 1 + 3 + r, 11).Value = "(R" & num * 1 + 3 + r & "C3-R" & num * 1 + 3 + r & "C10)^2"

Cells(num * 2 + 5 + r, 7).Value = "(R" & num * 2 + 5 + r & "C2-R" & num * 2 + 5 + r & "C6)^2"

Cells(num * 2 + 5 + r, 11).Value = "(R" & num * 2 + 5 + r & "C3-R" & num * 2 + 5 + r & "C10)^2"

Cells(num * 3 + 7 + r, 7).Value = "(R" & num * 3 + 7 + r & "C2-R" & num * 3 + 7 + r & "C6)^2"

Cells(num * 3 + 7 + r, 11).Value = "(R" & num * 3 + 7 + r & "C3-R" & num * 3 + 7 + r & "C10)^2"

Cells(num * 4 + 9 + r, 7).Value = "(R" & num * 4 + 9 + r & "C2-R" & num * 4 + 9 + r & "C6)^2"

```
Cells(num * 4 + 9 + r, 11).Value = "(R" & num * 4 + 9 + r & "C3-R" & num * 4 + 9 + r & "C10)^2"
```

```
r = r + 1
```

```
Loop
```

```
Cells(num * 1 + 5, 13).Value = "=sum(R" & num * 1 + 4 & "C7:R" & num * 2 + 3 & "C7)" 'Sum of the squares of the errors for each of the 8 fits
```

```
Cells(num * 1 + 5, 14).Value = "=sum(R" & num * 1 + 4 & "C11:R" & num * 2 + 3 & "C11)"
```

```
Cells(num * 2 + 7, 13).Value = "=sum(R" & num * 2 + 6 & "C7:R" & num * 3 + 5 & "C7)"
```

```
Cells(num * 2 + 7, 14).Value = "=sum(R" & num * 2 + 6 & "C11:R" & num * 3 + 5 & "C11)"
```

```
Cells(num * 3 + 9, 13).Value = "=sum(R" & num * 3 + 8 & "C7:R" & num * 4 + 7 & "C7)"
```

```
Cells(num * 3 + 9, 14).Value = "=sum(R" & num * 3 + 8 & "C11:R" & num * 4 + 7 & "C11)"
```

```
Cells(num * 4 + 11, 13).Value = "=sum(R" & num * 4 + 10 & "C7:R" & num * 5 + 9 & "C7)"
```

```
Cells(num * 4 + 11, 14).Value = "=sum(R" & num * 4 + 10 & "C11:R" & num * 5 + 9 & "C11)"
```

```
r = 1
```

Do While r < 5 'Solver loop that calculates D's for both elements iteratively over each of the four adjusted curves

```
target = Cells((num + 2) * r + 3, 13).Address
```

```
source = Cells((num + 2) * r + 2, 13).Address
```

```
SolverReset
```

```
solverok SetCell:=target, MaxMinVal:=3, ValueOf:=0, ByChange:=source, Engine:=1, EngineDesc:="GRG Nonlinear" 'Solver to optimize the Erfc fit for element 1
```

```
solversolve UserFinish:=True
```

```
target = Cells((num + 2) * r + 3, 14).Address
```

```
source = Cells((num + 2) * r + 2, 14).Address
```

```
SolverReset
```

```
solverok SetCell:=target, MaxMinVal:=3, ValueOf:=0, ByChange:=source,
Engine:=1, EngineDesc:="GRG Nonlinear" 'Solver to optimize the Erfc fit for element
2
```

```
solversolve UserFinish:=True
```

```
Cells((num + 2) * r + 5, 13).Value = "(5/(R" & (num + 2) * r + 2 &
"C13*1000))^2/R12C16" 'Output diffusion values
```

```
Cells((num + 2) * r + 5, 14).Value = "(5/(R" & (num + 2) * r + 2 &
"C14*1000))^2/R12C16"
```

```
r = r + 1
```

```
Loop
```

```
Cells(10, 18).Value = "D (m^2/s)" 'This section creates a table of each sigma and
the total sigma for each element
```

```
Cells(10, 19).Value = "Sig_tot"
```

```
Cells(10, 20).Value = "Sig_C"
```

```
Cells(10, 21).Value = "Sig_x"
```

```
Cells(11, 19).Value = "=sqrt(R11C20^2+R11C21^2)"
```

```
Cells(12, 19).Value = "=sqrt(R12C20^2+R12C21^2)"
```

```
Cells(11, 20).Value = "=sqrt(((R11C18-R" & num * 1 + 7 & "C13)^2+(R11C18-R" &
num * 2 + 9 & "C13)^2)/2)"
```

```
Cells(11, 21).Value = "=sqrt(((R11C18-R" & num * 3 + 11 & "C13)^2+(R11C18-R" &
num * 4 + 13 & "C13)^2)/2)"
```

```
Cells(12, 20).Value = "=sqrt(((R12C18-R" & num * 1 + 7 & "C14)^2+(R12C18-R" &
num * 2 + 9 & "C14)^2)/2)"
```

```
Cells(12, 21).Value = "=sqrt(((R12C18-R" & num * 3 + 11 & "C14)^2+(R12C18-R" &
num * 4 + 13 & "C14)^2)/2)"
```

```
'Create plot for first element
```

```
ActiveSheet.Shapes.AddChart.Select
```

```
ActiveChart.ChartType = xlXYScatterSmooth
```

```
ActiveChart.SeriesCollection.NewSeries
```

```
ActiveChart.SeriesCollection(1).XValues = Range(Cells(2, 22), Cells(num + 1, 22))
```

```
ActiveChart.SeriesCollection(1).Values = Range(Cells(2, 23), Cells(num + 1, 23))
```

```
ActiveChart.SeriesCollection.NewSeries
```

```
ActiveChart.SeriesCollection(2).XValues = Range(Cells(2, 22), Cells(num + 1, 22))
```



```

ActiveChart.SeriesCollection(2).Values = Range(Cells(2, 24), Cells(num + 1, 24))
ActiveChart.SeriesCollection(1).name = Cells(1, 2).Value & " Data"
ActiveChart.SeriesCollection(2).name = Cells(1, 2).Value & " erfc Model"
ActiveChart.Axes(xlValue).MinimumScale = 0
ActiveChart.Axes(xlValue).MaximumScale = 110
ActiveChart.Axes(xlValue).MajorUnit = 20
ActiveChart.ChartArea.Select
ActiveChart.SetElement (msoElementChartTitleAboveChart)
ActiveChart.SetElement (msoElementLegendTop)
Selection.Format.TextFrame2.TextRange.Characters.Text = Cells(1, 2).Value & " vs.
" & Cells(1, 3).Value & " Data vs. erfc Model"
ActiveChart.SetElement (msoElementPrimaryCategoryAxisTitleAdjacentToAxis)
Selection.Format.TextFrame2.TextRange.Characters.Text = "Position ( $\mu\text{m}$ )"
ActiveChart.SetElement (msoElementPrimaryValueAxisTitleRotated)
Selection.Format.TextFrame2.TextRange.Characters.Text = "Composition (at%)"

Do While ActiveChart.SeriesCollection.Count > 2
  ActiveChart.SeriesCollection(ActiveChart.SeriesCollection.Count).Delete
Loop

'Create plot for second element
ActiveSheet.Shapes.AddChart.Select
ActiveChart.ChartType = xlXYScatterSmooth
ActiveChart.SeriesCollection.NewSeries
ActiveChart.SeriesCollection(1).XValues = Range(Cells(2, 26), Cells(num + 1, 26))
ActiveChart.SeriesCollection(1).Values = Range(Cells(2, 27), Cells(num + 1, 27))
ActiveChart.SeriesCollection.NewSeries
ActiveChart.SeriesCollection(2).XValues = Range(Cells(2, 26), Cells(num + 1, 26))
ActiveChart.SeriesCollection(2).Values = Range(Cells(2, 28), Cells(num + 1, 28))
ActiveChart.SeriesCollection(1).name = Cells(1, 3).Value & " Data"
ActiveChart.SeriesCollection(2).name = Cells(1, 3).Value & " erfc Model"
ActiveChart.Axes(xlValue).MinimumScale = 0
ActiveChart.Axes(xlValue).MaximumScale = 110
ActiveChart.Axes(xlValue).MajorUnit = 20
ActiveChart.ChartArea.Select
ActiveChart.SetElement (msoElementChartTitleAboveChart)
ActiveChart.SetElement (msoElementLegendTop)
Selection.Format.TextFrame2.TextRange.Characters.Text = Cells(1, 3).Value & " vs.
" & Cells(1, 2).Value & " Data vs. erfc Model"
ActiveChart.SetElement (msoElementPrimaryCategoryAxisTitleAdjacentToAxis)

```

```
Selection.Format.TextFrame2.TextRange.Characters.Text = "Position ( $\mu\text{m}$ )"  
ActiveChart.SetElement (msoElementPrimaryValueAxisTitleRotated)  
Selection.Format.TextFrame2.TextRange.Characters.Text = "Composition (at%)"
```

```
Do While ActiveChart.SeriesCollection.Count > 2  
    ActiveChart.SeriesCollection(ActiveChart.SeriesCollection.Count).Delete  
Loop
```

```
'Create combined plot with both elements for dissertation  
ActiveSheet.Shapes.AddChart.Select  
ActiveChart.ChartType = xlXYScatterSmooth  
ActiveChart.SeriesCollection.NewSeries  
ActiveChart.SeriesCollection.NewSeries  
ActiveChart.SeriesCollection.NewSeries  
ActiveChart.SeriesCollection.NewSeries  
ActiveChart.SeriesCollection(1).XValues = Range(Cells(2, 26), Cells(num + 1, 26))  
ActiveChart.SeriesCollection(1).Values = Range(Cells(2, 27), Cells(num + 1, 27))  
'ActiveChart.SeriesCollection.NewSeries  
ActiveChart.SeriesCollection(2).XValues = Range(Cells(2, 26), Cells(num + 1, 26))  
ActiveChart.SeriesCollection(2).Values = Range(Cells(2, 28), Cells(num + 1, 28))  
ActiveChart.SeriesCollection(1).name = Cells(1, 3).Value & " Data"  
ActiveChart.SeriesCollection(2).name = Cells(1, 3).Value & " Model"  
'ActiveChart.SeriesCollection.NewSeries  
ActiveChart.SeriesCollection(3).XValues = Range(Cells(2, 22), Cells(num + 1, 22))  
ActiveChart.SeriesCollection(3).Values = Range(Cells(2, 23), Cells(num + 1, 23))  
'ActiveChart.SeriesCollection.NewSeries  
ActiveChart.SeriesCollection(4).XValues = Range(Cells(2, 22), Cells(num + 1, 22))  
ActiveChart.SeriesCollection(4).Values = Range(Cells(2, 24), Cells(num + 1, 24))  
ActiveChart.SeriesCollection(3).name = Cells(1, 2).Value & " Data"  
ActiveChart.SeriesCollection(4).name = Cells(1, 2).Value & " Model"  
ActiveChart.Axes(xlValue).MinimumScale = 0  
ActiveChart.Axes(xlValue).MaximumScale = 110  
ActiveChart.Axes(xlValue).MajorUnit = 20  
ActiveChart.ChartArea.Select  
'ActiveChart.SetElement (msoElementChartTitleAboveChart)  
ActiveChart.SetElement (msoElementLegendTop)  
'Selection.Format.TextFrame2.TextRange.Characters.Text = Cells(1, 3).Value & "  
vs. " & Cells(1, 2).Value & " Data vs. erfc Model"  
ActiveChart.SetElement (msoElementPrimaryCategoryAxisTitleAdjacentToAxis)  
Selection.Format.TextFrame2.TextRange.Characters.Text = "Position ( $\mu\text{m}$ )"
```

```
ActiveChart.SetElement (msoElementPrimaryValueAxisTitleRotated)
Selection.Format.TextFrame2.TextRange.Characters.Text = "Composition (at%)"
ActiveChart.Parent.Height = 288
ActiveChart.Parent.Width = 432
```

```
Do While ActiveChart.SeriesCollection.Count > 4
    ActiveChart.SeriesCollection(ActiveChart.SeriesCollection.Count).Delete
Loop
```

```
Application.ScreenUpdating = True
```

```
End Sub
```

A.2 Macro for Diffusion Coefficient Calculation on Split Interface

```
Sub Split_Interface_Solver()
```

```
,
```

```
' This macro is designed to take position data (first column) and composition data
for two elements (second and third columns)
' and determine the location of the Matano plane. Once this plane is determined, an
erfc fit is made to each concentration
' curve. Based on this fit, a diffusion coefficient is calculated based on each curve. In
addition, error values are computed.
```

```
' Note: The assumed units for input are  $\mu\text{m}$  and seconds and the output diffusion
coefficients are in units of  $\text{m}^2/\text{s}$ 
```

```
' Note: This macro will not work unless the Solver add-in is installed, Solver has
been run at least once in the worksheet,
' and the Solver add-in is referenced in the VBA editor
```

```
' This macro is specifically designed to work with data in which only a fraction of
the diffusion curve is available (i.e. a split interface)
```

```
,
```

```
' This macro was created by Grant Helmreich. Contact granthelmreich@gmail.com
for any comments or questions.
```

```
Dim num As Integer 'the number of data points
```

```

Dim r    As Integer 'loop counter and current row number
Dim quit As Boolean 'loop exit variable
Dim ele1avg As Double 'Average of high and low concentrations of element 1
Dim ele2avg As Double 'Average of high and low concentrations of element 2
Dim ele1min As Double 'Lowest concentration of element 1
Dim ele2min As Double 'Lowest concentration of element 2
Dim ele1max As Double 'Highest concentration of element 1
Dim ele2max As Double 'Highest concentration of element 2
Dim swap  As Double 'Temporary variable for swapping columns
Dim xm1   As Double 'Matano plane offset for element 1
Dim xm2   As Double 'Matano plane offset for element 2
Dim time  As Double 'Duration of the diffusion heat treatment in seconds
Dim sigx  As Double 'Error (in  $\mu\text{m}$ ) in position values
Dim sigc  As Double 'Error (in at%) in concentration values
Dim target As String 'Target cell for solver
Dim source As String 'Source cell for solver

```

```

r = 0
num = 0
quit = False

```

```

Application.ScreenUpdating = False

```

```

r = 4
Do                                'Loop to find total number of points
    If Cells(r, 1).Value = "" Then 'Starts in cell A4 then steps down until a blank
cell is found
        quit = True
    Else
        r = r + 1
    End If
Loop Until quit = True
quit = False
num = r - 4
r = 0

```

```

    If Cells(4, 2).Value > Cells(3 + num, 2).Value Then 'This block swaps the
columns to put them in the right order
        r = 4                                'It uses Column D as temporary storage for the
swap

```

```
Cells(1, 4).Value = Cells(1, 2).Value
Cells(1, 2).Value = Cells(1, 3).Value
Cells(1, 3).Value = Cells(1, 4).Value
Cells(1, 4).Value = ""
```

```
Cells(2, 4).Value = Cells(2, 2).Value
Cells(2, 2).Value = Cells(2, 3).Value
Cells(2, 3).Value = Cells(2, 4).Value
Cells(2, 4).Value = ""
```

```
Cells(3, 4).Value = Cells(3, 2).Value
Cells(3, 2).Value = Cells(3, 3).Value
Cells(3, 3).Value = Cells(3, 4).Value
Cells(3, 4).Value = ""
```

```
Do
    swap = Cells(r, 2).Value
    Cells(r, 2).Value = Cells(r, 3).Value
    Cells(r, 3).Value = swap
    r = r + 1
Loop Until r = num + 4
End If
```

```
ele1min = Cells(1, 2).Value 'Finds minimum value for element 1
ele1max = Cells(2, 2).Value 'Finds maximum value for element 1
ele2min = Cells(1, 3).Value 'Finds minimum value for element 2
ele2max = Cells(2, 3).Value 'Finds maximum value for element 2
ele1avg = (ele1max - ele1min) / 2 'Find average of high and low
values of element 1
ele2avg = (ele2max - ele2min) / 2 'Find average of high and low
values of element 2
```

```
Cells(1, 5).Value = "Coeff_1" 'Diffusion Coeff of curve 1, of curve 2, and
shift to Matano plane
```

```
Cells(1, 6).Value = "Coeff_2"
Cells(1, 7).Value = "Delta_Xm"
```

```
Cells(2, 5).Value = 1.1 'Initial guesses for D1, D2, and Delta_Xm
Cells(2, 6).Value = 1.1
Cells(2, 7).Value = 1.1
```

```
Cells(3, 5).Value = "X"  
Cells(3, 6).Value = Cells(3, 2).Value  
Cells(3, 7).Value = Cells(3, 3).Value
```

```
r = 4
```

```
Do
```

```
Cells(r, 5).Value = "=R" & r & "C1+R2C7" 'Matano plane adjusted for model
```

```
Cells(r, 6).Value = "=R2C2-ERFC(R" & r & "C5/R2C5)*(R2C2-R1C2)/2" 'Model  
for element 1
```

```
Cells(r, 7).Value = "=R1C3+ERFC(R" & r & "C5/R2C6)*(R2C3-R1C3)/2" 'Model  
for element 2
```

```
Cells(r, 9).Value = "(R" & r & "C2-R" & r & "C6)^2" 'Square of error for  
element 1
```

```
Cells(r, 10).Value = "(R" & r & "C3-R" & r & "C7)^2" 'Square of error for  
element 2
```

```
r = r + 1
```

```
Loop Until r = num + 4
```

```
Cells(3, 9).Value = "=SUM(R4C9:R" & num + 4 & "C9)" 'sum of squares of errors  
for element 1
```

```
Cells(3, 10).Value = "=SUM(R4C10:R" & num + 4 & "C10)" 'sum of squares of  
errors for element 2
```

```
Cells(1, 9).Value = "=r3c9^2+r3c10^2" 'Square of the sums of the squares of errors  
for each element
```

```
SolverReset
```

```
solverok SetCell:="$I$1", MaxMinVal:=3, ValueOf:=0, ByChange:="$e$2:$G$2",  
Engine:=1, EngineDesc:="GRG Nonlinear" 'Solver to optimize the Erfc fit for element  
1
```

```
SolverAdd CellRef:="$E$2", Relation:=3, FormulaText:="0.01"
```

```
SolverAdd CellRef:="$F$2", Relation:=3, FormulaText:="0.01"
```

```
SolverOptions MaxTime:=0, Iterations:=0, Precision:=0.000001,  
Convergence:=0.0001, StepThru:=False, Scaling:=True, AssumeNonNeg:=True,  
Derivatives:=2
```

```
SolverOptions PopulationSize:=100, RandomSeed:=0, MutationRate:=0.075,  
Multistart:=False, RequireBounds:=False, MaxSubproblems:=0, MaxIntegerSols:=0,  
IntTolerance:=1, SolveWithout:=False, MaxTimeNoImp:=30
```

```
solverok SetCell:="$I$1", MaxMinVal:=3, ValueOf:=0, ByChange:="$E$2:$G$2",  
Engine:=1, EngineDesc:="GRG Nonlinear" 'Solver to optimize the Erfc fit for element  
1
```

```
solversolve UserFinish:=True
```

```
Cells(2, 12).Value = "D1"
```

```
Cells(3, 12).Value = "D2"
```

```
Cells(2, 13).Value = "=(R2C5/2)^2/(R2C1*24*3600)*(1e-6)^2"
```

```
Cells(3, 13).Value = "=(R2C6/2)^2/(R2C1*24*3600)*(1e-6)^2"
```

```
Application.ScreenUpdating = True
```

```
End Sub
```

A.3 Macro for Combination of Diffusion Coefficients and Calculation of Q

```
Sub Calculate_Q()
```

'This macro is designed to take diffusion coefficients and their errors for different temperature values in columns

'B/C, E/F, and H/I, calculate combined diffusion coefficients and errors based on the Maximum Likelihood Method,

'then combine them into a calculation of activation energy along with it's error. For descriptions of how errors are

'propagated, see <http://www.physics.ohio-state.edu/~gan/teaching/spring04/Chapter5.pdf> and

'<http://www.physics.ohio-state.edu/~gan/teaching/spring04/Chapter7.pdf>

'To setup for the macro, for each data set merge three cells in row 1 (e.g. A1-C1 for first temperature) and input the

'temperature in Celsius. Below this, input "Source" in the first column of the row below, "D" in the second, and Sig_D

'in the third. Input all data according to the headers in the rows below that. Repeat this process for each data set,

'using the next set of three columns (e.g. D-F for teh second data set).

'This macro was written by Grant Helmreich. For questions or comments, email granthelmreich@gmail.com

```

Dim Sets As Integer 'Number of data sets (i.e. number of temperatures)
Dim Points() As Integer 'Number of points (diffusion values) in each data set
Dim m As Integer 'Loop counter
Dim n As Integer 'Loop counter
Dim quit As Boolean 'Loop exit test
Dim sum1 As Double 'First summation (D/sigma^2) or Ln(D) or 1/T/sigma^2
Dim sum2 As Double 'Second summation (1/sigma^2) or 1/T^2 or 1/sigma^2
Dim sum3 As Double 'Third summation Ln(D)/T
Dim sum4 As Double 'Fourth summation 1/T

```

```

Application.ScreenUpdating = False

```

```

n = 0
quit = False

```

```

Do While quit = False 'Loop to count number of data sets
    If Cells(1, n * 3 + 1).Value = "" Then
        quit = True
    Else
        n = n + 1
    End If
Loop

```

```

Sets = n 'Define number of sets based on loop and size of array for number
of points in each set
ReDim Points(1 To Sets)

```

```

m = 0
n = 0
quit = False

```

```

Do While m < Sets 'Loop to count the number of points in
each set
    Do While quit = False
        If Cells(n + 3, m * 3 + 2).Value = "" Then
            quit = True
        Else
            n = n + 1
        End If
    Loop

```



```

quit = False
m = m + 1
Points(m) = n
n = 0
Loop

m = 0
n = 0

Do While m < Sets      'Loop to find average D and Sigma_D for each of the data
sets
    sum1 = 0
    sum2 = 0
    Do While n < Points(m + 1)
        sum1 = sum1 + Cells(n + 3, m * 3 + 2).Value / ((Cells(n + 3, m * 3 + 3).Value) ^
2)
        sum2 = sum2 + 1 / ((Cells(n + 3, m * 3 + 3).Value) ^ 2)
        n = n + 1
    Loop
    Cells(n + 4, m * 3 + 1).Value = "1/T"
    Cells(n + 4, m * 3 + 2).Value = "D"
    Cells(n + 4, m * 3 + 3).Value = "Sigma"
    Cells(n + 5, m * 3 + 2).Value = sum1 / sum2
    Cells(n + 5, m * 3 + 3).Value = (1 / sum2) ^ 0.5
    Cells(n + 5, m * 3 + 1).Value = 1 / (Cells(1, m * 3 + 1).Value + 273.15)
    m = m + 1
    n = 0
Loop

m = 0
n = 0
sum1 = 0
sum2 = 0
sum3 = 0
sum4 = 0

Do While m < Sets      'Loop to calculate sums for determining Q and D_0
    m = m + 1
    sum1 = sum1 + Application.WorksheetFunction.Ln(Cells(Points(m) + 5, (m - 1) *
3 + 2))

```

```

sum2 = sum2 + (Cells(Points(m) + 5, (m - 1) * 3 + 1)) ^ 2
sum3 = sum3 + Application.WorksheetFunction.Ln(Cells(Points(m) + 5, (m - 1) *
3 + 2)) * (Cells(Points(m) + 5, (m - 1) * 3 + 1))
sum4 = sum4 + (Cells(Points(m) + 5, (m - 1) * 3 + 1))

```

Loop

```

Cells(1, Sets * 3 + 2).Value = "Q (kJ/mol)"
Cells(1, Sets * 3 + 3).Value = "Sigma_Q"
Cells(4, Sets * 3 + 2).Value = "D_0"
Cells(4, Sets * 3 + 3).Value = "Sigma_D_0"

```

```

Cells(2, Sets * 3 + 2).Value = -8.314 * (Sets * sum3 - sum1 * sum4) / (Sets * sum2 -
(sum4 * sum4)) / 1000 'Q

```

```

Cells(5, Sets * 3 + 2).Value = Exp((sum1 * sum2 - sum3 * sum4) / (Sets * sum2 -
(sum4 * sum4))) 'D_0

```

```

m = 0
n = 0
sum1 = 0
sum2 = 0
sum3 = 0

```

Do While m < Sets 'Loop to find sums for determining sigma of Q and D_0

```

m = m + 1
sum1 = sum1 + Cells(Points(m) + 5, (m - 1) * 3 + 1).Value / ((Cells(Points(m) + 5,
(m - 1) * 3 + 3) / Cells(Points(m) + 5, (m - 1) * 3 + 2)) ^ 2)
sum2 = sum2 + 1 / ((Cells(Points(m) + 5, (m - 1) * 3 + 3) / Cells(Points(m) + 5, (m -
1) * 3 + 2)) ^ 2)
sum3 = sum3 + (Cells(Points(m) + 5, (m - 1) * 3 + 1).Value) ^ 2 / ((Cells(Points(m)
+ 5, (m - 1) * 3 + 3) / Cells(Points(m) + 5, (m - 1) * 3 + 2)) ^ 2)

```

Loop

```

sum4 = sum3 * sum2 - sum1 ^ 2

```

```

Cells(2, Sets * 3 + 3).Value = (sum2 / sum4) ^ 0.5 * 8.314 / 1000 'Sigma_Q
Cells(5, Sets * 3 + 3).Value = ((sum3 / sum4) ^ 0.5) * Cells(5, Sets * 3 + 2).Value
'Sigma_D_0

```

```

Cells(2, Sets * 3 + 2).NumberFormat = "0.0"
Cells(2, Sets * 3 + 3).NumberFormat = "0.0"

```

```
Cells(5, Sets * 3 + 2).NumberFormat = "0.00E+00"  
Cells(5, Sets * 3 + 3).NumberFormat = "0.00E+00"
```

```
Cells(7, Sets * 3 + 2).Value = "1/T (K^-1)"  
Cells(7, Sets * 3 + 3).Value = "Ln(D)"
```

```
n = 0
```

```
Do While n < Sets
```

```
    n = n + 1
```

```
    Cells(7 + n, Sets * 3 + 2).Value = "=" & Cells(Points(n) + 5, (n - 1) * 3 + 1).Address
```

```
    Cells(7 + n, Sets * 3 + 3).Value = "=Ln(" & Cells(Points(n) + 5, (n - 1) * 3 +
```

```
2).Address & ")"
```

```
    Cells(8 + n + Sets, Sets * 3 + 2).Value = Cells(Points(n) + 5, (n - 1) * 3 + 2).Value
```

```
    Cells(8 + n + Sets, Sets * 3 + 3).Value = Cells(Points(n) + 5, (n - 1) * 3 + 3).Value
```

```
    Cells(9 + n + 2 * Sets, Sets * 3 + 2).Value = 1000 * Cells(Points(n) + 5, (n - 1) * 3 +  
1).Value
```

```
    Cells(9 + n + 2 * Sets, Sets * 3 + 3).Value = Cells(Points(n) + 5, (n - 1) * 3 + 2).Value
```

```
Loop
```

```
Application.ScreenUpdating = True
```

```
End Sub
```

APPENDIX B: SUMMARY OF HT-9 INTERFACES

B.1 HT-9/Nd After 17.5 Days at 550°C

The HT-9/Nd interface annealed for 17.5 days at 550°C bonded, producing two interaction zones. The first interaction zone was ~10 μm wide and had a composition of Nd₂(Fe+Cr)₁₇. Relative to the bulk HT-9, this zone was slightly enriched in Mo, W, Cr, and V and strongly depleted in Ni. While the steel-end of this interaction zone matched the expected composition of 10.5 at% Nd, the remainder of the zone was super-stoichiometric in Nd, reaching up to ~16 at%. As the Nd concentration increased, Nd₅(Fe+Cr)₁₇ precipitates were observed within the zone, culminating in nearly complete Nd₅(Fe+Cr)₁₇ over the last micron. The second interaction zone was ~3 μm, and had a composition of NdFe₂. Relative to the bulk HT-9, this zone was strongly depleted in all alloying elements except Mn. Compositional data (in at%) from WDS linescans across the interface is given below.

Position	Zr	Mo	W	Cr	Fe	Nd	V	Ni	Mn
0	0.00	0.00	0.00	2.23	55.69	41.57	0.00	0.00	0.51
1	0.00	0.00	0.01	2.48	54.43	42.60	0.00	0.08	0.40
2	0.00	0.00	0.02	4.81	6.34	87.74	0.06	0.15	0.88
3	0.04	0.00	0.00	2.66	54.94	41.81	0.04	0.08	0.44
4	0.00	0.00	0.00	2.68	56.57	40.03	0.10	0.09	0.54
5	0.00	0.04	0.00	2.48	51.53	45.35	0.02	0.04	0.54
6	0.00	0.03	0.00	2.48	17.85	79.05	0.00	0.08	0.52
7	0.00	0.46	0.13	9.30	28.95	60.43	0.22	0.03	0.47
8	0.00	0.84	0.26	14.32	57.72	25.83	0.41	0.00	0.63
9	0.00	0.91	0.18	15.62	66.79	15.51	0.33	0.00	0.66
10	0.01	0.80	0.17	15.67	66.88	15.38	0.35	0.01	0.73
11	0.01	0.76	0.19	15.54	68.22	14.24	0.34	0.00	0.71
12	0.00	0.72	0.16	15.45	70.55	12.09	0.34	0.05	0.64
13	0.00	0.77	0.17	15.18	70.70	12.17	0.34	0.00	0.67
14	0.00	0.59	0.10	13.04	81.29	3.89	0.34	0.22	0.54
15	0.00	0.70	0.18	13.44	82.25	1.98	0.34	0.44	0.67
0	0.00	0.00	0.03	0.07	1.32	98.13	0.00	0.03	0.42
1	0.03	0.05	0.03	0.20	1.62	97.43	0.01	0.08	0.56
2	0.01	0.00	0.06	0.26	2.52	96.70	0.00	0.00	0.45
3	0.00	0.00	0.03	0.32	4.80	94.27	0.01	0.00	0.57
4	0.01	0.00	0.00	0.28	17.47	81.72	0.00	0.00	0.52
5	0.00	0.00	0.02	0.51	4.21	94.79	0.00	0.00	0.47
6	0.00	0.00	0.00	1.93	34.34	63.20	0.02	0.00	0.51
7	0.00	0.41	0.08	6.72	44.23	47.85	0.13	0.07	0.51
8	0.00	0.75	0.14	13.09	63.09	21.95	0.39	0.04	0.56
9	0.00	0.68	0.13	14.53	65.22	18.22	0.46	0.08	0.69

10	0.00	0.83	0.20	15.59	68.10	14.16	0.40	0.00	0.73
11	0.00	0.84	0.24	16.43	69.89	11.59	0.38	0.01	0.63
12	0.00	0.73	0.17	15.42	69.32	13.31	0.37	0.00	0.67
13	0.01	0.77	0.23	15.60	69.99	12.30	0.43	0.02	0.66
14	0.00	0.82	0.19	15.38	68.32	14.19	0.37	0.00	0.73
15	0.00	0.83	0.16	14.60	75.93	7.31	0.40	0.14	0.63
16	0.01	0.67	0.13	13.15	82.72	1.94	0.35	0.42	0.62
17	0.00	0.90	0.24	16.62	80.29	0.83	0.42	0.09	0.63
18	0.00	0.83	0.19	14.88	75.22	7.83	0.39	0.16	0.50
19	0.01	0.67	0.13	13.21	82.57	2.07	0.33	0.45	0.58
20	0.00	0.74	0.15	13.33	83.58	0.72	0.33	0.49	0.66
21	0.00	0.68	0.18	13.09	83.84	0.70	0.31	0.53	0.68
22	0.00	0.76	0.19	13.80	83.00	0.69	0.32	0.50	0.75
23	0.01	0.72	0.17	13.35	83.62	0.64	0.32	0.52	0.65
24	0.00	0.86	0.20	15.24	81.71	0.52	0.34	0.45	0.69
25	0.01	0.89	0.21	15.21	81.69	0.46	0.34	0.46	0.73
0	0.01	0.69	0.15	13.11	84.15	0.41	0.28	0.56	0.65
1	0.00	0.70	0.14	12.70	84.68	0.35	0.28	0.48	0.68
2	0.00	0.64	0.14	12.64	84.74	0.46	0.27	0.49	0.63
3	0.00	0.65	0.18	12.44	84.82	0.60	0.30	0.45	0.56
4	0.00	0.65	0.17	12.52	84.29	1.11	0.29	0.36	0.61
5	0.00	0.68	0.14	13.26	81.74	2.99	0.32	0.29	0.58
6	0.00	0.74	0.20	14.32	76.81	6.88	0.31	0.08	0.67
7	0.00	0.81	0.22	14.63	74.21	9.05	0.35	0.11	0.62
8	0.00	0.83	0.18	14.90	72.76	10.38	0.32	0.00	0.63
9	0.01	0.82	0.20	15.18	72.16	10.59	0.33	0.00	0.70
10	0.02	0.76	0.18	15.37	71.91	10.77	0.33	0.00	0.67
11	0.00	0.80	0.17	15.66	71.77	10.55	0.38	0.00	0.68
12	0.00	0.75	0.19	15.30	71.31	11.40	0.33	0.00	0.73
13	0.00	0.82	0.17	15.17	68.41	14.40	0.31	0.01	0.70
14	0.00	0.84	0.19	15.17	63.05	19.70	0.34	0.05	0.68
15	0.00	0.94	0.19	16.41	61.93	19.61	0.38	0.00	0.55
16	0.00	0.95	0.23	13.83	55.59	28.34	0.47	0.00	0.59
17	0.00	0.00	0.00	2.73	62.48	34.13	0.03	0.08	0.56
18	0.04	0.03	0.04	2.68	61.87	34.69	0.04	0.04	0.58
19	0.01	0.01	0.00	2.55	61.38	35.60	0.00	0.00	0.45
20	0.00	0.03	0.00	2.29	58.52	38.65	0.00	0.00	0.51
21	0.00	0.03	0.00	1.51	37.28	60.59	0.08	0.00	0.51
22	0.03	0.00	0.00	0.99	28.18	70.32	0.06	0.00	0.43
23	0.01	0.01	0.00	2.58	61.72	35.08	0.09	0.01	0.51
24	0.00	0.00	0.00	0.58	16.29	82.64	0.00	0.00	0.49
25	0.00	0.03	0.00	0.12	3.84	95.31	0.12	0.00	0.60
26	0.01	0.04	0.00	1.22	35.67	62.38	0.02	0.10	0.56
27	0.00	0.04	0.00	0.07	0.80	98.62	0.06	0.00	0.41
28	0.00	0.08	0.00	0.04	0.64	98.72	0.00	0.09	0.42
29	0.00	0.00	0.00	0.01	0.52	98.81	0.12	0.00	0.54
30	0.00	0.04	0.05	0.00	0.65	98.81	0.00	0.04	0.41
0	0.00	0.68	0.16	13.22	84.33	0.13	0.31	0.50	0.67
1	0.00	0.72	0.13	13.45	84.17	0.09	0.29	0.51	0.65
2	0.00	0.71	0.17	13.26	84.36	0.07	0.30	0.47	0.66
3	0.00	0.70	0.17	12.98	84.40	0.22	0.35	0.50	0.69
4	0.00	0.73	0.16	12.90	84.55	0.25	0.34	0.46	0.62
5	0.00	0.65	0.14	12.44	85.16	0.14	0.33	0.51	0.64
6	0.00	0.70	0.15	12.99	84.41	0.25	0.32	0.48	0.71
7	0.00	0.64	0.18	12.73	82.93	2.14	0.38	0.39	0.61

8	0.01	0.70	0.14	13.82	76.24	7.98	0.32	0.18	0.60
9	0.00	0.76	0.13	14.56	72.96	10.51	0.37	0.02	0.69
10	0.00	0.72	0.13	14.91	73.00	10.26	0.30	0.00	0.69
11	0.00	0.79	0.13	15.11	73.12	9.86	0.26	0.00	0.73
12	0.00	0.77	0.21	15.25	72.80	9.95	0.34	0.00	0.69
13	0.01	0.80	0.21	15.44	71.67	10.83	0.35	0.00	0.69
14	0.01	0.86	0.16	15.75	70.91	11.26	0.40	0.03	0.63
15	0.01	0.78	0.18	16.12	70.47	11.36	0.40	0.00	0.68
16	0.00	0.80	0.20	15.93	70.41	11.59	0.42	0.00	0.65
17	0.00	0.86	0.17	15.87	68.78	13.26	0.47	0.00	0.58
18	0.00	0.89	0.20	15.61	67.03	15.24	0.37	0.00	0.66
19	0.00	0.94	0.28	15.65	64.54	17.58	0.35	0.04	0.62
20	0.00	0.90	0.25	12.42	48.21	37.19	0.39	0.00	0.64
21	0.00	0.37	0.14	6.20	38.76	53.86	0.18	0.09	0.40
22	0.00	0.07	0.03	2.39	55.38	41.59	0.00	0.06	0.49
23	0.01	0.03	0.00	2.23	59.03	38.08	0.05	0.00	0.57
24	0.00	0.00	0.00	0.04	0.77	98.17	0.15	0.41	0.47
25	0.00	0.00	0.00	0.03	0.59	98.79	0.05	0.01	0.53
0	0.00	0.63	0.16	13.04	82.16	2.66	0.37	0.37	0.61
1	0.00	0.72	0.19	14.40	74.59	9.01	0.41	0.12	0.58
2	0.00	0.65	0.13	12.39	84.94	0.44	0.30	0.55	0.60
3	0.00	0.84	0.18	15.21	70.10	12.73	0.33	0.02	0.60
4	0.00	0.89	0.15	15.14	69.14	13.67	0.35	0.03	0.64
5	0.01	0.69	0.11	13.32	81.42	3.34	0.31	0.22	0.59
6	0.02	0.63	0.22	11.08	51.60	35.55	0.34	0.03	0.54
7	0.00	0.20	0.11	5.08	52.18	41.67	0.16	0.05	0.55
8	0.00	0.02	0.00	2.76	59.07	37.46	0.10	0.01	0.59
9	0.00	0.00	0.01	2.32	60.79	36.35	0.00	0.00	0.54
10	0.01	0.03	0.00	2.11	58.78	38.40	0.04	0.00	0.62
11	0.00	0.00	0.00	2.34	60.94	36.00	0.03	0.04	0.65
12	0.00	0.03	0.02	2.05	46.57	50.85	0.00	0.00	0.49
13	0.01	0.00	0.00	1.33	31.35	66.76	0.02	0.00	0.54
14	0.00	0.00	0.00	0.29	5.02	94.17	0.00	0.00	0.53
15	0.01	0.04	0.00	0.30	6.08	93.19	0.00	0.00	0.39
16	0.00	0.00	0.00	0.66	6.98	91.68	0.11	0.00	0.58
17	0.00	0.00	0.00	0.23	2.26	97.01	0.09	0.00	0.42
18	0.00	0.00	0.00	0.10	1.59	97.81	0.10	0.00	0.40
19	0.02	0.00	0.00	0.24	4.72	94.51	0.00	0.00	0.51
20	0.00	0.00	0.06	0.17	2.76	96.43	0.00	0.00	0.57
0	0.00	0.69	0.18	12.79	84.07	0.92	0.36	0.39	0.60
1	0.00	0.69	0.15	13.16	82.55	2.15	0.29	0.33	0.67
2	0.00	0.77	0.14	14.59	75.66	7.74	0.39	0.09	0.62
3	0.00	0.76	0.15	15.20	73.28	9.58	0.38	0.00	0.66
4	0.00	0.70	0.16	12.77	84.35	0.64	0.34	0.44	0.61
5	0.01	0.64	0.22	13.47	81.90	2.42	0.36	0.35	0.64
6	0.00	0.78	0.21	14.42	75.70	7.74	0.38	0.08	0.69
7	0.00	0.80	0.19	15.07	73.48	9.42	0.35	0.01	0.69
8	0.00	0.84	0.22	15.16	71.36	11.32	0.34	0.06	0.72
9	0.04	0.87	0.19	14.79	64.95	18.14	0.35	0.00	0.68
10	0.00	0.81	0.15	15.01	72.13	10.82	0.37	0.04	0.66
11	0.01	0.85	0.15	14.99	71.64	11.31	0.40	0.00	0.65
12	0.00	0.84	0.21	14.89	67.58	15.50	0.35	0.05	0.59
13	0.00	0.50	0.13	8.22	57.47	32.99	0.17	0.00	0.53
14	0.01	0.11	0.00	3.68	62.08	33.53	0.09	0.00	0.49
15	0.00	0.01	0.00	2.60	64.33	32.47	0.04	0.05	0.50

16	0.00	0.04	0.00	2.44	64.15	32.71	0.06	0.00	0.60
17	0.01	0.00	0.00	2.40	64.58	32.49	0.00	0.00	0.52
18	0.00	0.00	0.00	2.14	63.33	34.03	0.00	0.00	0.50
19	0.03	0.00	0.00	1.67	57.08	40.62	0.07	0.00	0.53
20	0.00	0.01	0.00	1.08	43.56	54.62	0.05	0.13	0.55
21	0.00	0.05	0.00	0.42	14.98	84.09	0.00	0.01	0.46
22	0.00	0.02	0.00	0.16	2.86	96.48	0.00	0.00	0.48
23	0.08	0.00	0.00	0.11	1.12	98.19	0.01	0.00	0.50
24	0.02	0.01	0.00	0.12	0.83	98.47	0.00	0.00	0.55
25	0.00	0.00	0.05	0.13	0.76	98.53	0.00	0.07	0.46
0	0.00	0.66	0.14	13.71	80.13	4.03	0.36	0.28	0.69
1	0.00	0.72	0.17	14.11	77.87	5.82	0.43	0.21	0.68
2	0.00	0.74	0.21	13.86	79.47	4.50	0.31	0.21	0.72
3	0.03	0.69	0.23	13.42	82.41	1.83	0.37	0.42	0.61
4	0.01	0.65	0.17	13.25	83.22	1.34	0.32	0.38	0.67
5	0.00	0.65	0.13	13.23	81.95	2.81	0.39	0.26	0.58
6	0.01	0.77	0.19	14.80	74.83	8.24	0.42	0.05	0.70
7	0.01	0.72	0.14	15.32	73.14	9.49	0.36	0.07	0.75
8	0.00	0.74	0.22	15.40	72.83	9.71	0.44	0.00	0.66
9	0.00	0.75	0.19	15.27	72.78	9.92	0.33	0.00	0.77
10	0.00	0.77	0.18	15.44	72.15	10.24	0.37	0.05	0.80
11	0.01	0.82	0.16	15.22	72.20	10.41	0.38	0.02	0.78
12	0.01	0.78	0.19	15.40	72.27	10.18	0.38	0.05	0.76
13	0.00	0.77	0.17	15.33	72.19	10.36	0.44	0.03	0.70
14	0.01	0.78	0.20	15.14	72.01	10.79	0.32	0.03	0.73
15	0.01	0.78	0.13	15.20	71.17	11.60	0.38	0.00	0.73
16	0.00	0.81	0.18	14.10	65.89	18.05	0.32	0.00	0.65
17	0.00	0.42	0.08	6.96	59.45	32.18	0.24	0.09	0.57
18	0.03	0.04	0.02	2.32	62.89	34.05	0.07	0.00	0.59
19	0.00	0.01	0.01	2.30	62.60	34.47	0.01	0.03	0.58
20	0.00	0.04	0.00	1.41	45.86	52.10	0.00	0.00	0.59
21	0.02	0.00	0.12	1.22	43.10	54.94	0.08	0.00	0.53
22	0.00	0.00	0.00	0.22	3.72	95.43	0.00	0.10	0.54
23	0.00	0.05	0.00	0.34	5.84	92.87	0.14	0.13	0.63
24	0.00	0.02	0.00	0.26	1.75	97.15	0.00	0.38	0.45
25	0.01	0.11	0.01	0.00	0.99	98.36	0.00	0.00	0.53
26	0.01	0.02	0.02	0.13	1.14	98.01	0.00	0.17	0.50
27	0.03	0.04	0.00	0.04	0.68	98.73	0.03	0.00	0.45
28	0.00	0.00	0.00	0.08	0.73	98.53	0.00	0.26	0.41
29	0.00	0.01	0.00	0.01	1.01	98.41	0.00	0.01	0.57
30	0.00	0.00	0.07	0.15	1.09	98.09	0.08	0.00	0.52

B.2 HT-9/V/Nd After 17.5 Days at 550°C

The HT-9/V/Nd assembly annealed for 17.5 days at 550°C bonded on the V/Nd interface but not the HT-9/V interface. No WDS data was collected for the bonded V/Nd interface due to a beam alignment error.

B.3 HT-9/Zr/V/Nd After 17.5 Days at 550°C

The HT-9/Zr/V/Nd assembly annealed for 17.5 days at 550°C bonded on the V/Nd interface but not the HT-9/Zr or V/Zr interfaces. No WDS data was collected for the bonded V/Nd interface due to a beam alignment error.

B.4 HT-9/Zr/Nd After 17.5 Days at 550°C

The HT-9/Zr/Nd assembly annealed for 17.5 days at 550°C bonded on the Zr/Nd interface but not the HT-9/Zr interface. No WDS data was collected for the bonded Zr/Nd interface due to a beam alignment error.

B.5 HT-9/Ti/V/Nd After 17.5 Days at 550°C

The HT-9/Ti/V/Nd assembly annealed for 17.5 days at 550°C bonded on the V/Nd interface but not the HT-9/Ti or Ti/V interfaces. Compositional data (in at%) from WDS linescans across the V/Nd interface is given below.

Position	Ta	Ti	Mo	W	Cr	Fe	Nd	V	Ni	Mn
0	0.00	0.01	0.00	0.00	2.05	0.28	8.86	88.77	0.00	0.05
1	0.00	0.00	0.00	0.00	1.75	0.31	8.99	88.94	0.00	0.01
2	0.00	0.00	0.00	0.01	1.91	0.08	3.05	94.96	0.00	0.00
3	0.00	0.00	0.00	0.01	2.04	0.00	1.69	96.26	0.00	0.00
4	0.00	0.00	0.00	0.00	2.05	0.03	1.34	96.58	0.00	0.00
5	0.00	0.01	0.01	0.00	1.95	0.00	1.60	96.39	0.06	0.00
6	0.00	0.01	0.01	0.00	1.89	0.06	3.90	94.06	0.04	0.03
7	0.00	0.00	0.02	0.03	1.88	0.07	10.18	87.83	0.00	0.00
8	0.00	0.00	0.00	0.08	1.24	0.14	38.64	59.62	0.11	0.18
9	0.00	0.00	0.01	0.00	0.64	0.33	64.53	34.09	0.14	0.27
10	0.00	0.00	0.00	0.00	1.67	0.05	10.26	87.91	0.00	0.10
11	0.00	0.00	0.03	0.00	1.49	0.22	31.54	66.47	0.06	0.19
12	0.00	0.00	0.07	0.00	0.91	0.41	63.23	34.97	0.00	0.41
13	0.00	0.01	0.12	0.04	0.13	0.42	92.94	5.96	0.00	0.39
14	0.00	0.00	0.00	0.00	0.00	0.29	97.16	1.99	0.04	0.52
15	0.00	0.00	0.01	0.00	0.00	0.35	96.26	2.91	0.00	0.47

B.6 HT-9/Ti/Nd After 17.5 Days at 550°C

The HT-9/Ti/Nd assembly annealed for 17.5 days at 550°C bonded on the Ti/Nd interface but not the HT-9/Ti interface. Compositional data (in at%) from WDS linescans across the Ti/Nd interface is given below.

Position	Ta	Ti	Mo	W	Cr	Fe	Nd	V	Ni	Mn
0	0.00	1.00	0.00	0.00	0.00	0.34	97.96	0.02	0.00	0.68
1	0.00	1.12	0.00	0.00	0.00	0.69	97.60	0.00	0.01	0.58
2	0.00	1.35	0.00	0.04	0.00	1.41	96.57	0.04	0.01	0.58
3	0.00	1.51	0.03	0.06	0.27	1.32	96.02	0.00	0.00	0.80
4	0.00	1.88	0.01	0.00	0.07	0.82	96.57	0.00	0.00	0.65
5	0.00	2.07	0.00	0.00	0.00	0.62	96.81	0.01	0.01	0.49
6	0.00	2.63	0.00	0.01	0.00	0.44	96.31	0.00	0.13	0.48
7	0.00	35.61	0.00	0.00	0.10	1.64	62.08	0.06	0.18	0.33
8	0.00	59.26	0.00	0.00	0.14	1.28	38.72	0.17	0.02	0.41
9	0.00	88.34	0.00	0.03	0.03	0.42	10.82	0.30	0.04	0.03
10	0.00	97.43	0.00	0.00	0.09	0.14	2.03	0.31	0.00	0.00
11	0.00	86.68	0.02	0.00	0.06	0.51	12.33	0.30	0.00	0.10
12	0.00	96.73	0.00	0.01	0.08	0.15	2.72	0.28	0.00	0.04
13	0.00	97.94	0.00	0.00	0.00	0.19	1.53	0.33	0.00	0.02
14	0.00	98.43	0.00	0.00	0.02	0.31	0.99	0.23	0.00	0.02
15	0.00	98.25	0.00	0.04	0.10	0.54	0.86	0.21	0.00	0.00
0	0.00	1.81	0.05	0.20	0.00	0.48	97.01	0.10	0.00	0.356
1	0.00	2.39	0.00	0.00	0.02	0.21	96.76	0.02	0.05	0.553
2	0.00	2.66	0.00	0.00	0.02	0.43	96.56	0.01	0.00	0.326
3	0.00	1.96	0.01	0.10	0.03	0.39	96.72	0.06	0.13	0.594
4	0.00	2.40	0.00	0.09	0.00	0.39	96.34	0.00	0.06	0.729
5	0.00	3.10	0.00	0.00	0.00	0.23	96.13	0.00	0.00	0.546
6	0.00	4.69	0.00	0.04	0.21	0.31	94.10	0.00	0.00	0.655
7	0.00	16.76	0.10	0.00	0.06	0.34	82.34	0.07	0.00	0.324
8	0.00	98.19	0.00	0.00	0.00	0.16	1.29	0.33	0.00	0.03
9	0.00	99.22	0.00	0.00	0.02	0.12	0.36	0.28	0.00	0
10	0.00	98.75	0.00	0.00	0.09	0.44	0.37	0.31	0.05	0
11	0.00	98.15	0.00	0.02	0.17	0.93	0.52	0.20	0.00	0.008
12	0.00	96.67	0.00	0.00	0.30	2.03	0.74	0.22	0.04	0
13	0.00	93.62	0.00	0.02	0.74	4.33	1.05	0.20	0.03	0
14	0.00	90.58	0.05	0.03	0.95	6.67	1.44	0.20	0.02	0.075
15	0.00	90.59	0.02	0.04	0.90	6.33	1.76	0.26	0.04	0.065

B.7 HT-9/Ta/V/Nd After 17.5 Days at 550°C

The HT-9/Ta/V/Nd interface annealed for 17.5 days at 550°C bonded on the V/Nd interface but not the HT-9/Ta interface or the Ta/V interface. Compositional data (in at%) from WDS linescans across the V/Nd interface is given below.

Position	Ta	Ti	Mo	W	Cr	Fe	Nd	V	Ni	Mn
0	0.00	0.01	0.00	0.00	1.92	0.18	3.06	94.80	0.00	0.04
1	0.00	0.00	0.01	0.00	2.06	0.20	2.37	95.34	0.01	0.00
2	0.00	0.00	0.02	0.07	1.92	0.19	2.57	95.20	0.00	0.03
3	0.00	0.01	0.02	0.03	2.03	1.47	4.17	92.24	0.00	0.05
4	0.00	0.00	0.01	0.02	1.75	3.88	13.73	80.50	0.05	0.06
5	0.00	0.02	0.00	0.00	1.35	6.06	35.53	56.60	0.17	0.26
6	0.00	0.00	0.00	0.03	0.62	5.84	66.25	26.71	0.24	0.30
7	0.00	0.00	0.02	0.12	0.57	5.30	71.03	22.73	0.00	0.22

8	0.00	0.00	0.00	0.00	0.19	2.24	90.34	6.82	0.21	0.21
9	0.00	0.00	0.00	0.16	0.25	1.92	91.83	4.99	0.26	0.60
10	0.00	0.00	0.03	0.07	0.02	1.90	92.74	4.67	0.00	0.57
11	0.00	0.00	0.04	0.01	0.06	1.04	93.89	4.16	0.10	0.71
12	0.00	0.00	0.00	0.00	0.17	0.81	94.53	3.98	0.00	0.50
13	0.00	0.00	0.10	0.00	0.00	0.34	96.44	2.54	0.17	0.42
14	0.00	0.00	0.00	0.04	0.27	0.53	96.58	2.09	0.00	0.49
15	0.00	0.00	0.08	0.00	0.00	0.66	96.62	1.98	0.00	0.67

B.8 HT-9/Ta/Nd After 17.5 Days at 550°C

The HT-9/Ta/Nd assembly annealed for 17.5 days at 550°C bonded on the Ta/Nd interface but not the HT-9/Ta interface. Compositional data (in at%) from WDS linescans across the Ta/Nd interface is given below.

Position	Ta	Ti	Mo	W	Cr	Fe	Nd	V	Ni	Mn
0	0.00	0.00	0.11	0.03	0.10	0.46	98.73	0.00	0.05	0.53
1	0.00	0.00	0.02	0.13	0.00	0.52	98.73	0.09	0.00	0.51
2	0.00	0.01	0.00	0.00	0.00	0.35	98.98	0.00	0.15	0.51
3	0.00	0.00	0.00	0.00	0.00	0.44	99.02	0.00	0.00	0.55
4	0.00	0.00	0.01	0.00	0.04	0.43	98.87	0.08	0.13	0.44
5	0.00	0.01	0.00	0.00	0.07	0.40	98.81	0.01	0.04	0.66
6	0.00	0.00	0.00	0.19	0.17	0.87	97.85	0.05	0.00	0.86
7	11.39	0.00	0.00	1.05	0.15	0.89	85.90	0.00	0.20	0.43
8	72.33	0.00	0.12	1.77	0.00	0.15	25.47	0.00	0.00	0.15
9	90.99	0.00	0.00	2.31	0.00	0.07	6.64	0.00	0.00	0.00
10	93.37	0.06	0.07	2.42	0.00	0.06	3.85	0.02	0.00	0.15
11	93.32	0.00	0.00	2.54	0.00	0.10	3.83	0.17	0.00	0.03
12	93.56	0.02	0.00	2.22	0.00	0.10	3.78	0.00	0.33	0.00
13	95.40	0.01	0.00	2.18	0.00	0.00	2.23	0.07	0.00	0.11
14	95.56	0.00	0.08	2.30	0.09	0.11	1.72	0.00	0.09	0.05
15	93.47	0.00	0.09	2.52	0.08	0.03	3.46	0.13	0.12	0.10

B.9 HT-9/Mo/V/Nd After 17.5 Days at 550°C

The HT-9/Mo/V/Nd assembly annealed for 17.5 days at 550°C bonded on the V/Nd interface but not the HT-9/Mo or Mo/V interfaces. Compositional data (in at%) from WDS linescans across the V/Nd interface is given below.

Position	V	W	Mo	Nd	Ni	Fe	Mn	Cr
0	2.30	0.01	97.51	0.07	0.00	0.05	0.06	0.00
1	3.33	0.01	95.46	0.32	0.11	0.67	0.00	0.10
2	1.65	0.00	96.76	0.28	0.08	1.02	0.04	0.18
3	0.95	0.00	98.59	0.10	0.00	0.35	0.02	0.00
4	1.62	0.01	98.33	0.00	0.00	0.02	0.02	0.00
5	5.82	0.01	93.78	0.09	0.04	0.09	0.04	0.12
6	20.33	0.00	78.53	0.32	0.00	0.33	0.01	0.48
7	66.99	0.00	31.32	0.19	0.00	0.09	0.00	1.40

8	95.87	0.00	2.23	0.03	0.04	0.05	0.00	1.79
9	97.49	0.01	0.47	0.04	0.01	0.02	0.00	1.95
10	95.19	0.00	2.81	0.04	0.00	0.05	0.00	1.92
11	97.70	0.00	0.31	0.00	0.01	0.03	0.00	1.96
12	97.69	0.00	0.13	0.05	0.05	0.06	0.00	2.02
13	97.90	0.01	0.11	0.03	0.00	0.03	0.00	1.92
14	97.66	0.00	0.12	0.01	0.01	0.12	0.00	2.08
15	97.63	0.00	0.12	0.05	0.00	0.20	0.00	2.00
0	97.80	0.00	0.13	0.06	0.01	0.00	0.00	2.00
1	97.90	0.00	0.00	0.05	0.00	0.03	0.01	2.01
2	97.90	0.01	0.01	0.11	0.02	0.05	0.03	1.89
3	96.88	0.00	0.01	0.35	0.00	0.82	0.00	1.94
4	64.11	0.00	0.04	27.92	0.07	6.22	0.17	1.48
5	5.44	0.04	0.00	93.19	0.10	0.68	0.47	0.08
6	3.25	0.00	0.03	95.49	0.16	0.55	0.42	0.11
7	2.39	0.01	0.00	96.75	0.00	0.47	0.38	0.00
8	1.28	0.06	0.01	97.77	0.00	0.43	0.45	0.00
9	1.05	0.00	0.01	98.06	0.00	0.34	0.43	0.10
10	0.70	0.04	0.00	98.23	0.14	0.40	0.51	0.00
11	0.66	0.00	0.01	98.67	0.04	0.30	0.33	0.00
12	0.45	0.00	0.00	98.79	0.00	0.33	0.43	0.00
13	0.39	0.00	0.03	98.54	0.03	0.39	0.63	0.00
14	0.32	0.00	0.05	98.87	0.03	0.30	0.38	0.05
15	0.40	0.00	0.00	98.60	0.06	0.43	0.52	0.00
0	97.84	0.00	0.02	0.04	0.04	0.03	0.01	2.03
1	97.86	0.00	0.00	0.09	0.00	0.03	0.00	2.02
2	97.58	0.00	0.00	0.25	0.00	0.24	0.00	1.93
3	87.26	0.00	0.03	5.30	0.02	5.36	0.04	1.98
4	55.14	0.00	0.11	32.85	0.01	10.24	0.20	1.44
5	85.89	0.00	0.04	6.07	0.00	5.97	0.01	2.03
6	5.51	0.00	0.04	93.29	0.00	0.76	0.41	0.01
7	39.63	0.02	0.03	51.26	0.00	7.73	0.36	0.97
8	2.81	0.00	0.02	96.10	0.00	0.75	0.33	0.00
9	3.35	0.08	0.00	95.45	0.12	0.49	0.41	0.11
10	2.62	0.00	0.00	96.39	0.03	0.38	0.46	0.12
11	1.05	0.00	0.03	97.89	0.00	0.44	0.49	0.10
12	0.80	0.01	0.00	98.42	0.00	0.35	0.35	0.07
13	2.33	0.02	0.00	96.71	0.04	0.50	0.40	0.01
14	1.55	0.07	0.02	97.33	0.00	0.46	0.53	0.04
15	0.74	0.00	0.06	98.25	0.00	0.39	0.52	0.05

B.10 HT-9/Mo/Nd After 17.5 Days at 550°C

The HT-9/Mo/Nd assembly annealed for 17.5 days at 550°C bonded on the Mo/Nd interface but not the HT-9/Mo interface. Compositional data (in at%) from WDS linescans across the Mo/Nd interface is given below.

Position	V	W	Mo	Nd	Ni	Fe	Mn	Cr
0	0.00	0.00	0.05	98.94	0.25	0.32	0.45	0.00
1	0.00	0.03	0.01	99.12	0.07	0.25	0.53	0.00
2	0.03	0.00	0.04	98.94	0.14	0.38	0.46	0.00
3	0.00	0.00	0.05	99.17	0.09	0.34	0.35	0.00
4	0.00	0.00	0.08	98.90	0.12	0.34	0.54	0.03
5	0.02	0.00	0.14	98.91	0.02	0.37	0.55	0.00
6	0.00	0.00	5.50	93.39	0.00	0.50	0.60	0.00
7	0.00	0.00	78.93	20.50	0.00	0.35	0.07	0.15
8	0.08	0.01	95.35	4.19	0.12	0.21	0.00	0.04
9	0.29	0.04	98.32	0.41	0.01	0.07	0.86	0.00
10	0.04	0.02	99.39	0.39	0.00	0.11	0.05	0.01
11	0.12	0.02	99.57	0.25	0.00	0.00	0.00	0.03
12	0.00	0.00	99.61	0.24	0.00	0.06	0.09	0.00
13	0.03	0.00	99.66	0.19	0.00	0.05	0.07	0.00
14	0.01	0.00	99.79	0.14	0.03	0.01	0.02	0.00
15	0.04	0.00	99.57	0.37	0.01	0.02	0.00	0.00
0	0.08	0.01	0.00	98.81	0.00	0.43	0.67	0.00
1	0.00	0.04	0.03	99.16	0.01	0.38	0.38	0.00
2	0.00	0.00	0.08	99.19	0.00	0.22	0.51	0.00
3	0.02	0.00	0.00	98.76	0.21	0.34	0.67	0.00
4	0.00	0.00	0.11	98.83	0.06	0.35	0.65	0.00
5	0.03	0.02	0.16	98.99	0.00	0.33	0.48	0.00
6	0.00	0.00	0.22	98.79	0.06	0.36	0.57	0.00
7	0.05	0.01	3.43	95.62	0.00	0.40	0.48	0.02
8	0.08	0.00	46.28	52.84	0.09	0.30	0.35	0.08
9	0.03	0.01	91.58	8.13	0.07	0.09	0.00	0.09
10	0.05	0.01	99.33	0.54	0.00	0.05	0.00	0.01
11	0.04	0.01	99.48	0.44	0.00	0.03	0.00	0.00
12	0.06	0.02	99.62	0.27	0.02	0.01	0.01	0.00
13	0.02	0.00	99.64	0.29	0.02	0.03	0.00	0.01
14	0.00	0.01	99.66	0.20	0.05	0.03	0.00	0.06
15	0.03	0.00	99.53	0.19	0.06	0.07	0.09	0.03
0	0.07	0.02	0.05	98.94	0.00	0.31	0.62	0.00
1	0.05	0.05	0.07	98.78	0.00	0.37	0.61	0.07
2	0.00	0.00	0.10	98.92	0.02	0.50	0.46	0.00
3	0.00	0.00	0.07	94.64	0.00	4.62	0.42	0.25
4	0.01	0.00	0.15	96.58	0.02	2.67	0.43	0.14
5	0.00	0.03	0.06	99.11	0.00	0.33	0.46	0.01
6	0.00	0.00	0.11	98.82	0.12	0.43	0.49	0.02
7	0.02	0.03	0.16	98.95	0.03	0.30	0.46	0.05
8	0.00	0.00	10.36	88.73	0.00	0.44	0.47	0.00
9	0.02	0.02	84.67	14.91	0.05	0.23	0.07	0.04
10	0.07	0.00	99.22	0.65	0.00	0.00	0.02	0.04
11	0.04	0.01	99.42	0.32	0.07	0.10	0.04	0.00
12	0.00	0.01	99.39	0.33	0.03	0.18	0.00	0.06
13	0.06	0.01	99.69	0.22	0.00	0.03	0.00	0.00
14	0.10	0.00	99.56	0.24	0.00	0.04	0.07	0.00
15	0.03	0.02	99.58	0.25	0.04	0.04	0.04	0.01

B.11 HT-9/W/V/Nd After 17.5 Days at 550°C

The HT-9/W/V/Nd assembly annealed for 17.5 days at 550°C bonded on the V/Nd interface but not the HT-9/W or W/V interfaces. Since significant data had already been acquired for V/Nd interfaces at this time and temperature, no WDS analysis was performed on this interface.

B.12 HT-9/W/Nd After 17.5 Days at 550°C

The HT-9/W/Nd assembly annealed for 17.5 days at 550°C bonded on the W/Nd interface but not the HT-9/W interface. Compositional data (in at%) from WDS linescans across the W/Nd interface is given below.

Position	V	W	Mo	Nd	Ni	Fe	Mn	Cr
0	0.12	98.18	0.00	1.56	0.02	0.12	0.00	0.01
1	0.10	99.31	0.00	0.50	0.00	0.01	0.06	0.03
2	0.07	98.57	0.32	0.83	0.00	0.16	0.02	0.04
3	0.02	98.93	0.00	1.02	0.00	0.02	0.02	0.00
4	0.14	97.91	0.00	1.70	0.00	0.11	0.00	0.15
5	0.59	96.72	0.00	2.64	0.00	0.02	0.03	0.00
6	0.32	59.87	0.07	39.11	0.04	0.39	0.18	0.03
7	0.00	1.03	0.04	98.19	0.00	0.32	0.42	0.00
8	0.00	0.17	0.02	98.85	0.00	0.39	0.56	0.00
9	0.04	0.03	0.00	98.90	0.13	0.35	0.48	0.06
10	0.00	0.17	0.00	98.90	0.00	0.54	0.39	0.00
11	0.00	0.15	0.06	98.76	0.00	0.56	0.47	0.00
12	0.04	0.18	0.05	98.71	0.00	0.52	0.48	0.02
13	0.00	0.00	0.00	99.20	0.00	0.29	0.51	0.00
14	0.00	0.04	0.00	99.13	0.00	0.44	0.40	0.00
15	0.03	0.00	0.00	99.11	0.00	0.24	0.62	0.00
0	0.10	99.23	0.00	0.36	0.11	0.10	0.00	0.11
1	0.00	99.15	0.00	0.61	0.06	0.18	0.00	0.00
2	0.03	98.23	0.00	1.41	0.04	0.12	0.18	0.00
3	0.16	95.36	0.02	4.23	0.00	0.23	0.00	0.00
4	0.06	40.27	0.04	56.85	0.00	2.47	0.31	0.00
5	0.12	97.87	0.00	1.78	0.00	0.10	0.00	0.13
6	0.13	96.53	0.00	3.12	0.00	0.21	0.02	0.00
7	0.00	0.09	0.02	98.85	0.00	0.56	0.40	0.07
8	0.02	0.09	0.00	99.16	0.04	0.38	0.31	0.00
9	0.02	0.07	0.00	99.04	0.00	0.38	0.49	0.00
10	0.07	0.00	0.00	99.10	0.00	0.36	0.36	0.10
11	0.00	0.06	0.00	98.98	0.00	0.39	0.57	0.00
12	0.07	0.03	0.00	99.08	0.01	0.38	0.42	0.00
13	0.00	0.06	0.01	98.87	0.10	0.43	0.43	0.11
14	0.00	0.01	0.00	99.15	0.00	0.38	0.45	0.00
15	0.00	0.00	0.00	98.97	0.01	0.35	0.67	0.00

B.13 HT-9/Nd After 28 Days at 550°C

After annealing for 28 days at 550°C, the interface between HT-9 and Nd included two interaction zones. The first interaction zone, $\text{Nd}_2(\text{Fe}+\text{Cr})_{17}$ was ~12 μm wide, and was slightly enriched in Mo, W, Cr, and V and strongly depleted in Ni. The steel-end matched the expected composition of 10.5at% Nd, while the remainder of the zone was super-stoichiometric in Nd with $\text{Nd}_5(\text{Fe}+\text{Cr})_{17}$ precipitates. In some areas, the $\text{Nd}_5(\text{Fe}+\text{Cr})_{17}$ precipitates formed a separate zone up to 2 μm wide. The third zone, Fe_2Nd was ~4 μm wide and was strongly depleted in all alloying elements except Mn relative to bulk HT-9. Composition data (in at%) across the interface from WDS linescans is given below.

Position	Zr	Mo	W	Cr	Fe	Nd	V	Ni	Mn
0	0.00	0.68	0.16	12.72	83.52	1.54	0.30	0.49	0.59
1	0.02	0.66	0.16	12.62	83.67	1.51	0.30	0.47	0.59
2	0.00	0.57	0.17	11.99	84.44	1.51	0.30	0.47	0.56
3	0.01	0.69	0.18	12.87	83.03	1.77	0.32	0.46	0.69
4	0.00	0.65	0.14	12.89	83.14	1.77	0.34	0.43	0.64
5	0.00	0.54	0.14	11.85	84.27	1.86	0.32	0.45	0.58
6	0.00	0.72	0.16	13.48	78.15	6.36	0.34	0.22	0.58
7	0.00	0.96	0.21	14.98	71.27	11.52	0.37	0.02	0.67
8	0.01	0.78	0.17	14.75	71.32	11.94	0.33	0.04	0.66
9	0.01	0.76	0.17	14.69	71.33	12.09	0.36	0.00	0.59
10	0.01	0.83	0.17	14.92	71.00	12.08	0.34	0.03	0.63
11	0.00	0.72	0.15	15.08	70.19	12.96	0.34	0.00	0.56
12	0.01	0.77	0.17	14.74	71.18	12.15	0.32	0.06	0.60
13	0.00	0.73	0.17	15.10	70.53	12.41	0.34	0.05	0.68
14	0.00	0.76	0.18	15.33	69.45	13.18	0.35	0.00	0.75
15	0.00	0.78	0.25	15.32	68.60	14.10	0.35	0.00	0.60
16	0.01	0.75	0.20	14.99	68.67	14.33	0.34	0.04	0.67
17	0.00	0.74	0.23	15.36	68.20	14.44	0.37	0.00	0.65
18	0.00	0.76	0.16	15.02	63.52	19.46	0.32	0.10	0.65
19	0.00	0.76	0.18	15.09	63.48	19.47	0.37	0.00	0.66
20	0.00	1.02	0.27	15.00	53.10	29.64	0.41	0.00	0.56
21	0.00	0.38	0.15	7.83	11.48	79.31	0.15	0.17	0.53
22	0.06	0.00	0.00	0.92	2.16	96.27	0.00	0.03	0.56
23	0.00	0.00	0.00	0.44	1.52	97.60	0.01	0.00	0.44
24	0.04	0.01	0.04	0.40	1.84	97.17	0.00	0.00	0.51
25	0.00	0.00	0.02	0.34	1.43	97.77	0.00	0.00	0.43
26	0.00	0.01	0.07	0.34	1.59	97.45	0.05	0.05	0.46
27	0.02	0.06	0.02	0.24	1.37	97.72	0.04	0.00	0.54
28	0.00	0.02	0.00	0.14	1.44	97.80	0.00	0.00	0.61
29	0.06	0.00	0.06	0.11	0.72	98.14	0.07	0.18	0.67
30	0.00	0.03	0.00	0.09	0.82	98.64	0.00	0.00	0.42
0	0.00	0.64	0.15	13.31	82.14	2.33	0.30	0.46	0.65
1	0.00	0.63	0.15	13.25	82.27	2.32	0.32	0.45	0.62
2	0.00	0.63	0.15	12.74	83.37	1.65	0.30	0.56	0.61

3	0.00	0.63	0.17	12.63	83.92	1.23	0.30	0.47	0.66
4	0.01	0.59	0.15	12.37	84.77	0.61	0.32	0.51	0.66
5	0.00	0.68	0.15	13.47	83.45	0.79	0.36	0.42	0.69
6	0.00	0.78	0.14	13.34	83.36	0.90	0.34	0.42	0.72
7	0.00	0.66	0.18	13.30	82.65	2.01	0.33	0.31	0.56
8	0.01	0.70	0.19	14.77	74.44	8.90	0.36	0.00	0.66
9	0.01	0.78	0.16	15.14	71.83	11.00	0.38	0.00	0.71
10	0.01	0.82	0.20	15.20	72.04	10.59	0.37	0.08	0.69
11	0.00	0.74	0.18	15.33	70.82	11.83	0.37	0.00	0.74
12	0.00	0.76	0.16	15.05	71.39	11.57	0.32	0.02	0.73
13	0.00	0.78	0.15	15.02	71.08	11.85	0.35	0.02	0.75
14	0.00	0.80	0.20	15.26	71.04	11.62	0.35	0.00	0.74
15	0.00	0.76	0.20	15.30	70.34	12.36	0.36	0.00	0.69
16	0.02	0.78	0.18	15.20	70.04	12.76	0.34	0.01	0.67
17	0.01	0.84	0.20	14.95	63.85	18.91	0.35	0.08	0.81
18	0.00	1.08	0.29	1.22	70.42	25.68	0.48	0.00	0.83
19	0.00	0.82	0.20	14.84	63.92	19.18	0.32	0.00	0.73
20	0.00	0.45	0.19	7.89	43.77	46.94	0.26	0.04	0.47
21	0.00	0.00	0.02	2.69	58.86	37.90	0.05	0.00	0.48
22	0.00	0.04	0.02	2.34	58.75	38.06	0.00	0.13	0.66
23	0.03	0.01	0.00	2.37	60.67	36.32	0.01	0.08	0.52
24	0.01	0.03	0.00	2.27	61.54	35.55	0.02	0.08	0.50
25	0.00	0.00	0.01	1.58	53.51	44.21	0.01	0.00	0.69
26	0.00	0.53	0.03	10.06	47.26	41.55	0.00	0.00	0.57
27	0.06	0.09	0.00	1.45	23.21	74.21	0.00	0.48	0.51
28	0.01	0.03	0.03	0.16	2.28	96.73	0.00	0.30	0.48
29	0.00	0.02	0.03	0.12	0.99	98.34	0.00	0.02	0.49
30	0.00	0.03	0.07	0.06	1.08	98.14	0.00	0.19	0.43
0	0.01	0.69	0.15	12.96	84.38	0.27	0.39	0.50	0.66
1	0.00	0.66	0.15	12.81	84.71	0.31	0.31	0.49	0.56
2	0.01	0.70	0.14	13.43	84.04	0.18	0.29	0.52	0.69
3	0.00	0.73	0.16	13.39	84.20	0.17	0.30	0.44	0.62
4	0.00	0.67	0.15	12.98	84.54	0.26	0.29	0.46	0.65
5	0.00	0.76	0.16	13.01	83.75	0.89	0.33	0.46	0.64
6	0.00	0.70	0.19	14.93	73.10	10.07	0.31	0.00	0.71
7	0.00	0.70	0.17	15.04	73.12	9.86	0.36	0.03	0.73
8	0.00	0.71	0.17	15.12	72.15	10.71	0.41	0.01	0.74
9	0.02	0.76	0.16	15.25	71.90	10.88	0.35	0.03	0.65
10	0.00	0.79	0.19	15.36	71.20	11.43	0.36	0.00	0.67
11	0.01	0.77	0.17	15.21	71.27	11.42	0.44	0.05	0.67
12	0.00	0.78	0.14	15.33	69.52	13.16	0.42	0.00	0.65
13	0.00	0.88	0.16	15.28	68.11	14.54	0.36	0.03	0.64
14	0.01	0.79	0.18	13.48	53.30	31.21	0.40	0.00	0.63
15	0.00	0.76	0.17	12.52	51.74	33.74	0.39	0.10	0.58
16	0.03	0.40	0.12	7.71	58.15	32.79	0.24	0.00	0.57
17	0.05	0.02	0.04	3.24	63.12	32.90	0.10	0.00	0.53
18	0.00	0.05	0.01	2.95	63.30	33.03	0.00	0.08	0.58
19	0.00	0.00	0.07	2.47	60.46	36.43	0.03	0.03	0.51
20	0.00	0.00	0.03	2.18	52.48	44.74	0.06	0.00	0.50
21	0.04	0.00	0.00	0.88	22.17	76.31	0.00	0.03	0.58

22	0.00	0.03	0.02	0.67	12.78	85.95	0.01	0.01	0.52
23	0.00	0.00	0.00	0.21	1.96	97.21	0.00	0.06	0.55
24	0.00	0.00	0.16	0.21	1.76	97.11	0.11	0.12	0.53
25	0.00	0.00	0.00	0.26	1.14	98.21	0.00	0.03	0.37
0	0.00	0.67	0.16	13.06	84.48	0.16	0.28	0.50	0.68
1	0.02	0.72	0.13	12.98	84.52	0.17	0.30	0.46	0.70
2	0.00	0.67	0.15	13.11	84.34	0.26	0.33	0.48	0.67
3	0.00	0.79	0.18	15.90	79.89	1.38	0.42	0.58	0.86
4	0.00	0.68	0.16	13.46	81.33	3.15	0.35	0.30	0.57
5	0.00	0.73	0.16	14.79	75.72	7.60	0.35	0.00	0.66
6	0.00	0.79	0.17	15.35	72.54	10.02	0.33	0.10	0.71
7	0.00	0.81	0.16	15.58	71.99	10.45	0.31	0.04	0.67
8	0.00	0.78	0.20	15.35	72.12	10.44	0.33	0.00	0.79
9	0.00	0.86	0.18	15.46	70.78	11.69	0.35	0.06	0.63
10	0.01	0.79	0.17	15.60	70.14	12.22	0.39	0.00	0.69
11	0.00	0.82	0.18	15.47	69.51	12.94	0.35	0.07	0.65
12	0.00	0.83	0.14	15.70	68.78	13.39	0.38	0.02	0.75
13	0.01	0.79	0.19	15.67	67.81	14.47	0.41	0.00	0.66
14	0.02	0.80	0.19	15.72	67.48	14.71	0.40	0.00	0.69
15	0.00	0.78	0.19	15.69	69.46	12.78	0.39	0.00	0.72
16	0.00	0.89	0.20	15.71	64.29	17.88	0.38	0.02	0.64
17	0.02	0.79	0.22	15.90	67.60	14.47	0.37	0.00	0.63
18	0.01	0.81	0.20	16.01	67.32	14.65	0.41	0.00	0.60
19	0.01	0.82	0.20	15.70	67.84	14.33	0.42	0.04	0.63
20	0.02	0.87	0.18	15.91	65.75	16.27	0.39	0.01	0.60
21	0.00	0.95	0.18	13.80	57.44	26.75	0.39	0.00	0.49
22	0.00	0.34	0.08	5.69	45.70	47.60	0.10	0.00	0.49
23	0.00	0.00	0.03	1.29	42.21	55.90	0.00	0.00	0.58
24	0.00	0.02	0.03	1.29	43.72	54.35	0.02	0.12	0.45
25	0.00	0.00	0.03	0.31	6.93	92.10	0.16	0.00	0.46
26	0.00	0.01	0.07	0.18	1.28	97.98	0.00	0.01	0.48
27	0.02	0.00	0.03	0.21	1.71	97.55	0.00	0.00	0.49
28	0.00	0.00	0.00	0.19	1.53	97.69	0.00	0.13	0.46
0	0.01	0.65	0.14	13.20	84.23	0.33	0.29	0.50	0.65
1	0.01	0.68	0.14	13.00	84.37	0.37	0.31	0.46	0.66
2	0.00	0.63	0.19	13.18	84.09	0.38	0.35	0.52	0.66
3	0.00	0.68	0.16	13.37	83.37	1.13	0.30	0.38	0.62
4	0.01	0.76	0.17	15.11	75.52	7.21	0.38	0.15	0.70
5	0.00	0.68	0.12	15.10	73.34	9.72	0.38	0.00	0.68
6	0.00	0.73	0.21	15.46	72.42	10.03	0.36	0.07	0.73
7	0.01	0.76	0.14	15.52	71.90	10.61	0.34	0.00	0.72
8	0.00	0.75	0.22	15.68	71.74	10.54	0.43	0.01	0.65
9	0.01	0.78	0.21	15.91	71.32	10.67	0.37	0.04	0.69
10	0.00	0.80	0.17	16.04	71.12	10.81	0.36	0.00	0.70
11	0.00	0.75	0.13	15.70	70.48	11.81	0.37	0.00	0.77
12	0.01	0.82	0.18	14.82	69.83	13.31	0.38	0.00	0.65
13	0.00	0.74	0.17	14.62	69.40	14.01	0.36	0.04	0.67
14	0.02	0.79	0.17	15.26	68.79	13.83	0.39	0.07	0.67
15	0.00	0.84	0.19	15.26	65.93	16.66	0.35	0.03	0.75

16	0.00	0.74	0.14	12.66	59.97	25.42	0.36	0.08	0.64
17	0.01	0.27	0.11	6.63	56.71	35.58	0.09	0.10	0.50
18	0.04	0.10	0.02	3.32	58.99	36.85	0.07	0.00	0.61
19	0.01	0.05	0.04	2.66	60.23	36.47	0.00	0.02	0.52
20	0.00	0.04	0.00	2.57	61.38	35.34	0.05	0.01	0.61
21	0.04	0.04	0.00	2.06	50.81	46.47	0.07	0.00	0.52
22	0.03	0.03	0.00	0.75	17.22	81.59	0.00	0.00	0.39
23	0.00	0.04	0.05	1.24	8.37	89.83	0.00	0.05	0.42
24	0.00	0.28	0.03	5.35	37.01	56.35	0.12	0.30	0.57
25	0.00	0.33	0.06	4.79	33.37	60.66	0.05	0.25	0.49

B.14 HT-9/V/Nd After 28 Days at 550°C

The HT-9/V/Nd assembly annealed for 28 days at 550°C bonded on the V/Nd interface but not the HT-9/V interface. Compositional data (in at%) from WDS linescans across the V/Nd interface is given below.

Position	Zr	Mo	W	Cr	Fe	Nd	V	Ni	Mn
0	0.00	0.00	0.02	0.01	0.61	97.82	1.08	0.00	0.46
1	0.00	0.02	0.01	0.00	0.66	97.09	1.74	0.02	0.46
2	0.00	0.00	0.02	0.05	0.70	96.65	1.90	0.19	0.50
3	0.00	0.00	0.00	0.04	0.78	96.24	2.60	0.00	0.35
4	0.09	0.00	0.07	0.00	0.82	95.34	3.28	0.07	0.33
5	0.04	0.03	0.00	0.02	0.94	94.50	3.86	0.02	0.59
6	0.00	0.03	0.00	0.26	19.75	65.79	13.78	0.00	0.39
7	0.00	0.01	0.02	0.85	40.33	20.17	38.42	0.02	0.18
8	0.00	0.03	0.00	1.83	0.88	6.15	91.04	0.05	0.03
9	0.00	0.02	0.00	1.91	0.42	5.52	92.08	0.00	0.05
10	0.00	0.00	0.00	1.79	0.47	5.36	92.29	0.09	0.00
11	0.00	0.01	0.00	1.85	0.55	5.06	92.50	0.02	0.01
12	0.00	0.00	0.00	1.91	0.42	2.11	95.56	0.00	0.00
13	0.00	0.00	0.00	1.93	0.44	1.62	95.98	0.00	0.04
14	0.00	0.01	0.00	1.95	0.47	1.43	96.10	0.04	0.00
15	0.01	0.00	0.01	1.94	0.43	2.84	94.72	0.05	0.00

B.15 HT-9/Zr/V/Nd After 28 Days at 550°C

The HT-9/Zr/V/Nd assembly annealed for 28 days at 550°C bonded on the V/Nd interface but not the HT-9/Zr or Zr/V interfaces. Compositional data (in at%) from WDS linescans across the V/Nd interface is given below.

Position	Zr	Mo	W	Cr	Fe	Nd	V	Ni	Mn
0	0.00	0.00	0.00	0.07	0.58	97.07	1.75	0.00	0.53
1	0.03	0.00	0.04	0.12	0.44	95.53	3.34	0.06	0.44
2	0.00	0.02	0.02	0.00	0.41	96.96	1.98	0.00	0.61
3	0.00	0.05	0.02	0.00	0.49	95.84	3.21	0.00	0.40
4	0.04	0.01	0.06	0.05	0.51	95.25	3.51	0.00	0.58
5	0.01	0.00	0.00	0.06	0.42	95.70	3.47	0.00	0.35
6	0.02	0.01	0.02	0.07	0.45	94.76	4.02	0.14	0.53
7	0.00	0.04	0.00	0.22	0.80	90.99	7.61	0.00	0.34
8	0.01	0.02	0.00	1.36	7.28	31.46	59.73	0.00	0.13
9	0.00	0.00	0.00	2.01	1.32	1.17	95.48	0.00	0.02
10	0.00	0.00	0.02	2.02	0.51	0.58	96.86	0.00	0.01

B.16 HT-9/Zr/Nd After 28 Days at 550°C

The HT-9/Zr/Nd assembly annealed for 28 days at 550°C bonded on the Zr/Nd interface but not the HT-9/Zr interface. Compositional data (in at%) from WDS linescans across the Zr/Nd interface is given below.

Position	Zr	Mo	W	Cr	Fe	Nd	V	Ni	Mn
0	98.13	0.00	0.00	0.04	0.12	1.69	0.02	0.00	0.00
1	98.45	0.00	0.00	0.03	0.31	1.10	0.00	0.10	0.00
2	98.60	0.00	0.00	0.01	0.06	1.29	0.03	0.01	0.01
3	94.89	2.33	0.00	0.00	0.13	2.64	0.02	0.00	0.00
4	72.04	0.00	0.00	0.01	0.36	27.40	0.03	0.01	0.15
5	0.86	0.04	0.00	0.00	0.32	98.25	0.00	0.05	0.49
6	0.19	0.04	0.06	0.03	0.47	98.64	0.05	0.00	0.52
7	0.03	0.00	0.00	0.00	0.47	98.87	0.05	0.10	0.48
8	0.09	0.00	0.00	0.00	0.39	98.91	0.00	0.15	0.46
9	0.00	0.08	0.00	0.00	0.56	98.84	0.03	0.00	0.51
10	0.04	0.00	0.03	0.05	0.68	98.79	0.05	0.00	0.37
0	99.25	0.00	0.00	0.01	0.12	0.61	0.01	0.00	0.01
1	99.17	0.00	0.00	0.00	0.13	0.59	0.00	0.00	0.11
2	99.37	0.00	0.00	0.03	0.10	0.47	0.00	0.00	0.03
3	96.58	0.00	0.00	0.01	1.78	1.47	0.00	0.09	0.08
4	90.92	0.00	0.00	0.01	2.85	6.15	0.00	0.03	0.05
5	18.14	0.00	0.00	0.03	0.84	80.48	0.02	0.00	0.50
6	1.83	0.03	0.07	0.03	0.60	96.95	0.02	0.08	0.41
7	0.20	0.00	0.01	0.00	0.47	98.72	0.00	0.08	0.52
8	0.06	0.08	0.00	0.00	0.00	99.20	0.00	0.13	0.53
9	0.02	0.03	0.04	0.04	0.39	98.92	0.01	0.05	0.50
10	0.13	0.00	0.00	0.00	0.35	99.11	0.07	0.00	0.34

B.17 HT-9/Ti/V/Nd After 28 Days at 550°C

The HT-9/Ti/V/Nd assembly annealed for 28 days at 550°C bonded on the V/Nd and HT-9/Ti interfaces but not the Ti/V interface. Compositional data (in at%) from WDS linescans across the HT-9/Ti interface is given below.

Position	Ta	Ti	Mo	W	Cr	Fe	Nd	V	Ni	Mn
0	0.00	0.82	0.78	0.15	13.58	83.25	0.00	0.29	0.49	0.63
1	0.00	0.71	0.62	0.12	12.33	84.63	0.00	0.30	0.64	0.65
2	0.00	0.87	0.72	0.12	14.01	82.80	0.05	0.35	0.48	0.61
3	0.00	0.94	0.63	0.17	13.04	83.82	0.06	0.31	0.51	0.52
4	0.00	1.13	0.74	0.17	12.91	83.89	0.10	0.26	0.47	0.33
5	0.00	1.34	0.48	0.10	11.05	86.12	0.03	0.24	0.55	0.10
6	0.00	1.62	0.65	0.10	12.25	84.28	0.06	0.29	0.53	0.23
7	0.00	2.21	0.65	0.17	12.44	83.39	0.08	0.25	0.58	0.21
8	0.00	12.78	0.55	0.11	11.90	73.11	0.07	0.34	0.43	0.73
9	0.00	99.11	0.00	0.01	0.08	0.41	0.05	0.27	0.05	0.00
10	0.00	99.22	0.00	0.00	0.07	0.39	0.07	0.24	0.00	0.01
11	0.00	99.29	0.00	0.00	0.03	0.33	0.09	0.25	0.00	0.00
12	0.00	99.33	0.00	0.03	0.05	0.29	0.03	0.27	0.00	0.00
13	0.00	99.48	0.00	0.01	0.03	0.20	0.03	0.25	0.00	0.00
14	0.00	99.28	0.00	0.00	0.08	0.25	0.08	0.28	0.01	0.01
15	0.00	99.50	0.00	0.00	0.00	0.17	0.05	0.23	0.05	0.00
0	0.00	0.42	0.60	0.16	12.50	84.60	0.12	0.32	0.55	0.733
1	0.00	0.75	0.60	0.13	13.30	83.58	0.07	0.36	0.63	0.586
2	0.00	0.90	0.70	0.18	12.67	84.19	0.03	0.32	0.47	0.549
3	0.00	1.14	0.75	0.17	13.25	83.45	0.05	0.31	0.53	0.348
4	0.00	1.58	0.69	0.19	12.95	83.54	0.04	0.28	0.49	0.244
5	0.00	2.25	0.69	0.13	11.17	84.75	0.16	0.20	0.47	0.179
6	0.00	48.50	0.20	0.06	5.69	42.72	0.25	0.29	1.87	0.421
7	0.00	82.61	0.00	0.01	0.65	11.57	0.01	0.21	4.52	0.418
8	0.00	98.62	0.00	0.01	0.21	0.83	0.08	0.21	0.02	0.025
9	0.00	99.10	0.00	0.05	0.05	0.46	0.06	0.27	0.00	0
10	0.00	99.19	0.00	0.02	0.06	0.40	0.07	0.25	0.01	0.02
11	0.00	99.22	0.00	0.02	0.04	0.35	0.04	0.27	0.06	0.002
12	0.00	98.92	0.00	0.00	0.10	0.36	0.31	0.29	0.00	0.016
13	0.00	98.92	0.00	0.00	0.10	0.44	0.30	0.23	0.01	0
14	0.00	99.24	0.00	0.00	0.06	0.29	0.10	0.28	0.00	0.038
15	0.00	98.59	0.00	0.04	0.14	0.83	0.08	0.25	0.04	0.036

B.18 HT-9/Ti/Nd After 28 Days at 550°C

The HT-9/Ti/Nd assembly annealed for 28 days at 550°C bonded on the Ti/Nd interface but not the HT-9/Ti interface. Compositional data (in at%) from WDS linescans across the Ti/Nd interface is given below.

Position	Ta	Ti	Mo	W	Cr	Fe	Nd	V	Ni	Mn
0	0.00	1.40	0.00	0.00	0.00	0.47	97.48	0.12	0.00	0.53
1	0.00	1.41	0.10	0.00	0.10	0.21	97.83	0.00	0.00	0.35
2	0.00	2.09	0.00	0.00	0.06	0.05	97.28	0.02	0.00	0.51
3	0.00	2.85	0.00	0.03	0.18	0.09	95.96	0.02	0.25	0.62

4	0.00	3.18	0.16	0.02	0.00	0.21	95.99	0.00	0.00	0.44
5	0.00	3.47	0.01	0.02	0.15	0.09	95.67	0.00	0.00	0.60
6	0.00	3.76	0.03	0.11	0.08	0.30	95.17	0.00	0.20	0.35
7	0.00	4.91	0.04	0.00	0.00	0.27	94.09	0.02	0.37	0.31
8	0.00	8.12	0.07	0.00	0.00	0.29	91.10	0.05	0.00	0.37
9	0.00	7.47	0.00	0.00	0.08	0.26	91.70	0.09	0.03	0.36
10	0.00	89.13	0.00	0.00	0.06	0.16	10.21	0.32	0.01	0.12
11	0.00	96.71	0.00	0.00	0.00	0.00	2.99	0.26	0.00	0.04
12	0.00	96.75	0.00	0.00	0.00	0.01	2.92	0.27	0.00	0.05
13	0.00	96.74	0.00	0.01	0.02	0.01	2.89	0.22	0.05	0.05
14	0.00	98.69	0.00	0.01	0.04	0.02	0.92	0.33	0.00	0.00
15	0.00	99.04	0.00	0.00	0.00	0.03	0.63	0.25	0.03	0.02
0	0.00	1.11	0.00	0.00	0.20	0.18	98.06	0.00	0.07	0.38
1	0.00	1.35	0.11	0.00	0.00	0.24	97.58	0.06	0.23	0.45
2	0.00	1.80	0.00	0.01	0.18	0.69	96.70	0.10	0.00	0.53
3	0.00	1.81	0.10	0.11	3.78	25.12	68.43	0.11	0.07	0.47
4	0.00	1.81	0.27	0.06	3.88	27.09	66.22	0.03	0.18	0.47
5	0.00	1.87	0.00	0.10	0.35	1.23	95.72	0.07	0.15	0.51
6	0.00	6.32	0.00	0.03	0.04	0.37	92.80	0.00	0.00	0.44
7	0.00	19.47	0.00	0.08	0.18	0.48	79.18	0.14	0.08	0.39
8	0.00	3.36	0.02	0.00	0.42	3.89	91.92	0.00	0.09	0.30
9	0.00	5.70	0.06	0.01	0.00	0.61	93.03	0.02	0.08	0.49
10	0.00	94.99	0.00	0.00	0.05	0.08	4.56	0.27	0.00	0.05
11	0.00	96.02	0.00	0.04	0.00	0.28	3.42	0.21	0.00	0.04
12	0.00	96.52	0.00	0.01	0.02	0.09	3.09	0.26	0.00	0.00
13	0.00	97.22	0.00	0.01	0.01	0.01	2.53	0.21	0.00	0.02
14	0.00	98.05	0.00	0.02	0.05	0.04	1.61	0.22	0.03	0.00
15	0.00	98.01	0.00	0.00	0.00	0.00	1.64	0.32	0.00	0.03

B.19 HT-9/Ta/V/Nd After 28 Days at 550°C

The HT-9/Ta/V/Nd assembly annealed for 28 days at 550°C bonded on the V/Nd interface but not the HT-9/Ta or Ta/V interfaces. Since the V/Nd interface was already well characterized for this time and temperature, no WDS data on this interface was gathered.

B.20 HT-9/Ta/Nd After 28 Days at 550°C

The HT-9/Ta/Nd assembly annealed for 28 days at 550°C bonded on the Ta/Nd interface but not the HT-9/Ta interface. Compositional data (in at%) from WDS linescans across the Ta/Nd interface is given below.

Position	Ta	Ti	Mo	W	Cr	Fe	Nd	V	Ni	Mn
0	0.03	0.00	0.00	0.00	0.00	0.30	98.98	0.00	0.00	0.69
1	0.00	0.00	0.00	0.06	0.00	0.32	99.03	0.14	0.00	0.45
2	0.00	0.00	0.17	0.00	0.00	0.43	98.86	0.00	0.00	0.55
3	0.00	0.00	0.00	0.00	0.00	0.36	99.12	0.02	0.00	0.49
4	0.00	0.00	0.02	0.05	0.00	0.29	99.26	0.00	0.00	0.39
5	0.00	0.00	0.08	0.00	0.00	0.18	99.44	0.00	0.01	0.29

6	0.00	0.00	0.00	0.00	0.00	0.35	99.09	0.01	0.01	0.54
7	0.00	0.00	0.00	0.08	0.00	0.34	99.07	0.00	0.00	0.52
8	0.00	0.00	0.07	0.13	0.00	0.23	99.19	0.01	0.00	0.36
9	3.77	0.01	0.00	0.24	0.19	0.31	94.89	0.00	0.14	0.45
10	90.84	0.00	0.04	2.42	0.08	0.00	6.12	0.00	0.51	0.00
11	95.11	0.00	0.12	2.08	0.14	0.02	2.26	0.14	0.13	0.00
12	95.69	0.00	0.00	2.46	0.00	0.03	1.74	0.01	0.07	0.00
13	95.48	0.02	0.00	1.90	0.11	0.12	2.35	0.00	0.01	0.00
14	94.69	0.00	0.02	1.83	0.12	0.79	2.47	0.00	0.08	0.00
15	95.28	0.04	0.19	2.19	0.25	0.02	1.74	0.06	0.12	0.12
0	95.90	0.01	0.11	1.84	0.00	0.03	1.75	0.00	0.30	0.06
1	95.44	0.00	0.09	2.24	0.12	0.29	1.71	0.12	0.00	0.00
2	96.64	0.00	0.00	1.88	0.04	0.00	1.18	0.04	0.07	0.15
3	95.15	0.00	0.13	2.08	0.00	0.12	2.18	0.14	0.21	0.00
4	95.51	0.00	0.12	2.12	0.00	0.13	2.04	0.00	0.00	0.07
5	0.02	0.00	0.05	0.11	0.10	0.33	98.97	0.00	0.00	0.43
6	0.00	0.00	0.07	0.00	0.02	0.36	98.91	0.00	0.11	0.54
7	0.00	0.00	0.06	0.02	0.00	0.28	99.22	0.00	0.03	0.39
8	0.00	0.00	0.00	0.01	0.11	0.25	99.02	0.00	0.04	0.58
9	0.00	0.00	0.00	0.02	0.00	0.46	98.83	0.02	0.00	0.67
10	0.00	0.00	0.00	0.00	0.00	0.34	99.05	0.08	0.22	0.31
11	0.00	0.00	0.00	0.00	0.00	0.26	99.00	0.09	0.01	0.64
12	0.00	0.00	0.00	0.08	0.06	0.26	99.03	0.05	0.00	0.53
13	0.00	0.00	0.04	0.01	0.00	0.27	99.18	0.04	0.07	0.40
14	0.00	0.00	0.00	0.18	0.04	0.37	98.86	0.07	0.00	0.48
15	0.00	0.00	0.09	0.16	0.10	0.36	98.85	0.07	0.04	0.33

B.21 HT-9/Mo/V/Nd After 28 Days at 550°C

The HT-9/Mo/V/Nd assembly annealed for 28 days at 550°C bonded on the V/Nd interface but not the HT-9/Mo or Mo/V interfaces. Compositional data (in at%) from WDS linescans across the V/Nd interface is given below.

Position	Mo	W	Cr	Fe	Nd	V	Ni	Mn
0	0.02	0.00	1.95	0.37	2.70	94.90	0.03	0.03
2	0.00	0.00	2.05	0.08	1.55	96.32	0.00	0.00
4	0.05	0.00	2.10	1.48	3.52	92.81	0.04	0.01
6	0.00	0.00	1.97	0.15	1.86	96.00	0.00	0.02
8	0.00	0.00	1.92	0.06	11.02	86.98	0.00	0.02
10	0.05	0.00	1.97	0.16	5.01	92.78	0.02	0.02
12	0.02	0.00	1.96	0.99	2.42	94.59	0.00	0.02
14	7.83	0.00	0.95	4.10	49.04	37.79	0.03	0.26
16	0.12	0.06	0.29	0.59	86.62	11.99	0.03	0.31
18	0.00	0.00	0.06	0.29	97.15	2.01	0.07	0.42
20	0.02	0.00	0.05	0.43	98.21	0.91	0.00	0.38

B.22 HT-9/Mo/Nd After 28 Days at 550°C

The HT-9/Mo/Nd assembly annealed for 28 days at 550°C bonded on the Mo/Nd interface but not the HT-9/Mo interface. Compositional data (in at%) from WDS linescans across the Mo/Nd interface is given below.

Position	Mo	W	Cr	Fe	Nd	V	Ni	Mn
0	0.06	0.05	0.00	0.47	99.00	0.00	0.00	0.42
2	0.08	0.03	0.01	0.35	98.98	0.00	0.00	0.55
4	0.23	0.00	0.05	0.35	99.01	0.00	0.01	0.36
6	0.10	0.00	0.00	0.40	98.96	0.02	0.00	0.52
8	0.09	0.00	0.01	0.37	99.10	0.01	0.00	0.42
10	0.13	0.00	0.05	0.36	98.85	0.04	0.02	0.56
12	22.84	0.03	0.09	0.35	76.29	0.09	0.00	0.31
14	98.56	0.01	0.03	0.05	1.31	0.03	0.00	0.02
16	99.39	0.01	0.05	0.00	0.55	0.01	0.00	0.00
18	99.58	0.01	0.00	0.04	0.37	0.00	0.01	0.00
20	99.37	0.01	0.00	0.11	0.48	0.02	0.01	0.01

B.23 HT-9/W/V/Nd After 28 Days at 550°C

The HT-9/W/V/Nd assembly annealed for 28 days at 550°C bonded on the V/Nd interface but not the HT-9/W or W/V interfaces. Compositional data (in at%) from WDS linescans across the V/Nd interface is given below.

Position	Mo	W	Cr	Fe	Nd	V	Ni	Mn
0	0.00	0.01	1.92	0.02	0.09	97.95	0.00	0.00
2	0.00	0.04	1.98	0.02	0.09	97.87	0.00	0.00
4	0.01	0.01	1.98	0.02	0.13	97.86	0.00	0.00
6	0.00	0.00	1.93	0.32	0.72	97.03	0.01	0.00
8	0.01	0.11	1.95	1.40	0.61	95.92	0.00	0.00
10	0.00	0.03	0.10	0.79	91.86	6.71	0.05	0.47
12	0.00	0.05	0.07	0.38	95.53	3.50	0.00	0.48
14	0.00	0.05	0.00	0.38	96.69	2.35	0.00	0.53
16	0.05	0.03	0.07	0.48	94.39	4.54	0.00	0.45
18	0.00	0.01	0.00	0.36	98.16	0.92	0.07	0.49
20	0.00	0.00	0.04	0.34	98.45	0.54	0.12	0.51
0	0.01	0.00	1.96	0.01	0.13	97.89	0.00	0.00
2	0.01	0.01	2.03	0.01	0.12	97.83	0.00	0.00
4	0.00	0.00	1.96	0.00	0.09	97.94	0.01	0.00
6	0.00	0.02	1.98	0.03	0.11	97.86	0.00	0.00
8	0.01	0.00	1.85	3.78	1.76	92.59	0.00	0.01
10	0.00	0.00	0.04	0.44	93.73	5.31	0.00	0.48
12	0.01	0.02	0.00	0.44	96.40	2.60	0.01	0.52
14	0.00	0.02	0.00	0.33	97.46	1.71	0.00	0.48
16	0.02	0.00	0.06	0.38	97.37	1.76	0.05	0.35
18	0.00	0.02	0.09	0.43	97.14	1.93	0.00	0.38
20	0.00	0.01	0.00	0.39	98.13	0.98	0.00	0.49

B.24 HT-9/W/Nd After 28 Days at 550°C

The HT-9/W/Nd assembly annealed for 28 days at 550°C bonded on the W/Nd interface but not the HT-9/W interface. Compositional data (in at%) from WDS linescans across the W/Nd interface is given below.

Position	Mo	W	Cr	Fe	Nd	V	Ni	Mn
0	0.00	0.14	0.00	0.38	98.86	0.10	0.07	0.46

2	0.02	0.15	0.08	0.76	98.58	0.00	0.00	0.41
4	0.00	0.52	0.10	0.71	98.26	0.00	0.00	0.42
6	0.03	3.81	0.02	0.36	95.33	0.03	0.00	0.42
8	0.00	89.56	0.04	0.02	10.26	0.00	0.03	0.09
10	0.00	97.59	0.00	0.02	2.39	0.00	0.00	0.00
12	0.00	98.67	0.00	0.00	1.16	0.14	0.03	0.00
14	0.00	99.07	0.03	0.09	0.62	0.04	0.09	0.07
16	0.00	98.92	0.01	0.01	1.01	0.00	0.05	0.00
18	0.00	99.26	0.05	0.00	0.62	0.00	0.03	0.04
20	0.00	99.32	0.00	0.00	0.60	0.09	0.00	0.00

B.25 HT-9/Nd After 56 Days at 550°C

After annealing for 56 days at 550°C, three interaction zones were observed in the HT-9/Nd diffusion assembly. The $\text{Nd}_2(\text{Fe}+\text{Cr})_{17}$ zone was ~18 μm wide, the $\text{Nd}_5(\text{Fe}+\text{Cr})_{17}$ zone was ~8 μm wide, and the Fe_2Nd zone was ~5 μm wide. While the $\text{Nd}_2(\text{Fe}+\text{Cr})_{17}$ phase still contained $\text{Nd}_5(\text{Fe}+\text{Cr})_{17}$ precipitates, unlike the shorter anneals at 550°C, the intermediate $\text{Nd}_5(\text{Fe}+\text{Cr})_{17}$ phase developed consistently across the full interface, and to a much greater thickness. Compositional data from WDS linescans across the interface is given below.

Position	Zr	Mo	W	Cr	Fe	Nd	V	Ni	Mn
0	0.00	0.83	0.18	14.53	82.83	0.25	0.34	0.44	0.62
1	0.00	1.06	0.25	15.73	81.17	0.30	0.38	0.47	0.65
2	0.00	0.77	0.19	14.01	83.34	0.33	0.33	0.46	0.57
3	0.00	1.02	0.22	15.64	81.42	0.24	0.40	0.42	0.64
4	0.00	0.53	0.10	12.33	84.86	1.10	0.32	0.27	0.49
5	0.01	0.90	0.15	14.07	83.15	0.30	0.36	0.42	0.64
6	0.02	0.97	0.18	16.15	72.21	9.39	0.36	0.04	0.68
7	0.00	0.97	0.21	15.80	69.28	12.59	0.40	0.00	0.76
8	0.00	0.86	0.19	15.99	68.59	13.33	0.33	0.00	0.70
9	0.00	0.79	0.19	15.43	68.59	13.85	0.40	0.02	0.74
10	0.01	0.75	0.17	15.44	68.74	13.80	0.32	0.06	0.72
11	0.01	0.76	0.22	15.72	68.41	13.86	0.34	0.02	0.66
12	0.00	1.03	0.22	16.19	68.48	12.93	0.39	0.03	0.74
13	0.00	0.87	0.21	15.86	68.32	13.69	0.38	0.00	0.67
14	0.00	0.96	0.23	16.85	68.81	12.08	0.39	0.00	0.68
15	0.01	0.79	0.24	16.21	65.40	16.30	0.39	0.01	0.65
16	0.00	0.79	0.20	16.13	66.59	15.28	0.34	0.00	0.67
17	0.00	0.81	0.22	15.84	65.53	16.49	0.34	0.04	0.74
18	0.00	0.75	0.17	15.30	59.55	23.16	0.38	0.00	0.68
19	0.02	0.84	0.21	15.90	65.27	16.68	0.38	0.00	0.70
20	0.03	0.87	0.25	15.36	60.19	22.31	0.37	0.00	0.63
21	0.00	0.75	0.23	15.36	55.95	21.09	0.40	0.03	0.71
22	0.02	0.76	0.26	11.58	48.14	38.29	0.29	0.01	0.65
23	0.00	1.05	0.16	16.85	64.39	16.55	0.25	0.00	0.75
24	0.00	0.79	0.25	11.94	48.41	37.75	0.24	0.00	0.62
25	0.00	0.10	0.03	3.43	51.86	43.92	0.06	0.00	0.60

26	0.01	0.01	0.00	2.94	62.46	33.95	0.00	0.07	0.56
27	0.00	0.01	0.03	3.00	62.52	33.90	0.01	0.00	0.55
28	0.01	0.01	0.00	2.68	62.77	33.75	0.03	0.07	0.68
29	0.00	0.01	0.00	2.32	63.35	33.67	0.00	0.00	0.64
30	0.00	0.04	0.00	2.08	62.92	34.43	0.00	0.00	0.53
31	0.00	0.00	0.00	1.22	52.98	45.22	0.00	0.01	0.57
32	0.04	0.00	0.00	0.26	8.59	90.63	0.00	0.00	0.49
33	0.00	0.00	0.00	0.09	3.42	95.87	0.00	0.04	0.58
34	0.00	0.00	0.09	0.17	1.22	97.95	0.00	0.04	0.53
35	0.03	0.00	0.01	0.22	4.76	94.45	0.00	0.05	0.48
0	0.00	0.83	0.17	12.71	84.69	0.21	0.30	0.52	0.58
1	0.00	0.84	0.15	12.78	84.45	0.33	0.36	0.47	0.61
2	0.00	0.90	0.21	13.62	83.08	0.76	0.40	0.42	0.61
3	0.00	0.81	0.20	12.83	84.49	0.24	0.37	0.45	0.61
4	0.00	0.97	0.23	13.28	83.71	0.47	0.36	0.41	0.58
5	0.00	0.86	0.14	13.54	82.43	1.77	0.37	0.33	0.55
6	0.01	1.07	0.20	16.34	70.08	11.19	0.40	0.02	0.69
7	0.00	0.89	0.22	15.52	70.05	12.24	0.34	0.00	0.74
8	0.00	1.16	0.14	16.52	70.13	10.93	0.42	0.00	0.70
9	0.00	0.76	0.18	14.77	69.26	13.92	0.36	0.02	0.73
10	0.00	0.80	0.21	15.16	69.01	13.66	0.39	0.03	0.74
11	0.01	1.10	0.23	15.73	68.76	13.01	0.40	0.04	0.73
12	0.00	0.78	0.20	15.06	69.09	13.85	0.28	0.00	0.73
13	0.02	0.74	0.22	15.44	68.97	13.57	0.34	0.00	0.70
14	0.00	0.89	0.26	15.67	68.78	13.30	0.41	0.00	0.69
15	0.00	0.76	0.16	15.61	67.80	14.55	0.39	0.00	0.73
16	0.01	0.85	0.20	16.61	67.21	14.05	0.37	0.00	0.70
17	0.00	0.80	0.20	16.50	68.02	13.48	0.29	0.03	0.68
18	0.00	0.84	0.19	16.12	66.32	15.40	0.40	0.02	0.71
19	0.00	0.82	0.19	16.47	66.52	14.96	0.32	0.00	0.71
20	0.01	0.88	0.24	16.20	65.42	16.11	0.44	0.00	0.70
21	0.00	0.83	0.19	15.80	62.94	19.21	0.40	0.00	0.64
22	0.00	0.75	0.18	14.39	55.45	28.26	0.31	0.00	0.65
23	0.01	0.76	0.12	14.98	58.96	24.15	0.38	0.00	0.65
24	0.00	0.77	0.16	15.28	61.75	20.93	0.38	0.00	0.73
25	0.00	0.67	0.11	14.53	56.24	27.45	0.33	0.00	0.67
26	0.00	0.76	0.19	15.69	60.96	21.32	0.38	0.00	0.71
27	0.00	0.88	0.27	16.48	62.59	18.76	0.37	0.00	0.65
28	0.00	0.78	0.18	16.28	63.18	18.54	0.39	0.00	0.65
29	0.01	0.80	0.18	16.32	62.32	19.38	0.30	0.00	0.71
30	0.00	0.81	0.17	16.03	61.83	20.06	0.36	0.02	0.73
31	0.03	0.75	0.18	15.32	58.43	24.15	0.41	0.00	0.73
32	0.00	0.83	0.21	15.22	59.44	23.20	0.40	0.01	0.70
33	0.01	0.90	0.19	14.44	55.97	27.45	0.37	0.00	0.67
34	0.00	0.22	0.07	4.86	35.06	59.04	0.15	0.00	0.60
35	0.00	0.00	0.04	2.26	56.65	40.51	0.00	0.00	0.54
36	0.00	0.00	0.00	2.00	43.78	53.64	0.02	0.00	0.56
37	0.02	0.04	0.08	0.59	10.77	87.87	0.00	0.08	0.56
38	0.00	0.04	0.00	0.29	3.22	95.81	0.08	0.00	0.56
39	0.01	0.00	0.00	0.22	1.16	97.93	0.00	0.04	0.63
40	0.00	0.02	0.02	0.11	0.97	98.14	0.15	0.07	0.52

0	0.00	0.55	0.13	12.82	84.51	0.62	0.33	0.46	0.59
1	0.01	0.81	0.16	14.21	82.59	1.03	0.33	0.33	0.53
2	0.00	0.77	0.21	12.96	79.12	5.86	0.41	0.10	0.57
3	0.00	0.74	0.17	14.15	73.05	10.83	0.33	0.04	0.70
4	0.00	0.57	0.12	14.39	71.85	12.08	0.31	0.00	0.68
5	0.00	0.63	0.13	14.83	72.51	10.86	0.29	0.00	0.75
6	0.02	0.89	0.19	15.32	71.14	11.41	0.31	0.06	0.66
7	0.00	0.87	0.17	15.36	71.02	11.46	0.45	0.01	0.66
8	0.00	0.78	0.16	15.79	69.67	12.54	0.38	0.00	0.68
9	0.00	0.75	0.18	16.18	69.87	11.99	0.32	0.03	0.69
10	0.00	0.75	0.15	15.68	68.44	13.92	0.34	0.00	0.70
11	0.00	0.78	0.17	15.87	69.97	12.06	0.40	0.00	0.76
12	0.00	0.81	0.15	15.94	69.87	12.10	0.40	0.05	0.67
13	0.00	0.69	0.15	15.83	68.10	14.21	0.29	0.03	0.70
14	0.01	0.67	0.16	16.09	68.00	13.99	0.37	0.04	0.68
15	0.00	0.83	0.18	16.59	68.19	13.14	0.36	0.04	0.67
16	0.02	0.90	0.23	17.08	68.90	11.82	0.42	0.01	0.63
17	0.00	0.84	0.25	16.74	67.63	13.38	0.45	0.06	0.66
18	0.02	0.82	0.19	15.86	61.49	20.55	0.43	0.00	0.65
19	0.00	0.74	0.14	16.25	65.51	16.32	0.40	0.01	0.64
20	0.01	0.82	0.20	16.43	65.56	15.90	0.40	0.00	0.69
21	0.02	0.74	0.15	16.44	64.51	17.05	0.43	0.00	0.66
22	0.00	0.69	0.14	16.06	60.86	21.16	0.32	0.04	0.74
23	0.03	0.69	0.17	14.70	54.89	28.55	0.32	0.09	0.56
24	0.00	0.87	0.17	16.38	63.57	17.98	0.42	0.02	0.58
25	0.00	0.96	0.21	16.71	65.21	15.76	0.43	0.07	0.65
26	0.00	0.99	0.29	16.46	63.26	17.92	0.41	0.00	0.66
27	0.01	0.95	0.25	16.12	62.42	19.13	0.45	0.00	0.67
28	0.00	0.77	0.21	15.38	61.47	21.12	0.35	0.00	0.70
29	0.00	0.92	0.17	15.18	60.61	22.21	0.34	0.01	0.56
30	0.01	0.81	0.17	13.66	60.21	24.14	0.38	0.01	0.61
31	0.00	0.17	0.00	5.31	59.49	34.32	0.17	0.00	0.54
32	0.00	0.02	0.00	2.92	62.38	34.02	0.04	0.00	0.62
33	0.00	0.53	0.15	10.24	57.76	30.39	0.30	0.01	0.63
34	0.00	0.12	0.02	4.49	60.22	34.49	0.06	0.00	0.60
35	0.01	0.02	0.01	2.88	62.60	33.82	0.06	0.04	0.57
36	0.00	0.02	0.00	0.21	1.73	97.35	0.04	0.07	0.59
37	0.00	0.02	0.03	0.19	1.47	97.66	0.03	0.00	0.60
38	0.01	0.01	0.12	0.25	1.64	97.48	0.00	0.02	0.48
39	0.00	0.04	0.01	0.21	1.56	97.45	0.15	0.00	0.58
40	0.11	0.03	0.00	0.21	1.74	97.13	0.06	0.07	0.66
0	0.00	0.72	0.14	13.80	81.67	2.40	0.34	0.27	0.66
1	0.00	0.69	0.17	13.71	80.79	3.40	0.31	0.31	0.62
2	0.00	0.69	0.17	13.45	80.87	3.60	0.31	0.27	0.65
3	0.00	0.65	0.15	13.19	81.92	2.93	0.32	0.23	0.61
4	0.00	1.29	0.32	18.23	76.14	2.75	0.40	0.26	0.63
5	0.00	1.08	0.26	16.54	74.08	6.98	0.38	0.09	0.61
6	0.01	0.80	0.18	15.55	79.10	3.00	0.38	0.35	0.64
7	0.01	1.14	0.25	17.69	77.56	2.02	0.45	0.25	0.63

8	0.00	1.14	0.26	17.40	74.08	5.99	0.31	0.21	0.61
9	0.00	0.79	0.18	15.19	72.28	10.43	0.36	0.08	0.70
10	0.00	0.71	0.18	14.90	71.26	11.89	0.36	0.02	0.69
11	0.00	0.74	0.16	14.96	70.37	12.64	0.37	0.03	0.73
12	0.01	0.69	0.16	15.18	70.38	12.59	0.35	0.00	0.65
13	0.00	0.71	0.19	15.48	70.14	12.39	0.33	0.05	0.72
14	0.00	0.79	0.18	15.76	69.97	11.92	0.53	0.08	0.78
15	0.00	0.69	0.16	15.76	70.20	12.05	0.39	0.06	0.69
16	0.00	0.66	0.18	15.63	69.74	12.76	0.24	0.03	0.76
17	0.01	0.68	0.16	15.76	69.18	13.12	0.29	0.03	0.77
18	0.00	0.72	0.15	16.14	69.50	12.45	0.30	0.03	0.70
19	0.01	0.83	0.22	16.23	69.92	11.62	0.37	0.04	0.76
20	0.00	0.92	0.19	16.12	69.24	12.43	0.37	0.05	0.69
21	0.00	0.72	0.17	15.96	68.06	14.01	0.40	0.04	0.65
22	0.01	0.70	0.20	15.27	68.03	14.71	0.37	0.05	0.66
23	0.00	0.74	0.19	14.78	67.43	15.77	0.33	0.05	0.71
24	0.00	0.84	0.26	15.65	68.28	13.91	0.40	0.04	0.62
25	0.00	0.92	0.24	16.77	67.64	13.33	0.46	0.00	0.65
26	0.00	1.00	0.21	16.92	65.99	14.64	0.50	0.08	0.66
27	0.00	0.89	0.21	16.70	64.83	16.30	0.36	0.05	0.67
28	0.00	0.86	0.17	16.31	65.21	16.40	0.41	0.00	0.63
29	0.02	0.88	0.23	16.35	64.27	17.13	0.39	0.04	0.71
30	0.01	0.90	0.22	16.30	62.57	18.96	0.41	0.00	0.63
31	0.00	0.87	0.22	16.30	62.86	18.74	0.38	0.00	0.64
32	0.00	0.89	0.23	15.95	60.91	20.87	0.46	0.00	0.69
33	0.00	0.95	0.16	15.11	58.72	24.08	0.36	0.00	0.62
34	0.00	0.92	0.14	14.89	56.32	26.57	0.45	0.05	0.67
35	0.02	0.88	0.27	14.59	56.29	26.74	0.43	0.15	0.64
36	0.02	0.93	0.20	14.74	56.36	26.61	0.57	0.06	0.51
37	0.00	0.97	0.25	11.44	56.59	29.62	0.39	0.09	0.66
38	0.00	0.26	0.11	6.16	57.94	34.60	0.37	0.01	0.55
39	0.04	0.12	0.03	4.42	59.50	34.89	0.31	0.09	0.59
40	0.00	0.00	0.00	2.52	60.68	36.11	0.06	0.00	0.63
41	0.01	0.02	0.00	2.29	57.96	39.16	0.02	0.00	0.55
42	0.00	0.02	0.01	1.92	48.65	48.68	0.03	0.10	0.60
43	0.00	0.03	0.05	0.76	16.21	82.39	0.02	0.00	0.54
44	0.00	0.07	0.00	0.29	2.20	96.79	0.06	0.00	0.59
45	0.00	0.00	0.00	0.15	1.66	97.75	0.09	0.05	0.30
46	0.00	0.02	0.00	0.23	1.35	97.54	0.26	0.10	0.50
47	0.00	0.01	0.02	0.22	1.56	97.20	0.29	0.12	0.58
48	0.00	0.04	0.03	0.20	1.51	97.17	0.67	0.00	0.39
49	0.00	0.01	0.00	0.12	1.05	98.03	0.29	0.00	0.51
50	0.00	0.09	0.04	0.56	5.12	93.59	0.06	0.09	0.45
0	0.00	0.69	0.20	13.71	81.70	2.42	0.35	0.34	0.59
1	0.02	0.80	0.22	15.30	75.08	7.51	0.41	0.03	0.64
2	0.07	0.71	0.20	15.24	73.70	8.95	0.42	0.07	0.65
3	0.00	0.65	0.17	15.27	73.44	9.40	0.27	0.05	0.75
4	0.01	0.76	0.12	15.57	71.79	10.67	0.39	0.07	0.63
5	0.00	0.82	0.13	15.44	70.37	12.07	0.42	0.00	0.75
6	0.00	0.86	0.22	15.87	70.08	11.94	0.39	0.00	0.65

7	0.00	0.87	0.22	15.74	69.69	12.39	0.37	0.00	0.72
8	0.00	0.91	0.13	15.71	69.50	12.72	0.33	0.00	0.70
9	0.00	0.83	0.22	15.81	69.04	13.11	0.34	0.00	0.65
10	0.01	0.83	0.16	16.05	69.30	12.43	0.38	0.05	0.79
11	0.00	0.80	0.17	16.11	68.94	12.99	0.30	0.00	0.69
12	0.02	0.81	0.16	15.79	68.42	13.73	0.36	0.00	0.71
13	0.00	0.81	0.17	15.48	67.72	14.60	0.44	0.05	0.74
14	0.02	0.80	0.14	15.38	66.03	16.37	0.35	0.10	0.82
15	0.00	0.77	0.16	16.18	67.49	14.28	0.37	0.00	0.75
16	0.00	0.79	0.13	16.30	67.26	14.45	0.31	0.00	0.76
17	0.00	0.93	0.18	16.08	68.02	13.74	0.40	0.00	0.65
18	0.04	0.76	0.19	15.92	65.57	15.96	0.39	0.45	0.72
19	0.01	0.77	0.19	15.48	66.13	16.36	0.33	0.03	0.71
20	0.01	0.68	0.14	15.65	66.31	16.12	0.36	0.01	0.74
21	0.00	0.81	0.14	15.89	67.00	15.09	0.28	0.00	0.79
22	0.00	0.80	0.19	16.00	68.23	13.57	0.44	0.06	0.71
23	0.00	0.82	0.24	14.99	60.39	22.48	0.44	0.00	0.64
24	0.00	1.01	0.22	17.12	77.74	2.45	0.48	0.05	0.94
25	0.00	0.87	0.29	15.51	61.25	21.12	0.32	0.00	0.64
26	0.00	0.89	0.20	15.32	59.60	22.85	0.44	0.03	0.67
27	0.03	0.76	0.15	14.40	60.34	23.28	0.36	0.00	0.67
28	0.00	0.42	0.09	8.68	59.23	30.64	0.31	0.07	0.57
29	0.00	0.06	0.02	3.61	61.34	34.31	0.08	0.00	0.58
30	0.01	0.03	0.00	2.76	63.61	32.98	0.07	0.00	0.56
31	0.00	0.00	0.00	2.57	63.04	33.77	0.01	0.00	0.61
32	0.00	0.00	0.01	2.21	56.92	40.25	0.01	0.09	0.52
33	0.00	0.00	0.00	1.72	50.14	47.61	0.00	0.00	0.53
34	0.00	0.00	0.03	0.93	31.82	66.69	0.03	0.05	0.44
35	0.00	0.05	0.00	0.13	5.01	94.28	0.00	0.02	0.51
36	0.01	0.06	0.00	0.11	1.35	98.06	0.00	0.00	0.41
37	0.00	0.04	0.00	0.02	0.77	98.47	0.09	0.04	0.58
38	0.00	0.00	0.00	0.06	0.72	98.64	0.02	0.00	0.56
39	0.02	0.00	0.05	0.08	0.63	98.77	0.00	0.00	0.44
40	0.00	0.02	0.00	0.05	0.94	98.32	0.04	0.05	0.58
0	0.01	0.82	0.19	14.93	76.84	6.12	0.36	0.09	0.65
1	0.00	0.76	0.14	13.49	79.62	4.89	0.36	0.11	0.62
2	0.00	0.69	0.16	13.84	76.13	8.16	0.34	0.10	0.59
3	0.00	0.80	0.24	14.84	71.72	11.37	0.30	0.04	0.69
4	0.00	0.96	0.22	15.38	70.33	12.04	0.35	0.00	0.72
5	0.01	0.85	0.18	16.22	70.75	10.91	0.30	0.00	0.79
6	0.00	0.72	0.21	15.75	71.22	11.05	0.33	0.00	0.72
7	0.02	0.76	0.14	16.19	71.08	10.78	0.32	0.04	0.68
8	0.00	1.04	0.28	16.26	70.91	10.40	0.41	0.02	0.68
9	0.00	0.99	0.25	16.04	68.90	12.76	0.37	0.00	0.69
10	0.00	0.91	0.23	15.85	68.70	13.33	0.35	0.00	0.64
11	0.02	0.77	0.22	15.92	66.87	15.10	0.40	0.02	0.68
12	0.02	0.77	0.19	16.08	66.63	15.31	0.31	0.00	0.69
13	0.02	0.82	0.16	16.05	66.67	15.17	0.45	0.00	0.67
14	0.00	0.74	0.19	16.01	66.24	15.92	0.31	0.01	0.59
15	0.00	0.83	0.21	16.44	68.47	13.03	0.34	0.05	0.63

16	0.01	0.86	0.22	16.54	69.33	12.03	0.41	0.00	0.61
17	0.00	0.90	0.22	16.47	68.56	12.79	0.39	0.00	0.68
18	0.00	0.89	0.20	16.13	67.86	14.00	0.35	0.00	0.57
19	0.00	0.79	0.17	14.21	65.42	18.46	0.35	0.00	0.61
20	0.00	0.77	0.16	15.93	64.24	17.94	0.33	0.03	0.60
21	0.01	0.79	0.18	16.22	63.57	18.31	0.32	0.00	0.59
22	0.02	0.85	0.17	16.29	64.05	17.62	0.39	0.00	0.62
23	0.00	0.79	0.20	16.18	63.20	18.57	0.40	0.03	0.62
24	0.00	0.87	0.21	16.36	64.00	17.52	0.41	0.04	0.58
25	0.00	0.91	0.23	16.60	64.21	16.97	0.35	0.04	0.70
26	0.00	0.78	0.15	16.42	64.52	16.94	0.52	0.03	0.65
27	0.00	0.81	0.22	16.21	63.15	18.59	0.34	0.03	0.65
28	0.02	0.80	0.16	16.49	64.28	17.26	0.34	0.00	0.65
29	0.00	1.01	0.20	14.05	57.16	26.60	0.35	0.07	0.57
30	0.06	0.85	0.19	14.00	53.49	30.10	0.57	0.00	0.75
31	0.00	0.80	0.15	12.29	50.57	35.08	0.51	0.05	0.55
32	0.00	0.86	0.23	16.23	63.22	18.42	0.41	0.00	0.62
33	0.00	0.91	0.20	15.00	58.64	24.26	0.40	0.00	0.59
34	0.01	0.97	0.20	15.00	56.47	26.32	0.43	0.00	0.62
35	0.00	0.76	0.09	12.23	50.13	35.60	0.52	0.00	0.66
36	0.00	0.48	0.12	8.24	50.13	39.93	0.38	0.00	0.73
37	0.00	0.08	0.02	4.10	57.46	37.61	0.16	0.00	0.57
38	0.01	0.01	0.00	2.96	59.78	36.68	0.12	0.00	0.44
39	0.00	0.00	0.00	2.74	56.28	40.40	0.07	0.00	0.52
40	0.02	0.00	0.00	1.84	40.65	57.02	0.00	0.02	0.46
41	0.02	0.02	0.00	0.94	23.59	74.84	0.08	0.03	0.49
42	0.03	0.00	0.02	0.52	20.01	78.92	0.15	0.00	0.35
43	0.00	0.03	0.00	0.31	5.47	92.28	1.38	0.00	0.53
44	0.03	0.00	0.03	0.11	0.98	96.62	1.77	0.00	0.46
45	0.02	0.02	0.01	0.09	1.07	97.65	0.54	0.00	0.61

B.26 HT-9/V/Nd After 56 Days at 550°C

The HT-9/V/Nd assembly annealed for 56 days at 550°C bonded on both the V/Nd and the HT-9/V interface. Compositional data (in at%) from WDS linescans across the HT-9/V interface is given below.

Position	Zr	Mo	W	Cr	Fe	Nd	V	Ni	Mn
0	0.03	0.93	0.23	13.58	83.17	0.07	0.97	0.47	0.57
1	0.01	0.90	0.19	13.59	83.14	0.04	0.97	0.54	0.63
2	0.00	1.06	0.26	15.05	81.38	0.03	1.09	0.52	0.63
3	0.00	0.89	0.25	14.97	81.70	0.04	1.12	0.47	0.58
4	0.00	0.64	0.14	11.59	85.35	0.05	1.24	0.46	0.54
5	0.00	0.60	0.16	12.61	83.98	0.04	1.60	0.50	0.52
6	0.00	0.77	0.17	11.64	84.44	0.04	2.08	0.45	0.42
7	0.00	0.72	0.20	11.11	75.75	0.14	11.19	0.44	0.46
8	0.00	0.07	0.01	3.27	9.67	0.73	86.06	0.05	0.14
9	0.00	0.02	0.00	1.98	1.05	0.27	96.67	0.00	0.03
10	0.00	0.01	0.00	1.97	1.04	0.10	96.85	0.03	0.01
11	0.00	0.01	0.00	1.94	0.70	0.24	97.09	0.00	0.03
12	0.00	0.02	0.03	1.98	0.81	0.34	96.78	0.04	0.01

13	0.00	0.00	0.03	1.86	0.36	0.14	97.61	0.00	0.00
14	0.00	0.00	0.00	1.89	0.27	0.09	97.75	0.00	0.01
15	0.00	0.00	0.01	1.91	0.28	0.15	97.60	0.05	0.00
0	0.00	0.73	0.16	12.68	84.42	0.10	0.80	0.48	0.64
1	0.00	0.78	0.16	12.53	84.49	0.09	0.80	0.53	0.64
2	0.02	0.73	0.16	12.82	84.30	0.08	0.80	0.49	0.60
3	0.01	0.61	0.13	11.75	85.48	0.04	0.87	0.49	0.63
4	0.00	0.61	0.15	12.03	85.01	0.11	1.09	0.44	0.57
5	0.02	0.65	0.14	12.91	83.79	0.11	1.29	0.47	0.62
6	0.00	0.95	0.22	16.94	78.92	0.05	1.80	0.51	0.61
7	0.00	0.94	0.19	15.88	79.73	0.06	2.30	0.44	0.47
8	0.01	0.71	0.17	11.41	77.88	0.08	8.85	0.44	0.45
9	0.00	0.21	0.02	4.44	19.90	0.11	74.91	0.10	0.32
10	0.01	0.00	0.01	1.88	0.61	0.01	97.47	0.00	0.03
11	0.00	0.00	0.00	1.88	0.44	0.05	97.64	0.00	0.00
12	0.01	0.00	0.00	1.87	0.38	0.02	97.70	0.03	0.00
13	0.01	0.01	0.01	1.93	0.26	0.03	97.76	0.00	0.00
14	0.00	0.01	0.00	1.89	0.19	0.02	97.90	0.00	0.00
15	0.00	0.00	0.00	1.81	0.31	0.02	97.85	0.01	0.00

B.27 HT-9/Zr/V/Nd After 56 Days at 550°C

The HT-9/Zr/V/Nd assembly annealed for 56 days at 550°C bonded on the V/Nd interface but not the HT-9/Zr or Zr/V interfaces. Compositional data (in at%) from WDS linescans across the V/Nd interface is given below.

Position	Zr	Mo	W	Cr	Fe	Nd	V	Ni	Mn
0	0.00	0.00	0.00	0.02	0.28	97.43	1.70	0.00	0.56
1	0.00	0.06	0.00	0.03	0.35	96.20	2.92	0.00	0.46
2	0.00	0.02	0.06	0.15	0.43	94.60	4.19	0.07	0.49
3	0.29	0.00	0.01	0.18	0.87	95.36	2.69	0.00	0.59
4	0.44	0.10	0.11	0.71	4.74	89.18	4.25	0.03	0.43
5	0.01	0.00	0.00	0.22	0.72	90.32	8.28	0.00	0.46
6	0.00	0.01	0.01	0.75	0.95	66.93	30.96	0.03	0.36
7	0.01	0.01	0.03	1.41	0.80	25.84	71.74	0.03	0.13
8	0.00	0.01	0.00	1.81	0.75	5.81	91.56	0.03	0.03
9	0.00	0.00	0.01	1.87	0.03	0.34	97.74	0.01	0.00
10	0.01	0.00	0.03	1.86	0.00	0.42	97.69	0.00	0.00
11	0.00	0.01	0.00	1.81	0.02	0.55	97.60	0.01	0.00
12	0.00	0.00	0.00	1.82	0.06	0.31	97.81	0.00	0.01
13	0.02	0.00	0.00	1.84	2.15	0.44	95.55	0.01	0.00
14	0.00	0.00	0.00	1.81	0.01	0.38	97.80	0.00	0.00
15	0.00	0.00	0.00	1.82	0.04	0.27	97.86	0.02	0.00

B.28 HT-9/Zr/Nd After 56 Days at 550°C

The HT-9/Zr/Nd assembly annealed for 56 days at 550°C bonded on the Zr/Nd interface but not the HT-9/Zr interface. Compositional data (in at%) from WDS linescans across the Zr/Nd interface is given below.

Position	Zr	Mo	W	Cr	Fe	Nd	V	Ni	Mn
----------	----	----	---	----	----	----	---	----	----

0	99.07	0.00	0.00	0.13	0.29	0.42	0.01	0.04	0.04
1	99.36	0.00	0.00	0.02	0.18	0.36	0.06	0.00	0.03
2	99.58	0.00	0.00	0.00	0.07	0.30	0.05	0.00	0.00
3	99.49	0.00	0.00	0.04	0.09	0.37	0.02	0.00	0.00
4	98.37	0.00	0.00	0.00	0.23	1.38	0.00	0.02	0.00
5	95.52	0.04	0.00	0.00	1.22	3.09	0.03	0.06	0.03
6	77.13	0.00	0.00	0.01	10.53	11.76	0.01	0.47	0.09
7	36.29	0.00	0.00	0.00	4.20	59.01	0.00	0.13	0.38
8	13.81	0.00	0.00	0.00	1.28	84.36	0.00	0.02	0.53
9	10.08	0.00	0.00	0.01	0.80	88.60	0.00	0.04	0.48
10	18.21	0.06	0.00	0.00	0.73	80.36	0.00	0.09	0.55
11	9.76	0.02	0.02	0.01	0.41	89.26	0.03	0.00	0.49
12	2.37	0.00	0.00	0.13	0.85	96.08	0.00	0.00	0.57
13	2.20	0.01	0.00	0.04	0.73	96.31	0.07	0.07	0.58
14	0.04	0.00	0.08	0.00	0.25	99.00	0.03	0.04	0.57
15	3.04	0.01	0.00	0.15	0.91	95.30	0.00	0.00	0.59
0	98.43	0.00	0.00	0.03	0.13	0.54	0.86	0.02	0.00
1	99.64	0.01	0.00	0.03	0.08	0.24	0.01	0.00	0.00
2	99.44	0.02	0.00	0.04	0.15	0.29	0.00	0.03	0.03
3	99.44	0.00	0.00	0.07	0.15	0.28	0.01	0.04	0.01
4	99.59	0.00	0.00	0.03	0.05	0.33	0.00	0.00	0.00
5	99.55	0.01	0.00	0.00	0.04	0.36	0.01	0.03	0.00
6	99.36	0.00	0.00	0.00	0.09	0.48	0.04	0.00	0.03
7	93.41	0.00	0.00	0.00	2.28	4.17	0.00	0.14	0.00
8	65.17	0.07	0.00	0.09	1.43	32.93	0.00	0.08	0.23
9	7.51	0.03	0.00	0.00	0.43	91.47	0.00	0.04	0.53
10	1.43	0.00	0.02	0.00	0.41	97.57	0.00	0.00	0.57
11	0.35	0.01	0.05	0.06	0.36	98.59	0.00	0.02	0.58
12	0.14	0.02	0.02	0.00	0.29	98.99	0.00	0.00	0.54
13	0.17	0.02	0.02	0.00	0.23	99.04	0.00	0.00	0.54
14	0.02	0.00	0.04	0.00	0.35	99.02	0.03	0.00	0.54
15	0.12	0.01	0.02	0.00	0.34	98.86	0.05	0.00	0.60

B.29 HT-9/Ti/V/Nd After 56 Days at 550°C

The HT-9/Ti/V/Nd assembly annealed for 56 days at 550°C bonded on the HT-9/Ti, Ti/V and V/Nd interfaces. Compositional data (in at%) from WDS linescans across the each of these interfaces is given below.

Position	Ta	Ti	Mo	W	Cr	Fe	Nd	V	Ni	Mn
0	0.00	98.31	0.00	0.00	0.23	0.96	0.14	0.31	0.04	0.01
1	0.00	98.87	0.00	0.01	0.09	0.52	0.12	0.35	0.02	0.03
2	0.00	97.90	0.00	0.00	0.17	0.95	0.21	0.73	0.01	0.04
3	0.00	97.52	0.00	0.01	0.30	1.77	0.06	0.25	0.02	0.07
4	0.00	97.95	0.00	0.00	0.15	1.47	0.09	0.30	0.01	0.02
5	0.00	98.19	0.00	0.00	0.22	1.22	0.06	0.31	0.00	0.00
6	0.00	98.00	0.00	0.00	0.22	1.31	0.12	0.34	0.01	0.00
7	0.00	91.63	0.06	0.00	1.25	6.12	0.42	0.44	0.00	0.07
8	0.00	46.26	0.37	0.06	8.96	42.60	0.74	0.43	0.28	0.33
9	0.00	5.14	0.76	0.21	12.99	79.29	0.17	0.43	0.41	0.60
10	0.00	3.31	0.74	0.15	12.25	81.97	0.12	0.40	0.44	0.62
11	0.00	2.35	0.62	0.15	11.87	83.64	0.09	0.26	0.43	0.59
12	0.00	2.54	0.54	0.16	11.57	83.73	0.09	0.42	0.47	0.49

13	0.00	1.55	0.60	0.12	10.69	85.47	0.08	0.38	0.53	0.58
14	0.00	1.50	0.37	0.07	10.72	85.64	0.35	0.50	0.47	0.41
15	0.00	1.11	0.40	0.12	10.83	86.13	0.13	0.29	0.45	0.55
0	0.00	1.17	0.01	0.00	1.99	0.10	0.18	96.51	0.01	0.03
1	0.00	2.16	0.00	0.01	1.92	0.05	0.27	95.51	0.07	0.02
2	0.00	1.44	0.00	0.00	1.98	0.02	0.17	96.37	0.00	0.01
3	0.00	2.26	0.00	0.00	1.90	0.06	0.23	95.55	0.00	0.00
4	0.00	0.83	0.01	0.00	2.00	0.43	0.60	96.12	0.00	0.00
5	0.00	0.76	0.00	0.00	1.97	0.15	0.24	96.85	0.04	0.00
6	0.00	0.89	0.00	0.00	1.80	0.04	0.03	97.24	0.00	0.00
7	0.00	14.23	0.00	0.02	1.72	0.01	0.02	83.99	0.00	0.00
8	0.00	84.33	0.00	0.00	0.27	0.02	0.06	15.27	0.02	0.02
9	0.00	99.05	0.00	0.00	0.01	0.02	0.04	0.88	0.01	0.00
10	0.00	98.93	0.00	0.00	0.05	0.00	0.00	0.97	0.05	0.00
11	0.00	99.29	0.00	0.00	0.00	0.01	0.04	0.63	0.00	0.03
12	0.00	99.27	0.00	0.00	0.01	0.02	0.03	0.65	0.02	0.00
13	0.00	99.27	0.00	0.00	0.03	0.01	0.05	0.62	0.00	0.02
14	0.00	99.44	0.00	0.00	0.03	0.00	0.02	0.50	0.01	0.00
15	0.00	99.41	0.00	0.00	0.00	0.00	0.04	0.54	0.00	0.01
0	0.00	0.34	0.03	0.01	2.03	0.06	0.07	97.47	0.00	0.01
1	0.00	0.38	0.02	0.00	2.08	0.01	0.02	97.47	0.01	0.00
2	0.00	0.45	0.00	0.03	2.11	0.03	0.02	97.32	0.04	0.01
3	0.00	0.51	0.02	0.00	1.92	0.04	0.02	97.45	0.04	0.00
4	0.00	0.58	0.02	0.00	1.96	0.00	0.01	97.44	0.00	0.00
5	0.00	0.68	0.00	0.02	2.12	0.04	0.06	97.03	0.06	0.00
6	0.00	0.90	0.03	0.02	1.97	0.03	0.03	96.99	0.03	0.00
7	0.00	4.75	0.01	0.00	1.85	0.00	0.03	93.36	0.01	0.01
8	0.00	57.82	0.00	0.00	0.90	0.01	0.00	41.23	0.01	0.03
9	0.00	98.31	0.00	0.00	0.00	0.00	0.03	1.63	0.00	0.03
10	0.00	98.92	0.00	0.01	0.05	0.00	0.03	0.93	0.02	0.04
11	0.00	97.36	0.00	0.00	0.01	0.02	0.04	2.58	0.00	0.00
12	0.00	98.93	0.00	0.00	0.02	0.00	0.01	1.02	0.01	0.01
13	0.00	92.96	0.00	0.00	0.20	0.27	1.14	5.40	0.00	0.03
14	0.00	96.33	0.00	0.00	0.06	0.35	0.51	2.75	0.00	0.00
15	0.00	95.20	0.00	0.00	0.19	1.38	0.24	2.92	0.04	0.04
0	0.00	0.00	0.03	0.00	0.02	0.38	98.01	0.87	0.43	0.28
1	0.00	0.00	0.00	0.04	0.08	0.15	98.09	0.71	0.15	0.78
2	0.00	0.00	0.09	0.10	0.15	0.49	97.20	1.33	0.09	0.54
3	0.00	0.00	0.00	0.04	0.00	0.37	97.21	1.78	0.00	0.61
4	0.00	0.00	0.14	0.00	0.28	0.40	94.83	3.74	0.03	0.58
5	0.00	0.00	0.00	0.05	0.09	0.21	96.60	2.61	0.09	0.36
6	0.00	0.00	0.00	0.00	0.00	0.37	96.65	2.21	0.01	0.77
7	0.00	0.00	0.00	0.00	0.10	0.15	96.83	2.44	0.09	0.40
8	0.00	0.00	0.00	0.00	0.12	0.42	95.48	3.44	0.08	0.46
9	0.00	0.00	0.00	0.00	1.78	4.85	6.79	86.50	0.00	0.08
10	0.00	0.00	0.00	0.03	2.07	3.73	1.90	92.20	0.07	0.00
11	0.00	0.01	0.03	0.00	2.05	2.07	0.81	95.02	0.00	0.01
12	0.00	0.00	0.00	0.01	1.89	0.03	0.69	97.35	0.02	0.00
13	0.00	0.01	0.00	0.00	2.11	0.40	1.66	95.75	0.07	0.00
14	0.00	0.01	0.00	0.03	1.78	0.62	4.37	93.13	0.06	0.00
15	0.00	0.03	0.02	0.03	2.06	0.87	7.84	89.07	0.04	0.04

B.30 HT-9/Ti/Nd After 56 Days at 550°C

The HT-9/Ti/Nd assembly annealed for 56 days at 550°C bonded on the HT-9/Ti and Ti/Nd interfaces. Compositional data (in at%) from WDS linescans across the both of these interfaces is given below.

Position	Ta	Ti	Mo	W	Cr	Fe	Nd	V	Ni	Mn
0	0.00	0.78	0.74	0.06	12.18	84.70	0.03	0.35	0.55	0.61
1	0.00	0.78	0.69	0.15	12.42	84.71	0.06	0.29	0.31	0.58
2	0.00	0.88	0.88	0.16	13.95	82.62	0.04	0.33	0.49	0.65
3	0.00	0.99	0.79	0.18	13.80	82.74	0.06	0.33	0.48	0.62
4	0.00	1.30	1.08	0.30	17.49	78.45	0.03	0.30	0.51	0.55
5	0.00	1.53	1.38	0.31	22.01	73.18	0.08	0.44	0.40	0.67
6	0.00	1.84	1.33	0.24	20.96	74.13	0.04	0.51	0.44	0.52
7	0.00	3.80	0.86	0.21	15.14	78.72	0.06	0.40	0.35	0.47
8	0.00	16.49	0.63	0.09	12.84	68.58	0.10	0.44	0.37	0.47
9	0.00	77.07	0.19	0.00	4.31	16.64	0.10	0.43	0.96	0.30
10	0.00	96.26	0.00	0.00	0.26	2.50	0.05	0.32	0.52	0.09
11	0.00	98.42	0.00	0.00	0.18	1.03	0.00	0.34	0.00	0.03
12	0.00	98.53	0.00	0.01	0.17	0.97	0.04	0.21	0.04	0.02
13	0.00	99.19	0.00	0.01	0.05	0.36	0.11	0.22	0.04	0.01
14	0.00	99.33	0.00	0.01	0.01	0.29	0.04	0.27	0.05	0.00
15	0.00	99.10	0.00	0.00	0.07	0.37	0.17	0.29	0.00	0.00
0	0.00	0.54	0.74	0.19	14.12	82.95	0.02	0.47	0.40	0.58
1	0.00	0.70	0.82	0.16	14.77	81.83	0.07	0.32	0.57	0.75
2	0.00	0.89	0.86	0.23	15.78	80.77	0.04	0.31	0.46	0.66
3	0.00	0.97	0.65	0.10	12.68	84.17	0.07	0.36	0.40	0.61
4	0.00	1.10	0.57	0.12	11.15	85.68	0.04	0.27	0.48	0.60
5	0.00	1.37	0.52	0.11	11.35	85.32	0.02	0.22	0.45	0.64
6	0.00	1.70	0.63	0.14	11.82	84.41	0.00	0.39	0.48	0.43
7	0.00	2.42	0.70	0.15	12.46	83.09	0.01	0.39	0.41	0.36
8	0.00	17.77	0.75	0.12	11.54	68.48	0.05	0.38	0.52	0.40
9	0.00	87.11	0.08	0.00	1.76	9.60	0.08	0.35	0.84	0.20
10	0.00	96.24	0.00	0.00	0.16	2.61	0.03	0.32	0.44	0.20
11	0.00	99.09	0.00	0.00	0.07	0.49	0.00	0.29	0.00	0.06
12	0.00	99.16	0.00	0.00	0.09	0.37	0.01	0.30	0.05	0.02
13	0.00	99.12	0.00	0.00	0.07	0.44	0.10	0.24	0.03	0.00
14	0.00	98.68	0.00	0.00	0.15	0.85	0.07	0.23	0.00	0.01
15	0.00	99.32	0.00	0.00	0.08	0.32	0.03	0.24	0.01	0.00
0	0.00	99.23	0.00	0.00	0.00	0.18	0.22	0.32	0.04	0.01
1	0.00	99.47	0.00	0.00	0.00	0.01	0.21	0.27	0.04	0.01
2	0.00	99.49	0.00	0.00	0.01	0.01	0.23	0.26	0.00	0.00
3	0.00	99.37	0.00	0.00	0.06	0.04	0.20	0.28	0.05	0.00
4	0.00	99.47	0.00	0.00	0.01	0.03	0.25	0.25	0.00	0.00
5	0.00	98.90	0.00	0.00	0.00	0.50	0.32	0.27	0.00	0.01
6	0.00	93.27	0.00	0.00	0.00	0.63	5.70	0.36	0.00	0.04
7	0.00	45.08	0.01	0.01	0.01	1.18	53.27	0.20	0.00	0.25
8	0.00	5.07	0.08	0.04	0.00	0.28	93.49	0.13	0.24	0.67
9	0.00	2.75	0.00	0.01	0.00	0.35	96.43	0.00	0.00	0.46
10	0.00	2.03	0.05	0.06	0.00	0.17	97.03	0.01	0.06	0.60
11	0.00	1.56	0.00	0.02	0.11	0.30	97.35	0.07	0.00	0.59
12	0.00	1.27	0.07	0.00	0.00	0.39	97.60	0.00	0.07	0.60

13	0.00	1.23	0.03	0.01	0.00	0.30	97.79	0.00	0.00	0.64
14	0.00	1.12	0.00	0.00	0.11	0.53	97.63	0.10	0.05	0.47
15	0.00	1.57	0.00	0.00	0.00	0.33	97.69	0.00	0.00	0.42
0	0.00	99.57	0.00	0.02	0.00	0.03	0.18	0.20	0.00	0.01
1	0.00	99.47	0.00	0.00	0.00	0.04	0.20	0.30	0.00	0.00
2	0.00	99.39	0.00	0.01	0.00	0.01	0.26	0.31	0.00	0.02
3	0.00	99.29	0.00	0.00	0.00	0.04	0.35	0.28	0.02	0.03
4	0.00	95.51	0.00	0.00	0.02	0.25	3.83	0.32	0.03	0.05
5	0.00	47.89	0.04	0.00	0.00	0.58	51.03	0.28	0.00	0.19
6	0.00	67.32	0.00	0.00	0.04	0.43	31.62	0.32	0.09	0.19
7	0.00	33.43	0.00	0.11	0.00	0.48	65.25	0.12	0.16	0.46
8	0.00	17.03	0.00	0.00	0.00	0.41	81.83	0.17	0.11	0.44
9	0.00	7.51	0.00	0.10	0.08	0.38	91.34	0.11	0.00	0.50
10	0.00	6.48	0.00	0.00	0.18	0.29	92.52	0.00	0.00	0.54
11	0.00	4.37	0.00	0.00	0.02	0.43	94.75	0.00	0.00	0.43
12	0.00	3.23	0.00	0.01	0.03	0.62	95.36	0.11	0.09	0.55
13	0.00	3.53	0.00	0.11	0.13	0.72	94.93	0.01	0.09	0.49
14	0.00	2.35	0.11	0.00	0.03	0.90	95.92	0.00	0.00	0.69
15	0.00	1.74	0.00	0.00	0.24	0.50	97.17	0.00	0.00	0.36

B.31 HT-9/Ta/V/Nd After 56 Days at 550°C

The HT-9/Ta/V/Nd assembly annealed for 56 days at 550°C bonded on the V/Nd interface but not the HT-9/Ta or Ta/V interfaces. Since the V/Nd interface at this time and temperature was already well characterized, no WDS linescans were completed on it in this assembly.

B.32 HT-9/Ta/Nd After 56 Days at 550°C

The HT-9/Ta/Nd assembly annealed for 56 days at 550°C bonded on the Ta/Nd interface but not the HT-9/Ta interface. Compositional data (in at%) from WDS linescans across the Ta/Nd interface is given below.

Position	Ta	Ti	Mo	W	Cr	Fe	Nd	V	Ni	Mn
0	96.34	0.01	0.19	2.39	0.00	0.00	0.91	0.05	0.11	0.01
1	96.75	0.00	0.00	2.27	0.04	0.07	0.74	0.08	0.00	0.06
2	96.33	0.00	0.00	2.24	0.00	0.00	1.27	0.00	0.16	0.00
3	96.50	0.04	0.04	2.51	0.01	0.00	0.91	0.00	0.00	0.00
4	88.89	0.00	0.10	2.01	0.00	0.05	8.87	0.09	0.00	0.00
5	49.47	0.00	0.02	1.23	0.00	0.35	48.41	0.15	0.00	0.36
6	9.59	0.00	0.05	0.15	0.02	0.48	89.24	0.06	0.12	0.30
7	76.25	0.08	0.06	1.66	0.05	0.09	21.59	0.12	0.00	0.10
8	43.55	0.00	0.00	0.91	0.00	0.19	55.00	0.00	0.14	0.21
9	0.00	0.00	0.01	0.00	0.15	0.24	98.81	0.11	0.12	0.56
10	0.00	0.00	0.00	0.00	0.08	0.15	99.25	0.05	0.10	0.37
11	0.00	0.00	0.06	0.01	0.04	0.34	98.87	0.00	0.06	0.62
12	0.00	0.00	0.00	0.01	0.10	0.36	98.95	0.14	0.00	0.43
13	0.00	0.00	0.06	0.11	0.00	0.17	98.79	0.08	0.37	0.43
14	0.00	0.00	0.00	0.01	0.00	0.29	99.19	0.00	0.00	0.51

15	0.00	0.00	0.04	0.08	0.13	0.31	98.85	0.12	0.00	0.47
16	0.92	0.00	0.06	0.00	0.00	0.35	98.35	0.01	0.00	0.32
17	14.28	0.00	0.11	0.31	0.00	0.36	84.32	0.00	0.00	0.61
18	1.16	0.03	0.00	0.00	0.09	0.21	97.61	0.07	0.03	0.80
19	0.00	0.00	0.00	0.00	0.00	0.32	99.34	0.06	0.01	0.27
20	0.00	0.00	0.01	0.00	0.06	0.38	99.10	0.00	0.00	0.47
0	96.29	0.02	0.06	2.17	0.08	0.14	0.93	0.15	0.04	0.13
1	96.72	0.00	0.00	2.21	0.00	0.19	0.66	0.00	0.04	0.17
2	96.62	0.02	0.00	2.37	0.20	0.00	0.40	0.00	0.21	0.18
3	96.95	0.01	0.14	2.21	0.10	0.00	0.37	0.01	0.23	0.00
4	97.10	0.00	0.00	2.03	0.00	0.00	0.71	0.16	0.00	0.00
5	43.71	0.00	0.11	12.25	0.17	0.18	43.27	0.00	0.00	0.30
6	1.66	0.00	0.18	0.79	0.00	0.20	96.57	0.13	0.04	0.42
7	36.66	0.00	0.00	12.94	0.03	0.17	49.75	0.00	0.02	0.44
8	1.12	0.00	0.02	0.38	0.03	0.24	97.83	0.09	0.00	0.29
9	0.00	0.00	0.00	0.11	0.03	0.27	98.80	0.01	0.00	0.78
10	0.00	0.00	0.11	0.00	0.00	0.42	98.85	0.00	0.02	0.61
11	0.00	0.00	0.08	0.00	0.00	0.30	98.98	0.00	0.00	0.64
12	0.00	0.00	0.00	0.14	0.02	0.45	98.62	0.04	0.05	0.68
13	0.00	0.00	0.05	0.06	0.00	0.37	99.15	0.00	0.00	0.38
14	0.00	0.00	0.00	0.15	0.00	0.27	98.96	0.00	0.10	0.52
15	0.00	0.00	0.00	0.07	0.05	1.17	97.98	0.06	0.08	0.59
16	0.00	0.00	0.02	0.00	0.00	2.24	96.91	0.01	0.21	0.62
17	0.00	0.00	0.14	0.00	0.61	2.74	95.99	0.03	0.00	0.49
18	0.00	0.00	0.00	0.00	0.00	0.40	99.31	0.00	0.00	0.29
19	0.00	0.00	0.01	0.07	0.00	0.48	98.57	0.08	0.18	0.62
20	0.00	0.00	0.10	0.08	0.09	0.56	98.65	0.07	0.07	0.38

B.33 HT-9/Mo/V/Nd After 56 Days at 550°C

The HT-9/Mo/V/Nd assembly annealed for 56 days at 550°C bonded on the V/Nd interface but not the HT-9/Mo or Mo/V interfaces. Since the V/Nd interface at this time and temperature was already well characterized, no WDS linescans were completed on it in this assembly.

B.34 HT-9/Mo/Nd After 56 Days at 550°C

The HT-9/Mo/Nd assembly annealed for 56 days at 550°C bonded on the Mo/Nd interface but not the HT-9/Mo interface. Compositional data (in at%) from WDS linescans across the Mo/Nd interface is given below.

Position	W	Mo	Nd	Ni	Fe	Mn	Cr	V
0	0.00	0.05	98.97	0.09	0.53	0.36	0.00	0.00
1	0.01	0.16	98.12	0.00	1.25	0.46	0.01	0.00
2	0.02	0.14	98.25	0.12	0.90	0.57	0.00	0.00
3	0.00	0.16	97.96	0.00	1.47	0.28	0.13	0.00
4	0.03	0.46	89.81	0.00	7.85	0.57	1.17	0.11
5	0.00	0.19	98.34	0.18	0.59	0.57	0.06	0.07
6	0.00	7.31	91.62	0.05	0.55	0.49	0.00	0.00

7	0.00	94.15	5.28	0.01	0.33	0.12	0.05	0.07
8	0.02	65.62	30.11	0.00	3.63	0.00	0.55	0.08
9	0.02	97.77	1.89	0.00	0.30	0.00	0.01	0.01
10	0.00	99.59	0.10	0.15	0.07	0.00	0.08	0.02
11	0.02	99.73	0.18	0.02	0.03	0.00	0.00	0.02
12	0.03	99.66	0.16	0.00	0.09	0.04	0.00	0.02
13	0.00	99.29	0.13	0.00	0.32	0.04	0.18	0.05
14	0.01	99.51	0.12	0.18	0.07	0.00	0.09	0.02
15	0.01	99.61	0.11	0.00	0.11	0.10	0.05	0.00
0	0.01	8.69	90.27	0.00	0.44	0.58	0.01	0.00
1	0.06	0.39	98.17	0.20	0.65	0.52	0.00	0.00
2	0.00	0.81	97.24	0.00	1.10	0.59	0.13	0.14
3	0.02	0.29	96.58	0.17	2.00	0.35	0.34	0.26
4	0.00	0.28	97.45	0.11	1.53	0.51	0.06	0.05
5	0.00	0.22	96.46	0.16	1.11	0.59	0.00	1.45
6	0.11	0.47	97.14	0.00	1.79	0.40	0.02	0.07
7	0.02	0.73	96.93	0.00	1.51	0.54	0.13	0.14
8	0.00	61.60	36.50	0.00	1.36	0.20	0.34	0.00
9	0.00	99.06	0.66	0.07	0.18	0.01	0.02	0.00
10	0.01	99.54	0.19	0.10	0.14	0.00	0.00	0.02
11	0.01	99.61	0.16	0.04	0.11	0.05	0.03	0.00
12	0.00	99.66	0.21	0.01	0.00	0.03	0.07	0.02
13	0.03	99.64	0.21	0.00	0.00	0.03	0.09	0.00
14	0.00	99.79	0.09	0.00	0.09	0.01	0.02	0.00
15	0.03	99.91	0.00	0.00	0.00	0.02	0.00	0.05
0	0.04	0.04	98.59	0.00	0.73	0.50	0.00	0.10
1	0.02	0.05	98.60	0.00	0.80	0.44	0.09	0.00
2	0.00	0.11	99.07	0.00	0.43	0.40	0.00	0.00
3	0.05	0.16	98.52	0.10	0.38	0.49	0.14	0.16
4	0.01	10.27	88.25	0.15	0.80	0.39	0.07	0.07
5	0.00	10.94	87.12	0.00	1.11	0.66	0.04	0.12
6	0.00	98.24	1.47	0.05	0.13	0.05	0.06	0.00
7	0.01	99.29	0.59	0.11	0.00	0.00	0.00	0.00
8	0.02	99.51	0.46	0.01	0.00	0.00	0.00	0.00
9	0.01	98.43	1.12	0.00	0.20	0.06	0.14	0.05
10	0.01	99.58	0.25	0.06	0.06	0.00	0.01	0.04
11	0.01	99.33	0.41	0.03	0.17	0.06	0.00	0.00
12	0.00	99.73	0.02	0.00	0.24	0.00	0.00	0.02
13	0.01	98.23	0.09	0.12	1.36	0.00	0.20	0.00
14	0.00	99.61	0.17	0.17	0.01	0.04	0.00	0.00
15	0.04	99.77	0.07	0.00	0.04	0.02	0.00	0.07

B.35 HT-9/W/V/Nd After 56 Days at 550°C

The HT-9/W/V/Nd assembly annealed for 56 days at 550°C bonded on the HT-9/W and V/Nd interfaces but not the W/V interface. Compositional data (in at%) from WDS linescans across the HT-9/W interface is given below.

Position	W	Mo	Nd	Ni	Fe	Mn	Cr	V
0	0.17	0.59	0.13	0.45	86.38	0.68	11.08	0.52
1	0.23	0.79	0.13	0.55	82.77	0.61	14.36	0.57
2	0.22	0.72	0.07	0.45	84.63	0.63	12.76	0.52

3	7.39	0.58	0.13	0.41	79.17	0.50	11.41	0.40
4	5.40	0.67	0.18	0.41	79.79	0.59	12.54	0.43
5	88.82	0.00	0.31	0.00	8.92	0.20	1.61	0.15
6	92.65	0.00	0.22	0.00	6.08	0.16	0.89	0.00
7	95.26	0.00	0.14	0.06	3.59	0.06	0.70	0.20
8	96.13	0.00	0.00	0.00	3.27	0.00	0.40	0.20
9	97.87	0.00	0.18	0.00	1.89	0.00	0.05	0.00
10	97.33	0.00	0.36	0.31	1.57	0.00	0.39	0.04
11	95.46	0.00	0.29	0.04	3.23	0.00	0.66	0.32
12	96.48	0.00	1.39	0.00	1.33	0.17	0.36	0.28
13	96.78	0.00	1.54	0.11	1.02	0.15	0.28	0.12
14	97.07	0.00	0.95	0.00	1.33	0.31	0.27	0.09
15	98.31	0.00	0.23	0.01	1.02	0.19	0.00	0.23
0	0.17	0.66	0.18	0.49	85.62	0.59	11.94	0.35
1	0.18	0.52	0.15	0.55	86.77	0.59	11.02	0.22
2	0.19	0.58	0.14	0.41	86.33	0.57	11.43	0.36
3	0.25	0.59	0.15	0.49	86.72	0.54	10.75	0.52
4	0.21	0.54	0.11	0.45	86.74	0.62	10.83	0.50
5	87.50	0.00	0.13	0.16	10.25	0.31	1.65	0.00
6	94.80	0.00	0.26	0.02	3.83	0.10	0.95	0.05
7	94.84	0.00	0.35	0.10	4.03	0.02	0.40	0.27
8	95.43	0.00	1.04	0.00	2.67	0.20	0.42	0.25
9	88.14	0.00	3.60	0.00	5.98	0.24	1.15	0.88
10	83.74	0.05	2.68	0.07	11.13	0.20	1.75	0.39
11	86.74	0.01	8.21	0.06	3.93	0.12	0.60	0.34
12	92.21	0.28	0.87	0.39	5.20	0.00	0.78	0.28
13	91.30	0.00	0.60	0.12	6.87	0.01	0.79	0.31
14	96.90	0.00	1.52	0.01	1.58	0.00	0.00	0.00
15	96.35	0.00	0.76	0.00	2.29	0.22	0.28	0.10

B.36 HT-9/W/Nd After 56 Days at 550°C

The HT-9/W/Nd assembly annealed for 56 days at 550°C bonded on both the W/Nd interface and the HT-9/W interface. Compositional data (in at%) from WDS linescans across these interfaces is given below.

Position	W	Mo	Nd	Ni	Fe	Mn	Cr	V
0	0.19	0.06	98.54	0.08	0.43	0.54	0.16	0.52
1	0.00	0.00	98.80	0.05	0.84	0.32	0.00	0.57
2	0.16	0.01	97.09	0.19	1.69	0.39	0.47	0.52
3	2.57	0.02	94.33	0.38	1.85	0.86	0.00	0.40
4	2.15	0.01	95.94	0.00	1.23	0.55	0.12	0.43
5	1.11	0.13	96.61	0.07	1.34	0.60	0.15	0.15
6	4.80	0.13	93.13	0.15	1.39	0.41	0.00	0.00
7	78.54	0.00	20.95	0.07	0.39	0.00	0.05	0.20
8	98.79	0.00	0.86	0.00	0.00	0.06	0.29	0.20
9	99.13	0.00	0.45	0.42	0.00	0.00	0.00	0.00
10	98.87	0.00	0.92	0.00	0.02	0.00	0.19	0.04
11	99.23	0.00	0.32	0.00	0.16	0.15	0.14	0.32
12	99.54	0.00	0.40	0.00	0.02	0.00	0.04	0.28
13	99.19	0.02	0.47	0.00	0.11	0.00	0.22	0.12
14	99.93	0.00	0.00	0.00	0.00	0.07	0.00	0.09
15	99.55	0.01	0.12	0.07	0.10	0.00	0.14	0.23

0	98.33	0.01	0.00	0.28	1.15	0.00	0.23	0.35
1	97.58	0.00	0.00	0.42	2.00	0.00	0.00	0.22
2	96.76	0.00	0.09	0.36	2.40	0.00	0.39	0.36
3	95.85	0.00	0.12	0.00	3.44	0.00	0.59	0.52
4	93.74	0.00	0.00	0.00	5.39	0.00	0.87	0.50
5	92.26	0.00	0.00	0.12	6.33	0.00	1.29	0.00
6	0.74	0.67	0.12	0.70	84.66	0.56	12.56	0.05
7	1.42	0.61	0.11	0.53	84.29	0.55	12.50	0.27
8	0.36	0.73	0.41	0.42	84.79	0.73	12.56	0.25
9	0.14	0.68	0.06	0.39	85.67	0.55	12.50	0.88
10	0.22	0.72	0.07	0.50	83.79	0.62	14.08	0.39
11	0.13	0.86	0.03	0.37	84.18	0.72	13.72	0.34
12	0.24	0.95	0.09	0.48	80.76	0.67	16.82	0.28
13	0.22	0.73	0.12	0.46	85.06	0.62	12.80	0.31
14	0.42	0.70	0.43	0.47	84.89	0.64	12.46	0.00
15	0.55	0.46	0.36	0.61	86.43	0.60	10.99	0.10

B.37 HT-9/Nd After 28 Days at 625°C

After annealing for 28 days at 625°C a significant interaction zone developed between the HT-9 and Nd; however, due to the brittle nature of the interaction zones the diffusion couple broke apart upon removal from the furnace. The first $\text{Nd}_2(\text{Fe}+\text{Cr})_{17}$ phase remained mostly intact, with a zone width of ~40 μm . Small portions of additional $\text{Nd}_5(\text{Fe}+\text{Cr})_{17}$ and Fe_2Nd phases were found past the $\text{Nd}_2(\text{Fe}+\text{Cr})_{17}$ phase on the broken edge of the interface. Compositional data from WDS linescans across the interface is given below.

Position	Zr	Mo	W	Cr	Fe	Nd	V	Ni	Mn
0	0.02	0.76	0.18	14.70	73.01	10.44	0.32	0.06	0.52
1	0.00	0.80	0.17	14.54	72.76	10.81	0.35	0.00	0.57
2	0.00	0.77	0.16	13.85	67.70	16.57	0.30	0.04	0.62
3	0.01	0.74	0.17	14.02	68.80	15.36	0.36	0.00	0.55
4	0.00	0.81	0.17	14.59	73.03	10.41	0.39	0.04	0.57
5	0.00	0.79	0.13	14.46	73.20	10.47	0.40	0.00	0.57
6	0.00	0.80	0.14	13.55	72.37	12.13	0.38	0.07	0.56
7	0.00	0.73	0.18	11.62	72.51	14.12	0.36	0.00	0.48
8	0.01	0.42	0.07	9.76	73.55	15.46	0.23	0.01	0.50
9	0.02	0.18	0.02	6.21	66.66	26.33	0.07	0.00	0.51
10	0.00	0.03	0.08	3.70	50.26	45.31	0.08	0.04	0.50
11	0.00	0.02	0.03	2.05	26.22	71.04	0.09	0.00	0.55
12	0.00	0.00	0.00	2.01	52.19	45.31	0.00	0.00	0.48
13	0.00	0.03	0.00	2.22	61.87	35.31	0.00	0.06	0.51
14	0.01	0.01	0.00	1.97	26.94	70.34	0.02	0.18	0.53
15	0.00	0.04	0.01	1.86	46.29	51.22	0.06	0.04	0.49
0	0.00	0.82	0.18	14.73	71.95	11.39	0.36	0.00	0.57
1	0.00	0.83	0.19	13.94	68.08	15.97	0.42	0.02	0.55
2	0.00	0.69	0.22	13.47	63.63	20.97	0.38	0.00	0.64
3	0.00	0.84	0.20	14.17	71.20	12.66	0.37	0.04	0.53

4	0.02	0.84	0.20	13.65	72.73	11.69	0.34	0.00	0.54
5	0.00	0.71	0.18	12.09	62.35	23.63	0.36	0.13	0.56
6	0.00	0.42	0.13	7.21	32.97	58.48	0.29	0.04	0.46
7	0.00	0.37	0.16	7.01	33.03	58.61	0.24	0.00	0.58
8	0.01	0.45	0.12	8.96	45.01	44.48	0.32	0.11	0.55
9	0.00	0.39	0.12	9.34	53.37	36.12	0.15	0.03	0.50
10	0.02	0.18	0.05	6.61	56.97	35.53	0.11	0.01	0.53
11	0.00	0.13	0.00	3.73	50.57	44.88	0.04	0.03	0.64
12	0.00	0.00	0.00	2.26	62.22	34.95	0.00	0.03	0.53
13	0.00	0.02	0.00	2.25	63.46	33.74	0.06	0.00	0.46
14	0.00	0.00	0.02	2.31	63.72	33.45	0.03	0.00	0.48
15	0.00	0.00	0.01	2.22	63.15	33.95	0.04	0.07	0.55
1	0.06	0.03	0.03	5.36	58.66	35.27	0.09	0.00	0.50
2	0.00	0.05	0.01	2.21	21.34	75.93	0.00	0.00	0.46
3	0.00	0.02	0.01	1.28	8.04	89.98	0.02	0.08	0.59
4	0.00	0.58	0.18	11.46	55.70	31.34	0.21	0.06	0.47
5	0.00	0.88	0.28	14.34	72.74	10.78	0.37	0.00	0.62
6	0.00	0.89	0.19	14.46	73.35	10.04	0.38	0.02	0.68
7	0.00	0.80	0.19	14.19	71.08	12.73	0.38	0.02	0.62
8	0.00	0.83	0.20	14.35	73.73	9.90	0.36	0.08	0.56
9	0.00	0.84	0.17	14.36	73.14	10.47	0.38	0.00	0.64
10	0.00	0.74	0.19	13.56	66.55	17.88	0.36	0.07	0.66
11	0.00	0.82	0.18	14.38	73.75	9.88	0.37	0.00	0.61
12	0.00	0.75	0.15	14.48	72.69	10.94	0.36	0.04	0.58
13	0.00	0.73	0.19	13.72	69.86	14.52	0.34	0.00	0.63
14	0.00	0.74	0.17	13.55	66.01	18.54	0.30	0.10	0.58
15	0.00	0.77	0.20	14.68	73.88	9.48	0.38	0.01	0.61
16	0.00	0.76	0.18	14.86	74.00	9.22	0.33	0.03	0.62
17	0.00	0.79	0.20	14.44	73.88	9.76	0.34	0.00	0.60
18	0.00	0.79	0.20	14.83	73.25	9.94	0.35	0.07	0.57
19	0.00	0.82	0.18	14.66	71.93	11.44	0.35	0.01	0.61
20	0.00	0.84	0.19	15.02	73.25	9.67	0.37	0.00	0.65
21	0.00	0.80	0.22	14.74	69.69	13.54	0.38	0.00	0.64
22	0.00	0.84	0.21	14.88	71.22	11.87	0.37	0.03	0.59
23	0.02	0.77	0.17	13.94	66.23	17.91	0.35	0.01	0.60
24	0.02	0.84	0.20	14.79	72.06	11.09	0.38	0.00	0.62
25	0.01	0.84	0.16	15.39	72.55	10.00	0.40	0.06	0.59
26	0.00	0.80	0.23	15.23	70.22	12.52	0.40	0.01	0.59
27	0.01	0.77	0.18	15.14	70.19	12.66	0.38	0.00	0.68
28	0.00	0.85	0.21	15.06	71.11	11.78	0.38	0.05	0.56
29	0.01	0.84	0.21	15.33	71.86	10.77	0.38	0.00	0.60
30	0.00	0.93	0.19	15.82	65.38	10.38	0.40	0.05	0.58
31	0.01	0.86	0.23	15.52	72.55	9.93	0.36	0.00	0.55
32	0.00	0.86	0.19	15.50	70.78	11.72	0.38	0.00	0.59
33	0.02	0.91	0.23	15.76	72.17	9.84	0.39	0.06	0.61
34	0.01	0.93	0.22	15.58	70.91	11.31	0.39	0.02	0.64
35	0.00	0.85	0.20	16.05	71.51	10.32	0.39	0.06	0.61
36	0.00	0.84	0.21	16.05	70.90	10.98	0.39	0.00	0.63
37	0.00	0.84	0.17	16.13	71.35	10.54	0.37	0.00	0.60
38	0.00	0.77	0.18	16.12	71.86	10.13	0.34	0.00	0.60
39	0.02	0.79	0.19	16.13	70.81	11.05	0.40	0.00	0.62
40	0.00	0.71	0.15	15.20	75.48	7.45	0.40	0.03	0.60
41	0.01	0.54	0.14	13.22	84.10	0.71	0.36	0.38	0.53
42	0.00	0.62	0.14	13.02	84.54	0.25	0.31	0.47	0.65
43	0.01	0.69	0.17	13.09	84.33	0.26	0.33	0.53	0.61
44	0.00	0.62	0.14	13.07	84.49	0.22	0.32	0.48	0.68

45	0.00	0.63	0.15	13.16	84.49	0.26	0.31	0.40	0.60
46	0.01	0.60	0.13	13.32	83.94	0.60	0.32	0.41	0.69
47	0.00	0.61	0.12	13.20	84.32	0.34	0.33	0.40	0.69
48	0.00	0.60	0.16	13.19	84.41	0.14	0.31	0.48	0.70
49	0.01	0.61	0.13	13.46	84.17	0.33	0.29	0.36	0.65
50	0.00	0.59	0.11	13.37	84.24	0.34	0.33	0.46	0.57
0	0.02	0.69	0.14	14.47	73.60	10.05	0.41	0.04	0.59
1	0.00	0.74	0.19	14.34	72.32	11.44	0.35	0.00	0.62
2	0.01	0.76	0.15	14.31	72.92	10.86	0.36	0.00	0.65
3	0.01	0.74	0.20	14.94	73.96	9.21	0.35	0.00	0.58
4	0.02	0.74	0.15	14.59	74.05	9.45	0.36	0.02	0.61
5	0.00	0.79	0.19	14.65	73.99	9.34	0.37	0.04	0.63
6	0.01	0.77	0.17	14.89	73.71	9.43	0.35	0.08	0.60
7	0.01	0.78	0.17	14.96	73.56	9.49	0.36	0.05	0.63
8	0.00	0.79	0.24	14.78	73.50	9.61	0.37	0.11	0.60
9	0.01	0.80	0.23	14.64	72.36	10.98	0.35	0.00	0.65
10	0.00	0.83	0.19	14.99	73.17	9.85	0.33	0.01	0.63
11	0.00	0.84	0.22	15.01	72.84	10.14	0.34	0.00	0.61
12	0.00	0.75	0.21	13.99	67.17	16.91	0.33	0.04	0.61
13	0.01	0.76	0.18	14.67	70.64	12.82	0.35	0.00	0.58
14	0.00	0.77	0.21	14.85	71.31	11.81	0.36	0.04	0.66
15	0.00	0.79	0.22	14.71	73.17	10.15	0.36	0.00	0.59
16	0.00	0.79	0.20	15.01	72.83	10.18	0.34	0.02	0.62
17	0.00	0.81	0.20	14.92	72.33	10.76	0.39	0.02	0.57
18	0.01	0.80	0.19	14.68	73.12	10.24	0.37	0.01	0.56
19	0.00	0.82	0.19	14.83	72.68	10.47	0.36	0.00	0.65
20	0.00	0.89	0.22	15.22	71.82	10.86	0.33	0.00	0.66
21	0.00	0.86	0.21	15.20	71.69	11.03	0.38	0.02	0.62
22	0.00	0.99	0.26	14.15	65.47	18.15	0.33	0.02	0.63
23	0.00	0.82	0.19	14.91	71.10	11.96	0.33	0.03	0.66
24	0.00	0.87	0.21	14.88	70.72	12.37	0.34	0.00	0.61
25	0.00	1.01	0.28	14.33	65.07	18.34	0.35	0.06	0.56
26	0.01	0.79	0.21	15.46	71.17	11.41	0.36	0.00	0.60
27	0.00	0.65	0.17	15.85	72.35	9.91	0.40	0.00	0.67
28	0.01	0.81	0.21	15.52	71.58	10.86	0.34	0.03	0.63
29	0.01	0.85	0.21	15.27	71.57	11.10	0.37	0.05	0.59
30	0.00	0.72	0.15	15.64	72.08	10.44	0.35	0.01	0.61
31	0.00	0.69	0.19	15.73	72.29	10.08	0.36	0.05	0.62
32	0.01	0.77	0.20	15.29	73.47	9.24	0.36	0.01	0.65
33	0.00	0.45	0.12	13.79	82.35	2.40	0.35	0.07	0.48
34	0.00	0.57	0.22	13.11	84.90	0.34	0.32	0.07	0.48
35	0.00	0.42	0.12	12.91	85.09	0.35	0.32	0.28	0.52
36	0.00	0.52	0.14	12.86	85.05	0.19	0.31	0.40	0.53
37	0.00	1.55	0.41	13.19	83.42	0.17	0.29	0.35	0.62
38	0.00	0.63	0.15	13.23	84.61	0.12	0.32	0.39	0.54
39	0.00	0.53	0.11	13.04	84.83	0.13	0.31	0.47	0.59
40	0.00	0.52	0.11	13.20	84.68	0.14	0.33	0.39	0.64
41	0.00	0.63	0.14	13.04	84.82	0.06	0.30	0.38	0.64
42	0.00	0.83	0.17	13.12	84.28	0.19	0.32	0.45	0.65
43	0.01	0.60	0.12	13.17	84.58	0.10	0.33	0.46	0.63
44	0.00	0.77	0.16	12.97	84.59	0.12	0.32	0.50	0.58
45	0.01	0.63	0.13	13.03	84.75	0.04	0.31	0.46	0.63
46	0.00	0.84	0.20	13.17	83.85	0.46	0.34	0.52	0.63
47	0.00	0.57	0.13	13.01	84.80	0.05	0.29	0.49	0.67
48	0.01	0.59	0.11	13.14	84.59	0.06	0.35	0.47	0.68
49	0.00	0.64	0.12	12.98	84.75	0.04	0.31	0.54	0.62

50	0.01	1.09	0.26	13.12	83.98	0.04	0.32	0.45	0.73
----	------	------	------	-------	-------	------	------	------	------

B.38 HT-9/V/Nd After 28 Days at 625°C

The HT-9/V/Nd assembly annealed for 28 days at 625°C bonded on the V/Nd interface but not the HT-9/V interface. Since the V/Nd interface at this time and temperature was already well characterized, no WDS linescans were completed on it in this assembly.

B.39 HT-9/Zr/V/Nd After 28 Days at 625°C

The HT-9/Zr/V/Nd assembly annealed for 28 days at 625°C bonded on the V/Nd interface but not the HT-9/Zr or Zr/V interfaces. Compositional data (in at%) from WDS linescans across the V/Nd interface is given below.

Position	Zr	Mo	W	Cr	Fe	Nd	V	Ni	Mn
0	0.00	0.01	0.01	2.14	0.06	0.53	97.25	0.01	0.00
1	0.02	0.00	0.00	2.02	0.03	0.52	97.37	0.02	0.00
2	0.00	0.00	0.00	2.12	0.11	0.78	96.98	0.00	0.00
3	0.01	0.00	0.00	2.08	0.07	0.49	97.32	0.00	0.03
4	0.02	0.02	0.00	2.15	0.14	0.67	96.97	0.03	0.00
5	0.00	0.00	0.02	0.08	0.37	95.85	3.00	0.08	0.59
6	0.00	0.05	0.05	0.04	0.42	96.33	2.49	0.19	0.44
7	0.00	0.03	0.00	0.62	2.83	66.61	29.58	0.04	0.30
8	0.00	0.00	0.03	0.10	0.44	95.58	3.20	0.12	0.53
9	0.04	0.01	0.00	0.03	0.47	97.03	1.93	0.00	0.48
10	0.00	0.04	0.00	0.00	0.48	97.61	1.50	0.01	0.35
0	0.01	0.00	0.02	2.07	0.12	1.07	96.70	0.00	0.02
1	0.00	0.02	0.00	2.17	1.41	1.95	94.45	0.00	0.01
2	0.02	0.02	0.00	1.75	1.32	15.93	80.85	0.02	0.09
3	0.00	0.01	0.02	2.09	0.55	1.02	96.31	0.00	0.01
4	0.00	0.03	0.00	1.90	1.31	8.82	87.86	0.03	0.07
5	0.00	0.02	0.01	1.95	1.41	7.40	89.14	0.01	0.06
6	0.00	0.00	0.00	0.00	0.53	96.70	2.46	0.00	0.32
7	0.00	0.00	0.00	0.06	0.45	96.92	2.09	0.00	0.48
8	0.00	0.00	0.00	0.12	0.50	94.68	3.95	0.12	0.62
9	0.00	0.00	0.03	0.13	0.59	95.39	3.10	0.22	0.54
10	0.00	0.05	0.00	0.07	0.50	95.86	3.10	0.01	0.43

B.40 HT-9/Zr/Nd After 28 Days at 625°C

The HT-9/Zr/Nd assembly annealed for 28 days at 625°C bonded on the Zr/Nd interface but not the HT-9/Zr interface. Compositional data (in at%) from WDS linescans across the Zr/Nd interface is given below.

Position	Zr	Mo	W	Cr	Fe	Nd	V	Ni	Mn
0	98.85	0.00	0.00	0.00	0.04	1.08	0.00	0.00	0.02

1	98.70	0.00	0.00	0.01	0.11	1.17	0.00	0.00	0.03
2	97.97	0.00	0.00	0.06	0.37	1.60	0.00	0.00	0.00
3	89.79	0.00	0.00	0.07	1.47	8.57	0.03	0.02	0.06
4	76.90	0.01	0.00	0.08	1.03	21.78	0.00	0.06	0.15
5	0.49	0.00	0.00	0.01	0.39	98.73	0.03	0.03	0.34
6	0.07	0.00	0.03	0.00	0.49	98.93	0.05	0.00	0.43
7	0.00	0.00	0.00	0.00	0.52	98.97	0.05	0.00	0.45
8	0.00	0.00	0.04	0.00	0.67	98.73	0.01	0.01	0.55
9	0.00	0.00	0.01	0.00	0.68	98.73	0.01	0.00	0.57
10	0.00	0.05	0.04	0.00	0.60	98.85	0.00	0.00	0.47

B.41 HT-9/Ti/V/Nd After 28 Days at 625°C

The HT-9/Ti/V/Nd assembly annealed for 28 days at 625°C bonded on the V/Nd interface but not the HT-9/Ti or Ti/V interfaces. Since the V/Nd interface at this time and temperature was already well characterized, no WDS linescans were completed on it in this assembly.

B.42 HT-9/Ti/Nd After 28 Days at 625°C

The HT-9/Ti/Nd assembly annealed for 28 days at 625°C bonded on the Ti/Nd interface but not the HT-9/Ti interface. Compositional data (in at%) from WDS linescans across the Ti/Nd interface is given below.

Position	Ta	Ti	Mo	W	Cr	Fe	Nd	V	Ni	Mn
0	0.00	1.43	0.03	0.14	0.06	0.26	97.34	0.01	0.06	0.68
1	0.00	1.88	0.00	0.10	0.02	0.32	97.08	0.16	0.00	0.44
2	0.00	2.20	0.00	0.00	0.00	0.26	97.07	0.00	0.00	0.46
3	0.00	3.03	0.00	0.00	0.00	0.35	96.23	0.00	0.00	0.40
4	0.00	34.68	0.05	0.06	0.00	0.32	64.40	0.25	0.00	0.25
5	0.00	74.44	0.00	0.00	0.00	0.31	24.68	0.29	0.12	0.16
6	0.00	78.57	0.00	0.00	0.04	0.26	20.58	0.34	0.04	0.17
7	0.00	97.78	0.00	0.00	0.00	0.29	1.55	0.37	0.00	0.02
8	0.00	98.85	0.00	0.00	0.01	0.37	0.39	0.32	0.05	0.01
9	0.00	99.41	0.00	0.01	0.03	0.11	0.15	0.26	0.00	0.03
10	0.00	99.48	0.00	0.02	0.01	0.05	0.18	0.26	0.00	0.00
11	0.00	99.64	0.00	0.00	0.00	0.02	0.09	0.24	0.00	0.00
12	0.00	99.44	0.00	0.01	0.04	0.03	0.16	0.31	0.01	0.02
13	0.00	99.45	0.00	0.00	0.00	0.10	0.14	0.30	0.00	0.00
14	0.00	99.60	0.00	0.00	0.02	0.05	0.06	0.26	0.00	0.02
15	0.00	99.53	0.00	0.02	0.03	0.07	0.10	0.23	0.03	0.01

B.43 HT-9/Ta/V/Nd After 28 Days at 625°C

The HT-9/Ta/V/Nd assembly annealed for 28 days at 625°C bonded on the V/Nd interface but not the HT-9/Ta and Ta/V interfaces. Compositional data (in at%) from WDS linescans across the V/Nd interface is given below.

Position	Ta	Ti	Mo	W	Cr	Fe	Nd	V	Ni	Mn
0	0.00	0.00	0.00	0.00	1.83	0.03	0.27	97.83	0.02	0.02
1	0.00	0.00	0.01	0.00	1.94	0.01	0.21	97.81	0.00	0.02
2	0.00	0.00	0.00	0.01	1.79	0.03	0.31	97.85	0.00	0.00
3	0.00	0.00	0.00	0.00	1.90	0.01	0.31	97.75	0.03	0.00
4	0.00	0.00	0.00	0.00	1.74	0.01	0.35	97.86	0.04	0.00
5	0.00	0.00	0.01	0.00	1.74	0.01	0.70	97.54	0.00	0.00
6	0.00	0.00	0.00	0.00	1.90	0.43	1.14	96.53	0.00	0.00
7	0.00	0.00	0.00	0.02	1.80	0.33	1.92	95.89	0.00	0.05
8	0.00	0.00	0.10	0.00	0.47	0.33	86.83	11.79	0.00	0.48
9	0.00	0.00	0.00	0.02	0.14	0.68	92.60	6.08	0.18	0.30
10	0.00	0.00	0.05	0.00	0.28	0.44	93.82	5.07	0.00	0.34
11	0.00	0.00	0.00	0.00	0.13	0.62	92.39	6.48	0.00	0.39
12	0.00	0.00	0.00	0.14	0.20	0.48	94.45	4.26	0.09	0.37
13	0.00	0.00	0.00	0.00	0.00	0.38	97.17	2.00	0.00	0.45
14	0.00	0.00	0.03	0.05	0.10	0.45	97.41	1.56	0.00	0.40
15	0.00	0.01	0.08	0.14	0.00	0.42	97.51	1.23	0.21	0.41

B.44 HT-9/Ta/Nd After 28 Days at 625°C

The HT-9/Ta/Nd assembly annealed for 28 days at 625°C bonded on the Ta/Nd interface but not the HT-9/Ta interface. Compositional data (in at%) from WDS linescans across the Ta/Nd interface is given below.

Position	Ta	Ti	Mo	W	Cr	Fe	Nd	V	Ni	Mn
0	0.00	0.00	0.00	0.07	0.13	0.40	98.92	0.00	0.04	0.43
1	0.00	0.00	0.00	0.00	0.18	0.26	98.86	0.00	0.21	0.49
2	0.00	0.00	0.00	0.07	0.00	0.22	99.23	0.00	0.00	0.48
3	0.00	0.00	0.00	0.00	0.17	0.32	98.97	0.00	0.17	0.38
4	0.00	0.00	0.02	0.00	0.11	0.26	99.10	0.00	0.24	0.27
5	0.00	0.00	0.00	0.08	0.13	0.37	99.18	0.00	0.00	0.24
6	0.00	0.00	0.08	0.00	0.00	0.34	99.25	0.00	0.00	0.33
7	0.00	0.00	0.00	0.05	0.00	0.39	99.09	0.00	0.00	0.47
8	0.29	0.00	0.00	0.09	0.08	0.39	98.50	0.10	0.00	0.57
9	18.96	0.00	0.09	0.46	0.09	0.55	79.48	0.00	0.00	0.38
10	68.84	0.00	0.20	1.61	0.39	0.63	28.25	0.08	0.00	0.00
11	0.00	0.00	0.04	0.00	0.15	0.40	98.96	0.08	0.00	0.37
12	66.41	0.00	0.20	1.46	0.19	0.79	30.52	0.09	0.11	0.24
13	95.47	0.02	0.03	2.45	0.00	0.19	1.37	0.24	0.22	0.00
14	96.86	0.00	0.04	2.24	0.11	0.00	0.69	0.02	0.00	0.05
15	96.80	0.00	0.04	2.20	0.00	0.00	0.68	0.00	0.25	0.03
0	0.00	0.00	0.00	0.05	0.09	0.32	99.05	0.00	0.07	0.42
1	0.00	0.00	0.04	0.12	0.00	0.46	99.11	0.00	0.00	0.28
2	0.00	0.00	0.03	0.00	0.01	0.48	98.80	0.00	0.00	0.68
3	0.00	0.00	0.02	0.00	0.03	0.37	99.29	0.02	0.00	0.27
4	0.00	0.00	0.04	0.00	0.04	0.74	98.74	0.01	0.00	0.43
5	0.00	0.00	0.08	0.00	0.11	0.51	98.89	0.00	0.12	0.28
6	1.13	0.00	0.10	0.00	0.00	0.53	97.71	0.00	0.00	0.54
7	38.06	0.23	0.91	1.03	0.34	1.98	57.02	0.05	0.18	0.22
8	40.22	0.15	0.03	1.06	0.00	0.90	57.35	0.00	0.04	0.26
9	97.11	0.05	0.01	2.07	0.00	0.01	0.59	0.02	0.00	0.15
10	96.96	0.01	0.00	2.27	0.04	0.04	0.55	0.00	0.14	0.00
11	97.17	0.07	0.00	1.91	0.06	0.00	0.66	0.00	0.03	0.09

12	97.19	0.00	0.09	2.10	0.00	0.04	0.48	0.00	0.10	0.00
13	96.88	0.00	0.00	2.06	0.07	0.21	0.54	0.01	0.05	0.18
14	95.92	0.00	0.07	1.77	0.00	0.26	1.89	0.10	0.00	0.00
15	92.94	0.00	0.07	2.39	0.00	0.04	4.47	0.02	0.06	0.00

B.45 HT-9/Mo/V/Nd After 28 Days at 625°C

The HT-9/W/Nd assembly annealed for 28 days at 625°C bonded on the V/Nd interface but not the HT-9/Mo or Mo/V interfaces. Since the V/Nd interface at this time and temperature was already well characterized, no WDS linescans were completed on it in this assembly.

B.46 HT-9/Mo/Nd After 28 Days at 625°C

The HT-9/Mo/Nd assembly annealed for 28 days at 625°C bonded on the Mo/Nd interface but not the HT-9/Mo interface. Compositional data (in at%) from WDS linescans across the Mo/Nd interface is given below.

Position	V	W	Mo	Nd	Ni	Fe	Mn	Cr
0	0.00	0.05	1.02	97.32	0.00	1.06	0.46	0.09
1	0.12	0.00	0.03	98.81	0.00	0.38	0.54	0.12
2	0.00	0.01	0.10	98.77	0.00	0.55	0.46	0.11
3	0.07	0.00	0.13	99.19	0.00	0.20	0.42	0.00
4	0.00	0.00	0.25	99.03	0.00	0.22	0.44	0.05
5	0.09	0.06	0.91	97.91	0.04	0.30	0.69	0.00
6	0.02	0.00	17.16	81.74	0.10	0.49	0.49	0.00
7	0.03	0.03	81.19	18.39	0.00	0.22	0.00	0.14
8	0.04	0.01	97.29	2.48	0.00	0.10	0.08	0.00
9	0.00	0.01	98.65	1.15	0.01	0.09	0.10	0.00
10	0.01	0.03	97.87	1.95	0.00	0.11	0.04	0.00
11	0.00	0.01	99.68	0.29	0.00	0.02	0.00	0.00
12	0.00	0.01	99.31	0.63	0.00	0.04	0.00	0.02
13	0.00	0.04	99.34	0.27	0.00	0.23	0.06	0.05
14	0.03	0.03	99.69	0.18	0.05	0.01	0.00	0.00
15	0.01	0.01	99.38	0.38	0.04	0.05	0.11	0.03
0	0.06	0.00	0.19	98.51	0.00	0.58	0.66	0.00
1	0.00	0.04	0.05	98.87	0.00	0.55	0.46	0.04
2	0.00	0.00	0.17	98.71	0.07	0.34	0.72	0.00
3	0.14	0.00	0.11	98.80	0.09	0.40	0.46	0.00

4	0.07	0.00	0.12	99.04	0.00	0.35	0.41	0.00
5	0.00	0.02	0.88	97.80	0.00	0.76	0.55	0.00
6	0.00	0.00	24.94	73.55	0.04	0.98	0.51	0.00
7	0.02	0.05	83.11	16.55	0.00	0.27	0.00	0.00
8	0.03	0.03	98.81	1.02	0.00	0.08	0.03	0.00
9	0.01	0.00	98.77	0.78	0.02	0.23	0.08	0.11
10	0.05	0.00	99.49	0.24	0.00	0.14	0.00	0.09
11	0.02	0.00	99.82	0.10	0.00	0.06	0.00	0.01
12	0.09	0.00	99.64	0.20	0.00	0.07	0.00	0.00
13	0.05	0.01	99.72	0.19	0.00	0.03	0.00	0.00
14	0.05	0.04	99.75	0.07	0.03	0.05	0.01	0.00
15	0.00	0.00	99.49	0.18	0.15	0.06	0.06	0.06
0	0.00	0.00	0.04	99.02	0.00	0.34	0.58	0.02
1	0.08	0.00	0.05	98.79	0.07	0.51	0.49	0.00
2	0.00	0.00	0.04	98.87	0.00	0.41	0.63	0.04
3	0.05	0.00	0.08	98.93	0.07	0.46	0.42	0.00
4	0.11	0.11	0.32	57.34	0.19	36.26	0.56	5.11
5	0.06	0.00	0.24	93.11	0.35	5.26	0.29	0.69
6	0.07	0.00	5.72	90.26	0.06	2.87	0.49	0.54
7	0.00	0.00	53.76	45.65	0.00	0.39	0.17	0.04
8	0.04	0.06	98.89	0.94	0.00	0.07	0.00	0.00
9	0.44	0.03	98.45	1.00	0.00	0.05	0.04	0.00
10	4.05	0.01	91.34	3.61	0.08	0.70	0.00	0.22
11	0.00	0.00	98.83	0.74	0.07	0.31	0.00	0.05
12	0.00	0.00	99.54	0.25	0.00	0.14	0.08	0.00
13	0.00	0.00	99.68	0.09	0.07	0.09	0.00	0.08
14	0.01	0.02	99.73	0.24	0.00	0.00	0.00	0.00
15	0.03	0.00	99.56	0.30	0.00	0.04	0.08	0.00

B.47 HT-9/W/V/Nd After 28 Days at 625°C

The HT-9/W/V/Nd assembly annealed for 28 days at 625°C bonded on the V/Nd interface but not the HT-9/W or W/V interfaces. Since the V/Nd interface at this time and temperature was already well characterized, no WDS linescans were completed on it in this assembly.

B.48 HT-9/W/Nd After 28 Days at 625°C

The HT-9/W/Nd assembly annealed for 28 days at 625°C bonded on the W/Nd interface but not the HT-9/W interface. Compositional data (in at%) from WDS linescans across the W/Nd interface is given below.

Position	V	W	Mo	Nd	Ni	Fe	Mn	Cr
0	0.02	0.91	0.02	98.09	0.08	0.33	0.55	0.00
1	0.13	0.17	0.00	98.57	0.23	0.45	0.47	0.00
2	0.03	0.06	0.05	98.84	0.00	0.51	0.52	0.00
3	0.07	2.75	0.03	96.22	0.12	0.21	0.61	0.00
4	0.16	62.54	0.00	36.38	0.00	0.67	0.12	0.14
5	0.00	96.03	0.00	3.31	0.33	0.34	0.00	0.00
6	0.22	96.64	0.00	2.54	0.01	0.36	0.02	0.21
7	0.09	97.50	0.00	1.82	0.00	0.43	0.16	0.00
8	0.00	99.32	0.00	0.52	0.00	0.12	0.00	0.04
9	0.11	99.18	0.00	0.40	0.13	0.15	0.03	0.00
10	0.00	99.36	0.00	0.12	0.14	0.19	0.00	0.19
11	0.02	99.47	0.00	0.07	0.08	0.23	0.00	0.13
12	0.05	99.58	0.00	0.09	0.00	0.23	0.00	0.06
13	0.12	95.35	0.00	1.70	0.00	1.92	0.29	0.63
14	0.00	96.39	0.00	1.11	0.15	1.84	0.00	0.51
15	0.07	90.40	0.57	4.30	0.00	4.03	0.18	0.45
0	0.14	0.64	0.01	97.98	0.00	0.65	0.52	0.06
1	0.06	0.18	0.04	97.87	0.00	1.20	0.44	0.20
2	0.13	0.28	0.00	98.46	0.00	0.65	0.48	0.00
3	0.09	0.18	0.00	97.69	0.00	1.12	0.75	0.17
4	0.00	0.26	0.04	98.01	0.16	0.91	0.58	0.05
5	0.00	0.51	0.06	98.13	0.00	0.56	0.69	0.06
6	0.10	0.12	0.00	98.70	0.00	0.49	0.59	0.00
7	0.07	17.53	0.14	80.82	0.00	0.71	0.69	0.04
8	0.17	92.29	0.02	5.87	0.26	0.90	0.00	0.49
9	0.12	98.67	0.00	0.71	0.42	0.04	0.04	0.00
10	0.00	99.49	0.00	0.35	0.00	0.07	0.00	0.10
11	0.07	99.56	0.00	0.27	0.00	0.04	0.06	0.00
12	0.00	99.73	0.00	0.14	0.00	0.04	0.06	0.03
13	0.00	99.22	0.00	0.39	0.06	0.20	0.13	0.00
14	0.53	98.86	0.00	0.37	0.00	0.24	0.00	0.00

15	0.00	99.15	0.00	0.42	0.00	0.24	0.10	0.08
0	0.15	0.14	0.02	98.32	0.10	0.61	0.54	0.12
1	0.00	0.20	0.08	98.11	0.00	1.01	0.49	0.11
2	0.00	0.10	0.00	98.57	0.00	0.73	0.60	0.01
3	0.00	0.07	0.00	99.00	0.07	0.37	0.50	0.00
4	0.02	0.56	0.00	98.38	0.00	0.49	0.54	0.00
5	0.00	0.00	0.00	99.10	0.00	0.38	0.52	0.00
6	0.24	5.02	0.00	94.05	0.00	0.35	0.35	0.00
7	1.02	91.99	0.00	6.36	0.00	0.25	0.05	0.33
8	0.36	98.46	0.00	0.99	0.00	0.19	0.00	0.00
9	0.54	98.27	0.00	0.80	0.00	0.40	0.00	0.00
10	0.00	98.07	0.00	0.63	0.07	0.75	0.22	0.26
11	0.08	99.55	0.00	0.31	0.00	0.06	0.00	0.00
12	0.01	99.43	0.00	0.30	0.05	0.14	0.08	0.00
13	0.00	99.12	0.00	0.31	0.03	0.20	0.20	0.16

B.49 HT-9/Nd After 28 Days at 700°C

After annealing for 28 days at 700°C there was once again a significant interaction zone which broke upon removal from the furnace. Only the $\text{Nd}_2(\text{Fe}+\text{Cr})_{17}$ phase remained intact, with a zone width of ~530 μm . Compositional data from WDS linescans across the interface is given below.

Position	Zr	Mo	W	Cr	Fe	Nd	V	Ni	Mn
0	0.00	0.65	0.14	12.58	75.50	10.20	0.30	0.07	0.56
5	0.00	0.65	0.16	13.08	74.77	10.31	0.31	0.15	0.58
10	0.00	0.74	0.15	15.99	73.23	8.80	0.41	0.12	0.57
15	0.00	0.95	0.26	16.75	72.71	8.27	0.49	0.03	0.55
20	0.00	0.66	0.20	12.98	75.10	10.05	0.27	0.15	0.58
25	0.01	0.76	0.20	15.91	73.36	8.67	0.45	0.07	0.57
30	0.01	0.72	0.14	14.77	73.88	9.33	0.40	0.16	0.60
35	0.01	0.89	0.22	16.27	73.10	8.47	0.41	0.06	0.58
40	0.00	0.85	0.17	14.92	73.35	9.70	0.36	0.06	0.59
45	0.00	0.99	0.22	15.21	73.63	8.96	0.38	0.05	0.57
50	0.01	0.60	0.00	12.60	75.60	10.33	0.28	0.01	0.58
55	0.00	0.57	0.12	12.80	75.35	10.19	0.29	0.10	0.60
60	0.01	0.66	0.20	13.52	74.84	9.85	0.27	0.10	0.55
65	0.02	0.96	0.27	15.59	71.71	10.43	0.39	0.09	0.55
70	0.01	0.74	0.21	14.49	74.11	9.49	0.34	0.11	0.51
75	0.00	0.70	0.19	13.46	74.96	9.75	0.30	0.10	0.54
80	0.00	0.81	0.25	13.63	62.08	18.81	0.32	3.48	0.61
85	0.01	0.64	0.16	13.62	74.70	9.87	0.28	0.13	0.59
90	0.00	0.47	0.08	12.54	75.67	10.25	0.25	0.10	0.64
95	0.00	0.95	0.24	16.22	73.10	8.43	0.42	0.04	0.60
100	0.00	1.01	0.22	16.50	72.73	8.40	0.48	0.07	0.59
105	0.01	0.79	0.20	15.40	72.99	9.58	0.34	0.14	0.55

110	0.01	0.82	0.21	15.12	68.53	11.97	0.38	2.41	0.55
115	0.00	0.87	0.21	16.01	72.86	8.88	0.41	0.20	0.56
120	0.01	0.93	0.22	15.94	73.04	8.78	0.41	0.04	0.64
125	0.00	0.66	0.18	13.84	74.54	9.79	0.34	0.07	0.57
130	0.00	0.89	0.19	13.94	77.99	10.84	0.34	1.04	0.53
135	0.00	0.76	0.18	14.82	73.12	9.98	0.33	0.27	0.54
140	0.00	0.73	0.20	16.26	72.72	8.98	0.40	0.17	0.54
145	0.00	0.73	0.14	14.95	73.85	9.26	0.37	0.13	0.58
150	0.00	0.71	0.21	14.09	74.39	9.66	0.34	0.03	0.57
155	1.35	0.63	0.18	13.98	73.45	9.49	0.30	0.06	0.55
160	0.02	0.65	0.17	13.82	73.73	10.49	0.32	0.22	0.57
165	0.01	0.84	0.21	15.10	71.54	10.72	0.35	0.65	0.59
170	0.00	0.83	0.20	14.78	69.28	12.68	0.34	1.33	0.56
175	0.02	0.89	0.19	15.40	70.45	11.37	0.37	0.75	0.55
180	0.03	0.95	0.26	16.22	72.14	9.22	0.36	0.24	0.58
185	0.00	0.84	0.21	14.84	72.28	10.78	0.38	0.07	0.60
190	0.00	0.86	0.19	15.50	73.18	9.22	0.39	0.12	0.56
195	0.02	0.82	0.22	14.83	69.54	13.28	0.38	0.28	0.62
200	0.01	0.85	0.16	15.41	70.11	11.61	0.35	0.94	0.55
205	0.00	0.80	0.18	15.36	72.06	10.17	0.39	0.41	0.64
210	0.00	0.79	0.20	15.04	73.36	9.58	0.36	0.09	0.59
215	0.01	0.91	0.18	15.03	69.79	13.04	0.34	0.07	0.63
220	0.00	0.93	0.19	15.84	72.58	9.32	0.40	0.11	0.63
225	0.00	0.90	0.21	15.21	68.83	12.82	0.33	1.18	0.51
230	0.01	0.81	0.21	15.14	71.40	11.37	0.38	0.15	0.54
235	0.00	0.80	0.18	14.98	73.01	9.94	0.35	0.22	0.53
240	0.00	0.83	0.21	14.65	72.71	10.39	0.34	0.41	0.48
245	0.00	0.83	0.19	14.64	72.23	10.60	0.36	0.60	0.55
250	0.01	0.87	0.16	15.83	73.30	8.79	0.40	0.03	0.61
255	0.00	0.94	0.24	15.21	70.05	11.89	0.37	0.79	0.50
260	0.00	0.86	0.18	15.01	70.20	12.56	0.38	0.24	0.58
265	0.00	0.90	0.20	15.08	71.82	10.62	0.37	0.43	0.58
270	0.00	0.92	0.23	15.13	72.45	10.24	0.34	0.13	0.55
275	0.00	0.82	0.20	14.55	70.51	12.83	0.33	0.23	0.53
280	0.00	0.89	0.18	15.75	73.08	9.00	0.40	0.11	0.59
285	0.00	0.82	0.17	15.14	73.46	9.28	0.39	0.12	0.62
290	0.00	0.78	0.19	16.19	73.07	8.75	0.41	0.04	0.58
295	0.03	0.81	0.19	14.71	73.30	9.84	0.34	0.23	0.57
300	0.00	0.86	0.25	15.09	70.44	11.35	0.38	1.00	0.63
305	0.00	0.82	0.14	15.15	72.93	9.76	0.39	0.24	0.56
310	0.00	0.89	0.22	15.03	71.55	11.23	0.35	0.14	0.60
315	0.00	0.82	0.20	14.03	67.46	14.75	0.34	1.85	0.55
320	0.01	0.83	0.18	14.65	71.35	11.25	0.35	0.77	0.61
325	0.00	0.83	0.20	14.84	68.54	14.46	0.36	0.16	0.61
330	0.03	0.85	0.18	14.85	72.29	10.74	0.39	0.10	0.56
335	0.00	0.83	0.18	14.28	70.39	12.36	0.32	1.10	0.54
340	0.00	0.86	0.21	15.00	71.82	10.86	0.36	0.41	0.49
345	0.00	0.80	0.21	14.47	70.00	13.35	0.36	0.19	0.62
350	0.00	0.88	0.17	15.00	71.45	10.90	0.37	0.65	0.58
355	0.02	0.88	0.22	14.52	69.75	12.50	0.37	1.13	0.62
360	0.01	0.86	0.21	15.41	73.31	9.13	0.36	0.13	0.58
365	0.00	0.89	0.21	15.15	71.98	10.60	0.37	0.27	0.53
370	0.02	0.90	0.18	15.12	71.10	11.58	0.36	0.14	0.60
375	0.00	0.88	0.22	15.01	72.61	10.15	0.37	0.21	0.56
380	0.00	0.86	0.21	14.67	71.63	11.01	0.35	0.68	0.60
385	0.01	0.87	0.23	14.87	72.02	10.46	0.39	0.57	0.58
390	0.00	0.85	0.18	14.68	70.19	12.95	0.38	0.24	0.53

395	0.00	0.84	0.18	14.68	71.65	11.23	0.36	0.46	0.60
400	0.01	0.86	0.18	14.66	71.79	11.03	0.35	0.49	0.64
405	0.00	0.83	0.20	14.54	72.04	11.00	0.34	0.47	0.58
410	0.00	0.83	0.17	14.55	73.29	10.28	0.35	0.00	0.53
415	0.00	0.68	0.16	14.17	73.08	10.82	0.31	0.12	0.67
420	0.00	0.87	0.15	14.65	73.00	10.12	0.39	0.19	0.62
425	0.00	0.77	0.20	14.34	73.38	10.28	0.33	0.15	0.56
430	0.00	0.94	0.22	14.57	73.33	9.74	0.41	0.15	0.64
435	0.01	0.92	0.21	14.72	73.00	10.04	0.38	0.15	0.59
440	0.00	0.95	0.24	14.98	73.20	9.48	0.42	0.14	0.59
445	0.00	0.89	0.19	14.68	72.67	10.49	0.36	0.17	0.55
450	0.02	0.75	0.16	14.25	73.37	10.42	0.34	0.07	0.63
455	0.01	0.72	0.24	14.16	73.22	10.67	0.32	0.05	0.61
460	0.00	0.62	0.17	13.69	72.93	11.53	0.31	0.12	0.62
465	0.02	0.34	0.08	12.73	72.66	13.09	0.21	0.11	0.77
470	0.00	0.89	0.22	14.54	73.22	10.09	0.36	0.07	0.62
475	0.00	1.14	0.26	15.38	72.78	9.37	0.40	0.06	0.61
480	0.00	0.93	0.20	15.02	72.79	10.00	0.38	0.04	0.64
485	0.00	1.20	0.28	15.93	72.41	9.10	0.43	0.10	0.57
490	0.00	0.98	0.20	15.78	73.08	8.97	0.42	0.04	0.54
495	0.00	0.61	0.14	14.21	72.92	11.11	0.29	0.03	0.69
500	0.00	0.74	0.20	14.50	72.90	10.64	0.35	0.06	0.63
505	0.00	0.82	0.21	14.81	72.89	10.31	0.36	0.00	0.60
510	0.02	0.28	0.13	15.65	82.71	0.26	0.46	0.12	0.39
515	0.00	0.52	0.16	13.06	84.91	0.10	0.33	0.37	0.56
520	0.00	0.64	0.16	12.91	84.85	0.08	0.31	0.47	0.58
525	0.00	0.68	0.17	12.94	84.86	0.01	0.29	0.46	0.60
530	0.00	0.65	0.14	15.90	86.01	0.03	0.34	0.51	0.68
535	0.00	0.65	0.13	12.52	85.27	0.01	0.34	0.46	0.63
540	0.00	0.66	0.14	12.80	84.93	0.04	0.29	0.53	0.61
545	0.00	0.64	0.21	12.93	84.83	0.02	0.29	0.46	0.61
550	0.00	0.71	0.15	12.98	84.71	0.01	0.31	0.50	0.63
0	0.00	0.62	0.18	12.88	84.76	0.17	0.34	0.48	0.57
1	0.00	0.56	0.13	12.75	84.98	0.16	0.33	0.49	0.61
2	0.00	0.56	0.15	12.99	84.88	0.10	0.31	0.43	0.57
3	0.01	0.51	0.16	13.01	84.90	0.11	0.34	0.40	0.55
4	0.01	0.56	0.09	12.84	84.72	0.31	0.33	0.55	0.61
5	0.01	0.47	0.14	13.24	84.82	0.12	0.35	0.34	0.52
6	0.01	0.38	0.12	13.55	84.54	0.19	0.40	0.32	0.49
7	0.00	0.34	0.15	14.08	84.10	0.20	0.43	0.27	0.45
8	0.00	0.25	0.12	15.21	83.11	0.25	0.44	0.20	0.43
9	0.00	0.28	0.13	15.70	82.54	0.29	0.43	0.21	0.42
10	0.00	0.25	0.07	18.41	78.93	1.46	0.46	0.04	0.39
11	0.00	1.09	0.25	16.03	72.64	9.11	0.40	0.00	0.50
12	0.00	0.77	0.17	14.99	72.82	10.22	0.36	0.04	0.64
13	0.02	0.86	0.23	14.96	73.24	9.72	0.37	0.00	0.60
14	0.00	0.63	0.17	13.94	72.08	12.18	0.30	0.01	0.69
15	0.00	0.32	0.12	12.62	69.91	16.01	0.19	0.08	0.76
16	0.00	0.46	0.12	12.69	69.13	11.53	0.23	5.22	0.62
17	0.00	0.68	0.21	14.23	72.59	11.29	0.30	0.08	0.62
18	0.00	0.90	0.21	14.78	72.07	11.03	0.37	0.05	0.60
19	0.00	0.88	0.25	14.89	71.38	11.56	0.36	0.07	0.62
20	0.00	0.67	0.19	14.63	73.04	10.57	0.31	0.00	0.60
0	0.01	0.70	0.19	13.90	74.79	9.47	0.32	0.05	0.59
5	0.01	0.46	0.13	13.03	75.34	10.09	0.26	0.08	0.60

10	0.01	0.69	0.17	13.51	75.00	9.68	0.27	0.10	0.56
15	0.00	0.49	0.14	12.76	75.53	10.17	0.29	0.05	0.58
20	0.00	0.62	0.16	13.37	75.01	9.95	0.28	0.03	0.59
25	0.00	0.65	0.19	14.19	74.65	9.40	0.29	0.07	0.56
30	0.01	0.65	0.17	14.01	74.63	9.49	0.33	0.15	0.57
35	0.00	0.71	0.17	14.47	74.18	9.40	0.33	0.13	0.61
40	0.00	0.63	0.12	13.52	74.84	9.91	0.28	0.08	0.62
45	0.02	0.93	0.22	14.92	72.82	9.83	0.33	0.29	0.65
50	0.00	0.60	0.15	13.56	74.90	9.82	0.29	0.09	0.60
55	0.01	0.76	0.23	14.69	74.16	9.11	0.38	0.09	0.57
60	0.00	0.70	0.18	13.77	74.53	9.84	0.30	0.09	0.59
65	0.00	0.76	0.21	14.58	74.16	9.32	0.33	0.04	0.61
70	0.00	0.71	0.18	14.04	74.73	9.37	0.30	0.08	0.59
75	0.02	0.64	0.12	13.64	74.95	9.62	0.30	0.06	0.65
80	0.00	0.64	0.14	13.54	74.99	9.76	0.28	0.09	0.56
85	0.02	1.02	0.24	16.08	73.28	8.39	0.39	0.00	0.57
90	0.00	0.77	0.17	14.40	74.44	9.27	0.32	0.05	0.58
95	0.00	0.75	0.19	14.28	72.92	10.62	0.35	0.35	0.54
100	0.00	0.62	0.20	13.44	74.69	10.11	0.32	0.09	0.55
105	0.03	0.80	0.20	14.57	69.89	13.64	0.36	0.01	0.50
110	0.02	0.82	0.18	14.50	72.91	10.58	0.33	0.09	0.57
115	0.00	0.97	0.26	15.80	73.01	8.94	0.35	0.11	0.55
120	0.00	0.66	0.15	14.04	74.40	9.74	0.33	0.14	0.55
125	0.00	0.93	0.27	15.72	73.43	8.68	0.36	0.02	0.58
130	0.01	0.72	0.14	13.94	74.24	9.73	0.34	0.27	0.60
135	0.00	0.93	0.19	16.40	73.20	8.25	0.44	0.00	0.58
140	0.00	0.68	0.18	11.96	53.34	32.82	0.24	0.23	0.55
145	0.01	0.82	0.20	15.40	71.19	11.35	0.36	0.07	0.60
150	0.01	0.85	0.18	15.73	72.62	9.45	0.39	0.16	0.62
155	0.00	0.83	0.20	14.90	69.49	13.51	0.36	0.22	0.49
160	0.00	0.63	0.16	13.52	74.93	9.82	0.32	0.03	0.58
165	0.00	0.80	0.21	14.25	65.23	18.53	0.34	0.05	0.57
170	0.00	0.75	0.20	15.68	72.66	9.73	0.35	0.12	0.52
175	0.00	0.66	0.14	13.66	74.88	9.58	0.35	0.15	0.59
180	0.00	0.90	0.20	16.38	73.03	8.42	0.40	0.10	0.57
185	0.01	0.72	0.14	14.16	71.04	12.93	0.33	0.09	0.59
190	0.00	0.77	0.22	14.29	71.09	11.67	0.34	0.99	0.63
195	0.00	0.91	0.23	16.27	72.80	8.75	0.37	0.07	0.60
200	0.00	0.75	0.14	14.43	69.16	13.94	0.31	0.71	0.56
205	0.02	0.74	0.17	14.19	69.79	14.15	0.35	0.07	0.53
210	0.00	0.84	0.20	15.58	72.32	10.05	0.40	0.03	0.58
215	0.00	0.91	0.18	15.57	72.43	9.93	0.38	0.07	0.52
220	0.00	0.83	0.18	15.23	72.20	10.21	0.36	0.45	0.56
225	0.01	0.83	0.18	15.06	71.64	10.80	0.38	0.50	0.60
230	0.01	0.87	0.19	15.60	71.80	10.07	0.39	0.44	0.63
235	0.02	0.90	0.20	15.24	71.11	10.97	0.34	0.63	0.60
240	0.01	0.79	0.20	15.00	71.88	10.59	0.33	0.63	0.58
245	0.00	0.82	0.20	15.32	73.32	9.16	0.37	0.20	0.62
250	0.01	0.80	0.17	14.37	68.09	14.01	0.33	1.58	0.63
255	0.02	0.84	0.19	14.77	70.59	11.50	0.37	1.07	0.64
260	0.01	0.83	0.17	15.79	73.49	8.70	0.35	0.11	0.56
265	0.00	0.82	0.16	16.16	73.13	8.60	0.43	0.09	0.61
270	0.00	0.91	0.24	16.64	80.44	0.67	0.42	0.04	0.65
275	0.00	0.85	0.21	15.68	71.44	10.13	0.37	0.69	0.63
280	0.00	0.74	0.18	16.33	73.19	8.53	0.36	0.10	0.58
285	0.02	0.85	0.18	15.53	71.74	10.15	0.39	0.57	0.59
290	0.00	0.82	0.20	15.45	73.21	9.20	0.36	0.22	0.53

295	0.00	0.88	0.19	15.47	71.89	10.09	0.40	0.50	0.58
300	0.01	0.86	0.19	14.70	67.71	13.98	0.33	1.66	0.57
305	0.00	0.81	0.20	15.56	72.23	9.89	0.35	0.30	0.67
310	0.00	0.91	0.19	15.16	71.07	11.13	0.37	0.70	0.48
315	0.00	0.90	0.21	15.44	70.81	11.51	0.37	0.18	0.59
320	0.00	0.83	0.21	15.47	72.54	9.93	0.38	0.08	0.57
325	0.01	0.82	0.21	15.07	70.57	12.23	0.40	0.08	0.61
330	0.00	0.64	0.09	11.11	46.60	40.51	0.30	0.23	0.52
335	0.00	0.81	0.18	14.91	70.17	12.85	0.36	0.17	0.56
340	0.02	0.90	0.24	15.58	71.81	10.38	0.38	0.20	0.50
345	0.00	0.83	0.18	14.72	69.07	14.23	0.37	0.09	0.52
350	0.00	0.86	0.21	14.86	71.25	11.41	0.38	0.44	0.59
355	0.00	0.87	0.21	15.61	72.31	9.86	0.35	0.22	0.56
360	0.00	0.88	0.21	15.05	69.89	12.67	0.38	0.36	0.57
365	0.00	0.81	0.17	14.10	66.90	16.98	0.34	0.10	0.61
370	0.01	0.86	0.20	14.47	70.57	12.77	0.35	0.26	0.52
375	0.00	0.86	0.18	14.73	70.18	12.20	0.35	0.97	0.54
380	0.00	0.84	0.19	14.76	70.75	11.69	0.36	0.79	0.61
385	0.00	0.76	0.18	14.66	71.06	11.46	0.34	0.93	0.61
390	0.00	0.87	0.19	15.07	71.29	11.00	0.37	0.62	0.60
395	0.03	0.85	0.19	14.92	71.24	11.07	0.38	0.79	0.54
400	0.00	0.87	0.18	15.52	71.87	10.17	0.41	0.43	0.57
405	0.01	0.82	0.17	14.93	71.31	11.19	0.34	0.66	0.58
410	0.00	0.84	0.18	15.03	72.50	10.16	0.37	0.39	0.54
415	0.00	0.84	0.22	15.02	72.21	10.48	0.39	0.25	0.58
420	0.03	0.90	0.20	15.26	72.36	10.24	0.34	0.12	0.56
425	0.02	0.84	0.20	14.84	73.04	9.82	0.40	0.24	0.61
430	0.02	0.38	0.11	12.92	73.06	12.46	0.25	0.17	0.65
435	0.00	0.70	0.18	14.33	72.77	11.06	0.34	0.04	0.59
440	0.00	0.64	0.16	14.09	72.92	11.12	0.31	0.15	0.61
445	0.00	0.32	0.10	13.04	73.19	12.54	0.19	0.00	0.64
450	0.01	0.82	0.19	14.45	73.54	9.89	0.40	0.14	0.57
455	0.00	0.50	0.11	13.28	71.15	13.98	0.25	0.08	0.65
460	0.01	0.58	0.18	13.81	68.76	15.65	0.32	0.05	0.63
465	0.02	0.72	0.17	13.90	73.56	10.58	0.37	0.05	0.64
470	0.01	0.63	0.14	13.91	72.11	12.21	0.32	0.06	0.61
475	0.00	0.79	0.18	14.51	73.25	10.25	0.36	0.10	0.56
480	0.00	0.85	0.23	14.54	73.06	10.34	0.34	0.07	0.58
485	0.00	0.99	0.24	15.55	72.69	9.45	0.39	0.05	0.65
490	0.00	0.74	0.18	14.63	72.69	10.78	0.33	0.03	0.63
495	0.02	0.35	0.08	13.13	72.98	12.38	0.24	0.16	0.66
500	0.01	0.62	0.14	14.54	73.06	10.69	0.31	0.00	0.63
505	0.01	0.82	0.23	15.07	72.76	10.08	0.35	0.08	0.60
510	0.00	0.77	0.18	14.85	72.81	10.34	0.34	0.10	0.62
515	0.00	0.97	0.19	15.53	72.82	9.42	0.41	0.09	0.58
520	0.00	0.69	0.14	14.20	73.36	10.61	0.32	0.05	0.63
525	0.00	0.39	0.09	14.29	77.72	6.50	0.37	0.03	0.62
530	0.01	0.55	0.16	13.08	84.85	0.09	0.35	0.41	0.51
535	0.00	0.65	0.19	13.11	84.63	0.04	0.33	0.43	0.63
540	0.00	0.65	0.15	13.11	84.63	0.05	0.30	0.43	0.69
545	0.00	0.70	0.15	13.01	84.59	0.03	0.30	0.51	0.70
550	0.01	0.69	0.19	13.01	84.63	0.00	0.32	0.55	0.63
0	0.00	0.64	0.13	13.14	84.60	0.05	0.31	0.50	0.63
1	0.00	0.61	0.15	13.07	84.68	0.06	0.36	0.45	0.62
2	0.00	0.62	0.15	12.97	84.81	0.00	0.31	0.53	0.61
3	0.00	0.62	0.14	13.08	84.73	0.05	0.30	0.49	0.59

4	0.00	0.54	0.17	13.33	84.35	0.13	0.36	0.52	0.60
5	0.01	0.50	0.15	13.29	84.63	0.14	0.32	0.42	0.54
6	0.00	0.49	0.17	13.52	84.26	0.32	0.38	0.33	0.53
7	0.02	0.44	0.15	14.07	83.89	0.26	0.43	0.23	0.54
8	0.00	0.37	0.09	14.52	79.24	4.83	0.38	0.10	0.48
9	0.00	0.36	0.13	14.72	78.62	5.24	0.35	0.00	0.58
10	0.00	0.51	0.16	15.26	77.50	5.69	0.33	0.04	0.51
11	0.01	0.61	0.14	16.54	77.14	4.66	0.44	0.00	0.47
12	0.01	0.57	0.18	17.17	76.58	4.43	0.45	0.11	0.51
13	0.02	0.92	0.20	15.74	73.74	8.35	0.37	0.02	0.65
14	0.00	0.64	0.15	14.30	73.11	10.65	0.31	0.09	0.74
15	0.00	0.82	0.17	15.20	73.23	9.52	0.40	0.10	0.55
16	0.00	0.86	0.21	15.01	73.17	9.75	0.39	0.02	0.60
17	0.00	0.86	0.25	14.77	73.14	9.92	0.37	0.08	0.63
18	0.01	0.91	0.25	15.31	72.83	9.66	0.37	0.02	0.66
19	0.01	0.95	0.24	15.79	72.39	9.52	0.43	0.00	0.68
20	0.00	0.69	0.20	14.08	72.56	11.42	0.30	0.09	0.66
0	0.01	0.57	0.15	12.55	75.41	10.31	0.29	0.12	0.59
5	0.03	0.69	0.19	13.59	72.78	11.79	0.34	0.04	0.55
10	0.00	0.66	0.17	13.30	74.87	10.12	0.32	0.04	0.53
15	0.00	0.58	0.16	13.05	75.28	9.94	0.29	0.09	0.63
20	0.01	0.63	0.17	13.57	74.70	10.01	0.28	0.05	0.57
25	0.01	0.60	0.14	13.25	75.14	10.04	0.29	0.01	0.53
30	0.00	0.83	0.18	15.32	73.66	9.07	0.36	0.05	0.54
35	0.00	1.16	0.26	16.11	72.55	8.86	0.41	0.08	0.57
40	0.00	0.75	0.18	14.34	74.26	9.43	0.36	0.05	0.63
45	0.00	0.71	0.14	13.76	70.68	13.79	0.32	0.07	0.55
50	0.00	0.63	0.14	13.29	75.03	9.99	0.26	0.07	0.59
55	0.01	0.72	0.18	14.09	73.74	10.11	0.32	0.26	0.57
60	0.01	0.81	0.20	14.87	71.92	10.52	0.35	0.74	0.58
65	0.00	0.64	0.17	10.27	46.20	41.95	0.19	0.04	0.54
70	0.01	0.81	0.17	15.76	73.32	8.98	0.38	0.04	0.53
75	0.01	0.93	0.20	16.36	72.69	8.66	0.45	0.06	0.65
80	0.01	1.06	0.24	16.33	72.71	8.52	0.45	0.05	0.63
85	0.01	0.66	0.16	14.01	74.72	9.54	0.29	0.06	0.56
90	0.03	0.78	0.17	14.61	73.89	9.49	0.35	0.07	0.62
95	0.00	0.74	0.18	14.96	73.68	9.41	0.34	0.17	0.51
100	0.02	0.63	0.19	14.04	73.63	10.41	0.31	0.22	0.55
105	0.00	0.67	0.15	13.36	72.96	11.79	0.28	0.13	0.67
110	0.00	0.63	0.18	12.94	75.06	10.27	0.29	0.05	0.56
115	0.00	0.78	0.19	15.61	72.54	9.52	0.38	0.46	0.54
120	0.00	0.95	0.22	16.35	72.47	8.95	0.41	0.09	0.56
125	0.00	0.77	0.22	14.89	71.54	11.16	0.35	0.57	0.50
130	0.00	0.71	0.16	14.23	72.63	11.30	0.30	0.02	0.65
135	0.00	0.68	0.16	12.98	66.26	18.62	0.30	0.39	0.61
140	0.00	0.69	0.21	13.81	61.65	22.62	0.35	0.14	0.52
145	0.00	0.83	0.19	15.56	70.16	11.32	0.38	1.02	0.53
150	0.01	0.80	0.17	14.04	66.45	15.65	0.33	1.97	0.57
155	0.00	0.77	0.20	15.41	73.44	9.10	0.38	0.09	0.61
160	0.03	0.76	0.19	15.04	72.97	9.82	0.34	0.33	0.53
165	0.00	0.90	0.21	16.01	72.25	9.50	0.40	0.18	0.55
170	0.01	0.84	0.16	14.42	64.13	16.59	0.33	2.99	0.54
175	0.00	0.89	0.21	15.49	71.53	10.28	0.35	0.65	0.61
180	0.03	0.83	0.18	16.27	72.26	9.19	0.39	0.25	0.61
185	0.01	0.89	0.26	16.43	72.75	8.61	0.39	0.16	0.51
190	0.00	0.87	0.20	15.71	71.12	10.45	0.38	0.67	0.59

195	0.00	0.71	0.16	13.95	74.59	9.52	0.34	0.11	0.62
200	0.02	0.78	0.18	13.80	58.82	25.41	0.36	0.07	0.55
205	0.01	0.90	0.20	15.55	71.60	10.77	0.36	0.11	0.52
210	0.01	0.90	0.21	15.70	69.98	12.12	0.38	0.08	0.62
215	0.00	0.67	0.17	15.13	73.63	9.49	0.37	0.04	0.51
220	0.00	0.81	0.19	15.72	72.96	9.30	0.40	0.10	0.51
225	0.00	0.79	0.23	14.83	68.51	14.66	0.38	0.08	0.51
230	0.01	0.84	0.22	15.64	73.06	9.10	0.38	0.13	0.63
235	0.00	0.85	0.21	15.60	72.11	10.04	0.39	0.27	0.53
240	0.00	0.74	0.22	13.85	64.14	19.99	0.35	0.16	0.55
245	0.00	0.79	0.18	15.59	72.17	10.27	0.36	0.13	0.51
250	0.00	0.86	0.22	15.13	69.67	12.07	0.38	1.05	0.63
255	0.00	0.83	0.19	15.04	72.26	10.33	0.34	0.45	0.57
260	0.00	0.84	0.17	15.83	72.58	9.30	0.39	0.25	0.65
265	0.01	0.91	0.22	15.38	69.76	12.74	0.37	0.05	0.57
270	0.01	0.88	0.23	15.16	71.96	10.74	0.39	0.11	0.52
275	0.00	0.81	0.22	14.63	69.95	12.92	0.36	0.56	0.55
280	0.02	0.86	0.17	15.40	72.83	9.56	0.38	0.26	0.52
285	0.00	0.75	0.17	14.07	66.91	15.00	0.35	2.24	0.52
290	0.00	0.79	0.18	16.18	72.93	8.89	0.40	0.08	0.56
295	0.00	0.82	0.19	15.01	71.51	10.65	0.34	0.91	0.57
300	0.00	0.84	0.16	14.71	71.12	11.44	0.34	0.81	0.57
305	0.00	0.83	0.17	15.48	72.66	9.58	0.41	0.30	0.56
310	0.02	0.82	0.21	15.29	70.56	12.05	0.33	0.14	0.57
315	0.00	0.77	0.18	14.33	67.45	16.19	0.37	0.10	0.60
320	0.00	0.90	0.22	15.20	72.08	10.34	0.38	0.34	0.54
325	0.01	0.79	0.18	14.60	71.43	11.35	0.33	0.76	0.55
330	0.00	0.84	0.17	14.72	71.00	11.75	0.38	0.62	0.53
335	0.00	0.84	0.17	14.71	72.35	10.42	0.38	0.52	0.61
340	0.00	0.83	0.24	14.79	71.74	11.31	0.39	0.15	0.56
345	0.00	0.83	0.14	14.57	70.64	11.98	0.37	0.98	0.50
350	0.00	0.83	0.20	14.97	72.70	9.94	0.37	0.46	0.52
355	0.00	0.82	0.18	14.58	71.97	10.82	0.36	0.67	0.61
360	0.02	0.87	0.20	14.78	71.32	11.13	0.39	0.72	0.58
365	0.00	0.86	0.18	14.72	72.21	10.57	0.36	0.59	0.51
370	0.00	0.85	0.21	14.94	71.54	10.87	0.38	0.62	0.59
375	0.01	0.84	0.21	14.95	73.00	9.72	0.37	0.26	0.64
380	0.00	0.85	0.20	14.59	72.51	10.31	0.34	0.66	0.55
385	0.03	0.87	0.18	14.55	71.40	11.22	0.37	0.86	0.53
390	0.00	0.89	0.22	14.16	67.64	16.13	0.36	0.10	0.51
395	0.00	0.88	0.23	15.24	72.70	9.78	0.42	0.16	0.61
400	0.01	0.65	0.19	14.06	73.27	10.79	0.34	0.08	0.61
405	0.02	0.86	0.19	14.48	73.43	9.90	0.37	0.25	0.50
410	0.00	0.43	0.12	13.18	73.27	11.98	0.27	0.11	0.65
415	0.02	0.93	0.21	15.61	73.10	9.03	0.40	0.15	0.55
420	0.00	0.61	0.14	13.70	73.17	11.39	0.28	0.11	0.62
425	0.00	0.65	0.10	13.70	73.11	11.28	0.31	0.24	0.62
430	0.00	0.72	0.16	14.37	73.27	10.31	0.35	0.23	0.59
435	0.01	0.81	0.18	14.34	73.49	10.02	0.37	0.15	0.65
440	0.00	0.91	0.24	14.56	73.46	9.94	0.35	0.02	0.53
445	0.00	0.40	0.10	13.16	73.08	12.12	0.25	0.14	0.75
450	0.01	0.39	0.12	12.96	73.29	12.24	0.23	0.03	0.75
455	0.00	0.93	0.21	15.05	73.00	9.65	0.39	0.16	0.61
460	0.00	0.77	0.21	14.41	73.14	10.43	0.36	0.06	0.62
465	0.01	0.80	0.20	14.39	72.95	10.61	0.34	0.07	0.64
470	0.00	0.94	0.22	15.05	72.68	10.13	0.40	0.02	0.56
475	0.01	0.74	0.19	14.34	73.01	10.63	0.31	0.14	0.63

480	0.02	1.16	0.21	15.76	72.94	8.86	0.40	0.08	0.58
485	0.00	1.03	0.18	15.20	72.41	10.09	0.38	0.12	0.61
490	0.01	1.03	0.23	15.61	73.11	8.92	0.39	0.08	0.63
495	0.00	0.31	0.12	15.41	82.51	0.63	0.45	0.12	0.45
500	0.02	0.56	0.20	12.86	84.92	0.07	0.33	0.48	0.58
505	0.00	0.65	0.14	12.95	84.68	0.05	0.34	0.50	0.69
510	0.00	0.67	0.12	12.87	84.80	0.05	0.34	0.50	0.65
515	0.00	0.68	0.15	12.90	84.82	0.01	0.32	0.49	0.64
520	0.00	0.64	0.13	12.76	85.01	0.03	0.32	0.47	0.65
525	0.01	0.70	0.16	12.89	84.76	0.02	0.31	0.53	0.63
530	0.00	0.66	0.14	13.01	84.62	0.05	0.33	0.51	0.68
535	0.00	0.68	0.16	12.96	84.78	0.02	0.33	0.47	0.60
540	0.01	0.65	0.17	13.03	84.68	0.04	0.32	0.47	0.63
545	0.00	0.66	0.19	12.95	84.72	0.00	0.34	0.50	0.65
550	0.00	0.68	0.17	12.98	84.71	0.03	0.33	0.50	0.61
0	0.00	0.62	0.15	12.87	84.87	0.05	0.33	0.52	0.60
1	0.01	0.66	0.16	12.91	84.85	0.04	0.33	0.47	0.59
2	0.01	0.65	0.17	13.08	84.65	0.03	0.33	0.51	0.59
3	0.00	0.67	0.16	12.99	84.70	0.08	0.30	0.49	0.63
4	0.00	0.68	0.15	12.93	84.74	0.07	0.31	0.52	0.61
5	0.01	0.65	0.15	12.99	84.65	0.05	0.33	0.52	0.65
6	0.00	0.62	0.14	12.93	84.83	0.04	0.31	0.46	0.66
7	0.00	0.61	0.15	13.11	84.55	0.08	0.33	0.50	0.68
8	0.01	0.63	0.17	12.91	84.92	0.05	0.30	0.42	0.60
9	0.02	0.52	0.15	13.18	84.77	0.10	0.32	0.39	0.56
10	0.00	0.58	0.15	13.03	84.77	0.07	0.36	0.41	0.63
11	0.00	0.51	0.13	13.09	84.87	0.09	0.33	0.42	0.57
12	0.00	0.48	0.12	13.42	84.48	0.13	0.35	0.44	0.58
13	0.00	0.33	0.10	16.22	80.27	2.20	0.38	0.05	0.44
14	0.00	0.36	0.12	14.84	75.43	8.28	0.35	0.08	0.55
15	0.00	0.52	0.14	13.78	73.05	11.52	0.26	0.08	0.64
16	0.00	0.93	0.19	15.74	73.41	8.63	0.39	0.11	0.60
17	0.00	0.67	0.16	14.13	73.40	10.65	0.31	0.04	0.63
18	0.00	0.98	0.22	15.46	73.04	9.28	0.36	0.06	0.59
19	0.02	1.01	0.19	15.45	73.15	9.12	0.38	0.06	0.62
20	0.01	1.05	0.24	15.42	73.19	9.14	0.36	0.03	0.55

B.50 HT-9/V/Nd After 28 Days at 700°C

The HT-9/V/Nd assembly annealed for 28 days at 700°C bonded on both the V/Nd interface and the HT-9/V interface. Compositional data (in at%) from WDS linescans across the HT-9/V interface is given below.

Position	Zr	Mo	W	Cr	Fe	Nd	V	Ni	Mn
0	0.00	0.01	0.00	1.93	0.13	0.19	97.71	0.03	0.00
1	0.00	0.01	0.00	1.99	0.16	0.17	97.68	0.00	0.00
2	0.00	0.01	0.01	1.94	0.13	0.15	97.74	0.00	0.03
3	0.00	0.00	0.00	1.99	0.15	0.11	97.72	0.02	0.02
4	0.00	0.00	0.00	1.92	0.22	0.23	97.59	0.02	0.01
5	0.00	0.00	0.00	1.93	0.23	0.32	97.51	0.01	0.00
6	0.00	0.00	0.00	2.00	0.18	0.11	97.67	0.00	0.04
7	0.01	0.01	0.01	2.01	0.34	0.20	97.43	0.00	0.01
8	0.01	0.00	0.01	2.02	0.43	0.17	97.29	0.04	0.04

9	0.00	0.00	0.00	2.06	0.59	0.19	96.91	0.00	0.26
10	0.00	0.06	0.00	3.20	9.32	0.29	84.55	0.03	2.54
11	0.00	0.51	0.15	10.04	68.05	0.55	19.23	0.40	1.08
12	0.00	0.70	0.17	12.72	82.13	0.85	2.46	0.48	0.49
13	0.00	0.68	0.15	12.58	83.08	0.73	1.83	0.44	0.52
14	0.00	0.58	0.09	11.56	84.63	0.64	1.59	0.49	0.43
15	0.00	0.58	0.13	11.72	84.51	0.61	1.46	0.51	0.49
16	0.00	0.63	0.15	12.08	84.44	0.52	1.25	0.40	0.53
17	0.02	0.63	0.17	12.57	84.05	0.51	1.04	0.44	0.56
18	0.00	0.54	0.11	11.52	84.95	0.52	1.37	0.48	0.52
19	0.00	0.62	0.17	12.02	84.38	0.54	1.27	0.47	0.53
20	0.00	0.62	0.17	11.99	84.59	0.57	1.08	0.45	0.54

B.51 HT-9/Zr/V/Nd After 28 Days at 700°C

The HT-9/Zr/V/Nd assembly annealed for 28 days at 700°C bonded on the V/Nd interface but not the HT-9/Zr or Zr/V interfaces. Compositional data (in at%) from WDS linescans across the V/Nd interface is given below.

Position	Zr	Mo	W	Cr	Fe	Nd	V	Ni	Mn
0	0.00	0.00	0.00	0.00	0.62	98.54	0.42	0.00	0.43
1	0.04	0.09	0.00	0.00	0.42	98.76	0.34	0.06	0.29
2	0.00	0.00	0.00	0.06	0.41	98.43	0.54	0.14	0.42
3	0.04	0.00	0.00	0.00	0.30	98.58	0.62	0.00	0.46
4	0.06	0.00	0.00	0.05	0.46	98.22	0.70	0.08	0.44
5	0.00	0.06	0.02	0.04	0.35	98.23	0.77	0.04	0.51
6	0.00	0.00	0.00	0.05	0.38	97.82	1.06	0.07	0.62
7	0.02	0.01	0.01	0.00	0.48	97.90	1.16	0.00	0.43
8	0.03	0.00	0.08	0.01	0.37	97.46	1.46	0.09	0.50
9	0.05	0.01	0.00	0.00	0.40	97.27	1.77	0.00	0.49
10	0.00	0.00	0.00	0.02	0.46	96.69	2.31	0.02	0.51
11	0.06	0.04	0.00	0.08	0.56	95.81	2.99	0.00	0.46
12	0.03	0.00	0.00	0.03	0.48	95.15	3.89	0.07	0.37
13	0.02	0.00	0.00	0.15	0.82	90.78	7.60	0.09	0.53
14	0.01	0.06	0.01	1.54	9.38	22.35	66.49	0.00	0.17
15	0.01	0.04	0.02	1.96	9.48	6.02	82.34	0.00	0.13
16	0.01	0.01	0.02	1.91	0.22	2.04	95.70	0.02	0.07
17	0.02	0.00	0.00	1.88	0.24	2.13	95.72	0.02	0.00
18	0.01	0.00	0.01	2.03	0.18	1.23	96.52	0.02	0.01
19	0.00	0.00	0.01	1.90	0.32	2.25	95.46	0.00	0.06
20	0.00	0.02	0.01	1.95	0.07	0.59	97.32	0.04	0.00

B.52 HT-9/Zr/Nd After 28 Days at 700°C

The HT-9/Zr/Nd assembly annealed for 28 days at 700°C bonded on the Zr/Nd interface but not the HT-9/Zr interface. Compositional data (in at%) from WDS linescans across the Zr/Nd interface is given below.

Position	Zr	Mo	W	Cr	Fe	Nd	V	Ni	Mn
0	94.31	0.00	0.00	0.00	0.08	5.48	0.04	0.00	0.08
1	94.33	0.00	0.00	0.02	0.06	5.60	0.00	0.00	0.00
2	91.11	0.00	0.00	0.04	0.08	8.69	0.08	0.00	0.00

3	92.22	0.00	0.00	0.05	0.12	7.54	0.03	0.02	0.03
4	87.91	0.00	0.00	0.00	0.16	11.49	0.32	0.07	0.05
5	93.03	0.00	0.00	0.00	0.11	6.69	0.15	0.00	0.01
6	97.52	0.00	0.00	0.00	0.04	2.37	0.04	0.00	0.04
7	95.17	0.00	0.00	0.00	0.00	4.81	0.02	0.00	0.00
8	96.90	0.00	0.00	0.00	0.02	3.00	0.02	0.00	0.07
9	97.10	0.00	0.00	0.05	0.07	2.72	0.01	0.00	0.05
10	96.29	0.00	0.00	0.03	0.06	3.51	0.00	0.02	0.09
11	94.34	0.00	0.00	0.02	0.16	5.44	0.00	0.04	0.00
12	96.99	0.00	0.00	0.01	0.03	2.89	0.01	0.07	0.00
13	95.21	0.00	0.00	0.02	0.04	4.64	0.01	0.07	0.02
14	92.31	0.00	0.00	0.00	0.07	7.60	0.00	0.02	0.00
15	80.58	0.02	0.00	0.01	0.14	19.17	0.01	0.00	0.07
16	65.74	0.00	0.00	0.01	0.23	33.93	0.02	0.00	0.07
17	11.19	0.00	0.00	0.00	0.33	88.20	0.00	0.00	0.28
18	0.17	0.07	0.00	0.02	0.33	98.97	0.01	0.00	0.44
19	0.09	0.04	0.00	0.00	0.46	98.88	0.00	0.00	0.53
20	0.03	0.00	0.03	0.00	0.31	99.19	0.00	0.03	0.42
0	97.75	0.00	0.00	0.05	0.23	1.93	0.00	0.00	0.04
1	98.08	0.00	0.00	0.02	0.07	1.73	0.05	0.04	0.01
2	97.82	0.00	0.00	0.00	0.17	1.85	0.03	0.03	0.09
3	97.95	0.00	0.00	0.02	0.05	1.91	0.01	0.06	0.00
4	98.32	0.03	0.00	0.02	0.05	1.58	0.00	0.00	0.00
5	98.77	0.00	0.00	0.01	0.00	1.13	0.00	0.04	0.05
6	98.19	0.00	0.00	0.03	0.04	1.70	0.02	0.00	0.02
7	97.35	0.00	0.00	0.00	0.09	2.45	0.04	0.00	0.08
8	98.37	0.00	0.00	0.00	0.06	1.56	0.01	0.00	0.00
9	97.47	0.00	0.00	0.01	0.07	2.33	0.05	0.03	0.04
10	97.37	0.00	0.00	0.00	0.06	2.54	0.02	0.00	0.02
11	97.40	0.00	0.00	0.02	0.04	2.45	0.00	0.00	0.08
12	96.96	0.00	0.00	0.01	0.07	2.83	0.02	0.00	0.11
13	78.51	0.00	0.00	0.00	0.82	20.53	0.01	0.02	0.12
14	80.12	0.00	0.00	0.05	0.56	19.08	0.02	0.05	0.13
15	82.78	0.03	0.00	0.02	0.29	16.60	0.10	0.09	0.09
16	55.22	0.03	0.00	0.03	0.60	43.61	0.24	0.04	0.24
17	2.23	0.00	0.00	0.04	0.28	96.83	0.00	0.18	0.44
18	0.16	0.00	0.00	0.09	0.40	98.88	0.00	0.02	0.46
19	0.09	0.00	0.06	0.00	0.47	99.00	0.00	0.00	0.39
20	0.03	0.03	0.01	0.00	0.43	99.06	0.00	0.00	0.45
0	97.97	0.00	0.00	0.02	0.09	1.89	0.00	0.04	0.00
1	98.10	0.00	0.00	0.03	0.05	1.74	0.03	0.05	0.00
2	97.98	0.00	0.00	0.01	0.09	1.86	0.04	0.00	0.02
3	97.18	0.00	0.00	0.06	0.19	2.47	0.03	0.00	0.07
4	97.86	0.00	0.00	0.03	0.13	1.95	0.00	0.00	0.04
5	97.44	0.00	0.00	0.04	0.16	2.30	0.00	0.00	0.06
6	97.51	0.00	0.00	0.01	0.01	2.40	0.02	0.00	0.05
7	96.52	0.00	0.00	0.01	0.17	3.19	0.00	0.11	0.00
8	93.17	0.00	0.00	0.06	0.42	6.23	0.02	0.08	0.02
9	97.05	0.00	0.00	0.01	0.16	2.77	0.00	0.01	0.00
10	97.69	0.00	0.00	0.00	0.04	2.17	0.00	0.04	0.07
11	97.68	0.00	0.00	0.01	0.02	2.21	0.01	0.05	0.02
12	97.20	0.00	0.00	0.00	0.07	2.70	0.00	0.00	0.03
13	93.86	0.00	0.00	0.00	0.19	5.90	0.00	0.00	0.06
14	93.46	0.00	0.00	0.00	0.20	6.20	0.05	0.07	0.02
15	84.29	0.00	0.00	0.00	0.26	15.39	0.04	0.02	0.00

16	35.58	0.02	0.00	0.00	0.46	63.49	0.06	0.02	0.38
17	0.36	0.01	0.00	0.00	0.43	98.74	0.00	0.00	0.46
18	0.12	0.03	0.06	0.00	0.38	98.88	0.00	0.00	0.53
19	0.02	0.03	0.00	0.00	0.38	99.08	0.07	0.00	0.44
20	0.03	0.06	0.02	0.00	0.54	98.89	0.00	0.00	0.46

B.53 HT-9/Ti/V/Nd After 28 Days at 700°C

The HT-9/Ti/V/Nd assembly annealed for 28 days at 700°C bonded on the V/Nd and Ti/V interfaces but not the HT-9/Ti interface. Compositional data (in at%) from WDS linescans across the Ti/V interface is given below.

Position	Ta	Ti	Mo	W	Cr	Fe	Nd	V	Ni	Mn
0	0.00	99.11	0.00	0.00	0.00	0.01	0.01	0.85	0.00	0.04
1	0.00	99.06	0.00	0.00	0.00	0.00	0.03	0.88	0.03	0.00
2	0.00	99.13	0.00	0.00	0.01	0.04	0.03	0.72	0.04	0.03
3	0.00	99.14	0.00	0.00	0.01	0.00	0.01	0.80	0.00	0.05
4	0.00	98.95	0.00	0.00	0.00	0.02	0.05	0.93	0.05	0.01
5	0.00	98.69	0.00	0.00	0.02	0.19	0.13	0.96	0.01	0.00
6	0.00	98.45	0.00	0.02	0.00	0.28	0.16	1.06	0.02	0.01
7	0.00	98.72	0.00	0.00	0.01	0.00	0.05	1.21	0.01	0.01
8	0.00	92.80	0.00	0.02	0.15	0.01	0.12	6.86	0.00	0.05
9	0.00	3.48	0.00	0.02	1.84	0.05	0.00	94.59	0.00	0.02
10	0.00	1.74	0.00	0.00	1.77	0.08	0.00	96.41	0.00	0.01
11	0.00	0.86	0.00	0.00	1.75	0.00	0.00	97.40	0.00	0.00
12	0.00	1.47	0.00	0.00	1.77	0.14	0.15	96.47	0.00	0.00
13	0.00	0.76	0.00	0.00	1.87	0.21	0.44	96.71	0.00	0.00
14	0.00	0.56	0.00	0.00	1.91	0.00	0.09	97.43	0.00	0.01
15	0.00	0.35	0.02	0.02	1.92	0.01	0.01	97.67	0.00	0.00
16	0.00	0.34	0.00	0.00	1.71	0.06	0.07	97.82	0.00	0.00
17	0.00	0.70	0.02	0.00	2.00	0.61	0.49	96.09	0.10	0.00
18	0.00	0.43	0.00	0.00	1.87	0.28	0.25	97.18	0.00	0.00
19	0.00	0.56	0.00	0.00	2.04	0.05	0.09	97.26	0.00	0.00
20	0.00	0.61	0.00	0.00	1.72	0.22	0.46	96.93	0.00	0.07

B.54 HT-9/Ti/Nd After 28 Days at 700°C

The HT-9/Ti/Nd assembly annealed for 28 days at 700°C bonded on the Ti/Nd interface but not the HT-9/Ti interface. Compositional data (in at%) from WDS linescans across the Ti/Nd interface is given below.

Position	Ta	Ti	Mo	W	Cr	Fe	Nd	V	Ni	Mn
0	0.00	0.97	0.00	0.11	0.20	0.31	98.01	0.00	0.00	0.42
1	0.00	1.66	0.00	0.02	0.00	0.37	97.78	0.00	0.18	0.00
2	0.00	2.26	0.04	0.07	0.00	0.35	96.74	0.08	0.00	0.46
3	0.00	3.15	0.05	0.00	0.03	0.35	95.88	0.09	0.00	0.46
4	0.00	4.27	0.00	0.00	0.00	0.41	94.69	0.02	0.18	0.43
5	0.00	7.22	0.00	0.12	0.00	0.32	91.91	0.01	0.03	0.39
6	0.00	42.17	0.00	0.12	0.02	0.27	56.50	0.42	0.08	0.42
7	0.00	97.03	0.00	0.01	0.00	0.01	2.41	0.51	0.00	0.04
8	0.00	96.46	0.00	0.00	0.00	0.00	3.17	0.31	0.01	0.04
9	0.00	98.61	0.00	0.01	0.00	0.03	1.03	0.32	0.00	0.00

10	0.00	88.81	0.00	0.00	0.02	0.14	10.55	0.37	0.00	0.12
11	0.00	99.44	0.00	0.02	0.01	0.04	0.14	0.30	0.00	0.06
12	0.00	99.64	0.00	0.00	0.00	0.01	0.05	0.28	0.00	0.03
13	0.00	99.55	0.00	0.03	0.01	0.01	0.08	0.33	0.00	0.00
14	0.00	99.54	0.00	0.00	0.04	0.02	0.07	0.32	0.02	0.00
15	0.00	99.54	0.00	0.01	0.00	0.03	0.03	0.29	0.05	0.04

B.55 HT-9/Ta/V/Nd After 28 Days at 700°C

The HT-9/Ta/V/Nd assembly annealed for 28 days at 700°C bonded on the V/Nd interface but not the HT-9/Ta or Ta/V interfaces. Compositional data (in at%) from WDS linescans across the V/Nd interface is given below.

Position	Ta	Ti	Mo	W	Cr	Fe	Nd	V	Ni	Mn
0	0.00	0.00	0.09	0.02	0.02	0.36	98.03	1.05	0.01	0.41
1	0.00	0.00	0.05	0.06	0.14	0.29	97.58	0.99	0.12	0.77
2	0.00	0.00	0.17	0.04	0.00	0.26	98.28	1.01	0.00	0.24
3	0.00	0.01	0.01	0.14	0.02	0.41	97.78	1.24	0.01	0.38
4	0.00	0.00	0.03	0.05	0.08	0.40	97.76	1.35	0.01	0.32
5	0.00	0.00	0.00	0.03	0.05	0.33	97.49	1.62	0.04	0.45
6	0.00	0.00	0.00	0.04	0.11	0.56	95.32	3.40	0.26	0.32
7	0.00	0.00	0.05	0.02	0.99	1.18	46.25	51.25	0.02	0.24
8	0.00	0.00	0.19	0.01	1.68	9.74	23.77	64.39	0.03	0.18
9	0.00	0.00	0.14	0.00	1.80	8.49	9.81	79.76	0.00	0.00
10	0.00	0.00	0.10	0.00	2.03	4.80	6.35	86.64	0.00	0.08
11	0.00	0.00	0.02	0.01	1.85	3.49	1.29	93.32	0.00	0.02
12	0.00	0.01	0.00	0.01	1.87	0.66	0.89	96.57	0.00	0.00
13	0.00	0.00	0.00	0.00	1.75	0.14	0.44	97.62	0.04	0.00
14	0.00	0.00	0.00	0.01	1.82	0.05	0.15	97.98	0.00	0.00
15	0.00	0.00	0.00	0.00	1.76	0.03	0.15	98.04	0.00	0.02

B.56 HT-9/Ta/Nd After 28 Days at 700°C

The HT-9/Ta/Nd assembly annealed for 28 days at 700°C bonded on the Ta/Nd interface but not the HT-9/Ta interface. Compositional data (in at%) from WDS linescans across the Ta/Nd interface is given below.

Position	Ta	Ti	Mo	W	Cr	Fe	Nd	V	Ni	Mn
0	0.00	0.00	0.00	0.01	0.10	0.09	99.39	0.09	0.00	0.33
1	0.00	0.00	0.00	0.00	0.16	0.23	99.23	0.00	0.00	0.38
2	0.00	0.00	0.00	0.01	0.09	0.26	99.17	0.00	0.03	0.44
3	0.00	0.00	0.00	0.21	0.04	0.41	98.91	0.00	0.01	0.41
4	0.00	0.03	0.00	0.11	0.00	0.21	99.10	0.11	0.00	0.44
5	0.00	0.00	0.01	0.00	0.00	0.48	98.87	0.00	0.00	0.64
6	0.87	0.00	0.00	0.02	0.12	0.52	97.63	0.07	0.10	0.69
7	6.88	0.00	0.00	0.20	0.01	0.34	91.91	0.06	0.17	0.43
8	93.54	0.00	0.17	1.93	0.00	0.26	3.77	0.04	0.08	0.20
9	95.88	0.01	0.00	1.71	0.01	0.27	2.00	0.00	0.08	0.05
10	96.34	0.00	0.11	2.27	0.14	0.00	1.15	0.00	0.00	0.00
11	96.58	0.00	0.02	2.20	0.12	0.23	0.73	0.00	0.00	0.13
12	96.88	0.00	0.10	2.13	0.16	0.00	0.65	0.00	0.00	0.09
13	96.83	0.01	0.07	2.01	0.00	0.00	0.84	0.00	0.25	0.00

14	96.70	0.00	0.00	2.01	0.05	0.10	0.88	0.00	0.26	0.00
15	95.82	0.00	0.16	2.31	0.00	0.09	1.31	0.09	0.24	0.00
0	0.00	0.03	0.00	0.04	0.17	1.90	97.34	0.00	0.13	0.40
1	0.00	0.00	0.00	0.08	0.00	0.82	98.49	0.06	0.00	0.54
2	0.00	0.00	0.00	0.00	0.00	0.46	98.90	0.02	0.26	0.37
3	0.00	0.00	0.00	0.05	0.00	0.51	98.93	0.00	0.01	0.51
4	0.00	0.00	0.00	0.00	0.15	0.47	98.77	0.06	0.08	0.47
5	0.00	0.00	0.01	0.00	0.00	0.22	99.00	0.00	0.13	0.64
6	0.00	0.00	0.00	0.00	0.00	0.38	99.31	0.00	0.00	0.32
7	0.00	0.00	0.00	0.05	0.00	0.41	99.18	0.00	0.00	0.36
8	12.19	0.00	0.07	0.20	0.19	0.43	86.58	0.00	0.01	0.35
9	87.41	0.00	0.00	1.72	0.00	0.23	10.48	0.13	0.00	0.03
10	95.38	0.00	0.11	1.83	0.00	0.13	1.87	0.12	0.45	0.11
11	86.70	0.00	0.15	1.66	0.01	0.09	11.04	0.00	0.15	0.20
12	96.63	0.00	0.04	2.10	0.00	0.00	1.04	0.06	0.06	0.08
13	96.67	0.02	0.00	2.11	0.00	0.00	1.19	0.00	0.00	0.01
14	92.71	0.00	0.12	1.87	0.00	0.19	4.74	0.00	0.03	0.34
15	95.73	0.01	0.12	2.47	0.20	0.00	1.41	0.00	0.00	0.06

B.57 HT-9/Mo/V/Nd After 28 Days at 700°C

The HT-9/Mo/V/Nd assembly annealed for 28 days at 700°C bonded on the V/Nd interface but not the HT-9/Mo or Mo/V interfaces. Since the V/Nd interface at this time and temperature was already well characterized, no WDS linescans were completed on it in this assembly.

B.58 HT-9/Mo/Nd After 28 Days at 700°C

The HT-9/Mo/Nd assembly annealed for 28 days at 700°C bonded on the Mo/Nd interface but not the HT-9/Mo interface. Compositional data (in at%) from WDS linescans across the Mo/Nd interface is given below.

Position	V	W	Mo	Nd	Ni	Fe	Mn	Cr
0	0.00	0.10	0.07	98.75	0.23	0.34	0.43	0.09
1	0.00	0.17	0.05	97.98	0.00	0.83	0.75	0.22
2	0.02	0.00	0.01	98.93	0.26	0.35	0.36	0.06
3	0.06	0.00	0.08	98.97	0.00	0.59	0.30	0.00
4	0.00	0.07	0.00	99.00	0.00	0.60	0.33	0.00
5	0.14	0.00	0.10	98.41	0.00	0.45	0.62	0.27
6	0.10	0.00	1.38	97.64	0.00	0.55	0.34	0.00
7	0.00	0.00	18.22	79.07	0.28	1.68	0.34	0.40
8	0.00	0.05	1.35	97.13	0.04	0.63	0.80	0.00
9	0.15	0.01	0.39	98.33	0.00	0.52	0.50	0.11
10	0.15	0.12	1.22	96.78	0.07	1.26	0.36	0.03
11	0.02	0.01	4.99	93.92	0.00	0.65	0.36	0.05
12	0.11	0.00	55.22	42.04	0.00	1.26	0.17	1.20
13	0.05	0.00	80.50	17.61	0.17	1.17	0.00	0.51
14	0.01	0.00	97.06	2.68	0.00	0.22	0.00	0.03
15	0.27	0.06	99.00	0.47	0.07	0.13	0.00	0.00

0	0.10	0.04	0.11	98.47	0.00	0.63	0.60	0.04
1	0.05	0.00	9.93	88.29	0.13	0.84	0.58	0.17
2	0.11	0.00	50.39	48.23	0.00	0.39	0.38	0.49
3	0.02	0.00	80.96	16.55	0.00	1.00	0.14	1.34
4	0.00	0.03	82.32	16.05	0.00	0.88	0.01	0.71
5	0.00	0.04	86.88	11.50	0.00	0.89	0.00	0.69
6	0.05	0.04	97.63	1.50	0.03	0.50	0.08	0.18
7	0.13	0.00	99.32	0.44	0.00	0.04	0.00	0.06
8	0.06	0.01	99.54	0.18	0.00	0.07	0.09	0.05
9	0.00	0.00	99.64	0.32	0.00	0.01	0.03	0.00
10	0.13	0.00	99.43	0.37	0.03	0.04	0.00	0.00
11	0.00	0.00	99.07	0.78	0.02	0.13	0.00	0.00
12	0.07	0.00	99.06	0.79	0.00	0.00	0.00	0.09
13	0.00	0.00	98.40	1.08	0.28	0.24	0.00	0.00
14	0.00	0.00	99.00	0.84	0.00	0.09	0.00	0.08
15	0.00	0.00	98.92	0.79	0.14	0.08	0.00	0.09
0	0.03	0.00	0.00	98.99	0.28	0.24	0.42	0.03
1	0.11	0.00	0.10	99.00	0.03	0.35	0.41	0.00
2	0.19	0.15	0.36	98.57	0.00	0.33	0.40	0.00
3	0.30	0.00	0.18	98.24	0.03	0.65	0.51	0.11
4	0.03	0.00	0.04	99.08	0.00	0.19	0.63	0.04
5	0.23	0.02	0.08	98.80	0.01	0.39	0.48	0.00
6	0.00	0.00	0.31	98.44	0.00	0.42	0.83	0.00
7	0.17	0.01	27.78	70.90	0.35	0.40	0.19	0.21
8	0.43	0.00	0.10	98.35	0.18	0.41	0.53	0.00
9	0.12	0.13	0.08	98.64	0.00	0.36	0.62	0.06
10	0.00	0.01	1.03	98.28	0.00	0.28	0.32	0.08
11	0.02	0.11	42.90	55.73	0.00	0.60	0.21	0.44
12	0.05	0.07	78.70	20.43	0.15	0.36	0.11	0.14
13	0.06	0.02	97.98	1.76	0.13	0.06	0.00	0.00
14	0.00	0.02	99.65	0.21	0.00	0.00	0.12	0.00
15	0.00	0.00	99.62	0.31	0.02	0.01	0.02	0.02

B.59 HT-9/W/V/Nd After 28 Days at 700°C

The HT-9/W/V/Nd assembly annealed for 28 days at 700°C did not bond on any interfaces.

B.60 HT-9/W/Nd After 28 Days at 700°C

The HT-9/W/Nd assembly annealed for 28 days at 700°C bonded on the W/Nd interface but not the HT-9/W interface. Compositional data (in at%) from WDS linescans across the W/Nd interface is given below.

Position	V	W	Mo	Nd	Ni	Fe	Mn	Cr
0	0.09	99.49	0.00	0.25	0.00	0.07	0.10	0.00
1	0.00	99.24	0.00	0.19	0.00	0.23	0.00	0.34
2	0.00	98.81	0.00	0.51	0.11	0.41	0.09	0.07
3	0.00	99.41	0.00	0.51	0.00	0.08	0.00	0.00
4	0.24	99.24	0.00	0.51	0.00	0.00	0.00	0.00

5	0.18	98.75	0.00	0.72	0.00	0.29	0.00	0.07
6	0.00	97.65	0.00	1.40	0.26	0.22	0.35	0.12
7	0.00	95.02	0.00	3.98	0.14	0.66	0.19	0.00
8	0.03	95.36	0.00	3.47	0.00	0.95	0.07	0.11
9	0.16	0.13	0.18	83.16	0.00	12.50	0.33	3.55
10	0.00	0.00	0.00	99.54	0.00	0.00	0.46	0.00
11	0.05	0.25	0.70	74.56	0.10	14.94	0.61	8.79
12	0.10	0.00	0.15	97.12	0.05	1.87	0.33	0.39
13	0.00	0.30	0.00	97.06	0.00	1.40	1.04	0.20
14	0.00	0.20	0.00	98.76	0.00	0.56	0.48	0.01
15	0.02	0.25	0.00	98.67	0.00	0.62	0.35	0.10
0	0.45	98.99	0.00	0.23	0.00	0.17	0.07	0.10
1	0.05	99.42	0.00	0.41	0.00	0.08	0.00	0.04
2	0.04	99.20	0.00	0.39	0.23	0.15	0.00	0.00
3	0.00	98.53	0.00	1.14	0.06	0.22	0.01	0.04
4	0.21	74.52	0.00	24.85	0.00	0.42	0.00	0.00
5	0.18	5.58	0.00	93.25	0.00	0.60	0.39	0.00
6	0.00	0.00	0.00	98.46	0.44	0.82	0.28	0.00
7	0.00	0.67	0.09	97.84	0.00	0.75	0.66	0.00
8	0.00	5.33	0.00	93.26	0.05	0.48	0.81	0.08
9	0.00	0.68	0.02	97.81	0.02	0.81	0.59	0.07
10	0.00	0.64	0.00	98.01	0.04	0.65	0.57	0.09
11	0.00	0.14	0.03	98.64	0.23	0.50	0.47	0.00
12	0.00	0.00	0.02	97.71	0.11	1.68	0.32	0.17
13	0.00	0.15	0.00	97.69	0.12	1.49	0.46	0.09
14	0.03	0.10	0.02	98.96	0.14	0.59	0.16	0.00
15	0.09	0.35	0.00	98.23	0.00	0.68	0.66	0.00
0	0.10	99.75	0.00	0.00	0.03	0.08	0.04	0.00
1	0.09	98.95	0.00	0.44	0.24	0.13	0.14	0.00
2	0.01	99.20	0.00	0.40	0.16	0.00	0.09	0.15
3	0.07	98.92	0.00	0.64	0.29	0.04	0.00	0.03
4	0.08	95.37	0.00	3.47	0.31	0.53	0.18	0.07
5	0.12	87.84	0.00	10.81	0.34	0.71	0.00	0.19
6	0.25	83.50	0.00	15.46	0.00	0.71	0.00	0.08
7	0.00	16.57	0.05	82.33	0.00	0.64	0.38	0.04
8	0.15	2.55	0.05	94.56	0.00	1.95	0.48	0.27
9	0.04	2.54	0.00	92.97	0.25	3.20	0.68	0.32
10	0.04	1.51	0.01	95.72	0.26	1.77	0.68	0.02
11	0.00	0.73	0.08	96.83	0.02	1.46	0.47	0.41
12	0.18	2.17	0.00	94.78	0.00	2.06	0.37	0.45
13	0.26	2.14	0.00	96.75	0.00	0.38	0.47	0.00
14	0.00	2.91	0.00	95.44	0.00	0.91	0.56	0.18
15	0.34	5.20	0.00	91.25	0.00	2.30	0.48	0.42

APPENDIX C: SUMMARY OF G.91 INTERFACES

C.1 G.91/Nd After 28 Days at 550°C

After annealing for 28 days at 550°C, the first interaction zone in the G.91/Nd assembly was ~13 μm wide with a composition matching Nd₂(Fe+Cr)₁₇. In the last few microns of the zone, these precipitates were dense enough in some areas to effectively form a second Nd₅(Fe+Cr)₁₇ zone, up to ~2 μm wide. The third and final interaction zone was ~2 μm wide with a composition matching Fe₂Nd. Compositional data (in at%) from WDS linescans across the G.91/Nd interface is given below.

Position	Zr	Mo	Si	Cr	Fe	Nd	V	Mn
0	0.01	0.54	0.35	9.09	89.12	0.17	0.19	0.53
1	0.00	0.52	0.37	9.10	89.25	0.15	0.20	0.40
2	0.00	0.40	0.38	9.07	88.18	0.19	0.50	1.30
3	0.01	0.52	0.64	8.94	88.93	0.38	0.22	0.37
4	0.00	0.53	0.33	8.88	89.34	0.28	0.22	0.43
5	0.00	0.55	0.88	8.86	87.21	1.87	0.22	0.40
6	0.00	0.53	1.89	8.93	84.60	3.49	0.22	0.34
7	0.00	0.53	1.05	10.09	79.32	8.37	0.29	0.36
8	0.00	0.65	0.59	10.74	73.90	13.31	0.30	0.52
9	0.00	0.65	0.59	11.15	73.51	13.23	0.36	0.52
10	0.00	0.67	0.81	11.60	72.40	13.64	0.40	0.49
11	0.01	0.66	1.59	9.59	65.86	21.36	0.44	0.49
12	0.00	0.25	1.85	9.21	61.18	26.14	0.88	0.48
13	0.01	0.62	2.86	8.29	64.65	22.98	0.21	0.40
14	0.00	0.61	1.74	10.10	65.94	20.91	0.25	0.45
15	0.00	0.76	0.07	12.51	64.83	20.96	0.40	0.47
16	0.00	0.81	0.10	12.12	63.21	23.02	0.33	0.41
17	0.00	0.83	0.14	12.80	66.76	18.59	0.37	0.51
18	0.00	0.82	0.14	12.09	59.97	26.16	0.38	0.44
19	0.03	0.86	0.12	10.46	53.88	33.89	0.30	0.46
20	0.01	0.74	0.21	9.41	46.07	42.73	0.36	0.48
21	0.02	0.83	0.14	11.86	49.47	36.83	0.38	0.47
22	0.00	0.56	0.47	6.67	35.19	56.42	0.33	0.37
23	0.00	0.08	4.95	2.16	58.15	34.20	0.00	0.46
24	0.00	0.08	4.41	2.27	55.92	36.93	0.00	0.40
25	0.00	0.00	0.34	0.31	4.07	94.80	0.00	0.48
26	0.01	0.00	0.21	0.10	0.84	98.25	0.01	0.59
27	0.00	0.03	0.68	0.08	0.64	97.99	0.00	0.59
28	0.00	0.00	0.84	0.10	0.57	97.98	0.04	0.46
29	0.04	0.10	0.38	0.17	0.72	98.11	0.00	0.49
30	0.00	0.04	0.26	9.54	1.76	87.89	0.03	0.49
31	0.00	0.38	0.26	28.81	6.39	63.66	0.00	0.50
32	0.02	0.04	0.18	10.41	1.91	87.06	0.00	0.39
33	0.00	0.00	0.24	0.43	0.60	98.24	0.00	0.49
34	0.00	0.00	0.65	0.00	0.46	98.35	0.10	0.45
35	0.00	0.00	0.29	0.16	0.48	98.61	0.01	0.45
0	0.00	0.00	0.13	0.12	0.58	98.69	0.03	0.45

1	0.00	0.00	0.22	0.04	0.50	98.86	0.00	0.39
2	0.03	0.00	0.29	0.05	0.38	98.79	0.02	0.44
3	0.04	0.01	0.43	0.07	0.51	98.39	0.02	0.54
4	0.00	0.00	0.84	0.00	0.57	98.13	0.08	0.38
5	0.00	0.00	0.72	0.25	1.90	96.81	0.01	0.31
6	0.00	0.03	1.34	0.29	1.01	96.95	0.04	0.34
7	0.00	0.00	13.54	0.30	0.89	84.85	0.00	0.41
8	0.00	0.00	1.23	0.29	1.04	97.10	0.02	0.31
9	0.03	0.00	41.29	0.37	0.83	57.19	0.02	0.26
10	0.00	0.02	77.59	2.57	0.58	19.11	0.04	0.10
11	0.01	0.29	24.42	5.53	8.44	60.87	0.16	0.28
12	0.00	0.84	1.26	10.28	58.50	28.31	0.32	0.49
13	0.00	0.94	1.46	11.39	65.04	20.39	0.35	0.44
14	0.00	0.66	0.74	8.57	44.46	44.83	0.24	0.50
15	0.00	0.85	1.38	12.39	67.12	17.51	0.32	0.44
16	0.00	0.90	1.50	11.75	65.79	19.40	0.30	0.36
17	0.00	0.84	1.37	12.38	67.42	17.21	0.32	0.46
18	0.00	0.77	1.02	12.49	70.15	14.74	0.31	0.53
19	0.00	0.66	1.32	11.51	69.39	16.30	0.30	0.53
20	0.00	0.66	1.10	12.28	70.68	14.42	0.30	0.56
21	0.00	0.65	0.92	12.04	71.02	14.57	0.36	0.44
22	0.00	0.63	0.89	11.49	71.73	14.49	0.30	0.49
23	0.01	0.68	0.52	11.48	74.73	11.84	0.25	0.49
24	0.00	0.66	0.37	11.33	75.74	11.19	0.27	0.44
25	0.00	0.52	0.36	9.04	86.15	3.36	0.23	0.35
26	0.00	0.56	0.35	8.73	89.05	0.65	0.22	0.45
27	0.01	0.49	0.34	8.68	89.60	0.26	0.27	0.36
28	0.00	0.55	0.39	8.86	89.36	0.26	0.21	0.38
29	0.00	0.54	0.38	9.15	89.12	0.25	0.22	0.35
30	0.00	0.67	0.35	10.78	87.41	0.18	0.22	0.39
31	0.00	0.65	0.39	10.55	87.69	0.13	0.25	0.35
32	0.00	0.74	0.30	11.15	87.12	0.09	0.22	0.39
33	0.01	0.74	0.28	11.11	87.07	0.11	0.29	0.39
34	0.00	0.57	0.33	9.69	88.54	0.25	0.25	0.38
35	0.00	0.61	0.30	9.20	89.10	0.27	0.23	0.30
0	0.00	0.03	0.17	0.12	0.40	98.72	0.01	0.56
1	0.05	0.04	0.19	0.22	0.57	98.30	0.01	0.62
2	0.00	0.00	0.13	0.13	0.49	98.66	0.06	0.53
3	0.00	0.04	0.31	0.04	0.76	98.39	0.03	0.44
4	0.00	0.07	0.42	0.27	1.04	97.57	0.00	0.63
5	0.00	0.03	0.36	0.22	0.91	98.10	0.00	0.39
6	0.07	0.00	0.48	0.30	1.06	97.59	0.00	0.51
7	0.02	0.00	0.63	0.14	1.07	97.65	0.06	0.43
8	0.03	0.00	0.70	0.25	1.38	97.14	0.00	0.51
9	0.25	0.00	0.71	0.41	3.15	94.92	0.01	0.55
10	0.08	0.02	0.87	0.40	2.81	95.29	0.04	0.50
11	0.00	0.09	0.69	0.93	5.31	92.24	0.07	0.66
12	0.01	0.69	1.76	9.11	59.40	28.29	0.28	0.46
13	0.00	0.85	1.31	10.14	66.07	20.85	0.36	0.42
14	0.00	0.91	1.55	11.48	65.22	19.93	0.44	0.48
15	0.00	0.76	1.26	11.73	65.27	20.08	0.41	0.50
16	0.02	0.78	1.81	10.97	67.18	18.37	0.43	0.44
17	0.01	0.86	1.36	11.59	68.55	16.85	0.34	0.45
18	0.02	0.75	1.75	10.54	65.86	20.44	0.29	0.37
19	0.00	0.71	1.52	10.51	67.62	18.82	0.31	0.51
20	0.00	0.60	1.34	10.69	70.39	16.19	0.33	0.46

21	0.00	0.63	1.33	10.67	70.46	16.07	0.28	0.57
22	0.00	0.65	1.25	10.62	70.46	16.23	0.35	0.45
23	0.01	0.70	0.81	11.49	71.85	14.43	0.23	0.49
24	0.01	0.67	1.10	10.58	70.77	16.13	0.25	0.49
25	0.00	0.65	0.93	10.02	75.31	12.42	0.30	0.38
26	0.02	0.64	0.83	10.59	76.71	10.48	0.37	0.36
27	0.01	0.56	0.50	9.53	84.89	3.92	0.24	0.36
28	0.00	0.60	0.32	8.93	89.13	0.49	0.22	0.32
29	0.00	0.53	0.58	9.56	82.96	5.67	0.31	0.39
30	0.00	0.55	0.33	8.75	89.47	0.29	0.24	0.38
31	0.00	0.57	0.34	8.95	89.39	0.17	0.26	0.32
32	0.00	0.63	0.34	9.03	89.24	0.20	0.25	0.32
33	0.00	0.56	0.47	8.68	89.53	0.18	0.26	0.32
34	0.00	0.57	1.08	8.76	88.64	0.15	0.38	0.41
35	0.00	0.52	0.37	8.50	89.88	0.15	0.26	0.33
0	0.00	0.46	5.77	8.75	82.59	1.86	0.24	0.32
1	0.00	0.50	4.30	8.64	84.83	1.12	0.24	0.37
2	0.00	0.53	2.02	8.79	87.57	0.50	0.23	0.36
3	0.00	0.53	0.53	8.84	89.05	0.44	0.25	0.36
4	0.00	0.45	0.43	8.91	88.36	1.22	0.27	0.34
5	0.00	0.52	3.48	9.36	82.46	3.53	0.26	0.39
6	0.00	0.55	14.63	8.97	68.37	6.96	0.21	0.32
7	0.01	0.54	13.15	9.84	66.19	9.66	0.24	0.39
8	0.00	0.66	3.80	11.21	71.60	11.99	0.28	0.47
9	0.02	0.64	0.76	11.89	73.03	13.05	0.24	0.38
10	0.00	0.72	0.66	12.31	72.40	13.12	0.30	0.50
11	0.00	0.73	0.72	12.55	71.39	13.85	0.29	0.49
12	0.00	0.70	0.89	12.32	70.12	15.12	0.34	0.51
13	0.00	0.75	0.95	12.51	69.19	15.82	0.30	0.49
14	0.00	0.74	1.01	12.64	67.82	16.95	0.32	0.52
15	0.00	0.79	0.97	12.71	67.19	17.55	0.29	0.51
16	0.00	0.74	0.97	12.74	66.89	17.90	0.27	0.50
17	0.01	0.77	0.83	12.84	66.17	18.65	0.29	0.45
18	0.00	0.81	0.53	13.00	64.21	20.67	0.31	0.49
19	0.00	0.85	0.22	12.45	62.20	23.50	0.32	0.46
20	0.01	0.79	0.41	11.78	60.73	25.47	0.34	0.49
21	0.03	0.81	0.99	10.75	61.09	25.59	0.32	0.42
22	0.00	0.75	1.27	10.21	59.20	27.84	0.34	0.40
23	0.00	0.11	0.23	1.41	6.65	90.98	0.10	0.52
24	0.12	0.00	0.21	0.25	1.19	97.88	0.00	0.35
25	0.00	0.00	0.30	0.09	0.72	98.46	0.00	0.43
0	0.00	0.56	0.84	9.27	88.31	0.33	0.25	0.44
1	0.00	0.58	0.93	9.51	88.10	0.29	0.25	0.35
2	0.00	0.56	1.51	9.37	87.37	0.67	0.23	0.30
3	0.01	0.54	0.78	9.86	84.66	3.52	0.25	0.38
4	0.00	0.55	0.53	10.25	80.92	7.15	0.29	0.31
5	0.00	0.66	0.55	10.89	75.43	11.75	0.31	0.42
6	0.00	0.63	0.48	9.93	84.16	4.19	0.30	0.31
7	0.00	0.59	0.53	10.40	80.47	7.30	0.34	0.37
8	0.00	0.68	0.51	10.80	76.52	10.79	0.31	0.39
9	0.00	0.68	0.62	11.20	73.56	13.14	0.34	0.47
10	0.04	0.73	0.77	11.82	69.41	16.70	0.00	0.54
11	0.00	0.69	0.50	12.06	66.37	19.57	0.31	0.49
12	0.00	0.69	0.40	12.26	65.01	20.81	0.35	0.48
13	0.01	0.69	0.76	11.70	69.95	16.12	0.33	0.44

14	0.04	0.69	0.78	11.87	68.72	17.11	0.33	0.45
15	0.02	0.64	0.53	12.12	66.18	19.75	0.30	0.46
16	0.01	0.71	0.37	12.28	64.43	21.50	0.28	0.44
17	0.00	0.77	0.25	12.47	64.56	21.17	0.29	0.49
18	0.05	0.79	0.22	12.46	64.95	20.76	0.32	0.47
19	0.00	0.83	0.24	11.97	62.73	23.50	0.33	0.40
20	0.00	0.89	0.18	11.69	57.12	29.09	0.38	0.65
21	0.00	0.78	0.40	10.42	48.57	38.85	0.45	0.52
22	0.00	0.54	0.72	6.79	31.86	59.42	0.28	0.39
23	0.00	0.07	0.69	1.23	5.31	92.15	0.06	0.49
24	0.13	0.06	0.64	0.48	2.13	96.09	0.00	0.47
25	0.00	0.04	0.49	0.16	0.89	97.97	0.00	0.45
0	0.00	0.52	4.36	8.75	85.56	0.18	0.25	0.38
1	0.00	0.58	0.67	9.21	88.66	0.22	0.28	0.39
2	0.01	0.55	0.55	8.98	88.92	0.31	0.29	0.39
3	0.00	0.57	0.47	9.23	88.27	0.81	0.29	0.36
4	0.00	0.00	0.68	10.23	83.91	4.57	0.29	0.34
5	0.00	0.62	1.15	10.96	78.24	8.26	0.31	0.46
6	0.00	0.68	1.06	11.43	76.13	10.01	0.26	0.43
7	0.00	0.64	0.99	11.53	75.38	10.76	0.27	0.43
8	0.00	0.74	0.79	12.14	72.99	12.64	0.30	0.40
9	0.01	0.75	0.81	12.24	71.31	14.13	0.32	0.44
10	0.01	0.76	0.82	12.36	70.80	14.48	0.32	0.46
11	0.00	0.69	1.00	12.10	69.96	15.40	0.32	0.53
12	0.01	0.72	1.11	12.06	69.52	15.83	0.31	0.44
13	0.00	0.71	1.25	11.87	68.32	17.10	0.34	0.41
14	0.00	0.68	1.19	11.69	68.04	17.62	0.31	0.47
15	0.00	0.71	1.37	11.47	63.71	21.92	0.36	0.46
16	0.00	0.70	1.35	11.02	64.64	21.44	0.32	0.53
17	0.00	0.73	1.49	11.06	63.79	22.16	0.30	0.48
18	0.00	0.84	0.70	11.11	54.01	32.49	0.40	0.46
19	0.06	1.05	0.92	10.95	48.38	37.78	0.43	0.44
20	0.00	0.83	0.86	11.09	41.32	33.74	0.35	0.54
21	0.06	0.52	0.51	8.48	42.83	36.21	0.33	0.56
22	0.00	0.95	0.94	11.04	46.19	40.04	0.41	0.42
23	0.00	0.62	0.77	10.04	29.52	58.39	0.29	0.38
24	0.00	0.22	0.17	4.26	6.52	88.32	0.07	0.45
25	0.00	0.05	0.16	0.70	1.04	97.51	0.01	0.53
0	0.00	0.50	0.53	8.89	88.82	0.67	0.24	0.35
1	0.00	0.51	0.65	8.88	87.18	2.17	0.21	0.40
2	0.00	0.56	0.92	9.25	85.15	3.59	0.21	0.32
3	0.01	0.55	2.52	9.45	80.72	6.11	0.23	0.41
4	0.00	0.60	6.08	10.19	70.15	12.24	0.28	0.47
5	0.03	0.63	5.47	10.79	68.93	13.37	0.25	0.54
6	0.00	0.65	4.60	11.01	69.38	13.57	0.26	0.54
7	0.01	0.66	1.08	11.97	69.78	15.78	0.27	0.46
8	0.03	0.77	1.32	12.27	68.11	16.79	0.28	0.42
9	0.00	0.78	1.23	12.47	68.29	16.39	0.34	0.51
10	0.00	0.78	1.37	12.46	67.48	17.18	0.30	0.43
11	0.03	0.77	1.72	11.69	66.82	18.27	0.28	0.42
12	0.02	0.82	1.23	12.62	68.34	16.27	0.30	0.39
13	0.00	0.77	1.22	12.56	67.86	16.78	0.33	0.47
14	0.00	0.80	1.69	11.77	66.94	18.10	0.29	0.41
15	0.02	0.88	0.66	13.30	66.28	18.04	0.39	0.42
16	0.03	0.90	0.51	13.30	64.62	19.66	0.43	0.55

17	0.00	0.82	0.55	12.23	61.39	24.13	0.42	0.47
18	0.02	0.88	0.73	13.38	66.19	17.98	0.38	0.45
19	0.00	0.86	0.45	12.98	63.81	21.04	0.44	0.42
20	0.00	0.86	0.51	12.30	62.00	23.49	0.39	0.45
21	0.00	0.90	0.69	11.73	59.80	26.02	0.40	0.47
22	0.00	0.76	0.97	11.07	58.61	27.66	0.41	0.52
23	0.02	0.83	1.16	10.48	55.37	31.66	0.00	0.48
24	0.01	0.71	1.38	9.58	50.30	37.27	0.38	0.36
25	0.01	0.40	2.65	5.60	51.84	38.86	0.22	0.42
26	0.07	0.45	2.12	6.18	50.44	40.12	0.23	0.39
27	0.00	0.27	3.34	4.33	54.08	37.44	0.14	0.39
28	0.00	0.05	4.05	1.96	55.32	38.22	0.01	0.40
29	0.05	0.00	0.16	0.05	0.64	98.65	0.03	0.42
30	0.00	0.00	0.17	0.01	0.68	98.53	0.05	0.57

C.2 G.91/V/Nd After 28 Days at 550°C

The G.91/V/Nd assembly annealed for 28 days at 550°C bonded on the V/Nd interface but not the G.91/V interface. Compositional data (in at%) from WDS linescans across the V/Nd interface is given below.

Position	Zr	Mo	Si	Cr	Fe	Nd	V	Mn
0	0.00	0.01	0.38	2.04	0.02	0.14	97.38	0.02
1	0.00	0.00	0.29	2.09	0.03	0.40	97.19	0.01
2	0.02	0.01	0.87	2.11	0.18	1.62	95.18	0.02
3	0.02	0.00	0.20	2.10	0.07	0.32	97.29	0.00
4	0.00	0.01	0.56	2.14	0.12	0.88	96.30	0.00
5	0.00	0.00	0.06	2.03	0.26	0.24	97.42	0.00
6	0.00	0.02	0.17	1.96	3.02	0.34	94.49	0.00
7	0.00	0.05	1.53	0.40	31.53	40.31	26.13	0.06
8	0.01	0.00	0.39	0.10	1.69	91.80	5.78	0.24
9	0.00	0.07	0.40	0.00	1.18	93.97	3.92	0.46
10	0.00	0.05	0.26	0.02	0.48	95.80	2.92	0.46
11	0.00	0.00	0.63	0.08	1.10	95.47	2.32	0.41
12	0.00	0.00	1.30	0.05	0.41	95.83	1.86	0.55
13	0.00	0.00	1.07	0.04	0.44	96.53	1.52	0.41
14	0.02	0.09	0.17	0.00	0.47	97.35	1.35	0.55
15	0.00	0.00	3.75	0.00	0.49	94.25	1.08	0.44

C.3 G.91/Zr/V/Nd After 28 Days at 550°C

The G.91/Zr/V/Nd assembly annealed for 28 days at 550°C bonded on the V/Nd interface but not the G.91/Zr or Zr/V interfaces. Compositional data (in at%) from WDS linescans across the V/Nd interface is given below.

Position	Zr	Mo	Si	Cr	Fe	Nd	V	Mn
0	0.01	0.00	0.25	1.98	0.30	0.26	97.20	0.00
1	0.01	0.01	0.20	2.02	0.36	0.22	97.20	0.00
2	0.09	0.06	1.86	0.31	1.76	83.22	12.24	0.47
3	0.04	0.00	0.42	0.04	0.37	94.30	4.36	0.47
4	0.03	0.00	0.69	0.09	0.33	95.42	3.02	0.43
5	0.57	0.05	3.77	0.09	0.36	92.45	2.26	0.47

6	0.08	0.00	0.85	0.04	0.49	93.46	4.57	0.51
7	0.01	0.00	1.98	0.00	0.38	94.91	2.23	0.48
8	0.00	0.00	2.42	0.05	0.29	95.53	1.24	0.48
9	0.00	0.05	1.83	0.08	0.25	96.27	1.01	0.51
10	0.00	0.00	1.14	0.01	0.34	95.44	2.52	0.56
11	0.07	0.07	1.42	0.22	0.48	91.46	5.57	0.72
12	0.06	0.06	1.97	0.00	0.49	95.15	1.98	0.29
13	0.01	0.02	1.51	0.00	0.44	96.70	0.70	0.62
14	0.00	0.00	1.53	0.00	0.36	96.78	1.03	0.30
15	0.20	0.00	2.88	0.16	1.51	93.96	0.79	0.50

C.4 G.91/Zr/Nd After 28 Days at 550°C

The G.91/Zr/Nd assembly annealed for 28 days at 550°C bonded on the Zr/Nd interface but not the G.91/Zr interface. Compositional data (in at%) from WDS linescans across the Zr/Nd interface is given below.

Position	Zr	Mo	Si	Cr	Fe	Nd	V	Mn
0	0.05	0.00	0.00	0.00	0.32	99.11	0.00	0.52
1	0.13	0.00	0.36	0.00	0.41	98.42	0.10	0.59
2	0.03	0.01	0.35	0.00	0.40	98.65	0.00	0.57
3	1.04	0.01	0.41	0.00	0.39	97.65	0.04	0.47
4	5.88	0.00	0.52	0.00	0.49	92.69	0.00	0.42
5	21.54	0.00	1.77	0.00	0.57	75.74	0.00	0.37
6	82.13	0.01	1.93	0.07	0.61	15.19	0.00	0.06
7	99.08	0.01	0.11	0.01	0.12	0.68	0.00	0.00
8	99.05	0.00	0.09	0.03	0.00	0.77	0.04	0.03
9	99.12	0.00	0.10	0.00	0.05	0.66	0.00	0.07
10	99.03	0.00	0.00	0.03	0.08	0.82	0.00	0.05
11	99.25	0.00	0.09	0.01	0.04	0.62	0.00	0.00
12	99.14	0.02	0.00	0.01	0.11	0.66	0.05	0.02
13	99.58	0.00	0.06	0.00	0.04	0.33	0.00	0.00
14	99.23	0.00	0.27	0.08	0.08	0.32	0.00	0.03
15	99.46	0.00	0.08	0.02	0.00	0.39	0.05	0.00
0	0.11	0.00	0.40	0.06	0.41	98.60	0.08	0.35
1	0.11	0.01	0.38	0.00	0.44	98.63	0.00	0.43
2	0.16	0.00	0.45	0.06	0.36	98.43	0.01	0.52
3	0.17	0.04	0.49	0.00	0.32	98.62	0.00	0.36
4	0.31	0.00	0.38	0.07	0.59	98.10	0.03	0.52
5	0.86	0.05	0.36	0.11	1.06	97.09	0.00	0.47
6	95.35	0.02	0.16	0.09	0.62	3.69	0.00	0.06
7	93.43	0.04	1.65	0.01	0.30	4.54	0.05	0.00
8	94.98	0.00	0.14	0.17	0.83	3.53	0.36	0.00
9	94.87	0.00	0.74	0.00	0.32	3.95	0.09	0.04
10	90.75	0.00	0.40	0.04	0.29	8.48	0.03	0.01
11	93.12	0.00	0.28	0.04	0.08	6.28	0.04	0.16
12	97.51	0.00	0.53	0.03	0.05	1.89	0.00	0.00
13	98.81	0.00	0.08	0.01	0.27	0.83	0.00	0.00
14	99.44	0.00	0.01	0.01	0.06	0.44	0.03	0.01
15	99.13	0.00	0.19	0.04	0.08	0.56	0.00	0.00

C.5 G.91/Ti/V/Nd After 28 Days at 550°C

The G.91/Ti/V/Nd assembly annealed for 28 days at 550°C bonded on the G.91/Ti and V/Nd interfaces but not the Ti/V interface. Compositional data (in at%) from WDS linescans across the G.91/Ti and V/Nd interfaces is given below.

Position	Ti	Ta	Mo	Si	Cr	Fe	Nd	V	Mn
0	0.90	0.00	0.72	0.33	10.36	87.27	0.00	0.00	0.43
1	1.29	0.00	0.69	0.31	9.89	87.26	0.01	0.20	0.36
2	0.93	0.00	0.71	0.43	9.71	87.55	0.05	0.24	0.40
3	1.72	0.00	0.68	0.50	9.33	87.18	0.00	0.30	0.29
4	1.91	0.00	0.66	0.39	8.96	87.52	0.00	0.26	0.30
5	3.15	0.00	0.53	0.46	8.00	87.50	0.00	0.23	0.13
6	59.01	0.00	0.23	0.22	4.29	35.98	0.00	0.21	0.07
7	99.03	0.00	0.00	0.03	0.03	0.63	0.03	0.25	0.00
8	99.16	0.00	0.00	0.06	0.04	0.43	0.01	0.30	0.01
9	99.35	0.00	0.00	0.02	0.04	0.35	0.00	0.25	0.00
10	99.33	0.00	0.00	0.11	0.02	0.27	0.01	0.27	0.00
11	99.46	0.00	0.00	0.02	0.04	0.22	0.01	0.26	0.00
12	99.49	0.00	0.00	0.02	0.02	0.21	0.00	0.26	0.00
13	99.31	0.00	0.00	0.28	0.04	0.16	0.00	0.21	0.00
14	99.39	0.00	0.00	0.06	0.01	0.20	0.04	0.24	0.06
15	99.57	0.00	0.00	0.04	0.03	0.15	0.00	0.21	0.00
0	0.00	0.00	0.00	0.87	2.48	0.00	0.04	96.60	0.01
1	0.00	0.00	0.00	0.68	2.41	0.01	0.09	96.82	0.00
2	0.00	0.00	0.00	2.79	2.29	0.00	0.10	94.80	0.02
3	0.00	0.00	0.00	0.11	2.33	0.00	0.08	97.46	0.03
4	0.00	0.00	0.00	0.08	2.46	0.00	0.21	97.21	0.04
5	0.00	0.00	0.00	0.30	2.23	1.70	3.43	92.32	0.01
6	0.00	0.00	0.01	0.09	2.39	0.05	0.17	97.28	0.01
7	0.00	0.00	0.02	0.18	2.38	1.01	2.08	94.31	0.02
8	0.00	0.00	0.00	0.45	0.70	3.33	73.30	21.70	0.52
9	0.00	0.00	0.02	1.33	0.00	0.58	93.35	4.57	0.16
10	0.00	0.00	0.03	0.22	0.18	0.41	95.93	3.06	0.16
11	0.00	0.00	0.00	0.31	0.08	0.40	94.82	4.11	0.28
12	0.00	0.00	0.12	0.03	0.00	0.34	97.06	2.07	0.40
13	0.00	0.00	0.06	0.31	0.00	0.34	97.71	1.08	0.51
14	0.00	0.00	0.11	0.21	0.00	0.27	97.97	1.05	0.39
15	0.01	0.00	0.00	0.63	0.00	0.29	97.69	0.84	0.54

C.6 G.91/Ti/Nd After 28 Days at 550°C

The G.91/Ti/Nd assembly annealed for 28 days at 550°C bonded on the Ti/Nd interface but not the G.91/Ti interface. Compositional data (in at%) from WDS linescans across the Ti/Nd interface is given below.

Position	Ti	Ta	Mo	Si	Cr	Fe	Nd	V	Mn
0	0.62	0.00	0.04	0.32	0.14	0.32	98.11	0.05	0.41
1	1.23	0.00	0.01	0.29	0.06	0.35	97.59	0.00	0.48
2	1.60	0.00	0.00	0.22	0.00	0.36	97.40	0.00	0.43
3	2.24	0.00	0.00	0.12	0.06	0.28	96.73	0.00	0.58

4	3.25	0.00	0.00	0.15	0.00	0.33	95.89	0.04	0.34
5	6.84	0.00	0.04	0.33	0.00	0.36	92.15	0.00	0.29
6	47.06	0.00	0.00	0.35	0.05	0.55	51.67	0.27	0.06
7	93.33	0.00	0.00	0.06	0.07	5.49	0.74	0.31	0.01
8	99.14	0.00	0.00	0.02	0.00	0.37	0.20	0.26	0.02
9	99.33	0.00	0.00	0.25	0.01	0.01	0.13	0.27	0.00
10	99.52	0.00	0.00	0.13	0.00	0.00	0.12	0.23	0.00
11	99.51	0.00	0.00	0.10	0.03	0.02	0.07	0.26	0.01
12	99.47	0.00	0.00	0.06	0.00	0.04	0.18	0.25	0.00
13	99.12	0.00	0.00	0.02	0.01	0.13	0.43	0.30	0.00
14	99.35	0.00	0.00	0.07	0.00	0.08	0.24	0.27	0.00
15	99.47	0.00	0.00	0.20	0.00	0.00	0.08	0.26	0.00
0	0.74	0.00	0.08	0.10	0.00	0.33	98.46	0.00	0.29
1	0.65	0.00	0.00	0.14	0.03	0.48	98.25	0.00	0.45
2	0.83	0.00	0.03	0.19	0.00	0.16	98.31	0.00	0.48
3	1.08	0.00	0.00	0.13	0.06	0.50	97.84	0.00	0.39
4	1.33	0.00	0.00	0.42	0.00	0.40	97.21	0.00	0.65
5	2.93	0.00	0.06	0.22	0.02	0.38	95.92	0.04	0.43
6	3.50	0.00	0.12	0.35	0.03	0.35	95.10	0.02	0.55
7	8.35	0.00	0.00	0.29	0.00	0.40	90.66	0.00	0.30
8	81.91	0.00	0.02	0.13	0.07	0.47	16.88	0.36	0.19
9	98.13	0.00	0.00	0.58	0.01	0.05	0.91	0.29	0.03
10	99.39	0.00	0.00	0.16	0.01	0.02	0.18	0.22	0.02
11	99.56	0.00	0.00	0.07	0.00	0.03	0.14	0.20	0.00
12	99.65	0.00	0.00	0.01	0.01	0.00	0.07	0.24	0.02
13	99.41	0.00	0.00	0.13	0.00	0.04	0.11	0.31	0.00
14	99.60	0.00	0.00	0.05	0.01	0.01	0.08	0.24	0.00
15	93.99	0.00	0.00	5.44	0.03	0.05	0.26	0.24	0.00

C.7 G.91/Ta/V/Nd After 28 Days at 550°C

The G.91/Ta/V/Nd assembly annealed for 28 days at 550°C bonded on the G.91/Ta and V/Nd interface but not the Ta/V interface. Compositional data (in at%) from WDS linescans across the G.91/Ta and V/Nd interfaces is given below.

Position	Ti	Ta	Mo	Si	Cr	Fe	Nd	V	Mn
0	0.01	0.00	0.56	0.45	8.32	90.05	0.03	0.22	0.35
1	0.00	0.00	0.57	0.59	8.08	90.02	0.00	0.48	0.26
2	0.00	0.00	0.47	0.53	7.51	90.89	0.02	0.32	0.26
3	0.00	1.79	0.52	1.64	7.85	87.56	0.10	0.27	0.28
4	0.02	82.71	0.17	3.61	1.48	11.76	0.13	0.13	0.00
5	0.00	86.13	0.15	7.52	0.54	5.06	0.05	0.35	0.21
6	0.00	92.59	0.04	0.00	0.54	4.79	0.15	1.88	0.02
7	0.04	78.04	0.11	1.28	1.29	9.40	0.81	9.03	0.00
8	0.00	85.09	0.01	0.00	1.08	7.96	3.13	2.62	0.12
9	0.04	60.84	0.29	4.23	2.58	22.53	5.93	3.28	0.30
10	0.00	81.79	0.09	1.08	1.27	12.20	2.69	0.88	0.00
11	0.00	94.07	0.20	0.00	0.54	4.21	0.57	0.40	0.00
12	0.00	97.37	0.08	0.00	0.25	1.92	0.11	0.19	0.09
13	0.00	96.71	0.01	0.88	0.12	2.24	0.04	0.00	0.00
14	0.00	87.49	0.12	11.36	0.09	0.71	0.15	0.09	0.01
15	0.00	86.40	0.00	12.68	0.15	0.67	0.05	0.06	0.00

0	0.00	0.00	0.46	0.84	7.74	90.55	0.01	0.13	0.27
1	0.01	0.00	0.93	2.77	10.23	85.38	0.07	0.26	0.35
2	0.01	0.00	0.47	5.27	7.66	85.68	0.36	0.28	0.28
3	0.00	0.00	0.44	18.79	6.82	70.04	3.26	0.34	0.30
4	0.00	0.00	0.52	7.26	7.33	75.37	8.83	0.35	0.33
5	0.03	13.17	0.45	2.62	6.85	69.98	6.18	0.41	0.32
6	0.00	34.65	0.34	17.06	4.38	38.32	4.73	0.30	0.22
7	0.03	60.13	0.20	19.42	1.45	13.93	4.45	0.27	0.12
8	0.00	87.07	0.05	0.00	0.76	6.90	0.70	4.51	0.00
9	0.02	53.45	0.01	3.29	1.24	6.23	0.94	34.76	0.06
10	0.00	77.77	0.07	3.81	1.35	12.17	2.37	2.43	0.04
11	0.00	94.80	0.05	0.00	0.34	3.58	0.79	0.45	0.00
12	0.00	95.85	0.02	0.00	0.21	3.23	0.48	0.23	0.00
13	0.01	98.30	0.12	0.00	0.11	1.41	0.05	0.00	0.00
14	0.00	99.13	0.01	0.00	0.06	0.77	0.00	0.00	0.03
15	0.01	98.48	0.00	0.00	0.18	1.22	0.00	0.05	0.06
0	0.02	0.00	0.00	0.32	2.28	0.06	0.11	97.22	0.00
1	0.00	0.00	0.03	1.97	2.24	0.02	0.06	95.62	0.06
2	0.00	0.00	0.01	0.22	2.25	0.05	0.24	97.23	0.00
3	0.01	0.00	0.00	0.08	2.36	0.03	0.11	97.41	0.00
4	0.00	0.00	0.00	0.38	2.27	1.34	2.63	93.35	0.03
5	0.01	0.00	0.06	1.37	1.68	11.76	23.65	61.39	0.08
6	0.00	0.00	0.02	1.55	0.15	1.55	86.87	9.48	0.40
7	0.00	0.00	0.01	0.20	0.07	0.26	95.24	3.74	0.49
8	0.00	0.00	0.00	0.16	0.15	0.55	95.58	3.21	0.35
9	0.02	0.00	0.00	0.14	0.07	0.40	97.52	1.72	0.13
10	0.00	0.00	0.01	0.21	0.04	0.26	97.58	1.49	0.40
11	0.00	0.00	0.00	0.10	0.11	0.37	97.77	1.14	0.51
12	0.00	0.00	0.02	0.26	0.07	0.38	98.08	0.94	0.25
13	0.00	0.00	0.11	0.31	0.09	0.38	97.80	0.79	0.52
14	0.00	0.00	0.00	0.37	0.02	0.28	98.27	0.67	0.41
15	0.00	0.00	0.00	0.55	0.01	0.31	98.46	0.33	0.33

C.8 G.91/Ta/Nd After 28 Days at 550°C

The G.91/Ta/Nd assembly annealed for 28 days at 550°C bonded on the Ta/Nd interface but not the G.91/Ta interface. Compositional data (in at%) from WDS linescans across the Ta/Nd interface is given below.

Position	Ti	Ta	Mo	Si	Cr	Fe	Nd	V	Mn
0	0.00	0.00	0.00	4.26	0.06	0.23	94.96	0.00	0.49
1	0.00	0.00	0.00	0.60	0.00	0.44	98.67	0.00	0.29
2	0.00	0.00	0.00	0.39	0.00	0.31	98.53	0.09	0.69
3	0.00	0.00	0.00	2.34	0.00	0.37	97.03	0.00	0.26
4	0.00	0.00	0.05	0.18	0.01	0.28	99.08	0.00	0.39
5	0.00	0.00	0.00	0.52	0.00	0.40	98.68	0.00	0.40
6	0.00	0.00	0.03	14.37	0.00	0.66	84.63	0.01	0.31
7	0.07	94.16	0.05	0.00	0.13	0.80	4.68	0.00	0.13
8	0.00	98.79	0.12	0.00	0.00	0.07	0.87	0.01	0.13
9	0.00	99.03	0.11	0.00	0.08	0.13	0.47	0.19	0.00
10	0.03	99.27	0.28	0.00	0.10	0.07	0.26	0.00	0.00
11	0.00	99.33	0.00	0.00	0.01	0.00	0.45	0.07	0.14
12	0.00	98.04	0.07	0.00	0.00	0.17	1.59	0.13	0.00

13	0.03	91.93	0.00	7.28	0.00	0.11	0.63	0.01	0.00
14	0.00	98.63	0.00	0.00	0.00	0.12	1.22	0.04	0.00
15	0.05	98.13	0.05	0.00	0.01	0.15	1.56	0.00	0.05
0	0.00	0.00	0.05	0.47	0.00	0.48	98.45	0.15	0.40
1	0.00	0.00	0.00	0.49	0.00	0.37	98.76	0.04	0.34
2	0.00	0.00	0.02	0.36	0.00	0.36	98.84	0.00	0.43
3	0.00	0.00	0.09	0.70	0.00	0.23	98.30	0.00	0.69
4	0.00	0.00	0.06	0.20	0.00	0.44	98.87	0.00	0.43
5	0.00	0.00	0.02	0.08	0.00	0.44	98.96	0.00	0.50
6	0.00	0.00	0.00	0.17	0.00	0.47	98.95	0.00	0.41
7	0.00	0.13	0.00	0.35	0.00	0.39	98.79	0.04	0.30
8	0.00	39.80	0.11	0.00	0.14	0.40	59.20	0.08	0.29
9	0.00	84.92	0.00	0.00	0.14	0.60	14.24	0.10	0.00
10	0.01	95.03	0.21	0.00	0.04	0.32	4.07	0.21	0.12
11	0.03	99.28	0.10	0.00	0.01	0.15	0.43	0.00	0.00
12	0.00	99.52	0.00	0.00	0.00	0.00	0.48	0.00	0.00
13	0.00	99.42	0.01	0.00	0.00	0.06	0.32	0.05	0.14
14	0.00	99.43	0.00	0.00	0.05	0.00	0.42	0.10	0.00
15	0.01	93.35	0.00	5.73	0.00	0.00	0.77	0.14	0.00

C.9 G.91/Mo/V/Nd After 28 Days at 550°C

The G.91/Mo/V/Nd assembly annealed for 28 days at 550°C bonded on the V/Nd interface but not the G.91/Mo or Mo/V interfaces. Compositional data (in at%) from WDS line scans across the V/Nd interface is given below.

Position	W	Nd	Mo	Fe	Mn	Cr	V	Si
0	0.00	0.11	0.00	0.07	0.03	1.88	89.14	8.77
1	0.00	0.07	0.00	0.03	0.00	2.01	97.41	0.49
2	0.01	0.16	0.00	0.26	0.04	2.05	97.35	0.13
3	0.01	0.16	0.00	0.09	0.00	2.06	97.61	0.08
4	0.01	0.30	0.01	0.27	0.00	2.00	97.26	0.15
5	0.01	4.84	0.00	3.82	0.06	1.82	89.20	0.25
6	0.00	37.67	0.04	5.58	0.16	1.22	54.92	0.42
7	0.04	92.06	0.00	0.62	0.43	0.15	5.95	0.75
8	0.01	94.34	0.00	0.45	0.57	0.08	4.42	0.13
9	0.04	96.87	0.00	0.38	0.36	0.00	2.23	0.13
10	0.02	95.66	0.02	0.44	0.49	0.07	2.91	0.39
11	0.00	92.39	0.02	0.51	0.46	0.17	4.45	2.00
12	0.03	97.17	0.00	0.33	0.51	0.00	1.31	0.65
13	0.00	96.60	0.00	0.36	0.53	0.03	2.11	0.38
14	0.00	95.99	0.02	0.42	0.50	0.08	2.72	0.29
15	0.02	98.06	0.06	0.41	0.46	0.00	0.60	0.38
0	0.00	0.27	0.00	0.08	0.00	2.03	96.35	1.27
1	0.01	0.26	0.00	0.06	0.00	1.96	96.37	1.34
2	0.01	0.24	0.00	0.02	0.00	1.98	96.45	1.29
3	0.00	0.87	0.00	1.45	0.01	1.97	95.02	0.67
4	0.00	10.69	0.03	8.66	0.05	1.73	78.12	0.72
5	0.02	70.59	0.07	4.53	0.32	0.43	20.71	3.33
6	0.00	84.09	0.02	0.46	0.49	0.03	3.95	10.96
7	0.00	93.03	0.00	0.46	0.46	0.01	4.26	1.77
8	0.00	97.07	0.02	0.39	0.47	0.06	1.60	0.39

9	0.00	98.03	0.00	0.27	0.42	0.04	0.89	0.36
10	0.00	96.06	0.00	0.52	0.46	0.00	2.46	0.50
11	0.03	92.36	0.03	1.15	0.50	0.17	5.39	0.37
12	0.00	95.80	0.02	0.67	0.49	0.01	2.82	0.19
13	0.02	98.14	0.00	0.40	0.52	0.00	0.54	0.37
14	0.00	98.36	0.03	0.28	0.54	0.00	0.36	0.44
15	0.00	98.24	0.00	0.26	0.46	0.03	0.32	0.69

C.10 G.91/Mo/Nd After 28 Days at 550°C

The G.91/Mo/Nd assembly annealed for 28 days at 550°C bonded on the Mo/Nd interface but not the G.91/Mo interface. Compositional data (in at%) from WDS linescans across the Mo/Nd interface is given below.

Position	W	Nd	Mo	Fe	Mn	Cr	V	Si
0	0.00	98.83	0.00	0.38	0.48	0.00	0.04	0.27
1	0.00	98.79	0.03	0.33	0.61	0.05	0.00	0.19
2	0.00	98.87	0.05	0.26	0.54	0.03	0.03	0.23
3	0.02	98.75	0.08	0.33	0.52	0.02	0.05	0.23
4	0.02	98.85	0.14	0.36	0.41	0.02	0.00	0.20
5	0.07	91.13	7.59	0.45	0.33	0.00	0.07	0.35
6	0.01	37.02	61.93	0.41	0.27	0.05	0.00	0.32
7	0.00	1.92	97.36	0.10	0.04	0.02	0.03	0.54
8	0.02	0.36	98.24	0.03	0.01	0.00	0.06	1.28
9	0.00	0.27	99.13	0.02	0.12	0.02	0.02	0.42
10	0.02	0.15	99.47	0.02	0.00	0.02	0.00	0.32
11	0.01	0.28	99.53	0.00	0.07	0.00	0.11	0.01
12	0.03	0.13	99.72	0.00	0.02	0.06	0.01	0.05
13	0.01	0.21	99.45	0.00	0.08	0.05	0.00	0.21
14	0.02	0.19	99.50	0.09	0.00	0.00	0.05	0.14
15	0.02	0.14	99.75	0.04	0.00	0.00	0.00	0.05
0	0.00	99.05	0.03	0.35	0.51	0.00	0.00	0.06
1	0.00	98.86	0.03	0.39	0.52	0.00	0.04	0.15
2	0.00	98.62	0.04	0.40	0.65	0.00	0.00	0.30
3	0.07	98.78	0.08	0.38	0.41	0.04	0.01	0.24
4	0.00	98.75	0.06	0.39	0.55	0.00	0.03	0.22
5	0.00	97.76	1.10	0.41	0.50	0.00	0.00	0.24
6	0.03	75.00	23.57	0.83	0.41	0.07	0.00	0.09
7	0.00	3.09	96.24	0.41	0.00	0.07	0.09	0.10
8	0.02	0.74	98.99	0.07	0.00	0.00	0.02	0.15
9	0.00	0.42	99.26	0.03	0.01	0.05	0.10	0.14
10	0.02	0.32	99.38	0.04	0.10	0.00	0.02	0.12
11	0.04	0.18	99.61	0.03	0.04	0.04	0.01	0.05
12	0.01	0.18	99.51	0.03	0.01	0.01	0.06	0.19
13	0.01	0.55	99.21	0.00	0.04	0.02	0.00	0.16
14	0.01	0.13	99.74	0.00	0.04	0.00	0.07	0.02
15	0.01	0.17	99.65	0.00	0.02	0.03	0.01	0.12

C.11 G.91/W/V/Nd After 28 Days at 550°C

The G.91/W/V/Nd assembly annealed for 28 days at 550°C bonded on the G.91/W and V/Nd interfaces but not the W/V interface. Compositional data (in at%) from WDS linescans across the G.91/W interface is given below.

Position	W	Nd	Mo	Fe	Mn	Cr	V	Si
0	2.43	0.30	0.56	87.43	0.33	8.01	0.28	0.68
1	0.44	0.16	0.57	87.79	0.27	7.79	0.26	2.71
2	1.04	0.28	0.56	88.33	0.32	7.53	0.24	1.71
3	2.19	0.94	0.58	86.87	0.38	7.71	0.27	1.07
4	3.63	2.09	0.59	84.41	0.34	7.67	0.26	1.01
5	51.10	5.19	0.29	36.94	0.33	4.10	0.64	1.43
6	63.58	5.36	0.18	25.85	0.05	2.74	0.73	1.51
7	82.65	2.16	0.00	12.49	0.14	1.26	0.38	0.93
8	93.06	1.20	0.00	4.35	0.13	0.60	0.23	0.44
9	95.73	0.75	0.00	2.45	0.03	0.37	0.33	0.34
10	81.19	2.72	0.03	12.79	0.06	1.31	0.50	1.40
11	92.73	1.36	0.00	4.28	0.03	0.55	0.35	0.69
12	95.73	0.78	0.00	2.39	0.00	0.18	0.46	0.47
13	96.70	0.69	0.00	1.60	0.14	0.18	0.17	0.52
14	97.19	0.67	0.00	1.20	0.19	0.24	0.29	0.22
15	98.19	0.50	0.00	0.95	0.00	0.16	0.08	0.12

C.12 G.91/W/Nd After 28 Days at 550°C

The G.91/W/Nd assembly annealed for 28 days at 550°C did not bond on the G.91/W or W/Nd interfaces.

C.13 G.91/Nd After 56 Days at 550°C

After annealing for 56 days at 550°C, three interaction zones were observed across the G.91/Nd interface. The first zone was ~16 μm wide and had a composition matching $\text{Nd}_2(\text{Fe}+\text{Cr})_{17}$ with $\text{Nd}_5(\text{Fe}+\text{Cr})_{17}$ precipitates. The second zone was ~3 μm wide and had a composition matching $\text{Nd}_5(\text{Fe}+\text{Cr})_{17}$. The third interaction zone was ~3 μm wide with a composition matching Fe_2Nd . Compositional data (in at%) from WDS linescans across the G.91/Nd interface is given below.

Position	Zr	Mo	Si	Cr	Fe	Nd	V	Mn
0	0.01	0.52	3.30	9.15	86.09	0.26	0.24	0.43
1	0.00	0.49	7.74	8.66	82.02	0.49	0.23	0.38
2	0.00	0.50	7.55	8.55	82.45	0.40	0.22	0.34
3	0.00	0.47	3.62	8.67	86.39	0.26	0.27	0.33
4	0.01	0.46	4.17	8.81	85.64	0.29	0.26	0.35
5	0.00	0.49	4.11	8.95	85.50	0.35	0.22	0.38
6	0.00	0.52	2.77	9.32	86.11	0.63	0.27	0.37
7	0.01	0.48	4.16	8.69	85.85	0.23	0.25	0.35

8	0.00	0.49	4.31	8.85	85.49	0.28	0.20	0.39
9	0.00	0.48	2.66	9.36	86.05	0.84	0.24	0.37
10	0.00	0.56	1.75	9.67	85.35	2.06	0.24	0.37
11	0.02	0.63	0.55	10.26	82.74	5.23	0.28	0.29
12	0.00	0.63	0.29	10.80	78.10	9.56	0.27	0.36
13	0.00	0.61	0.28	11.05	75.19	12.19	0.28	0.40
14	0.01	0.60	0.39	10.91	73.51	13.89	0.26	0.43
15	0.00	0.60	0.43	10.91	73.10	14.23	0.30	0.44
16	0.00	0.67	0.45	11.19	72.78	14.14	0.31	0.46
17	0.00	0.62	0.42	11.24	72.61	14.36	0.35	0.40
18	0.01	0.74	0.53	11.05	71.40	15.42	0.42	0.44
19	0.00	0.67	0.81	10.64	70.88	16.20	0.42	0.38
20	0.00	0.66	0.73	10.44	71.61	15.87	0.30	0.39
21	0.01	0.63	0.32	11.41	71.62	15.26	0.32	0.43
22	0.00	0.68	0.08	11.61	71.30	15.57	0.34	0.43
23	0.03	0.61	0.18	11.19	68.47	18.80	0.29	0.43
24	0.00	0.60	0.27	10.93	65.35	22.14	0.30	0.42
25	0.03	0.64	0.61	10.13	63.19	24.69	0.33	0.38
26	0.00	0.44	2.57	7.43	59.39	29.55	0.25	0.38
27	0.01	0.22	4.14	4.16	56.55	34.48	0.08	0.35
28	0.00	0.00	10.07	1.31	49.37	38.54	0.29	0.41
29	0.00	0.00	13.49	0.95	35.47	49.36	0.30	0.43
30	0.00	0.01	3.56	1.68	61.63	32.64	0.10	0.39
0	0.01	0.42	12.20	8.07	78.64	0.11	0.25	0.32
1	0.01	0.47	12.41	8.02	78.36	0.14	0.28	0.31
2	0.01	0.45	20.94	7.48	70.54	0.14	0.17	0.29
3	0.00	0.50	5.98	8.36	84.43	0.16	0.19	0.38
4	0.00	0.48	3.99	8.32	86.39	0.20	0.27	0.35
5	0.00	0.45	4.81	8.34	85.11	0.63	0.30	0.36
6	0.00	0.49	4.47	8.62	82.71	3.06	0.29	0.35
7	0.04	0.49	4.44	8.51	82.76	3.14	0.26	0.36
8	0.00	0.48	4.59	8.22	85.73	0.30	0.31	0.37
9	0.01	0.49	4.76	8.17	85.36	0.59	0.28	0.34
10	0.00	0.47	4.52	8.37	83.52	2.50	0.29	0.33
11	0.01	0.46	4.35	8.51	82.63	3.42	0.26	0.36
12	0.01	0.63	0.28	11.52	73.92	12.83	0.45	0.36
13	0.00	0.66	0.32	11.70	73.38	13.10	0.43	0.41
14	0.00	0.71	0.44	11.52	72.48	14.01	0.40	0.44
15	0.01	0.71	0.29	11.91	72.66	13.64	0.33	0.45
16	0.00	0.77	0.13	12.61	73.72	12.04	0.33	0.41
17	0.00	0.65	0.09	12.77	73.82	12.01	0.31	0.36
18	0.01	0.71	0.07	12.77	73.10	12.63	0.30	0.43
19	0.02	0.72	0.08	12.28	72.65	13.52	0.33	0.40
20	0.00	0.75	0.06	12.16	71.55	14.83	0.32	0.33
21	0.00	0.74	0.05	12.04	70.93	15.47	0.33	0.45
22	0.01	0.69	0.13	11.86	70.99	15.59	0.33	0.42
23	0.04	0.80	0.08	12.12	71.06	15.20	0.30	0.41
24	0.01	0.75	0.07	12.07	70.66	15.63	0.34	0.47
25	0.00	0.75	0.14	11.96	70.92	15.54	0.34	0.36
26	0.04	0.70	0.15	11.55	69.41	17.26	0.43	0.47
27	0.00	0.76	0.12	11.36	65.95	21.03	0.39	0.40
28	0.00	0.74	0.28	10.19	60.24	27.75	0.41	0.39
29	0.00	0.55	1.12	7.14	56.12	34.36	0.34	0.38
30	0.01	0.31	2.10	4.04	56.08	36.89	0.16	0.41
31	0.00	0.06	3.05	2.32	59.67	34.63	0.00	0.27
32	0.06	0.01	3.24	1.77	58.74	35.81	0.00	0.38

33	0.03	0.00	3.03	1.63	56.42	38.49	0.00	0.39
34	0.01	0.01	3.36	1.20	48.11	46.90	0.00	0.41
35	0.01	0.00	7.16	0.63	27.23	64.75	0.00	0.23
0	0.00	0.58	1.29	9.67	87.24	0.66	0.26	0.29
1	0.01	0.62	1.36	9.55	86.89	0.89	0.31	0.38
2	0.01	0.61	1.68	9.71	86.48	0.93	0.27	0.31
3	0.00	0.58	1.95	9.81	86.14	0.80	0.27	0.45
4	0.00	0.61	2.59	9.54	86.40	0.33	0.23	0.31
5	0.00	0.57	5.78	9.31	83.43	0.24	0.27	0.40
6	0.01	0.52	8.78	8.71	81.06	0.32	0.26	0.35
7	0.00	0.55	5.08	8.85	84.26	0.77	0.21	0.29
8	0.00	0.68	0.11	11.43	75.41	11.66	0.28	0.44
9	0.00	0.70	0.08	11.78	74.64	12.01	0.33	0.46
10	0.01	0.67	0.08	11.83	74.09	12.58	0.31	0.44
11	0.00	0.70	0.07	11.72	74.41	12.37	0.34	0.41
12	0.00	0.67	0.13	11.48	73.90	13.04	0.33	0.45
13	0.00	0.65	0.25	11.20	72.10	15.16	0.29	0.34
14	0.05	0.63	0.23	11.33	72.94	14.21	0.27	0.35
15	0.00	0.63	0.09	11.63	71.71	15.29	0.32	0.34
16	0.03	0.66	0.09	11.45	69.71	17.38	0.30	0.39
17	0.01	0.69	0.07	11.81	71.42	15.32	0.31	0.37
18	0.00	0.67	0.12	11.60	71.92	15.06	0.28	0.36
19	0.00	0.64	0.17	11.28	69.71	17.50	0.28	0.42
20	0.03	0.65	0.15	11.06	69.27	18.10	0.33	0.41
21	0.03	0.72	0.13	11.15	64.84	22.37	0.28	0.49
22	0.01	0.74	0.16	11.52	62.95	23.87	0.37	0.38
23	0.02	0.68	0.52	8.86	53.12	36.14	0.35	0.32
24	0.01	0.34	1.83	4.99	49.21	43.01	0.19	0.42
25	0.04	0.15	2.80	3.10	51.97	41.44	0.12	0.40
26	0.02	0.01	3.76	2.00	58.25	35.61	0.00	0.35
27	0.04	0.00	4.05	1.53	49.48	44.44	0.03	0.43
28	0.00	0.03	3.46	1.17	35.71	59.21	0.00	0.43
29	0.00	0.10	1.20	0.35	8.20	89.67	0.02	0.46
30	0.00	0.02	0.78	0.10	2.50	96.11	0.02	0.48
31	0.00	0.00	1.60	0.21	1.58	96.18	0.02	0.42
32	0.00	0.00	1.40	0.17	1.51	96.45	0.00	0.47
33	0.00	0.03	1.44	0.27	2.39	95.36	0.02	0.49
34	0.00	0.01	2.62	0.31	4.15	92.54	0.00	0.37
35	0.00	0.00	13.41	0.13	1.72	84.38	0.08	0.29
0	0.01	0.57	0.75	9.13	88.81	0.13	0.24	0.36
1	0.00	0.58	1.55	9.38	87.67	0.16	0.28	0.38
2	0.00	0.54	0.34	9.32	88.97	0.14	0.25	0.43
3	0.01	0.58	0.40	9.63	88.54	0.19	0.25	0.40
4	0.00	0.71	0.37	11.35	86.84	0.15	0.23	0.35
5	0.00	0.66	0.35	10.00	88.10	0.23	0.23	0.43
6	0.00	0.56	0.35	9.38	88.89	0.23	0.22	0.36
7	0.02	0.57	0.36	9.49	88.40	0.56	0.21	0.40
8	0.00	0.55	0.32	9.68	86.41	2.53	0.27	0.25
9	0.00	0.91	0.85	11.07	74.75	11.81	0.24	0.38
10	0.00	0.84	0.29	11.79	74.53	11.80	0.30	0.45
11	0.00	0.60	0.30	11.74	74.61	12.00	0.26	0.48
12	0.00	0.76	0.19	11.44	74.45	12.44	0.24	0.48
13	0.02	0.63	0.07	11.41	75.10	12.04	0.30	0.42
14	0.00	0.67	0.07	11.42	74.52	12.60	0.30	0.42
15	0.00	0.75	0.08	11.65	73.30	13.48	0.29	0.46

16	0.00	0.71	0.07	11.74	71.36	15.42	0.29	0.41
17	0.03	0.72	0.15	10.49	52.04	35.99	0.25	0.35
18	0.00	0.72	0.06	11.68	70.53	16.20	0.34	0.47
19	0.00	0.69	0.10	11.31	69.63	17.58	0.35	0.36
20	0.00	0.67	0.11	11.17	70.10	16.84	0.75	0.36
21	0.03	0.80	0.15	8.10	68.12	21.92	0.41	0.46
22	0.02	0.96	0.24	1.20	53.97	42.54	0.47	0.61
23	0.00	0.03	1.69	0.70	29.48	67.64	0.05	0.42
24	0.00	0.00	3.29	1.18	31.37	63.75	0.05	0.36
25	0.02	0.00	1.07	0.50	5.80	92.26	0.01	0.35
26	0.01	0.04	0.52	0.24	1.90	96.78	0.00	0.51
27	0.00	0.08	0.19	0.19	1.85	97.19	0.00	0.50
28	0.01	0.00	0.29	0.09	0.71	98.41	0.01	0.48
29	0.01	0.00	0.40	0.00	0.47	98.66	0.01	0.45
30	0.01	0.02	0.77	0.07	0.57	98.26	0.03	0.29
0	0.00	0.59	0.60	9.51	88.69	0.03	0.22	0.36
1	0.00	0.41	28.71	7.25	63.12	0.02	0.19	0.29
2	0.00	0.59	0.42	10.20	88.06	0.06	0.26	0.42
3	0.00	0.68	0.43	10.56	87.65	0.07	0.28	0.35
4	0.00	0.55	7.39	8.91	82.39	0.09	0.27	0.40
5	0.00	0.54	0.84	9.19	88.69	0.11	0.26	0.37
6	0.01	0.53	1.47	9.03	87.97	0.37	0.24	0.38
7	0.00	0.64	0.43	9.56	88.50	0.22	0.35	0.31
8	0.00	0.75	0.30	9.41	88.62	0.26	0.34	0.33
9	0.00	0.65	0.60	10.26	81.49	6.20	0.52	0.28
10	0.03	0.75	0.41	9.59	88.36	0.22	0.30	0.34
11	0.00	0.59	0.28	9.46	87.49	1.57	0.43	0.19
12	0.02	0.74	5.90	10.56	72.58	9.61	0.21	0.38
13	0.00	0.76	1.14	11.63	73.85	11.97	0.25	0.42
14	0.00	0.74	0.59	11.32	73.32	13.21	0.32	0.49
15	0.00	0.84	0.75	11.34	72.07	14.29	0.27	0.44
16	0.00	0.66	0.44	11.46	73.36	13.27	0.35	0.47
17	0.00	0.71	0.36	11.95	73.63	12.61	0.31	0.44
18	0.02	0.76	0.40	12.28	73.26	12.53	0.34	0.41
19	0.00	0.70	0.61	11.31	73.01	13.67	0.28	0.43
20	0.02	0.71	0.44	11.52	73.39	13.31	0.25	0.35
21	0.00	0.72	0.68	10.80	71.78	15.29	0.29	0.44
22	0.00	0.61	0.72	10.96	72.49	14.53	0.27	0.44
23	0.01	0.76	0.20	12.04	74.22	11.98	0.38	0.42
24	0.00	0.61	0.57	11.60	73.72	12.84	0.26	0.40
25	0.00	0.65	1.21	10.55	71.86	15.04	0.31	0.38
26	0.00	0.57	1.42	9.73	69.71	18.02	0.22	0.34
27	0.00	0.76	0.37	12.00	73.98	12.17	0.32	0.40
28	0.02	0.70	0.17	12.52	69.49	16.28	0.43	0.40
29	0.00	0.73	0.16	12.53	67.89	17.90	0.35	0.44
30	0.00	0.83	0.18	12.29	70.58	15.29	0.46	0.39
0	0.00	0.63	0.46	9.60	88.64	0.06	0.25	0.35
1	0.00	0.52	0.33	8.82	88.95	0.05	0.93	0.41
2	0.00	0.58	0.44	8.90	88.97	0.09	0.63	0.41
3	0.00	0.55	0.54	8.80	89.50	0.07	0.22	0.33
4	0.00	0.52	1.58	8.54	88.58	0.17	0.28	0.34
5	0.00	0.54	0.43	8.74	89.21	0.38	0.29	0.42
6	0.00	0.69	0.86	10.18	76.50	11.13	0.29	0.35
7	0.00	0.62	0.28	10.03	80.00	8.32	0.39	0.35
8	0.00	0.80	0.32	11.06	72.76	14.24	0.38	0.45

9	0.02	0.77	0.29	11.21	72.31	14.64	0.38	0.39
10	0.00	0.80	0.34	11.35	72.44	14.28	0.33	0.44
11	0.00	0.67	0.73	10.57	71.47	15.80	0.31	0.45
12	0.01	0.69	0.13	11.51	73.98	13.03	0.27	0.39
13	0.00	0.72	0.08	11.57	74.43	12.42	0.35	0.42
14	0.00	0.70	0.14	11.88	71.29	15.05	0.48	0.46
15	0.00	0.75	0.04	11.95	74.57	11.97	0.33	0.38
16	0.01	0.69	0.08	11.77	73.19	13.56	0.29	0.41
17	0.00	0.68	0.18	10.72	59.54	28.07	0.30	0.52
18	0.01	0.63	0.12	10.54	59.43	28.48	0.32	0.47
19	0.01	0.75	0.14	10.12	63.70	24.56	0.21	0.51
20	0.00	0.82	0.19	11.70	71.51	14.97	0.33	0.49
21	0.00	0.80	0.13	11.58	70.64	16.16	0.37	0.33
22	0.00	0.90	0.37	11.55	67.30	19.13	0.33	0.42
23	0.01	0.76	0.27	10.61	63.75	23.90	0.30	0.41
24	0.00	0.77	0.19	10.90	67.79	19.48	0.36	0.51
25	0.02	0.74	1.53	10.14	62.39	24.43	0.31	0.45
26	0.00	0.04	1.84	2.09	60.02	33.68	0.09	0.45
27	0.00	0.28	2.10	3.23	58.52	35.30	0.14	0.42
28	0.00	0.05	21.32	2.04	39.98	36.28	0.00	0.35
29	0.00	0.09	1.40	0.16	1.54	96.38	0.00	0.43
30	0.00	0.00	1.99	0.13	1.01	96.33	0.00	0.54

C.14 G.91/V/Nd After 56 Days at 550°C

The G.91/V/Nd assembly annealed for 56 days at 550°C bonded on the V/Nd interface but not the G.91/V interface. Since the V/Nd interface at this time and temperature was already well characterized, no WDS linescans were completed on it in this assembly.

C.15 G.91/Zr/v/Nd After 56 Days at 550°C

The G.91/Zr/V/Nd assembly annealed for 56 days at 550°C bonded on the V/Nd interface but not the G.91/Zr or Zr/V interfaces. Compositional data (in at%) from WDS linescans across the V/Nd interface is given below.

Position	Zr	Mo	Si	Cr	Fe	Nd	V	Mn
0	0.03	0.02	1.00	1.97	0.23	2.64	94.11	0.00
1	0.00	0.01	1.23	2.05	0.14	1.69	94.90	0.00
2	0.00	0.01	0.52	2.00	0.03	0.49	96.96	0.00
3	0.00	0.03	0.18	1.98	0.04	0.28	97.50	0.00
4	0.00	0.00	2.39	1.91	0.02	0.26	95.41	0.00
5	0.00	0.01	5.94	1.75	0.02	0.24	92.04	0.00
6	0.00	0.00	4.19	1.88	0.00	0.31	93.60	0.02
7	0.00	0.02	10.32	1.81	0.03	0.21	87.60	0.02

8	0.01	0.01	1.14	1.56	9.21	4.76	83.23	0.08
9	0.03	0.00	8.46	0.18	0.52	85.19	5.25	0.37
10	0.01	0.00	2.59	0.20	0.51	88.32	7.97	0.40
11	0.01	0.01	2.27	0.20	0.62	89.33	7.01	0.54
12	0.02	0.08	22.75	0.12	0.43	73.10	3.21	0.29
13	0.05	0.00	7.09	0.06	0.34	90.66	1.53	0.28
14	0.00	0.00	0.93	0.00	0.26	97.24	1.27	0.30
15	0.00	0.08	0.68	0.01	0.34	97.18	1.28	0.44

C.16 G.91/Zr/Nd After 56 Days at 550°C

The G.91/Zr/Nd assembly annealed for 56 days at 550°C did not bond on the G.91/Zr or Zr/Nd interfaces.

C.17 G.91/Ti/V/Nd After 56 Days at 550°C

The G.91/Ti/V/Nd assembly annealed for 56 days at 550°C bonded on the V/Nd interface but not the G.91/Ti or Ti/V interfaces. Compositional data (in at%) from WDS linescans across the V/Nd interface is given below.

Position	Ti	Ta	Mo	Si	Cr	Fe	Nd	V	Mn
0	0.00	0.00	0.01	2.49	2.22	0.10	1.36	93.82	0.00
1	0.01	0.00	0.00	2.89	2.13	1.36	2.31	91.29	0.00
2	0.00	0.00	0.05	1.45	2.17	3.09	2.20	91.02	0.02
3	0.00	0.00	0.00	2.12	1.27	11.22	53.46	31.59	0.33
4	0.00	0.00	0.00	0.36	0.13	0.46	94.08	4.51	0.46
5	0.00	0.00	0.06	0.28	0.17	0.57	94.69	3.71	0.53
6	0.00	0.00	0.00	3.22	0.00	0.41	93.35	2.59	0.42
7	0.00	0.00	0.00	2.41	0.02	0.33	95.34	1.66	0.23
8	0.00	0.00	0.06	1.10	0.00	0.35	96.59	1.42	0.49
9	0.00	0.00	0.00	0.36	0.10	0.37	96.50	2.04	0.64
10	0.00	0.00	0.03	0.10	0.10	0.39	97.53	1.29	0.57
11	0.00	0.00	0.00	0.31	0.00	0.27	98.03	0.82	0.56
12	0.00	0.00	0.08	0.13	0.09	0.29	98.49	0.56	0.37
13	0.00	0.00	0.01	0.28	0.05	0.23	98.30	0.65	0.48
14	0.02	0.00	0.00	0.53	0.12	0.34	97.98	0.41	0.60
15	0.00	0.00	0.00	0.14	0.14	0.41	98.35	0.58	0.37

C.18 G.91/Ti/Nd After 56 Days at 550°C

The G.91/Ti/Nd assembly annealed for 56 days at 550°C bonded on the Ti/Nd interface but not the G.91/Ti interface. Compositional data (in at%) from WDS linescans across the Ti/Nd interface is given below.

Position	Ti	Ta	Mo	Si	Cr	Fe	Nd	V	Mn
0	1.67	0.00	0.03	22.96	0.00	0.49	74.15	0.21	0.50

1	5.02	0.00	0.00	1.43	0.04	0.49	92.56	0.07	0.39
2	6.74	0.00	0.00	36.27	0.00	0.59	56.15	0.00	0.25
3	89.56	0.00	0.00	1.81	0.01	0.70	7.49	0.39	0.05
4	97.75	0.00	0.00	0.59	0.00	0.29	1.13	0.25	0.00
5	96.82	0.00	0.00	0.76	0.00	0.10	2.03	0.26	0.03
6	95.06	0.00	0.00	3.27	0.02	0.06	1.35	0.24	0.00
7	94.92	0.00	0.00	2.53	0.02	0.26	1.93	0.32	0.02
8	75.82	0.00	0.00	20.78	0.05	0.70	2.44	0.22	0.00
9	49.78	0.00	0.00	48.82	0.00	0.06	1.17	0.14	0.02
10	24.62	0.00	0.00	74.06	0.00	0.04	1.23	0.05	0.00
11	2.80	0.00	0.02	94.74	0.00	0.09	2.30	0.03	0.01
12	34.00	0.00	0.01	65.13	0.02	0.05	0.75	0.04	0.00
13	80.27	0.00	0.00	19.18	0.00	0.04	0.28	0.23	0.00
14	96.66	0.00	0.00	2.34	0.02	0.16	0.53	0.24	0.05
15	98.87	0.00	0.00	0.56	0.00	0.07	0.24	0.24	0.03
0	3.38	0.00	0.00	9.26	0.85	7.81	78.19	0.16	0.34
1	5.30	0.00	0.02	5.68	0.16	2.01	86.39	0.07	0.37
2	5.74	0.00	0.05	2.11	0.06	1.04	90.24	0.14	0.63
3	7.25	0.00	0.05	4.60	0.20	2.40	85.05	0.14	0.32
4	19.70	0.00	0.06	8.05	0.09	1.28	70.38	0.18	0.26
5	78.90	0.00	0.03	5.41	0.00	0.63	14.60	0.29	0.16
6	98.37	0.00	0.00	0.27	0.03	0.01	1.03	0.25	0.05
7	98.30	0.00	0.00	0.41	0.00	0.03	1.01	0.25	0.00
8	97.31	0.00	0.00	0.33	0.00	0.06	1.99	0.31	0.01
9	90.99	0.00	0.00	4.12	0.05	0.22	4.28	0.28	0.07
10	91.79	0.00	0.00	5.56	0.03	0.11	2.30	0.21	0.00
11	94.22	0.00	0.00	4.04	0.04	0.07	1.40	0.23	0.01
12	94.21	0.00	0.00	3.76	0.00	0.05	1.77	0.22	0.00
13	91.22	0.00	0.00	3.59	0.10	0.46	4.40	0.24	0.00
14	87.79	0.00	0.00	8.87	0.00	0.26	2.32	0.29	0.48
15	92.72	0.00	0.00	5.85	0.02	0.07	1.11	0.24	0.00

C.19 G.91/Ta/V/Nd After 56 Days at 550°C

The G.91/Ta/V/Nd assembly annealed for 56 days at 550°C bonded on the V/Nd interface but not the G.91/Ta or Ta/V interfaces. Compositional data (in at%) from WDS linescans across the V/Nd interface is given below.

Position	Ti	Ta	Mo	Si	Cr	Fe	Nd	V	Mn
0	0.00	0.00	0.00	0.34	0.05	0.48	96.13	2.70	0.31
1	0.00	0.00	0.00	0.67	0.16	0.42	94.12	4.22	0.41
2	0.00	0.00	0.01	10.65	0.23	1.27	81.72	5.74	0.37
3	0.00	0.00	0.08	10.38	0.95	7.17	74.57	6.22	0.62
4	0.00	0.00	0.05	5.45	1.23	8.34	44.17	40.66	0.12
5	0.01	0.00	0.04	1.63	2.06	16.78	10.27	69.01	0.20
6	0.00	0.00	0.01	2.01	2.08	12.36	7.44	75.99	0.13
7	0.01	0.00	0.04	0.20	2.06	0.56	1.05	96.08	0.00
8	0.00	0.00	0.02	0.46	2.09	1.08	1.67	94.67	0.02
9	0.00	0.00	0.00	0.70	2.11	2.46	4.85	89.89	0.01
10	0.01	0.00	0.00	0.30	2.15	0.01	0.40	97.13	0.00
11	0.00	0.00	0.04	0.88	2.12	0.17	3.17	93.58	0.05
12	0.00	0.00	0.00	20.62	1.31	0.72	22.03	55.27	0.06
13	0.00	0.00	0.03	0.21	2.21	0.03	0.26	97.26	0.00

14	0.00	0.00	0.02	3.66	1.67	0.60	16.99	76.97	0.09
15	0.00	0.00	0.00	28.19	1.54	0.26	6.59	63.39	0.03

C.20 G.91/Ta/Nd After 56 Days at 550°C

The G.91/Ta/Nd assembly annealed for 56 days at 550°C bonded on the Ta/Nd interface but not the G.91/Ta interface. Compositional data (in at%) from WDS linescans across the Ta/Nd interface is given below.

Position	Ti	Ta	Mo	Si	Cr	Fe	Nd	V	Mn
0	0.00	0.07	0.00	0.91	0.00	0.46	98.02	0.05	0.50
1	0.00	4.36	0.02	1.02	0.09	1.61	92.29	0.01	0.61
2	0.00	4.63	0.06	2.37	0.02	2.94	89.61	0.00	0.38
3	0.00	0.18	0.06	0.57	0.00	0.48	98.31	0.00	0.40
4	0.00	0.07	0.10	0.40	0.04	0.31	98.44	0.05	0.59
5	0.00	0.07	0.09	0.50	0.03	0.41	98.27	0.14	0.51
6	0.00	26.02	0.10	0.05	0.00	0.69	72.71	0.00	0.43
7	0.00	96.99	0.00	0.00	0.05	0.38	2.51	0.07	0.00
8	0.00	96.25	0.00	1.20	0.14	0.58	1.83	0.00	0.00
9	0.05	88.30	0.15	6.22	0.37	2.72	1.86	0.33	0.00
10	0.00	84.30	0.18	4.70	0.33	8.51	1.96	0.00	0.03
11	0.08	90.08	0.12	4.95	0.35	2.88	1.49	0.06	0.00
12	0.63	81.94	0.00	8.78	0.52	6.09	1.67	0.18	0.21
13	0.00	92.03	0.06	1.74	0.42	4.42	1.27	0.07	0.00
14	0.00	63.33	0.01	33.53	0.10	2.29	0.74	0.00	0.00
15	0.00	76.53	0.15	17.22	0.60	4.71	0.61	0.14	0.06
0	0.00	6.14	0.00	0.80	0.00	0.57	92.09	0.03	0.38
1	0.00	12.01	0.01	1.85	0.06	0.77	85.06	0.03	0.21
2	0.00	6.89	0.00	0.92	0.04	0.71	90.89	0.00	0.55
3	0.00	30.43	0.04	0.87	0.04	0.75	67.44	0.00	0.44
4	0.00	91.01	0.05	1.69	0.19	1.88	5.02	0.10	0.06
5	0.00	83.89	0.03	8.70	0.22	3.35	3.63	0.16	0.03
6	0.02	97.41	0.00	0.19	0.06	0.69	1.64	0.00	0.00
7	0.00	89.36	0.00	5.69	0.26	2.67	2.00	0.00	0.01
8	0.02	73.68	0.07	23.37	0.13	1.70	0.85	0.07	0.12
9	0.02	85.07	0.10	1.63	0.87	9.35	2.68	0.06	0.23
10	0.00	94.85	0.00	2.52	0.00	0.75	1.71	0.10	0.09
11	0.06	94.55	0.17	0.00	0.35	2.89	1.92	0.06	0.00
12	0.27	88.16	0.07	8.40	0.17	1.82	1.00	0.13	0.00
13	0.02	93.59	0.00	3.24	0.13	0.81	1.90	0.12	0.19
14	0.00	50.01	0.17	32.41	1.52	12.00	3.89	0.00	0.01
15	0.00	74.40	0.15	16.64	0.53	3.97	4.17	0.16	0.00
0	0.00	78.11	0.11	8.92	1.01	11.30	0.37	0.13	0.06
1	0.00	71.53	0.06	4.01	2.70	20.48	0.98	0.05	0.20
2	0.00	71.08	0.16	11.02	2.08	14.38	1.01	0.11	0.16
3	0.00	8.69	0.74	5.58	9.63	74.22	0.55	0.19	0.40
4	0.00	1.43	0.52	2.09	6.97	88.07	0.13	0.30	0.49
5	0.01	0.00	0.67	0.76	8.79	89.17	0.09	0.20	0.30
6	0.00	0.00	0.52	1.17	8.47	89.10	0.14	0.24	0.36
7	0.00	0.00	0.54	2.11	7.60	89.09	0.13	0.20	0.33
8	0.01	0.00	0.72	1.02	9.15	88.50	0.19	0.25	0.18
9	0.00	0.00	0.55	6.80	7.62	83.76	0.63	0.28	0.35

10	0.00	0.00	0.54	6.80	7.72	84.19	0.24	0.22	0.30
11	0.00	0.00	0.68	1.79	8.60	88.35	0.14	0.23	0.21
12	0.00	0.00	0.60	2.34	8.85	87.44	0.25	0.25	0.27
13	0.00	0.00	0.55	0.36	8.93	89.23	0.27	0.25	0.42
14	0.01	0.00	0.63	0.50	8.89	89.21	0.20	0.23	0.34
15	0.02	0.00	0.58	0.82	9.10	88.54	0.29	0.26	0.41
0	0.00	89.59	0.00	6.64	0.41	3.29	0.07	0.00	0.01
1	0.00	89.85	0.00	4.13	0.55	4.67	0.55	0.08	0.17
2	0.01	70.10	0.29	1.38	3.16	23.98	0.66	0.15	0.28
3	0.00	8.39	0.49	1.07	7.35	81.98	0.30	0.19	0.23
4	0.00	0.18	0.54	0.89	8.04	89.70	0.17	0.18	0.29
5	0.00	0.00	0.59	0.40	9.15	89.22	0.09	0.21	0.34
6	0.04	0.00	0.53	5.02	8.23	85.55	0.17	0.27	0.21
7	0.01	0.00	0.45	0.59	7.72	90.57	0.15	0.26	0.25
8	0.01	0.00	0.46	0.87	7.91	89.85	0.12	0.39	0.40
9	0.00	0.00	0.57	4.62	8.25	85.82	0.13	0.26	0.35
10	0.00	0.00	0.64	0.79	9.92	87.68	0.24	0.33	0.41
11	0.01	0.00	0.55	2.14	9.83	86.65	0.23	0.23	0.36
12	0.00	0.00	0.60	4.11	9.39	84.31	0.99	0.27	0.33
13	0.01	0.00	0.51	22.43	7.99	68.13	0.45	0.20	0.29
14	0.00	0.00	0.56	10.02	8.74	79.75	0.41	0.22	0.31
15	0.00	0.00	0.55	2.03	8.95	87.81	0.13	0.17	0.37

C.21 G.91/Mo/V/Nd After 56 Days at 550°C

The G.91/Mo/V/Nd assembly annealed for 56 days at 550°C bonded on the V/Nd interface but not the G.91/Mo or Mo/V interfaces. Since the V/Nd interface at this time and temperature was already well characterized, no WDS linescans were completed on it in this assembly.

C.22 G.91/Mo/Nd After 56 Days at 550°C

The G.91/Mo/Nd assembly annealed for 56 days at 550°C bonded on the Mo/Nd interface but not the G.91/Mo interface. Compositional data (in at%) from WDS linescans across the Mo/Nd interface is given below.

Position	W	Nd	Mo	Fe	Mn	Cr	V	Si
0	0.00	98.05	0.12	0.89	0.46	0.06	0.00	0.42
1	0.00	98.24	0.09	0.28	0.45	0.05	0.00	0.88
2	0.00	90.45	0.16	0.27	0.38	0.03	0.04	8.66
3	0.00	60.57	0.13	0.29	0.32	0.01	0.00	38.67
4	0.00	89.27	0.14	0.28	0.30	0.00	0.08	9.93
5	0.00	65.58	0.14	0.29	0.40	0.00	0.00	33.59
6	0.00	83.32	0.63	0.42	0.32	0.03	0.02	15.26
7	0.05	85.20	12.18	0.44	0.37	0.00	0.00	1.76
8	0.02	0.87	98.83	0.06	0.01	0.00	0.03	0.18
9	0.00	0.04	99.92	0.01	0.01	0.00	0.00	0.02
10	0.00	0.25	99.55	0.04	0.00	0.04	0.00	0.13
11	0.03	0.39	99.30	0.08	0.00	0.00	0.02	0.19

12	0.01	0.37	99.27	0.11	0.01	0.04	0.00	0.19
13	0.00	0.17	99.43	0.09	0.01	0.00	0.04	0.25
14	0.00	0.19	99.33	0.02	0.00	0.01	0.05	0.40
15	0.00	0.10	99.45	0.00	0.00	0.02	0.01	0.42

C.23 G.91/W/V/Nd After 56 Days at 550°C

The G.91/W/V/Nd assembly annealed for 56 days at 550°C bonded on the W/V interface but not the G.91/W or V/Nd interfaces. Compositional data (in at%) from WDS linescans across the W/V interface is given below.

Position	W	Nd	Mo	Fe	Mn	Cr	V	Si
0	97.46	0.13	0.00	0.16	0.00	0.04	1.93	0.28
1	96.63	0.03	0.00	0.24	0.05	0.16	2.79	0.10
2	80.25	0.35	0.00	0.54	0.00	0.25	13.12	5.50
3	11.07	0.16	0.00	0.53	0.00	0.97	48.55	38.71
4	0.20	0.03	0.00	0.12	0.00	1.58	80.47	17.60
5	0.02	0.04	0.00	0.09	0.00	1.54	75.15	23.16
6	0.01	0.05	0.00	0.06	0.01	1.63	79.75	18.50
7	0.02	0.07	0.01	0.14	0.00	1.70	84.33	13.74
8	0.01	0.26	0.01	0.38	0.00	1.60	76.26	21.47
9	0.01	0.40	0.00	0.37	0.00	1.64	81.61	15.98
10	0.02	0.65	0.02	0.44	0.00	1.84	90.88	6.16
11	0.02	0.31	0.00	0.11	0.03	1.81	93.42	4.30
12	0.01	0.22	0.00	0.07	0.00	1.85	95.33	2.52
13	0.02	0.41	0.00	0.03	0.00	1.86	96.05	1.64
14	0.00	0.37	0.01	0.03	0.02	1.95	96.74	0.89
15	0.02	0.62	0.01	0.07	0.00	1.92	96.79	0.58

C.24 G.91/W/Nd After 56 Days at 550°C

The G.91/W/Nd assembly annealed for 56 days at 550°C bonded on the W/Nd interface but not the G.91/W interface. Compositional data (in at%) from WDS linescans across the W/Nd interface is given below.

Position	W	Nd	Mo	Fe	Mn	Cr	V	Si
0	0.02	98.63	0.00	0.43	0.63	0.00	0.00	0.29
1	0.02	98.70	0.02	0.41	0.51	0.00	0.00	0.34
2	0.00	98.55	0.00	0.69	0.44	0.04	0.00	0.28
3	0.03	98.54	0.00	0.50	0.62	0.03	0.00	0.28
4	9.61	85.02	0.00	0.79	0.48	0.40	0.00	3.70
5	39.13	58.41	0.00	0.62	0.33	0.02	0.03	1.46
6	93.11	5.95	0.00	0.20	0.00	0.00	0.19	0.56
7	98.54	1.31	0.00	0.02	0.00	0.05	0.07	0.03
8	99.47	0.43	0.00	0.08	0.03	0.00	0.00	0.00
9	99.09	0.52	0.00	0.10	0.03	0.00	0.02	0.25
10	99.31	0.34	0.00	0.06	0.10	0.13	0.06	0.00
11	99.44	0.12	0.00	0.14	0.00	0.05	0.11	0.14
12	99.56	0.26	0.00	0.00	0.00	0.05	0.13	0.00
13	99.55	0.19	0.00	0.00	0.04	0.00	0.00	0.22
14	99.61	0.04	0.00	0.05	0.14	0.00	0.07	0.09
15	99.65	0.18	0.00	0.09	0.00	0.05	0.03	0.00

C.25 G.91/Nd After 28 Days at 625°C

The G.91/W/Nd assembly annealed for 28 days at 625°C included two interaction zones across the diffusion interface. The first interaction zone observed was ~38 μm wide with a composition matching $\text{Nd}_2(\text{Fe}+\text{Cr})_{17}$. The second interaction zone had a composition matching Fe_2Nd , with a zone width of ~4 μm . Compositional data (in at%) from WDS linescans across the W/Nd interface is given below.

Position	Zr	Mo	Si	Cr	Fe	Nd	V	Mn
0	0.00	0.60	4.59	8.50	85.76	0.03	0.20	0.33
1	0.00	0.61	5.98	8.34	84.39	0.12	0.23	0.33
2	0.00	0.58	0.39	9.02	89.21	0.07	0.38	0.36
3	0.01	0.59	0.38	8.87	89.51	0.06	0.23	0.35
4	0.01	0.65	0.38	8.93	89.37	0.05	0.27	0.35
5	0.00	0.60	0.47	8.85	89.28	0.05	0.43	0.31
6	0.00	0.62	0.43	8.84	89.49	0.07	0.21	0.35
7	0.00	0.63	0.42	8.89	89.41	0.08	0.23	0.34
8	0.01	0.60	0.58	8.87	89.06	0.07	0.44	0.38
9	0.00	0.62	0.38	8.91	89.38	0.11	0.25	0.36
10	0.01	0.57	0.37	8.92	89.43	0.08	0.24	0.38
11	0.00	0.58	1.81	8.92	88.00	0.13	0.22	0.35
12	0.00	0.61	1.44	9.02	88.16	0.20	0.22	0.35
13	0.00	0.60	0.33	9.20	88.83	0.37	0.27	0.40
14	0.00	0.60	1.00	10.53	80.88	6.25	0.30	0.44
15	0.00	0.69	0.13	11.26	76.10	11.09	0.29	0.44
16	0.00	0.65	0.11	11.37	75.09	12.09	0.26	0.44
17	0.00	0.70	0.13	11.17	75.91	11.38	0.30	0.40
18	0.02	0.62	0.38	11.02	75.52	11.75	0.31	0.38
19	0.02	0.66	0.23	11.13	75.55	11.74	0.28	0.39
20	0.01	0.66	0.19	11.26	75.47	11.73	0.27	0.41
21	0.01	0.74	0.12	11.12	74.80	12.47	0.29	0.46
22	0.00	0.79	0.09	11.57	74.66	12.30	0.26	0.33
23	0.01	0.78	0.10	10.88	74.68	12.93	0.25	0.37
24	0.00	0.65	0.15	10.86	74.83	12.91	0.26	0.35
25	0.00	0.79	0.15	0.97	84.06	13.21	0.34	0.48
26	0.00	0.72	0.11	10.61	76.44	11.51	0.30	0.32
27	0.00	0.88	0.15	11.15	73.30	13.85	0.35	0.33
28	0.01	0.80	0.19	10.95	75.02	12.26	0.37	0.40
29	0.00	0.73	0.11	10.94	76.89	10.59	0.31	0.44
30	0.00	0.72	0.17	10.10	73.35	15.02	0.27	0.37
31	0.00	0.76	0.15	11.01	76.48	10.89	0.31	0.41
32	0.00	0.76	0.10	11.20	76.44	10.75	0.37	0.39
33	0.00	0.75	0.33	10.98	67.92	19.41	0.26	0.36
34	0.00	0.79	0.12	10.99	76.69	10.70	0.34	0.37
35	0.00	0.76	0.09	11.01	76.73	10.70	0.31	0.40
36	0.00	0.72	0.13	10.94	76.71	10.83	0.29	0.37
37	0.00	0.69	0.48	10.85	75.58	11.71	0.30	0.40
38	0.02	0.71	0.09	10.92	74.58	12.92	0.39	0.39
39	0.01	0.74	0.13	10.81	75.28	12.30	0.35	0.39
40	0.00	0.81	0.13	10.95	75.19	12.18	0.30	0.43
41	0.01	0.76	0.19	10.37	71.59	16.29	0.37	0.42
42	0.00	0.79	0.11	11.02	76.55	10.92	0.30	0.31

43	0.00	0.73	0.06	10.65	76.37	11.49	0.28	0.43
44	0.00	0.81	0.15	10.59	76.10	11.63	0.38	0.34
45	0.01	0.84	0.17	10.67	76.15	11.47	0.30	0.39
46	0.02	0.76	0.10	10.34	76.30	11.74	0.35	0.39
47	0.00	0.40	0.25	6.81	77.19	11.62	0.18	0.45
48	0.00	0.34	0.12	7.75	79.40	11.82	0.21	0.37
49	0.02	0.44	0.09	8.12	78.44	12.26	0.21	0.43
50	0.00	0.02	0.91	5.89	48.67	44.17	0.03	0.30
51	0.04	0.01	3.21	1.82	56.56	38.08	0.01	0.28
52	0.04	0.01	4.88	1.60	61.40	31.72	0.03	0.33
53	0.00	0.00	5.06	1.53	61.36	31.75	0.00	0.30
54	0.02	0.02	4.76	1.50	61.37	32.03	0.00	0.30
55	0.00	0.01	4.59	1.64	61.25	32.05	0.02	0.44
56	0.00	0.01	4.05	1.31	56.13	38.13	0.00	0.36
57	0.00	0.00	1.20	0.34	12.19	85.70	0.00	0.57
58	0.00	0.02	0.51	0.06	1.08	97.73	0.00	0.61
59	0.01	0.08	0.65	0.09	1.03	97.76	0.00	0.39
60	0.00	0.00	2.49	0.01	1.19	95.72	0.00	0.58
0	0.00	0.62	0.61	9.45	88.86	0.12	0.34	0.00
1	0.00	0.60	0.63	9.25	88.90	0.05	0.21	0.35
2	0.01	0.68	0.75	9.24	88.67	0.03	0.25	0.38
3	0.00	0.53	15.60	8.49	74.69	0.26	0.19	0.25
4	0.02	0.45	29.48	7.07	61.62	0.96	0.17	0.23
5	0.02	0.64	1.03	9.29	88.34	0.09	0.26	0.35
6	0.00	0.63	0.58	9.14	89.03	0.02	0.26	0.35
7	0.00	0.57	0.93	9.16	88.72	0.05	0.24	0.34
8	0.00	0.63	0.39	9.10	89.18	0.09	0.24	0.37
9	0.00	0.65	1.09	9.10	88.45	0.10	0.24	0.38
10	0.00	0.52	9.07	8.56	80.74	0.60	0.17	0.34
11	0.00	0.64	2.06	9.10	87.25	0.41	0.23	0.32
12	0.00	0.62	0.83	9.18	88.19	0.59	0.21	0.39
13	0.00	0.59	5.84	8.77	83.14	1.01	0.24	0.41
14	0.00	0.54	14.63	7.90	76.04	0.32	0.23	0.35
15	0.00	0.51	15.10	7.96	75.37	0.32	0.40	0.34
16	0.00	0.55	10.49	8.37	79.63	0.33	0.32	0.32
17	0.01	0.52	14.02	7.91	76.67	0.29	0.22	0.38
18	0.00	0.52	13.65	8.18	76.54	0.37	0.45	0.29
19	0.00	0.55	1.36	9.31	88.06	0.14	0.25	0.34
20	0.00	0.56	0.44	9.44	88.77	0.16	0.28	0.36
21	0.01	0.60	1.62	9.18	87.67	0.33	0.21	0.39
22	0.00	0.54	3.78	9.28	85.53	0.28	0.25	0.33
23	0.00	0.39	0.12	10.03	86.59	2.30	0.36	0.23
24	0.01	0.85	0.09	12.54	75.06	10.68	0.32	0.46
25	0.01	0.84	0.10	12.72	75.60	9.95	0.33	0.45
26	0.00	0.91	0.04	12.92	74.71	10.64	0.40	0.39
27	0.01	0.72	0.11	11.76	75.50	11.18	0.34	0.38
28	0.00	0.61	0.11	10.90	75.72	12.03	0.32	0.31
29	0.01	0.66	0.07	10.35	76.25	11.89	0.35	0.43
30	0.00	0.69	0.10	10.12	73.85	14.62	0.28	0.34
31	0.01	0.78	0.11	10.39	74.17	13.87	0.26	0.43
32	0.00	0.73	0.13	10.71	76.40	11.43	0.28	0.32
33	0.01	0.69	0.12	10.48	77.28	10.75	0.29	0.39
34	0.00	0.75	0.22	10.64	75.76	12.01	0.26	0.37
35	0.00	0.75	0.13	10.69	75.60	12.21	0.25	0.38
36	0.00	0.67	0.09	10.45	76.80	11.21	0.32	0.46
37	0.00	0.77	0.13	11.01	76.29	11.23	0.27	0.32

38	0.02	0.82	0.14	10.82	75.44	12.03	0.35	0.39
39	0.00	0.79	0.11	11.11	76.37	10.96	0.31	0.35
40	0.02	0.80	0.15	10.89	76.73	10.65	0.34	0.42
41	0.01	0.75	0.06	10.56	75.21	12.68	0.33	0.39
42	0.00	0.74	0.09	10.62	73.96	13.88	0.35	0.38
43	0.01	0.80	0.13	10.96	76.53	10.82	0.32	0.43
44	0.01	0.73	0.17	10.42	76.22	11.82	0.30	0.34
45	0.00	0.70	0.11	10.49	77.27	10.73	0.31	0.39
46	0.02	0.70	0.18	10.44	77.23	10.77	0.30	0.37
47	0.00	0.72	0.12	10.30	77.00	11.18	0.30	0.38
48	0.01	0.79	0.33	10.28	77.33	10.63	0.30	0.33
49	0.00	0.75	0.19	9.70	75.98	12.62	0.33	0.42
50	0.03	0.77	0.15	1.71	76.66	19.85	0.34	0.51
51	0.01	0.74	0.31	10.27	77.21	10.70	0.33	0.44
52	0.00	0.78	0.26	10.29	76.76	11.19	0.34	0.38
53	0.04	0.35	0.17	8.37	62.07	28.40	0.23	0.39
54	0.00	0.43	0.17	7.21	75.27	16.28	0.17	0.47
55	0.00	0.19	0.33	6.52	79.44	13.12	0.06	0.35
56	0.02	0.00	4.45	1.82	62.22	31.16	0.02	0.32
57	0.00	0.00	5.24	1.83	60.95	31.58	0.01	0.39
58	0.00	0.02	5.35	1.71	60.64	31.92	0.04	0.32
59	0.00	0.00	14.26	1.34	43.46	40.57	0.02	0.35
60	0.00	0.04	5.66	1.23	53.98	38.67	0.00	0.42
0	0.01	0.62	3.25	9.02	86.34	0.09	0.35	0.32
1	0.00	0.63	0.43	9.12	89.12	0.08	0.30	0.31
2	0.02	0.65	3.32	8.88	86.38	0.11	0.33	0.32
3	0.00	0.43	33.37	6.54	57.90	1.43	0.15	0.20
4	0.00	0.59	12.17	7.92	77.58	1.12	0.28	0.35
5	0.01	0.50	27.58	7.05	63.28	1.17	0.18	0.23
6	0.00	0.61	1.12	9.09	88.57	0.12	0.23	0.27
7	0.01	0.53	13.86	8.32	76.17	0.68	0.19	0.26
8	0.00	0.61	2.10	8.91	87.60	0.20	0.26	0.31
9	0.00	0.53	0.19	9.05	89.54	0.19	0.22	0.28
10	0.00	0.56	0.18	8.99	89.46	0.27	0.24	0.29
11	0.01	0.52	1.10	8.85	88.58	0.38	0.26	0.32
12	0.02	0.66	0.83	11.42	76.65	9.72	0.30	0.41
13	0.00	0.58	2.48	11.16	77.41	7.62	0.28	0.46
14	0.00	0.73	1.27	11.65	75.37	10.25	0.29	0.44
15	0.00	0.69	3.81	12.70	77.76	10.96	0.29	0.43
16	0.00	0.64	1.06	11.30	75.39	11.01	0.25	0.35
17	0.00	0.62	0.14	11.14	76.27	11.13	0.28	0.42
18	0.01	0.73	0.15	11.11	75.32	11.99	0.31	0.38
19	0.00	0.80	0.07	11.14	76.25	10.95	0.31	0.48
20	0.00	0.62	0.13	11.02	75.71	11.79	0.32	0.42
21	0.00	0.65	0.12	11.22	75.85	11.39	0.35	0.42
22	0.00	0.76	0.17	10.78	76.15	11.43	0.34	0.37
23	0.01	0.73	0.12	10.71	75.29	12.48	0.29	0.38
24	0.00	0.80	0.07	10.99	74.85	12.53	0.35	0.42
25	0.00	0.77	0.06	11.12	75.24	12.13	0.35	0.34
26	0.00	0.78	0.12	11.06	75.43	11.80	0.35	0.45
27	0.00	0.69	0.14	10.77	77.07	10.70	0.29	0.35
28	0.00	0.72	0.13	10.70	76.55	11.25	0.29	0.37
29	0.01	0.74	0.13	10.68	76.31	11.47	0.29	0.38
30	0.00	0.71	0.17	10.85	76.64	10.94	0.34	0.35
31	0.00	0.68	0.10	10.80	76.83	10.90	0.29	0.40
32	0.00	0.74	0.18	10.60	76.16	11.62	0.35	0.37

33	0.00	0.68	0.13	10.63	76.40	11.38	0.33	0.45
34	0.00	0.75	0.50	10.87	76.58	10.60	0.30	0.40
35	0.00	0.69	0.16	10.89	76.51	11.10	0.26	0.39
36	0.00	0.78	0.89	11.01	76.29	10.34	0.33	0.35
37	0.00	0.71	0.48	10.64	75.54	11.97	0.28	0.39
38	0.00	0.76	0.21	11.41	75.51	11.43	0.33	0.36
39	0.01	0.77	0.36	10.89	75.60	11.67	0.34	0.38
40	0.00	0.63	1.11	8.57	72.00	16.93	0.28	0.49
41	0.00	0.62	1.41	10.00	72.46	14.83	0.25	0.43
42	0.01	0.83	0.17	10.69	76.33	11.29	0.35	0.34
43	0.01	0.86	0.50	11.10	76.34	10.55	0.28	0.38
44	0.00	0.78	0.09	10.99	76.86	10.56	0.35	0.36
45	0.00	0.83	0.12	10.98	76.26	11.08	0.32	0.41
46	0.00	0.83	0.09	10.95	76.47	11.03	0.33	0.30
47	0.00	0.84	0.18	10.16	76.74	11.34	0.37	0.36
48	0.04	0.17	0.29	1.86	34.10	62.92	0.13	0.49
49	0.02	0.27	0.20	5.24	50.48	43.26	0.14	0.40
50	0.00	0.15	0.58	2.32	38.73	57.61	0.11	0.51
51	0.00	0.15	0.41	4.86	50.54	43.54	0.06	0.46
52	0.00	0.15	0.29	6.49	79.23	13.43	0.04	0.37
53	0.00	0.16	0.26	6.53	80.25	12.37	0.02	0.41
54	0.00	0.18	0.47	3.06	45.76	50.03	0.15	0.35
55	0.01	0.19	0.29	6.35	78.47	14.27	0.07	0.35
56	0.00	0.14	0.22	6.44	80.13	12.57	0.03	0.47
57	0.00	0.11	2.52	5.57	75.63	15.75	0.05	0.38
58	0.01	0.08	2.60	2.50	72.15	22.23	0.03	0.41
59	0.00	0.01	5.21	1.54	61.33	31.47	0.01	0.43
60	0.00	0.00	4.67	1.58	61.23	32.16	0.04	0.33

C.26 G.91/V/Nd After 28 Days at 625°C

The G.91/V/Nd assembly annealed for 28 days at 625°C bonded on the V/Nd interface but not the G.91/V interface. Since the V/Nd interface at this time and temperature was already well characterized, no WDS linescans were completed on it in this assembly.

C.27 G.91/Zr/V/Nd After 28 Days at 625°C

The G.91/Zr/V/Nd assembly annealed for 28 days at 625°C bonded on the V/Nd interface but not the G.91/Zr or Zr/V interfaces. Compositional data (in at%) from WDS linescans across the V/Nd interface is given below.

Position	Zr	Mo	Si	Cr	Fe	Nd	V	Mn
0	0.04	0.00	0.19	0.00	0.30	98.27	0.58	0.62
1	0.00	0.05	0.19	0.00	0.27	97.87	1.14	0.48
2	0.00	0.00	0.43	0.00	0.45	96.89	1.65	0.57
3	0.00	0.00	0.27	0.00	0.47	96.42	2.29	0.56
4	0.05	0.13	0.45	0.35	2.19	80.81	15.59	0.43
5	0.01	0.11	0.57	1.87	12.80	7.53	77.01	0.09
6	0.00	0.07	0.64	1.93	8.30	2.75	86.23	0.07

7	0.00	0.01	0.76	1.70	0.59	4.54	92.37	0.04
8	0.02	0.02	0.52	1.83	0.15	1.34	96.12	0.01
9	0.00	0.00	0.56	1.87	0.11	1.41	96.05	0.00
10	0.00	0.01	2.01	1.86	0.06	0.19	95.89	0.00
11	0.00	0.00	2.89	1.78	0.04	0.09	95.20	0.00
12	0.01	0.02	1.38	1.85	0.01	0.05	96.68	0.00
13	0.01	0.00	1.76	1.91	0.03	0.05	96.24	0.01
14	0.00	0.01	0.49	1.82	0.02	0.09	97.59	0.00
15	0.00	0.01	2.56	1.86	0.02	0.06	95.49	0.01

C.28 G.91/Zr/Nd After 28 Days at 625°C

The G.91/Zr/Nd assembly annealed for 28 days at 625°C bonded on the Zr/Nd interface but not the G.91/Zr interface. Compositional data (in at%) from WDS linescans across the Zr/Nd interface is given below.

Position	Zr	Mo	Si	Cr	Fe	Nd	V	Mn
0	98.75	0.00	1.12	0.00	0.03	0.08	0.01	0.00
1	99.68	0.00	0.21	0.00	0.01	0.05	0.05	0.01
2	99.65	0.02	0.16	0.00	0.00	0.10	0.07	0.00
3	99.36	0.00	0.37	0.04	0.12	0.10	0.02	0.00
4	98.97	0.00	0.75	0.01	0.00	0.22	0.00	0.05
5	98.44	0.00	1.23	0.01	0.00	0.29	0.03	0.00
6	97.93	0.00	0.32	0.03	0.83	0.84	0.05	0.00
7	98.78	0.00	0.36	0.00	0.13	0.71	0.01	0.00
8	72.68	0.00	0.67	0.03	0.49	26.01	0.00	0.12
9	8.40	0.05	0.49	0.00	0.43	90.14	0.06	0.45
10	0.44	0.00	0.59	0.03	0.35	98.04	0.00	0.55
11	0.18	0.00	0.53	0.00	0.39	98.34	0.00	0.56
12	0.08	0.00	0.21	0.05	0.34	99.06	0.00	0.27
13	0.11	0.01	0.25	0.00	0.32	98.81	0.00	0.51
14	0.08	0.00	0.23	0.00	0.41	98.78	0.00	0.50
15	0.05	0.00	0.26	0.00	0.41	98.79	0.06	0.43

C.29 G.91/Ti/V/Nd After 28 Days at 625°C

The G.91/Ti/V/Nd assembly annealed for 28 days at 625°C bonded on the V/Nd interface but not the G.91/Ti or Ti/V interfaces. Compositional data (in at%) from WDS linescans across the V/Nd interface is given below.

Position	Ti	Ta	Mo	Si	Cr	Fe	Nd	V	Mn
0	0.04	0.00	0.00	5.23	2.00	0.07	0.71	91.90	0.05
1	0.17	0.00	0.01	5.68	2.06	0.19	0.87	90.98	0.04
2	0.25	0.00	0.01	18.75	1.75	0.08	0.72	78.45	0.00
3	0.03	0.00	0.00	0.71	2.19	0.08	0.54	96.45	0.00
4	0.06	0.00	0.00	0.25	2.09	0.01	0.96	96.62	0.00
5	0.02	0.00	0.00	0.19	2.02	0.04	0.63	97.09	0.01
6	0.00	0.00	0.00	0.67	2.12	0.00	2.39	94.75	0.08
7	0.00	0.00	0.00	1.61	0.44	0.15	77.60	19.93	0.27
8	0.00	0.00	0.09	0.55	0.23	0.44	92.75	5.56	0.37
9	0.00	0.00	0.13	0.47	0.19	0.36	93.72	4.74	0.39
10	0.00	0.00	0.06	0.46	0.00	0.42	94.74	4.17	0.16

11	0.00	0.00	0.00	0.69	0.05	0.52	94.52	3.91	0.32
12	0.00	0.00	0.00	0.78	0.15	0.41	95.48	2.80	0.39
13	0.00	0.00	0.00	0.58	0.08	0.42	95.60	2.90	0.42
14	0.00	0.00	0.01	0.36	0.10	0.23	96.16	2.63	0.51
15	0.00	0.00	0.00	0.58	0.00	0.45	96.63	1.93	0.42

C.30 G.91/Ti/Nd After 28 Days at 625°C

The G.91/Ti/Nd assembly annealed for 28 days at 625°C bonded on the G.91/Ti and Ti/Nd interfaces. Compositional data (in at%) from WDS linescans across these interfaces is given below.

Position	Ti	Ta	Mo	Si	Cr	Fe	Nd	V	Mn
0	2.11	0.00	0.12	1.07	0.00	0.23	95.91	0.00	0.56
1	3.41	0.44	0.00	5.95	0.00	0.53	89.09	0.03	0.55
2	4.85	0.00	0.08	26.69	0.00	0.59	67.45	0.00	0.34
3	3.58	0.00	0.00	35.54	0.06	0.35	60.19	0.00	0.28
4	9.54	0.00	0.00	22.42	0.00	0.38	67.41	0.00	0.25
5	46.49	0.00	0.00	9.29	0.01	0.47	43.32	0.20	0.22
6	80.62	0.00	0.02	4.50	0.13	3.98	10.33	0.25	0.16
7	80.64	0.00	0.00	4.66	0.12	3.89	10.19	0.33	0.16
8	43.81	0.00	0.03	43.84	0.16	3.23	8.70	0.13	0.09
9	41.43	0.00	0.00	51.08	0.04	2.55	4.66	0.17	0.06
10	55.05	0.00	0.00	35.33	0.08	3.00	6.32	0.13	0.09
11	83.99	0.00	0.00	4.85	0.08	1.02	9.94	0.00	0.12
12	91.48	0.00	0.00	0.40	0.05	0.12	7.60	0.29	0.08
13	95.58	0.00	0.00	0.53	0.00	0.08	3.48	0.30	0.03
14	79.97	0.00	0.00	1.35	0.01	0.56	17.80	0.19	0.12
15	63.16	0.00	0.00	6.94	0.07	0.33	29.24	0.13	0.14
0	98.64	0.00	0.00	0.39	0.03	0.40	0.29	0.24	0.01
1	98.81	0.00	0.00	0.14	0.08	0.51	0.18	0.27	0.02
2	98.45	0.00	0.00	0.48	0.08	0.56	0.16	0.23	0.04
3	98.68	0.00	0.00	0.12	0.13	0.71	0.09	0.26	0.01
4	98.59	0.00	0.00	0.08	0.13	0.84	0.02	0.33	0.01
5	96.99	0.00	0.00	0.08	0.30	2.11	0.14	0.35	0.03
6	33.17	0.00	0.56	0.37	9.34	55.75	0.32	0.32	0.18
7	3.07	0.00	0.41	0.32	7.95	87.49	0.23	0.35	0.19
8	2.14	0.00	0.43	2.11	7.76	87.01	0.11	0.26	0.18
9	2.06	0.00	0.44	0.64	7.77	88.48	0.18	0.23	0.20
10	1.35	0.00	0.48	0.68	8.51	88.19	0.43	0.20	0.17
11	1.06	0.00	0.45	0.60	8.60	88.48	0.35	0.21	0.24
12	3.19	0.00	0.46	2.21	8.32	84.77	0.57	0.24	0.23
13	4.45	0.00	0.42	2.97	8.45	82.73	0.43	0.26	0.29
14	1.05	0.00	0.42	0.00	8.55	89.07	0.39	0.28	0.25
15	2.30	0.00	0.49	1.28	8.81	86.22	0.41	0.28	0.23
0	98.52	0.00	0.00	0.66	0.05	0.45	0.07	0.24	0.00
1	98.81	0.00	0.00	0.18	0.11	0.58	0.09	0.23	0.01
2	96.83	0.00	0.00	2.00	0.10	0.74	0.07	0.25	0.01
3	94.93	0.00	0.00	2.71	0.28	1.36	0.33	0.34	0.05
4	67.70	0.00	0.25	0.91	5.05	24.73	0.55	0.40	0.41
5	15.39	0.00	0.64	1.03	10.09	70.99	0.65	0.33	0.88
6	3.10	0.00	0.52	0.33	7.74	87.23	0.49	0.32	0.28

7	1.87	0.00	0.59	0.26	8.46	87.85	0.36	0.29	0.32
8	1.98	0.00	0.63	0.38	8.87	87.36	0.35	0.20	0.23
9	1.31	0.00	0.81	1.81	11.27	83.94	0.33	0.23	0.30
10	0.98	0.00	0.55	0.36	8.91	88.19	0.44	0.28	0.29
11	0.88	0.00	0.85	0.41	10.83	86.06	0.33	0.20	0.46
12	0.91	0.00	0.71	0.68	10.07	86.80	0.23	0.28	0.33
13	1.06	0.00	0.67	0.42	9.75	87.32	0.19	0.29	0.30
14	0.45	0.00	0.52	0.29	8.43	89.62	0.16	0.18	0.35
15	1.11	0.00	0.64	1.42	9.86	86.17	0.26	0.20	0.34

C.31 G.91/Ta/V/Nd After 28 Days at 625°C

The G.91/Ta/V/Nd assembly annealed for 28 days at 625°C bonded on the V/Nd interface but not the G.91/Ta or Ta/V interfaces. Since the V/Nd interface at this time and temperature was already well characterized, no WDS line scans were completed on it in this assembly.

C.32 G.91/Ta/Nd After 28 Days at 625°C

The G.91/Ta/Nd assembly annealed for 28 days at 625°C bonded on the Ta/Nd interface but not the G.91/Ta interface. Compositional data (in at%) from WDS line scans across the Ta/Nd interface is given below.

Position	Ti	Ta	Mo	Si	Cr	Fe	Nd	V	Mn
0	0.00	0.00	0.03	8.32	0.05	0.31	90.77	0.00	0.52
1	0.00	0.00	0.03	0.12	0.09	0.33	98.98	0.10	0.35
2	0.00	0.00	0.00	0.19	0.06	0.22	98.99	0.00	0.55
3	0.00	0.00	0.09	0.21	0.04	0.16	98.90	0.00	0.62
4	0.00	0.00	0.00	0.22	0.04	0.43	98.90	0.00	0.41
5	0.00	0.00	0.07	0.20	0.00	0.28	98.77	0.00	0.68
6	0.00	0.00	0.02	25.20	0.00	0.64	73.61	0.01	0.51
7	0.00	77.99	0.09	0.00	0.10	0.88	20.56	0.08	0.30
8	0.02	98.24	0.00	0.00	0.00	0.08	1.55	0.11	0.00
9	0.00	94.89	0.00	0.00	0.00	0.00	5.01	0.06	0.04
10	0.01	89.57	0.00	5.06	0.00	0.03	5.31	0.03	0.00
11	0.00	91.09	0.02	0.00	0.00	0.94	7.93	0.03	0.00
12	0.00	96.89	0.02	0.00	0.02	0.00	3.07	0.00	0.01
13	0.00	98.40	0.01	0.00	0.10	0.00	1.49	0.00	0.00
14	0.05	97.53	0.00	0.00	0.00	0.04	2.21	0.00	0.17
15	0.04	97.30	0.09	0.00	0.10	0.05	2.41	0.00	0.02

C.33 G.91/Mo/V/Nd After 28 Days at 625°C

The G.91/Mo/V/Nd assembly annealed for 28 days at 625°C bonded on the V/Nd interface but not the G.91/Mo or Mo/V interfaces. Since the V/Nd interface at

this time and temperature was already well characterized, no WDS linescans were completed on it in this assembly.

C.34 G.91/Mo/Nd After 28 Days at 625°C

The G.91/Mo/Nd assembly annealed for 28 days at 625°C bonded on the Mo/Nd interface but not the G.91/Mo interface. Compositional data (in at%) from WDS linescans across the Mo/Nd interface is given below.

Position	W	Nd	Mo	Fe	Mn	Cr	V	Si
0	0.02	98.22	0.12	0.61	0.49	0.03	0.01	0.50
1	0.00	93.87	0.14	0.83	0.27	0.10	0.00	4.79
2	0.03	68.78	1.61	0.74	0.30	0.01	0.02	28.49
3	0.00	50.89	19.56	0.57	0.33	0.02	0.00	28.63
4	0.00	21.13	69.70	0.28	0.12	0.04	0.04	8.70
5	0.00	2.63	96.66	0.12	0.02	0.01	0.00	0.56
6	0.04	0.85	98.52	0.06	0.00	0.00	0.06	0.46
7	0.01	0.43	99.33	0.05	0.00	0.00	0.03	0.15
8	0.00	0.26	99.43	0.07	0.03	0.02	0.03	0.17
9	0.01	0.19	99.70	0.00	0.00	0.00	0.02	0.07
10	0.03	5.28	94.65	0.02	0.03	0.00	0.00	0.00
11	0.00	0.24	99.66	0.02	0.00	0.00	0.00	0.08
12	0.00	0.03	99.71	0.12	0.00	0.01	0.04	0.09
13	0.01	0.18	99.51	0.00	0.07	0.02	0.10	0.11
14	0.03	0.06	99.59	0.03	0.09	0.02	0.05	0.15
15	0.00	0.06	99.74	0.02	0.00	0.00	0.01	0.17
0	0.00	98.95	0.01	0.40	0.44	0.00	0.00	0.20
1	0.01	98.68	0.03	0.55	0.51	0.00	0.00	0.22
2	0.00	98.75	0.06	0.37	0.53	0.01	0.00	0.28
3	0.04	98.65	0.19	0.46	0.50	0.03	0.01	0.13
4	0.00	98.63	0.21	0.44	0.43	0.00	0.03	0.25
5	0.03	90.18	8.72	0.32	0.49	0.01	0.04	0.23
6	0.00	42.92	55.78	0.52	0.30	0.06	0.00	0.42
7	0.01	9.64	89.71	0.21	0.14	0.00	0.01	0.28
8	0.02	2.19	97.50	0.10	0.05	0.01	0.01	0.13
9	0.00	0.44	99.13	0.04	0.03	0.11	0.00	0.25
10	0.02	0.28	99.21	0.05	0.00	0.00	0.00	0.45
11	0.01	0.43	98.90	0.06	0.02	0.00	0.00	0.58
12	0.02	0.24	99.36	0.06	0.04	0.00	0.00	0.29
13	0.02	0.10	99.76	0.10	0.00	0.00	0.00	0.02
14	0.01	0.10	99.56	0.12	0.00	0.02	0.01	0.18
15	0.01	0.32	97.93	0.04	0.06	0.00	0.00	1.64
0	0.04	93.65	0.32	4.23	0.47	0.32	0.00	0.96
1	0.00	93.67	0.32	4.24	0.39	0.29	0.08	1.00
2	0.00	96.22	0.08	0.90	0.51	0.12	0.00	2.17
3	0.00	98.51	0.07	0.55	0.43	0.04	0.04	0.36
4	0.00	98.43	0.12	0.55	0.43	0.05	0.00	0.42
5	0.00	97.13	0.34	0.38	0.42	0.00	0.00	1.73
6	0.03	90.82	6.42	0.40	0.54	0.05	0.00	1.74
7	0.01	52.45	45.48	0.58	0.15	0.00	0.03	1.29

8	0.00	30.16	68.69	0.35	0.14	0.05	0.04	0.56
9	0.01	2.48	97.23	0.00	0.09	0.00	0.04	0.15
10	0.01	0.27	99.46	0.07	0.00	0.00	0.08	0.11
11	0.03	0.17	99.55	0.03	0.00	0.00	0.02	0.21
12	0.01	0.15	99.71	0.03	0.00	0.00	0.01	0.09
13	0.02	0.15	99.64	0.07	0.00	0.00	0.01	0.11
14	0.01	0.14	99.47	0.05	0.03	0.03	0.00	0.28
15	0.01	0.13	99.38	0.06	0.00	0.02	0.00	0.41

C.35 G.91/W/V/Nd After 28 Days at 625°C

The G.91/W/V/Nd assembly annealed for 28 days at 625°C bonded on the W/V and V/Nd interfaces but not the G.91/W interface. Compositional data (in at%) from WDS linescans across the W/V interface is given below.

Position	W	Nd	Mo	Fe	Mn	Cr	V	Si
0	98.66	0.00	0.00	0.06	0.13	0.06	1.09	0.00
1	98.04	0.02	0.00	0.13	0.00	0.05	1.64	0.13
2	97.17	0.10	0.00	0.24	0.00	0.05	2.45	0.00
3	96.51	0.04	0.00	0.16	0.11	0.07	3.11	0.00
4	94.95	0.00	0.00	0.09	0.00	0.20	4.65	0.12
5	91.43	0.15	0.00	0.20	0.00	0.14	7.93	0.14
6	57.69	0.23	0.00	0.26	0.08	0.76	40.21	0.78
7	3.94	0.16	0.00	0.17	0.02	1.75	90.86	3.11
8	0.32	0.02	0.00	0.07	0.00	1.85	94.45	3.30
9	0.08	0.00	0.00	0.02	0.00	1.91	97.33	0.66
10	0.02	0.00	0.01	0.05	0.00	1.87	97.94	0.13
11	0.02	0.03	0.00	0.46	0.00	1.87	97.44	0.19
12	0.01	0.03	0.01	0.22	0.01	1.84	97.74	0.15
13	0.02	0.01	0.02	0.06	0.00	1.94	97.89	0.07
14	0.02	0.01	0.00	0.01	0.00	1.97	97.84	0.15
15	0.00	0.00	0.00	0.03	0.01	1.89	95.43	2.64
0	98.01	0.00	0.00	0.01	0.08	0.10	1.80	0.00
1	98.66	0.05	0.00	0.09	0.00	0.00	1.19	0.00
2	98.07	0.05	0.00	0.04	0.00	0.09	1.74	0.00
3	97.20	0.00	0.00	0.14	0.00	0.07	2.23	0.36
4	95.30	0.14	0.00	0.18	0.00	0.00	4.00	0.38
5	93.95	0.18	0.00	0.24	0.16	0.11	5.23	0.13
6	90.24	0.21	0.00	0.18	0.10	0.08	8.75	0.44
7	41.18	0.11	0.00	0.16	0.02	0.91	45.31	12.32
8	1.03	0.04	0.00	0.05	0.00	1.66	85.35	11.88
9	0.02	0.00	0.01	0.05	0.00	1.72	90.56	7.65
10	0.02	0.00	0.01	0.03	0.04	1.76	90.56	7.59
11	0.01	0.00	0.00	0.04	0.00	1.82	95.90	2.23
12	0.01	0.01	0.00	0.06	0.00	1.85	94.36	3.71
13	0.02	0.00	0.01	0.06	0.00	1.85	89.90	8.17
14	0.02	0.00	0.00	0.04	0.00	1.83	94.33	3.78
15	0.17	0.03	0.00	0.07	0.00	1.81	94.29	3.63

C.36 G.91/W/Nd After 28 Days at 625°C

The G.91/W/Nd assembly annealed for 28 days at 625°C bonded on the W/Nd interface but not the G.91/W interface. Compositional data (in at%) from WDS linescans across the W/Nd interface is given below.

Position	W	Nd	Mo	Fe	Mn	Cr	V	Si
0	0.06	96.68	0.04	2.00	0.55	0.12	0.00	0.55
1	3.83	88.90	0.00	0.55	0.32	0.05	0.02	6.33
2	14.49	50.51	0.00	0.55	0.36	0.04	0.00	34.05
3	23.48	31.64	0.01	0.56	0.17	0.03	0.00	44.12
4	92.83	4.82	0.00	0.36	0.00	0.10	0.17	1.72
5	98.97	0.81	0.00	0.01	0.02	0.00	0.06	0.13
6	99.22	0.58	0.00	0.06	0.12	0.04	0.00	0.00
7	99.31	0.47	0.00	0.16	0.00	0.04	0.00	0.01
8	99.73	0.16	0.00	0.07	0.00	0.00	0.03	0.01
9	99.47	0.14	0.00	0.18	0.00	0.02	0.10	0.09
10	99.50	0.21	0.00	0.22	0.02	0.02	0.02	0.00
11	99.43	0.17	0.00	0.23	0.00	0.10	0.08	0.00
12	98.45	0.52	0.00	0.84	0.04	0.01	0.07	0.06
13	99.26	0.36	0.00	0.38	0.00	0.00	0.00	0.00
14	97.92	0.67	0.00	1.06	0.11	0.10	0.08	0.06
15	99.38	0.20	0.00	0.29	0.01	0.12	0.00	0.00
0	0.06	97.95	0.00	0.65	0.38	0.02	0.05	0.90
1	0.00	98.27	0.01	0.61	0.40	0.04	0.00	0.68
2	0.07	93.61	0.04	2.96	0.43	0.26	0.00	2.64
3	0.17	68.01	0.10	18.78	0.45	1.59	0.08	10.82
4	2.82	64.88	0.07	17.58	0.40	1.50	0.06	12.70
5	45.30	48.48	0.00	3.25	0.32	0.30	0.00	2.35
6	85.80	2.75	0.00	1.05	0.09	9.05	0.04	1.22
7	88.55	2.03	0.00	1.19	0.00	0.09	0.01	8.13
8	98.18	0.82	0.00	0.20	0.03	0.00	0.34	0.44
9	99.53	0.30	0.00	0.00	0.00	0.04	0.12	0.00
10	97.67	0.32	0.00	0.10	1.91	0.00	0.00	0.00
11	96.90	0.98	0.00	0.12	0.08	0.00	0.00	1.92
12	97.35	0.66	0.00	0.10	0.10	0.04	0.08	1.67
13	99.05	0.27	0.00	0.17	0.05	0.08	0.11	0.28
14	99.48	0.14	0.00	0.12	0.02	0.10	0.14	0.00
15	99.01	0.33	0.00	0.13	0.00	0.00	0.00	0.54

C.37 G.91/Nd After 28 Days at 700°C

The G.91/Nd diffusion couple annealed for 28 days at 700°C broke upon removal from the furnace, leaving only the first interaction zone intact. The remaining portion of this zone was ~640 μm wide with a composition matching $\text{Nd}_2(\text{Fe}+\text{Cr})_{17}$. Compositional data (in at%) from WDS linescans across the interface is given below.

Position	Zr	Mo	Si	Cr	Fe	Nd	V	Mn
0	0.02	0.58	0.48	8.93	89.32	0.01	0.24	0.42
20	0.00	0.61	4.57	8.86	85.31	0.00	0.27	0.38

40	0.00	0.63	0.10	11.78	81.35	5.44	0.37	0.33
60	0.02	0.66	0.25	10.09	77.53	10.80	0.26	0.40
80	0.00	0.69	0.19	10.54	77.31	10.60	0.29	0.39
100	0.01	0.60	0.19	10.38	77.48	10.63	0.28	0.43
120	0.00	0.63	0.13	10.65	77.19	10.74	0.27	0.40
140	0.00	0.60	0.19	10.70	77.45	10.57	0.23	0.26
160	0.00	0.67	0.14	10.69	77.27	10.62	0.28	0.32
180	0.03	0.63	0.18	10.86	77.01	10.64	0.29	0.38
200	0.00	0.64	0.15	10.62	77.16	10.81	0.31	0.30
220	0.00	0.67	0.15	10.92	77.06	10.44	0.32	0.45
240	0.00	0.57	9.57	10.18	67.94	11.18	0.30	0.27
260	0.01	0.73	0.21	11.37	74.85	12.12	0.30	0.41
280	0.00	0.69	0.37	11.43	76.53	10.30	0.29	0.38
300	0.01	0.74	0.13	11.81	76.68	10.06	0.20	0.38
320	0.01	0.74	0.10	11.48	76.70	10.27	0.39	0.33
340	0.01	0.75	0.12	11.32	76.51	10.60	0.32	0.38
360	0.00	0.81	0.17	11.66	76.05	10.65	0.36	0.31
380	0.02	0.77	0.14	11.63	76.63	10.15	0.38	0.29
400	0.00	0.88	0.14	12.18	76.10	9.85	0.43	0.42
420	0.00	0.85	0.18	11.98	75.97	10.27	0.38	0.38
440	0.00	0.95	0.21	12.27	75.53	10.19	0.43	0.42
460	0.01	0.83	0.14	12.07	75.98	10.26	0.35	0.37
480	0.00	0.89	0.16	13.19	75.32	9.60	0.43	0.41
500	0.00	0.85	0.22	12.79	75.36	10.06	0.36	0.37
520	0.00	0.90	0.12	13.30	74.11	10.75	0.42	0.40
540	0.01	0.70	0.15	12.33	75.98	10.11	0.36	0.37
560	0.00	0.77	0.29	12.42	75.72	10.12	0.34	0.34
580	0.00	0.70	0.09	12.37	75.50	10.66	0.28	0.41
600	0.00	0.77	0.08	12.71	75.48	10.23	0.38	0.36
620	0.00	0.82	0.02	12.72	75.12	10.60	0.37	0.35
640	0.02	0.80	0.03	13.06	75.63	9.70	0.44	0.33
660	0.03	0.63	0.12	12.63	71.95	13.90	0.32	0.44
680	0.00	0.83	0.08	12.93	75.44	9.87	0.53	0.32
700	0.00	0.54	0.59	11.81	72.58	13.48	0.67	0.33
0	0.01	0.51	0.29	9.35	89.18	0.01	0.28	0.37
1	0.00	0.58	0.21	9.33	89.21	0.08	0.23	0.36
2	0.00	0.52	0.23	9.34	89.23	0.09	0.30	0.30
3	0.00	0.51	0.23	9.24	89.31	0.09	0.28	0.33
4	0.00	0.52	0.20	9.42	89.22	0.07	0.27	0.30
5	0.00	0.54	0.23	9.32	89.24	0.11	0.26	0.31
6	0.00	0.50	0.17	9.48	89.05	0.15	0.30	0.35
7	0.01	0.43	0.13	9.54	89.13	0.19	0.28	0.29
8	0.00	0.38	0.10	9.88	88.79	0.30	0.28	0.26
9	0.00	0.39	0.26	10.63	84.43	3.70	0.32	0.28
10	0.00	1.07	0.21	10.67	73.39	13.95	0.30	0.41
11	0.00	1.12	0.21	10.47	71.93	15.59	0.23	0.45
12	0.00	0.93	0.15	9.96	74.28	14.00	0.25	0.43
13	0.00	0.87	0.17	11.25	74.19	12.68	0.32	0.52
14	0.00	0.78	0.18	10.69	77.03	10.66	0.31	0.35
15	0.00	0.66	0.17	10.30	77.91	10.29	0.27	0.40
16	0.00	0.65	0.14	10.09	77.97	10.49	0.26	0.39
17	0.01	0.66	0.18	10.03	76.51	11.92	0.26	0.44
18	0.00	0.80	0.23	10.44	77.09	10.74	0.29	0.41
19	0.00	0.82	0.15	10.22	76.34	11.81	0.30	0.36
20	0.01	0.84	0.11	10.16	76.71	11.59	0.28	0.31

0	0.00	0.85	2.34	12.54	74.06	9.49	0.34	0.39
1	0.00	0.80	0.48	12.53	75.54	9.96	0.34	0.35
2	0.00	0.97	0.13	12.77	75.48	10.01	0.35	0.31
3	0.00	0.90	0.13	13.83	74.92	9.42	0.43	0.38
4	0.00	0.82	0.12	13.20	75.39	9.77	0.39	0.31
5	0.01	0.87	0.13	13.60	75.19	9.49	0.41	0.32
6	0.01	0.79	0.14	12.90	75.56	9.84	0.40	0.35
7	0.00	0.87	0.18	12.75	75.64	9.89	0.35	0.31
8	0.00	0.74	0.18	11.79	76.26	10.25	0.37	0.41
9	0.00	0.88	0.17	15.91	73.79	8.44	0.50	0.31
10	0.01	0.75	0.14	14.09	74.75	9.43	0.40	0.43
11	0.00	0.79	0.14	12.29	75.36	10.79	0.32	0.33
12	0.00	0.78	0.13	12.37	75.67	10.31	0.38	0.37
13	0.02	0.80	0.11	11.86	74.34	12.13	0.39	0.35
14	0.00	0.75	0.23	12.15	75.46	10.73	0.39	0.29
15	0.01	0.72	0.19	12.22	75.79	10.40	0.33	0.34
16	0.00	0.78	0.13	12.53	76.10	9.80	0.35	0.32
17	0.00	0.77	0.16	12.31	76.17	9.91	0.34	0.35
18	0.00	0.72	0.10	12.37	75.83	10.26	0.35	0.36
19	0.01	0.72	0.14	12.47	75.77	10.10	0.36	0.45
20	0.01	0.81	0.13	12.06	76.24	9.96	0.40	0.40
0	0.00	0.81	0.13	12.72	75.32	10.23	0.43	0.37
1	0.00	0.85	0.26	12.56	74.06	11.42	0.48	0.39
2	0.00	0.75	0.32	12.21	69.81	16.08	0.51	0.33
3	0.01	0.90	0.13	12.61	73.14	12.41	0.49	0.30
4	0.01	0.81	0.14	12.60	75.13	10.52	0.47	0.33
5	0.00	0.79	0.12	12.59	74.12	11.53	0.50	0.36
6	0.00	0.86	0.18	11.90	61.43	24.82	0.50	0.31
7	0.01	0.48	0.04	12.75	70.43	15.46	0.53	0.31
8	0.01	0.37	0.06	12.56	74.76	11.39	0.53	0.33
9	0.00	0.66	0.08	12.46	75.60	10.49	0.42	0.31
10	0.00	0.71	0.12	11.99	76.39	10.07	0.40	0.32
11	0.00	0.69	0.33	11.69	76.48	10.18	0.30	0.33
12	0.01	0.66	0.16	11.76	76.42	10.26	0.41	0.33
13	0.02	0.76	0.66	11.78	75.76	10.35	0.38	0.29
14	0.00	0.75	0.16	12.35	75.85	10.17	0.42	0.30
15	0.00	0.72	0.21	11.91	75.99	10.47	0.41	0.29
16	0.00	0.79	0.40	12.33	75.51	10.15	0.52	0.30
17	0.00	0.72	0.89	11.99	74.85	10.77	0.45	0.34
18	0.00	0.64	0.39	11.89	74.93	11.28	0.56	0.31
19	0.01	0.47	0.87	11.12	73.51	13.22	0.53	0.28
20	0.00	0.08	0.38	10.83	69.78	18.17	0.49	0.28

C.38 G.91/V/Nd After 28 Days at 700°C

The G.91/V/Nd assembly annealed for 28 days at 700°C bonded on the G.91/V and V/Nd interfaces. Compositional data (in at%) from WDS linescans across the G.91/V interface is given below.

Position	Zr	Mo	Si	Cr	Fe	Nd	V	Mn
0	0.00	0.00	1.83	2.04	0.47	0.03	95.63	0.00
1	0.00	0.00	6.89	1.92	0.49	0.01	90.67	0.02
2	0.01	0.01	1.87	2.02	0.30	0.00	95.80	0.00

3	0.01	0.01	9.41	1.88	0.34	0.00	88.34	0.00
4	0.01	0.00	2.74	1.92	0.41	0.00	94.93	0.00
5	0.01	0.01	0.06	2.01	0.52	0.00	97.38	0.01
6	0.00	0.01	0.15	2.02	0.78	0.00	96.99	0.06
7	0.00	0.00	0.94	2.17	1.13	0.00	95.62	0.14
8	0.00	0.16	2.65	4.14	22.01	0.00	70.48	0.57
9	0.01	0.49	1.10	8.21	83.43	0.00	6.45	0.32
10	0.01	0.53	0.97	8.38	87.29	0.01	2.46	0.35
11	0.00	0.49	0.41	8.43	88.13	0.00	2.18	0.36
12	0.00	0.53	0.43	8.53	88.27	0.00	1.95	0.30
13	0.01	0.55	0.37	8.56	88.96	0.00	1.24	0.31
14	0.00	0.54	0.75	8.69	88.20	0.00	1.52	0.30
15	0.00	0.54	0.34	8.75	88.92	0.01	1.13	0.31
0	0.00	0.03	0.12	2.04	0.24	0.01	97.56	0.00
1	0.01	0.00	0.21	2.03	0.29	0.00	97.47	0.00
2	0.00	0.01	1.96	2.01	0.35	0.00	95.67	0.00
3	0.00	0.01	0.27	2.06	0.43	0.01	97.22	0.00
4	0.00	0.00	0.36	2.08	0.87	0.01	96.68	0.00
5	0.00	0.01	0.34	2.02	0.97	0.01	96.28	0.36
6	0.00	0.12	4.82	3.84	20.87	0.03	69.31	1.02
7	0.00	0.56	0.45	8.56	86.85	0.01	3.24	0.34
8	0.00	0.54	0.40	8.50	88.16	0.00	2.11	0.30
9	0.00	0.49	0.45	8.34	85.59	0.00	4.81	0.32
10	0.00	0.49	0.73	8.37	86.22	0.00	3.88	0.31
11	0.01	0.51	0.44	8.52	85.88	0.00	4.35	0.29
12	0.00	0.53	0.49	8.53	87.04	0.00	3.12	0.28
13	0.01	0.50	0.35	8.67	88.15	0.00	2.03	0.29
14	0.00	0.51	1.16	8.64	88.42	0.03	0.92	0.32
15	0.01	0.51	1.35	8.75	87.66	0.01	1.38	0.33
0	0.00	0.00	4.35	1.93	0.29	0.00	93.42	0.01
1	0.01	0.00	1.90	2.03	0.28	0.00	95.77	0.00
2	0.00	0.00	28.47	1.43	0.32	0.02	69.76	0.00
3	0.00	0.00	6.48	1.87	0.37	0.00	91.26	0.02
4	0.00	0.00	0.31	2.05	0.46	0.05	97.13	0.00
5	0.01	0.00	0.28	2.06	0.66	0.01	96.91	0.08
6	0.00	0.01	8.86	1.89	0.82	0.01	88.26	0.15
7	0.00	0.50	0.53	8.31	87.30	0.04	3.00	0.32
8	0.01	0.47	0.96	8.39	86.26	0.01	3.61	0.30
9	0.01	0.60	0.41	9.58	87.60	0.01	1.48	0.32
10	0.01	0.55	0.39	8.67	88.81	0.00	1.27	0.31
11	0.01	0.56	0.49	8.94	88.27	0.00	1.43	0.29
12	0.01	0.52	0.39	8.77	88.84	0.00	1.14	0.33
13	0.00	0.51	0.57	8.88	88.89	0.00	0.90	0.26
14	0.00	0.53	0.36	8.96	89.01	0.00	0.80	0.35
15	0.00	0.53	0.74	8.77	89.00	0.03	0.68	0.27
0	0.01	0.00	0.13	2.05	0.24	0.00	97.54	0.03
1	0.01	0.02	2.34	1.96	0.32	0.02	95.34	0.00
2	0.01	0.02	0.27	1.98	0.28	0.01	97.43	0.01
3	0.00	0.00	2.85	2.02	0.30	0.00	94.82	0.00
4	0.00	0.02	1.68	2.02	0.40	0.00	95.88	0.00
5	0.01	0.03	0.23	1.98	0.59	0.00	97.16	0.00
6	0.00	0.00	0.08	2.01	0.79	0.00	97.12	0.01
7	0.01	0.21	4.37	4.45	29.78	0.06	60.70	0.43
8	0.00	0.23	3.85	5.21	36.88	0.03	53.41	0.39

9	0.02	0.23	5.01	4.73	31.88	0.06	57.63	0.44
10	0.01	0.28	5.94	6.17	49.17	0.02	38.09	0.32
11	0.00	0.50	9.32	7.63	75.66	0.01	6.58	0.30
12	0.00	0.40	33.41	5.74	53.11	0.02	7.12	0.22
13	0.01	0.52	0.62	8.55	86.18	0.08	3.70	0.34
14	0.00	0.51	0.43	8.72	87.04	0.07	2.88	0.33
15	0.01	0.63	0.52	9.23	87.96	0.03	1.34	0.28
0	0.00	0.01	0.11	2.07	0.37	0.00	97.43	0.00
1	0.00	0.01	5.94	1.88	0.51	0.00	91.66	0.00
2	0.00	0.01	3.42	1.99	0.80	0.00	93.78	0.00
3	0.00	0.02	0.73	2.12	1.67	0.05	95.32	0.09
4	0.00	0.08	2.31	3.12	12.32	0.01	81.49	0.69
5	0.00	0.32	2.00	6.10	47.15	0.04	43.71	0.69
6	0.00	0.54	1.09	8.54	85.68	0.07	3.74	0.35
7	0.00	0.54	0.65	8.57	83.66	0.04	6.23	0.31
8	0.00	0.73	0.61	9.81	86.35	0.01	2.19	0.30
9	0.00	0.50	0.49	8.90	86.85	0.00	2.95	0.32
10	0.01	0.52	0.39	8.67	88.35	0.03	1.72	0.32
11	0.01	0.50	0.85	8.48	85.71	0.10	4.02	0.35
12	0.00	0.52	1.86	8.70	87.25	0.00	1.37	0.31
13	0.00	0.54	0.37	8.83	89.03	0.00	0.94	0.29
14	0.01	0.54	0.49	9.14	88.54	0.04	0.90	0.35
15	0.00	0.53	1.17	8.69	88.15	0.01	1.12	0.33

C.39 G.91/Zr/V/Nd After 28 Days at 700°C

The G.91/Zr/V/Nd assembly annealed for 28 days at 700°C bonded on the Zr/V V/Nd interface but not the G.91/Zr interface. Compositional data (in at%) from WDS linescans across the Zr/V interface is given below.

Position	Zr	Mo	Si	Cr	Fe	Nd	V	Mn
0	97.55	0.00	1.60	0.02	0.06	0.20	0.57	0.02
1	98.49	0.00	0.53	0.03	0.00	0.13	0.83	0.00
2	97.15	0.00	1.53	0.03	0.02	0.10	1.06	0.11
3	93.56	0.00	0.75	0.02	0.03	4.43	1.21	0.00
4	95.23	0.00	1.83	0.05	0.28	0.45	2.09	0.06
5	89.31	0.00	4.29	0.15	0.81	1.02	4.41	0.00
6	23.07	0.01	1.63	1.54	0.29	0.12	73.32	0.02
7	5.19	0.01	0.85	1.84	0.09	0.07	91.94	0.02
8	0.58	0.01	0.53	1.99	0.01	0.14	96.73	0.00
9	0.19	0.00	0.85	2.03	0.05	0.28	96.61	0.00
10	0.11	0.00	3.72	1.92	0.07	0.70	93.49	0.00
11	0.05	0.01	1.39	1.88	0.02	0.28	96.37	0.00
12	0.07	0.01	3.60	1.94	0.00	0.13	94.26	0.00
13	1.42	0.02	9.25	1.78	0.03	0.74	86.77	0.00
14	0.18	0.00	1.14	1.95	0.02	0.41	96.31	0.00
15	0.07	0.00	1.08	2.00	0.06	0.44	96.35	0.00
0	98.42	0.00	0.42	0.03	0.00	0.07	1.07	0.00
1	98.47	0.00	0.03	0.07	0.01	0.08	1.35	0.00
2	97.79	0.00	0.06	0.05	0.06	0.09	1.95	0.00
3	97.52	0.00	0.10	0.08	0.02	0.03	2.24	0.03
4	97.10	0.00	0.26	0.06	0.04	0.10	2.43	0.00

5	49.38	0.00	4.69	0.92	0.59	0.23	44.19	0.00
6	9.76	0.00	1.38	1.83	0.11	0.15	86.78	0.00
7	0.75	0.00	6.68	1.87	0.16	0.43	90.10	0.01
8	0.24	0.00	20.73	1.58	0.32	0.96	76.17	0.00
9	0.10	0.00	15.26	1.72	0.09	0.51	82.33	0.00
10	0.05	0.01	8.22	1.80	0.09	0.38	89.46	0.00
11	0.05	0.01	24.74	1.53	0.12	0.32	73.22	0.02
12	0.05	0.00	4.93	1.94	0.17	0.18	92.68	0.03
13	0.05	0.00	3.33	1.95	0.13	0.44	94.08	0.01
14	0.05	0.00	4.99	1.89	0.18	0.18	92.70	0.01
15	0.07	0.01	13.67	1.72	0.02	0.11	84.39	0.02

C.40 G.91/Zr/Nd After 28 Days at 700°C

The G.91/Zr/Nd assembly annealed for 28 days at 700°C did not bond on the G.91/Zr or Zr/Nd interfaces.

C.41 G.91/Ti/V/Nd After 28 Days at 700°C

The G.91/Ti/V/Nd assembly annealed for 28 days at 700°C bonded on the Ti/V and V/Nd interfaces but not the G.91/Ti interface. Compositional data (in at%) from WDS linescans across the Ti/V and V/Nd interfaces is given below.

Position	Ti	Ta	Mo	Si	Cr	Fe	Nd	V	Mn
0	99.10	0.00	0.00	0.07	0.01	0.00	0.00	0.82	0.00
1	98.93	0.00	0.00	0.11	0.00	0.00	0.05	0.91	0.00
2	98.85	0.00	0.00	0.12	0.00	0.00	0.03	1.00	0.00
3	98.47	0.00	0.00	0.17	0.03	0.02	0.05	1.22	0.05
4	98.03	0.00	0.00	0.21	0.04	0.01	0.01	1.67	0.03
5	24.83	0.00	0.00	10.12	1.52	0.00	0.11	63.40	0.01
6	1.06	0.00	0.00	6.72	2.08	0.32	0.13	89.68	0.01
7	0.80	0.00	0.02	1.69	2.38	0.06	0.05	95.01	0.00
8	0.61	0.00	0.03	0.49	2.37	0.02	0.05	96.43	0.01
9	0.50	0.00	0.03	0.13	2.43	0.00	0.10	96.77	0.03
10	0.43	0.00	0.01	0.16	2.50	0.01	0.08	96.80	0.01
11	0.36	0.00	0.00	0.15	2.41	0.02	0.04	97.00	0.01
12	0.35	0.00	0.02	0.15	2.42	0.04	0.05	96.97	0.00
13	0.33	0.00	0.00	0.10	2.33	0.00	0.00	97.18	0.06
14	0.29	0.00	0.02	0.71	2.34	0.02	0.04	96.58	0.00
15	0.22	0.00	0.00	0.24	2.33	0.00	0.07	97.14	0.00
16	0.22	0.00	0.01	0.93	2.25	0.01	0.28	96.25	0.05
17	0.17	0.00	0.00	1.81	2.31	0.00	0.05	95.63	0.02
18	0.20	0.00	0.01	7.24	2.17	0.05	0.33	89.99	0.03
19	0.30	0.00	0.02	8.74	1.99	0.06	0.69	88.19	0.01
20	0.21	0.00	0.00	5.29	2.23	0.02	0.06	92.19	0.01
0	98.01	0.00	0.00	0.16	0.04	0.00	0.05	1.70	0.03
1	98.01	0.00	0.00	0.18	0.03	0.00	0.09	1.68	0.00
2	97.88	0.00	0.00	0.19	0.04	0.07	0.07	1.76	0.00
3	97.75	0.00	0.00	0.12	0.05	0.01	0.09	1.98	0.00
4	97.86	0.00	0.00	0.17	0.00	0.00	0.04	1.90	0.03
5	97.75	0.00	0.00	0.17	0.03	0.00	0.01	2.04	0.01

6	96.88	0.00	0.00	0.35	0.05	0.02	0.07	2.60	0.02
7	78.28	0.00	0.00	0.46	0.54	0.05	0.13	20.55	0.00
8	1.18	0.00	0.00	0.64	2.27	0.00	0.00	95.91	0.00
9	0.77	0.00	0.00	1.18	2.18	0.06	0.06	95.72	0.03
10	0.58	0.00	0.01	0.16	2.17	0.01	0.05	97.02	0.00
11	0.49	0.00	0.00	1.59	2.20	0.02	0.02	95.66	0.03
12	0.40	0.00	0.01	0.10	2.17	0.00	0.02	97.30	0.00
13	0.33	0.00	0.02	0.83	2.10	0.00	0.04	96.69	0.00
14	0.31	0.00	0.00	0.16	2.32	0.00	0.03	97.18	0.00
15	0.27	0.00	0.00	0.24	2.33	0.00	0.06	97.07	0.04
16	0.23	0.00	0.00	0.49	2.23	0.02	0.11	96.93	0.00
17	0.21	0.00	0.02	0.49	2.26	0.00	0.04	96.99	0.00
18	0.20	0.00	0.00	0.36	2.32	0.01	0.08	97.02	0.01
19	0.19	0.00	0.00	1.87	2.23	0.00	0.02	95.69	0.00
20	0.20	0.00	0.01	1.34	2.31	0.08	0.11	95.95	0.00
0	0.00	0.00	0.02	0.06	2.31	0.09	0.29	97.22	0.02
1	0.00	0.00	0.02	0.11	2.27	0.32	0.36	96.91	0.00
2	0.01	0.00	0.03	0.70	2.49	0.92	2.10	93.70	0.06
3	0.00	0.00	0.03	0.30	1.59	0.79	48.98	48.06	0.26
4	0.02	0.00	0.00	1.10	0.88	0.32	63.94	33.28	0.46
5	0.00	0.00	0.01	0.32	0.40	0.43	89.04	9.38	0.41
6	0.00	0.00	0.01	0.46	0.81	0.58	67.31	30.60	0.23
7	0.07	0.00	0.00	0.29	0.54	0.51	82.68	15.57	0.34
8	0.00	0.00	0.02	0.35	1.45	0.41	47.05	50.58	0.13
9	0.10	0.00	0.02	1.22	1.46	0.86	50.63	45.52	0.19
10	0.00	0.00	0.03	0.41	0.15	0.39	95.97	2.66	0.39
11	0.02	0.00	0.10	0.34	0.97	0.50	59.34	38.47	0.25
12	0.21	0.00	0.00	2.22	1.03	0.69	69.52	25.86	0.48
13	0.00	0.00	0.07	0.41	0.05	0.40	96.26	2.53	0.29
14	0.00	0.00	0.00	0.20	0.06	0.34	97.95	0.93	0.52
15	0.00	0.00	0.01	0.21	0.00	0.44	98.53	0.46	0.35

C.42 G.91/Ti/Nd After 28 Days at 700°C

The G.91/Ti/Nd assembly annealed for 28 days at 700°C bonded on the Ti/Nd interface but not the G.91/Ti interface. Compositional data (in at%) from WDS linescans across the Ti/Nd interface is given below.

Position	Ti	Ta	Mo	Si	Cr	Fe	Nd	V	Mn
0	21.94	0.00	0.01	1.01	0.04	0.33	76.19	0.14	0.36
1	35.75	0.00	0.00	2.13	0.10	0.51	61.03	0.19	0.30
2	79.71	0.00	0.00	0.72	0.02	0.21	18.95	0.28	0.11
3	87.14	0.00	0.00	0.35	0.01	0.09	11.95	0.41	0.06
4	92.28	0.00	0.00	0.55	0.00	0.15	6.61	0.34	0.06
5	88.68	0.00	0.00	2.72	0.00	0.20	8.05	0.33	0.02
6	68.58	0.00	0.00	26.93	0.00	0.12	4.14	0.22	0.00
7	70.54	0.00	0.00	25.95	0.02	0.36	2.92	0.22	0.00
8	91.84	0.00	0.00	1.66	0.07	4.41	1.67	0.24	0.12
9	90.42	0.00	0.02	0.30	0.11	8.61	0.15	0.26	0.13
10	90.37	0.00	0.00	0.36	0.09	8.63	0.19	0.29	0.08
11	90.86	0.00	0.00	0.30	0.09	8.31	0.07	0.27	0.11
12	90.69	0.00	0.00	0.31	0.09	8.41	0.07	0.31	0.11
13	90.77	0.00	0.00	0.26	0.07	8.45	0.06	0.27	0.13

14	90.22	0.00	0.02	0.31	0.09	8.98	0.02	0.26	0.10
15	92.74	0.00	0.00	1.48	0.08	5.31	0.07	0.27	0.06
0	32.60	0.00	0.01	0.59	0.00	0.20	66.34	0.10	0.17
1	38.98	0.00	0.00	1.99	0.00	0.41	58.33	0.21	0.08
2	15.41	0.00	0.02	1.69	0.00	0.55	82.02	0.00	0.31
3	41.56	0.00	0.00	7.28	0.03	0.58	50.08	0.15	0.31
4	88.17	0.00	0.00	3.67	0.00	0.13	7.66	0.26	0.11
5	79.31	0.00	0.00	6.38	0.00	0.36	13.56	0.27	0.11
6	81.11	0.00	0.00	9.31	0.08	1.18	7.99	0.31	0.04
7	83.93	0.00	0.00	8.23	0.00	0.51	7.06	0.28	0.00
8	83.75	0.00	0.03	6.89	0.04	2.38	6.54	0.31	0.06
9	86.11	0.00	0.01	7.03	0.05	4.70	1.67	0.34	0.10
10	96.59	0.00	0.00	0.92	0.01	1.38	0.77	0.31	0.03
11	97.88	0.00	0.00	0.67	0.00	0.39	0.75	0.31	0.00
12	97.60	0.00	0.00	0.44	0.00	0.10	1.60	0.25	0.01
13	99.00	0.00	0.00	0.47	0.00	0.07	0.21	0.22	0.02
14	99.24	0.00	0.00	0.34	0.00	0.05	0.10	0.23	0.03
15	99.00	0.00	0.00	0.24	0.00	0.05	0.41	0.29	0.00

C.43 G.91/Ta/V/Nd After 28 Days at 700°C

The G.91/Ta/V/Nd assembly annealed for 28 days at 700°C bonded on the V/Nd interface but not the G.91/Ta or Ta/V interfaces. Compositional data (in at%) from WDS linescans across the V/Nd interface is given below.

Position	Ti	Ta	Mo	Si	Cr	Fe	Nd	V	Mn
0	0.00	0.00	0.02	0.13	2.39	0.02	0.46	96.98	0.00
1	0.01	0.00	0.01	0.19	2.28	0.03	2.19	95.25	0.04
2	0.00	0.00	0.01	0.21	2.28	0.10	1.95	95.38	0.06
3	0.00	0.00	0.03	0.21	2.41	0.22	2.14	94.99	0.00
4	0.00	0.00	0.01	0.21	2.39	0.79	3.82	92.69	0.09
5	0.01	0.00	0.08	0.46	2.34	0.45	9.35	87.25	0.07
6	0.00	0.00	0.00	0.27	0.55	0.50	77.62	20.72	0.33
7	0.00	0.00	0.00	0.82	0.22	0.42	94.10	3.97	0.48
8	0.00	0.00	0.11	0.39	0.13	0.56	95.94	2.59	0.29
9	0.00	0.00	0.00	0.30	0.02	0.51	96.26	2.39	0.53
10	0.00	0.00	0.02	0.21	0.09	0.42	95.12	3.77	0.38
11	0.00	0.00	0.02	0.19	0.15	0.35	96.87	2.07	0.36
12	0.02	0.00	0.13	0.49	0.27	0.42	94.25	4.13	0.29
13	0.01	0.00	0.00	0.41	0.01	0.36	98.43	0.34	0.43
14	0.00	0.00	0.00	0.34	0.05	0.35	98.48	0.45	0.33
15	0.00	0.00	0.00	0.46	0.01	0.38	98.29	0.50	0.36

C.44 G.91/Ta/Nd After 28 Days at 700°C

The G.91/Ta/Nd assembly annealed for 28 days at 700°C bonded on the Ta/Nd interface but not the G.91/Ta interface. Compositional data (in at%) from WDS linescans across the Ta/Nd interface is given below.

Position	Ti	Ta	Mo	Si	Cr	Fe	Nd	V	Mn
0	0.00	0.00	0.09	0.70	0.00	0.38	98.54	0.14	0.16

1	0.00	0.00	0.07	1.88	0.49	6.26	90.11	0.67	0.51
2	0.00	0.00	0.00	0.64	0.00	0.59	98.31	0.05	0.41
3	0.00	0.00	0.00	0.22	0.12	0.67	98.69	0.02	0.28
4	0.00	0.00	0.00	0.81	0.00	0.41	98.22	0.07	0.49
5	0.00	0.00	0.07	0.39	0.01	0.44	98.77	0.00	0.32
6	0.00	0.00	0.00	0.66	0.00	0.37	98.52	0.00	0.45
7	0.00	0.07	0.00	0.22	0.00	0.33	98.72	0.00	0.66
8	0.00	12.86	0.06	0.00	0.11	0.48	85.83	0.10	0.54
9	0.03	84.58	0.51	0.00	0.07	0.57	13.62	0.50	0.12
10	0.07	94.10	0.29	0.00	0.13	0.19	4.93	0.01	0.28
11	0.00	95.69	0.11	0.00	0.00	0.05	4.02	0.08	0.05
12	0.02	98.30	0.09	0.00	0.13	0.08	1.16	0.05	0.18
13	0.00	98.66	0.05	0.00	0.00	0.09	1.02	0.00	0.18
14	0.00	98.88	0.04	0.00	0.00	0.10	0.98	0.00	0.00
15	0.00	98.97	0.02	0.00	0.08	0.05	0.83	0.04	0.00
0	0.01	0.02	0.15	0.27	0.00	0.39	98.80	0.00	0.37
1	0.00	0.00	0.09	0.27	0.01	0.38	98.79	0.00	0.47
2	0.00	0.00	0.00	0.36	0.00	0.36	98.88	0.00	0.41
3	0.00	0.00	0.00	0.59	0.00	0.41	98.40	0.00	0.59
4	0.00	0.00	0.00	15.25	0.00	0.25	84.24	0.00	0.26
5	0.02	0.00	0.00	93.68	0.00	0.05	6.24	0.02	0.00
6	0.01	0.00	0.05	92.86	0.01	0.11	6.83	0.07	0.06
7	0.03	96.37	0.05	0.16	0.00	0.04	2.45	0.91	0.00
8	0.00	98.56	0.05	0.00	0.08	0.21	0.86	0.08	0.16
9	0.00	99.22	0.00	0.00	0.00	0.04	0.74	0.00	0.00
10	0.00	98.43	0.00	0.00	0.00	0.00	1.12	0.42	0.04
11	0.00	99.32	0.00	0.00	0.04	0.01	0.38	0.18	0.08
12	0.00	99.10	0.04	0.00	0.08	0.23	0.55	0.01	0.00
13	0.03	99.47	0.01	0.00	0.00	0.01	0.44	0.05	0.00
14	0.04	99.27	0.09	0.00	0.01	0.05	0.46	0.08	0.01
15	0.00	99.31	0.00	0.00	0.20	0.10	0.40	0.00	0.00
0	0.00	0.00	0.00	0.77	0.01	0.41	98.68	0.00	0.14
1	0.00	0.00	0.02	3.13	0.00	0.78	95.81	0.02	0.25
2	0.00	2.67	0.10	9.41	0.55	5.04	81.78	0.10	0.34
3	0.00	0.44	0.27	4.09	2.81	29.17	62.61	0.03	0.58
4	0.00	0.00	0.00	0.90	0.14	2.40	96.18	0.05	0.34
5	0.00	0.00	0.03	0.36	0.08	0.33	98.92	0.00	0.29
6	0.00	0.03	0.03	0.38	0.09	0.32	98.60	0.00	0.55
7	0.00	0.18	0.00	0.26	0.00	0.45	98.71	0.02	0.38
8	0.00	0.00	0.08	0.40	0.00	0.42	98.67	0.01	0.42
9	0.00	0.00	0.00	0.31	0.02	0.34	98.70	0.16	0.47
10	0.00	0.06	0.00	0.58	0.01	0.43	98.31	0.05	0.57
11	0.00	1.87	0.00	0.42	0.00	0.36	96.90	0.00	0.46
12	0.00	91.69	0.07	0.00	0.04	0.03	7.45	0.17	0.55
13	0.00	97.05	0.10	0.00	0.00	0.00	2.85	0.00	0.00
14	0.00	97.06	0.02	0.00	0.00	0.15	2.58	0.00	0.19
15	0.02	82.96	0.06	15.41	0.06	0.22	1.12	0.14	0.01

C.45 G.91/Mo/V/Nd After 28 Days at 700°C

The G.91/Mo/V/Nd assembly annealed for 28 days at 700°C bonded on the V/Nd interface but not the G.91/Mo or Mo/V interface. Since the V/Nd interface at

this time and temperature was already well characterized, no WDS linescans were completed on it in this assembly.

C.46 G.91/Mo/Nd After 28 Days at 700°C

The G.91/Mo/Nd assembly annealed for 28 days at 700°C bonded on the Mo/Nd interface but not the G.91/Mo interface. Compositional data (in at%) from WDS linescans across the Mo/Nd interface is given below.

Position	W	Nd	Mo	Fe	Mn	Cr	V	Si
0	0.00	98.84	0.01	0.39	0.50	0.02	0.02	0.23
1	0.00	99.04	0.04	0.30	0.45	0.01	0.00	0.16
2	0.00	98.82	0.03	0.32	0.40	0.03	0.04	0.37
3	0.03	99.00	0.08	0.34	0.50	0.00	0.00	0.05
4	0.02	96.59	2.25	0.38	0.42	0.00	0.02	0.32
5	0.01	40.90	58.34	0.20	0.27	0.00	0.17	0.12
6	0.00	66.44	32.69	0.35	0.37	0.06	0.05	0.05
7	0.02	11.14	88.26	0.18	0.05	0.04	0.19	0.13
8	0.00	1.19	98.63	0.02	0.00	0.01	0.04	0.11
9	0.00	0.94	98.83	0.00	0.05	0.02	0.02	0.14
10	0.03	0.63	99.28	0.03	0.00	0.00	0.02	0.01
11	0.02	0.66	98.44	0.08	0.02	0.00	0.01	0.78
12	0.03	0.61	95.13	0.06	0.00	0.00	0.05	4.12
13	0.01	0.85	98.64	0.09	0.00	0.03	0.16	0.23
14	0.02	0.60	99.03	0.13	0.04	0.00	0.06	0.13
15	0.02	1.15	98.20	0.00	0.07	0.00	0.21	0.35
0	0.00	90.96	0.22	0.42	0.51	0.00	0.11	7.79
1	0.00	85.16	0.37	0.47	0.34	0.00	0.03	13.63
2	0.06	94.11	0.15	0.34	0.47	0.02	0.00	4.85
3	0.08	96.70	0.11	0.40	0.42	0.10	0.00	2.19
4	0.00	92.98	0.15	0.34	0.60	0.00	0.05	5.89
5	0.00	96.73	0.50	0.43	0.47	0.00	0.11	1.77
6	0.00	84.71	14.06	0.40	0.45	0.00	0.03	0.36
7	0.03	10.89	88.49	0.06	0.11	0.02	0.05	0.36
8	0.00	1.16	98.33	0.05	0.04	0.00	0.00	0.43
9	0.02	0.54	98.56	0.08	0.00	0.02	0.03	0.74
10	0.00	0.33	91.35	0.07	0.00	0.00	0.00	8.24
11	0.00	0.45	82.67	0.05	0.05	0.01	0.00	16.78
12	0.00	1.90	97.32	0.00	0.00	0.00	0.02	0.75
13	0.03	1.91	97.40	0.07	0.00	0.01	0.04	0.55
14	0.03	0.28	99.48	0.04	0.04	0.00	0.00	0.14
15	0.00	0.25	99.44	0.06	0.01	0.03	0.05	0.16
0	0.00	98.82	0.00	0.34	0.65	0.00	0.02	0.17
1	0.00	98.98	0.04	0.48	0.49	0.01	0.00	0.00
2	0.00	98.90	0.00	0.36	0.56	0.00	0.00	0.18
3	0.00	98.97	0.01	0.36	0.57	0.02	0.00	0.08
4	0.00	98.94	0.04	0.29	0.50	0.00	0.09	0.15
5	0.00	98.55	0.15	0.27	0.55	0.00	0.07	0.42
6	0.01	96.47	2.47	0.25	0.39	0.00	0.03	0.38
7	0.02	89.06	9.79	0.40	0.45	0.00	0.05	0.23

8	0.01	52.04	46.83	0.33	0.22	0.03	0.10	0.45
9	0.01	4.85	94.69	0.12	0.12	0.02	0.00	0.20
10	0.00	0.57	99.24	0.10	0.00	0.00	0.01	0.07
11	0.01	0.68	99.12	0.02	0.00	0.01	0.00	0.17
12	0.04	0.42	99.33	0.08	0.00	0.00	0.01	0.12
13	0.01	0.24	99.43	0.06	0.13	0.03	0.02	0.09
14	0.03	0.29	99.55	0.02	0.00	0.03	0.01	0.08
15	0.03	0.24	99.55	0.00	0.00	0.06	0.02	0.11
0	0.01	1.09	90.60	3.23	0.11	0.37	0.09	4.50
1	0.01	0.55	87.93	5.31	0.00	0.57	0.06	5.58
2	0.02	0.66	86.08	7.18	0.17	0.78	0.00	5.11
3	0.03	1.28	93.47	2.34	0.12	0.25	0.00	2.52
4	0.04	1.25	95.66	1.92	0.00	0.13	0.00	1.00
5	0.01	1.05	94.94	1.12	0.07	0.04	0.02	2.76
6	0.00	0.63	95.26	0.84	0.14	0.12	0.01	3.01
7	0.00	0.30	94.38	0.34	0.05	0.08	0.94	3.91
8	0.01	0.29	89.88	0.32	0.00	0.09	1.20	8.22
9	0.01	0.07	96.71	0.28	0.06	0.02	0.22	2.63
10	0.00	0.05	99.08	0.13	0.00	0.00	0.12	0.63
11	0.00	0.01	99.12	0.20	0.03	0.05	0.07	0.51
12	0.01	0.05	96.32	0.10	0.02	0.04	0.06	3.40
13	0.02	0.01	99.63	0.10	0.09	0.02	0.06	0.09
14	0.04	0.19	99.08	0.18	0.02	0.02	0.07	0.40
15	0.00	0.29	99.23	0.14	0.01	0.01	0.03	0.29

C.47 G.91/W/V/Nd After 28 Days at 700°C

The G.91/W/V/Nd assembly annealed for 28 days at 700°C bonded on the V/Nd interface but not the G.91/W or W/V interfaces. Since the V/Nd interface at this time and temperature was already well characterized, no WDS linescans were completed on it in this assembly.

C.48 G.91/W/Nd After 28 Days at 700°C

The G.91/W/Nd assembly annealed for 28 days at 700°C bonded on the W/Nd interface but not the G.91/W interface. Compositional data (in at%) from WDS linescans across the W/Nd interface is given below.

Position	W	Nd	Mo	Fe	Mn	Cr	V	Si
0	99.80	0.12	0.00	0.01	0.00	0.00	0.00	0.07
1	99.53	0.43	0.00	0.00	0.00	0.05	0.00	0.00
2	98.97	0.82	0.00	0.12	0.00	0.09	0.00	0.00
3	95.89	3.87	0.00	0.12	0.00	0.00	0.00	0.12
4	47.60	51.28	0.00	0.27	0.32	0.00	0.13	0.42
5	26.31	61.89	0.00	0.24	0.32	0.03	0.02	11.19
6	2.81	58.34	0.00	0.13	0.22	0.00	0.00	38.50
7	0.20	93.58	0.00	0.20	0.33	0.00	0.00	5.69
8	0.04	98.06	0.02	0.39	0.44	0.00	0.00	1.05
9	0.05	97.80	0.02	0.29	0.48	0.00	0.01	1.35

10	0.08	98.81	0.00	0.25	0.47	0.00	0.00	0.39
11	0.09	98.41	0.04	0.33	0.53	0.10	0.09	0.42
12	0.05	98.31	0.02	0.41	0.58	0.03	0.06	0.54
13	0.00	98.79	0.01	0.41	0.54	0.02	0.00	0.23
14	0.03	98.76	0.00	0.38	0.56	0.00	0.00	0.26
15	0.05	98.84	0.00	0.29	0.45	0.00	0.04	0.35
0	98.87	0.89	0.00	0.08	0.00	0.00	0.04	0.12
1	98.87	0.94	0.00	0.05	0.04	0.11	0.00	0.00
2	98.94	0.91	0.00	0.02	0.06	0.00	0.06	0.01
3	98.61	1.30	0.00	0.00	0.09	0.00	0.00	0.00
4	15.79	82.98	0.01	0.35	0.34	0.01	0.00	0.52
5	2.49	96.52	0.00	0.29	0.34	0.00	0.00	0.36
6	0.33	98.56	0.00	0.32	0.48	0.09	0.00	0.22
7	0.13	98.72	0.00	0.48	0.33	0.00	0.00	0.33
8	0.17	98.58	0.04	0.23	0.46	0.00	0.03	0.48
9	0.04	98.76	0.02	0.39	0.46	0.02	0.00	0.31
10	0.38	96.27	0.01	0.43	0.48	0.00	0.05	2.38
11	0.11	56.29	0.04	0.19	0.39	0.00	0.00	42.99
12	0.00	32.47	0.00	0.09	0.14	0.01	0.00	67.28
13	0.14	65.61	0.00	0.22	0.31	0.00	0.00	33.71
14	1.23	97.12	0.00	0.39	0.49	0.02	0.00	0.75
15	0.07	98.70	0.00	0.40	0.53	0.00	0.00	0.30

APPENDIX D: SUMMARY OF SS-316 INTERFACES

D.1 SS-316/Nd After 28 Days at 550°C

When annealed for 28 days at 550°C, the SS-316/Nd diffusion assembly included three diffusion interaction zones. The first zone was ~52 μm wide with a composition matching Nd₂(Fe+Cr)₁₇. The second interaction zone was ~21 μm wide with a composition matching Fe₂Nd. Finally, the third interaction zone observed was ~15 μm wide with a composition matching Nd₃(Ni+Fe). Compositional data (in at%) from WDS linescans across the interface is given below.

Position	Zr	Mo	Si	Cr	Fe	Nd	V	Ni	Mn
0	0.00	1.38	2.22	18.35	66.35	0.26	0.08	9.57	1.79
1	0.00	1.48	4.25	18.60	64.70	0.27	0.09	8.74	1.88
2	0.00	1.42	5.02	18.03	64.60	0.25	0.10	8.87	1.73
3	0.00	1.51	1.23	18.85	67.02	0.28	0.09	9.19	1.84
4	0.00	1.49	1.19	18.92	66.96	0.31	0.11	9.26	1.76
5	0.00	1.45	1.09	18.55	67.47	0.32	0.10	9.13	1.88
6	0.01	1.64	0.67	20.84	64.91	8.07	0.09	1.85	1.93
7	0.02	1.45	1.15	18.56	67.14	0.56	0.05	9.17	1.90
8	0.00	1.45	1.13	18.47	67.25	0.61	0.10	9.17	1.83
9	0.00	1.44	1.06	19.31	66.44	3.36	0.10	6.50	1.78
10	0.00	1.55	0.79	19.75	65.99	5.77	0.08	4.15	1.90
11	0.01	1.62	0.55	20.99	65.07	8.79	0.09	1.10	1.79
12	0.00	1.69	0.26	20.66	65.12	10.17	0.11	0.19	1.81
13	0.00	1.67	0.34	20.73	65.13	10.20	0.06	0.11	1.76
14	0.00	1.58	0.24	20.38	65.74	10.01	0.10	0.14	1.81
15	0.01	1.71	0.39	20.65	65.05	10.31	0.11	0.07	1.71
16	0.00	1.60	0.36	20.76	65.03	10.28	0.09	0.10	1.78
17	0.01	1.56	0.32	20.33	65.56	10.20	0.11	0.14	1.77
18	0.00	1.61	0.33	20.54	65.63	9.97	0.11	0.04	1.78
19	0.01	1.68	0.38	19.91	65.60	10.26	0.08	0.21	1.89
20	0.01	1.65	0.38	20.28	65.64	10.15	0.10	0.05	1.75
21	0.00	1.58	0.41	19.68	65.01	11.27	0.08	0.18	1.80
22	0.01	1.56	0.38	19.94	64.92	11.07	0.10	0.14	1.89
23	0.00	1.51	0.32	20.18	64.98	10.77	0.14	0.22	1.88
24	0.02	1.59	0.28	20.38	65.75	10.00	0.10	0.08	1.81
25	0.01	1.67	0.27	20.13	65.71	10.21	0.12	0.12	1.76
26	0.02	1.59	0.27	20.39	65.45	10.29	0.09	0.12	1.77
27	0.00	1.58	0.27	20.21	65.24	10.67	0.10	0.10	1.84
28	0.00	1.62	0.52	20.00	65.69	10.13	0.08	0.16	1.81
29	0.00	1.67	0.70	19.99	64.91	10.62	0.10	0.18	1.84
30	0.00	1.65	0.46	19.98	65.23	10.61	0.11	0.18	1.78
31	0.00	1.63	0.48	20.10	65.74	9.88	0.12	0.19	1.87
32	0.00	1.50	0.36	20.30	65.63	10.18	0.11	0.11	1.81
33	0.00	1.59	0.22	20.10	65.55	10.39	0.11	0.17	1.87
34	0.00	1.65	0.30	20.06	65.27	10.71	0.09	0.19	1.73
35	0.02	1.56	0.29	19.96	65.00	11.09	0.07	0.14	1.88
36	0.04	1.64	0.25	20.18	65.17	10.56	0.12	0.23	1.81
37	0.00	1.51	0.32	20.26	65.39	10.33	0.10	0.26	1.83

38	0.00	1.50	0.28	20.46	65.71	9.84	0.08	0.21	1.93
39	0.00	1.50	0.32	19.82	64.50	11.68	0.07	0.28	1.84
40	0.01	1.53	0.30	19.68	64.93	11.33	0.07	0.21	1.95
41	0.01	1.54	0.32	20.13	65.27	10.58	0.09	0.16	1.90
42	0.00	1.45	0.31	20.20	65.12	10.83	0.11	0.14	1.84
43	0.00	1.41	0.36	19.57	63.69	12.92	0.10	0.18	1.78
44	0.01	1.53	0.36	19.79	64.96	11.20	0.10	0.17	1.88
45	0.01	1.45	0.29	19.97	64.36	11.75	0.08	0.19	1.92
46	0.00	1.47	0.28	19.83	64.92	11.50	0.09	0.21	1.71
47	0.00	1.53	0.22	19.62	65.05	11.61	0.08	0.19	1.70
48	0.00	1.54	0.29	19.63	63.95	12.65	0.06	0.16	1.74
49	0.00	1.49	0.31	19.37	61.97	14.76	0.11	0.18	1.83
50	0.00	1.46	0.35	19.99	64.75	11.37	0.10	0.17	1.81
51	0.00	1.45	0.30	20.16	65.04	11.03	0.06	0.18	1.78
52	0.00	1.44	0.32	19.74	64.43	11.72	0.11	0.14	2.10
53	0.01	1.53	0.35	19.74	64.95	11.20	0.09	0.24	1.90
54	0.03	1.46	0.44	18.93	62.93	14.28	0.06	0.16	1.71
55	0.02	1.55	0.61	19.22	64.32	12.07	0.10	0.24	1.87
56	0.00	1.26	0.99	18.93	61.11	15.83	0.07	0.05	1.77
57	0.00	1.07	0.92	19.25	62.11	14.75	0.06	0.05	1.80
58	0.02	0.11	4.91	6.49	60.21	26.64	0.00	0.09	1.55
59	0.02	0.04	6.01	2.91	58.54	30.97	0.01	0.11	1.40
60	0.00	0.02	5.83	2.80	58.59	31.31	0.00	0.00	1.45
61	0.04	0.00	5.92	2.76	58.74	31.11	0.01	0.06	1.37
62	0.00	0.00	5.68	2.67	58.69	31.31	0.00	0.17	1.48
63	0.02	0.00	5.88	2.86	57.50	32.21	0.07	0.08	1.39
64	0.00	0.03	6.17	2.97	58.20	31.14	0.00	0.09	1.41
65	0.00	0.02	5.45	2.86	56.46	33.77	0.00	0.13	1.31
66	0.00	0.00	5.02	2.88	56.17	34.46	0.00	0.05	1.42
67	0.00	0.00	5.05	2.79	54.76	35.84	0.03	0.13	1.41
68	0.02	0.02	5.49	2.80	54.66	35.50	0.00	0.10	1.41
69	0.00	0.00	5.20	2.59	54.12	36.56	0.04	0.16	1.35
70	0.00	0.01	5.63	2.50	57.83	32.48	0.00	0.14	1.42
71	0.00	0.00	5.30	2.84	56.40	33.80	0.00	0.16	1.49
72	0.03	0.01	5.13	2.75	55.32	35.21	0.00	0.09	1.46
73	0.01	0.01	5.61	2.55	55.45	34.86	0.04	0.10	1.39
74	0.00	0.03	5.43	2.61	58.30	31.90	0.02	0.17	1.53
75	0.00	0.00	5.86	2.49	58.75	31.34	0.02	0.15	1.39
76	0.00	0.02	6.25	2.26	58.77	31.10	0.01	0.12	1.47
77	0.00	0.00	12.73	1.85	54.95	29.00	0.00	0.20	1.27
78	0.02	0.02	20.92	1.96	48.66	26.98	0.03	0.30	1.12
79	0.03	0.02	4.69	1.03	33.25	51.83	0.00	8.26	0.89
80	0.00	0.00	0.37	0.09	3.75	75.90	0.00	19.41	0.48
81	0.02	0.00	0.72	0.00	2.85	79.69	0.00	16.22	0.51
82	0.03	0.00	0.60	0.03	3.30	76.71	0.00	18.86	0.46
83	0.00	0.00	0.34	0.00	3.45	75.73	0.00	20.11	0.38
84	0.00	0.01	0.24	0.03	3.49	75.82	0.00	19.89	0.53
85	0.00	0.00	0.35	0.00	3.55	75.76	0.00	20.05	0.29
86	0.04	0.03	0.27	0.00	3.60	75.53	0.03	19.99	0.50
87	0.00	0.00	0.28	0.02	3.43	75.59	0.00	20.14	0.53
88	0.01	0.01	0.22	0.00	3.55	75.92	0.00	19.84	0.46
89	0.00	0.00	0.31	0.02	3.58	76.15	0.00	19.53	0.42
90	0.00	0.04	0.72	0.00	3.45	75.55	0.00	19.87	0.38
0	0.00	1.38	0.65	19.83	66.38	8.71	0.12	1.22	1.71
1	0.00	1.38	0.43	20.34	66.44	9.39	0.07	0.06	1.89
2	0.00	1.41	0.36	20.49	66.17	9.46	0.13	0.11	1.88

3	0.00	1.41	0.25	20.52	66.16	9.44	0.10	0.10	2.02
4	0.00	1.45	0.29	21.20	65.82	9.30	0.08	0.03	1.83
5	0.00	1.43	0.45	20.79	66.00	9.53	0.08	0.06	1.67
6	0.00	1.39	0.43	20.77	65.63	9.74	0.10	0.16	1.78
7	0.01	1.43	0.34	20.49	65.76	9.97	0.10	0.12	1.78
8	0.00	1.41	0.35	20.53	65.72	10.04	0.05	0.12	1.79
9	0.00	1.43	0.23	20.74	65.92	9.59	0.13	0.08	1.88
10	0.00	1.40	0.25	20.53	66.21	9.53	0.11	0.11	1.86
11	0.00	1.45	0.31	20.63	66.04	9.65	0.06	0.01	1.84
12	0.00	1.46	0.34	20.79	65.85	9.57	0.08	0.07	1.85
13	0.02	1.44	0.47	20.52	66.01	9.61	0.03	0.08	1.83
14	0.00	1.45	0.41	20.38	66.20	9.66	0.08	0.13	1.70
15	0.00	1.42	0.27	20.31	66.00	9.96	0.08	0.08	1.88
16	0.00	1.46	0.32	20.24	66.17	9.74	0.13	0.11	1.85
17	0.00	1.43	0.44	20.61	65.87	9.53	0.10	0.16	1.87
18	0.01	1.43	0.41	20.49	65.97	9.72	0.10	0.10	1.77
19	0.00	1.42	0.24	20.52	65.60	10.05	0.10	0.15	1.92
20	0.00	1.45	0.29	20.33	65.65	10.01	0.08	0.16	2.03
21	0.00	1.44	0.33	20.55	65.93	9.64	0.09	0.10	1.92
22	0.02	1.42	0.28	20.44	65.82	9.99	0.08	0.18	1.80
23	0.00	1.49	0.26	20.26	66.12	9.82	0.08	0.11	1.86
24	0.00	1.44	0.31	20.49	65.35	10.39	0.09	0.16	1.79
25	0.00	1.37	0.32	20.16	65.45	10.61	0.07	0.16	1.87
26	0.00	1.50	0.32	20.58	65.42	10.15	0.09	0.16	1.78
27	0.00	1.46	0.33	20.29	65.65	10.18	0.11	0.11	1.88
28	0.00	1.41	0.27	20.18	65.22	10.83	0.10	0.12	1.87
29	0.00	1.44	0.27	20.19	65.23	10.75	0.10	0.22	1.81
30	0.00	1.40	0.26	20.37	65.64	10.21	0.06	0.17	1.89
31	0.00	1.40	0.86	20.38	64.40	10.93	0.11	0.14	1.78
32	0.00	1.42	5.51	19.40	62.10	9.70	0.10	0.05	1.73
33	0.00	1.50	0.28	20.68	64.88	10.64	0.09	0.10	1.84
34	0.00	1.44	0.29	20.18	64.76	11.29	0.10	0.17	1.78
35	0.00	1.38	0.30	20.34	65.20	10.78	0.08	0.13	1.80
36	0.02	1.44	0.22	20.47	64.51	11.31	0.12	0.14	1.77
37	0.00	1.47	0.34	20.13	65.50	10.44	0.10	0.21	1.81
38	0.03	1.49	0.24	20.19	65.26	10.64	0.09	0.17	1.89
39	0.00	1.46	0.28	20.18	65.79	10.21	0.09	0.13	1.86
40	0.00	1.48	0.32	20.28	65.72	10.10	0.09	0.18	1.84
41	0.00	1.53	0.24	20.31	65.12	10.63	0.11	0.21	1.85
42	0.02	1.42	0.28	20.12	65.32	10.73	0.09	0.16	1.88
43	0.00	1.47	0.20	20.14	65.80	10.31	0.12	0.22	1.76
44	0.00	1.44	0.28	19.62	66.22	10.31	0.09	0.17	1.89
45	0.00	1.54	0.31	19.84	65.81	10.27	0.11	0.26	1.88
46	0.00	1.52	0.28	20.01	65.79	10.26	0.09	0.25	1.79
47	0.01	1.41	0.20	20.00	65.76	10.42	0.13	0.20	1.87
48	0.00	1.42	0.30	19.64	66.03	10.31	0.10	0.21	2.00
49	0.00	1.41	0.32	19.99	65.85	10.30	0.10	0.20	1.83
50	0.00	1.45	0.26	19.59	65.18	11.35	0.09	0.26	1.82
51	0.01	1.49	0.28	19.63	64.93	11.44	0.15	0.27	1.82
52	0.00	1.43	0.32	19.55	64.54	12.06	0.08	0.23	1.80
53	0.01	1.45	0.29	19.41	64.17	12.65	0.09	0.12	1.82
54	0.00	1.33	0.27	19.47	62.77	13.93	0.08	0.20	1.94
55	0.00	0.91	0.23	20.95	63.08	12.75	0.08	0.08	1.91
56	0.00	0.28	3.36	9.87	57.09	27.82	0.00	0.10	1.47
57	0.00	0.15	5.17	5.11	57.03	30.98	0.02	0.12	1.44
58	0.00	0.04	6.09	2.79	59.29	30.33	0.00	0.12	1.35
59	0.01	0.00	5.97	2.80	59.45	30.29	0.00	0.10	1.37

60	0.01	0.00	5.70	2.77	59.31	30.81	0.02	0.08	1.31
61	0.00	0.00	5.94	2.84	59.05	30.57	0.00	0.13	1.47
62	0.00	0.00	6.05	2.77	59.02	30.76	0.01	0.00	1.40
63	0.00	0.03	5.44	2.72	56.98	33.39	0.00	0.07	1.37
64	0.00	0.04	5.42	2.85	57.51	32.74	0.00	0.12	1.34
65	0.00	0.02	5.36	2.96	58.75	31.34	0.00	0.10	1.47
66	0.01	0.03	5.66	2.83	58.58	31.38	0.00	0.07	1.45
67	0.00	0.00	5.65	2.92	58.97	30.99	0.02	0.06	1.39
68	0.00	0.00	5.55	2.91	58.43	31.60	0.02	0.13	1.36
69	0.04	0.00	5.58	2.69	58.28	31.78	0.02	0.16	1.45
70	0.00	0.04	5.75	2.47	58.74	31.50	0.00	0.11	1.41
71	0.01	0.00	5.38	2.91	58.70	31.43	0.00	0.05	1.53
72	0.00	0.00	5.40	2.82	58.54	31.61	0.00	0.15	1.50
73	0.01	0.00	5.53	2.63	58.59	31.63	0.02	0.07	1.52
74	0.00	0.00	5.57	2.21	59.05	31.66	0.02	0.17	1.32
75	0.04	0.00	5.11	2.04	56.30	34.16	0.02	1.15	1.18
76	0.03	0.02	2.70	0.97	28.46	56.18	0.00	10.80	0.84
77	0.01	0.05	0.78	0.07	3.58	75.54	0.01	19.61	0.34
78	0.00	0.06	0.43	0.05	3.34	75.81	0.00	19.86	0.44
79	0.00	0.00	0.32	0.06	3.45	75.72	0.00	20.12	0.34
80	0.06	0.00	0.29	0.00	3.59	75.65	0.00	19.96	0.46
81	0.01	0.06	0.23	0.07	3.61	75.52	0.00	20.10	0.41
82	0.00	0.00	0.30	0.10	3.54	75.53	0.02	20.07	0.44
83	0.00	0.00	0.30	0.00	3.65	75.66	0.00	19.91	0.49
84	0.00	0.00	0.24	0.00	3.68	75.78	0.09	19.76	0.45
85	0.03	0.00	0.28	0.00	3.45	75.96	0.02	19.78	0.50
86	0.00	0.00	0.42	0.00	3.70	75.76	0.04	19.51	0.56
87	0.01	0.01	0.32	0.00	3.57	75.68	0.00	19.98	0.44
88	0.00	0.00	0.29	0.05	3.60	75.91	0.00	19.72	0.43
89	0.06	0.03	0.36	0.00	3.58	75.61	0.04	20.07	0.27
90	0.00	0.03	0.26	0.03	3.54	75.65	0.04	20.02	0.44
0	0.00	0.03	5.52	2.36	58.88	31.57	0.05	0.10	1.50
2	0.00	0.00	5.56	2.44	58.65	31.74	0.02	0.14	1.45
4	0.00	0.07	6.47	0.90	24.80	57.42	0.01	9.53	0.82
6	0.03	0.00	6.86	0.39	10.38	66.35	0.00	15.44	0.54
8	0.01	0.00	7.09	0.37	13.20	64.06	0.00	14.70	0.57
10	0.00	0.00	8.42	0.25	9.38	66.27	0.09	15.08	0.51
12	0.03	0.00	7.76	0.15	3.47	70.61	0.04	17.69	0.26
14	0.06	0.00	1.99	0.15	3.67	74.59	0.00	19.16	0.38
16	0.00	0.04	0.19	0.00	3.49	76.35	0.00	19.56	0.37
18	0.00	0.02	0.17	0.03	3.56	76.42	0.01	19.40	0.39
20	0.00	0.03	0.12	0.00	3.96	76.20	0.00	19.38	0.32
22	0.07	0.02	0.21	0.02	3.82	76.00	0.07	19.32	0.47
24	0.00	0.00	0.27	0.00	3.82	76.01	0.00	19.46	0.45
26	0.00	0.00	0.23	0.00	3.69	76.50	0.02	19.18	0.38
28	0.00	0.00	0.23	0.02	3.58	78.59	0.04	17.10	0.44
30	0.00	0.00	0.19	0.17	3.74	77.75	0.00	17.73	0.43
32	0.00	0.05	0.27	0.02	2.89	84.09	0.00	12.14	0.55
34	0.00	0.00	0.86	0.00	0.50	97.82	0.07	0.21	0.54
36	0.00	0.04	0.28	0.09	0.40	98.56	0.05	0.10	0.49
38	0.03	0.02	1.11	0.03	0.41	97.60	0.00	0.20	0.60
40	0.03	0.06	1.87	0.11	0.64	96.22	0.00	0.61	0.47

D.2 SS-316/V/Nd After 28 Days at 550°C

The SS-316/V/Nd assembly annealed for 28 days at 550°C bonded on the V/Nd interface but not the SS-316/V interface. Since the V/Nd interface at this time and temperature was already well characterized, no WDS linescans were completed on it in this assembly.

D.3 SS-316/Zr/V/Nd After 28 Days at 550°C

The SS-316/Zr/V/Nd assembly annealed for 28 days at 550°C bonded on the V/Nd interface but not the SS-316/Zr or Zr/V interfaces. Compositional data (in at%) from WDS linescans across the V/Nd interface is given below.

Position	Zr	Mo	Si	Cr	Fe	Nd	V	Ni	Mn
0	0.00	0.02	0.79	1.80	0.20	1.02	96.17	0.00	0.01
1	0.07	0.01	2.41	1.76	0.18	1.52	93.97	0.05	0.03
2	0.01	0.01	5.09	1.65	0.17	1.94	91.12	0.01	0.00
3	0.00	0.00	0.22	1.83	2.19	1.06	94.67	0.02	0.01
4	0.04	0.00	1.04	0.24	2.63	77.23	18.38	0.00	0.45
5	0.00	0.02	0.61	0.06	1.36	87.70	9.78	0.00	0.47
6	0.03	0.02	0.85	1.57	5.64	12.22	79.54	0.00	0.14
7	0.00	0.02	0.91	0.44	2.96	75.86	19.42	0.00	0.40
8	0.00	0.03	0.23	0.00	0.30	95.23	3.70	0.00	0.51
9	0.00	0.13	0.15	0.00	0.30	96.05	2.70	0.05	0.63
10	0.00	0.00	0.20	0.11	0.40	96.61	2.08	0.08	0.53
11	0.00	0.09	0.39	0.15	0.44	96.10	2.35	0.00	0.47
12	0.00	0.08	0.44	0.07	0.46	95.07	3.35	0.00	0.53
13	0.02	0.03	0.48	0.00	0.34	96.75	1.93	0.01	0.44
14	0.00	0.00	0.54	0.04	0.41	97.15	1.42	0.00	0.44
15	0.00	0.00	1.37	0.00	0.49	96.52	0.94	0.08	0.60

D.4 SS-316/Zr/Nd After 28 Days at 550°C

The SS-316/Zr/Nd assembly annealed for 28 days at 550°C bonded on the Zr/Nd interface but not the SS-316/Zr interface. Compositional data (in at%) from WDS linescans across the Zr/Nd interface is given below.

Position	Zr	Mo	Si	Cr	Fe	Nd	V	Ni	Mn
0	99.57	0.00	0.05	0.06	0.00	0.30	0.00	0.00	0.02
1	99.46	0.00	0.06	0.03	0.05	0.30	0.03	0.05	0.04
2	99.35	0.00	0.22	0.00	0.03	0.37	0.03	0.00	0.00
3	99.25	0.00	0.22	0.02	0.05	0.37	0.06	0.03	0.00
4	99.24	0.00	0.28	0.00	0.08	0.41	0.00	0.00	0.00
5	99.01	0.00	0.28	0.00	0.07	0.50	0.07	0.07	0.00
6	99.39	0.00	0.05	0.00	0.03	0.46	0.07	0.01	0.00
7	99.05	0.00	0.09	0.00	0.18	0.66	0.00	0.03	0.00
8	89.41	0.00	0.16	0.00	1.45	5.71	0.00	0.26	0.00

9	70.13	0.00	0.28	0.10	2.28	26.82	0.04	0.15	0.22
10	21.06	0.02	0.32	0.09	0.49	77.62	0.00	0.09	0.31
11	6.04	0.00	0.33	0.00	0.39	92.62	0.00	0.12	0.50
12	0.28	0.06	0.37	0.02	0.32	98.39	0.11	0.00	0.45
13	0.19	0.00	0.42	0.07	0.37	98.39	0.00	0.00	0.55
14	0.03	0.00	0.41	0.00	0.36	98.60	0.00	0.01	0.59
15	0.04	0.00	0.38	0.00	0.20	98.50	0.00	0.18	0.71
0	99.36	0.01	0.15	0.00	0.14	0.29	0.00	0.00	0.05
1	99.35	0.00	0.10	0.06	0.06	0.41	0.00	0.00	0.03
2	98.68	0.00	0.17	0.11	0.19	0.74	0.04	0.03	0.04
3	91.88	0.00	0.18	0.00	2.01	5.74	0.01	0.13	0.06
4	63.39	0.06	0.58	0.04	2.44	33.10	0.00	0.19	0.21
5	10.16	0.02	1.92	0.00	0.68	86.67	0.01	0.03	0.52
6	0.13	0.01	1.10	0.04	0.35	97.94	0.03	0.00	0.41
7	23.89	0.00	1.80	0.00	1.17	72.66	0.00	0.00	0.48
8	0.59	0.00	1.69	0.00	0.39	96.60	0.04	0.20	0.50
9	0.11	0.01	1.39	0.00	0.30	97.57	0.00	0.19	0.45
10	0.07	0.00	0.78	0.07	0.35	98.09	0.00	0.00	0.63
11	0.07	0.00	0.32	0.09	0.66	98.16	0.00	0.04	0.66
12	0.14	0.06	0.62	0.26	1.03	97.50	0.00	0.02	0.38
13	0.05	0.00	0.73	0.02	0.32	98.15	0.00	0.06	0.68
14	0.03	0.10	0.43	0.27	0.89	97.69	0.02	0.03	0.54
15	0.08	0.00	1.08	0.11	1.19	96.85	0.00	0.08	0.62

D.5 SS-316/Ti/V/Nd After 28 Days at 550°C

The SS-316/Ti/V/Nd assembly annealed for 28 days at 550°C bonded on the SS-316/Ti and V/Nd interfaces but not the Ti/V interface. Compositional data (in at%) from WDS linescans across the SS-316/Ti and V/Nd interfaces is given below.

Position	Ta	Ti	Mo	Si	Fe	Nd	V	Cr	Ni	Mn
0	0.00	1.57	1.20	1.33	67.64	0.02	0.12	17.84	8.66	1.62
1	0.00	1.00	1.21	2.26	67.20	0.02	0.08	18.04	8.55	1.64
2	0.00	1.04	1.27	1.23	67.84	0.02	0.06	18.21	8.70	1.64
3	0.00	1.20	1.22	1.05	67.69	0.03	0.09	18.37	8.68	1.67
4	0.00	0.93	1.31	0.94	68.32	0.00	0.08	18.29	8.43	1.71
5	0.00	2.54	1.36	1.04	66.97	0.06	0.08	18.14	8.20	1.60
6	0.00	4.97	1.36	1.32	64.52	0.03	0.13	18.43	7.73	1.52
7	0.00	2.56	1.49	1.73	66.45	0.04	0.13	18.65	7.52	1.43
8	0.00	23.28	1.43	1.05	47.30	0.10	0.17	19.55	6.10	1.02
9	0.00	2.15	1.04	0.86	69.45	0.01	0.08	15.58	9.46	1.37
10	0.00	17.80	1.52	1.03	51.71	0.07	0.17	19.38	7.15	1.18
11	0.00	89.12	0.14	3.25	4.14	0.17	0.35	2.26	0.45	0.12
12	0.00	84.01	0.00	14.59	0.72	0.08	0.21	0.23	0.10	0.06
13	0.00	99.04	0.00	0.14	0.35	0.02	0.25	0.08	0.07	0.07
14	0.00	98.62	0.00	0.33	0.43	0.02	0.30	0.12	0.12	0.07
15	0.00	96.84	0.00	1.77	0.26	0.72	0.26	0.08	0.03	0.04
0	0.00	0.52	1.22	1.37	67.59	0.02	0.09	18.12	9.28	1.79
1	0.00	0.96	1.16	7.53	63.09	0.05	0.05	16.34	9.16	1.67
2	0.00	1.14	1.13	11.83	60.31	0.02	0.09	15.56	8.36	1.57
3	0.00	1.00	0.96	23.06	52.28	0.03	0.08	14.11	7.08	1.40
4	0.00	3.33	1.12	14.80	52.00	0.13	0.09	17.34	9.39	1.80

5	0.00	1.74	1.14	5.53	63.85	0.05	0.10	16.43	9.55	1.62
6	0.00	2.16	1.14	1.01	66.79	0.06	0.07	17.46	9.44	1.86
7	0.00	3.82	1.17	1.30	65.46	0.09	0.12	17.11	9.31	1.62
8	0.00	4.61	1.12	2.21	65.46	0.11	0.09	16.50	8.46	1.45
9	0.00	66.23	0.36	14.06	11.62	0.27	0.25	5.72	1.23	0.25
10	0.00	78.63	0.00	19.87	0.73	0.09	0.31	0.21	0.07	0.07
11	0.00	69.29	0.02	28.24	1.25	0.24	0.25	0.56	0.13	0.03
12	0.00	75.94	0.00	22.42	0.85	0.07	0.33	0.25	0.10	0.04
13	0.00	88.57	0.00	10.24	0.57	0.08	0.26	0.17	0.08	0.03
14	0.00	93.53	0.00	5.20	0.59	0.07	0.28	0.18	0.11	0.04
15	0.00	93.29	0.00	5.51	0.48	0.25	0.30	0.09	0.08	0.01
0	0.00	1.09	1.09	0.91	67.40	0.04	0.08	17.95	9.53	1.93
1	0.00	1.03	1.13	0.85	67.44	0.05	0.11	17.97	9.68	1.74
2	0.00	1.14	1.19	1.13	66.85	0.03	0.12	18.06	9.48	2.02
3	0.00	3.66	1.16	1.19	65.28	0.08	0.12	17.55	9.31	1.66
4	0.00	13.22	0.94	2.08	58.20	0.12	0.15	15.51	8.30	1.49
5	0.00	12.60	0.93	1.93	60.02	0.05	0.13	15.37	7.53	1.44
6	0.00	5.26	1.15	0.89	65.32	0.04	0.09	16.78	8.82	1.65
7	0.00	6.45	1.10	1.87	63.68	0.11	0.13	16.03	9.06	1.56
8	0.00	6.52	0.87	0.93	66.09	0.00	0.09	14.59	9.50	1.42
9	0.00	11.76	0.97	0.80	61.78	0.03	0.15	15.42	8.01	1.09
10	0.00	33.38	1.44	0.95	40.52	0.03	0.18	17.79	4.88	0.83
11	0.00	91.79	0.13	1.10	3.68	0.04	0.26	2.48	0.39	0.13
12	0.00	98.62	0.00	0.36	0.50	0.04	0.27	0.12	0.04	0.05
13	0.00	98.30	0.00	0.88	0.37	0.00	0.28	0.12	0.05	0.00
14	0.00	98.76	0.00	0.42	0.35	0.02	0.29	0.12	0.00	0.04
15	0.00	98.18	0.00	0.60	0.63	0.00	0.29	0.18	0.11	0.03
0	0.00	19.37	0.90	7.34	48.98	0.57	0.63	13.95	6.93	1.35
1	0.00	1.22	1.15	1.00	67.34	0.00	0.10	17.46	10.00	1.74
2	0.00	1.01	1.22	1.14	67.00	0.04	0.08	17.86	9.97	1.69
3	0.00	1.17	1.14	0.95	67.24	0.11	0.07	17.57	9.97	1.80
4	0.00	1.10	1.25	0.89	66.93	0.02	0.10	17.94	10.03	1.75
5	0.00	1.22	1.24	1.07	66.81	0.03	0.07	17.73	10.14	1.71
6	0.00	5.91	1.07	3.17	62.63	0.07	0.16	15.92	9.50	1.58
7	0.00	5.36	1.01	1.83	64.88	0.17	0.10	15.31	9.79	1.56
8	0.00	4.82	0.78	2.36	65.48	0.12	0.14	14.11	10.55	1.65
9	0.00	37.89	0.43	4.79	40.48	0.12	0.31	8.66	6.36	0.98
10	0.00	73.78	0.07	11.35	10.18	0.20	0.46	2.30	1.40	0.28
11	0.00	95.90	0.00	2.18	1.03	0.10	0.32	0.31	0.15	0.02
12	0.00	96.68	0.00	2.01	0.71	0.01	0.27	0.19	0.09	0.04
13	0.00	96.51	0.00	2.27	0.59	0.13	0.25	0.14	0.06	0.06
14	0.00	92.72	0.00	6.15	0.43	0.21	0.34	0.11	0.05	0.00
15	0.00	98.37	0.00	0.91	0.29	0.04	0.31	0.06	0.01	0.03
0	0.00	0.16	0.00	41.39	0.16	1.07	46.74	10.42	0.07	0.00
1	0.00	0.00	0.00	0.60	0.06	0.64	96.41	2.23	0.05	0.02
2	0.00	0.00	0.00	0.14	0.00	0.47	96.11	2.09	0.02	1.17
3	0.00	0.00	0.00	0.30	0.12	1.30	95.98	2.31	0.00	0.00
4	0.00	0.00	0.00	1.34	0.48	3.42	92.67	2.08	0.00	0.00
5	0.00	0.00	0.00	0.89	0.53	3.86	92.58	2.14	0.00	0.00
6	0.00	0.00	0.02	15.83	4.75	15.93	61.86	1.52	0.00	0.09
7	0.00	0.01	0.02	3.65	18.26	8.54	67.48	1.86	0.00	0.18
8	0.00	0.01	0.07	7.28	9.11	32.09	49.70	1.45	0.02	0.26
9	0.00	0.01	0.02	1.53	0.75	91.17	5.96	0.12	0.00	0.44
10	0.00	0.00	0.00	1.12	0.50	92.76	4.68	0.17	0.13	0.63

11	0.00	0.00	0.04	0.22	0.75	90.61	7.76	0.21	0.00	0.41
12	0.00	0.01	0.01	0.67	3.25	93.40	2.13	0.06	0.00	0.48
13	0.00	0.00	0.11	0.35	0.45	97.00	1.50	0.00	0.00	0.60
14	0.00	0.00	0.00	0.65	0.66	96.06	1.95	0.15	0.00	0.54
15	0.00	0.00	0.05	0.81	2.08	95.05	1.56	0.05	0.05	0.35

D.6 SS-316/Ti/Nd After 28 Days at 550°C

The SS-316/Ti/Nd assembly annealed for 28 days at 550°C bonded on the Ti/Nd interface but not the SS-316/Ti interface. Compositional data (in at%) from WDS linescans across the Ti/Nd interface is given below.

Position	Ta	Ti	Mo	Si	Fe	Nd	V	Cr	Ni	Mn
0	0.00	2.12	0.00	0.15	0.15	96.96	0.00	0.03	0.00	0.58
1	0.00	2.09	0.00	0.17	0.23	96.81	0.04	0.00	0.00	0.66
2	0.00	3.64	0.02	0.23	0.36	95.15	0.00	0.00	0.04	0.57
3	0.00	6.18	0.04	1.08	0.35	91.75	0.03	0.00	0.00	0.57
4	0.00	24.87	0.00	0.48	0.30	73.63	0.26	0.05	0.00	0.40
5	0.00	97.72	0.00	0.09	0.15	1.68	0.35	0.02	0.00	0.00
6	0.00	99.45	0.00	0.05	0.01	0.10	0.32	0.02	0.06	0.00
7	0.00	99.20	0.00	0.04	0.00	0.48	0.26	0.02	0.00	0.00
8	0.00	99.49	0.00	0.04	0.01	0.23	0.22	0.00	0.00	0.01
9	0.00	99.53	0.00	0.06	0.00	0.12	0.24	0.03	0.00	0.01
10	0.00	99.46	0.00	0.13	0.01	0.12	0.26	0.00	0.02	0.00
11	0.00	98.09	0.00	1.44	0.03	0.15	0.25	0.00	0.04	0.00
12	0.00	96.85	0.00	2.49	0.04	0.27	0.27	0.00	0.06	0.02
13	0.00	98.76	0.00	0.44	0.06	0.38	0.27	0.04	0.04	0.00
14	0.00	99.09	0.00	0.12	0.04	0.27	0.40	0.03	0.03	0.02
15	0.00	98.62	0.00	0.72	0.06	0.33	0.27	0.00	0.01	0.00
0	0.00	2.00	0.00	0.14	0.36	96.91	0.02	0.10	0.01	0.46
1	0.00	4.52	0.00	0.30	0.48	94.24	0.02	0.00	0.00	0.45
2	0.00	88.82	0.00	0.17	0.35	10.17	0.39	0.01	0.02	0.08
3	0.00	97.48	0.00	0.81	0.49	0.78	0.25	0.11	0.08	0.00
4	0.00	74.76	0.00	0.30	0.40	24.02	0.31	0.05	0.01	0.16
5	0.00	97.48	0.00	0.23	0.15	1.74	0.29	0.06	0.02	0.02
6	0.00	92.97	0.01	2.92	2.40	0.55	0.24	0.56	0.26	0.08
7	0.00	82.16	0.00	15.86	0.96	0.53	0.24	0.16	0.09	0.02
8	0.00	90.55	0.00	8.60	0.22	0.33	0.25	0.02	0.00	0.03
9	0.00	95.40	0.00	3.98	0.11	0.24	0.25	0.02	0.00	0.02
10	0.00	85.76	0.00	12.53	0.77	0.46	0.25	0.12	0.10	0.01
11	0.00	91.81	0.00	7.31	0.25	0.28	0.24	0.04	0.06	0.01
12	0.00	94.32	0.00	4.85	0.14	0.36	0.28	0.03	0.02	0.00
13	0.00	98.04	0.00	1.45	0.07	0.18	0.24	0.01	0.00	0.00
14	0.00	98.98	0.00	0.25	0.05	0.40	0.28	0.00	0.03	0.02
15	0.00	99.05	0.00	0.20	0.07	0.30	0.33	0.04	0.02	0.00

D.7 SS-316/Ta/V/Nd After 28 Days at 550°C

The SS-316/Ta/V/Nd assembly annealed for 28 days at 550°C bonded on the V/Nd interface but not the SS-316/Ta or Ta/V interfaces. Compositional data (in at%) from WDS linescans across the V/Nd interface is given below.

Position	Ta	Ti	Mo	Si	Fe	Nd	V	Cr	Ni	Mn
0	0.00	0.00	0.01	0.35	0.37	97.02	1.73	0.00	0.10	0.42
1	0.11	0.00	0.00	0.64	0.73	90.57	7.29	0.17	0.00	0.50
2	0.00	0.00	0.00	18.44	0.76	74.17	5.96	0.11	0.15	0.42
3	0.00	0.00	0.05	5.76	12.35	20.13	59.91	1.46	0.13	0.21
4	0.00	0.00	0.01	2.39	5.52	4.90	85.16	1.96	0.00	0.05
5	0.00	0.00	0.01	0.48	0.32	0.40	96.63	2.15	0.00	0.02
6	0.00	0.01	0.00	0.47	0.06	0.19	96.97	2.29	0.00	0.02
7	0.00	0.00	0.00	1.29	0.02	0.09	96.35	2.22	0.04	0.00
8	0.00	0.00	0.00	4.63	0.11	0.84	92.30	2.10	0.02	0.00
9	0.00	0.00	0.01	0.70	0.03	0.21	96.82	2.19	0.05	0.00
10	0.00	0.00	0.00	1.50	0.02	0.15	95.98	2.35	0.00	0.00
11	0.00	0.00	0.00	5.40	0.03	0.10	92.24	2.20	0.02	0.00
12	0.00	0.00	0.00	9.95	0.05	0.10	87.89	1.99	0.01	0.00
13	0.00	0.00	0.02	1.21	0.05	0.10	96.36	2.24	0.00	0.02
14	0.00	0.00	0.00	0.27	0.00	0.04	97.59	2.10	0.00	0.00
15	0.00	0.00	0.01	0.13	0.03	0.02	97.70	2.11	0.00	0.00
0	0.00	0.00	0.00	0.24	0.34	97.43	1.61	0.00	0.00	0.39
1	0.00	0.00	0.00	25.06	2.45	56.07	15.81	0.42	0.00	0.20
2	0.00	0.00	0.00	0.89	4.47	3.13	89.36	2.12	0.04	0.00
3	0.00	0.00	0.01	0.25	0.63	0.41	96.44	2.20	0.04	0.02
4	0.00	0.00	0.00	0.17	0.02	0.17	97.36	2.27	0.00	0.00
5	0.00	0.00	0.00	0.93	0.01	0.11	96.69	2.25	0.00	0.01
6	0.00	0.00	0.00	0.21	0.01	0.07	97.54	2.17	0.00	0.00
7	0.00	0.00	0.00	0.48	0.05	0.04	97.18	2.26	0.00	0.00
8	0.00	0.00	0.01	0.26	0.02	0.02	97.47	2.18	0.04	0.00
9	0.00	0.00	0.00	0.63	0.02	0.07	97.03	2.22	0.03	0.00
10	0.00	0.00	0.01	0.48	0.02	0.10	97.16	2.24	0.00	0.00
11	0.00	0.00	0.01	0.09	0.00	0.07	97.54	2.29	0.00	0.00
12	0.00	0.00	0.02	0.36	0.01	0.03	97.29	2.24	0.03	0.00
13	0.00	0.00	0.00	0.32	0.01	0.01	97.36	2.28	0.01	0.01
14	0.00	0.01	0.01	0.07	0.01	0.01	97.74	2.15	0.01	0.00
15	0.00	0.00	0.00	0.08	0.01	0.02	97.67	2.23	0.00	0.00

D.8 SS-316/Ta/Nd After 28 Days at 550°C

The SS-316/Ta/Nd assembly annealed for 28 days at 550°C did not bond on the SS-316/Ta or Ta/Nd interfaces.

D.9 SS-316/Mo/V/Nd After 28 Days at 550°C

The SS-316/Mo/V/Nd assembly annealed for 28 days at 550°C bonded on the V/Nd interface but not the SS-316/Mo or Mo/V interfaces. Since the V/Nd interface at this time and temperature was already well characterized, no WDS linescans were completed on it in this assembly.

D.10 SS-316/Mo/Nd After 28 Days at 550°C

The SS-316/W/Nd assembly annealed for 28 days at 550°C bonded on the Mo/Nd interface but not the SS-316/Mo interface. Compositional data (in at%) from WDS linescans across the Mo/Nd interface is given below.

Position	Si	V	W	Mo	Nd	Ni	Fe	Mn	Cr
0	0.28	0.16	0.00	0.08	98.65	0.00	0.34	0.47	0.01
1	3.88	0.00	0.00	2.98	92.01	0.00	0.50	0.63	0.00
2	5.52	0.03	0.03	26.62	66.93	0.02	0.35	0.47	0.03
3	0.73	0.00	0.00	73.51	25.25	0.04	0.30	0.15	0.02
4	0.35	0.02	0.00	94.93	4.46	0.03	0.13	0.08	0.00
5	0.21	0.05	0.02	97.63	1.88	0.04	0.09	0.05	0.03
6	0.05	0.10	0.00	99.32	0.46	0.00	0.06	0.03	0.00
7	0.03	0.00	0.00	99.57	0.34	0.00	0.00	0.06	0.00
8	0.17	0.00	0.00	99.32	0.34	0.05	0.00	0.04	0.08
9	0.02	0.07	0.00	99.37	0.46	0.05	0.01	0.00	0.04
10	0.29	0.03	0.02	99.31	0.24	0.00	0.05	0.07	0.00
11	0.36	0.14	0.00	99.15	0.21	0.02	0.06	0.06	0.00
12	0.18	0.01	0.00	99.53	0.20	0.03	0.04	0.01	0.00
13	0.16	0.00	0.03	99.63	0.12	0.05	0.02	0.00	0.00
14	0.21	0.03	0.01	99.53	0.06	0.10	0.02	0.00	0.05
15	0.36	0.00	0.00	99.51	0.07	0.00	0.03	0.00	0.03
0	0.17	0.00	0.00	0.03	98.81	0.00	0.33	0.65	0.01
1	0.10	0.00	0.01	0.20	98.76	0.01	0.33	0.58	0.01
2	0.28	0.01	0.01	3.70	95.12	0.07	0.32	0.49	0.00
3	0.39	0.16	0.03	67.90	30.76	0.06	0.40	0.16	0.14
4	0.35	0.09	0.00	94.99	4.13	0.01	0.20	0.10	0.12
5	0.15	0.02	0.01	98.82	0.85	0.00	0.07	0.08	0.00
6	0.40	0.02	0.00	98.72	0.59	0.01	0.08	0.00	0.18
7	1.11	0.00	0.01	97.96	0.58	0.03	0.26	0.00	0.06
8	1.34	0.00	0.02	97.50	0.61	0.09	0.35	0.00	0.09
9	0.31	0.00	0.01	98.85	0.64	0.00	0.10	0.00	0.08
10	0.25	0.04	0.02	98.86	0.77	0.00	0.06	0.00	0.00
11	0.26	0.01	0.02	98.04	1.38	0.00	0.28	0.00	0.01
12	0.36	0.00	0.00	97.72	1.43	0.00	0.28	0.09	0.11
13	0.55	0.02	0.00	96.97	2.03	0.01	0.31	0.00	0.10
14	1.44	0.05	0.03	96.02	2.05	0.04	0.28	0.06	0.04
15	0.61	0.02	0.02	98.08	0.80	0.11	0.25	0.04	0.07
0	1.38	0.09	0.00	0.28	97.34	0.00	0.38	0.55	0.00
1	0.79	0.05	0.00	0.10	98.11	0.00	0.38	0.50	0.07
2	0.36	0.00	0.00	0.30	98.49	0.01	0.28	0.57	0.00
3	0.35	0.00	0.00	19.00	79.73	0.02	0.39	0.48	0.04
4	0.26	0.09	0.01	80.77	18.02	0.00	0.58	0.07	0.22
5	0.24	0.03	0.02	91.69	7.48	0.00	0.42	0.02	0.10
6	0.31	0.02	0.00	96.16	3.06	0.10	0.32	0.00	0.04
7	0.22	0.03	0.01	98.26	1.16	0.14	0.07	0.06	0.06
8	1.99	0.15	0.01	96.87	0.93	0.00	0.00	0.04	0.00
9	2.20	0.05	0.00	96.67	0.94	0.00	0.08	0.00	0.05
10	0.83	0.00	0.02	96.55	2.30	0.01	0.14	0.08	0.08
11	0.61	0.00	0.00	96.80	2.34	0.02	0.09	0.04	0.10
12	1.19	0.03	0.03	97.21	1.29	0.00	0.26	0.00	0.00

13	0.76	0.00	0.00	98.07	0.69	0.04	0.31	0.00	0.14
14	0.32	0.12	0.00	98.60	0.66	0.04	0.19	0.00	0.07
15	0.03	0.00	0.00	99.75	0.13	0.00	0.09	0.01	0.00

D.11 SS-316/W/V/Nd After 28 Days at 550°C

The SS-316/W/V/Nd assembly annealed for 28 days at 550°C bonded on the V/Nd interface but not the SS-316/W or W/V interfaces. Since the V/Nd interface at this time and temperature was already well characterized, no WDS linescans were completed on it in this assembly.

D.12 SS-316/W/Nd After 28 Days at 550°C

The SS-316/W/Nd assembly annealed for 28 days at 550°C bonded on the W/Nd interface but not the SS-316/W interface. Compositional data (in at%) from WDS linescans across the W/Nd interface is given below.

Position	Si	V	W	Mo	Nd	Ni	Fe	Mn	Cr
0	0.00	0.00	0.05	0.00	99.09	0.08	0.23	0.55	0.00
1	8.88	0.00	2.57	0.00	87.75	0.06	0.25	0.44	0.05
2	8.70	0.17	45.69	0.00	44.88	0.00	0.21	0.26	0.09
3	1.88	0.03	0.23	0.00	97.62	0.07	0.05	0.10	0.05
4	0.00	0.07	98.72	0.00	1.05	0.14	0.02	0.00	0.01
5	8.60	0.06	47.76	0.01	43.11	0.21	0.09	0.14	0.04
6	0.01	0.16	99.03	0.00	0.55	0.01	0.07	0.03	0.14
7	0.00	0.09	99.37	0.00	0.22	0.07	0.03	0.00	0.23
8	0.00	0.01	99.64	0.00	0.24	0.00	0.05	0.06	0.00
9	0.00	0.00	99.53	0.00	0.35	0.02	0.02	0.05	0.04
10	0.00	0.05	99.41	0.00	0.21	0.09	0.09	0.09	0.06
11	0.00	0.12	99.67	0.00	0.19	0.00	0.02	0.00	0.00
12	0.08	0.00	99.70	0.00	0.08	0.06	0.09	0.00	0.00
13	0.00	0.26	99.42	0.00	0.20	0.01	0.10	0.02	0.00
14	0.00	0.13	99.50	0.00	0.26	0.08	0.00	0.00	0.03
15	0.00	0.17	99.29	0.00	0.20	0.26	0.05	0.04	0.00
0	0.13	0.05	0.02	0.00	98.96	0.00	0.26	0.55	0.03
1	0.49	0.00	0.08	0.01	98.62	0.00	0.27	0.53	0.00
2	0.18	0.01	0.08	0.04	98.78	0.00	0.34	0.57	0.00
3	0.26	0.00	11.57	0.00	87.50	0.04	0.24	0.36	0.03
4	0.30	0.08	26.97	0.00	71.95	0.10	0.20	0.41	0.00
5	0.00	0.18	95.71	0.00	3.99	0.00	0.12	0.00	0.00
6	0.00	0.12	98.39	0.00	1.19	0.11	0.03	0.02	0.14
7	0.00	0.10	99.10	0.00	0.58	0.04	0.00	0.18	0.00
8	0.00	0.08	99.43	0.00	0.32	0.02	0.05	0.10	0.00
9	0.00	0.13	99.05	0.00	0.39	0.17	0.12	0.03	0.11
10	0.02	0.00	99.19	0.00	0.34	0.27	0.15	0.00	0.03
11	0.18	0.12	99.26	0.00	0.32	0.00	0.06	0.02	0.05
12	1.59	0.12	98.09	0.00	0.13	0.00	0.03	0.04	0.00
13	1.79	0.00	97.92	0.00	0.22	0.00	0.04	0.02	0.00
14	0.34	0.10	99.53	0.00	0.00	0.00	0.04	0.00	0.00

15	0.00	0.00	99.88	0.00	0.10	0.00	0.00	0.02	0.00
0	0.17	0.16	0.08	0.02	98.90	0.00	0.30	0.37	0.00
1	0.05	0.03	0.05	0.00	99.06	0.00	0.37	0.37	0.06
2	0.21	0.14	0.00	0.02	98.91	0.00	0.21	0.51	0.02
3	0.11	0.07	0.13	0.02	98.95	0.00	0.39	0.34	0.00
4	0.09	0.11	0.03	0.02	98.82	0.01	0.25	0.62	0.04
5	0.15	0.00	0.03	0.00	98.83	0.00	0.32	0.56	0.10
6	0.00	0.00	0.08	0.00	99.14	0.00	0.32	0.47	0.00
7	0.22	0.05	9.23	0.00	89.75	0.00	0.30	0.45	0.00
8	0.03	0.00	53.69	0.00	45.74	0.12	0.22	0.18	0.02
9	0.00	0.00	94.99	0.00	4.81	0.00	0.07	0.09	0.05
10	0.00	0.09	99.02	0.00	0.78	0.00	0.07	0.05	0.00
11	0.00	0.13	99.49	0.00	0.37	0.00	0.01	0.00	0.00
12	0.14	0.13	99.16	0.00	0.33	0.00	0.05	0.12	0.07
13	0.00	0.00	99.52	0.00	0.28	0.00	0.06	0.00	0.14
14	0.00	0.18	99.45	0.00	0.20	0.00	0.05	0.04	0.09
15	0.00	0.20	99.46	0.00	0.21	0.06	0.00	0.00	0.07

D.13 SS-316/Nd After 56 Days at 550°C

When annealed for 56 days at 550°C, three interaction zones were observed for the SS-316/Nd diffusion assembly. The first interaction zone, which had a composition matching $\text{Nd}_2(\text{Fe}+\text{Cr})_{17}$, was $\sim 87 \mu\text{m}$ wide. The second interaction zone, which had a composition matching Fe_2Nd , was $\sim 21 \mu\text{m}$ wide. The third interaction zone observed had a composition matching $\text{Nd}_3(\text{Ni}+\text{Fe})$ and was $\sim 22 \mu\text{m}$ wide. Compositional data (in at%) from WDS linescans across the interface is given below.

Position	Zr	Mo	Si	Cr	Fe	Nd	V	Ni	Mn
0	0.00	1.41	0.48	20.17	64.11	11.68	0.10	0.19	1.86
1	0.00	1.44	0.29	20.25	64.86	11.08	0.09	0.21	1.79
2	0.01	1.50	0.25	20.27	65.36	10.39	0.13	0.22	1.87
3	0.00	1.49	0.21	20.42	65.51	10.15	0.11	0.23	1.89
4	0.00	1.48	0.24	20.40	65.78	10.10	0.09	0.16	1.76
5	0.00	1.52	0.24	20.23	65.62	10.28	0.08	0.23	1.80
6	0.00	1.42	0.21	20.04	65.66	10.56	0.11	0.21	1.80
7	0.00	1.46	0.21	20.07	64.61	11.47	0.14	0.19	1.86
8	0.00	1.51	0.23	19.62	64.30	12.22	0.11	0.23	1.79
9	0.00	1.34	0.77	17.85	62.77	15.28	0.07	0.15	1.78
10	0.00	0.90	2.31	13.19	61.36	20.45	0.06	0.09	1.65
11	0.00	0.47	4.09	7.19	60.14	26.62	0.00	0.06	1.44
12	0.00	0.19	4.95	4.90	59.33	29.13	0.04	0.06	1.40
13	0.02	0.03	5.41	3.17	59.11	30.74	0.05	0.02	1.45
14	0.01	0.01	5.34	2.97	59.17	30.89	0.00	0.15	1.46
15	0.00	0.00	5.72	0.02	60.44	32.18	0.00	0.13	1.52
16	0.00	0.00	5.26	2.67	57.30	33.33	0.01	0.13	1.30
17	0.00	0.01	5.11	2.69	57.27	33.44	0.00	0.14	1.35
18	0.00	0.00	5.26	2.68	57.39	33.27	0.03	0.05	1.33
19	0.00	0.02	5.55	2.49	57.88	32.48	0.03	0.16	1.40
20	0.00	0.00	5.24	2.35	58.94	31.77	0.00	0.20	1.50
21	0.01	0.00	5.32	2.16	59.28	31.65	0.04	0.20	1.33

22	0.03	0.00	4.75	2.11	53.97	35.92	0.00	2.04	1.19
23	0.00	0.00	3.67	1.36	40.87	46.65	0.03	6.39	1.03
24	0.00	0.01	5.19	2.24	58.35	32.35	0.00	0.54	1.34
25	0.00	0.01	4.21	1.74	48.96	40.31	0.05	3.53	1.18
26	0.03	0.05	2.52	0.83	27.61	57.54	0.00	10.65	0.77
27	0.06	0.00	0.27	0.04	3.47	76.47	0.03	19.25	0.42
28	0.00	0.00	0.34	0.06	3.44	76.47	0.00	19.31	0.37
29	0.06	0.09	0.26	0.16	3.49	76.29	0.03	19.15	0.47
30	0.08	0.04	0.38	0.06	3.56	76.15	0.03	19.30	0.41
31	0.00	0.00	0.22	0.01	3.58	75.93	0.11	19.68	0.48
32	0.09	0.01	0.34	0.07	3.31	76.20	0.00	19.60	0.39
33	0.00	0.03	0.22	0.08	3.56	75.71	0.00	20.01	0.37
34	0.05	0.02	0.24	0.00	3.33	75.91	0.05	20.06	0.35
35	0.00	0.05	0.21	0.00	3.49	76.14	0.00	19.64	0.47
36	0.00	0.00	0.21	0.06	3.46	76.17	0.00	19.68	0.43
37	0.00	0.01	0.09	0.06	3.56	76.58	0.00	19.27	0.44
38	0.01	0.01	0.23	0.07	3.72	75.92	0.00	19.60	0.45
39	0.00	0.01	0.21	0.00	3.53	75.90	0.04	20.00	0.30
40	0.00	0.06	0.15	0.00	3.53	76.35	0.02	19.53	0.36
41	0.00	0.00	0.23	0.00	3.64	76.24	0.00	19.45	0.44
42	0.00	0.02	0.24	0.01	3.40	76.25	0.00	19.62	0.46
43	0.02	0.04	0.31	0.05	3.45	76.30	0.02	19.36	0.46
44	0.05	0.00	0.24	0.15	3.54	76.27	0.00	19.38	0.37
45	0.00	0.02	0.18	0.00	3.59	76.53	0.00	19.31	0.36
46	0.00	0.08	0.28	0.05	3.69	76.42	0.05	19.15	0.29
47	0.00	0.00	0.28	0.00	3.65	76.52	0.00	19.14	0.40
48	0.02	0.02	8.83	0.02	3.66	69.67	0.03	17.37	0.37
49	0.00	0.06	21.20	0.05	3.19	60.16	0.00	14.95	0.39
50	0.00	0.06	25.49	0.03	3.00	56.95	0.06	14.14	0.29
51	0.00	0.00	24.46	0.06	2.81	58.00	0.00	14.31	0.38
52	0.00	0.00	15.12	0.01	3.13	65.23	0.08	16.05	0.37
53	0.03	0.02	24.04	0.11	3.11	58.20	0.00	14.16	0.33
54	0.00	0.00	26.58	0.06	2.83	56.56	0.00	13.75	0.21
55	0.00	0.05	0.25	0.05	3.56	76.14	0.00	19.60	0.35
56	0.04	0.06	0.29	0.00	3.69	76.14	0.02	19.38	0.39
57	0.00	0.00	0.23	0.07	3.75	75.98	0.01	19.61	0.37
58	0.00	0.00	0.23	0.00	3.72	76.07	0.00	19.47	0.51
59	0.00	0.00	0.24	0.00	3.76	76.50	0.00	19.15	0.35
60	0.04	0.00	0.23	0.00	3.65	76.03	0.00	19.53	0.53
61	0.00	0.01	0.23	0.00	3.57	76.32	0.02	19.45	0.39
62	0.00	0.00	0.28	0.09	3.79	76.24	0.00	19.33	0.27
63	0.00	0.00	0.19	0.01	3.75	76.38	0.00	19.24	0.44
64	0.00	0.05	0.19	0.00	3.71	76.29	0.10	19.29	0.37
65	0.00	0.02	0.29	0.05	3.62	76.35	0.03	19.27	0.37
66	0.00	0.00	0.22	0.06	3.66	76.18	0.00	19.51	0.37
67	0.07	0.00	0.21	0.00	3.56	76.41	0.02	19.49	0.24
68	0.04	0.05	0.30	0.00	3.65	76.14	0.00	19.39	0.42
69	0.04	0.00	0.18	0.00	3.72	76.18	0.00	19.44	0.43
70	0.00	0.02	0.24	0.00	3.53	76.48	0.10	19.22	0.43
71	0.00	0.00	0.17	0.05	3.56	76.57	0.00	19.30	0.35
72	0.01	0.02	0.22	0.00	3.67	76.30	0.06	19.27	0.46
73	0.00	0.05	0.14	0.10	3.60	77.50	0.03	18.23	0.35
74	0.00	0.00	0.14	0.00	3.71	76.25	0.02	19.43	0.47
75	0.00	0.00	0.28	0.00	3.63	76.28	0.03	19.36	0.42
76	0.03	0.00	0.23	0.00	3.59	76.89	0.00	18.80	0.47
77	0.00	0.00	1.44	0.00	0.76	95.32	0.00	1.95	0.54
78	0.04	0.00	4.02	0.00	0.45	94.58	0.00	0.40	0.51

79	0.00	0.00	14.66	0.00	0.30	84.63	0.00	0.00	0.41
80	0.05	0.02	23.53	0.03	0.30	75.72	0.04	0.00	0.32
0	0.03	1.56	0.25	20.06	63.89	12.02	0.10	0.23	1.87
2	0.02	1.56	0.33	19.95	64.00	12.07	0.14	0.27	1.66
4	0.00	1.55	0.28	19.67	63.93	12.43	0.06	0.30	1.78
6	0.00	1.41	0.44	19.04	63.46	13.74	0.08	0.11	1.72
8	0.00	1.11	1.07	17.03	61.64	17.40	0.09	0.05	1.63
10	0.00	0.21	4.23	7.27	59.10	27.57	0.04	0.06	1.52
12	0.00	0.00	5.50	2.75	59.36	31.04	0.01	0.04	1.32
14	0.00	0.06	5.32	2.64	59.17	31.24	0.00	0.14	1.42
16	0.00	0.00	5.44	2.65	58.65	31.76	0.00	0.09	1.42
18	0.00	0.02	5.50	2.77	58.33	31.99	0.00	0.04	1.35
20	0.04	0.02	5.52	2.44	58.83	31.64	0.02	0.10	1.40
22	0.00	0.03	8.83	2.04	57.18	30.46	0.06	0.13	1.28
24	0.00	0.01	8.49	1.86	57.36	30.95	0.00	0.07	1.25
26	0.00	0.04	4.87	1.47	45.44	47.05	0.03	0.08	1.04
28	0.02	0.00	3.05	0.72	26.97	68.27	0.00	0.14	0.85
30	0.01	0.04	0.38	0.21	1.87	96.76	0.00	0.12	0.60
32	0.00	0.00	0.24	0.06	0.89	98.18	0.00	0.17	0.46
34	0.01	0.00	0.17	0.22	0.58	98.57	0.00	0.02	0.42
36	0.05	0.01	0.14	0.07	0.55	98.59	0.11	0.01	0.46
38	0.00	0.00	0.13	0.00	0.45	98.90	0.00	0.04	0.50
40	0.00	0.00	0.12	0.00	0.47	98.77	0.00	0.10	0.55
42	0.03	0.01	46.68	0.36	1.63	50.90	0.06	0.02	0.30
44	0.00	0.01	22.77	0.19	1.16	75.37	0.02	0.08	0.41
46	0.00	0.05	53.17	0.50	1.75	44.09	0.00	0.13	0.32
48	0.00	0.04	59.81	0.21	1.03	38.55	0.02	0.09	0.25
50	0.00	0.03	42.83	0.17	0.88	55.74	0.04	0.06	0.26
52	0.00	0.05	5.44	0.11	0.77	93.18	0.00	0.00	0.46
54	0.01	0.06	0.30	0.03	0.67	98.29	0.00	0.18	0.45
56	0.00	0.05	3.38	0.07	0.54	95.47	0.00	0.00	0.49
58	0.00	0.00	0.28	0.00	0.66	98.52	0.00	0.02	0.53
60	0.01	0.02	0.15	0.00	0.57	98.70	0.08	0.04	0.44
0	0.00	1.04	0.82	17.52	68.82	0.07	0.10	9.91	1.72
5	0.00	1.00	0.91	17.50	68.91	0.08	0.07	9.83	1.71
10	0.00	1.00	0.72	17.87	68.61	0.09	0.08	9.94	1.70
15	0.01	1.12	0.74	18.68	67.25	3.89	0.10	6.49	1.73
20	0.00	0.97	0.82	21.36	63.26	11.48	0.07	0.19	1.86
25	0.02	1.28	0.44	21.02	65.56	9.72	0.09	0.18	1.70
30	0.00	1.39	0.26	21.35	64.06	10.93	0.07	0.20	1.74
35	0.00	1.40	0.21	21.16	65.32	9.84	0.08	0.23	1.77
40	0.02	1.33	0.27	21.24	64.74	10.49	0.04	0.14	1.73
45	0.00	1.35	0.21	20.99	65.78	9.56	0.09	0.20	1.82
50	0.00	1.38	0.22	21.43	65.15	9.85	0.09	0.11	1.77
55	0.00	1.38	0.18	21.24	63.81	11.38	0.08	0.13	1.80
60	0.00	1.43	0.20	20.80	64.88	10.78	0.07	0.18	1.67
65	0.00	1.43	0.26	21.20	64.89	10.06	0.08	0.21	1.87
70	0.00	1.39	0.22	20.90	64.02	11.44	0.12	0.19	1.71
75	0.00	1.45	0.30	21.11	65.16	9.96	0.07	0.20	1.77
80	0.02	1.38	0.22	20.58	64.50	11.24	0.10	0.13	1.83
85	0.00	1.42	5.27	19.98	61.17	10.19	0.10	0.12	1.75
90	0.00	1.44	0.25	19.88	63.67	12.57	0.12	0.19	1.88
95	0.00	1.49	0.21	20.51	65.15	10.53	0.11	0.18	1.83
100	0.00	1.63	0.23	20.50	63.85	11.37	0.10	0.32	2.01
105	0.00	1.39	0.20	20.58	64.27	11.53	0.07	0.18	1.79

110	0.00	1.37	0.27	20.41	63.13	12.73	0.08	0.29	1.74
115	0.00	0.11	5.04	7.18	59.92	26.28	0.06	0.03	1.40
120	0.07	0.00	2.01	0.96	16.19	80.11	0.00	0.02	0.64
125	0.00	0.00	5.52	2.64	58.80	31.64	0.00	0.09	1.32
130	0.01	0.00	5.85	2.29	57.46	32.76	0.03	0.36	1.24
135	0.00	0.00	0.37	0.00	3.06	76.95	0.00	19.26	0.36
140	0.00	0.01	0.10	0.05	3.49	76.66	0.00	19.27	0.41
0	0.00	1.36	0.21	21.06	65.14	10.08	0.13	0.22	1.79
1	0.01	1.33	0.36	19.90	61.78	14.63	0.04	0.19	1.76
2	0.00	1.10	0.38	21.09	65.66	9.91	0.04	0.00	1.81
3	0.00	0.64	1.36	17.28	64.84	14.08	0.01	0.00	1.79
4	0.00	0.05	5.51	5.20	59.12	28.70	0.00	0.04	1.38
5	0.00	0.02	5.85	3.00	58.40	31.26	0.00	0.00	1.46
6	0.00	0.00	5.87	2.66	58.13	32.00	0.00	0.00	1.34
7	0.00	0.00	5.15	2.18	48.98	42.32	0.00	0.11	1.25
8	0.00	0.02	4.70	1.96	42.81	49.22	0.00	0.14	1.15
9	0.00	0.00	1.86	0.84	14.69	81.91	0.00	0.00	0.70
10	0.00	0.01	2.46	1.08	19.77	75.86	0.01	0.00	0.82
11	0.00	0.00	5.71	2.65	57.74	32.55	0.00	0.05	1.31
12	0.00	0.03	5.69	2.66	58.33	31.83	0.00	0.07	1.39
13	0.00	0.00	5.64	2.75	58.26	31.83	0.03	0.18	1.31
14	0.03	0.01	5.50	2.64	58.60	31.65	0.00	0.15	1.43
15	0.02	0.03	5.80	2.39	58.31	32.17	0.00	0.13	1.17
16	0.01	0.00	5.69	2.48	58.41	32.05	0.00	0.04	1.33
17	0.01	0.00	5.97	2.29	58.26	32.01	0.01	0.15	1.31
18	0.01	0.02	5.76	2.46	57.71	32.35	0.00	0.29	1.40
19	0.00	0.00	5.83	2.26	57.28	32.97	0.00	0.37	1.30
20	0.00	0.03	4.69	1.44	42.39	47.29	0.05	3.13	0.97
21	0.00	0.00	0.41	0.05	11.68	85.77	0.00	1.66	0.43
22	0.01	0.00	0.21	0.00	1.80	87.41	0.01	10.22	0.35
23	0.00	0.00	0.26	0.04	2.98	76.93	0.01	19.48	0.31
24	0.00	0.00	0.36	0.01	3.07	76.94	0.00	19.26	0.36
25	0.00	0.00	0.19	0.00	3.07	76.75	0.00	19.61	0.39
0	0.00	1.24	0.22	21.21	65.85	9.45	0.06	0.13	1.85
1	0.00	1.38	0.33	21.05	65.65	9.62	0.09	0.12	1.76
2	0.01	1.25	0.71	20.67	65.04	10.16	0.11	0.11	1.95
3	0.01	0.75	0.66	21.69	63.63	11.07	0.10	0.29	1.81
4	0.03	0.97	0.70	21.23	63.50	11.48	0.09	0.18	1.83
5	0.00	1.16	0.33	21.05	65.70	9.24	0.11	0.59	1.83
6	0.00	1.13	0.77	18.17	67.87	2.00	0.07	8.25	1.74
7	0.00	1.13	0.89	17.86	68.20	0.21	0.10	9.89	1.72
8	0.01	1.16	0.38	20.56	66.39	8.64	0.10	0.96	1.81
9	0.00	1.07	0.76	17.71	68.56	0.18	0.09	9.92	1.71
10	0.00	1.14	0.87	17.90	68.20	0.08	0.10	10.03	1.68
0	0.00	1.24	1.00	18.41	67.23	0.09	0.09	10.06	1.89
5	0.01	1.03	16.33	15.89	56.99	0.07	0.09	8.16	1.45
10	0.01	1.27	1.01	18.55	66.72	0.21	0.10	10.27	1.87
15	0.00	1.50	0.42	21.26	65.02	9.66	0.13	0.21	1.81
20	0.08	1.40	0.29	21.34	64.20	10.47	0.11	0.22	1.88
25	0.01	1.48	0.23	21.80	65.14	9.47	0.06	0.07	1.75
30	0.00	1.50	0.21	20.98	65.38	9.89	0.13	0.14	1.76
35	0.00	1.48	0.23	21.10	64.64	10.51	0.10	0.18	1.77
40	0.01	1.50	0.21	21.22	65.52	9.53	0.07	0.22	1.73
45	0.00	1.48	0.26	21.21	65.04	9.96	0.06	0.19	1.81

50	0.00	1.44	0.26	20.70	65.19	10.34	0.08	0.18	1.82
55	0.00	1.39	0.19	21.00	63.56	11.67	0.11	0.21	1.86
60	0.00	1.41	0.28	20.53	64.44	11.17	0.10	0.22	1.85
65	0.00	1.44	0.23	21.05	64.78	10.44	0.11	0.17	1.78
70	0.00	1.39	0.39	20.81	62.99	12.26	0.11	0.24	1.81
75	0.00	1.43	0.22	20.48	64.88	10.89	0.14	0.20	1.76
80	0.00	1.45	0.21	20.48	64.88	10.88	0.07	0.32	1.72
85	0.00	1.51	0.20	20.69	65.35	10.04	0.11	0.25	1.86
90	0.00	1.47	0.37	20.69	64.92	10.52	0.10	0.23	1.69
95	0.00	1.52	0.29	20.38	65.33	10.08	0.12	0.36	1.93
100	0.00	1.51	0.20	20.41	64.56	11.15	0.08	0.31	1.78
105	0.03	0.00	4.05	3.55	43.75	47.10	0.05	0.16	1.31
110	0.00	0.00	5.62	3.05	58.87	31.20	0.00	0.03	1.23
115	0.01	0.03	5.59	2.68	58.88	31.46	0.00	0.16	1.20
120	0.00	0.03	5.68	2.55	58.38	31.97	0.00	0.15	1.25
125	0.00	0.00	5.25	2.36	56.85	34.04	0.00	0.14	1.37
130	0.01	0.00	0.39	2.27	3.67	74.35	0.00	18.89	0.42
135	0.00	0.00	0.26	0.08	3.43	76.50	0.05	19.38	0.30
140	0.00	0.01	0.23	0.06	3.58	76.95	0.00	18.84	0.33
0	0.00	0.99	0.21	18.05	57.98	21.02	0.05	0.02	1.68
1	0.00	0.01	5.69	3.20	57.65	31.90	0.00	0.14	1.42
2	0.00	0.00	5.61	2.93	58.98	30.97	0.03	0.07	1.41
3	0.01	0.00	5.76	3.01	58.44	31.25	0.02	0.12	1.39
4	0.04	0.00	5.67	3.08	58.29	31.45	0.00	0.05	1.43
5	0.02	0.03	5.76	2.96	58.36	31.40	0.00	0.09	1.38
6	0.01	0.00	6.00	2.89	58.42	31.19	0.00	0.09	1.40
7	0.00	0.03	5.70	2.82	58.95	31.09	0.00	0.12	1.29
8	0.00	0.00	5.78	2.68	58.64	31.41	0.00	0.20	1.29
9	0.00	0.00	5.70	2.80	58.41	31.75	0.00	0.05	1.29
10	0.00	0.00	5.93	2.70	58.48	31.41	0.00	0.06	1.41
11	0.01	0.00	5.92	2.52	58.49	31.71	0.03	0.08	1.25
12	0.00	0.01	5.65	2.67	58.62	31.82	0.00	0.02	1.23
13	0.00	0.01	5.79	2.68	58.41	31.56	0.01	0.08	1.45
14	0.00	0.00	5.66	2.57	58.56	31.95	0.02	0.01	1.23
15	0.00	0.02	5.60	2.49	57.16	33.16	0.03	0.14	1.42
16	0.00	0.03	5.33	2.41	57.54	33.39	0.00	0.10	1.20
17	0.01	0.00	5.49	2.40	58.60	32.16	0.01	0.13	1.20
18	0.00	0.00	4.76	1.89	48.74	43.35	0.02	0.10	1.15
19	0.00	0.01	3.16	1.45	33.95	60.38	0.00	0.17	0.89
20	0.00	0.00	5.15	2.38	55.91	35.06	0.00	0.21	1.30
21	0.00	0.00	5.80	2.49	58.36	31.84	0.00	0.20	1.31
22	0.00	0.02	5.36	2.36	58.78	31.92	0.00	0.22	1.34
23	0.00	0.00	4.73	1.71	46.25	42.25	0.00	3.95	1.12
24	0.01	0.00	0.27	0.07	5.10	75.83	0.00	18.31	0.43
25	0.00	0.06	0.29	0.00	3.70	76.53	0.02	19.00	0.40
26	0.01	0.00	0.34	0.00	3.63	76.77	0.00	18.89	0.37
27	0.00	0.00	0.27	0.01	3.58	76.70	0.01	19.08	0.35
28	0.04	0.00	0.31	0.00	3.37	76.70	0.05	19.19	0.35
29	0.00	0.02	0.27	0.02	3.56	76.49	0.00	19.06	0.58
30	0.02	0.00	0.18	0.00	3.55	76.93	0.01	18.97	0.35
0	0.00	1.32	1.14	17.86	67.26	0.18	0.12	10.29	1.84
1	0.00	1.26	1.06	18.56	66.88	0.11	0.11	10.20	1.83
2	0.00	1.33	0.98	18.35	67.08	0.23	0.09	10.10	1.83
3	0.00	1.28	0.93	17.81	67.55	0.24	0.04	10.17	1.99
4	0.00	1.30	0.91	18.22	66.97	0.82	0.12	9.87	1.80

5	0.00	1.34	0.74	19.28	65.79	5.93	0.09	5.02	1.81
6	0.00	1.37	0.35	20.76	66.01	9.45	0.11	0.16	1.79
7	0.02	1.36	0.24	21.02	65.79	9.48	0.06	0.21	1.82
8	0.01	1.48	1.63	20.20	65.22	9.25	0.09	0.43	1.70
9	0.00	1.36	2.04	20.45	64.34	9.27	0.08	0.65	1.81
10	0.00	1.41	0.30	21.22	65.15	9.79	0.12	0.14	1.87

D.14 SS-316/V/Nd After 56 Days at 550°C

The SS-316/V/Nd assembly annealed for 56 days at 550°C bonded on the V/Nd interface but not the SS-316/V interface. Compositional data (in at%) from WDS linescans across the V/Nd interface is given below.

Position	Zr	Mo	Si	Cr	Fe	Nd	V	Ni	Mn
0	0.01	0.01	0.18	0.02	0.49	96.93	1.92	0.04	0.40
1	0.02	0.00	0.17	0.21	5.85	87.30	5.77	0.00	0.69
2	0.04	0.00	0.12	0.55	32.58	50.85	15.12	0.00	0.75
3	0.02	0.03	0.33	0.89	50.35	19.73	28.07	0.01	0.57
4	0.00	0.01	0.38	1.43	42.35	2.88	52.61	0.04	0.31
5	0.01	0.00	0.26	1.92	10.61	1.80	85.28	0.03	0.09
6	0.00	0.00	0.32	2.09	1.37	0.78	95.42	0.02	0.00
7	0.00	0.00	0.27	2.06	0.53	3.10	94.02	0.00	0.02
8	0.01	0.00	1.12	1.73	1.04	20.94	74.86	0.18	0.11
9	0.00	0.00	0.11	2.14	0.25	0.78	96.61	0.07	0.04
10	0.00	0.01	0.14	2.31	0.72	1.52	95.27	0.01	0.03
11	0.00	0.03	0.12	2.31	1.29	4.32	91.52	0.41	0.01
12	0.00	0.00	0.10	2.22	0.16	1.97	95.54	0.00	0.02
13	0.00	0.01	0.14	2.18	0.04	0.20	97.44	0.00	0.00
14	0.00	0.01	0.08	2.21	0.03	0.21	97.46	0.00	0.00
15	0.02	0.03	6.47	1.95	0.27	0.42	90.82	0.02	0.00

D.15 SS-316/Zr/V/Nd After 56 Days at 550°C

The SS-316/Zr/V/Nd assembly annealed for 56 days at 550°C bonded on the SS-316/Zr, Zr/V and V/Nd interfaces. Compositional data (in at%) from WDS linescans across each of these interfaces is given below.

Position	Zr	Mo	Si	Cr	Fe	Nd	V	Ni	Mn
0	0.05	1.23	0.81	17.95	69.19	0.16	0.10	8.86	1.65
1	0.04	1.25	0.87	17.40	68.60	0.11	0.08	10.01	1.64
2	0.25	1.39	0.96	17.70	68.25	0.19	0.11	9.39	1.76
3	5.54	1.36	1.21	16.82	62.73	1.52	0.15	9.04	1.64
4	75.78	0.14	2.74	2.58	15.51	1.21	0.14	1.52	0.39
5	88.47	0.03	0.58	0.76	9.20	0.21	0.01	0.71	0.04
6	98.23	0.00	0.13	0.24	0.98	0.16	0.06	0.14	0.06
7	98.78	0.00	0.09	0.14	0.74	0.11	0.00	0.12	0.00
8	98.85	0.00	0.03	0.13	0.57	0.20	0.03	0.20	0.00
9	98.90	0.00	0.12	0.17	0.59	0.14	0.01	0.07	0.00
10	98.76	0.00	0.05	0.15	0.58	0.33	0.00	0.11	0.03
11	98.71	0.00	0.08	0.14	0.56	0.30	0.03	0.13	0.06
12	97.13	0.00	1.83	0.18	0.50	0.23	0.02	0.10	0.01
13	72.59	0.02	25.64	0.23	1.05	0.31	0.00	0.10	0.06

14	66.66	0.02	31.33	0.24	1.01	0.46	0.04	0.24	0.00
15	95.55	0.00	3.41	0.08	0.42	0.32	0.10	0.09	0.03
0	98.10	0.00	0.03	0.06	0.71	0.25	0.85	0.00	0.00
1	97.81	0.02	0.14	0.01	0.41	0.30	1.23	0.00	0.09
2	95.38	0.00	0.20	0.13	0.19	0.81	3.19	0.10	0.00
3	96.54	0.00	0.18	0.21	0.96	0.92	1.13	0.07	0.00
4	97.66	0.00	0.07	0.10	0.29	0.33	1.48	0.07	0.00
5	95.01	0.01	0.16	0.17	0.19	0.78	3.61	0.07	0.00
6	0.11	0.01	1.79	2.15	0.11	0.24	95.53	0.07	0.00
7	0.22	0.00	0.63	2.06	0.09	0.20	96.78	0.02	0.01
8	0.27	0.01	1.08	2.20	0.36	0.35	95.67	0.06	0.00
9	0.11	0.02	4.15	2.06	0.12	0.21	93.30	0.00	0.03
10	0.17	0.00	1.40	2.02	0.07	0.24	96.08	0.03	0.00
11	0.27	0.01	10.74	1.78	0.06	1.03	86.10	0.00	0.01
12	17.06	0.00	3.65	1.68	0.63	5.04	71.84	0.10	0.00
13	1.02	0.05	15.08	2.39	3.73	7.41	69.59	0.57	0.16
14	0.15	0.00	1.04	2.09	0.12	0.52	96.03	0.05	0.00
15	0.01	0.01	0.55	2.08	0.01	0.12	97.21	0.00	0.00
0	0.81	0.00	0.63	2.11	0.16	2.83	93.44	0.00	0.00
1	0.02	0.01	0.41	2.29	1.42	7.20	88.40	0.19	0.06
2	0.02	0.00	0.19	2.10	0.66	1.50	95.46	0.08	0.00
3	0.08	0.22	2.81	3.12	9.02	45.51	37.54	1.23	0.46
4	0.26	0.09	1.60	1.46	4.17	72.26	19.30	0.44	0.43
5	0.41	0.07	1.26	1.21	3.00	66.33	17.27	0.32	10.14
6	0.08	0.10	0.53	3.45	9.34	13.54	71.57	1.12	0.26
7	0.01	0.01	0.98	0.96	4.49	54.74	38.54	0.01	0.26
8	0.16	0.06	1.70	0.85	2.56	87.83	6.10	0.24	0.51
9	0.14	0.01	1.15	0.39	1.36	89.73	6.59	0.05	0.57
10	0.05	0.00	1.24	0.31	0.53	94.15	3.22	0.05	0.46
11	0.02	0.00	0.57	0.00	0.57	93.93	4.51	0.00	0.39
12	0.00	0.00	0.18	0.20	0.49	95.79	2.82	0.02	0.50
13	0.00	0.09	0.26	0.00	0.40	97.67	1.24	0.00	0.34
14	0.00	0.02	0.85	0.10	0.32	97.26	0.80	0.19	0.47
15	0.00	0.00	0.47	0.04	0.38	97.98	0.75	0.01	0.38

D.16 SS-316/Zr/Nd After 56 Days at 550°C

The SS-316/Zr/Nd assembly annealed for 56 days at 550°C bonded on the Zr/Nd interface but not the SS-316/Zr interface. Compositional data (in at%) from WDS linescans across the Zr/Nd interface is given below.

Position	Zr	Mo	Si	Cr	Fe	Nd	V	Ni	Mn
0	0.00	0.01	0.41	0.11	0.31	98.72	0.00	0.00	0.43
1	0.04	0.12	0.38	0.00	0.52	98.54	0.00	0.00	0.40
2	0.14	0.05	2.05	0.07	0.56	96.65	0.05	0.00	0.45
3	0.45	0.06	5.82	0.24	1.66	91.33	0.01	0.05	0.39
4	0.40	0.03	2.86	0.04	0.77	95.17	0.02	0.17	0.54
5	2.62	0.00	0.84	0.00	0.43	95.62	0.00	0.02	0.48
6	27.91	0.00	3.25	0.08	1.27	67.07	0.00	0.05	0.37
7	72.17	0.01	2.76	0.01	11.41	13.20	0.05	0.33	0.07
8	83.06	0.00	0.35	0.06	12.54	3.45	0.00	0.48	0.07
9	96.54	0.00	0.05	0.01	1.00	2.31	0.03	0.01	0.05

10	98.90	0.00	0.03	0.00	0.13	0.87	0.02	0.06	0.00
11	99.37	0.00	0.02	0.00	0.06	0.53	0.02	0.00	0.00
12	99.54	0.00	0.14	0.00	0.04	0.18	0.00	0.06	0.05
13	98.97	0.00	0.84	0.02	0.05	0.12	0.00	0.00	0.00
14	99.70	0.00	0.07	0.00	0.03	0.18	0.00	0.00	0.01
15	99.17	0.00	0.52	0.00	0.00	0.16	0.00	0.11	0.04

D.17 SS-316/Ti/V/Nd After 56 Days at 550°C

The SS-316/Ti/V/Nd assembly annealed for 56 days at 550°C bonded on the V/Nd interface but not the SS-316/Ti or Ti/V interfaces. Compositional data (in at%) from WDS linescans across the V/Nd interface is given below.

Position	Ta	Ti	Mo	Si	Fe	Nd	V	Cr	Ni	Mn
0	0.00	0.03	0.00	0.26	0.15	0.04	97.36	2.17	0.00	0.00
1	0.00	0.02	0.00	0.34	0.29	0.23	96.91	2.17	0.04	0.00
2	0.00	0.00	0.04	0.39	7.07	56.20	35.06	0.98	0.00	0.26
3	0.00	0.00	0.04	0.19	0.75	92.64	5.76	0.16	0.04	0.42
4	0.00	0.02	0.05	0.23	0.82	93.39	4.88	0.26	0.00	0.35
5	0.00	0.00	0.00	0.10	0.42	96.30	2.63	0.08	0.00	0.47
6	0.00	0.00	0.10	0.19	0.00	96.90	2.21	0.01	0.12	0.46
7	0.00	0.09	0.00	1.06	1.10	94.42	2.40	0.27	0.17	0.50
8	0.00	0.62	0.20	3.85	11.64	49.33	28.63	3.44	1.76	0.54
9	0.00	0.14	0.03	35.99	0.70	51.81	10.65	0.39	0.05	0.24
10	0.00	0.25	0.02	1.86	2.96	89.17	4.19	0.61	0.43	0.51
11	0.00	0.00	0.00	3.52	0.32	93.54	2.08	0.06	0.03	0.46
12	0.00	0.03	0.00	0.47	0.37	98.00	0.57	0.02	0.02	0.52
13	0.00	0.05	0.00	6.65	0.44	89.68	2.47	0.07	0.12	0.55
14	0.00	0.00	0.00	0.31	0.31	97.53	1.26	0.08	0.00	0.52
15	0.00	0.02	0.00	1.03	0.42	97.32	0.58	0.10	0.00	0.53

D.18 SS-316/Ti/Nd After 56 Days at 550°C

The SS-316/Ti/Nd assembly annealed for 56 days at 550°C bonded on the Ti/Nd interface but not the SS-316/Ti interface. Compositional data (in at%) from WDS linescans across the Ti/Nd interface is given below.

Position	Ta	Ti	Mo	Si	Fe	Nd	V	Cr	Ni	Mn
0	0.00	0.60	0.01	0.16	0.32	98.14	0.00	0.16	0.00	0.61
1	0.00	0.76	0.00	0.19	0.41	97.82	0.01	0.15	0.02	0.63
2	0.00	1.00	0.00	0.32	0.68	97.27	0.00	0.12	0.00	0.61
3	0.00	1.36	0.00	0.32	0.45	97.40	0.00	0.00	0.00	0.48
4	0.00	41.39	0.00	13.05	0.37	44.71	0.24	0.04	0.00	0.20
5	0.00	17.17	0.00	26.05	0.68	55.61	0.12	0.12	0.08	0.17
6	0.00	90.98	0.00	1.26	5.86	1.48	0.27	0.08	0.07	0.00
7	0.00	99.19	0.00	0.07	0.32	0.18	0.22	0.01	0.01	0.01
8	0.00	99.57	0.00	0.04	0.02	0.10	0.25	0.01	0.00	0.01
9	0.00	99.49	0.00	0.02	0.12	0.10	0.27	0.00	0.01	0.00
10	0.00	96.97	0.00	1.95	0.42	0.22	0.25	0.11	0.07	0.03
11	0.00	98.73	0.00	0.85	0.06	0.08	0.23	0.03	0.02	0.01
12	0.00	99.55	0.00	0.04	0.03	0.09	0.23	0.02	0.00	0.03
13	0.00	99.02	0.00	0.02	0.21	0.34	0.30	0.05	0.05	0.00

14	0.00	99.42	0.00	0.21	0.04	0.08	0.25	0.01	0.00	0.00
15	0.00	99.53	0.00	0.06	0.04	0.08	0.26	0.00	0.00	0.04
0	0.00	1.43	0.00	0.37	0.52	97.19	0.06	0.00	0.00	0.43
1	0.00	2.02	0.00	0.26	0.34	96.81	0.05	0.00	0.00	0.52
2	0.00	2.70	0.00	0.29	0.38	96.12	0.00	0.00	0.00	0.52
3	0.00	3.74	0.00	0.32	0.38	95.00	0.00	0.07	0.00	0.48
4	0.00	5.13	0.00	0.34	0.40	93.53	0.07	0.14	0.00	0.39
5	0.00	3.78	0.00	0.29	0.25	95.11	0.00	0.00	0.11	0.47
6	0.00	85.81	0.00	0.43	0.09	13.20	0.23	0.05	0.03	0.17
7	0.00	98.37	0.00	0.08	0.02	1.19	0.28	0.00	0.03	0.03
8	0.00	99.50	0.00	0.03	0.04	0.15	0.29	0.00	0.00	0.00
9	0.00	99.54	0.00	0.05	0.02	0.12	0.24	0.01	0.02	0.00
10	0.00	99.51	0.00	0.05	0.03	0.12	0.27	0.02	0.00	0.00
11	0.00	98.72	0.00	0.85	0.01	0.13	0.25	0.02	0.02	0.00
12	0.00	99.04	0.00	0.47	0.03	0.12	0.29	0.01	0.04	0.00
13	0.00	98.36	0.00	1.18	0.04	0.17	0.24	0.02	0.00	0.00
14	0.00	99.50	0.00	0.07	0.01	0.11	0.28	0.03	0.00	0.00
15	0.00	99.40	0.00	0.11	0.03	0.09	0.32	0.03	0.01	0.01

D.19 SS-316/Ta/V/Nd After 56 Days at 550°C

The SS-316/Ta/V/Nd assembly annealed for 56 days at 550°C bonded on the V/Nd interface but not the SS-316/Ta or Ta/V interfaces. Since the V/Nd interface at this time and temperature was already well characterized, no WDS linescans were completed on it in this assembly.

D.20 SS-316/Ta/Nd After 56 Days at 550°C

The SS-316/W/Nd assembly annealed for 56 days at 550°C did not bond on the SS-316/Ta or Ta/Nd interfaces.

D.21 SS-316/Mo/V/Nd After 56 Days at 550°C

The SS-316/Mo/V/Nd assembly annealed for 56 days at 550°C bonded on the V/Nd interface but not the SS-316/Mo or Mo/V interfaces. Compositional data (in at%) from WDS linescans across the V/Nd interface is given below.

Position	Si	V	W	Mo	Nd	Ni	Fe	Mn	Cr
0	0.34	97.43	0.00	0.01	0.04	0.00	0.01	0.00	2.17
1	0.13	97.33	0.00	0.06	0.19	0.02	0.11	0.05	2.11
2	0.10	97.55	0.00	0.06	0.17	0.00	0.08	0.00	2.05
3	2.35	95.16	0.00	0.02	0.21	0.02	0.20	0.00	2.05
4	1.14	88.52	0.01	0.02	4.39	0.07	3.84	0.06	1.98
5	0.26	30.65	0.02	0.03	62.76	0.06	5.15	0.36	0.71
6	0.45	9.38	0.00	0.01	87.71	0.12	1.59	0.46	0.28
7	0.33	4.11	0.00	0.02	94.39	0.02	0.70	0.39	0.04

8	0.31	2.98	0.03	0.00	95.41	0.00	0.61	0.43	0.23
9	1.56	2.14	0.00	0.02	95.23	0.00	0.46	0.42	0.18
10	1.38	2.62	0.00	0.00	95.07	0.07	0.57	0.28	0.02
11	0.34	2.97	0.00	0.03	95.36	0.05	0.70	0.49	0.06
12	0.22	2.99	0.03	0.02	95.45	0.13	0.61	0.45	0.11
13	0.08	2.15	0.00	0.00	96.75	0.01	0.47	0.53	0.00
14	0.12	0.59	0.02	0.03	98.33	0.07	0.39	0.44	0.00
15	0.25	0.43	0.01	0.00	98.47	0.00	0.41	0.42	0.00

D.22 SS-316/Mo/Nd After 56 Days at 550°C

The SS-316/Mo/Nd assembly annealed for 56 days at 550°C bonded on the Mo/Nd interface but not the SS-316/Mo interface. Compositional data (in at%) from WDS linescans across the Mo/Nd interface is given below.

Position	Si	V	W	Mo	Nd	Ni	Fe	Mn	Cr
0	0.47	0.09	0.00	0.05	98.16	0.17	0.63	0.38	0.05
1	0.38	0.02	0.01	0.19	97.60	0.12	0.99	0.43	0.26
2	0.55	0.07	0.00	0.18	97.29	0.08	1.10	0.62	0.12
3	0.52	0.09	0.00	0.40	97.40	0.12	0.83	0.42	0.22
4	0.60	0.15	0.00	12.51	85.31	0.07	0.81	0.46	0.10
5	0.41	0.06	0.00	75.07	23.57	0.09	0.50	0.13	0.15
6	0.15	0.07	0.00	97.48	1.81	0.07	0.26	0.00	0.16
7	0.14	0.00	0.01	98.67	0.82	0.10	0.14	0.07	0.07
8	0.10	0.08	0.00	98.14	1.41	0.04	0.18	0.00	0.06
9	0.37	0.00	0.00	97.13	1.95	0.02	0.27	0.09	0.16
10	0.40	0.04	0.00	97.23	1.96	0.00	0.28	0.00	0.10
11	0.05	0.06	0.01	99.48	0.21	0.00	0.12	0.06	0.01
12	0.04	0.02	0.03	99.47	0.28	0.00	0.10	0.06	0.00
13	0.10	0.00	0.00	99.47	0.24	0.00	0.07	0.04	0.07
14	0.13	0.00	0.00	98.98	0.40	0.04	0.20	0.10	0.15
15	0.08	0.03	0.02	99.53	0.21	0.00	0.08	0.04	0.01
0	0.33	0.02	0.02	0.10	97.88	0.10	0.78	0.57	0.21
1	0.22	0.00	0.00	0.06	98.13	0.12	0.74	0.66	0.08
2	0.04	0.03	0.01	0.08	98.58	0.11	0.61	0.54	0.00
3	0.30	0.08	0.01	0.09	98.57	0.01	0.52	0.42	0.00
4	0.34	0.05	0.02	0.16	98.05	0.10	0.64	0.55	0.08
5	0.32	0.02	0.00	0.16	98.25	0.04	0.66	0.49	0.07
6	0.36	0.06	0.00	0.57	97.50	0.06	0.92	0.54	0.00
7	0.89	0.00	0.03	12.01	85.70	0.22	0.74	0.31	0.11
8	0.32	0.00	0.02	81.86	17.44	0.00	0.27	0.06	0.04
9	0.10	0.00	0.00	98.92	0.86	0.01	0.06	0.00	0.06
10	0.09	0.00	0.01	99.13	0.47	0.00	0.19	0.05	0.07
11	0.06	0.00	0.01	99.28	0.33	0.03	0.16	0.00	0.14
12	0.18	0.03	0.00	98.39	0.83	0.00	0.46	0.00	0.11
13	0.36	0.02	0.02	99.29	0.07	0.01	0.13	0.05	0.04
14	0.07	0.07	0.03	99.59	0.13	0.00	0.06	0.07	0.01
15	0.03	0.00	0.00	99.65	0.22	0.00	0.09	0.01	0.00
0	0.21	0.00	0.00	0.05	98.34	0.11	0.68	0.43	0.18
1	0.43	0.13	0.00	0.04	98.32	0.00	0.45	0.49	0.15
2	0.25	0.00	0.01	0.10	98.35	0.12	0.61	0.46	0.10
3	0.62	0.05	0.00	0.21	96.36	0.22	1.47	0.81	0.28

4	0.55	0.00	0.03	0.25	97.47	0.12	0.97	0.61	0.00
5	0.75	0.00	0.05	10.43	87.45	0.00	0.67	0.53	0.12
6	1.06	0.01	0.00	61.38	36.71	0.03	0.51	0.20	0.11
7	0.76	0.02	0.02	95.25	3.62	0.00	0.30	0.00	0.05
8	1.05	0.00	0.02	97.04	1.68	0.00	0.10	0.02	0.08
9	2.98	0.08	0.01	95.01	1.82	0.00	0.07	0.00	0.03
10	8.55	0.08	0.01	90.07	1.15	0.00	0.07	0.03	0.05
11	6.68	0.04	0.00	91.86	1.23	0.00	0.11	0.00	0.08
12	3.35	0.04	0.02	94.76	1.36	0.00	0.38	0.00	0.09
13	0.49	0.00	0.00	98.51	0.66	0.04	0.23	0.00	0.08
14	0.43	0.02	0.00	98.48	0.69	0.03	0.21	0.01	0.12
15	0.62	0.01	0.00	97.96	0.49	0.07	0.68	0.00	0.18

D.23 SS-316/W/V/Nd After 56 Days at 550°C

The SS-316/W/V/Nd assembly annealed for 56 days at 550°C bonded on the SS-316/W, W/V, and W/Nd interfaces. Compositional data (in at%) from WDS linescans across the SS-316/W and W/V interfaces is given below.

Position	Si	V	W	Mo	Nd	Ni	Fe	Mn	Cr
0	47.86	0.05	0.18	0.71	0.07	4.48	35.45	0.91	10.30
1	5.00	0.07	0.18	1.21	0.21	8.63	65.20	1.73	17.76
2	6.05	0.11	0.18	1.21	0.24	8.53	64.47	1.66	17.56
3	3.34	0.09	0.16	1.24	0.11	8.94	66.37	1.68	18.08
4	5.27	0.09	0.13	1.23	0.03	9.08	65.55	1.49	17.13
5	1.68	0.08	0.69	1.15	0.09	10.15	67.69	1.53	16.94
6	1.50	0.14	2.24	0.99	0.12	10.66	68.11	1.24	15.00
7	1.87	0.09	11.14	0.89	0.11	10.02	62.10	0.78	13.00
8	3.02	0.04	63.70	0.26	0.14	3.30	24.58	0.21	4.75
9	0.93	0.02	93.53	0.00	0.00	0.70	3.75	0.11	0.95
10	7.05	0.07	90.01	0.00	0.03	0.23	2.16	0.00	0.45
11	13.67	0.00	83.94	0.00	0.05	0.26	1.62	0.04	0.43
12	4.12	0.13	93.71	0.00	0.17	0.23	1.41	0.00	0.24
13	0.08	0.00	98.61	0.00	0.03	0.09	0.93	0.13	0.12
14	0.77	0.18	97.53	0.00	0.17	0.09	1.11	0.00	0.15
15	6.28	0.00	92.70	0.00	0.11	0.18	0.42	0.00	0.31
0	0.53	2.66	93.59	0.00	1.77	0.30	0.83	0.00	0.32
1	2.58	7.36	86.00	0.00	1.95	0.28	1.37	0.00	0.46
2	1.63	6.62	85.82	0.00	3.52	0.30	1.40	0.16	0.56
3	1.13	5.92	83.00	0.00	6.47	0.00	2.64	0.08	0.76
4	0.84	8.17	47.81	0.14	31.24	1.12	8.06	0.34	2.29
5	1.31	8.84	28.84	0.25	45.81	1.26	10.26	0.57	2.86
6	1.31	11.89	46.75	0.25	21.47	1.85	12.64	0.38	3.46
7	1.15	13.39	71.13	0.00	6.48	0.86	5.30	0.17	1.53
8	0.97	21.71	65.14	0.00	6.60	0.55	3.63	0.03	1.38
9	1.88	20.90	64.05	0.00	5.87	0.69	4.67	0.18	1.75
10	1.16	27.18	57.50	0.06	5.61	0.80	5.44	0.17	2.09
11	0.70	33.08	51.93	0.09	6.09	0.77	5.14	0.07	2.14
12	0.81	49.82	30.92	0.10	8.78	0.88	5.83	0.18	2.68
13	1.55	82.86	4.86	0.09	4.22	0.47	3.19	0.07	2.70
14	1.50	93.17	0.26	0.05	1.67	0.11	0.97	0.00	2.28
15	1.26	70.25	13.21	0.14	6.84	0.51	4.78	0.20	2.82

D.24 SS-316/W/Nd After 56 Days at 550°C

The SS-316/W/Nd assembly annealed for 56 days at 550°C bonded on the W/Nd interface but not the SS-316/W interface. Compositional data (in at%) from WDS linescans across the W/Nd interface is given below.

Position	Si	V	W	Mo	Nd	Ni	Fe	Mn	Cr
0	0.42	0.00	1.12	0.05	96.27	0.16	1.19	0.60	0.20
1	0.39	0.02	1.19	0.00	95.74	0.00	1.63	0.65	0.39
2	0.33	0.12	1.18	0.01	96.07	0.11	1.37	0.61	0.20
3	0.37	0.00	0.94	0.04	96.24	0.05	1.54	0.47	0.34
4	0.83	0.06	1.58	0.05	93.77	0.24	2.30	0.59	0.58
5	2.00	0.15	2.46	0.10	91.29	0.20	2.55	0.67	0.59
6	5.29	0.01	3.67	0.11	86.97	0.33	2.62	0.57	0.43
7	13.52	0.10	23.86	0.00	58.80	0.15	2.52	0.47	0.59
8	6.02	0.00	51.57	0.05	39.59	0.23	1.84	0.29	0.43
9	3.13	0.00	80.62	0.00	14.93	0.05	0.77	0.19	0.32
10	2.56	0.00	90.89	0.00	5.71	0.29	0.27	0.16	0.13
11	0.80	0.00	97.15	0.00	1.69	0.07	0.14	0.06	0.10
12	0.00	0.05	99.17	0.00	0.62	0.00	0.07	0.00	0.09
13	0.30	0.22	99.00	0.00	0.33	0.00	0.14	0.00	0.02
14	0.16	0.01	99.37	0.00	0.12	0.18	0.17	0.00	0.00
15	0.00	0.21	99.10	0.00	0.20	0.00	0.35	0.12	0.02
0	0.40	0.03	0.93	0.00	97.04	0.09	0.80	0.59	0.12
1	0.30	0.00	0.34	0.02	97.54	0.05	1.04	0.51	0.22
2	3.48	0.06	1.80	0.11	93.13	0.00	0.81	0.58	0.04
3	4.60	0.00	3.17	0.03	90.72	0.00	0.88	0.44	0.16
4	2.88	0.12	51.77	0.00	44.24	0.04	0.59	0.25	0.11
5	1.15	0.00	78.05	0.00	20.24	0.15	0.31	0.03	0.06
6	0.26	0.00	92.73	0.00	6.60	0.00	0.19	0.21	0.01
7	0.04	0.00	98.39	0.00	0.94	0.00	0.31	0.04	0.29
8	0.00	0.02	98.94	0.00	0.73	0.17	0.10	0.03	0.01
9	0.00	0.13	99.23	0.00	0.39	0.08	0.00	0.00	0.17
10	0.10	0.00	98.08	0.00	0.98	0.16	0.47	0.00	0.21
11	0.04	0.12	99.15	0.00	0.53	0.07	0.05	0.00	0.06
12	0.00	0.00	99.75	0.00	0.19	0.00	0.01	0.04	0.00
13	0.00	0.04	99.37	0.00	0.25	0.18	0.02	0.03	0.11

D.25 SS-316/Nd After 28 Days at 625°C

The diffusion interface of the SS-316/Nd diffusion couple annealed for 28 days at 625°C broke apart upon removal from the furnace, rendering full analysis of the developed phases impossible. The remainder of the interface included two interaction zones. First, a zone matching $\text{Nd}_2(\text{Fe}+\text{Cr})_{17}$ by composition extended for $\sim 500 \mu\text{m}$. The second interaction zone matched $\text{Nd}_5(\text{Fe}+\text{Cr}+\text{Ni})_{17}$ by composition, but was only partially intact so its width was unmeasurable. Compositional data (in at%) from WDS linescans across the interface is given below.

Position	Zr	Mo	Si	Cr	Fe	Nd	V	Ni	Mn
0	0.04	1.30	0.24	14.98	47.73	21.35	0.06	13.12	1.19
1	0.00	1.25	0.36	14.95	47.33	21.40	0.10	13.44	1.18
2	0.00	1.16	0.27	14.71	47.42	21.57	0.03	13.54	1.32
3	0.00	1.21	0.29	14.50	47.37	21.59	0.12	13.70	1.22
4	0.04	1.21	0.32	14.22	47.15	21.80	0.12	13.88	1.26
5	0.04	1.32	0.37	16.19	54.06	25.63	0.04	0.93	1.41
6	0.00	1.23	0.31	14.49	46.96	21.90	0.03	13.84	1.24
7	0.00	1.20	0.36	14.22	47.58	21.68	0.10	13.67	1.20
8	0.02	1.18	0.36	14.52	47.57	21.55	0.07	13.55	1.19
9	0.00	1.10	0.39	14.43	47.01	22.05	0.04	13.75	1.23
10	0.00	1.18	0.41	15.01	47.44	21.14	0.12	13.42	1.27
11	0.00	1.18	0.60	15.51	50.16	19.59	0.07	11.65	1.24
12	0.00	1.20	0.50	16.50	52.77	17.71	0.10	9.83	1.39
13	0.00	1.30	0.49	17.49	55.08	16.11	0.05	8.20	1.29
14	0.00	1.21	0.27	18.31	58.05	14.51	0.04	6.23	1.40
15	0.02	1.23	0.18	20.49	64.99	9.89	0.11	1.54	1.57
16	0.00	1.35	0.18	20.46	65.02	9.81	0.07	1.53	1.59
17	0.00	1.32	0.16	21.21	66.27	8.92	0.09	0.44	1.59
18	0.00	1.33	0.16	20.99	66.18	9.02	0.12	0.52	1.68
19	0.00	1.31	0.16	20.20	65.32	10.31	0.09	0.99	1.62
20	0.00	1.21	0.18	20.34	64.39	10.95	0.03	1.32	1.60
21	0.00	0.94	0.20	20.43	64.99	10.55	0.08	1.13	1.69
22	0.04	0.76	0.17	21.30	66.82	8.73	0.07	0.36	1.76
23	0.00	0.63	0.18	21.58	67.41	8.29	0.00	0.08	1.83
24	0.00	0.61	0.13	21.44	67.72	8.23	0.04	0.05	1.77
25	0.00	0.59	0.13	21.53	67.59	8.37	0.00	0.04	1.75
26	0.01	0.59	0.15	21.84	67.32	8.31	0.05	0.05	1.68
27	0.01	0.59	0.14	21.78	67.45	8.20	0.05	0.03	1.76
28	0.01	0.54	0.19	21.39	67.53	8.47	0.02	0.07	1.78
29	0.03	0.54	0.22	21.00	67.77	8.55	0.04	0.08	1.77
30	0.00	0.64	0.22	20.95	64.86	11.51	0.03	0.10	1.69
0	0.00	1.23	0.34	16.83	54.12	17.39	0.08	8.61	1.40
1	0.00	1.22	0.34	16.61	54.04	17.62	0.07	8.71	1.39
2	0.02	1.25	0.33	16.62	54.07	17.59	0.05	8.72	1.36
3	0.00	1.22	0.32	16.36	54.21	17.68	0.12	8.73	1.35
4	0.00	1.16	0.45	16.33	53.17	18.32	0.10	9.10	1.36
5	0.02	1.22	0.53	15.89	52.18	19.18	0.10	9.51	1.37
6	0.00	1.26	0.43	15.82	51.96	19.05	0.06	10.09	1.33
7	0.01	1.29	0.34	15.79	51.67	18.95	0.07	10.56	1.33
8	0.00	1.19	0.36	15.89	51.52	18.96	0.04	10.76	1.29
9	0.00	1.20	0.30	15.73	50.93	19.23	0.07	11.30	1.26
10	0.01	1.16	0.28	16.13	52.71	18.38	0.00	10.01	1.30
11	0.01	1.17	0.27	16.81	54.59	17.00	0.09	8.72	1.35
12	0.02	1.15	0.25	17.87	56.65	15.39	0.07	7.16	1.44
13	0.00	1.18	0.25	18.58	59.06	13.78	0.10	5.51	1.54
14	0.00	1.20	0.22	19.26	61.29	12.33	0.05	4.14	1.51
15	0.00	1.20	0.14	20.23	64.39	10.31	0.05	2.16	1.53
16	0.01	1.16	0.11	21.61	63.69	9.91	0.10	1.91	1.49
17	0.01	1.24	0.21	21.36	66.72	8.53	0.10	0.25	1.58
18	0.00	1.14	0.21	21.43	66.73	8.52	0.10	0.20	1.68
19	0.01	1.14	0.20	21.00	66.80	8.76	0.11	0.35	1.63
20	0.01	0.96	0.17	21.56	66.54	8.78	0.05	0.23	1.69
21	0.02	0.76	0.23	21.44	66.95	8.58	0.03	0.22	1.77
22	0.00	0.72	0.16	21.70	66.99	8.51	0.03	0.10	1.79
23	0.00	0.64	0.14	21.52	67.28	8.51	0.00	0.11	1.81

24	0.00	0.74	0.16	21.40	67.51	8.31	0.02	0.10	1.77
25	0.00	0.68	0.18	21.45	67.46	8.47	0.00	0.09	1.68
26	0.02	0.65	0.22	21.23	66.91	8.86	0.03	0.31	1.77
27	0.00	0.55	0.23	21.33	66.55	9.16	0.04	0.40	1.74
28	0.00	0.53	0.86	20.89	67.07	8.68	0.05	0.23	1.70
29	0.00	0.46	2.17	20.81	66.56	8.22	0.04	0.11	1.63
30	0.00	0.47	3.62	20.52	65.09	8.43	0.09	0.12	1.67
0	0.00	1.24	0.30	16.46	53.14	18.03	0.08	9.35	1.41
1	0.01	1.32	0.33	16.41	53.43	17.78	0.07	9.28	1.38
2	0.01	1.29	0.35	16.46	53.09	18.00	0.07	9.34	1.38
3	0.00	1.28	0.31	16.21	53.12	18.03	0.12	9.66	1.28
4	0.00	1.30	0.39	16.36	53.35	17.80	0.12	9.25	1.43
5	0.00	1.36	0.35	16.62	53.41	17.91	0.11	8.88	1.36
6	0.00	1.31	0.37	16.41	53.38	17.95	0.05	9.16	1.38
7	0.00	1.29	0.30	15.99	52.70	18.36	0.11	9.88	1.37
8	0.00	1.29	0.39	16.09	52.13	18.51	0.09	10.06	1.44
9	0.03	1.29	0.36	16.03	52.17	18.51	0.08	10.14	1.40
10	0.00	1.22	0.33	17.03	53.61	17.46	0.05	8.85	1.45
11	0.02	1.25	0.20	18.46	59.95	13.37	0.15	5.07	1.54
12	0.00	1.27	0.19	19.72	63.05	11.23	0.08	2.84	1.61
13	0.00	1.26	0.17	20.76	65.97	9.15	0.03	0.98	1.67
14	0.00	1.24	0.16	21.32	65.95	9.08	0.05	0.69	1.52
15	0.00	1.28	0.16	21.18	66.10	8.94	0.04	0.62	1.67
16	0.00	1.31	0.13	20.74	66.70	8.90	0.07	0.50	1.64
17	0.00	1.30	0.19	21.00	66.50	8.87	0.05	0.51	1.59
18	0.00	1.31	0.18	21.05	66.10	9.14	0.14	0.48	1.62
19	0.02	1.32	0.19	21.02	66.41	8.85	0.15	0.51	1.54
20	0.01	1.28	0.24	21.02	66.13	9.13	0.08	0.43	1.70
21	0.02	1.15	0.21	21.09	65.06	9.72	0.09	1.08	1.59
22	0.01	1.28	0.23	21.01	65.13	9.70	0.09	0.96	1.60
23	0.00	0.82	0.21	21.41	66.73	8.72	0.10	0.28	1.74
24	0.00	0.70	0.14	21.78	67.12	8.28	0.03	0.14	1.80
25	0.00	0.70	0.16	21.11	67.77	8.41	0.01	0.13	1.71
26	0.00	0.77	0.13	21.58	67.46	8.22	0.00	0.11	1.72
27	0.00	0.74	0.12	21.06	67.73	8.46	0.05	0.14	1.70
28	0.00	0.70	0.15	21.32	67.71	8.33	0.05	0.10	1.65
29	0.02	0.72	0.18	21.24	67.86	8.13	0.05	0.15	1.64
30	0.00	0.62	0.16	21.12	67.84	8.43	0.00	0.12	1.71
0	0.00	1.13	16.53	15.98	57.34	0.06	0.06	7.51	1.39
20	0.00	1.16	1.00	18.45	68.68	0.05	0.09	8.96	1.61
40	0.00	1.08	5.59	16.66	65.97	0.02	0.07	9.02	1.59
60	0.00	1.08	1.17	17.96	68.38	0.05	0.09	9.64	1.63
80	0.00	1.11	0.86	18.12	68.40	0.08	0.07	9.59	1.78
100	0.00	1.41	0.28	21.42	65.83	9.09	0.08	0.30	1.60
120	0.02	1.33	0.31	21.19	65.98	9.13	0.11	0.43	1.52
140	0.00	1.29	0.29	20.99	65.15	9.77	0.11	0.82	1.57
160	0.03	1.35	0.44	20.82	64.12	10.66	0.08	0.91	1.59
180	0.01	1.15	17.64	17.30	53.87	8.12	0.08	0.44	1.41
200	0.02	1.40	0.27	20.65	65.12	9.98	0.12	0.84	1.61
220	0.00	1.40	0.32	20.24	64.58	10.86	0.10	0.89	1.60
240	0.00	1.35	0.30	20.71	64.21	10.60	0.12	1.15	1.56
260	0.00	1.36	0.27	20.50	64.73	10.25	0.07	1.11	1.72
280	0.00	1.43	2.56	20.07	62.40	10.72	0.09	1.25	1.49
300	0.00	1.45	0.33	20.41	64.55	10.46	0.12	1.02	1.65
320	0.00	1.47	0.25	20.43	63.58	11.27	0.08	1.41	1.50

340	0.00	1.46	0.40	20.11	64.09	11.01	0.07	1.28	1.58
360	0.00	1.22	12.59	17.86	55.45	9.86	0.07	1.60	1.34
380	0.00	1.44	0.75	20.47	64.14	10.55	0.10	1.10	1.47
400	0.00	1.47	0.79	19.63	62.07	12.56	0.09	1.80	1.59
420	0.00	1.39	0.30	19.66	62.05	12.44	0.11	2.49	1.57
440	0.00	1.41	0.30	19.66	61.67	12.67	0.09	2.76	1.44
460	0.00	1.39	0.23	20.27	64.33	10.84	0.06	1.26	1.62
480	0.00	1.43	0.26	19.68	62.69	12.63	0.09	1.62	1.59
500	0.02	1.39	0.29	19.35	63.00	12.34	0.10	1.89	1.62
520	0.00	1.34	0.29	19.03	60.73	12.96	0.08	4.09	1.48
540	0.00	1.40	0.43	18.49	59.04	16.08	0.08	2.96	1.53
560	0.00	1.29	0.33	17.01	55.44	16.62	0.12	7.73	1.46
580	0.00	1.28	0.33	16.74	53.20	17.62	0.09	9.38	1.37
600	0.00	0.81	0.15	20.89	67.99	8.39	0.05	0.11	1.62
0	0.00	1.23	0.84	18.02	68.68	0.05	0.10	9.42	1.67
1	0.00	1.23	0.87	18.68	68.39	0.09	0.08	8.97	1.69
2	0.00	1.33	0.89	18.69	68.60	0.10	0.09	8.74	1.55
3	0.00	1.36	0.88	19.00	68.52	0.08	0.08	8.41	1.68
4	0.00	1.02	1.05	21.77	72.14	0.42	0.08	2.14	1.40
5	0.01	2.03	0.41	33.37	59.14	2.67	0.15	0.39	1.84
6	0.00	1.43	0.41	21.38	66.69	7.72	0.10	0.47	1.81
7	0.00	1.51	0.35	21.18	66.64	8.18	0.10	0.48	1.56
8	0.00	1.45	0.25	21.28	66.59	8.40	0.10	0.36	1.58
9	0.00	1.72	0.29	21.52	66.21	8.27	0.10	0.33	1.56
10	0.03	1.56	0.29	21.95	65.91	8.36	0.10	0.27	1.53
11	0.00	1.13	0.27	21.94	66.65	8.05	0.10	0.27	1.58
12	0.01	1.34	0.28	22.67	65.71	8.06	0.13	0.29	1.52
13	0.00	1.37	0.28	21.94	66.06	8.28	0.11	0.36	1.59
14	0.00	1.52	0.25	21.67	66.06	8.56	0.12	0.25	1.58
15	0.00	1.46	0.29	21.20	66.52	8.43	0.08	0.36	1.66
16	0.00	1.26	0.30	21.71	66.38	8.43	0.11	0.25	1.55
17	0.00	1.48	0.32	20.96	66.82	8.35	0.08	0.39	1.62
18	0.00	1.43	0.27	21.29	66.56	8.51	0.09	0.29	1.55
19	0.00	1.31	0.28	21.14	66.72	8.62	0.09	0.33	1.51
20	0.00	1.24	0.33	21.57	66.51	8.33	0.09	0.32	1.61
0	0.00	1.15	0.87	17.29	68.53	0.04	0.09	10.23	1.80
1	0.00	1.15	2.94	17.24	66.85	0.06	0.09	9.96	1.73
2	0.00	1.12	1.06	17.51	68.17	0.06	0.12	10.18	1.78
3	0.01	1.04	3.94	16.90	66.64	0.13	0.09	9.55	1.70
4	0.00	0.90	1.49	19.01	70.91	0.27	0.07	5.84	1.51
5	0.00	0.66	0.67	22.01	72.57	0.79	0.09	1.78	1.45
6	0.00	0.65	0.17	22.56	72.67	2.13	0.11	0.44	1.27
7	0.00	1.82	0.56	19.02	69.27	6.93	0.09	0.73	1.59
8	0.00	1.94	0.39	19.02	66.89	9.23	0.12	0.61	1.80
9	0.00	1.81	0.33	19.45	66.56	9.63	0.08	0.42	1.73
10	0.00	1.59	0.28	19.92	65.83	10.49	0.07	0.21	1.61
11	0.00	1.53	0.25	20.56	66.72	8.92	0.09	0.26	1.67
12	0.00	1.54	0.25	20.86	66.56	8.80	0.07	0.34	1.57
13	0.00	1.48	0.25	20.37	64.84	11.08	0.07	0.28	1.63
14	0.01	1.51	0.27	20.95	65.41	9.85	0.07	0.37	1.56
15	0.00	1.49	0.30	20.98	65.92	9.44	0.04	0.28	1.54
16	0.00	1.27	0.29	20.99	65.12	10.37	0.10	0.30	1.57
17	0.00	1.37	0.28	21.00	66.20	9.21	0.10	0.26	1.58
18	0.00	1.34	0.36	20.32	62.39	13.62	0.11	0.32	1.56
19	0.00	1.29	0.25	21.15	65.61	9.74	0.08	0.30	1.58

20	0.00	1.34	0.37	20.49	62.40	13.48	0.07	0.23	1.62
0	0.00	0.79	0.11	20.64	66.84	9.32	0.03	0.72	1.54
1	0.01	0.90	0.20	21.17	67.53	8.30	0.04	0.23	1.63
2	0.01	0.69	0.14	21.11	67.36	8.74	0.04	0.18	1.74
3	0.01	0.80	0.19	21.10	67.62	8.41	0.05	0.16	1.66
4	0.00	0.74	0.17	21.26	66.03	9.97	0.06	0.14	1.64
5	0.01	0.71	0.19	21.31	67.46	8.27	0.05	0.23	1.78
6	0.00	0.76	0.18	21.09	67.07	8.89	0.05	0.35	1.61
7	0.00	0.77	0.21	21.46	67.29	8.29	0.09	0.20	1.69
8	0.00	0.89	0.19	21.10	66.26	9.18	0.11	0.64	1.63
9	0.00	1.34	0.25	20.70	65.80	9.47	0.08	0.73	1.64
10	0.00	1.48	0.26	21.13	66.64	8.36	0.10	0.34	1.70
11	0.00	1.30	0.14	21.45	66.65	8.53	0.11	0.24	1.58
12	0.00	1.29	0.17	20.66	66.31	9.15	0.11	0.69	1.63
13	0.01	1.11	0.28	17.00	53.09	17.51	0.09	9.48	1.44
14	0.00	1.23	0.27	16.53	53.44	17.73	0.08	9.31	1.40
15	0.00	1.07	0.29	15.73	50.28	19.55	0.09	11.66	1.34
16	0.02	0.96	0.32	14.51	45.94	22.50	0.05	14.55	1.14
17	0.02	0.99	1.38	14.10	46.06	21.90	0.09	14.25	1.22
18	0.01	1.02	0.57	15.28	49.25	20.31	0.08	12.27	1.23
19	0.00	1.06	0.35	15.26	48.94	20.20	0.07	12.72	1.40
20	0.02	1.14	0.41	16.50	53.27	17.88	0.06	9.32	1.41

D.26 SS-316/V/Nd After 28 Days at 625°C

The SS-316/V/Nd assembly annealed for 28 days at 625°C bonded on the SS-316/V and V/Nd interfaces. Compositional data (in at%) from WDS linescans across the both interfaces is given below.

Position	Zr	Mo	Si	Cr	Fe	Nd	V	Ni	Mn
0	0.00	0.00	0.57	0.03	0.65	97.29	0.96	0.07	0.42
1	0.00	0.02	0.40	0.05	1.01	96.63	1.39	0.00	0.51
2	0.02	0.00	0.49	0.02	0.98	95.97	1.99	0.04	0.50
3	0.00	0.00	0.36	0.18	1.39	95.11	2.26	0.09	0.62
4	0.00	0.00	0.52	0.00	1.86	94.10	2.98	0.07	0.47
5	0.00	0.09	0.53	0.61	12.76	79.56	5.98	0.00	0.47
6	0.02	0.00	0.41	1.40	69.85	10.27	17.67	0.06	0.33
7	0.00	0.00	0.15	1.56	59.09	5.36	32.94	0.17	0.74
8	0.00	0.02	0.10	1.30	56.81	1.08	40.12	0.04	0.54
9	0.01	0.01	0.07	1.34	42.22	0.34	55.76	0.00	0.27
10	0.01	0.00	0.32	1.89	5.26	0.34	92.12	0.08	0.01
11	0.01	0.00	0.51	1.99	0.24	0.26	96.98	0.00	0.01
12	0.01	0.00	0.08	1.96	0.19	0.20	97.52	0.04	0.00
13	0.01	0.00	0.11	2.03	0.15	0.30	97.36	0.03	0.01
14	0.00	0.01	0.35	1.95	0.11	0.17	97.42	0.00	0.00
15	0.00	0.01	0.20	2.05	0.14	0.20	97.40	0.01	0.00
0	0.00	0.00	1.66	1.92	0.13	0.01	96.22	0.06	0.01
1	0.00	0.01	0.82	2.00	0.26	0.00	96.87	0.04	0.00
2	0.01	0.00	1.14	2.00	0.30	0.02	96.46	0.08	0.00
3	0.00	0.01	5.23	2.03	0.50	0.00	92.15	0.09	0.00
4	0.00	0.03	3.47	2.11	7.45	0.03	83.58	3.18	0.16
5	0.00	0.01	0.76	3.64	23.18	0.26	63.05	8.58	0.51

6	0.00	0.24	1.14	7.87	30.89	6.77	45.94	6.04	1.13
7	0.00	2.32	1.35	19.42	38.45	18.92	14.41	3.92	1.21
8	0.00	3.73	1.13	29.14	55.85	2.33	2.73	3.47	1.62
9	0.00	2.06	0.73	21.87	65.60	0.40	1.92	5.68	1.75
10	0.01	0.86	0.68	15.51	71.18	0.07	1.27	8.71	1.71
11	0.00	1.08	0.73	16.52	69.79	0.03	1.14	9.10	1.63
12	0.01	0.80	1.28	15.58	69.71	0.05	0.98	9.92	1.68
13	0.01	0.63	1.15	15.35	70.31	0.03	0.83	9.99	1.71
14	0.00	0.86	0.79	15.62	70.19	0.00	0.63	10.25	1.67
15	0.00	1.10	0.74	17.59	68.60	0.05	0.44	9.72	1.76

D.27 SS-316/Zr/V/Nd After 28 Days at 625°C

The SS-316/Zr/V/Nd assembly annealed for 28 days at 625°C bonded on the V/Nd interface but not the SS-316/Zr or Zr/V interfaces. Since the V/Nd interface at this time and temperature was already well characterized, no WDS linescans were completed on it in this assembly.

D.28 SS-316/Zr/Nd After 28 Days at 625°C

The SS-316/Zr/Nd assembly annealed for 28 days at 625°C bonded on the Zr/Nd interface but not the SS-316/Zr interface. Compositional data (in at%) from WDS linescans across the Zr/Nd interface is given below.

Position	Zr	Mo	Si	Cr	Fe	Nd	V	Ni	Mn
0	99.68	0.00	0.05	0.03	0.00	0.18	0.00	0.06	0.00
1	99.68	0.00	0.08	0.00	0.01	0.22	0.02	0.00	0.00
2	99.56	0.00	0.10	0.06	0.02	0.22	0.05	0.00	0.00
3	97.30	0.00	0.15	0.32	1.55	0.37	0.03	0.24	0.06
4	98.91	0.00	0.16	0.00	0.46	0.43	0.05	0.00	0.00
5	97.38	0.00	0.16	0.06	1.05	1.25	0.05	0.04	0.00
6	73.91	0.02	0.48	0.04	0.95	24.25	0.09	0.14	0.12
7	19.59	0.01	0.50	0.00	0.92	78.47	0.02	0.20	0.29
8	0.36	0.02	0.18	0.10	0.42	98.35	0.00	0.04	0.54
9	0.24	0.00	0.43	0.00	0.24	98.53	0.00	0.06	0.51
10	0.23	0.02	0.10	0.00	0.36	98.71	0.05	0.00	0.54
11	0.00	0.04	0.08	0.00	0.40	99.00	0.01	0.06	0.41
12	0.06	0.00	0.17	0.02	0.38	98.80	0.00	0.00	0.57
13	0.02	0.00	0.11	0.01	0.31	99.07	0.00	0.02	0.47
14	0.00	0.01	0.19	0.03	0.43	98.86	0.07	0.00	0.43
15	0.01	0.01	0.08	0.04	0.32	99.04	0.00	0.00	0.50
0	99.68	0.00	0.02	0.00	0.01	0.22	0.01	0.05	0.02
1	99.45	0.01	0.18	0.04	0.00	0.25	0.01	0.06	0.00
2	99.18	0.00	0.30	0.06	0.03	0.41	0.00	0.00	0.02
3	98.50	0.00	0.40	0.00	0.46	0.62	0.00	0.01	0.00
4	98.90	0.00	0.25	0.00	0.33	0.38	0.00	0.05	0.10
5	80.97	0.03	0.46	0.21	1.40	16.54	0.02	0.18	0.18
6	10.29	0.01	0.77	0.17	0.71	87.49	0.03	0.17	0.36
7	0.61	0.00	0.36	0.06	0.40	98.01	0.00	0.00	0.56

8	0.23	0.02	0.51	0.00	0.53	98.07	0.00	0.00	0.64
9	0.11	0.03	0.27	0.00	0.42	98.72	0.00	0.00	0.45
10	0.08	0.00	0.20	0.08	0.29	98.72	0.02	0.07	0.55
11	0.03	0.00	0.31	0.02	0.40	98.72	0.00	0.06	0.45
12	0.14	0.00	0.45	0.00	0.34	98.53	0.03	0.00	0.51
13	0.28	0.00	0.70	0.00	0.45	97.80	0.00	0.00	0.77
14	0.13	0.00	0.86	0.00	0.48	97.93	0.04	0.14	0.41
15	0.08	0.02	0.49	0.00	0.31	98.48	0.02	0.05	0.55
0	0.02	0.06	0.24	0.00	0.43	98.78	0.00	0.00	0.47
1	0.17	0.06	0.34	0.00	0.26	98.59	0.00	0.00	0.58
2	0.11	0.00	0.17	0.06	0.43	98.74	0.00	0.02	0.47
3	4.39	0.00	1.51	0.28	1.74	91.54	0.04	0.12	0.38
4	84.22	0.01	3.40	0.00	0.86	11.35	0.00	0.11	0.05
5	86.91	0.00	0.46	0.10	11.21	0.46	0.00	0.72	0.16
6	99.11	0.00	0.12	0.01	0.17	0.57	0.00	0.00	0.03
7	98.67	0.00	0.10	0.04	0.09	0.92	0.08	0.05	0.07
8	99.31	0.00	0.11	0.04	0.02	0.45	0.01	0.02	0.04
9	99.50	0.00	0.05	0.01	0.02	0.31	0.02	0.04	0.05
10	99.53	0.00	0.18	0.00	0.02	0.20	0.03	0.05	0.00
11	99.41	0.02	0.13	0.06	0.02	0.30	0.02	0.05	0.00
12	99.69	0.00	0.08	0.00	0.03	0.18	0.03	0.00	0.00
13	99.66	0.00	0.21	0.00	0.00	0.11	0.00	0.00	0.02
14	99.63	0.00	0.00	0.02	0.05	0.24	0.04	0.00	0.02
15	99.45	0.00	0.03	0.04	0.16	0.32	0.00	0.00	0.01

D.29 SS-316/Ti/V/Nd After 28 Days at 625°C

The SS-316/Ti/V/Nd assembly annealed for 28 days at 625°C bonded on the Ti/V and V/Nd interfaces but not the SS-316/Ti interface. Compositional data (in at%) from WDS linescans across the Ti/V interface is given below.

Position	Ta	Ti	Mo	Si	Fe	Nd	V	Cr	Ni	Mn
0	0.00	98.81	0.00	0.27	0.27	0.14	0.39	0.08	0.03	0.01
1	0.00	93.63	0.00	1.95	2.57	0.26	0.35	0.70	0.44	0.10
2	0.00	91.95	0.00	3.19	3.00	0.17	0.43	0.83	0.37	0.06
3	0.00	92.65	0.00	4.07	1.62	0.37	0.52	0.43	0.27	0.06
4	0.00	92.94	0.00	3.26	1.97	0.41	0.60	0.50	0.26	0.05
5	0.00	94.96	0.00	3.27	0.74	0.19	0.49	0.20	0.12	0.03
6	0.00	96.91	0.00	1.38	0.46	0.48	0.55	0.14	0.07	0.02
7	0.00	95.62	0.00	1.69	0.11	1.97	0.58	0.01	0.00	0.02
8	0.00	88.51	0.00	9.75	0.47	0.43	0.62	0.14	0.06	0.03
9	0.00	91.75	0.01	1.28	3.60	0.89	0.87	1.01	0.50	0.09
10	0.00	67.43	0.27	1.79	19.06	0.53	3.10	4.77	2.61	0.44
11	0.00	48.91	0.01	8.99	1.98	0.88	37.53	1.35	0.29	0.06
12	0.00	23.43	0.00	1.10	0.20	0.05	73.52	1.67	0.01	0.03
13	0.00	2.02	0.00	0.22	0.05	0.04	95.54	2.12	0.00	0.01
14	0.00	0.90	0.00	0.11	0.01	0.07	96.78	2.13	0.00	0.00
15	0.00	2.45	0.00	2.94	0.09	0.35	92.18	1.99	0.00	0.00
16	0.00	5.23	0.01	13.89	0.16	0.26	78.77	1.66	0.03	0.01
17	0.00	4.61	0.00	17.87	0.51	0.29	74.86	1.81	0.02	0.03
18	0.00	4.49	0.01	2.68	0.31	0.16	90.27	2.02	0.07	0.00
19	0.00	0.82	0.04	0.98	3.23	0.29	91.24	2.83	0.45	0.12
20	0.00	0.60	0.09	0.75	6.95	0.34	86.64	3.41	1.07	0.16

0	0.00	73.33	0.00	20.39	1.77	0.58	3.19	0.45	0.23	0.07
1	0.00	67.36	0.04	22.88	5.59	0.60	2.44	0.87	0.17	0.06
2	0.00	90.79	0.00	3.84	3.29	0.42	0.86	0.60	0.17	0.03
3	0.00	97.59	0.00	1.11	0.20	0.38	0.59	0.08	0.05	0.00
4	0.00	97.79	0.00	0.80	0.44	0.19	0.62	0.09	0.05	0.02
5	0.00	82.38	0.00	16.24	0.35	0.16	0.68	0.11	0.08	0.01
6	0.00	83.60	0.00	12.03	2.07	0.43	0.98	0.49	0.31	0.07
7	0.00	97.28	0.00	1.07	0.09	0.14	1.30	0.06	0.00	0.06
8	0.00	88.83	0.00	1.19	0.03	0.32	9.39	0.19	0.04	0.00
9	0.00	29.22	0.00	2.10	0.16	0.14	66.81	1.55	0.00	0.02
10	0.00	1.43	0.02	0.75	0.03	0.10	95.52	2.13	0.03	0.00
11	0.00	0.71	0.01	1.87	0.03	0.09	95.22	2.07	0.00	0.00
12	0.00	0.63	0.00	3.15	0.04	0.45	93.61	2.13	0.00	0.00
13	0.00	0.48	0.01	0.75	0.10	0.21	96.26	2.14	0.05	0.01
14	0.00	0.47	0.00	0.68	0.09	0.16	96.36	2.21	0.03	0.00
15	0.00	0.38	0.00	0.34	0.04	0.11	97.03	2.07	0.04	0.00
16	0.00	0.37	0.00	0.68	0.06	0.13	96.51	2.26	0.00	0.00
17	0.00	0.52	0.01	1.03	0.23	0.19	95.94	2.08	0.00	0.00
18	0.00	0.64	0.00	0.16	0.71	0.23	95.99	2.23	0.04	0.01
19	0.00	0.37	0.01	0.63	0.06	0.14	96.67	2.13	0.00	0.00
20	0.00	1.72	0.00	0.30	0.10	0.14	95.67	2.05	0.02	0.00

D.30 SS-316/Ti/Nd After 28 Days at 625°C

The SS-316/Ti/Nd assembly annealed for 28 days at 625°C bonded on the Ti/Nd interface but not the SS-316/Ti interface. Compositional data (in at%) from WDS linescans across the Ti/Nd interface is given below.

Position	Ta	Ti	Mo	Si	Fe	Nd	V	Cr	Ni	Mn
0	0.00	4.87	0.07	4.21	2.66	86.42	0.05	0.69	0.55	0.48
1	0.00	11.40	0.07	8.72	1.23	77.81	0.09	0.23	0.05	0.41
2	0.00	39.62	0.00	1.13	0.80	57.84	0.19	0.06	0.05	0.30
3	0.00	69.76	0.02	2.92	3.64	22.77	0.26	0.28	0.20	0.16
4	0.00	87.59	0.00	1.03	2.61	8.22	0.31	0.10	0.06	0.08
5	0.00	96.05	0.00	0.20	0.69	2.74	0.27	0.00	0.03	0.01
6	0.00	99.22	0.00	0.09	0.02	0.39	0.26	0.00	0.01	0.00
7	0.00	98.81	0.00	0.11	0.10	0.69	0.23	0.05	0.00	0.01
8	0.00	98.82	0.00	0.09	0.05	0.64	0.38	0.02	0.00	0.00
9	0.00	99.10	0.00	0.08	0.03	0.55	0.23	0.01	0.00	0.00
10	0.00	99.08	0.00	0.06	0.03	0.50	0.29	0.00	0.03	0.02
11	0.00	97.45	0.00	1.53	0.26	0.51	0.22	0.03	0.00	0.01
12	0.00	80.58	0.00	17.47	0.48	1.24	0.19	0.01	0.00	0.04
13	0.00	91.62	0.00	5.71	0.37	2.01	0.24	0.04	0.01	0.00
14	0.00	94.54	0.00	3.00	0.09	2.06	0.27	0.00	0.04	0.00
15	0.00	98.42	0.00	0.47	0.04	0.78	0.26	0.03	0.00	0.01
0	0.00	2.35	0.00	7.76	0.39	88.94	0.00	0.00	0.00	0.56
1	0.00	2.42	0.03	8.17	0.35	88.59	0.00	0.04	0.00	0.39
2	0.00	2.20	0.04	5.23	0.27	91.85	0.00	0.06	0.02	0.34
3	0.00	2.30	0.00	7.74	0.45	88.91	0.07	0.03	0.00	0.50
4	0.00	3.20	0.04	4.99	2.38	88.27	0.04	0.37	0.19	0.52
5	0.00	6.10	0.12	10.80	22.11	57.19	0.00	2.64	0.72	0.32
6	0.00	32.95	0.02	14.53	3.36	48.02	0.07	0.60	0.19	0.26

7	0.00	59.86	0.03	11.23	5.33	22.05	0.17	0.81	0.33	0.20
8	0.00	88.05	0.00	8.77	0.59	2.08	0.21	0.18	0.08	0.03
9	0.00	97.21	0.00	1.24	0.08	1.06	0.29	0.03	0.05	0.05
10	0.00	97.73	0.00	0.14	0.08	1.76	0.26	0.00	0.03	0.00
11	0.00	97.86	0.00	0.13	0.11	1.59	0.26	0.02	0.00	0.02
12	0.00	98.96	0.00	0.08	0.04	0.66	0.21	0.00	0.00	0.06
13	0.00	97.57	0.00	0.15	0.09	1.84	0.26	0.04	0.02	0.04
14	0.00	88.10	0.00	2.49	0.32	8.71	0.26	0.02	0.01	0.09
15	0.00	98.09	0.00	0.72	0.05	0.88	0.22	0.03	0.00	0.01

D.31 SS-316/Ta/V/Nd After 28 Days at 625°C

The SS-316/Ta/V/Nd assembly annealed for 28 days at 625°C bonded on the V/Nd interface but not the SS-316/Ta or Ta/V interfaces. Since the V/Nd interface at this time and temperature was already well characterized, no WDS linescans were completed on it in this assembly.

D.32 SS-316/Ta/Nd After 28 Days at 625°C

The SS-316/Ta/Nd assembly annealed for 28 days at 625°C did not bond on the SS-316/Ta or Ta/Nd interfaces.

D.33 SS-316/Mo/V/Nd After 28 Days at 625°C

The SS-316/Mo/V/Nd assembly annealed for 28 days at 625°C bonded on the SS-316/Mo and Mo/Nd interfaces but not the Mo/V interface. Compositional data (in at%) from WDS linescans across the SS-316/Mo interface is given below.

Position	Si	V	W	Mo	Nd	Ni	Fe	Mn	Cr
1	2.12	0.13	0.03	2.00	0.36	9.13	65.26	1.80	19.19
2	1.68	0.16	0.04	2.16	0.27	8.84	64.51	1.72	20.63
3	2.55	0.13	0.02	2.17	0.35	9.36	65.57	1.74	18.12
4	2.32	0.12	0.00	68.70	0.48	2.86	20.26	0.49	4.77
5	4.71	0.12	0.01	31.55	0.69	6.50	43.59	1.19	11.67
6	1.30	0.05	0.00	80.02	0.41	1.83	12.88	0.33	3.18
7	0.25	0.03	0.00	97.70	0.13	0.18	1.29	0.03	0.39
8	0.39	0.01	0.02	98.39	0.10	0.06	0.80	0.02	0.21
9	0.68	0.01	0.01	98.59	0.02	0.02	0.50	0.01	0.17
10	0.67	0.00	0.02	98.81	0.00	0.07	0.35	0.00	0.08
11	0.11	0.10	0.01	99.27	0.05	0.10	0.32	0.00	0.04
12	0.17	0.13	0.00	99.20	0.06	0.00	0.29	0.04	0.10
13	0.08	0.02	0.03	99.33	0.10	0.03	0.26	0.02	0.13
14	0.06	0.03	0.02	99.50	0.05	0.03	0.22	0.00	0.08
15	0.07	0.00	0.00	99.50	0.05	0.07	0.27	0.00	0.04

D.34 SS-316/Mo/Nd After 28 Days at 625°C

The SS-316/Mo/Nd assembly annealed for 28 days at 625°C bonded on the Mo/Nd interface but not the SS-316/Mo interface. Compositional data (in at%) from WDS linescans across the Mo/Nd interface is given below.

Position	Si	V	W	Mo	Nd	Ni	Fe	Mn	Cr
0	0.16	0.10	0.03	0.00	98.95	0.00	0.29	0.43	0.05
1	0.32	0.03	0.00	0.05	98.70	0.00	0.31	0.59	0.00
2	0.41	0.06	0.04	0.09	98.53	0.00	0.44	0.45	0.00
3	0.31	0.00	0.06	0.08	98.67	0.05	0.36	0.46	0.02
4	0.31	0.00	0.01	0.14	98.53	0.00	0.48	0.54	0.00
5	0.32	0.07	0.00	0.23	98.21	0.10	0.50	0.42	0.15
6	0.51	0.00	0.00	0.25	97.62	0.00	0.86	0.60	0.16
7	0.35	0.02	0.01	15.03	83.53	0.00	0.53	0.46	0.09
8	0.53	0.00	0.00	92.92	6.29	0.00	0.17	0.09	0.00
9	0.30	0.07	0.00	98.58	0.80	0.00	0.14	0.06	0.05
10	0.17	0.01	0.00	99.42	0.34	0.04	0.02	0.00	0.00
11	0.11	0.04	0.03	99.43	0.24	0.00	0.05	0.04	0.06
12	0.09	0.00	0.01	99.50	0.28	0.07	0.01	0.03	0.01
13	0.63	0.00	0.03	99.04	0.11	0.10	0.08	0.00	0.02
14	13.52	0.00	0.02	86.10	0.17	0.00	0.12	0.04	0.03
15	0.98	0.04	0.01	98.78	0.11	0.01	0.02	0.05	0.02

D.35 SS-316/W/V/Nd After 28 Days at 625°C

The SS-316/W/Nd assembly annealed for 28 days at 625°C bonded on the SS-316/W and V/Nd interfaces but not the W/V interface. Compositional data (in at%) from WDS linescans across the SS-316/W interface is given below.

Position	Si	V	W	Mo	Nd	Ni	Fe	Mn	Cr
3	1.07	0.36	0.02	1.23	11.67	8.28	60.25	1.63	15.49
4	1.04	0.29	0.14	1.23	9.87	8.45	61.71	1.68	15.60
5	0.65	1.23	30.71	0.60	26.17	3.61	28.41	0.92	7.69
6	4.37	0.03	89.42	0.00	1.60	0.55	3.28	0.03	0.73
7	2.93	0.08	92.77	0.00	0.74	0.30	2.47	0.00	0.71
8	0.04	0.01	97.64	0.00	0.10	0.24	1.38	0.24	0.35
9	0.04	0.03	98.07	0.00	0.06	0.25	1.14	0.12	0.29
10	0.00	0.00	98.47	0.00	0.04	0.18	1.07	0.00	0.24
11	0.10	0.00	98.67	0.00	0.08	0.09	0.74	0.12	0.19
12	0.00	0.00	99.03	0.00	0.02	0.03	0.71	0.05	0.16
13	0.00	0.00	98.96	0.00	0.04	0.17	0.64	0.08	0.11
14	0.00	0.04	98.96	0.00	0.02	0.07	0.75	0.00	0.16
15	0.07	0.13	98.74	0.00	0.14	0.08	0.60	0.07	0.17

D.36 SS-316/W/Nd After 28 Days at 625°C

The SS-316/W/Nd assembly annealed for 28 days at 625°C did not bond on the SS-316/W or W/Nd interfaces.

D.37 SS-316/Nd After 28 Days at 700°C

The diffusion interface of the SS-316/Nd diffusion couple annealed for 28 days at 700°C also broke apart upon removal from the furnace. The remaining interface contained a region that was approximately ~780 μm in width and was predominantly Nd₂(Fe+Cr)₁₇ by composition with some precipitates of Nd₅(Fe+Cr+Ni)₁₇. Compositional data (in at%) from WDS linescans across the interface is given below.

Position	Zr	Mo	Si	Cr	Fe	Nd	V	Ni	Mn
0	0.01	1.08	0.18	21.45	64.15	9.76	0.40	1.41	1.57
20	0.00	2.51	0.17	21.60	65.84	7.80	0.19	0.41	1.49
40	0.00	1.58	2.20	21.28	65.02	7.92	0.16	0.39	1.46
60	0.00	0.62	1.47	8.65	25.09	47.50	0.11	15.58	0.99
80	0.00	1.22	0.07	23.85	65.40	7.79	0.19	0.12	1.37
100	0.01	1.40	0.31	23.33	65.34	7.78	0.14	0.27	1.44
120	0.00	1.76	2.24	22.61	63.84	7.52	0.12	0.43	1.48
140	0.02	1.54	0.30	23.01	64.90	8.41	0.15	0.20	1.47
160	0.00	1.61	2.27	22.48	63.64	8.31	0.12	0.22	1.35
180	0.00	1.64	0.38	22.76	65.14	8.16	0.11	0.28	1.53
200	0.01	1.59	0.63	20.85	65.70	8.59	0.10	1.13	1.40
220	0.02	1.96	0.43	23.39	64.40	8.06	0.17	0.17	1.40
240	0.00	1.60	0.26	23.31	65.31	7.84	0.11	0.04	1.52
260	0.00	1.41	7.69	20.96	60.24	7.71	0.10	0.43	1.46
280	0.00	1.67	0.34	23.58	64.41	8.32	0.09	0.11	1.49
300	0.01	1.56	6.46	22.01	60.63	7.44	0.06	0.35	1.48
320	0.00	1.78	4.11	20.65	62.97	8.26	0.10	0.73	1.40
340	0.00	1.40	0.34	23.61	65.20	7.74	0.09	0.08	1.54
360	0.06	0.99	0.88	15.39	50.98	22.53	0.06	7.79	1.34
380	0.00	1.32	0.37	25.12	50.39	12.85	0.05	8.50	1.39
400	0.00	1.42	12.30	18.78	57.64	7.68	0.07	0.74	1.38
420	0.00	1.85	0.34	23.49	64.44	7.57	0.13	0.67	1.52
440	0.00	1.49	0.52	19.75	66.93	8.59	0.07	1.06	1.58
460	0.00	1.26	4.05	14.37	46.90	18.97	0.06	13.22	1.17
480	0.00	0.52	2.76	5.58	16.97	66.61	0.05	6.65	0.86
500	0.00	0.95	16.72	10.93	35.72	19.96	0.03	14.74	0.95
520	0.01	0.98	12.34	11.37	38.57	21.19	0.05	14.43	1.06
540	0.01	1.35	1.74	14.64	50.39	25.70	0.10	4.73	1.35
560	0.03	1.86	0.22	35.46	54.55	4.94	0.14	1.31	1.50
580	0.00	1.66	0.60	17.26	59.20	14.39	0.09	5.21	1.60
600	0.00	1.56	0.95	17.97	60.38	13.30	0.11	4.23	1.50
620	0.00	1.66	4.43	18.38	60.78	12.40	0.12	0.59	1.65
640	0.00	1.52	9.70	16.50	55.63	12.49	0.13	2.69	1.35
660	0.00	1.59	0.59	19.14	62.78	11.38	0.15	2.82	1.56
680	0.00	1.62	0.92	20.79	64.15	9.64	0.11	1.19	1.59
700	0.00	1.69	0.56	32.75	58.46	4.18	0.16	0.74	1.47
720	0.01	1.81	0.25	38.05	54.94	2.67	0.15	0.59	1.53
740	0.00	1.66	0.87	20.54	65.47	8.68	0.09	1.10	1.58
760	0.00	1.70	0.61	23.38	64.59	7.28	0.06	0.76	1.62
780	0.00	3.27	0.24	33.91	59.13	0.81	0.17	0.51	1.96
800	0.00	1.21	8.17	16.28	63.29	0.37	0.61	8.14	1.93
820	0.00	1.40	1.21	18.09	66.34	0.02	0.08	10.90	1.96
840	0.00	1.53	4.91	17.46	64.25	0.08	0.13	9.82	1.82

0	0.00	1.12	4.79	22.09	69.75	0.19	0.09	0.54	1.45
1	0.01	1.51	1.30	26.11	66.88	0.16	0.12	0.52	1.65
2	0.01	2.07	0.51	27.00	67.67	0.12	0.13	0.62	1.89
3	0.01	2.67	0.50	28.31	65.62	0.19	0.17	0.71	1.83
4	0.00	2.45	0.68	28.52	65.57	0.20	0.14	0.69	1.75
5	0.00	2.09	0.33	27.38	67.59	0.22	0.13	0.58	1.68
6	0.00	1.11	0.20	25.82	70.59	0.30	0.13	0.31	1.55
7	0.00	0.89	0.52	24.04	72.24	0.66	0.09	0.16	1.40
8	0.00	1.53	0.29	27.23	67.51	1.50	0.11	0.27	1.57
9	0.00	2.84	0.26	32.96	60.04	1.66	0.10	0.28	1.87
10	0.00	2.86	0.45	31.27	57.15	5.58	0.15	0.74	1.81
11	0.00	2.47	0.58	23.13	64.15	7.38	0.12	0.51	1.67
12	0.01	2.31	0.56	19.82	67.00	8.02	0.08	0.58	1.62
13	0.00	2.21	0.53	23.09	65.14	6.77	0.10	0.59	1.58
14	0.00	1.88	0.87	21.90	65.57	7.43	0.11	0.66	1.58
15	0.00	1.59	5.58	19.07	63.74	7.66	0.08	0.70	1.59
16	0.00	1.61	8.17	18.34	61.94	7.71	0.05	0.66	1.52
17	0.00	1.67	6.34	18.58	63.40	7.90	0.04	0.63	1.43
18	0.00	1.74	1.17	19.91	66.65	8.19	0.10	0.57	1.68
19	0.01	1.55	8.42	18.49	61.43	7.64	0.09	0.77	1.61
20	0.00	1.66	0.59	20.03	66.73	8.35	0.13	0.73	1.78
0	0.00	3.91	3.92	30.46	57.42	1.18	0.15	1.00	1.96
1	0.00	3.54	6.81	28.58	57.61	0.47	0.15	0.90	1.96
2	0.00	3.64	6.14	29.57	56.17	1.60	0.14	0.87	1.88
3	0.00	3.93	4.49	30.64	56.58	1.38	0.13	0.97	1.90
4	0.00	3.59	2.87	30.57	59.68	0.40	0.17	0.78	1.95
5	0.01	3.47	0.59	32.40	60.51	0.36	0.15	0.52	2.00
6	0.00	3.67	0.31	31.94	60.71	0.46	0.18	0.72	2.01
7	0.00	3.70	0.31	31.75	60.83	0.39	0.13	0.85	2.05
8	0.00	3.77	0.35	32.14	60.59	0.27	0.14	0.75	1.98
9	0.00	2.90	0.42	31.86	56.57	6.19	0.10	0.28	1.68
10	0.01	2.69	0.43	28.69	60.44	5.63	0.11	0.34	1.66
11	0.01	2.37	0.52	21.71	66.15	7.11	0.04	0.49	1.59
12	0.01	2.03	0.68	19.41	67.37	8.17	0.10	0.64	1.59
13	0.00	2.04	0.74	19.31	67.00	8.47	0.00	0.70	1.74
14	0.00	1.89	0.62	19.47	66.85	8.74	0.10	0.72	1.61
15	0.01	1.73	0.72	19.64	67.13	8.32	0.12	0.75	1.59
16	0.00	1.87	0.60	19.72	67.30	8.28	0.11	0.53	1.61
17	0.00	1.67	1.18	20.05	66.27	8.38	0.08	0.70	1.68
18	0.00	1.78	0.75	19.57	67.20	8.18	0.09	0.76	1.69
19	0.00	1.74	0.88	19.63	66.10	9.11	0.09	0.80	1.64
20	0.00	1.71	1.35	19.88	66.27	8.35	0.07	0.73	1.65
0	0.00	1.77	0.57	17.70	59.00	13.64	0.21	5.69	1.43
20	0.00	1.60	11.29	23.65	55.27	6.58	0.20	0.24	1.17
40	0.00	0.30	7.35	3.36	10.68	60.23	0.04	17.24	0.82
60	0.00	1.29	0.24	22.74	65.82	7.92	0.17	0.41	1.42
80	0.00	1.84	0.49	19.94	64.78	10.31	0.17	0.98	1.49
100	0.00	1.52	0.10	23.05	65.50	8.07	0.14	0.22	1.40
120	0.00	1.64	0.43	21.24	65.80	8.49	0.15	0.75	1.51
140	0.00	1.74	0.47	22.27	65.47	8.04	0.15	0.38	1.48
160	0.00	1.45	1.64	20.95	64.96	8.69	0.11	0.67	1.53
180	0.00	0.78	0.58	15.99	52.12	18.78	0.09	10.35	1.32
200	0.00	1.28	0.12	23.68	65.43	7.90	0.09	0.03	1.48
220	0.00	1.55	0.62	20.02	64.46	10.33	0.12	1.19	1.71

240	0.00	1.32	0.20	22.30	66.37	7.89	0.12	0.33	1.46
260	0.00	1.38	0.40	19.52	59.37	14.51	0.15	3.15	1.52
280	0.00	1.59	0.38	21.81	66.21	8.14	0.09	0.33	1.46
300	0.00	1.58	2.91	26.19	60.97	6.11	0.15	0.58	1.52
320	0.00	1.43	0.79	22.58	65.26	8.07	0.07	0.20	1.60
340	0.01	1.59	0.21	23.36	65.08	8.07	0.09	0.13	1.45
360	0.01	1.01	3.09	28.28	46.93	12.62	0.17	6.53	1.35
380	0.00	1.37	2.43	32.12	48.40	8.77	0.10	5.46	1.36
400	0.00	1.21	0.65	16.89	56.78	18.17	0.12	4.69	1.49
420	0.00	1.73	0.46	21.10	66.57	7.93	0.12	0.56	1.54
440	0.02	1.61	10.18	17.88	58.64	8.35	0.10	1.76	1.46
460	0.00	1.68	0.89	20.50	66.75	8.00	0.06	0.54	1.57
480	0.00	1.74	0.82	20.07	66.78	8.25	0.10	0.77	1.47
500	0.00	1.17	0.51	12.79	44.02	23.27	0.06	17.02	1.16
520	0.00	1.22	0.52	13.81	46.52	21.48	0.11	14.98	1.36
540	0.00	1.46	0.60	15.86	55.15	16.80	0.08	8.69	1.36
560	0.01	1.55	0.73	16.28	55.87	15.98	0.10	8.04	1.44
580	0.00	1.47	0.74	17.23	58.67	15.99	0.11	4.26	1.53
600	0.00	1.57	0.56	17.67	60.04	14.82	0.10	3.64	1.60
620	0.00	1.49	0.58	17.58	59.08	15.99	0.08	3.70	1.49
640	0.00	1.52	1.30	18.37	60.81	14.49	0.09	1.92	1.50
660	0.01	1.70	0.55	20.52	66.31	8.30	0.09	0.87	1.65
680	0.00	1.54	2.22	18.66	62.84	12.19	0.10	0.78	1.67
700	0.00	1.59	0.70	19.33	64.67	10.51	0.08	1.53	1.59
720	0.01	1.54	0.70	19.19	63.97	10.78	0.06	2.17	1.58
740	0.01	1.48	0.71	21.57	64.67	8.82	0.11	1.08	1.55
760	0.00	1.50	0.93	19.73	66.17	8.96	0.12	0.97	1.63
780	0.00	2.03	0.86	19.20	67.60	7.98	0.10	0.52	1.70
800	0.00	1.07	1.35	17.79	67.87	0.07	0.09	9.98	1.79
820	0.00	1.02	1.64	17.16	68.16	0.00	0.05	10.15	1.82
840	0.01	1.18	1.37	17.89	66.95	0.07	0.10	10.52	1.90
0	0.00	0.84	2.17	19.42	71.83	2.96	0.09	1.15	1.54
1	0.00	1.23	2.26	20.70	70.62	2.56	0.12	0.99	1.53
2	0.00	0.82	2.30	19.79	71.13	3.21	0.11	1.21	1.43
3	0.00	0.74	2.28	19.82	71.30	3.06	0.11	1.28	1.42
4	0.00	0.73	1.59	20.47	72.63	2.07	0.09	1.04	1.39
5	0.00	0.81	0.98	20.65	74.11	1.12	0.10	0.71	1.52
6	0.00	0.57	1.22	21.80	74.30	0.34	0.09	0.34	1.35
7	0.00	0.57	0.68	22.35	74.16	0.44	0.09	0.36	1.35
8	0.02	0.91	0.73	22.81	70.64	2.93	0.12	0.40	1.44
9	0.00	1.28	0.81	22.06	67.68	6.04	0.08	0.50	1.56
10	0.00	1.31	0.55	20.76	67.53	7.66	0.09	0.52	1.58
11	0.01	1.43	1.78	19.56	66.76	8.15	0.10	0.62	1.58
12	0.00	1.22	0.65	21.71	67.74	6.36	0.08	0.55	1.70
13	0.03	1.42	4.50	19.10	64.40	8.43	0.09	0.54	1.50
14	0.00	1.55	4.46	20.16	63.55	8.00	0.12	0.54	1.64
15	0.01	1.57	3.94	21.10	63.66	7.58	0.09	0.48	1.57
16	0.00	1.44	3.72	19.22	63.33	8.50	0.11	0.62	1.52
17	0.00	1.79	0.75	23.99	64.28	6.91	0.12	0.46	1.71
18	0.00	1.75	0.50	24.51	63.98	6.99	0.12	0.52	1.63
19	0.00	1.79	0.38	25.30	63.70	6.60	0.13	0.46	1.65
20	0.00	1.93	0.39	26.22	63.12	6.11	0.12	0.49	1.61
21	0.00	1.83	0.39	29.44	66.22	6.66	0.06	0.50	1.68
22	0.03	1.81	0.43	23.46	64.85	7.11	0.13	0.57	1.60
23	0.04	1.65	0.61	20.97	65.80	8.55	0.09	0.72	1.58
24	0.00	1.69	0.56	20.56	65.70	9.05	0.10	0.76	1.58

25	0.00	1.66	0.50	20.88	65.44	8.94	0.10	0.83	1.66
----	------	------	------	-------	-------	------	------	------	------

D.38 SS-316/V/Nd After 28 Days at 700°C

The SS-316/W/Nd assembly annealed for 28 days at 700°C bonded on the W/Nd interface but not the SS-316/W interface. Compositional data (in at%) from WDS linescans across the W/Nd interface is given below.

Position	Zr	Mo	Si	Cr	Fe	Nd	V	Ni	Mn
0	0.00	0.04	3.05	2.13	1.46	0.05	93.11	0.16	0.00
1	0.00	0.01	7.08	2.14	1.47	0.02	89.15	0.08	0.06
2	0.00	0.00	15.53	1.67	0.35	0.03	82.39	0.02	0.02
3	0.00	0.01	11.31	1.72	0.26	0.01	86.64	0.06	0.00
4	0.00	0.00	3.22	1.86	0.35	0.01	94.49	0.07	0.01
5	0.01	0.01	2.12	1.85	0.33	0.00	95.62	0.07	0.00
6	0.00	0.00	0.83	1.97	3.07	0.00	93.04	1.05	0.04
7	0.00	0.02	0.68	2.20	16.92	0.01	74.65	5.27	0.25
8	0.00	0.01	0.47	3.08	29.35	0.00	59.27	7.39	0.44
9	0.00	0.06	0.68	4.74	36.32	0.00	50.41	7.13	0.67
10	0.00	0.18	1.13	7.33	43.67	0.00	40.30	6.50	0.90
11	0.00	0.64	1.33	11.62	46.97	0.00	32.52	5.89	1.03
12	0.00	1.63	1.08	18.25	52.41	0.01	20.59	4.79	1.24
13	0.00	1.41	0.94	19.10	54.89	0.00	17.26	5.00	1.38
14	0.00	1.41	1.02	18.91	54.60	0.03	17.32	5.28	1.45
15	0.00	1.41	0.96	19.40	55.03	0.00	16.43	5.32	1.46
0	0.00	0.00	4.96	1.82	0.35	0.01	92.87	0.00	0.00
1	0.00	0.01	8.18	1.75	0.21	0.03	89.82	0.00	0.00
2	0.01	0.01	7.94	1.77	0.41	0.02	89.76	0.04	0.05
3	0.01	0.02	3.80	1.78	0.32	0.02	94.00	0.05	0.01
4	0.39	0.00	1.20	1.85	0.22	0.01	96.26	0.06	0.01
5	0.00	0.01	1.70	1.90	0.23	0.00	96.12	0.01	0.02
6	0.00	0.00	2.83	1.97	0.58	0.03	94.46	0.12	0.00
7	0.00	0.00	0.94	1.95	4.61	0.00	90.62	1.82	0.06
8	0.00	0.18	5.25	7.15	40.54	0.01	39.38	6.57	0.93
9	0.00	0.45	1.61	9.97	44.13	0.00	36.20	6.49	1.14
10	0.00	1.58	1.25	16.84	49.46	0.01	23.13	5.35	2.37
11	0.00	1.64	0.99	18.28	52.33	0.00	18.57	5.38	2.82
12	0.00	1.80	1.00	19.43	53.68	0.00	17.08	5.46	1.55
13	0.00	2.33	1.00	21.13	53.95	0.00	14.83	5.20	1.56
14	0.00	2.58	0.98	22.16	53.79	0.02	12.80	5.07	2.61
15	0.00	2.19	1.79	20.22	51.57	0.02	14.02	5.96	4.23
0	0.00	0.00	11.79	1.70	0.18	0.00	86.27	0.05	0.00
1	0.00	0.00	2.75	1.91	0.22	0.00	95.09	0.02	0.00
2	0.36	0.01	7.44	1.80	1.45	0.00	88.41	0.53	0.01
3	0.35	0.01	6.12	2.14	13.01	0.00	73.72	4.41	0.25
4	0.17	0.01	7.95	1.77	0.49	0.01	89.53	0.07	0.00
5	0.00	0.05	2.61	5.82	34.69	0.05	47.85	7.78	1.16
6	0.00	0.17	3.72	7.98	38.24	0.04	41.28	7.28	1.29
7	0.00	0.38	3.78	10.27	41.03	0.01	36.46	6.81	1.27
8	0.00	0.05	2.45	11.28	34.69	0.06	43.29	7.02	1.15
9	0.00	0.12	3.88	7.78	37.42	0.03	42.21	7.32	1.25
10	0.00	0.34	3.98	9.72	40.46	0.04	37.02	7.05	1.40

11	0.00	0.67	3.44	11.68	44.02	0.12	32.38	6.37	1.32
12	0.00	0.67	3.44	12.04	44.58	0.17	31.36	6.50	1.22
13	0.00	0.78	5.00	11.91	43.41	0.08	31.31	6.40	1.11
14	0.00	1.13	3.05	15.24	49.10	0.07	24.01	6.07	1.35

D.39 SS-316/Zr/V/Nd After 28 Days at 700°C

The SS-316/Zr/V/Nd assembly annealed for 28 days at 700°C bonded on the SS-316/Zr, Zr/V, and V/Nd interfaces. Compositional data (in at%) from WDS linescans across the SS-316/Zr and Zr/V interfaces is given below.

Position	Zr	Mo	Si	Cr	Fe	Nd	V	Ni	Mn
0	0.01	1.85	1.35	19.13	67.18	0.00	0.07	8.69	1.73
1	0.01	1.45	1.41	18.40	67.46	0.00	0.10	9.47	1.71
2	0.06	1.53	3.85	17.09	67.01	0.00	0.10	9.22	1.15
3	0.13	1.75	3.58	19.44	65.94	0.01	0.11	8.34	0.70
4	20.47	1.16	1.85	15.79	53.46	0.05	0.08	6.73	0.40
5	91.03	0.01	0.82	1.60	5.55	0.00	0.06	0.83	0.12
6	97.70	0.01	0.10	0.45	1.39	0.06	0.00	0.26	0.04
7	34.13	0.85	1.61	12.83	44.33	0.03	0.04	5.86	0.31
8	88.21	0.00	0.94	2.01	7.68	0.07	0.01	1.04	0.05
9	97.81	0.00	0.11	0.44	1.30	0.06	0.00	0.28	0.01
10	97.99	0.00	0.50	0.37	1.05	0.03	0.00	0.06	0.01
11	95.94	0.00	2.28	0.34	1.12	0.06	0.00	0.20	0.05
12	68.41	0.00	30.23	0.25	1.01	0.01	0.00	0.09	0.01
13	61.31	0.00	37.60	0.17	0.67	0.05	0.00	0.19	0.04
14	94.15	0.00	5.04	0.17	0.52	0.03	0.00	0.07	0.03
15	98.90	0.00	0.37	0.14	0.48	0.04	0.00	0.05	0.02
0	90.61	0.02	8.35	0.00	0.03	0.02	0.87	0.05	0.05
1	98.03	0.00	0.60	0.14	0.00	0.00	1.17	0.00	0.06
2	97.72	0.00	0.37	0.08	0.20	0.00	1.46	0.06	0.11
3	94.13	0.00	1.00	0.67	1.66	0.01	1.82	0.55	0.17
4	85.57	0.00	2.45	0.79	3.42	0.00	6.05	1.40	0.32
5	56.97	0.02	5.00	0.77	1.41	0.01	34.98	0.61	0.25
6	35.54	0.00	7.64	1.10	0.36	0.00	55.11	0.10	0.16
7	23.23	0.01	8.33	1.28	0.27	0.01	66.75	0.04	0.09
8	9.59	0.00	4.91	1.72	0.14	0.02	83.60	0.00	0.04
9	4.78	0.02	2.11	1.83	0.06	0.00	91.19	0.00	0.01
10	0.94	0.00	1.23	1.92	0.04	0.00	95.84	0.02	0.03
11	0.12	0.00	0.79	1.85	0.01	0.01	97.20	0.04	0.00
12	0.11	0.01	0.29	1.94	0.06	0.00	97.58	0.00	0.02
13	5.09	0.01	6.51	1.78	0.16	0.02	86.40	0.00	0.03
14	8.64	0.02	13.21	1.59	0.61	0.05	75.74	0.10	0.04
15	3.06	0.03	6.70	2.09	1.49	0.07	86.29	0.22	0.05
0	89.48	0.02	9.65	0.01	0.07	0.00	0.71	0.00	0.07
1	97.01	0.00	1.66	0.09	0.06	0.00	0.98	0.06	0.14
2	89.39	0.00	7.94	0.26	0.86	0.10	1.24	0.18	0.03
3	67.71	0.04	29.19	0.34	1.19	0.02	1.34	0.11	0.06
4	89.71	0.00	7.80	0.25	0.78	0.07	1.25	0.07	0.08
5	72.32	0.02	24.43	0.32	1.26	0.12	1.40	0.12	0.02
6	64.52	0.00	30.91	0.31	0.92	0.06	3.11	0.13	0.04
7	70.92	0.01	4.97	0.59	0.56	0.03	22.49	0.16	0.26

8	13.40	0.01	3.08	1.82	1.57	0.10	79.25	0.22	0.55
9	3.10	0.01	1.53	1.99	0.70	0.03	92.22	0.11	0.31
10	0.81	0.00	0.62	1.87	0.13	0.00	96.52	0.00	0.05
11	3.80	0.00	3.80	2.14	1.01	0.07	89.05	0.00	0.15
12	10.40	0.02	8.24	2.19	1.52	0.08	77.25	0.03	0.28
13	11.51	0.01	9.12	1.77	0.63	0.07	76.59	0.10	0.21
14	5.09	0.02	7.36	1.67	0.19	0.03	85.43	0.03	0.18
15	0.35	0.01	2.94	1.87	0.06	0.01	94.71	0.00	0.05

D.40 SS-316/Zr/Nd After 28 Days at 700°C

The SS-316/Zr/Nd assembly annealed for 28 days at 700°C bonded on the SS-316/Zr interface but not the Zr/Nd interface. Compositional data (in at%) from WDS linescans across the SS-3136/Zr interface is given below.

Position	Zr	Mo	Si	Cr	Fe	Nd	V	Ni	Mn
0	66.90	0.01	0.84	0.44	13.56	0.00	0.01	17.33	0.91
1	66.41	0.00	1.41	0.40	13.53	0.00	0.06	17.24	0.95
2	66.09	0.01	2.63	0.55	13.37	0.01	0.03	16.44	0.86
3	70.06	0.00	2.28	0.70	11.87	0.08	0.00	14.30	0.70
4	74.31	0.32	1.24	2.53	11.02	3.61	0.03	6.48	0.46
5	29.70	2.26	1.34	17.59	37.05	10.55	0.11	0.67	0.73
6	5.57	3.73	1.49	26.93	53.62	6.92	0.10	0.48	1.16
7	0.34	3.66	1.32	28.63	62.42	1.60	0.14	0.66	1.25
8	0.10	3.78	1.23	28.69	63.25	0.70	0.11	0.86	1.28
9	0.03	3.36	1.16	27.01	63.10	0.69	2.69	0.70	1.26
10	0.02	1.16	0.92	19.83	74.35	1.88	0.07	0.79	0.98
11	0.02	0.77	1.18	18.59	77.34	0.42	0.10	0.68	0.90
12	0.02	0.73	0.84	18.78	76.70	1.10	0.11	0.83	0.90
13	0.03	0.80	0.70	18.82	75.65	1.87	0.10	1.01	1.02
14	0.21	1.37	1.15	20.88	73.68	0.47	0.10	1.07	1.07
15	0.08	1.54	21.15	18.67	56.53	0.10	0.09	0.90	0.95
0	83.13	0.00	0.50	0.33	10.76	0.03	0.03	4.93	0.29
1	74.39	0.01	0.76	0.35	15.98	0.00	0.04	8.10	0.36
2	74.39	0.00	0.26	0.53	15.71	0.00	0.00	8.70	0.42
3	70.48	0.05	0.19	1.29	16.56	0.00	0.01	10.26	1.16
4	39.68	1.64	0.63	14.31	35.22	0.02	0.09	8.04	0.39
5	4.82	1.52	1.00	19.27	64.27	0.00	0.09	8.08	0.95
6	56.42	0.87	0.45	7.79	24.20	0.03	0.05	9.48	0.71
7	20.12	2.15	0.88	19.52	49.62	0.02	0.12	7.05	0.52
8	3.42	1.18	0.92	17.90	65.98	0.03	0.08	9.16	1.32
9	2.65	1.08	0.88	17.02	66.72	0.00	0.07	9.92	1.66
10	1.87	1.18	1.03	16.88	67.09	0.00	0.10	10.09	1.77
11	0.86	1.28	1.05	17.32	67.41	0.01	0.05	10.24	1.78
12	0.45	1.21	1.31	17.30	67.56	0.00	0.13	10.25	1.80
13	0.51	1.33	1.25	17.24	67.59	0.00	0.07	10.27	1.75
14	0.56	1.25	1.30	17.42	67.30	0.00	0.06	10.25	1.86
15	0.39	1.20	1.56	17.23	67.75	0.01	0.09	10.06	1.72

D.41 SS-316/Ti/V/Nd After 28 Days at 700°C

The SS-316/Ti/V/Nd assembly annealed for 28 days at 700°C bonded on the SS-316/Ti, Ti/V, and V/Nd interfaces. Compositional data (in at%) from WDS linescans across each of these interfaces is given below.

Position	Ta	Ti	Mo	Si	Fe	Nd	V	Cr	Ni	Mn
0	0.00	13.25	2.78	1.82	50.59	0.00	0.20	28.12	1.90	1.35
1	0.00	6.42	2.11	0.51	52.29	0.03	0.20	34.91	1.89	1.64
2	0.00	55.53	0.16	0.11	36.82	0.00	0.18	2.69	4.03	0.48
3	0.00	67.68	0.03	3.27	17.94	0.01	0.25	1.47	9.02	0.33
4	0.00	74.70	0.14	0.35	14.54	0.04	0.26	1.89	7.66	0.42
5	0.00	86.12	0.26	0.79	8.89	0.00	0.30	2.37	0.89	0.37
6	0.00	86.06	0.18	3.54	6.91	0.04	0.29	1.83	0.87	0.29
7	0.00	86.28	0.10	5.65	5.36	0.05	0.33	1.37	0.68	0.20
8	0.00	85.79	0.12	3.56	7.14	0.06	0.34	1.80	0.91	0.28
9	0.00	54.85	0.42	10.32	22.82	0.35	1.67	6.29	2.73	0.56
10	0.00	54.78	0.38	13.58	21.08	0.33	1.21	5.67	2.49	0.50
11	0.00	77.15	0.22	4.29	12.66	0.11	0.40	3.21	1.58	0.38
12	0.00	85.33	0.18	2.43	8.29	0.03	0.29	2.12	1.04	0.30
13	0.00	87.21	0.18	0.71	8.15	0.04	0.29	2.14	0.98	0.30
14	0.00	86.84	0.20	0.85	8.28	0.01	0.31	2.16	0.99	0.36
15	0.00	87.60	0.13	0.43	8.17	0.01	0.28	2.05	1.08	0.25
0	0.00	6.27	2.46	0.60	48.80	0.01	0.30	38.69	1.44	1.42
1	0.00	6.52	2.51	0.61	48.98	0.00	0.30	38.15	1.58	1.36
2	0.00	80.83	0.00	0.26	13.77	0.00	0.29	1.33	3.27	0.26
3	0.00	73.70	0.00	0.68	14.99	0.03	0.27	1.22	8.77	0.35
4	0.00	63.06	0.23	0.26	30.70	0.00	0.24	3.41	1.70	0.41
5	0.00	85.04	0.23	0.19	9.59	0.03	0.29	2.52	1.78	0.33
6	0.00	90.76	0.15	0.28	5.92	0.06	0.36	1.68	0.56	0.25
7	0.00	93.30	0.04	2.09	2.70	0.22	0.37	0.80	0.37	0.11
8	0.00	94.81	0.00	0.99	2.51	0.12	0.39	0.72	0.40	0.06
9	0.00	92.05	0.12	0.35	4.92	0.12	0.31	1.49	0.44	0.20
10	0.00	91.36	0.05	3.30	3.09	0.40	0.36	0.90	0.43	0.12
11	0.00	93.94	0.01	1.04	2.99	0.18	0.44	0.82	0.48	0.11
12	0.00	86.86	0.20	0.35	8.36	0.04	0.32	2.42	1.13	0.33
13	0.00	87.21	0.18	0.18	8.37	0.00	0.28	2.32	1.12	0.35
14	0.00	87.33	0.23	0.21	8.25	0.01	0.25	2.35	1.03	0.34
15	0.00	86.83	0.16	0.68	8.14	0.23	0.41	2.21	1.02	0.32
0	0.00	46.39	0.00	12.26	2.18	0.18	37.57	0.99	0.36	0.08
1	0.00	40.87	0.00	6.25	1.90	0.29	49.10	1.22	0.34	0.03
2	0.00	56.19	0.00	2.02	2.53	0.11	37.72	0.90	0.50	0.03
3	0.00	50.50	0.00	1.17	22.93	0.20	24.08	0.65	0.45	0.03
4	0.00	58.60	0.00	8.06	2.62	0.12	29.27	0.77	0.52	0.04
5	0.00	53.20	0.00	14.46	2.39	0.26	28.50	0.69	0.46	0.04
6	0.00	58.86	0.00	1.12	2.70	0.16	35.68	0.97	0.47	0.04
7	0.00	60.18	0.00	0.83	3.27	0.19	33.94	0.96	0.58	0.05
8	0.00	58.39	0.00	2.43	2.85	0.22	34.70	0.88	0.48	0.05
9	0.00	47.26	0.00	14.49	2.05	0.26	34.69	0.89	0.36	0.02
10	0.00	33.58	0.01	19.58	1.37	0.21	44.05	0.95	0.24	0.02
11	0.00	22.31	0.00	3.31	1.47	0.37	70.38	1.86	0.29	0.01
12	0.00	16.95	0.02	4.31	1.79	1.24	73.28	2.10	0.28	0.04

13	0.00	24.30	0.00	4.18	1.16	0.94	67.62	1.61	0.18	0.02
14	0.00	9.17	0.00	0.93	0.46	1.75	85.75	1.88	0.06	0.00
15	0.00	1.02	0.01	2.47	0.32	0.86	93.01	2.28	0.03	0.00
0	0.00	67.45	0.01	6.56	3.72	0.21	20.69	0.67	0.63	0.07
1	0.00	39.19	0.04	39.59	5.17	0.14	13.77	1.19	0.83	0.09
2	0.00	62.59	0.00	7.76	3.28	0.15	24.93	0.68	0.54	0.08
3	0.00	67.08	0.00	0.68	3.50	0.10	27.26	0.72	0.63	0.05
4	0.00	61.23	0.00	6.86	3.09	0.18	27.35	0.69	0.55	0.05
5	0.00	60.02	0.00	8.37	3.14	0.27	26.91	0.70	0.53	0.05
6	0.00	64.18	0.00	0.37	3.15	0.10	30.84	0.78	0.56	0.02
7	0.00	64.24	0.00	1.03	3.37	0.11	29.85	0.74	0.61	0.04
8	0.00	56.29	0.01	10.32	2.87	0.11	29.08	0.78	0.51	0.03
9	0.00	56.86	0.00	8.12	3.22	0.15	30.20	0.83	0.56	0.07
10	0.00	60.68	0.00	1.54	3.06	0.22	33.05	0.84	0.58	0.03
11	0.00	59.18	0.00	0.61	2.83	0.01	35.94	0.91	0.51	0.02
12	0.00	55.69	0.00	0.46	2.72	0.04	39.61	1.00	0.45	0.03
13	0.00	48.74	0.00	2.05	2.45	0.05	45.26	1.08	0.35	0.02
14	0.00	29.98	0.00	4.36	1.50	0.17	62.34	1.41	0.24	0.00
15	0.00	20.19	0.00	1.54	1.08	0.33	74.90	1.90	0.06	0.00
0	0.00	0.05	0.01	12.75	0.24	2.55	82.38	1.95	0.09	0.00
1	0.00	0.09	0.03	0.31	2.56	3.64	90.35	2.65	0.32	0.06
2	0.00	0.20	0.05	0.22	2.11	1.63	92.89	2.57	0.26	0.08
3	0.00	0.23	0.18	0.33	3.15	3.02	89.76	2.83	0.32	0.17
4	0.00	0.01	0.21	0.47	1.43	30.12	65.61	1.88	0.00	0.27
5	0.00	0.01	0.05	0.37	1.00	92.86	4.96	0.19	0.13	0.44
6	0.00	0.00	0.01	0.46	0.51	95.20	3.21	0.17	0.00	0.44
7	0.00	0.49	0.01	0.29	0.67	95.87	1.94	0.05	0.07	0.62
8	0.00	0.00	0.03	0.32	0.46	97.21	1.33	0.10	0.04	0.52
9	0.00	0.00	0.03	1.15	1.96	94.87	1.03	0.33	0.09	0.55
10	0.00	0.00	0.11	1.81	1.58	94.39	0.95	0.38	0.29	0.50
11	0.00	0.39	0.04	5.91	1.43	89.47	1.67	0.38	0.21	0.49
12	0.00	0.00	0.06	1.10	2.23	94.33	1.18	0.34	0.19	0.57
13	0.00	0.03	0.15	2.33	2.28	92.39	1.27	0.64	0.38	0.53
14	0.00	0.46	0.04	5.66	1.42	90.14	1.55	0.27	0.14	0.33
15	0.00	0.02	0.00	0.92	1.06	93.64	3.39	0.36	0.08	0.55

D.42 SS-316/Ti/Nd After 28 Days at 700°C

The SS-316/Ti/Nd assembly annealed for 28 days at 700°C bonded on the SS=316/Ti and Ti/Nd interfaces. Compositional data (in at%) from WDS linescans across these interfaces is given below.

Position	Ta	Ti	Mo	Si	Fe	Nd	V	Cr	Ni	Mn
0	0.00	0.89	0.04	72.77	0.24	25.86	0.04	0.03	0.02	0.12
1	0.00	3.51	0.00	77.74	0.44	18.06	0.04	0.12	0.03	0.06
2	0.00	15.30	0.00	39.43	0.64	44.10	0.11	0.08	0.09	0.25
3	0.00	50.95	0.01	10.13	0.52	37.84	0.18	0.11	0.03	0.25
4	0.00	61.94	0.06	22.38	1.17	13.85	0.26	0.17	0.13	0.03
5	0.00	68.73	0.19	6.66	6.47	15.94	0.45	0.30	1.06	0.20
6	0.00	80.87	0.05	1.06	3.85	12.36	0.35	0.12	1.22	0.12
7	0.00	97.99	0.00	0.82	0.15	0.57	0.32	0.04	0.07	0.04
8	0.00	99.21	0.00	0.24	0.07	0.08	0.33	0.03	0.00	0.04

9	0.00	99.06	0.00	0.38	0.06	0.15	0.30	0.00	0.02	0.02
10	0.00	99.12	0.00	0.35	0.05	0.10	0.32	0.05	0.00	0.00
11	0.00	99.39	0.00	0.10	0.07	0.11	0.30	0.04	0.00	0.00
12	0.00	98.91	0.00	0.66	0.01	0.09	0.28	0.00	0.02	0.03
13	0.00	64.55	0.00	34.87	0.16	0.15	0.19	0.04	0.05	0.00
14	0.00	86.81	0.00	12.59	0.14	0.20	0.24	0.02	0.00	0.00
15	0.00	86.34	0.00	6.93	3.09	2.22	0.26	0.70	0.37	0.08
0	0.00	4.08	0.00	4.73	0.25	90.28	0.03	0.00	0.06	0.58
1	0.00	8.73	0.04	0.44	0.39	89.81	0.08	0.00	0.00	0.50
2	0.00	53.72	0.02	0.57	0.27	44.90	0.31	0.06	0.00	0.16
3	0.00	30.14	0.00	5.74	0.51	62.97	0.16	0.11	0.07	0.32
4	0.00	21.04	0.00	43.12	0.62	34.76	0.09	0.07	0.07	0.23
5	0.00	56.97	0.00	27.95	0.41	14.11	0.27	0.10	0.17	0.04
6	0.00	88.24	0.00	7.23	0.49	3.44	0.35	0.11	0.08	0.06
7	0.00	97.37	0.00	0.73	0.31	1.14	0.33	0.05	0.04	0.03
8	0.00	99.19	0.00	0.22	0.04	0.19	0.33	0.00	0.00	0.03
9	0.00	91.73	0.00	4.45	0.53	2.65	0.35	0.16	0.09	0.04
10	0.00	98.31	0.00	0.48	0.13	0.69	0.34	0.03	0.02	0.00
11	0.00	98.67	0.00	0.65	0.06	0.22	0.31	0.03	0.02	0.04
12	0.00	90.66	0.00	7.55	0.04	1.44	0.24	0.06	0.03	0.00
13	0.00	56.41	0.00	35.99	0.23	7.03	0.19	0.06	0.06	0.04
14	0.00	98.40	0.00	1.03	0.04	0.24	0.27	0.00	0.00	0.03
15	0.00	77.87	0.00	18.42	0.09	3.31	0.25	0.03	0.00	0.02
0	0.00	86.04	0.17	1.41	9.55	0.06	0.22	1.59	0.72	0.23
1	0.00	68.01	0.00	0.23	21.15	0.04	0.18	1.35	8.63	0.41
2	0.00	67.23	0.01	0.18	22.16	0.03	0.21	1.67	8.11	0.40
3	0.00	55.64	0.24	0.11	37.45	0.03	0.13	3.25	2.46	0.69
4	0.00	41.42	1.74	1.47	40.53	0.00	0.15	12.43	1.41	0.86
5	0.00	9.61	2.40	0.85	46.04	0.02	0.26	37.79	1.55	1.50
6	0.00	52.85	0.29	0.07	40.27	0.03	0.18	3.74	1.97	0.59
7	0.00	34.87	2.34	1.96	40.79	0.01	0.19	17.54	1.36	0.94
8	0.00	9.79	2.36	0.64	46.40	0.01	0.24	37.48	1.61	1.49
9	0.00	11.09	2.21	0.82	46.46	0.00	0.28	36.11	1.56	1.48
10	0.00	18.06	2.06	0.54	43.42	0.00	0.46	32.60	1.48	1.39
11	0.00	9.36	2.33	0.59	49.56	0.00	0.30	34.47	1.85	1.54
12	0.00	2.57	2.49	0.90	55.04	0.04	0.18	34.73	2.39	1.66
13	0.00	4.78	1.62	1.67	58.48	0.09	0.21	25.90	5.65	1.60
14	0.00	1.13	1.62	0.82	63.04	0.04	0.16	24.29	7.17	1.74
15	0.00	2.20	1.36	1.39	65.38	0.04	0.10	18.20	9.52	1.81
0	0.00	85.25	0.18	1.93	9.74	0.02	0.25	1.59	0.79	0.25
1	0.00	86.66	0.21	0.88	9.46	0.02	0.21	1.67	0.68	0.21
2	0.00	70.42	0.03	0.21	19.37	0.04	0.17	1.42	7.96	0.38
3	0.00	66.42	0.02	0.19	23.07	0.02	0.18	1.63	8.03	0.44
4	0.00	57.99	0.16	0.16	33.26	0.03	0.18	2.89	4.67	0.68
5	0.00	50.55	0.52	0.48	38.93	0.02	0.15	4.93	3.49	0.93
6	0.00	59.15	0.12	0.12	32.19	0.02	0.16	2.67	4.94	0.63
7	0.00	52.04	0.35	0.31	38.80	0.07	0.17	3.90	3.53	0.83
8	0.00	36.24	2.31	2.10	43.60	0.00	0.15	12.40	1.98	1.23
9	0.00	15.89	2.67	1.67	46.72	0.00	0.21	29.44	1.66	1.73
10	0.00	4.70	2.44	0.64	50.90	0.02	0.26	37.07	1.92	2.05
11	0.00	4.21	2.40	0.60	53.01	0.04	0.24	35.05	2.38	2.07
12	0.00	3.48	2.32	1.19	54.20	0.06	0.23	33.92	2.65	1.97
13	0.00	1.61	2.19	1.09	58.11	0.06	0.19	31.21	3.59	1.95
14	0.00	2.94	1.60	0.92	61.20	0.18	0.18	24.51	6.69	1.79

15	0.00	3.26	1.63	1.03	62.78	0.70	0.13	21.21	7.48	1.79
0	0.00	79.92	0.17	7.49	9.75	0.04	0.21	1.48	0.68	0.26
1	0.00	68.91	0.12	20.38	8.20	0.12	0.18	1.29	0.59	0.22
2	0.00	57.44	0.16	33.38	6.87	0.28	0.13	1.10	0.48	0.16
3	0.00	60.01	0.15	30.38	7.01	0.42	0.17	1.14	0.51	0.21
4	0.00	60.98	0.16	29.58	7.13	0.08	0.19	1.22	0.50	0.16
5	0.00	62.99	0.16	26.88	7.60	0.05	0.19	1.38	0.57	0.20
6	0.00	77.77	0.16	8.48	10.37	0.06	0.21	1.68	1.03	0.24
7	0.00	69.42	0.03	0.70	19.78	0.03	0.19	1.30	8.26	0.28
8	0.00	66.49	0.03	0.29	22.86	0.00	0.21	1.67	8.11	0.33
9	0.00	52.38	0.22	0.12	40.77	0.00	0.14	3.45	2.40	0.52
10	0.00	21.40	2.68	1.91	45.53	0.01	0.14	25.07	1.74	1.52
11	0.00	5.63	2.22	0.60	50.23	0.01	0.17	37.14	2.04	1.97
12	0.00	7.13	2.34	0.58	51.09	0.00	0.22	34.48	2.17	2.00
13	0.00	2.67	2.34	0.60	53.95	0.00	0.21	35.97	2.26	2.01
14	0.00	4.39	2.23	0.64	53.68	0.03	0.21	34.26	2.60	1.96
15	0.00	1.99	2.09	0.68	57.63	0.06	0.17	32.01	3.35	2.02
0	0.00	99.49	0.00	0.04	0.08	0.06	0.30	0.02	0.02	0.00
1	0.00	99.36	0.00	0.20	0.09	0.03	0.29	0.02	0.01	0.00
2	0.00	99.48	0.00	0.11	0.07	0.06	0.25	0.03	0.00	0.00
3	0.00	89.44	0.00	3.46	5.61	0.04	0.25	0.59	0.50	0.10
4	0.00	88.97	0.00	0.51	8.69	0.00	0.28	0.71	0.66	0.18
5	0.00	89.40	0.00	0.18	8.56	0.02	0.25	0.68	0.75	0.16
6	0.00	89.81	0.00	0.15	8.18	0.05	0.25	0.73	0.68	0.15
7	0.00	89.55	0.00	0.15	8.40	0.06	0.27	0.74	0.67	0.16
8	0.00	89.69	0.00	0.07	8.44	0.03	0.25	0.69	0.69	0.15
9	0.00	89.63	0.00	0.11	8.40	0.07	0.23	0.76	0.69	0.11
10	0.00	89.62	0.00	0.07	8.45	0.06	0.30	0.68	0.65	0.16
11	0.00	89.50	0.02	0.08	8.54	0.04	0.24	0.70	0.76	0.12
12	0.00	89.45	0.00	0.12	8.47	0.05	0.20	0.84	0.70	0.17
13	0.00	89.46	0.00	0.12	8.47	0.06	0.26	0.71	0.78	0.16
14	0.00	89.45	0.00	0.10	8.61	0.03	0.20	0.70	0.75	0.17
15	0.00	89.36	0.00	0.10	8.65	0.03	0.24	0.78	0.64	0.21

D.43 SS-316/Ta/V/Nd After 28 Days at 700°C

The SS-316/Ta/V/Nd assembly annealed for 28 days at 700°C bonded on the V/Nd interface but not the SS-316/Ta or Ta/V interfaces. Compositional data (in at%) from WDS line scans across the V/Nd interface is given below.

Position	Ta	Ti	Mo	Si	Fe	Nd	V	Cr	Ni	Mn
0	0.00	0.00	0.00	3.89	0.64	93.66	1.04	0.19	0.06	0.53
1	0.00	0.00	0.00	10.69	0.38	87.58	1.01	0.00	0.00	0.35
2	0.00	0.00	0.00	0.53	0.47	96.51	1.69	0.01	0.12	0.66
3	0.00	0.00	0.00	0.56	1.00	95.46	2.05	0.27	0.17	0.49
4	0.00	0.00	0.03	0.66	0.61	95.69	2.27	0.14	0.12	0.49
5	0.00	0.00	0.09	3.36	0.40	73.39	21.83	0.54	0.03	0.35
6	0.00	0.00	0.01	0.21	0.19	4.50	93.01	2.09	0.00	0.00
7	0.00	0.00	0.01	0.37	0.19	2.16	95.00	2.26	0.00	0.01
8	0.00	0.00	0.02	0.06	0.07	0.21	97.38	2.27	0.00	0.00
9	0.00	0.01	0.02	0.05	0.11	0.18	97.33	2.26	0.05	0.00
10	0.00	0.00	0.01	0.09	0.07	0.16	97.32	2.33	0.03	0.00

11	0.00	0.00	0.00	0.09	0.03	0.48	97.14	2.26	0.00	0.00
12	0.00	0.00	0.00	0.13	0.06	3.17	94.31	2.28	0.05	0.00
13	0.00	0.00	0.01	0.09	0.01	0.79	96.81	2.29	0.00	0.00
14	0.00	0.00	0.00	1.50	0.03	4.15	92.19	2.12	0.01	0.00
15	0.00	0.00	0.01	34.27	0.05	6.74	57.53	1.32	0.04	0.05

D.44 SS-316/Ta/Nd After 28 Days at 700°C

The SS-316/Ta/Nd assembly annealed for 28 days at 700°C bonded on the Ta/Nd interface but not the SS-316/Ta interface. Compositional data (in at%) from WDS linescans across the Ta/Nd interface is given below.

Position	Ta	Ti	Mo	Si	Fe	Nd	V	Cr	Ni	Mn
0	99.26	0.01	0.04	0.00	0.14	0.49	0.04	0.00	0.03	0.00
1	99.71	0.00	0.00	0.00	0.04	0.22	0.00	0.04	0.00	0.00
2	99.61	0.00	0.06	0.00	0.00	0.23	0.03	0.04	0.04	0.00
3	99.44	0.00	0.00	0.00	0.07	0.36	0.06	0.00	0.00	0.07
4	99.21	0.00	0.05	0.00	0.00	0.58	0.05	0.09	0.01	0.00
5	94.43	0.00	0.04	0.00	0.03	5.46	0.03	0.00	0.00	0.02
6	75.27	0.00	0.08	0.00	0.21	24.23	0.13	0.00	0.00	0.08
7	6.14	0.00	0.00	0.00	0.30	93.03	0.03	0.03	0.00	0.48
8	0.21	0.00	0.00	0.09	0.39	98.50	0.04	0.15	0.00	0.62
9	0.36	0.00	0.00	0.31	0.40	98.36	0.07	0.00	0.00	0.51
10	0.28	0.00	0.05	1.04	0.31	97.71	0.10	0.00	0.00	0.51
11	3.45	0.00	0.00	9.75	0.33	85.99	0.00	0.02	0.05	0.41
12	0.32	0.00	0.00	0.27	0.35	98.58	0.00	0.00	0.02	0.46
13	0.00	0.00	0.00	0.19	0.29	98.93	0.00	0.02	0.00	0.57
14	0.14	0.00	0.02	0.32	0.28	98.60	0.00	0.00	0.10	0.54
15	5.50	0.00	0.03	0.64	0.83	92.34	0.08	0.09	0.00	0.50
0	93.03	0.00	0.04	6.54	0.10	0.27	0.00	0.02	0.00	0.00
1	90.90	0.00	0.01	7.68	0.41	0.82	0.01	0.14	0.01	0.02
2	95.38	0.00	0.01	4.15	0.15	0.12	0.12	0.00	0.00	0.08
3	99.78	0.00	0.06	0.00	0.08	0.08	0.00	0.00	0.00	0.00
4	94.93	0.02	0.00	4.73	0.05	0.16	0.00	0.00	0.11	0.00
5	99.17	0.03	0.06	0.00	0.01	0.61	0.02	0.00	0.06	0.04
6	82.71	0.00	0.05	8.11	0.26	8.53	0.04	0.17	0.13	0.00
7	85.88	0.00	0.05	6.98	0.24	6.25	0.13	0.12	0.24	0.10
8	91.04	0.00	0.04	7.66	0.09	0.99	0.05	0.13	0.00	0.00
9	0.20	0.00	0.05	0.19	0.37	98.58	0.00	0.00	0.05	0.56
10	84.49	0.00	0.14	0.00	0.30	14.82	0.07	0.05	0.00	0.13
11	4.06	0.00	0.00	0.03	0.42	95.12	0.00	0.03	0.00	0.33
12	0.16	0.00	0.07	0.15	0.37	98.67	0.00	0.03	0.09	0.47
13	0.16	0.00	0.00	0.30	0.34	98.55	0.00	0.00	0.12	0.53
14	0.00	0.00	0.00	0.14	0.41	98.97	0.02	0.05	0.00	0.41
15	0.00	0.00	0.00	0.16	0.33	99.01	0.02	0.06	0.00	0.42

D.45 SS-316/Mo/V/Nd After 28 Days at 700°C

The SS-316/W/Nd assembly annealed for 28 days at 700°C bonded on the V/Nd interface but not the SS-316/Mo or Mo/V interfaces. Since the V/Nd interface

at this time and temperature was already well characterized, no WDS linescans were completed on it in this assembly.

D.46 SS-316/Mo/Nd After 28 Days at 700°C

The SS-316/Mo/Nd assembly annealed for 28 days at 700°C bonded on the Mo/Nd interface but not the SS-316/Mo interface. Compositional data (in at%) from WDS linescans across the Mo/Nd interface is given below.

Position	Si	V	W	Mo	Nd	Ni	Fe	Mn	Cr
0	0.49	0.00	0.01	0.17	98.33	0.07	0.28	0.65	0.00
1	0.13	0.00	0.01	0.17	98.88	0.00	0.34	0.46	0.00
2	0.26	0.00	0.03	0.11	98.69	0.00	0.35	0.56	0.00
3	0.25	0.00	0.03	0.18	98.63	0.00	0.36	0.56	0.00
4	0.15	0.06	0.01	91.78	7.94	0.00	0.05	0.02	0.00
5	0.11	0.00	0.01	98.86	0.93	0.05	0.04	0.00	0.00
6	0.16	0.06	0.00	63.73	35.30	0.10	0.25	0.31	0.11
7	0.16	0.00	0.00	97.52	2.21	0.00	0.08	0.04	0.00
8	0.15	0.00	0.01	98.72	0.96	0.06	0.06	0.04	0.00
9	0.10	0.02	0.00	99.37	0.35	0.00	0.10	0.07	0.00
10	0.08	0.00	0.02	99.41	0.27	0.14	0.05	0.03	0.00
11	0.10	0.00	0.02	99.53	0.23	0.01	0.03	0.00	0.08
12	0.10	0.03	0.04	99.49	0.28	0.00	0.01	0.06	0.00
13	0.16	0.02	0.03	99.29	0.39	0.03	0.08	0.00	0.02
14	0.95	0.05	0.01	98.68	0.18	0.00	0.07	0.06	0.01
15	0.08	0.08	0.00	99.54	0.12	0.00	0.09	0.04	0.04

D.47 SS-316/W/V/Nd After 28 Days at 700°C

The SS-316/W/V/Nd assembly annealed for 28 days at 700°C bonded on the V/Nd interface but not the SS-316/W or W/V interfaces. Since the V/Nd interface at this time and temperature was already well characterized, no WDS linescans were completed on it in this assembly.

D.48 SS-316/W/Nd After 28 Days at 700°C

The SS-316/W/Nd assembly annealed for 28 days at 700°C did not bond on the SS-316/W or W/Nd interfaces.

APPENDIX E: SUMMARY OF IRON INTERFACES

E.1 Fe/Nd After 28 Days at 550°C

The Fe/Nd assembly annealed for 28 days at 550°C crumbled significantly upon removal from the diffusion jig, leaving no interaction interface to examine.

E.2 Fe/V/Nd After 28 Days at 550°C

The Fe/V/Nd assembly annealed for 28 days at 550°C bonded on the V/Nd interface but not the Fe/V interface. Compositional data (in at%) from WDS linescans across the V/Nd interface is given below.

Position	Nd	Zr	Fe	V
0	0.44	0.00	0.08	99.48
1	0.36	0.00	0.20	99.45
2	1.00	0.00	0.27	98.73
3	1.17	0.00	0.24	98.59
4	0.48	0.00	0.05	99.48
5	0.21	0.00	0.06	99.73
6	0.34	0.00	0.09	99.58
7	0.47	0.00	0.16	99.37
8	4.81	0.00	3.65	91.54
9	12.64	0.00	7.19	80.18
10	16.47	0.00	4.47	79.06
11	46.35	0.00	3.62	50.03
12	79.55	0.00	5.32	15.13
13	87.96	0.00	6.29	5.75
14	91.95	0.00	5.51	2.54
15	85.07	0.00	5.97	8.97
16	90.05	0.00	6.39	3.55
17	91.66	0.00	5.82	2.53
18	95.07	0.00	2.87	2.07
19	96.21	0.00	2.29	1.50
20	97.06	0.00	0.69	2.25

E.3 Fe/Zr/V/Nd After 28 Days at 550°C

The Fe/Zr/V/Nd assembly annealed for 28 days at 550°C bonded on the Fe/Zr interface but not the Zr/V or V/Nd interfaces. Compositional data (in at%) from WDS linescans across the Fe/Zr interface is given below.

Position	Nd	Zr	Fe	V
0	0.17	99.33	0.50	0.00
1	0.10	99.32	0.57	0.02
2	0.07	99.29	0.63	0.01
3	0.06	99.21	0.67	0.06
4	0.30	98.07	1.42	0.21

5	0.23	98.04	1.51	0.21
6	0.53	97.73	1.67	0.07
7	0.39	98.18	1.37	0.06
8	0.05	98.26	1.68	0.02
9	0.03	75.45	24.52	0.00
10	0.27	98.27	1.40	0.06
11	0.07	98.28	1.63	0.01
12	0.04	95.33	4.63	0.00
13	0.00	63.24	36.76	0.00
14	0.04	13.22	86.74	0.00
15	0.09	3.22	96.68	0.01
0	0.33	98.09	1.12	0.47
1	0.08	99.31	0.52	0.09
2	0.04	99.25	0.61	0.10
3	0.10	99.35	0.51	0.05
4	0.15	99.25	0.58	0.02
5	0.06	99.18	0.73	0.03
6	0.10	99.03	0.83	0.05
7	0.21	98.74	1.01	0.05
8	0.44	97.91	1.61	0.04
9	0.73	96.88	2.30	0.10
10	1.91	94.07	3.73	0.29
11	0.84	96.37	2.80	0.00
12	0.47	86.03	13.41	0.09
13	0.24	54.97	44.72	0.07
14	1.90	94.51	3.43	0.17
15	0.74	96.22	3.00	0.05
16	0.34	75.80	23.74	0.12
17	0.19	40.67	59.08	0.06
18	0.13	10.22	89.63	0.02
19	0.32	2.96	96.56	0.17
20	0.50	1.78	97.51	0.22

E.4 Fe/Zr/Nd After 28 Days at 550°C

The Fe/Zr/Nd assembly annealed for 28 days at 550°C bonded on the Zr/Nd interface but not the Fe/Zr interface. Compositional data (in at%) from WDS linescans across the Zr/Nd interface is given below.

Position	Nd	Zr	Fe	V
0	0.51	98.88	0.61	0.00
1	0.49	98.69	0.81	0.01
2	0.50	98.96	0.54	0.00
3	0.42	99.41	0.16	0.01
4	0.35	99.53	0.11	0.01
5	0.45	99.50	0.05	0.00
6	0.51	99.45	0.04	0.00
7	0.54	99.44	0.02	0.00
8	0.68	99.14	0.18	0.00

9	1.51	98.10	0.38	0.00
10	14.63	84.90	0.46	0.01
11	67.65	31.70	0.65	0.00
12	99.44	0.08	0.46	0.01
13	98.32	1.23	0.45	0.00
14	98.19	1.34	0.41	0.06
15	99.53	0.09	0.39	0.00
16	99.50	0.13	0.37	0.00
17	99.49	0.05	0.45	0.02
18	99.58	0.05	0.35	0.03
19	99.63	0.01	0.36	0.00
20	99.58	0.00	0.42	0.00

E.5 Fe/Ti/V/Nd After 28 Days at 550°C

The Fe/Ti/V/Nd assembly annealed for 28 days at 550°C bonded on the Fe/Ti and V/Nd interfaces but not the Ti/V interface. Compositional data (in at%) from WDS linescans across the Fe/Ti and V/Nd interfaces is given below.

Position	Ta	Ti	V	Fe	Nd
0	0.00	0.80	0.18	98.98	0.03
1	0.00	0.84	0.01	99.12	0.03
2	0.00	0.78	0.00	99.18	0.04
3	0.00	1.12	0.03	98.83	0.02
4	0.00	1.95	0.02	97.99	0.05
5	0.00	1.08	0.02	98.86	0.04
6	0.00	1.52	0.02	98.38	0.09
7	0.00	3.68	0.03	96.18	0.11
8	0.00	2.25	0.05	97.62	0.08
9	0.00	4.20	0.09	95.63	0.09
10	0.00	1.98	0.01	97.97	0.04
11	0.00	19.12	0.10	80.71	0.07
12	0.00	39.19	0.13	60.59	0.09
13	0.00	59.98	0.20	39.69	0.13
14	0.00	77.11	0.37	22.40	0.12
15	0.00	85.24	0.31	14.41	0.04
0	0.00	0.90	0.02	99.05	0.03
1	0.00	1.21	0.01	98.75	0.02
2	0.00	1.25	0.02	98.71	0.02
3	0.00	1.47	0.02	98.46	0.05
4	0.00	1.28	0.03	98.69	0.00
5	0.00	1.28	0.05	98.67	0.00
6	0.00	1.50	0.00	98.48	0.02
7	0.00	1.88	0.04	98.07	0.01
8	0.00	5.69	0.04	94.25	0.02
9	0.00	88.43	0.26	11.29	0.03
10	0.00	98.74	0.26	0.98	0.03
11	0.00	98.93	0.30	0.74	0.03
12	0.00	99.02	0.30	0.64	0.03

13	0.00	98.95	0.34	0.56	0.15
14	0.00	99.10	0.32	0.54	0.04
15	0.00	95.38	2.39	1.48	0.76
0	0.00	0.00	98.21	0.10	1.69
1	0.00	0.00	97.64	1.08	1.28
2	0.00	0.00	98.43	0.07	1.50
3	0.00	0.06	97.20	0.09	2.65
4	0.00	0.09	96.65	0.13	3.14
5	0.00	0.00	96.89	0.07	3.04
6	0.00	0.00	99.20	0.21	0.59
7	0.00	0.10	96.53	0.91	2.46
8	0.00	0.00	77.39	5.53	17.08
9	0.00	0.00	39.99	4.63	55.39
10	0.00	0.12	93.01	1.37	5.50
11	0.00	0.03	2.53	0.35	97.10
12	0.00	0.00	2.19	0.45	97.37
13	0.00	0.00	1.29	0.38	98.34
14	0.00	0.00	1.11	0.31	98.59
15	0.00	0.00	0.86	0.35	98.79

E.6 Fe/Ti/Nd After 28 Days at 550°C

The Fe/Ti/Nd assembly annealed for 28 days at 550°C bonded on the Ti/Nd interface but not the Fe/Ti interface. Compositional data (in at%) from WDS linescans across the Ti/Nd interface is given below.

Position	Ta	Ti	V	Fe	Nd
0	0.00	1.98	0.00	0.42	97.60
1	0.00	3.11	0.04	0.42	96.44
2	0.00	4.28	0.00	0.35	95.36
3	0.00	8.90	0.04	0.41	90.66
4	0.00	65.12	0.26	0.66	33.96
5	0.00	95.16	0.27	0.23	4.34
6	0.00	97.98	0.27	0.09	1.66
7	0.00	98.86	0.23	0.04	0.87
8	0.00	99.52	0.26	0.01	0.22
9	0.00	97.78	0.28	0.06	1.88
10	0.00	98.84	0.25	0.08	0.83
11	0.00	99.04	0.26	0.08	0.62
12	0.00	98.04	0.25	0.11	1.60
13	0.00	92.23	0.27	0.52	6.98
14	0.00	88.57	0.23	0.23	10.97
15	0.00	99.03	0.28	0.11	0.59
0	0.00	1.42	0.00	0.34	98.24
1	0.00	1.45	0.01	0.36	98.18
2	0.00	2.55	0.02	4.55	92.87
3	0.00	3.75	0.00	0.42	95.84
4	0.00	5.05	0.00	0.41	94.55
5	0.00	16.84	0.09	0.85	82.22
6	0.00	4.68	0.00	0.39	94.93
7	0.00	11.90	0.03	0.58	87.50
8	0.00	39.77	0.04	0.71	59.48

9	0.00	79.06	0.24	0.46	20.24
10	0.00	98.35	0.28	0.32	1.06
11	0.00	99.03	0.25	0.06	0.66
12	0.00	99.26	0.26	0.08	0.40
13	0.00	99.42	0.29	0.02	0.28
14	0.00	99.39	0.26	0.12	0.23
15	0.00	98.89	0.29	0.05	0.77

E.7 Fe/Ta/V/Nd After 28 Days at 550°C

The Fe/Ta/V/Nd assembly annealed for 28 days at 550°C bonded on the V/Nd interface but not the Fe/Ta or Ta/V interfaces. Since the V/Nd interface at this time and temperature was already well characterized, no WDS linescans were completed on it in this assembly.

E.8 Fe/Ta/Nd After 28 Days at 550°C

The Fe/Ta/Nd assembly annealed for 28 days at 550°C did not bond on the Fe/Ta or Ta/Nd interfaces.

E.9 Fe/Mo/V/Nd After 28 Days at 550°C

The Fe/Mo/V/Nd assembly annealed for 28 days at 550°C bonded on the V/Nd interface but not the Fe/Mo or Mo/V interfaces. Since the V/Nd interface at this time and temperature was already well characterized, no WDS linescans were completed on it in this assembly.

E.10 Fe/Mo/Nd After 28 Days at 550°C

The Fe/Mo/Nd assembly annealed for 28 days at 550°C bonded on the Mo/Nd interface but not the Fe/Mo interface. Compositional data (in at%) from WDS linescans across the Mo/Nd interface is given below.

Position	W	Nd	Mo	Fe	V
0	0.00	90.94	8.70	0.29	0.08
1	0.00	40.11	59.54	0.31	0.03
2	0.01	8.56	91.27	0.16	0.00
3	0.02	1.36	98.55	0.07	0.00
4	0.05	0.25	99.66	0.02	0.03
5	0.02	0.13	99.81	0.04	0.01
6	0.00	0.20	99.74	0.05	0.01
7	0.05	0.12	99.83	0.00	0.00
8	0.02	0.06	99.90	0.03	0.00

9	0.03	0.14	99.76	0.05	0.03
10	0.03	0.21	99.73	0.03	0.00
11	0.03	0.07	99.88	0.01	0.02
12	0.00	0.06	99.91	0.03	0.00
13	0.01	0.10	99.85	0.04	0.00
14	0.01	0.05	99.88	0.02	0.04
15	0.03	0.13	99.75	0.10	0.00
0	0.03	98.31	1.30	0.34	0.03
1	0.06	50.30	48.95	0.69	0.00
2	0.01	5.57	94.19	0.18	0.04
3	0.02	0.48	99.42	0.07	0.01
4	0.00	0.31	99.69	0.00	0.00
5	0.03	0.23	99.65	0.00	0.10
6	0.00	0.23	99.74	0.03	0.00
7	0.00	0.33	99.65	0.02	0.01
8	0.02	0.36	99.56	0.06	0.00
9	0.04	0.23	99.70	0.02	0.00
10	0.01	0.15	99.83	0.02	0.00
11	0.00	0.09	99.88	0.03	0.00
12	0.00	0.13	99.83	0.04	0.00
13	0.02	0.08	99.88	0.01	0.00
14	0.04	0.10	99.78	0.04	0.04
15	0.00	0.07	99.85	0.08	0.00
0	0.00	44.80	54.69	0.41	0.09
1	0.03	39.70	59.90	0.26	0.13
2	0.00	9.80	90.00	0.18	0.02
3	0.05	0.28	99.60	0.07	0.00
4	0.01	0.29	99.68	0.03	0.00
5	0.01	0.25	99.71	0.01	0.02
6	0.01	0.22	99.77	0.00	0.00
7	0.00	0.18	99.82	0.00	0.00
8	0.03	0.16	99.76	0.04	0.01
9	0.00	0.10	99.84	0.03	0.04
10	0.01	0.10	99.86	0.03	0.01
11	0.02	0.06	99.93	0.00	0.00
12	0.00	0.10	99.90	0.00	0.00
13	0.02	0.08	99.88	0.00	0.03
14	0.02	0.05	99.75	0.00	0.17
15	0.01	0.05	99.85	0.02	0.07

E.11 Fe/W/V/Nd After 28 Days at 550°C

The Fe/W/V/Nd assembly annealed for 28 days at 550°C bonded on the V/Nd interface but not the Fe/W or W/V interfaces. Compositional data (in at%) from WDS linescans across the V/Nd interface is given below.

Position	W	Nd	Mo	Fe	V
0	0.00	0.18	0.01	0.05	99.77
1	0.00	0.05	0.00	0.00	99.94
2	0.02	6.49	0.01	0.47	93.01
3	0.01	2.53	0.00	0.20	97.26
4	0.02	2.53	0.00	0.49	96.96

5	0.05	32.75	0.00	3.35	63.85
6	0.09	90.84	0.01	0.86	8.20
7	0.04	94.83	0.00	0.60	4.53
8	0.00	95.77	0.00	0.52	3.71
9	0.00	96.30	0.00	0.48	3.22
10	0.09	95.75	0.00	1.15	3.01
11	0.33	95.50	0.02	1.86	2.31
12	0.05	96.20	0.00	1.46	2.29
13	0.14	96.68	0.00	1.47	1.71
14	0.06	96.71	0.00	1.12	2.12
15	0.21	96.10	0.01	1.48	2.19

E.12 Fe/W/Nd After 28 Days at 550°C

The Fe/W/Nd assembly annealed for 28 days at 550°C bonded on the W/Nd interface but not the Fe/W interface. Compositional data (in at%) from WDS linescans across the W/Nd interface is given below.

Position	W	Nd	Mo	Fe	V
0	1.25	97.89	0.01	0.84	0.03
1	2.21	96.63	0.02	1.12	0.03
2	0.04	99.50	0.00	0.45	0.00
3	0.00	99.66	0.00	0.32	0.03
4	0.02	99.66	0.00	0.29	0.04
5	0.04	99.61	0.01	0.35	0.00
6	0.05	99.55	0.00	0.40	0.00
7	8.99	90.60	0.00	0.36	0.04
8	47.36	52.34	0.00	0.30	0.00
9	98.63	1.17	0.00	0.20	0.00
10	98.77	1.23	0.00	0.00	0.00
11	99.23	0.75	0.00	0.03	0.00
12	99.47	0.46	0.00	0.07	0.00
13	99.35	0.49	0.00	0.16	0.00
14	99.48	0.43	0.00	0.07	0.02
15	99.71	0.29	0.00	0.00	0.00
0	0.02	99.59	0.04	0.30	0.05
1	0.01	99.48	0.03	0.49	0.00
2	0.12	99.51	0.02	0.36	0.00
3	0.00	99.72	0.00	0.28	0.00
4	0.07	99.57	0.00	0.36	0.01
5	0.19	99.43	0.00	0.39	0.00
6	9.55	90.00	0.00	0.43	0.02
7	12.34	87.24	0.00	0.41	0.01
8	97.48	2.32	0.00	0.14	0.06
9	96.69	3.23	0.00	0.08	0.01
10	98.57	1.30	0.00	0.14	0.00
11	98.25	1.67	0.00	0.08	0.00
12	94.42	5.43	0.00	0.03	0.13
13	91.79	8.10	0.00	0.05	0.06
14	96.90	2.86	0.00	0.20	0.04
15	97.43	2.33	0.00	0.25	0.00
0	0.00	99.60	0.00	0.37	0.03

1	0.04	99.60	0.00	0.35	0.00
2	0.00	99.47	0.17	0.35	0.02
3	0.03	99.66	0.00	0.31	0.00
4	0.05	99.70	0.00	0.25	0.00
5	0.61	99.09	0.00	0.25	0.05
6	2.36	97.25	0.04	0.35	0.00
7	1.26	98.35	0.01	0.32	0.07
8	53.33	46.39	0.04	0.19	0.05
9	91.64	8.11	0.00	0.19	0.07
10	98.93	1.03	0.00	0.04	0.00
11	99.34	0.51	0.00	0.14	0.00
12	99.74	0.26	0.00	0.00	0.00
13	99.44	0.47	0.00	0.07	0.02
14	99.70	0.25	0.00	0.05	0.00
15	99.63	0.28	0.00	0.09	0.00

E.13 Fe/Nd After 56 Days at 550°C

The Fe/Nd assembly annealed for 56 days at 550°C crumbled significantly upon removal from the diffusion jig, leaving no interaction interface to examine.

E.14 Fe/V/Nd After 56 Days at 550°C

The Fe/V/Nd assembly annealed for 56 days at 550°C bonded on the V/Nd interface but not the Fe/V interface. Compositional data (in at%) from WDS linescans across the V/Nd interface is given below.

Position	Nd	Zr	Fe	V
0	98.30	0.00	0.39	1.31
1	97.38	0.00	0.48	2.15
2	97.05	0.02	0.50	2.44
3	96.08	0.02	0.58	2.84
4	96.74	0.00	0.50	2.76
5	96.65	0.00	0.50	2.85
6	96.06	0.03	0.46	3.45
7	91.04	0.02	1.29	7.65
8	67.05	0.00	5.11	27.84
9	32.27	0.01	6.67	61.06
10	11.18	0.00	4.98	83.84
11	2.09	0.00	2.15	95.76
12	1.15	0.00	0.49	98.37
13	2.38	0.00	2.40	95.23
14	1.15	0.00	0.67	98.18
15	1.20	0.00	0.23	98.57

E.15 Fe/Zr/V/Nd After 56 Days at 550°C

The Fe/Zr/V/Nd assembly annealed for 56 days at 550°C bonded on the Fe/Zr and V/Nd interfaces but not the Zr/V interface. Compositional data (in at%) from WDS linescans across the Fe/Zr and V/Nd interfaces is given below.

Position	Nd	Zr	Fe	V
0	98.79	0.00	0.31	0.90
1	98.76	0.00	0.31	0.93
2	98.38	0.00	0.45	1.18
3	98.10	0.00	0.40	1.50
4	97.89	0.00	0.34	1.77
5	97.14	0.04	0.51	2.32
6	96.48	0.00	0.46	3.06
7	95.80	0.00	0.34	3.86
8	89.82	0.00	0.29	9.89
9	52.28	0.00	0.17	47.55
10	22.79	0.00	0.10	77.11
11	7.10	0.00	0.06	92.84
12	7.56	0.00	0.04	92.40
13	7.68	0.00	0.07	92.26
14	6.71	0.00	0.01	93.29
15	3.06	0.00	0.03	96.92
0	0.06	98.92	1.00	0.02
1	0.02	98.84	1.11	0.03
2	0.05	98.71	1.21	0.03
3	0.02	98.49	1.45	0.04
4	0.03	98.38	1.55	0.04
5	0.03	98.07	1.88	0.02
6	0.06	97.64	2.29	0.01
7	0.07	94.52	5.39	0.02
8	0.00	4.30	95.69	0.02
9	0.03	1.24	98.73	0.01
10	0.01	0.40	99.57	0.02
11	0.01	0.45	99.52	0.03
12	0.03	0.72	99.21	0.03
13	0.02	0.68	99.25	0.04
14	0.01	0.50	99.47	0.02
15	0.02	0.16	99.80	0.01
0	0.04	98.36	1.53	0.07
1	0.04	98.29	1.54	0.14
2	0.06	98.30	1.48	0.16
3	0.08	98.16	1.68	0.08
4	0.05	98.06	1.84	0.05
5	0.03	97.74	2.21	0.02
6	0.00	87.92	12.08	0.00
7	0.03	28.92	71.03	0.02
8	0.03	27.54	72.41	0.02
9	0.00	0.24	99.76	0.01
10	0.03	0.17	99.77	0.03
11	0.01	0.25	99.75	0.00
12	0.02	0.16	99.82	0.00

13	0.01	0.08	99.90	0.01
14	0.01	0.09	99.88	0.02
15	0.02	0.05	99.91	0.02

E.16 Fe/Zr/Nd After 56 Days at 550°C

The Fe/Zr/Nd assembly annealed for 56 days at 550°C bonded on the Zr/Nd interface but not the Fe/Zr interface. Compositional data (in at%) from WDS linescans across the Zr/Nd interface is given below.

Position	Nd	Zr	Fe	V
0	0.41	99.41	0.19	0.00
1	0.43	99.36	0.19	0.02
2	0.56	99.29	0.14	0.01
3	0.72	98.98	0.30	0.00
4	7.12	91.38	1.47	0.03
5	20.37	77.72	1.91	0.00
6	47.29	50.55	2.16	0.00
7	82.39	16.07	1.50	0.03
8	98.77	0.69	0.54	0.00
9	99.43	0.15	0.41	0.00
10	99.53	0.07	0.39	0.02
11	99.41	0.09	0.50	0.00
12	99.36	0.13	0.51	0.00
13	99.38	0.08	0.51	0.02
14	99.41	0.10	0.47	0.03
15	99.45	0.08	0.47	0.00

E.17 Fe/Ti/V/Nd After 56 Days at 550°C

The Fe/Ti/V/Nd assembly annealed for 56 days at 550°C bonded on the V/Nd interface but not the Fe/Ti or Ti/V interfaces. Compositional data (in at%) from WDS linescans across the V/Nd interface is given below.

Position	Ta	Ti	V	Fe	Nd
0	0.00	0.00	99.63	0.01	0.35
1	0.00	0.12	83.59	2.80	13.49
2	0.00	0.03	61.86	3.94	34.17
3	0.00	0.00	7.19	0.69	92.13
4	0.00	0.00	4.38	0.60	95.02
5	0.00	0.00	2.71	1.12	96.17
6	0.00	0.00	2.18	0.44	97.38
7	0.00	0.00	1.64	0.67	97.68
8	0.00	0.00	1.47	0.67	97.87
9	0.00	0.01	1.34	0.79	97.86
10	0.00	0.00	1.36	1.07	97.57

11	0.00	0.09	1.03	1.75	97.13
12	0.00	0.00	0.65	0.47	98.89
13	0.00	0.00	0.44	0.35	99.21
14	0.00	0.07	0.94	1.41	97.57
15	0.00	0.00	0.60	0.37	99.04

E.18 Fe/Ti/Nd After 56 Days at 550°C

The Fe/Ti/Nd assembly annealed for 56 days at 550°C bonded on the Ti/Nd interface but not the Fe/Ti interface. Compositional data (in at%) from WDS linescans across the Ti/Nd interface is given below.

Position	Ta	Ti	V	Fe	Nd
0	0.00	0.82	0.00	0.37	98.81
1	0.00	1.25	0.00	0.39	98.36
2	0.00	1.67	0.02	0.34	97.97
3	0.00	2.49	0.10	0.28	97.13
4	0.00	84.12	0.28	7.25	8.35
5	0.00	99.35	0.30	0.09	0.25
6	0.00	92.59	0.30	4.09	3.03
7	0.00	99.06	0.25	0.44	0.25
8	0.00	99.41	0.26	0.08	0.25
9	0.00	99.55	0.26	0.04	0.16
10	0.00	99.51	0.29	0.04	0.17
11	0.00	99.52	0.29	0.07	0.12
12	0.00	99.53	0.26	0.13	0.09
13	0.00	99.54	0.27	0.08	0.12
14	0.00	97.56	0.28	0.30	1.86
15	0.00	89.10	0.22	1.19	9.49
0	0.00	2.13	0.00	0.41	97.46
1	0.00	2.74	0.01	0.46	96.79
2	0.00	7.43	0.00	0.70	91.87
3	0.00	8.25	0.02	2.36	89.37
4	0.00	24.82	0.12	2.06	73.00
5	0.00	8.11	0.06	0.46	91.37
6	0.00	8.12	0.04	0.40	91.44
7	0.00	44.01	0.15	5.75	50.09
8	0.00	82.38	0.23	14.53	2.87
9	0.00	94.39	0.25	4.75	0.61
10	0.00	97.81	0.26	0.56	1.37
11	0.00	95.87	0.29	1.77	2.08
12	0.00	98.02	0.26	0.83	0.89
13	0.00	99.60	0.26	0.05	0.09
14	0.00	99.53	0.26	0.03	0.18
15	0.00	99.57	0.26	0.07	0.10
0	0.00	99.22	0.27	0.49	0.03
1	0.00	98.90	0.26	0.78	0.06
2	0.00	98.63	0.25	1.09	0.03
3	0.00	95.71	0.30	3.95	0.04
4	0.00	12.43	0.03	87.45	0.09
5	0.00	2.25	0.00	97.72	0.03
6	0.00	2.24	0.03	97.70	0.04

7	0.00	1.55	0.02	98.40	0.03
8	0.00	1.42	0.01	98.54	0.03
9	0.00	1.18	0.02	98.80	0.01
10	0.00	1.08	0.02	98.87	0.02
11	0.00	1.07	0.04	98.88	0.01
12	0.00	0.87	0.02	99.12	0.00
13	0.00	1.15	0.01	98.82	0.02
14	0.00	1.07	0.01	98.90	0.02
15	0.00	0.93	0.01	99.01	0.05
0	0.00	99.12	0.27	0.59	0.02
1	0.00	98.84	0.29	0.87	0.00
2	0.00	96.05	0.36	3.56	0.04
3	0.00	95.44	0.36	4.15	0.04
4	0.00	2.55	0.01	97.42	0.03
5	0.00	1.98	0.02	97.96	0.04
6	0.00	1.83	0.05	98.06	0.06
7	0.00	1.48	0.23	98.29	0.00
8	0.00	1.21	0.00	98.79	0.00
9	0.00	1.14	0.01	98.82	0.03
10	0.00	1.08	0.00	98.89	0.03
11	0.00	0.88	0.00	99.10	0.02
12	0.00	1.15	0.00	98.85	0.00
13	0.00	1.09	0.01	98.87	0.02
14	0.00	1.00	0.01	98.99	0.00
15	0.00	0.88	0.04	99.07	0.01

E.19 Fe/Ta/V/Nd After 56 Days at 550°C

The Fe/Ta/V/Nd assembly annealed for 56 days at 550°C bonded on the V/Nd interface but not the Fe/Ta or Ta/V interfaces. Since the V/Nd interface at this time and temperature was already well characterized, no WDS linescans were completed on it in this assembly.

E.20 Fe/Ta/Nd After 56 Days at 550°C

The Fe/Ta/Nd assembly annealed for 56 days at 550°C did not bond on the Fe/Ta or Ta/Nd interfaces.

E.21 Fe/Mo/V/Nd After 56 Days at 550°C

The Fe/Mo/V/Nd assembly annealed for 56 days at 550°C bonded on the V/Nd interface but not the Fe/Mo or Mo/V interfaces. Since the V/Nd interface at this time and temperature was already well characterized, no WDS linescans were completed on it in this assembly.

E.22 Fe/Mo/Nd After 56 Days at 550°C

The Fe/Mo/Nd assembly annealed for 56 days at 550°C did not bond on the Fe/Mo or Mo/Nd interfaces.

E.23 Fe/W/V/Nd After 56 Days at 550°C

The Fe/W/V/Nd assembly annealed for 56 days at 550°C bonded on the V/Nd interface but not the Fe/W or W/V interfaces. Since the V/Nd interface at this time and temperature was already well characterized, no WDS linescans were completed on it in this assembly.

E.24 Fe/W/Nd After 56 Days at 550°C

The Fe/W/Nd assembly annealed for 56 days at 550°C bonded on the W/Nd interface but not the Fe/W interface. Compositional data (in at%) from WDS linescans across the W/Nd interface is given below.

Position	W	Nd	Mo	Fe	V
0	0.13	99.32	0.00	0.51	0.04
1	0.06	99.61	0.00	0.33	0.00
2	0.03	99.34	0.03	0.57	0.03
3	0.00	99.60	0.02	0.38	0.00
4	0.07	99.58	0.03	0.33	0.00
5	0.48	99.18	0.04	0.30	0.00
6	37.88	61.75	0.07	0.28	0.02
7	92.65	7.35	0.00	0.00	0.00
8	98.81	1.15	0.00	0.00	0.04
9	99.06	0.91	0.00	0.03	0.00
10	99.19	0.68	0.00	0.11	0.02
11	99.37	0.53	0.00	0.00	0.11
12	99.64	0.24	0.00	0.01	0.11
13	99.72	0.19	0.00	0.08	0.02
14	99.69	0.31	0.00	0.00	0.00
15	99.70	0.23	0.00	0.08	0.00
0	99.85	0.13	0.00	0.02	0.00
1	99.58	0.41	0.00	0.00	0.02
2	99.65	0.35	0.00	0.00	0.00
3	99.45	0.43	0.00	0.07	0.06
4	99.40	0.53	0.00	0.00	0.08
5	99.21	0.63	0.00	0.05	0.12
6	98.78	1.13	0.00	0.09	0.00
7	97.38	2.57	0.00	0.06	0.00
8	1.11	98.53	0.05	0.32	0.00
9	8.17	91.43	0.03	0.36	0.00
10	0.03	99.50	0.00	0.47	0.00

11	0.00	99.57	0.02	0.41	0.00
12	0.00	99.50	0.03	0.39	0.08
13	0.06	99.56	0.04	0.30	0.03
14	0.05	99.67	0.02	0.25	0.01
15	0.10	99.50	0.00	0.41	0.00
0	99.59	0.25	0.00	0.02	0.13
1	99.70	0.17	0.00	0.00	0.13
2	99.57	0.29	0.00	0.14	0.00
3	99.43	0.38	0.00	0.16	0.03
4	98.95	0.97	0.00	0.09	0.00
5	98.53	1.33	0.00	0.09	0.06
6	98.76	1.12	0.00	0.02	0.10
7	92.24	7.71	0.00	0.05	0.00
8	51.07	48.64	0.00	0.26	0.04
9	4.62	95.01	0.04	0.33	0.00
10	0.03	99.65	0.00	0.32	0.00
11	0.09	99.55	0.00	0.35	0.01
12	0.00	99.70	0.00	0.31	0.00
13	0.00	99.70	0.01	0.30	0.00
14	0.03	99.23	0.05	0.37	0.32
15	0.11	98.47	0.00	0.38	1.04

E.25 Fe/Nd After 28 Days at 625°C

The Fe/Nd assembly annealed for 28 days at 625°C crumbled significantly upon removal from the diffusion jig, leaving no interaction interface to examine.

E.26 Fe/V/Nd After 28 Days at 625°C

The Fe/V/Nd assembly annealed for 28 days at 625°C bonded on the V/Nd interface but not the Fe/V interface. Compositional data (in at%) from WDS linescans across the V/Nd interface is given below.

Position	Nd	Zr	Fe	V
0	98.19	0.00	0.43	1.38
1	98.08	0.00	0.39	1.53
2	95.13	0.00	0.45	4.43
3	94.13	0.00	0.47	5.41
4	91.00	0.00	0.48	8.53
5	63.96	0.00	0.69	35.35
6	33.51	0.00	0.80	65.70
7	14.62	0.00	0.64	84.74
8	4.17	0.00	0.47	95.36
9	0.84	0.00	0.30	98.87
10	0.46	0.01	0.11	99.42
11	0.43	0.00	0.11	99.47
12	0.45	0.00	0.10	99.45
13	0.22	0.00	0.04	99.74
14	0.20	0.00	0.05	99.75
15	0.20	0.00	0.09	99.71

E.27 Fe/Zr/V/Nd After 28 Days at 625°C

The Fe/Zr/V/Nd assembly annealed for 28 days at 625°C bonded on the Fe/Zr, Zr/V, and V/Nd interfaces. Compositional data (in at%) from WDS linescans across each of these interfaces is given below.

Position	Nd	Zr	Fe	V
0	0.02	0.02	99.96	0.00
1	0.04	0.02	99.94	0.01
2	0.03	0.02	99.94	0.01
3	0.03	0.03	99.94	0.00
4	0.01	0.03	99.96	0.01
5	0.03	0.11	99.86	0.00
6	0.05	0.96	99.00	0.00
7	0.05	4.41	95.53	0.01
8	0.07	20.77	79.12	0.03
9	0.08	41.20	58.70	0.02
10	0.12	76.35	23.51	0.03
11	0.05	96.37	3.56	0.02
12	0.04	98.55	1.41	0.00
13	0.05	98.73	1.20	0.03
14	0.00	98.92	1.08	0.00
15	0.07	98.95	0.97	0.01
0	0.04	0.66	99.29	0.01
1	0.03	0.85	99.12	0.00
2	0.07	11.30	88.62	0.01
3	0.09	35.44	64.42	0.05
4	0.13	65.27	34.58	0.02
5	0.13	90.68	9.16	0.03
6	0.16	97.18	2.67	0.00
7	0.12	98.18	1.68	0.02
8	0.13	98.35	1.49	0.03
9	0.07	98.72	1.21	0.00
10	0.05	98.99	0.96	0.00
11	0.05	99.01	0.94	0.00
12	0.04	99.09	0.87	0.00
13	0.05	99.14	0.80	0.01
14	0.03	99.13	0.84	0.00
15	0.05	98.69	1.24	0.02
0	0.12	98.34	0.14	1.40
1	0.14	95.53	0.06	4.27
2	0.11	96.43	0.08	3.39
3	0.15	96.63	0.09	3.14
4	0.12	96.05	0.12	3.72
5	0.09	72.96	0.17	26.78
6	0.09	37.29	0.10	62.51
7	0.07	13.20	0.04	86.69
8	0.03	4.58	0.05	95.34
9	0.07	0.08	0.02	99.83
10	0.07	0.05	0.04	99.84
11	0.12	0.02	0.05	99.81
12	0.07	0.06	0.04	99.84

13	0.07	0.03	0.05	99.85
14	0.15	0.05	0.02	99.78
15	0.16	0.02	0.03	99.78
0	0.11	97.94	0.05	1.90
1	0.11	97.42	0.08	2.39
2	0.18	96.21	0.13	3.48
3	0.19	95.80	0.11	3.90
4	0.16	92.24	0.07	7.53
5	0.16	74.94	0.08	24.82
6	0.11	35.57	0.05	64.27
7	0.10	11.41	0.04	88.45
8	0.08	9.05	0.07	90.81
9	0.05	0.44	0.06	99.46
10	0.09	0.89	0.24	98.77
11	0.13	1.69	0.65	97.53
12	0.08	0.61	0.08	99.23
13	0.10	0.89	0.25	98.76
14	0.13	1.52	0.58	97.77
15	0.18	1.97	0.56	97.29
0	0.20	98.93	0.05	0.83
1	0.18	98.61	0.03	1.18
2	0.15	98.33	0.07	1.46
3	0.15	96.27	0.02	3.56
4	0.19	71.41	0.19	28.22
5	0.16	40.39	0.15	59.30
6	0.12	13.17	0.12	86.60
7	0.13	8.85	0.11	90.91
8	0.11	0.12	0.04	99.72
9	0.13	0.38	0.05	99.44
10	0.18	1.17	0.05	98.61
11	0.25	1.95	0.09	97.71
12	0.13	0.29	0.04	99.54
13	0.21	1.53	0.07	98.18
14	0.24	1.93	0.09	97.74
15	0.27	2.08	0.10	97.55
0	0.08	99.13	0.03	0.76
1	0.09	98.73	0.11	1.07
2	0.18	98.32	0.13	1.37
3	0.12	97.94	0.12	1.83
4	0.07	92.42	0.07	7.44
5	0.06	59.53	0.04	40.38
6	0.04	31.18	0.04	68.74
7	0.04	7.42	0.02	92.52
8	0.06	3.29	0.03	96.62
9	0.04	0.23	0.01	99.72
10	0.03	14.64	0.05	85.27
11	0.04	0.76	0.03	99.17
12	0.03	0.28	0.02	99.67
13	0.04	0.42	0.04	99.51
14	0.06	0.41	0.02	99.51
15	0.06	0.28	0.05	99.61
0	1.30	0.02	0.30	98.38
1	2.65	0.02	0.64	96.69

2	4.80	0.01	1.08	94.11
3	5.20	0.01	1.22	93.57
4	5.23	0.00	1.13	93.65
5	4.38	0.00	1.43	94.20
6	7.01	0.01	1.95	91.02
7	22.29	0.00	2.49	75.22
8	49.97	0.01	2.52	47.49
9	77.27	0.02	2.07	20.64
10	95.67	0.02	1.91	2.41
11	96.34	0.01	1.74	1.91
12	96.18	0.00	1.68	2.14
13	96.33	0.06	1.33	2.28
14	97.51	0.06	0.48	1.94
15	97.58	0.00	0.46	1.95

E.28 Fe/Zr/Nd After 28 Days at 625°C

The Fe/Zr/Nd assembly annealed for 28 days at 625°C bonded on the Fe/Zr and Zr/Nd interfaces. Compositional data (in at%) from WDS linescans across both of these interfaces is given below.

Position	Nd	Zr	Fe	V
0	99.61	0.11	0.27	0.01
1	69.69	29.91	0.40	0.00
2	54.85	44.61	0.52	0.01
3	37.51	61.90	0.60	0.00
4	22.87	76.38	0.74	0.01
5	11.37	87.92	0.68	0.02
6	8.14	91.28	0.58	0.00
7	22.61	76.65	0.74	0.00
8	10.55	88.79	0.63	0.03
9	0.69	99.27	0.04	0.00
10	0.27	99.64	0.08	0.01
11	0.25	99.69	0.06	0.00
12	0.30	99.68	0.01	0.02
13	0.27	99.70	0.03	0.00
14	0.27	99.68	0.04	0.01
15	0.31	99.63	0.06	0.00
0	69.27	29.31	1.41	0.01
1	59.09	38.69	2.21	0.01
2	39.93	57.37	2.70	0.01
3	25.90	71.92	2.15	0.03
4	17.70	80.50	1.80	0.00
5	12.60	85.83	1.56	0.01
6	6.69	92.48	0.83	0.00
7	19.49	78.74	1.77	0.00
8	3.98	95.55	0.47	0.00
9	0.80	99.00	0.20	0.00
10	0.33	99.58	0.07	0.01
11	0.26	99.64	0.07	0.03
12	0.20	99.78	0.02	0.00
13	0.20	99.79	0.01	0.00
14	0.18	99.79	0.02	0.00

15	0.19	99.77	0.04	0.00
0	0.23	98.05	1.71	0.01
1	0.17	97.42	2.41	0.00
2	0.20	93.02	6.76	0.03
3	0.17	72.52	27.31	0.01
4	0.25	42.43	57.33	0.00
5	0.20	81.28	18.52	0.01
6	0.33	5.79	93.88	0.00
7	0.44	2.16	97.37	0.03
8	0.56	2.51	96.90	0.03
9	1.84	3.12	95.01	0.03
10	3.03	3.90	93.04	0.04
11	1.02	2.57	96.38	0.04
12	2.48	3.80	93.68	0.04
13	0.47	0.51	99.02	0.01
14	0.35	0.20	99.45	0.00
0	0.15	97.77	2.08	0.00
1	0.18	83.01	16.82	0.00
2	0.21	62.08	37.69	0.02
3	0.29	20.53	79.17	0.01
4	0.26	11.36	88.38	0.00
5	0.37	0.49	99.14	0.00
6	0.32	6.79	92.88	0.01
7	0.36	0.94	98.70	0.00
8	0.37	0.31	99.32	0.00
9	0.35	0.07	99.57	0.01
10	0.36	0.07	99.55	0.01
11	0.40	0.07	99.52	0.01
12	0.35	0.07	99.58	0.00
13	0.36	0.13	99.49	0.02
14	0.35	0.16	99.49	0.00
15	0.33	0.24	99.43	0.00

E.29 Fe/Ti/V/Nd After 28 Days at 625°C

The Fe/Ti/V/Nd assembly annealed for 28 days at 625°C bonded on the Fe/Ti, Ti/V, and V/Nd interfaces. Unfortunately, quantitative data from WDS linescans across these interfaces has been lost and is thus unavailable.

E.30 Fe/Ti/Nd After 28 Days at 625°C

The Fe/Ti/Nd assembly annealed for 28 days at 625°C bonded on the Fe/Ti and Ti/Nd interfaces. Unfortunately, quantitative data from WDS linescans across these interfaces has been lost and is thus unavailable.

E.31 Fe/Ta/V/Nd After 28 Days at 625°C

The Fe/W/Nd assembly annealed for 28 days at 625°C bonded on the Ta/V and V/Nd interface but not the Fe/Ta interface. Unfortunately, quantitative data from WDS linescans across these interfaces has been lost and is thus unavailable.

E.32 Fe/Ta/Nd After 28 Days at 625°C

The Fe/Ta/Nd assembly annealed for 28 days at 625°C did not bond on the Fe/Ta or Ta/Nd interfaces.

E.33 Fe/Mo/V/Nd After 28 Days at 625°C

The Fe/Mo/V/Nd assembly annealed for 28 days at 625°C bonded on the V/Nd interface but not the Fe/Mo or Mo/V interfaces. Compositional data (in at%) from WDS linescans across the V/Nd interface is given below.

Position	W	Nd	Mo	Fe	V
0	0.00	0.11	0.00	0.02	99.87
1	0.00	0.03	0.01	0.03	99.93
2	0.00	0.13	0.02	0.06	99.80
3	0.00	0.14	0.02	0.11	99.74
4	0.00	1.30	0.04	1.36	97.31
5	0.00	8.47	0.09	3.57	87.86
6	0.00	16.54	0.08	3.28	80.11
7	0.04	26.35	0.08	7.30	66.24
8	0.00	78.45	0.02	4.21	17.32
9	0.00	95.75	0.00	0.73	3.52
10	0.00	97.49	0.01	0.51	1.99
11	0.00	98.39	0.05	0.38	1.19
12	0.01	98.75	0.00	0.40	0.85
13	0.03	98.76	0.00	0.37	0.85
14	0.00	98.86	0.06	0.49	0.59
15	0.00	97.37	0.00	2.16	0.47

E.34 Fe/Mo/Nd After 28 Days at 625°C

The Fe/Mo/Nd assembly annealed for 28 days at 625°C bonded on the Mo/Nd interface but not the Fe/Mo interface. Compositional data (in at%) from WDS linescans across the Mo/Nd interface is given below.

Position	W	Nd	Mo	Fe	V
0	0.08	99.21	0.13	0.58	0.00
1	0.14	91.15	0.00	8.68	0.04
2	0.03	88.36	0.02	11.57	0.02
3	0.00	99.28	0.05	0.67	0.00

4	0.00	99.01	0.57	0.42	0.00
5	0.00	79.71	19.97	0.28	0.04
6	0.00	28.15	71.57	0.23	0.05
7	0.00	4.36	95.54	0.11	0.00
8	0.00	1.11	98.77	0.12	0.00
9	0.00	0.93	99.03	0.05	0.00
10	0.00	0.78	99.19	0.03	0.00
11	0.00	0.19	99.77	0.04	0.00
12	0.00	0.16	99.76	0.09	0.00
13	0.02	0.21	99.69	0.04	0.04
14	0.03	0.09	99.88	0.00	0.00
15	0.02	0.10	99.74	0.06	0.07
0	0.03	99.21	0.37	0.39	0.00
1	0.00	99.30	0.41	0.29	0.00
2	0.00	99.44	0.19	0.36	0.01
3	0.00	99.66	0.07	0.27	0.00
4	0.00	99.77	0.00	0.22	0.01
5	0.00	98.96	0.72	0.33	0.00
6	0.00	57.33	42.15	0.39	0.12
7	0.00	60.78	38.76	0.43	0.04
8	0.00	60.09	39.44	0.41	0.06
9	0.01	4.01	95.70	0.27	0.02
10	0.00	0.66	99.16	0.15	0.03
11	0.00	0.23	99.65	0.12	0.00
12	0.01	0.19	99.76	0.04	0.00
13	0.00	0.16	99.79	0.05	0.00
14	0.00	0.22	99.72	0.07	0.00
15	0.04	0.12	99.82	0.03	0.00
0	0.00	99.52	0.03	0.45	0.00
1	0.00	99.36	0.00	0.65	0.00
2	0.02	99.44	0.06	0.48	0.00
3	0.00	99.54	0.00	0.46	0.00
4	0.00	99.22	0.07	0.71	0.00
5	0.01	99.15	0.09	0.75	0.00
6	0.04	99.45	0.10	0.41	0.00
7	0.02	29.74	69.64	0.55	0.05
8	0.00	65.32	34.14	0.54	0.00
9	0.00	1.61	98.05	0.07	0.28
10	0.00	3.50	96.18	0.15	0.18
11	0.00	1.65	98.11	0.15	0.09
12	0.00	1.91	97.89	0.20	0.00
13	0.00	1.23	98.54	0.20	0.03
14	0.03	0.57	99.25	0.16	0.00
15	0.01	0.13	99.84	0.02	0.00

E.35 Fe/W/V/Nd After 28 Days at 625°C

The Fe/W/V/Nd assembly annealed for 28 days at 625°C bonded on the V/Nd interface but not the Fe/W or W/V interfaces. Compositional data (in at%) from WDS linescans across the V/Nd interface is given below.

Position	W	Nd	Mo	Fe	V
----------	---	----	----	----	---

0	0.02	1.27	0.01	0.64	98.07
1	0.01	2.00	0.01	0.77	97.21
2	0.03	2.24	0.01	1.04	96.69
3	0.00	0.51	0.01	0.08	99.40
4	0.00	0.85	0.01	0.32	98.81
5	0.00	0.79	0.01	0.76	98.44
6	0.02	2.29	0.00	0.76	96.93
7	0.00	23.77	0.00	2.56	73.67
8	0.06	86.04	0.00	1.14	12.76
9	0.06	95.87	0.04	0.42	3.61
10	0.15	94.85	0.00	0.84	4.16
11	0.13	96.71	0.00	1.09	2.08
12	0.00	97.64	0.00	0.90	1.45
13	0.00	98.48	0.03	0.33	1.16
14	0.00	98.64	0.02	0.32	1.02
15	0.00	97.88	0.00	0.48	1.63

E.36 Fe/W/Nd After 28 Days at 625°C

The Fe/W/Nd assembly annealed for 28 days at 625°C bonded on the W/Nd interface but not the Fe/W interface. Compositional data (in at%) from WDS linescans across the W/Nd interface is given below.

Position	W	Nd	Mo	Fe	V
0	0.11	99.41	0.05	0.43	0.00
1	0.00	99.63	0.02	0.36	0.00
2	0.04	99.58	0.03	0.36	0.00
3	0.12	99.36	0.00	0.52	0.00
4	0.15	99.40	0.01	0.45	0.00
5	1.29	98.22	0.02	0.36	0.11
6	18.28	81.12	0.00	0.53	0.07
7	81.83	17.22	0.00	0.95	0.00
8	98.27	1.32	0.00	0.40	0.01
9	99.50	0.44	0.00	0.06	0.00
10	99.61	0.29	0.00	0.11	0.00
11	99.58	0.28	0.00	0.14	0.00
12	99.76	0.19	0.00	0.00	0.06
13	99.83	0.12	0.00	0.02	0.03
14	99.90	0.09	0.00	0.00	0.00
15	99.89	0.11	0.00	0.00	0.00
0	0.03	99.37	0.00	0.49	0.10
1	0.00	99.66	0.03	0.32	0.00
2	0.12	99.50	0.00	0.37	0.01
3	8.21	91.42	0.03	0.27	0.06
4	20.56	79.17	0.00	0.27	0.00
5	76.87	23.02	0.00	0.11	0.00
6	96.94	2.99	0.00	0.08	0.00
7	98.45	1.52	0.00	0.00	0.04
8	99.23	0.75	0.00	0.01	0.00
9	99.38	0.59	0.00	0.00	0.03
10	99.43	0.53	0.00	0.00	0.04
11	99.52	0.25	0.00	0.07	0.17
12	99.57	0.24	0.00	0.00	0.19

13	99.33	0.48	0.00	0.09	0.10
14	99.62	0.36	0.00	0.02	0.00
15	99.68	0.27	0.00	0.05	0.00
0	0.52	98.11	0.06	1.08	0.23
1	6.97	91.14	0.05	0.58	1.26
2	2.26	96.69	0.00	1.03	0.03
3	1.83	96.45	0.02	1.70	0.00
4	44.40	54.76	0.00	0.85	0.00
5	93.62	6.12	0.00	0.12	0.13
6	99.07	0.82	0.00	0.11	0.00
7	99.55	0.45	0.00	0.00	0.00
8	99.47	0.39	0.00	0.08	0.06
9	99.70	0.19	0.00	0.12	0.00
10	99.88	0.11	0.00	0.02	0.00
11	99.76	0.16	0.00	0.00	0.08
12	99.81	0.11	0.00	0.09	0.00
13	99.64	0.14	0.00	0.12	0.10
14	99.80	0.07	0.00	0.07	0.06
15	99.91	0.04	0.00	0.05	0.00

E.37 Fe/Nd After 28 Days at 700°C

The Fe/Nd assembly annealed for 28 days at 700°C crumbled significantly upon removal from the diffusion jig, leaving no interaction interface to examine.

E.38 Fe/V/Nd After 28 Days at 700°C

The Fe/V/Nd assembly annealed for 28 days at 700°C bonded on the V/Nd interface but not the Fe/V interface. Since the V/Nd interface at this time and temperature was already well characterized, no WDS linescans were completed on it in this assembly.

E.39 Fe/Zr/V/Nd After 28 Days at 700°C

The Fe/Zr/V/Nd assembly annealed for 28 days at 700°C bonded on the Fe/Zr and V/Nd interfaces but not the Zr/V interface. Compositional data (in at%) from WDS linescans across the Fe/Zr and V/Nd interfaces is given below.

Position	Nd	Zr	Fe	V
0	0.33	96.02	3.65	0.00
1	0.11	99.25	0.52	0.12
2	0.24	94.05	4.88	0.84
3	0.15	99.16	0.68	0.02
4	1.24	89.41	8.94	0.42
5	0.05	99.37	0.54	0.04
6	0.08	99.44	0.47	0.00
7	0.04	99.30	0.66	0.00

8	0.05	99.31	0.61	0.03
9	0.11	99.26	0.61	0.02
10	0.08	99.35	0.57	0.00
11	0.05	99.24	0.69	0.02
12	0.08	99.21	0.70	0.01
13	0.12	98.59	1.27	0.02
14	0.06	98.55	1.39	0.00
15	0.05	97.86	2.06	0.04
16	0.05	97.38	2.58	0.00
17	0.03	97.82	2.16	0.00
18	0.05	90.40	9.45	0.10
19	0.02	1.42	98.55	0.02
20	0.03	0.13	99.82	0.02
0	98.28	0.00	1.29	0.43
1	99.19	0.00	0.50	0.31
2	99.20	0.00	0.42	0.39
3	99.06	0.01	0.43	0.50
4	99.02	0.00	0.43	0.55
5	98.14	0.00	0.54	1.32
6	98.42	0.01	0.41	1.16
7	97.91	0.03	0.48	1.59
8	97.60	0.00	0.40	2.01
9	97.39	0.04	0.43	2.14
10	97.36	0.00	0.47	2.17
11	95.63	0.00	0.87	3.50
12	95.68	0.00	0.99	3.34
13	91.60	0.15	1.94	6.31
14	90.07	0.12	1.59	8.23
15	65.03	0.00	6.29	28.68
16	26.05	0.03	4.74	69.18
17	7.23	0.04	2.06	90.66
18	0.31	0.01	0.27	99.41
19	0.21	0.01	0.03	99.76
20	0.61	0.12	0.11	99.16

E.40 Fe/Zr/Nd After 28 Days at 700°C

The Fe/Zr/Nd assembly annealed for 28 days at 700°C did not bond on the Fe/Zr or Zr/Nd interfaces.

E.41 Fe/Ti/V/Nd After 28 Days at 700°C

The Fe/Ti/V/Nd assembly annealed for 28 days at 700°C bonded on the Fe/Ti and V/Nd interfaces but not the Ti/V interface. Unfortunately, quantitative data from WDS linescans across these interfaces has been lost and is thus unavailable.

E.42 Fe/Ti/Nd After 28 Days at 700°C

The Fe/Ti/Nd assembly annealed for 28 days at 700°C bonded on the Fe/Ti and Ti/Nd interfaces. Unfortunately, quantitative data from WDS linescans across these interfaces has been lost and is thus unavailable.

E.43 Fe/Ta/V/Nd After 28 Days at 700°C

The Fe/Ta/V/Nd assembly annealed for 28 days at 700°C bonded on the V/Nd interface but not the Fe/Ta or Ta/V interfaces. Unfortunately, quantitative data from WDS linescans across these interfaces has been lost and is thus unavailable.

E.44 Fe/Ta/Nd After 28 Days at 700°C

The Fe/Ta/Nd assembly annealed for 28 days at 700°C bonded on the Ta/Nd interface but not the Fe/Ta interface. Unfortunately, quantitative data from WDS linescans across these interfaces has been lost and is thus unavailable.

E.45 Fe/Mo/V/Nd After 28 Days at 700°C

The Fe/Mo/V/Nd assembly annealed for 28 days at 700°C bonded on the V/Nd interface but not the Fe/Mo or Mo/V interfaces. Since the V/Nd interface at this time and temperature was already well characterized, no WDS linescans were completed on it in this assembly.

E.46 Fe/Mo/Nd After 28 Days at 700°C

The Fe/Mo/Nd assembly annealed for 28 days at 700°C bonded on the Mo/Nd interface but not the Fe/Mo interface. Compositional data (in at%) from WDS linescans across the Mo/Nd interface is given below.

Position	W	Nd	Mo	Fe	V
0	0.05	5.42	85.89	8.50	0.14
1	0.03	0.66	99.14	0.12	0.06
2	0.02	0.45	99.43	0.07	0.04
3	0.01	0.69	99.25	0.00	0.05
4	0.00	2.15	97.75	0.07	0.03
5	0.00	31.27	68.33	0.12	0.28
6	0.00	81.42	17.92	0.31	0.35

7	0.05	99.34	0.14	0.43	0.04
8	0.00	99.27	0.13	0.46	0.15
9	0.00	99.31	0.13	0.34	0.23
10	0.00	99.60	0.09	0.26	0.05
11	0.01	99.11	0.11	0.74	0.04
12	0.02	97.27	0.45	2.16	0.10
13	0.03	86.74	0.51	12.61	0.11
14	0.05	92.15	0.34	7.46	0.00
15	0.04	97.15	0.07	2.74	0.00

E.47 Fe/W/V/Nd After 28 Days at 700°C

The Fe/W/V/Nd assembly annealed for 28 days at 700°C bonded on the V/Nd interface but not the Fe/W or W/V interfaces. Since the V/Nd interface at this time and temperature was already well characterized, no WDS linescans were completed on it in this assembly.

E.48 Fe/W/Nd After 28 Days at 700°C

The Fe/W/Nd assembly annealed for 28 days at 700°C bonded on the W/Nd interface but not the Fe/W interface. Compositional data (in at%) from WDS linescans across the W/Nd interface is given below.

Position	W	Nd	Mo	Fe	V
0	0.22	98.43	0.00	1.27	0.08
1	0.15	99.17	0.03	0.63	0.01
2	0.24	98.44	0.00	1.32	0.01
3	0.19	98.85	0.00	0.89	0.06
4	1.49	98.09	0.00	0.42	0.00
5	5.63	93.41	0.02	0.92	0.02
6	41.62	58.13	0.00	0.24	0.01
7	70.58	29.11	0.00	0.29	0.02
8	90.84	8.13	0.00	0.81	0.22
9	79.20	20.24	0.00	0.49	0.07
10	98.65	0.85	0.00	0.13	0.38
11	97.12	0.95	0.00	0.19	1.73
12	98.72	0.70	0.00	0.07	0.51
13	98.49	0.94	0.00	0.21	0.36
14	99.40	0.45	0.00	0.06	0.10
15	99.38	0.29	0.00	0.17	0.16
0	0.15	99.11	0.00	0.74	0.00
1	0.25	98.19	0.01	1.55	0.00
2	0.26	98.65	0.00	1.06	0.04
3	1.20	98.21	0.01	0.55	0.04
4	10.85	88.61	0.00	0.54	0.00
5	30.38	69.00	0.00	0.63	0.00
6	16.04	82.53	0.00	1.43	0.00
7	5.53	93.38	0.00	0.89	0.21
8	63.54	35.48	0.00	0.75	0.23

9	88.54	10.20	0.00	0.39	0.86
10	97.68	1.21	0.00	0.07	1.04
11	99.02	0.51	0.00	0.01	0.46
12	99.41	0.53	0.00	0.00	0.07
13	99.51	0.22	0.00	0.02	0.26
14	99.64	0.17	0.00	0.02	0.17
15	99.63	0.10	0.00	0.05	0.22